

*McGraw-Hill* **HANDBOOKS**

# RADIANT HEATING & COOLING HANDBOOK



- Coupling radiant heating with forced air heating
- Principles of radiant heating and cooling relating to thermal comfort
- Sample calculations

RICHARD D. WATSON  
KIRBY S. CHAPMAN

**S · E · C · T · I · O · N · 1**

**INTRODUCTION TO  
RADIANT SYSTEMS**



---

# CHAPTER 1

---

## EXAMPLES OF RADIANT SYSTEMS

---

The earth is heated radiantly. Almost everyone worldwide identifies with the warmth of the sun. Whether welcoming the sun on a cool spring day or seeking shelter from the sun on a hot summer day, everyone has developed a response to the sun. In fact, many daily activities are planned around the presence or absence of sunshine. Yet, few people think in terms of the sun being the earth's heating system. Perhaps, because the sun is such a dependable, reliable, and predictable heat energy source, people take it for granted.

Few people, whether laypeople or professionals, make the connection between natural radiant heating and cooling in the great outdoors and environmental conditions for human occupancy in the built environment. But they really can be made to function very similarly. The objective is to capture the best of outdoor comfort for creation in the built environment whenever desired or required. To understand what may be involved, it is instructive to examine just how and why nature's heating system actually works.

To the best of our current knowledge, only the earth is dynamically positioned in relation to the sun to enable exploitation of its resources to support life as we know it. The daily rotation of the earth during its annual orbit around the sun results in the simultaneous 24-hour routine we know as day and night and the climatic change we know as seasons that fans out from the equator. In the natural environment, shelter, insulation (fur, clothing, or structural), life-cycle change, and migration are a few of nature's responses to changing daily and seasonal environmental conditions.

The reason for changing the climate in the built environment is to provide for building use, occupant comfort, and safety of the building and its contents. Yet, to do this in a cost-effective manner requires that the entire structure be viewed as a system in support of the relevant preceding objective. Building design and environmental siting impact the performance of heating and cooling design. The focus of efficiently and effectively heating and cooling a building should include a comprehensive analysis of all the relevant interactions, whether natural or manmade, to ensure that the energy balance is optimized in relation to the objective. The same system logic feeds concern about global warming due to a change in any one of the components in the complex web of environmental balance.

## 1.1 NATURAL THERMAL ENVIRONMENT

---

We find in nature all of the elements that are applied and controlled in the built environment. Radiation, convection, conduction, condensation, evaporation, and the resulting influences of each action are described in detail in the Handbook as we seek to harness the laws of physics for application to the built environment. The performance of a radiant environment contrasts with that where air is used to deliver or extract heat. To better understand the radiant built environment we will look at a few examples of how the natural radiant environment operates.

A look at the normal agricultural cycle in the continental United States tells us that soil temperatures, essential to plant growth, are the main determinant of the planting period. Actual soil temperatures are a direct result of radiant heat charge and discharge. A look at the time lag involved is instructive to understanding the performance of building mass in radiant heating and cooling. The other variable also at work is the change in angle and intensity of the sun. The winter solstice, or shortest day of the year, is December 21, when the sun cycle is shortest and weakest.

The coldest part of winter in the United States normally occurs in January, when the days are actually lengthening and the earth is moving closer to the sun. The recharging of the earth mass continues for more than 4 months before the soil temperature is at levels required for seed germination. In fact, the longest sun exposure and greatest potential radiant intensity occurs at the summer solstice on June 21. Although sun intensity and length of exposure then decrease until the occurrence of the winter solstice on December 21, it is not unusual to have warm days through the end of October without a killing frost. These same areas may experience temperatures of 0°F or below by, or even before, January.

Lengthy charging and discharging periods are characteristic of high-mass radiant heating and cooling. The resulting thermal stability is a unique characteristic of radiant heating that yields rich design alternatives, ranging from passive solar and earth thermal storage to an array of cooling strategies. The time constants involved in the built environment relate to the building structure, natural external exposure, and radiant panel selection. Whether occurring naturally or by design, the harnessing of radiant energy for the provision of thermal comfort and energy conservation differentiates the design of radiant heating and cooling systems from natural and mechanical convection systems.

## 1.2 APPLICATION OF NATURAL PRINCIPLES

---

Public awareness of outer space exposure to the impacts of radiation heat transfer was sparked by the launch of the first Soviet Sputnik satellite. Although commercial, combat, and reconnaissance aviation required resolution of radiant heat transfer impacts, human travel in outer space required a comprehensive resolution of radiant heat transfer impacts over the full range of human exposure. The vision of a man walking in the environment on the moon graphically conveyed how far the management of energy transfer had come. The space suit provided greater freedom of movement at -300°F (-184.1°C) than the first commercially sewn, bulky down snowsuits provided at 0°F (-17.4°C).

Recognition of the application's potential for materials exploiting basic radiant heat transfer principles spurred extension of reflective insulation into common everyday use. One dramatic comfort and conservation application for the building

industry in hot climates is the reduction in attic temperatures achieved through the application of low-emissivity surface to the underside of roof panels to reduce radiant heat transfer from the hot roof to the attic floor or ceiling below. Considerable study revealed that attic ventilation was ineffective in reducing the air-conditioning heat load caused by radiant heat transfer from the roof above and, in fact, could increase the air-conditioning load by increasing the exfiltration of mechanically cooled air.

The development of window films and spectrally selective coatings responds to the need to harness the visible and invisible infrared spectrum to provide safety, comfort, and energy conservation. The development of high-performance windows has proceeded to the point where so little heat is transferred to the outer glass surface that condensation can occur at night due to nocturnal radiation. To get a sense of the magnitude of nocturnal radiation through the atmosphere, think of how much warmer the air remains on a calm, cloudy night versus a calm, clear night. The difference is caused by the role the cloud cover plays in lessening energy escape, which may reduce the day-night temperature range by  $10^{\circ}$  to  $30^{\circ}\text{F}$  or more. A second example is the ability to freeze water in the desert at night when the ambient temperature is much higher than  $32^{\circ}\text{F}$  ( $0^{\circ}\text{C}$ ). A pan of water radiates more heat to the clear night sky than it receives from the surrounding air. Hence, the equilibrium temperature of the water drops below the freezing point, even though the surrounding air temperature is actually above the freezing point.

The discomfort caused by heat loss from the human body to a cold window is well understood, but the application of the same principles for cooling by use of a low-temperature cold-radiant panel is still relatively uncommon. Yet, primitives sought relief from the heat in caves and other places with cooler surface temperatures, where radiant cooling supplanted evaporation as the main agent of temperature reduction. In arid climates, evaporative cooling of the air is cost-effective, as is evaporative cooling of roof surfaces that are misted, thereby cooling water that is recovered for use as the cooling fluid for radiant panels or to lower the temperature of building mass.

The ability to sunbathe on a calm  $60^{\circ}\text{F}$  ( $15.9^{\circ}\text{C}$ ) spring day is a dramatic example of the role that radiant energy can play in providing thermal comfort at a lower ambient dry-bulb air temperature. Another equally striking example is that of skiers in swimsuits on days when the air temperature is in the  $40^{\circ}\text{F}$  range and the snow is still crisp and fresh. The relatively high metabolic rate; dry, clear, thin high-altitude air; strong late-spring sun; and snow covered surface all combine to enable the high-intensity radiant field make the human body feel comfortable in otherwise cold conditions. These examples are illustrative of the important role that radiant heat transfer can play in providing human thermal comfort.

Greenhouses are designed to make use of radiant energy from the sun. However, most people do not understand why a greenhouse can absorb more radiant energy than it loses and, therefore, develop significantly higher inside temperature than the surrounding outside air. The answer lies in the spectral characteristics of the radiant energy from the sun and also of glass. A substantial percentage of the radiant energy from the sun is at short wavelengths. Glass is transparent to short-wavelength radiation; therefore, the greenhouse glass allows most of the radiant energy from the sun to enter the greenhouse. The radiant energy that is emitted within the greenhouse is at long wavelengths, and it happens that glass is opaque to long wavelength radiation. Hence, the radiant energy trying to leave the greenhouse is stopped by the glass. These are the same reasons that the enclosed interior of a car sitting in the sun can become quite warm inside on a calm, sunny  $0^{\circ}\text{F}$  ( $-17.4^{\circ}\text{C}$ ) winter day. As you will discover in Sec. 2, long- and short-wavelength radiation come from low- and

high-temperature sources, respectively. This concept will have some application in the employment of radiant heating systems.

The creation of heat from radiation leads to another natural phenomenon, the movement of air we know as wind. Anyone who has ever sat in Wrigley Field, which is located on the shore of Lake Michigan, has basked in the warm midday zephyr breezes only to find the wind suddenly shifting from the West to the East off a cold Lake Michigan. The hot air from the warmed agricultural plains west of the city and the draft from the hot, level concrete and asphalt city surfaces draw in the cooler air off of the Lake, suddenly shifting the airflow. The air replaces the rising air heated by the thermally charged high mass of the city as it continues to discharge heat and until the plains cool through nocturnal radiation to a temperature below the surface temperature of the Lake water and the process begins anew. The lesson here is that air movement is driven by temperature gradients, and that it is not heat that rises, but hot air. This is a truth of physics that is often confused, but must be sorted out to understand the significance of radiant panel location and sizing and comfort design.

Condensation, or dew, is a common natural occurrence that we seek to eliminate in the built environment. For many heating and cooling systems, relative humidity within normally acceptable limits is inherent to the system. Natural relative humidity varies from as low as 0 percent below freezing to 100 percent over the range of temperatures above freezing. The entrance of outside air into the built environment may require the addition or removal of moisture from the air. These conditions are most evident in the winter when people complain of nasal passage or sinus dryness and in the summer when mold and mildew appear due to excess moisture. Radiantly heated and cooled homes normally experience significantly lower rates of infiltration and exfiltration, reducing the impact of casual outside air on the indoor environment. The role of indoor and outdoor temperature is as important a determinant in the significance of natural building pressure differences as the influence of mechanical air distribution balance and pressure protocol is on determining its parasitic influence on infiltration and exfiltration.

The orientation, material selection, grade, and elevation design, as well as landscaping are among the design decisions that impact the role of natural and designed radiant heating and cooling. These decisions should be made in conjunction with the review of heating, ventilation, and air-conditioning alternatives. Yet, whatever decision is made will include all three elements of heat transfer. In essence, all analyses of the structure and occupant as a system are incomplete unless they recognize that comfort is achieved through management of the entire range of dynamic thermal transfer. The objective of this Handbook is to empower the reader to identify the role of each and to develop the exact blend or combination of each that best serves the design application.

---

# CHAPTER 2

---

## ADVANTAGES OF USING RADIANT SYSTEMS

---

Radiant heating and cooling systems offer unique features that merit the inclusion of radiant analysis in heating, ventilation, and air-conditioning (HVAC) design considerations. There are many radiant system features that differentiate radiant and convection heating design, performance, and cost. Some of the features present opportunities to take a fresh look at the building as a system using radiant as the primary system (Fig. 2.1). Other features make radiant an ideal complementary component for another dominant system in what then becomes a hybrid system. The important key to remember is that the range and flexibility of systems and application options is every bit as encompassing as those common to convection system design.

---

### 2.1 OCCUPANT THERMAL COMFORT

---

It would seem obvious that occupant thermal comfort would be the objective of any HVAC system. However, trade publications such as *Professional Builder and Contractor* magazine surveys show little year-to-year change in reporting that almost one-half of building occupants—residential or commercial—are not fully satisfied with their level of comfort. This is especially surprising when you consider that the American Society of Heating, Refrigeration, and Air-Conditioning Engineers (ASHRAE) Standard 55-92, *Thermal Environmental Conditions for Human Occupancy*, has been available for incorporation into design performance for decades. The Standard identifies the mean radiant temperature (MRT) as an important factor in assuring human thermal comfort. Radiant systems provide unique, cost-effective approaches to addressing numerous conditions affecting human thermal comfort, as primary or hybrid systems. Standard 55-92 provides the conditions and methods for analysis to ensure compliance with the Standard.

Radiant systems are used to condition space, often in the traditional way that convection systems must do, by their nature, to produce a selected air temperature. However, radiant systems may also be used to heat people in comparison to space. The idea is that the occupied air mass is heated to a lower dry-bulb temperature than with a convection heating system as long as the occupants are radiantly heated. The objective is to save energy or to overcome otherwise adverse local comfort conditions (Fig 2.2). The range of radiant equipment, design, and temperature options provides great flexibility over a broad range of conditions and human occupied environments. Concealed radiant systems convert an interior building surface into a radiant heat transfer panel.

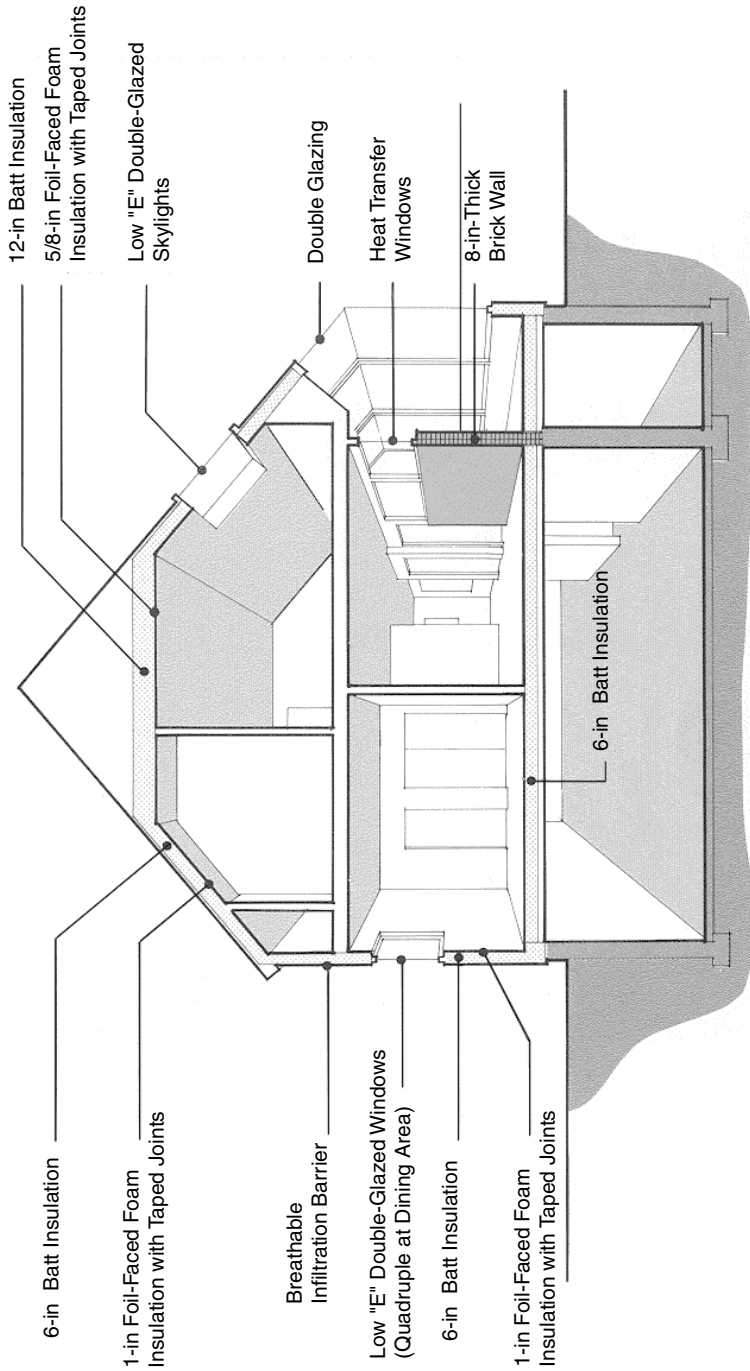


**FIGURE 2.1** House as a system. The interactions of home features influence system design and performance.



**FIGURE 2.2** Comfort is the key feature of a radiant environment. (Source: Photo courtesy of Delta-Therm Corporation.)

Modular panels affixed to the wall or ceiling require a small fraction of the surface area of concealed systems due to their higher surface-heating temperatures. Cooling panel surface temperatures are dew point constrained, regardless of configuration. The important point to remember is that panel surface area and MRT requirements are important factors influencing several aspects of radiant system selection.

Radiant systems provide the opportunity to provide comfort at lower ambient air temperatures. ASHRAE Standard 55-92 provides information about the index of human thermal comfort: *operative temperature* (OT). Operative temperature is the weighted average of MRT and dry-bulb air temperature, which for convenience is approximated as the simple average in the built environment. Under uniform conditions, the readings converge. However, under transient conditions, or conditions that are not uniform, a divergence occurs.

A radiant system may be employed to provide the higher or lower MRT necessary to achieve the OT required for human thermal comfort.

The presence of the radiant field, or MRT, characteristic of all radiant systems, normally results in comfort at a 4°F (–15.2°C) to 6°F (–14.1°C) lower dry-bulb air temperature than if a convection heating system were used. The U.S. Department of Energy guideline is that a 1°F air temperature reduction results in a 3 percent energy reduction. Table 2.1 shows detailed presentation of temperature setback heating load reduction in the commonly encountered range of dry-bulb air temperature set points. Therefore, a 12 to 18 percent energy reduction is a minimum expectation for a radiant system in comparison to a convective system providing equivalent comfort. The actual dollar impact would relate to the relevant fuel or energy costs.

## **2.2 RADIANT CHARACTERISTICS AND APPLICATIONS**

---

Radiant systems are fuel neutral. Gas, oil, electricity, and alternate energy sources are all viable options for operation of radiant systems. The focus of this book is primarily on the radiant delivery configuration, performance, and sizing. The reader may be assured that there is plenty of information available about heat pumps, boilers, combination electric and gas water heaters, and electrical service to determine the most appropriate heating or cooling option to serve the desired radiant system.

The transfer of more than 50 percent of energy radiantly characterizes the definition of a radiant heating or cooling panel (ASHRAE), or other truly radiant device, including heaters such as quartz or tube heaters (Fig. 2.3). The balance of



**FIGURE 2.3** Industrial gas-tube heaters. (Source: Photo courtesy of Detroit Radiant Products.)

energy transfer is accomplished through either convection or conduction. While radiation is dominant, convection is usually the next largest means by which heat is transferred from a radiant panel. Stratification is normally less with radiant systems than convection systems, which are characterized by the buoyancy of the warmed air that facilitates the natural or mechanically driven heat distribution.

**TABLE 2.1** Percentage Reduction in Annual Heating Load Resulting from Lower Setting of Thermostat\*

Original thermostat setting, °F	Degree decreases in original thermostat setting									
	1°	2°	3°	4°	5°	6°	7°	8°	9°	10°
70	3.74	7.41	11.02	14.56	18.03	21.42	24.74	27.99	31.16	34.26
69	3.81	7.56	11.24	14.84	18.37	21.81	25.19	28.49	31.70	34.85
68	3.90	7.72	11.46	15.13	18.71	22.23	25.65	29.00	32.27	35.46
67	3.97	7.87	11.69	15.42	19.07	22.64	26.12	29.52	32.84	36.10
66	4.06	8.04	11.92	15.72	19.44	23.06	26.60	30.07	33.46	36.76
65	4.14	8.19	12.15	16.03	19.80	23.49	27.10	30.64	34.09	37.44
64	4.22	8.36	12.40	16.34	20.19	23.95	27.64	31.24	34.74	38.13
63	4.32	8.54	12.65	16.67	20.60	24.45	28.21	31.86	35.41	38.86
62	4.41	8.71	12.91	17.02	21.04	24.97	28.87	32.49	36.09	39.61
61	4.50	8.90	13.19	17.40	21.51	25.50	29.38	33.15	36.83	40.40
60	4.60	9.11	13.51	17.81	21.99	26.05	30.00	33.85	37.59	41.20
59	4.72	9.34	13.85	18.23	22.48	26.62	30.66	34.58	38.36	
58	4.85	9.58	14.18	18.65	22.99	27.23	31.34	35.30		
57	4.97	9.80	14.50	19.06	23.52	27.84	32.01			
56	5.09	10.03	14.83	19.52	24.06	28.45				
55	5.21	10.27	15.21	19.99	24.62					

\* Results assume no internal or external heat gains. This chart is applicable to residences and commercial buildings where these gains are minimal.

Radiant systems may accommodate any building configuration or material surface. Radiant panels accomplish heat transfer utilizing hydronic or electric conduit in many design configurations. The actual radiating surface characteristics generally do not significantly impact the radiant output because the surface emissivities of commonly encountered materials are 0.85 or higher. The important design and performance factor to be evaluated is the existing or potential resistance to heat transfer presented by materials that separate the heat-generating source from the radiation panel surface.

Radiant panel location—ceiling, wall, or floor—is the major determinant of the division of heat output between radiation and convection. The location of the radiant system, as well as the panel configuration, will impact the radiative-convective heat transfer split. The definitional panel radiant output range of more than 50 percent defines the base radiant design factor that must be fine-tuned with the largely convective balance for proper radiant panel sizing. Determining the radiative-convective split is an important design factor in ensuring that OT requirements are met.

Radiant systems may be characterized as having minimal transmission loss in hydronic systems and no transmission loss in electric systems. Convection systems may experience from 20 to 40 percent or more in losses from the ducts required to transport the energy from the source to the occupied space. ASHRAE Standard 152P, *A Standard Method of Testing for Determining the Steady-State and Seasonal Efficiencies of Residential Thermal Distribution Systems*, is a standard for thermal distribution that provides the methodology to determine these thermal distribution losses. Determining the magnitude of distribution loss is an important comparative system sizing parameter and operating cost determinant.

Heating system choice can impact building performance in terms of relative humidity due to an increase in infiltration. Radiant systems do not produce air temperatures significantly above the thermostat set point. Convective systems, whether perimeter baseboard or warm air, increase the indoor-outdoor temperature differential significantly—20°F (−6.3°C) to 50°F (10.3°C)—in various locations at various times. In addition, the stack effect of delivery air temperature well above thermostat

set point also increases infiltration of cold, dry outside air, which then reduces the interior relative humidity. The relative humidity in radiantly heated buildings is normally within the range recommended in Standard 55-92.

Eliminating or reducing the use of air to distribute or remove energy lessens a major source of pollen, dust, bacteria, and germ distribution. Radiant systems are nonallergenic and often prescribed for people with allergies. Fig. 2.4 shows a popular stainless-steel portable model. In cases in which makeup air is mandated, designers may choose the appropriate design to provide the correct amount of air required by ASHRAE Standard 62, *Ventilation for Acceptable Indoor Air Quality*. Regardless of the circumstances, the net reduction in air movement is sig-

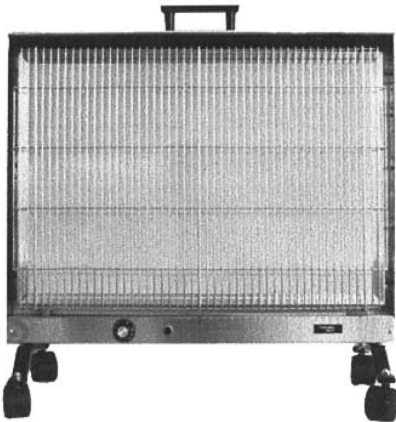


**FIGURE 2.4** Ceramic portable nonallergenic heater. (Source: Photo courtesy of Radiant Electric Heat.)

nificant in reducing the transfer of airborne contaminants, as well as the cost of air distribution and filtration.

The characteristic reduction in infiltration and exfiltration of a radiant system contributes to the significant overall sizing reduction compared with convection systems. Capacity reduction is significant in terms of initial cost, operating cost, and energy requirements. Reduced radiant sizing may provide an opportunity for significant peak power reduction in electrically heated or cooled buildings.

Hydronic system capacity reductions provide the incentive for development of new heater products, including combination potable and hydronic water heaters. The newly energized boiler industry is responding with many innovations, including a significant increase in the range of acceptable incoming and outgoing fluid temperatures, sizes, and packaged systems.

Radiant panels are noiseless. Absent the creaks, vibrations, and air noise characteristic of the different convection systems, radiant panels are silent and odorless. Scorched-dust air odors are eliminated.

Thermal stability is generally greater in buildings with radiant than with convection systems. Interior space temperatures are tempered by the flywheel effect of the embedded energy characteristic of concealed radiant panels (Figure 2.5). Surface radiant heating or cooling panels (Fig. 2.6) may also be used to charge the mass when it is cost-effective to do so. In the normal operation of radiant panels, opposing surfaces directly absorb and reradiate energy in relation to their surface emis-

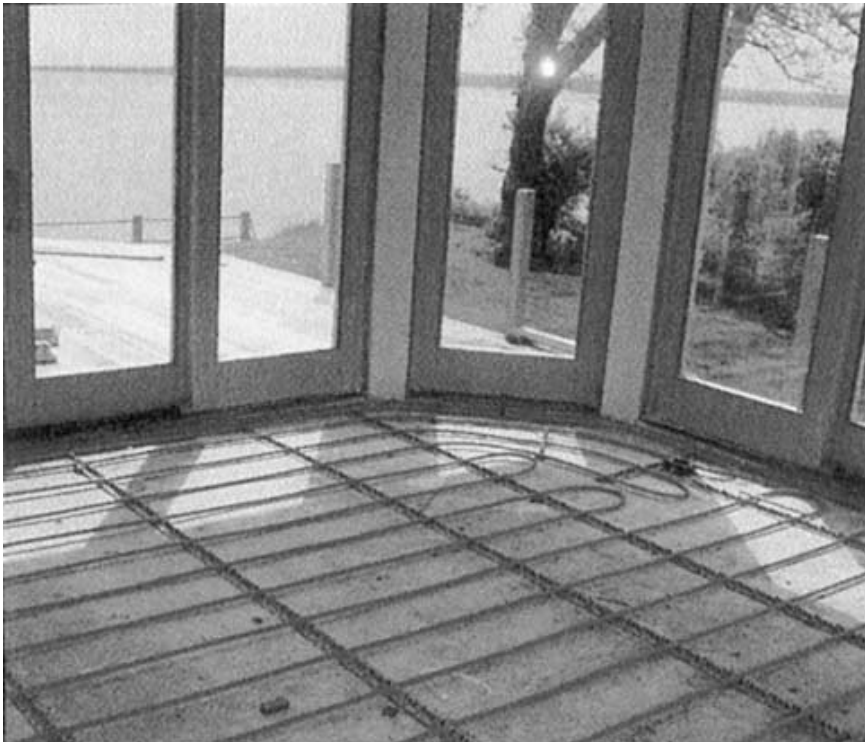


**FIGURE 2.5** Residential radiant hydronic floor heating.



**FIGURE 2.6** Hydronic radiant ceiling cooling panels with displacement ventilation system.

sivities and respective temperatures. The thermal energy storage and/or thermal stability characteristics of radiant systems provide unique opportunities for the economic management of human thermal comfort.

Radiant panels are generally maintenance-free. The advent of new materials and technologies has given many radiant systems almost a life of the structure longevity. Manufacturer warranties should be consulted in every case. Radiant system maintenance for hydronic systems is primarily a function of the radiant panel support equipment, which may include boilers, heat pumps, valves, fittings, meters, controls, and so forth.

### **2.3 RADIANT ENERGY AND OPERATING COST**

---

Case studies confirm the energy savings that radiant users have anecdotally reported for years. Studies also confirm reduced heat loss and sizing design for radiant systems. Case study results specific to one type of system may be inappropriate for extrapolation to other radiant systems. The differences among radiant heating systems require appreciation of the design impacts that affect system performance of each form of radiant heating.

While each radiant panel design or product may be unique, there is a common basis to expect lower operating costs through their use in buildings that meet the prevailing ASHRAE 90.1 and 90.2, *Commercial Energy Standards* and *Residential Energy Standards*, respectively. The common factors are occupant thermal comfort at lower ambient air temperatures, reduced infiltration, and lower system-induced heat loss.

Additional energy savings may be achieved through thermal storage, task heating or cooling, dynamic or sophisticated control, zoning, and hybrid systems. The oppor-



**FIGURE 2.7** Electric radiant ceiling panel. (Source: Photo courtesy of SSHC, Inc., Solid-State Heating Division.)

tunities for assuring comfort through conservation are greatly enhanced by the incorporation of radiant heating and cooling in the overall building-as-a-system design analysis approach. Incorporation of the occupant as the object by which the comfort of the system is measured fits right in with the approach long advocated by cutting-edge organizations, including Affordable Comfort, Inc.; the Energy Efficient Building Association; and the Quality Building Council of the New England Sustainable Energy Association.

---

## CHAPTER 3

---

# HOW TO USE THIS BOOK

---

The process of choosing a heating or cooling system requires disciplined analysis of information that is relative to the determination of comparative system performance. Typically these include parameters for comfort, energy consumption, maintenance cost, architectural detail, system space requirements, impact on occupant space utilization, reliability, flexibility, as well as first and life-cycle costs. The objective is to select a system that satisfies the agreed-upon goals for providing the desired built environment.

In addition to the normal engineering design parameters, there may be system selection-influencing goals, such as supporting a unique process or activity (e.g., a computer center, hospital surgical area, or a mother-in-law suite). The goal may be promotion of aseptic or clean room environment, or increasing sales of office condominium space, or increasing net rental income, or salability of a property, or any one of several other goals that heating system selection might impact.

The structure of this Handbook is designed to provide the information required in order to guide the reader through the decision points that determine the true comparative relationship of radiant heating and cooling systems with conventional heating, ventilating, and air-conditioning (HVAC) systems. The framework for evaluation, in addition to the technical theories and design application information, demands an appreciation of the typical broad-picture factors. The location; financial functional, and productivity constraints; and first cost compared with operating cost are early primary inputs. Secondary considerations include maintenance frequency, extent, and impact on occupants; system failure frequency and impact; and repair time, cost, and parts dependability and long-term availability.

The rapid technology advances in equipment, electronics, materials, components, and system packaging make it impractical to assemble specifications in this Handbook. The good news is that mastery of the principles and design checkpoints equips the reader to make selections that satisfy the design and performance specifications. The role of the intermediary supply source, whether it is the local supply house, a manufacturer's representative, the contractor, or the factory, is important in acquiring detailed product information. As with any HVAC system, the job is only as good as the installing contractor makes it. Close inspection at each stage of completion is important to ensure that it is built as it is designed. The reader is encouraged to make note of information on radiant panel and system design elements that influence system performance.

The advantages and disadvantages of conventional systems are well known by engineers, designers, building owners, and occupants. The comparative features of radiant alternatives are generally unknown because the commonly used engineering and simulation programs are designed for convection heating systems. In

fact, although convection and conduction are integral factors in the algorithms employed, a key factor in human thermal comfort, mean radiant temperature (MRT), is absent. This aim of this Handbook is to arm the reader with a working appreciation for the role of MRT in distinguishing radiant from convection systems. The reader will develop the ability to provide thermal comfort designed to the standards of ASHRAE 55-92 through radiant system selection from an array of proven radiant heating design options.

This brief review of where to go for specific information by section and by chapter provides the reader with a quick overview of how to use the Handbook. It is provided to enable readers with varying backgrounds and interests to quickly identify the path and location of information they need. The reader is also reminded of the “Definitions of Terms and Conversions” chart in the front of the Handbook, as well as the index at the end.

### **3.1 SECTION AND CHAPTER OVERVIEW**

---

The most important determinant of the accuracy of the overall design analysis is how well the work has accounted for all energy flows. Section 2, “Fundamentals of Heat Transfer and Thermodynamics,” is where the reader finds detailed explanations of how this is accomplished.

Chapter 1, “The Energy Balance,” covers conservation and mass equations, heat transfer and work, the energy content of air—internal energy and enthalpy. The conclusion of the chapter elements is the conservation of energy equation. Chapter 2, “Conduction and Convection Heat Transfer,” explains the underlying theory through Fourier’s law of heat conduction and detailed explanation of thermal conductivity. Newton’s law of cooling, the heat transfer coefficient, the Reynolds and Prandtl numbers, and the Nusselt number and correlations for the heat transfer coefficient discussion include the important numbers and correlations required to develop specific heat transfer coefficients. The theory is placed into design perspective in “Combining Building Materials into a Wall, Floor, or Ceiling.” Many contractors use heat loss analysis programs that stop at this point. Most simulation programs incorporate elements of radiant heat transfer, which are covered in Chap. 3, “Radiation Heat Transfer.”

Radiant heat transfer is the equally important third form of heat transfer. The incorporation of radiant heat transfer factors into design programs completes the opportunity to optimize building design performance, including heating and cooling, and most important, in relation to human thermal comfort. Calculation complexity and time constraints have been overcome by the evolution of computer programming and run time that makes inclusion of radiant transfer factors practical for personal computers.

Chapter 3, “Radiation Heat Transfer,” begins with a discussion about wavelengths, microns, and the electromagnetic spectrum, followed by absolute temperature scales. The important subject of radiative intensity, the basic building block of radiative heat transfer, is covered fundamentally, but in relation to application in the built environment. The body of defined theory is covered in Planck’s law, blackbody radiation, Wien’s displacement law, and the important Stefan-Boltzmann equation. Perhaps the most important, but often left out, material on surface emissivity, absorptivity, and transmissivity characteristics are covered in an easy-to-understand format that brings to life the performance of building material surfaces in a radiant environment. Thermophysical properties of matter encountered in the built environment are the subject of an overview discussion that commences with thermal conductivity of various

building materials and  $R$  values, followed by the density of common building materials and specific heat of common building materials. The properties of air and water vapor are introduced, followed by a revisit of the emissivities and absorptivities of common building materials. Window transmissivity, emissivity, and absorptivity are related to radiant heating system design, energy, and comfort impacts.

View factor calculations were a major stumbling block that computer capability has overcome, yet it is important to understand their role in radiant system design and performance. Chapter 3 next explores the radiative resistance network approach to calculations of radiative heat transfer, followed by a discussion of solar radiation versus radiant heating systems, which nicely ties together the natural radiant environmental heating system with radiant heating systems for the built environment. Finally, the advanced topic: the radiative transfer equation is presented for those who may choose to work the math, which includes the spherical harmonics method, Monte Carlo method, and discrete ordinates modeling.

Multimodal heat transfer is the subject of Chap. 4. The integration of convection, conduction, and radiation heat transfer into a complete heat transfer analysis system leads to discussion of techniques to analyze combined heat transfer cases.

Chapter 5, "Psychrometrics and Mixtures," deals with the fundamentals of moisture analysis in the design process. Topics covered are humidity ratio, relative humidity, dewpoint temperature, the psychrometric chart, and heating and cooling humid air.

"Fluid Mechanics," Chap. 6, is essential to the design of hydronic radiant heating and cooling systems. Bernoulli's equation and the complete range of pipe flow, pump power, and head loss calculation methodology is reviewed.

Section 3 is "Thermal Comfort." Chapter 1 asks and answers the question, What Is Thermal Comfort?, and it looks at the effects of thermal distribution systems. Chapter 2 reviews the Rohles-Nevin studies, the Fanger and Gagge models, and improvements to the Fanger and Gagge models. These participant studies and models are the basis of thermal comfort design methodology, which is explored in a discussion of recent thermal comfort tools. Chapter 3, "The Mean Radiant Temperature," provides definition, relationship to thermal comfort, and measurement techniques. Understanding MRT is essential to appreciating the performance capabilities of radiant heating and cooling systems in comparison to convection. The interrelationship of MRT is explained in Chap. 4, "The Operative Temperature." Included in the discussion is the definition, relationship to thermal comfort, measurement techniques, and example calculations and procedures for thermal comfort calculations.

Section 4, "Sizing and Load Estimation," starts with Chap. 1, "ASHRAE Standard Methods," in which design point, multiple-measure sizing, and detailed simulation methods are reviewed. Chapter 2, "The Building Comfort Analysis Program Methodology," details the methodology, including analysis of information provided, as well as output that these methods do not provide, along with the common estimating approaches to factoring various changes into time block calculations. The example calculations provide radiant heating application calculations, which demonstrate methodology to develop information that differentiates radiant heating system design using the Building Comfort Analysis Program (BCAP).

In Sec. 5, "Radiant Heating Systems," Chap. 1, "Introduction to Radiant Panels," presents a review of common radiant panel configurations, location, and distinguishing performance, design, and installation features. Chapter 2, "Electric Radiant Heating Panels," presents the universal principles governing electric radiant panel performance. The first category is preinsulated panels, which includes framed fast-acting panels and metal-encased panels. The second common electric panel category is cable, mat, or flexible element heating, which is primarily differentiated by ceiling and floor location of field-constructed embedded designs, or manufactured sheetrock and gyp-

sum panels. Ceramic or glass heat fixtures include cove, recessed wall, and baseboard heaters utilizing ceramic or glass heating element panels. Filament, metal-sheathed, and quartz heaters, which are higher in watt density and radiant intensity, round out Chap. 2.

Chapter 3, "High-Temperature Heaters" delineates high-, medium-, and low-temperature heaters, and gas-fired radiant tube heaters. There is information on pollutant emissions, with information of increasing design relevance in gas radiant specification. Chapter 4, "Hydronic Radiant Heating Systems," contains an extensive introduction to radiant hydronic systems. In a discussion of overhead hydronic panels, there is information on concealed radiant hydronic ceiling systems and visible hydronic radiant ceiling heating panels. Hydronic radiant floor panels, radiant hydronic wall panels, and alternate energy radiant hydronic heating systems complete Chap. 4. Chapter 5, "Case Studies," presents information from case studies and research conducted by recognized third-party entities that furthers the understanding of comparative radiant system performance.

Section 6, "Control Operations for Radiant Heating and Cooling Panels," follows mastery of radiant fundamentals in importance. Successful control exploits the full comparative advantages of radiant versus convection heating. Chapter 1, "Introduction," sets up the comparative analysis by detailing interface with the occupant and interface with the conditioned space. Chapter 2, "Role of the Heat Output," reviews mechanical and electronic line and low thermostats. Chapter 3, "Controls in Common Use," reveals the emerging opportunity for occupant-comfort-oriented heating and cooling. Subjects such as lead/lag and thermal charge/discharge, as well as outdoor reset, are discussed. Chapter 4, "Thermostats and Thermal Comfort," explores the common options for network comfort and energy management.

Section 7, "Radiant Heating and Cooling Hybrid Systems," introduces the developing appreciation for the benefits of mixing and matching the smorgasbord of heating and cooling options and explores the myths and mystique that may explain the limited harvest of radiant cooling potential. Chapter 1, "When to Use Hybrid Systems," begins with a definition of hybrid systems and continues with cases when combination systems are preferred. Chapter 2, "Convective Systems with Radiant Panels," describes design strategies for optimizing system combination. Chapter 3, "Ventilation with Radiant Heating and Cooling," covers indoor air quality, infiltration/exfiltration, dehumidification, and cooling. Chapter 4, "Hybrid Heating and Cooling Demonstration Projects," demonstrates the design methodology for successful radiant and convective system interaction.

Section 8, "Engineering Design Tools to Assist in Heater/Cooler Sizing," is an insightful comparative review of the range of design methodology capabilities. Chapter 1, "Computer-Aided Thermal Comfort Design Tools," discusses the range of computer tools available to the designer. Chapter 2, "Computer-Aided Codes Presently Available," is really an introduction to accelerating computer code development. Chapter 3, "Actual Building Occupant Verification Efficiency, ABOVE<sup>®</sup>," discusses the information output that can be generated from a dynamic, energy balance, thermal comfort design program. Chapter 4, "Design Parameters," reviews key design inputs such as surface coverage and panel location impacts, heater cycling, window versus wall surface area ratio, air change ratio, and so forth. A discussion of example heater sizing, location, and design calculations presents different approaches to optimizing the radiant heating system.

This review provides a brief overview of the Handbook. The reader is encouraged to develop a plan for use of the Handbook that focuses on developing information that responds to areas of greatest interest, yet assures that the basics are mastered.

Although the urgent need for information makes it tempting to skip around between sections and chapters, the development of a thorough understanding of the information provided would best equip the reader to harvest the benefits of comprehensive knowledge about radiant heating systems. The reader who masters the Handbook will recognize that the fundamentals are sound. System performance risks are no different than those encountered with other HVAC systems. The current limited market penetrations spells opportunity for significant growth in radiant heating and cooling system application, with the attendant energy, comfort, customer satisfaction, and profit benefits.

## HOW TO USE THIS BOOK

**S · E · C · T · I · O · N · 2**

**FUNDAMENTALS OF  
HEAT TRANSFER AND  
THERMODYNAMICS**



---

# CHAPTER 1

---

## THE ENERGY BALANCE

---

The energy balance is the fundamental process by which temperatures, pressures, relative humidity, indoor air quality, and other measurable quantities are related to heat transfer and power. The energy balance provides the means to determine the amount of energy that is contained within a specific mass. This mass can be anything such as room air, the glass in a window, a wall structure, or a cup of coffee. Energy content is not measured directly. Instead, temperatures, pressures, and the chemical compositions are measured, which are then related to the energy content.

In the case of a built environment, heating and cooling systems add energy by electrical resistance heating, burning of hydrocarbons, or through the use of refrigeration cycles. Using the energy balance allows us to predict the local temperatures within the built environment. For example, as a cup of hot coffee sets on a desk, heat transfers from the hot coffee to the room air. Since heat (energy) is removed from the coffee, the temperature of the coffee decreases. A second example of this same concept is the air in a room. If the room air temperature is 70°F (21.4°C) and the outdoor air temperature is 0°F (-17.4°C), then a certain amount of power (e.g., 1000 W) is transferred through the room walls, ceiling, and floor to the outside. To maintain the room air temperature at 70°F (21.4°C), an equal amount of power (1000 W in this example) must be added to the room air to balance the power transferred through the walls. This power could be added by one or more of the following: a central forced-air heating system, an in-space convective system, a radiant heat panel, people, appliances, light bulbs, or any other heat-generating component in the room.

Consequently, the energy balance is an integral part of any calculations in the heating, ventilation, and air-conditioning (HVAC) field. The energy balance provides the basis for sizing a heating or cooling system, calculating the air temperature in a room, evaluating thermal conditions, and specifying ventilation rates. This chapter focuses entirely on the energy balance by first discussing energy and mass conservation equations, followed by quantitative descriptions of heat transfer and work mechanisms, and finishes with property evaluations. At the conclusion of the chapter, the reader will be able to thermodynamically describe a building, balance heat transfer rates, and calculate temperatures associated with the building heating and cooling system.

## 1.1 CONTROL VOLUME AND ASSOCIATED THERMODYNAMIC PROCESSES

---

Conservation equations describe the transport of conserved quantities. Conserved quantities are those parameters that cannot be created or destroyed. As an example, consider a 0.5-gal pan filled to the brim with water at 70°F (21.4°C). According to data on water, the mass of water in the pan will be 4.173 pound-mass (lbm). The pan of water is now heated on a stove. What happens to the water as the temperature increases? Those who try this will know that as the water temperature increases, the water overflows the boundaries of the pan. This is because the same mass of water requires a larger volume at higher temperatures. Data show that at a higher temperature, our original mass of water now requires a volume of 0.556 gal. But since our pan will only hold 0.5 gal of water, the mass of water left in the pan is now 3.755 lbm. The question now is how much water flowed over the brim of the pan? If we assume water is not created or destroyed, then the answer is  $(4.173 \text{ lbm} - 3.755 \text{ lbm}) = 0.418 \text{ lbm}$ . We cannot say the same about the volume since the volume required to hold the water increases with the temperature. Hence, the *conserved quantity* is the mass of water. Note that volume is not a conserved quantity.

The conserved quantities of interest in this book are energy, mass, and, to a lesser extent, species such as carbon dioxide and water vapor. The premise is that energy, mass, and the atomic structure of carbon, hydrogen, and oxygen are not created or destroyed. So if we keep track of the transfer of energy and mass, then we can always calculate how much mass or energy remains in the volume we are studying. Specifically, this means that the energy contained within a building is the result of energy losses or gains through walls, windows, ventilation systems, heating systems, cooling systems, solar insulation, lights, equipment, people, and anything else that generates or absorbs heat. Energy, in this case, is the conserved quantity. The same can be said for the mass in the building.

Before the conservation equations can be studied, a good understanding of the components making up the conservation equations (e.g., work, heat transfer, and control volumes) is necessary.

### 1.1.1 Control Volumes

Conserved quantities are described relative to specified boundaries. For example, the quantity of energy contained within the boundaries of a building is certainly different than the quantity of energy contained within the Earth's atmosphere. However, if we were interested in global warming, we would examine the energy in the atmosphere, whereas if we were interested in building thermal comfort, the energy contained within the building would be of prime importance. Consequently, a mechanism is necessary to "bound" the system of interest. We have already used a control volume in the example of the water overflowing the pan. The control volume in that case was the pan. As the water was heated, some of the water left the control volume by overflowing the boundaries of the pan.

The control volume is the arbitrary boundary used to define the scope of an analysis. The control volume must surround all the processes that are to be analyzed. Figure 1.1 illustrates the concept of a control volume used to analyze a building with two rooms. The furnace adds energy to the building, as does the sun through solar gain through the window. Energy is transferred through the walls to the outside environment, and is then carried from the building by the ventilation system. If one large control volume is drawn that surrounds the entire building, then the analysis

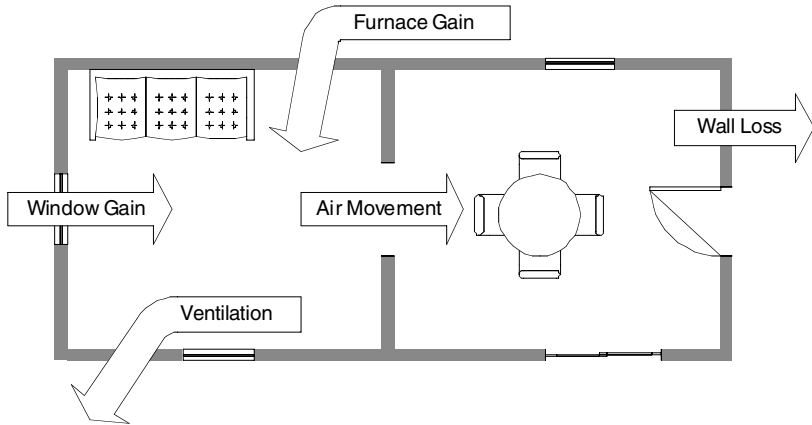


**FIGURE 1.1** Room energy balance components.

will provide information on the entire building. It does not provide room-by-room information. If, instead, two smaller control volumes are drawn that surround each room, then the analysis provides detailed information on each particular room. The same energy transfer rates still exist as they did for the single large control volume, but now the air movement between the rooms plays a role in the analysis. In addition, the specific locations of each of the energy transfer rates affect the analysis for each room. For example, the solar gain through the windows directly affects the room on the left, but only indirectly affects the room on the right.

The question now is, How and where is the control volume drawn? The answer depends on the level of detail required. The analysis from the large control volume could show that the average thermal comfort level could be satisfactory. But the distribution of thermal comfort could be unsatisfactory. For example, the individual rooms could be uncomfortable (the room on the left could be too warm, and the room on the right could be too cold), but on the average, the overall building temperature could average  $72^{\circ}\text{F}$  ( $22.6^{\circ}\text{C}$ ), which is commonly thought of as a comfortable temperature. This is one argument for doing local comfort analyses as opposed to a building average analysis.

The cost of this additional localized information is that the required effort in this case is doubled (two analyses as opposed to one analysis). This simple example shows the importance of clearly identifying the required level of detail, and then drawing the appropriate control volume that provides that information. If one is interested in the building average comfort level, then the building control volume would be used. If one were instead interested in a room-by-room control analysis, then a control volume would be drawn around each room in the building.

The control volume has several important characteristics. These are:

1. The boundaries may or may not be permeable to flow, such that mass may flow into and out of a control volume (the air movement between the two rooms in Fig. 1.1).
2. The boundaries may move, increasing or decreasing the size of the control volume.
3. Control volumes should undergo some process, such as heating or cooling.
4. This process may change relative to time (unsteady) or may not change relative to time (steady state).

5. The thermodynamic properties such as temperature and pressure may or may not be uniform over the control volume. Note that this has nothing to do with an unsteady or steady process.

From these characteristics, it may appear that a control volume can be defined in many different ways. This is probably one of the more important aspects of control volumes. The following sections use the concept of the control volume to define and characterize the conservation of mass and energy. The control volume concept is used repeatedly throughout this Handbook.

### 1.1.2 Heat Transfer and Work Interactions

Heat transfer is the process by which energy moves from a hot source to a cold sink. An example is a cooling cup of coffee as it sits on a kitchen table. Since the coffee is at a higher temperature than the surroundings, heat transfer occurs from the coffee to the surroundings. A savvy observer would note that the coffee could not cool below the temperature of the surroundings. Hence, heat transfer is a *directional* phenomenon that occurs only from the hotter source to the cooler sink. It is impossible to do otherwise without additional energy. A refrigerator moves heat from the relatively cold refrigerator interior to the warmer room, but at the expense of power to operate the refrigeration compressor. By convention, heat transfer out of a control volume is labeled as *negative*, and heat transfer into a control volume is labeled as *positive*. Therefore, for the coffee cup example, if the control volume were drawn around the coffee cup, then the heat transfer would be negative relative to the control volume.

The opposite case would be if the control volume were drawn around the entire room but excluding the coffee cup. Then the heat transfer would be into the control volume from the coffee and would be positive relative to the control volume. Again, it simply depends on where the control volume boundaries are placed.

Three separate modes of heat transfer can occur: (1) convection, (2) conduction, and (3) radiation. These three heat transfer modes are illustrated in Fig. 1.2. It is extremely important to realize and understand that, with the exception of a complete vacuum, all three modes of heat transfer occur simultaneously. This is referred to as *multimodal heat transfer*, and is discussed in Chap. 4 of this section. In the remainder of this chapter, the focus will be on using these heat transfer modes in the energy conservation equation. The next two chapters focus on calculating the magnitude of the heat transfer rates.

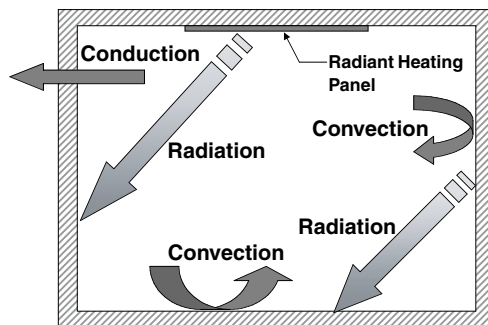


**FIGURE 1.2** Heat transfer modes within an enclosed space.

Referring to Fig. 1.2, *conduction* is defined as the rate that energy is transported through a solid medium. In Fig. 1.2, conduction is shown as the heat transfer through the building wall. As one might expect, the direction of heat flow is from the hot temperature to the cold temperature. Mathematically, conduction is proportional to the temperature difference and the thickness of the solid medium, and is described as:

$$q''_{\text{cond}} \propto \frac{\Delta T}{\Delta x} \quad (1.1)$$

The proportionality constant that relates the conductive heat transfer rate to the ratio of the temperature difference and the wall thickness is called the *thermal conductivity*. Thermal conductivity is designated by  $k$ . The ratio  $\Delta T/\Delta x$  is the temperature gradient across the wall. For preciseness, and to allow for variations in the thermal conductivity of the solid material with temperature, the thickness is reduced to zero. The heat conduction equation then becomes:

$$q''_{\text{cond}} = \lim_{\Delta x \rightarrow 0} \left( -k \frac{\Delta T}{\Delta x} \right) = -k \frac{dT}{dx} \quad (1.2)$$

Convection in Fig. 1.2 is the rate that energy is transferred by a moving fluid over a solid surface. Convection is shown as the heat transferred from the wall surface to the room air. Convection can be either forced, as with a fan, or natural, which is due to the buoyant nature of a relatively warm fluid. Mathematically, convection heat transfer to a surface is defined as:

$$q''_{\text{conv}} = h(T_f - T_i) \quad (1.3)$$

The parameter  $h$  is the heat transfer coefficient,  $T_f$  is the fluid temperature, and  $T_i$  is the temperature of solid surface  $i$ . Heat transfer coefficients are correlated from extensive libraries of experimental data (*ASHRAE Handbook*, Incropera and DeWitt, and others). These experimental data include the fluid velocity, fluid and surface temperatures, and fluid properties. A typical value for  $h$  in the built environment is 2 Btu/hr · ft<sup>2</sup>.

Radiation, arguably the most complex mode of heat transfer, is the rate that energy is transferred from a hot heat source to a cold heat sink by electromagnetic waves. Radiation is the only heat transfer mode that can transmit energy through a vacuum. In Fig. 1.2, radiation heat transfer is shown as the rate that energy is transferred directly from the hot radiant panel surface to the left wall. Radiation is also shown from the right wall surface to the floor of the room. Radiation heat transfer from surface  $j$  to surface  $i$  is frequently simplified to:

$$q''_{\text{rad}, j \rightarrow i} = \epsilon \sigma F_{ji} (T_j^4 - T_i^4) \quad (1.4)$$

The double arrow represents the net radiation heat transfer rate from surface  $j$  to surface  $i$ . The parameter  $\epsilon$  is the surface emissivity, which varies between zero for a reflective surface to one for a completely absorbing surface. The parameter  $\sigma$  is the Stefan-Boltzmann constant ( $5.67 \times 10^{-8} \text{ W/m}^2 \cdot \text{K}^4$ ). The view factor, denoted by  $F_{ji}$ , represents the geometrical configuration of the items within the control volume. For most applications in the built environment, the view factor is approximately 0.8 to 0.9. One special case for the configuration factor is when one of the surfaces is small compared with the other surface, in which case, the configuration factor is 1.0.

Note that the temperatures are to the fourth power and *must* be specified in absolute units [Kelvins (K) or degrees Rankine (°R)]. Although this is a typical representation of radiation heat transfer, it is far from the most general. Chapter 3 in

this section discusses radiation heat transfer in detail as it applies to radiant heating and cooling systems and to thermal comfort calculations.

Work interactions can occur by several means. Two of the more popular means are through shaft work from a fan or compressor and by electrical resistance heating. These forms are straightforward and are generally known by the design engineer. For example, a fan motor has a horsepower rating, and an electrical resistance radiant heating panel has a kilowatt rating. Other forms of work are important to general thermodynamic calculations, but they are not pertinent to HVAC calculations.

**EXAMPLE 1.1** A 6-in-thick solid wall separates a comfortably conditioned space from the outdoor environment. The inside surface temperature of the wall is 70°F (21.4°C), and the outside surface temperature of the wall is 0°F (−17.4°C). Calculate the conduction heat transfer through the wall if the thermal conductivity is 0.07 Btu/(h · ft<sup>2</sup> · °R) and the dimensions of the wall are 8 × 12 × 15 ft. The conduction equation is used to calculate the heat transfer rate through the wall:

$$\begin{aligned}\dot{Q} &= \frac{q''}{dt} A \\ \dot{Q}_{cond} &= -kA \frac{dT}{dx} \cong kA \frac{T_{in} - T_o}{\Delta x} \\ A &= 8 \text{ ft} \times 12 \text{ ft} = 96 \text{ ft}^2 \\ \dot{Q}_{cond} &= \left( \frac{0.07 \text{ Btu}}{\text{h} \cdot \text{ft}^2 \cdot ^\circ\text{R}} \right) (96 \text{ ft}^2) \frac{(70 - 0)^\circ\text{R}}{6 \text{ in}} \times \frac{12 \text{ in}}{\text{ft}} \\ \dot{Q}_{cond} &= \frac{940.8 \text{ Btu}}{\text{h}}\end{aligned}$$

One conclusion from this calculation is that there are three ways to reduce the heat transfer rate through the wall: (1) reduce the thermal conductivity by using a better insulating wall material (increases the R value); (2) increase the thickness of the wall with the same insulating material (increases the R value); and (3) reduce the temperature differential across the wall. Each of these techniques affects thermal comfort, as we will see later in the Handbook.

**EXAMPLE 1.2** The room air temperature in the previous example is 75°F (24.2°C). If the heat transfer coefficient between the wall and air is 1.96 Btu/(h · ft<sup>2</sup> · °F), calculate the convection heat transfer rate between the room air and the wall surface. The convection heat transfer equation is:

$$\begin{aligned}\dot{Q}_{conv} &= hA(T_{fluid} - T_{solid}) \\ &= \left( \frac{1.96 \text{ Btu}}{\text{h} \cdot \text{ft}^2 \cdot ^\circ\text{F}} \right) (96 \text{ ft}^2) (75^\circ\text{F} - 70^\circ\text{F}) \\ &= \frac{940.8 \text{ Btu}}{\text{h}}\end{aligned}$$

There are only two apparent ways to affect the rate of convection heat transfer: (1) reduce the temperature differential between the air and wall surface, and (2) reduce the convection heat transfer coefficient. As we will find in Chap. 2 of this section, reducing the convection heat transfer coefficient can be accomplished in many different ways.

**EXAMPLE 1.3** A pan of water sits on the ground in the desert at night. The effective temperature of the clear night sky is 5°F (-14.7°C). The surrounding air temperature is 40°F (4.4°C). Calculate the equilibrium temperature of the water if the convection heat transfer coefficient is 1.5 Btu/(h · ft<sup>2</sup> · °F).

Figure 1.3 shows the heat transfer balance on the pan of water. A control volume is drawn around the pan and all known forms of heat transfer are shown relative to the control volume. Note that the convection and radiation heat transfer rates are shown going into the pan of water, which is the positive direction relative to the pan of water. The equation that describes the heat transfer interactions is:

$$\dot{Q}_{conv} + \dot{Q}_{rad} = 0$$

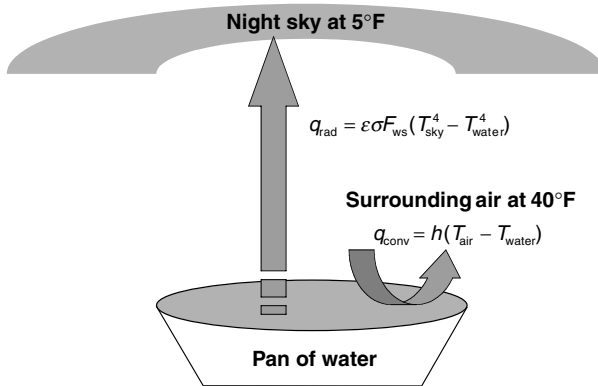


**FIGURE 1.3** Example showing convection and radiation heat transfer.

The convection heat transfer rate is  $\dot{Q}_{conv} = hA(T_{air} - T_{water})$ .

The radiation heat transfer rate is written using the simplified form of the radiation equation provided earlier in this chapter, in Eq. (1.4). For this case, the radiation heat transfer rate is written as:

$$q''_{rad,j \rightarrow i} = \epsilon \sigma F_{ji} (T_j^4 - T_i^4)$$

$$\sigma = \frac{1.712 \times 10^{-9} \text{ Btu}}{h \cdot \text{ft}^2 \cdot ^\circ R^4}$$

$$\epsilon = 1.0$$

$$F_{ji} = 1.0$$

The emissivity  $\epsilon$  and the view factor  $F_{ji}$  are equal to one for this example. In Chap. 3 of this section, we will describe these parameters in greater detail.

The balance equation has now become:

$$\dot{Q}_{conv} + \dot{Q}_{rad} = 0 = hA(T_{air} - T_w) + \sigma A(T_{sky}^4 - T_w^4) = 0$$

$$\left( \frac{1.5 \text{ Btu}}{h \cdot \text{ft}^2 \cdot ^\circ R} \right) (500^\circ R - T_w) + \left( \frac{1.712 \times 10^{-9} \text{ Btu}}{h \cdot \text{ft}^2 \cdot ^\circ R^4} \right) [(465^\circ R)^4 - T_w^4] = 0$$

There are several ways to solve this equation. Two methods will be demonstrated here. The first is to iterate to the solution. The iteration method requires a guessed answer. In this case, we will guess  $500^\circ\text{R}$  as our first guess and  $480^\circ\text{R}$  as our second guess. Additionally, an error function  $E$  is defined as:

$$E(T_w) = hA(T_{air} - T_w) + \sigma A(T_{sky}^4 - T_w^4) \\ = \left( \frac{1.5 \text{ Btu}}{h \cdot \text{ft}^2 \cdot ^\circ\text{R}} \right) (500^\circ\text{R} - T_w) + \left( \frac{1.712 \times 10^{-9} \text{ Btu}}{h \cdot \text{ft}^2 \cdot ^\circ\text{R}^4} \right) [(465^\circ\text{R})^4 - T_w^4]$$

Our goal is to guess a water temperature  $T_w$  that makes  $E$  equal to zero:

$T_w$	$E(T_w)$
$500^\circ\text{R}$	$-26.961 \text{ Btu}/(h \cdot \text{ft}^2)$
$480^\circ\text{R}$	$+19.16 \text{ Btu}/(h \cdot \text{ft}^2)$

$$\frac{T_w - 480^\circ\text{R}}{0 - 19.16} = \frac{500^\circ\text{R} - 480^\circ\text{R}}{-26.961 - 19.16} \\ T_w = \left( \frac{500^\circ\text{R} - 480^\circ\text{R}}{-26.961 - 19.16} \right) (0 - 19.16) + 480^\circ\text{R} = 488.3^\circ\text{R}$$

The last step in the preceding procedure is to interpolate between the two guessed temperatures to get the third guessed temperature. In this case, that temperature is  $488.3^\circ\text{R}$ . The next step is to plug this temperature into the balance equation, calculate the error, and then interpolate between the two guessed values with the lowest error  $E$ :

$T_w$	$E(T_w)$
$500^\circ\text{R}$	$-26.961 \text{ Btu}/(h \cdot \text{ft}^2)$
$480^\circ\text{R}$	$+19.16 \text{ Btu}/(h \cdot \text{ft}^2)$
$488.3^\circ\text{R}$	$+0.259 \text{ Btu}/(h \cdot \text{ft}^2)$

$$\frac{T_w - 488.3^\circ\text{R}}{0 - 0.259} = \frac{488.3^\circ\text{R} - 480^\circ\text{R}}{0.259 - 19.16} \\ T_w = \left( \frac{488.3^\circ\text{R} - 480^\circ\text{R}}{0.259 - 19.16} \right) (0 - 0.259) + 488.3^\circ\text{R} = 488.4^\circ\text{R}$$

Substituting  $T_w = 488.4^\circ\text{R}$  into the balance equation shows that this is, in fact, the correct solution. The equilibrium water temperature is  $(488.4 - 460)^\circ\text{F} = 28.4^\circ\text{F}$ , which is below the freezing point of water. Therefore, the water will freeze, even though the air temperature is above the freezing point!

The second solution method is to define what is sometimes referred to as the radiation heat transfer coefficient. Rearranging the balance equation results in:

$$0 = hA(T_{air} - T_w) + \sigma A(T_{sky}^4 - T_w^4) \\ = h(T_{air} - T_w) + \sigma(T_{sky}^2 - T_w^2)(T_{sky}^2 + T_w^2) \\ = h(T_{air} - T_w) + \sigma(T_{sky}^2 + T_w^2)(T_{sky} + T_w)(T_{sky} - T_w) \\ = h(T_{air} - T_w) + \underbrace{\sigma(T_{sky}^2 + T_w^2)(T_{sky} + T_w)}_{\text{Radiation heat transfer coefficient, } h_R} (T_{sky} - T_w) \\ = h(T_{air} - T_w) + h_R(T_{sky} - T_w)$$

$$T_w = \frac{hT_{air} + h_R T_{sky}}{h + h_R}$$

Note that a guessed value of  $T_w$  is still necessary to solve the equation. The solution process is as follows:

$$h_R = \sigma(T_{sky}^2 + T_w^2)(T_{sky} + T_w)$$

$$T_w = (40^\circ F + 460) = 500^\circ R \text{ (guessed value)}$$

$$h_R = \underbrace{\left( \frac{1.712 \times 10^{-9} \text{ Btu}}{h \cdot \text{ft}^2 \cdot ^\circ R^4} \right)}_{\sigma} \left[ \underbrace{(465^\circ R)^2}_{T_{sky}} + \underbrace{(500^\circ R)^2}_{T_w \text{ (guessed)}} \right] [(465^\circ R) + (500^\circ R)]$$

$$= \frac{0.77 \text{ Btu}}{h \cdot \text{ft}^2 \cdot ^\circ R}$$

$$T_w = \frac{hT_{air} + h_R T_{sky}}{h + h_R}$$

$$= \frac{\left( \frac{1.5 \text{ Btu}}{h \cdot \text{ft}^2 \cdot ^\circ R} \right) \times 500^\circ R + \left( \frac{0.77 \text{ Btu}}{h \cdot \text{ft}^2 \cdot ^\circ R} \right) \times 465^\circ R}{\left( \frac{1.5 \text{ Btu}}{h \cdot \text{ft}^2 \cdot ^\circ R} \right) + \left( \frac{0.77 \text{ Btu}}{h \cdot \text{ft}^2 \cdot ^\circ R} \right)}$$

$$= 488.12^\circ R$$

The next step is to use the newly calculated  $T_w$  and recalculate the radiation heat transfer coefficient and then re-solve the balance equation:

$$h_R = \underbrace{\left( \frac{1.712 \times 10^{-9} \text{ Btu}}{h \cdot \text{ft}^2 \cdot ^\circ R^4} \right)}_{\sigma} \left[ \underbrace{(465^\circ R)^2}_{T_{sky}} + \underbrace{(488.12^\circ R)^2}_{T_w \text{ (guessed)}} \right] [(465^\circ R) + (488.12^\circ R)]$$

$$= \frac{0.742 \text{ Btu}}{h \cdot \text{ft}^2 \cdot ^\circ R}$$

$$T_w = \frac{hT_{air} + h_R T_{sky}}{h + h_R}$$

$$= \frac{\left( \frac{1.5 \text{ Btu}}{h \cdot \text{ft}^2 \cdot ^\circ R} \right) \times 500^\circ R + \left( \frac{0.742 \text{ Btu}}{h \cdot \text{ft}^2 \cdot ^\circ R} \right) \times 465^\circ R}{\left( \frac{1.5 \text{ Btu}}{h \cdot \text{ft}^2 \cdot ^\circ R} \right) + \left( \frac{0.742 \text{ Btu}}{h \cdot \text{ft}^2 \cdot ^\circ R} \right)}$$

$$= 488.42^\circ R$$

$$= 28.42^\circ F$$

The radiation heat transfer coefficient method is commonly used to solve radiation heat transfer problems. Caution needs to be exercised because the radiation heat transfer coefficient varies with temperature. However, in this example, even a guessed temperature of  $500^\circ R$  resulted in an answer that was fairly close to the correct result.

### 1.1.3 Thermodynamic Properties of Solids, Liquids, and Ideal Gases

Matter can be in one of three forms that are important to this Handbook: (1) liquid, (2) solid, and (3) gas. The state of the matter is defined exclusively by the state variables of temperature, pressure, volume, and mass. Knowing any three of these parameters automatically fixes the fourth. Consequently, the state variables are always related through some form of equation of state. The state variables are further classified as extrinsic and intrinsic. Extrinsic variables depend on the mass of the substance, and the intrinsic variables are independent of mass. For example, a 1-ft<sup>3</sup> volume of water with a mass of 62.4 lbm, a temperature of 70°F, and a pressure of 1 atm is divided exactly in half. Each half now exhibits a volume of 0.5 ft<sup>3</sup> and a mass of 31.2 lbm. The temperature and pressure of each half are still the same as the original volume of water, 70°F and 1 atm. Consequently, the mass and volume are extrinsic properties, and the temperature and pressure are intrinsic properties. Dividing the extrinsic property volume by the extrinsic property mass results in the intrinsic property specific volume,  $v$ . The inverse of  $v$  is the density,  $\rho$ .

The gases discussed in this Handbook will further be restricted to ideal gases. This classification requires that the state variables of temperature  $T$ , pressure  $p$ , volume  $V$ , and mass  $m$  relate to each other according to the ideal gas equation of state:

$$\frac{pV}{mT} = \frac{R_u}{M} \quad (1.5)$$

The parameter  $R_u$  is the universal gas constant, equal to 10.732 psia · ft<sup>3</sup>/(lbmol · °R) [8.314 kJ/(kmol · K)], and the parameter  $M$  is the gas molecular weight. The molecular weight varies with the type of gas, and is tabulated in the appendix for several common gases.

The relationship between the pressure, volume, temperature, and mass of liquids is much more complex. Because of this complexity, the relationship is generally provided in the form of tabular data or curves. For this text, solid- and liquid-state variables will be considered incompressible, meaning they are independent of pressure.

Matter, by its very nature, contains a certain predictable quantity of energy. The total quantity of energy  $E$  contained by a substance depends on the velocity, elevation, temperature, pressure, and mass. The specific energy  $e$  is the total energy divided by the mass of the substance. A 10-lbm quantity of water may contain a total of 1000 Btu of energy. The specific energy of this water is 100 Btu/lbm. Consequently, the specific energy is an intrinsic property, and the total energy is an extrinsic property. The specific energy is further subdivided into internal, kinetic, and potential energy. Mathematically, the specific energy is defined as:

$$e = u + \frac{W^2}{2} + gz \quad (1.6)$$

specific energy	=	u	+	$\frac{W^2}{2}$	+	gz
specific energy		internal energy		kinetic energy		potential energy

where  $u$  is the internal energy,  $W$  is the velocity,  $z$  is the elevation, and  $g$  is the acceleration of gravity (32.2 ft/s<sup>2</sup>, 9.806 m/s<sup>2</sup>). The internal energy represents the energy that is associated with the molecular interactions within the fluid, gas, or solid. To keep the design process practical, the internal energies of most gases, fluids, and solids have been tabulated as a function of temperature.

The kinetic energy represents the energy that is contained within the control volume due to its velocity. An example is a car. A car moving at 50 mi/h obviously has

more energy than the same car at 0 mi/h. This energy could be recovered by slowing the car down by compressing a large spring. This spring could then be used to do some work by letting the spring expand.

The potential energy represents the energy that is contained within the medium due to elevation. A large weight elevated at 20 ft has more energy than the same weight at an elevation of 0 ft. As with the car, this energy could be recovered by letting the weight fall while compressing a spring. The spring could then be used to do some work. Generally, potential and kinetic energy can be neglected with little loss in accuracy for HVAC calculations. The examples at the end of this section show the relative magnitudes of the internal, kinetic, and potential energies.

Enthalpy is another useful thermodynamic property that is solely a combination of other thermodynamic properties. Enthalpy is defined as:

$$h = u + pv \quad (1.7)$$

The definition of specific heats can be used to approximate the internal energy and enthalpy of air. The specific heats are defined as:

$$c_p = \left. \frac{\partial h}{\partial T} \right|_p \approx \frac{\Delta h}{\Delta T} \quad (1.8)$$

$$c_v = \left. \frac{\partial u}{\partial T} \right|_v \approx \frac{\Delta u}{\Delta T} \quad (1.9)$$

These equations are especially useful when analyzing an ideal gas. Another key property of ideal gases is that the internal energy and enthalpy are strictly functions of temperature. Consequently, Eqs. (1.8) and (1.9) can be rearranged to calculate the change in internal energy and enthalpy by knowing the specific heats and temperature changes. For example, if a sample of air with an average constant-volume specific heat of 0.24 Btu/(lbm · °R) changes from 50 to 70°F, then the change in specific internal energy is:

$$\Delta u = c_v \times \Delta T = \left( \frac{0.24 \text{ Btu}}{\text{lbm} \cdot ^\circ\text{F}} \right) (70^\circ\text{F} - 50^\circ\text{F}) = \frac{4.8 \text{ Btu}}{\text{lbm}}$$

For ideal gases, the specific heats are related by the universal gas constant:

$$c_p - c_v = \frac{R_u}{M} \quad (1.10)$$

Substituting Eq. (1.10) into Eq. (1.8) allows the calculation of the change in specific enthalpy of the air sample:

$$\begin{aligned} \Delta h &= c_p \times \Delta T = \left( \frac{R_u}{M} + c_v \right) \Delta T \quad (1.11) \\ &= \left[ \left( \frac{1.986 \text{ Btu}}{\text{lbmol} \cdot ^\circ\text{R}} \times \frac{\text{lbmol}}{28.97 \text{ lbm}} \right) + \frac{0.24 \text{ Btu}}{\text{lbm} \cdot ^\circ\text{R}} \right] \times (70^\circ\text{F} - 50^\circ\text{F}) \\ &= \left( \frac{0.309 \text{ Btu}}{\text{lbm} \cdot ^\circ\text{R}} \right) \times (20^\circ\text{F}) = \frac{6.17 \text{ Btu}}{\text{lbm}} \end{aligned}$$

**EXAMPLE 1.4** A 1-lbm sample of air is contained in a 1-ft<sup>3</sup> container. The sample is at 80°F. Calculate the pressure, density, and specific volume of the air.

The ideal gas equation of state is used to calculate the air pressure:

$$\begin{aligned} p &= \frac{mR_u T}{MV} \\ &= \frac{1 \text{ lbm} \times (80 + 460)^\circ R}{1 \text{ ft}^3} \times \left( \frac{10.732 \text{ psia} \cdot \text{ft}^3}{\text{lbmol} \cdot ^\circ R} \right) \left( \frac{\text{lbmol}}{28.97 \text{ lbm}} \right) \\ &= 200 \text{ psia} \end{aligned}$$

The specific volume and density are calculated from the volume and mass of that sample:

$$\begin{aligned} v &= \frac{V}{m} = \frac{1 \text{ ft}^3}{1 \text{ lbm}} = \frac{1 \text{ ft}^3}{\text{lbm}} \\ \rho &= \frac{m}{V} = \frac{1 \text{ lbm}}{1 \text{ ft}^3} = \frac{1 \text{ lbm}}{\text{ft}^3} \end{aligned}$$

**EXAMPLE 1.5** Water vapor at a pressure of 0.5 psia and 70°F can be accurately approximated as an ideal gas. Calculate the density and specific volume of water vapor at these conditions.

The ideal gas equation of state is used to calculate the density and specific volume of the water vapor:

$$\begin{aligned} pV &= \frac{mR_u T}{M} \\ \rho &= \frac{m}{V} = \frac{pM}{R_u T} \\ &= \frac{0.5 \text{ psia}}{(70 + 460)^\circ R} \left( \frac{18 \text{ lbm}}{\text{lbmol}} \right) \left( \frac{\text{lbmol} \cdot ^\circ R}{10.732 \text{ psia} \cdot \text{ft}^3} \right) \\ &= \frac{0.00158 \text{ lbm}}{\text{ft}^3} \\ v &= \frac{1}{\rho} = \frac{632 \text{ ft}^3}{\text{lbm}} \end{aligned}$$

**EXAMPLE 1.6** Air at 90°F is moving at a velocity of 100 ft/s at an elevation of 200 ft. Calculate the change in total specific energy of the air if it is slowed to 10 ft/s, lowered to an elevation of 50 ft, and cooled to a temperature of 50°F.

The equation for the total specific energy was defined as:

$$e = u + \frac{W^2}{2} + gz$$

If the first state is designated as state 1 and the second state is designated as state 2, then the change in the total energy  $e$  is defined as:

$$\begin{aligned} \Delta e &= e_2 - e_1 \\ &= \left( u_2 + \frac{W_2^2}{2} + gz_2 \right) - \left( u_1 + \frac{W_1^2}{2} + gz_1 \right) \end{aligned}$$

$$= (u_2 - u_1) + \left( \frac{W_2^2 - W_1^2}{2} \right) + g(z_2 - z_1)$$

The change in internal energy  $u$  will be approximated using the constant-volume specific heat:

$$\begin{aligned} \Delta e &= (u_2 - u_1) + \left( \frac{W_2^2 - W_1^2}{2} \right) + g(z_2 - z_1) \\ &= c_v(T_2 - T_1) + \left( \frac{W_2^2 - W_1^2}{2} \right) + g(z_2 - z_1) \end{aligned}$$

To evaluate the relative magnitude of each type of energy on the total energy change, each term is calculated individually. The change in internal energy ( $u$ ) is:

$$\begin{aligned} \Delta u &= c_v(T_2 - T_1) = \left( c_p - \frac{R_u}{M_{air}} \right) (T_2 - T_1) \\ &= \left[ \frac{0.240 \text{ Btu}}{\text{lbm} \cdot ^\circ\text{F}} - \left( \frac{1.986 \text{ Btu}}{\text{lbmol} \cdot ^\circ\text{F}} \right) \left( \frac{\text{lbmol}}{28.97 \text{ lbm}} \right) \right] (90^\circ\text{F} - 50^\circ\text{F}) \\ &= \left( \frac{0.171 \text{ Btu}}{\text{lbm} \cdot ^\circ\text{F}} \right) (90^\circ\text{F} - 50^\circ\text{F}) \\ &= \frac{6.86 \text{ Btu}}{\text{lbm}} \end{aligned}$$

The change in kinetic energy (KE) is:

$$\begin{aligned} \Delta KE &= \frac{1}{2} \left[ \left( \frac{100 \text{ ft}}{\text{s}} \right)^2 - \left( \frac{10 \text{ ft}}{\text{s}} \right)^2 \right] \\ &= \frac{9900 \text{ ft}^2}{\text{s}^2} \times \underbrace{\frac{\text{lb} \cdot \text{ft}}{32.2 \text{ lbm} \cdot \text{ft}}}_{\text{unit conversion factor}} \times \underbrace{\frac{\text{Btu}}{778.16 \text{ ft} \cdot \text{lb}}}_{\text{unit conversion factor}} \\ &= \frac{0.198 \text{ Btu}}{\text{lbm}} \end{aligned}$$

The change in potential energy (PE) is:

$$\begin{aligned} \Delta PE &= \frac{32.2 \text{ ft}}{\text{s}^2} (200 \text{ ft} - 50 \text{ ft}) \\ &= \frac{4830 \text{ ft}^2}{\text{s}^2} \times \underbrace{\frac{\text{lb} \cdot \text{ft}}{32.2 \text{ lbm} \cdot \text{ft}}}_{\text{unit conversion factor}} \times \underbrace{\frac{\text{Btu}}{778.16 \text{ ft} \cdot \text{lb}}}_{\text{unit conversion factor}} \\ &= \frac{0.193 \text{ Btu}}{\text{lbm}} \end{aligned}$$

The total change in specific energy ( $e$ ) is:

$$\begin{aligned}\Delta e &= \Delta u + \Delta KE + \Delta PE \\ &= \left( \frac{6.86 \text{ Btu}}{\text{lbm}} \right) + \left( \frac{0.395 \text{ Btu}}{\text{lbm}} \right) + \left( \frac{0.193 \text{ Btu}}{\text{lbm}} \right) \\ &= \frac{7.25 \text{ Btu}}{\text{lbm}}\end{aligned}$$

This example shows the relative magnitude between the internal, kinetic, and potential energies. Even though the initial velocity is 100 ft/s and the initial elevation is 200 ft, the changes in kinetic and potential energies are only a small percentage of the change in internal energy. Hence, the changes in kinetic and potential energies of air can oftentimes be neglected with little loss in accuracy, especially when the velocities are lower than 100 ft/s.

The following section combines work, heat transfer, and thermodynamic properties into a single equation that is a major part of the puzzle to calculate and predict the thermal comfort conditions in a room.

## 1.2 PUTTING IT ALL TOGETHER— THE CONSERVATION EQUATIONS

---

At this point, all of the components that are necessary to write the conservation equations have been described. These conservation equations are much like a bank account. Whatever money is deposited in the account is balanced by either a withdrawal from the account or by an increase in the account. The mass conservation and energy conservation equations follow this same principle and are applied to a specific control volume. If energy is added to a room, then one of the following must happen: (1) the energy content of the room must increase by an equal amount; (2) an equal amount of energy must be removed from the room; or (3) a combination of the first two items such that the net result is equal to the quantity of energy that entered the room.

The following sections describe the mass conservation and energy conservation equations. The mass conservation equation is somewhat simpler to understand, whereas the energy conservation equation can be quite complex.

### 1.2.1 Conservation of Mass

The mass conservation equation is used to identify the change in mass of the control volume over a specified time interval. During this time interval, mass may enter and leave the control volume. By balancing the mass inflows and outflows, the change in mass of the control volume can be calculated.

Figure 1.4 shows a room with an open window on the right side and an exhaust fan on the left side. The goal is to analyze how the mass of air changes in the room over time. The first step is to concisely define the control volume. In this case, the room walls are a logical choice for the control volume boundaries. The dashed lines in the figure identify these boundaries. Over a period of time, from  $t_1$  to  $t_2$ , a certain mass of air enters the room (control volume) through the window and a certain mass

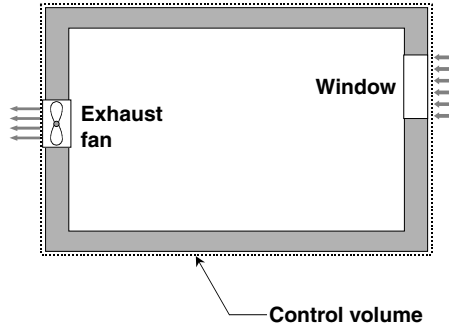


**FIGURE 1.4** Example control volume demonstrating mass conservation.

of air leaves the room through the exhaust fan. These entering and leaving masses do not have to be the same. In equation form, this process is written as:

$$m_{t_2} - m_{t_1} = m_{\text{window}} - m_{\text{exhaust}} \quad (1.12)$$

Mass of air at  $t_2$       Mass of air at  $t_1$       Mass of entering air      Mass of exiting air

The left side of Eq. (1.12) is the change in mass of the control volume, and the right side shows the incoming and outgoing air masses. The conservation of mass states that these quantities must exactly balance. Note that if three of the four terms are known, then this equation can be used to calculate the fourth.

A general form of Eq. (1.12) takes into consideration all flow paths that may enter or leave a control volume. This form of the mass conservation equation is written as:

$$m_{t_2} - m_{t_1} = \sum_{\text{in}} m - \sum_{\text{out}} m \quad (1.13)$$

The summation signs indicate that all flow paths must be considered to precisely balance the mass conservation equation.

The mass conservation equation can be transformed into a rate equation by dividing Eq. (1.13) by the time interval,  $\Delta t$ :

$$\frac{m_{t_2} - m_{t_1}}{\Delta t} = \frac{\sum_{\text{in}} m}{\Delta t} - \frac{\sum_{\text{out}} m}{\Delta t} \quad (1.14)$$

In Eq. (1.14), each term is now in units of mass (kg, lbm, slugs, etc.)/time (s, h, days, etc.). Although the interval  $\Delta t$  can be a year, a day, or a second, it is common practice to let the interval approach zero to get instantaneous flow rates. Equation (1.14) becomes:

$$\lim_{\Delta t \rightarrow 0} \frac{m_{t_2} - m_{t_1}}{\Delta t} \Rightarrow \frac{dm_{\text{CV}}}{dt} = \sum_{\text{in}} \dot{m} - \sum_{\text{out}} \dot{m} \quad (1.15)$$

The derivative represents the time rate of change of the mass in the control volume, and the summations are for the rate that mass enters and leaves the control volume.

A special case of this equation is when the mass leaving and entering the control volume is the same. This special case is referred to as a *steady-state process*, and it specifically indicates that the derivative in Eq. (1.15) is zero. This is the most common way in which the mass conservation equation is employed.

**EXAMPLE 1.7** *The mass in a room remains constant over time (steady state). Air infiltrates the room through cracks at the rate of 2 kg/s. Ventilation system 1 exhausts air from the room at a rate of 1 kg/s. Calculate the exhaust mass flow rate of ventilation system 2. The given information is:*

$$\dot{m}_{inf} = 2 \text{ kg/s}$$

$$\dot{m}_1 = 1 \text{ kg/s}$$

$$\dot{m}_2 = ??$$

From the mass conservation equation,

$$\begin{aligned} \frac{dm_{cv}}{dt} &= \sum_{in} \dot{m} - \sum_{out} \dot{m} = \dot{m}_{inf} - (\dot{m}_1 + \dot{m}_2) \\ 0 &= 2 \text{ kg/s} - (1 \text{ kg/s} + \dot{m}_2) \\ \dot{m}_2 &= 2 \text{ kg/s} - 1 \text{ kg/s} \\ \dot{m}_2 &= 1 \text{ kg/s} \end{aligned}$$

In this example, knowledge of two of the flow rates leads to the calculation of the third. In writing the equation, the mass flow rate through ventilation system 2 was assumed to be out of the system. If this assumption had been incorrect, then the numerical answer would have been negative, indicating that the initial assumption of outflow was incorrect.

**EXAMPLE 1.8** *The room shown in Fig. 1.5 contains a recirculation system, a fresh-air ventilator, and an exhaust fan and exhibits some form of air infiltration/exfiltration. The recirculation system recycles 2 kg/s of air, and the fresh-air ventilator supplies 1 kg/s. The exhaust fan discharges 0.5 kg/s from the room. Calculate the infiltration/exfiltration that is necessary to maintain a constant mass of air within the room.*

This problem is a steady-state problem because none of the flow rates vary with time. The solution is obtained by applying the mass conservation equation. In this situation, it is not readily apparent if the air infiltration is into or out of the room. The following analysis assumes it is into the room, but as will be shown, the initial choice is irrelevant. The mass conservation equation becomes:

$$\begin{aligned} \frac{dm_{cv}}{dt} = 0 &= \underbrace{(\dot{m}_2 + \dot{m}_5 + \dot{m}_4)}_{\substack{\text{into room} \\ (+)}} - \underbrace{(\dot{m}_1 + \dot{m}_3)}_{\substack{\text{out of room} \\ (-)}} \\ \dot{m}_4 &= (\dot{m}_1 + \dot{m}_3) - (\dot{m}_2 + \dot{m}_5) \\ \dot{m}_4 &= (2 \text{ kg/s} + 0.5 \text{ kg/s}) - (2 \text{ kg/s} + 1 \text{ kg/s}) \\ \dot{m}_4 &= -0.5 \text{ kg/s} \end{aligned}$$

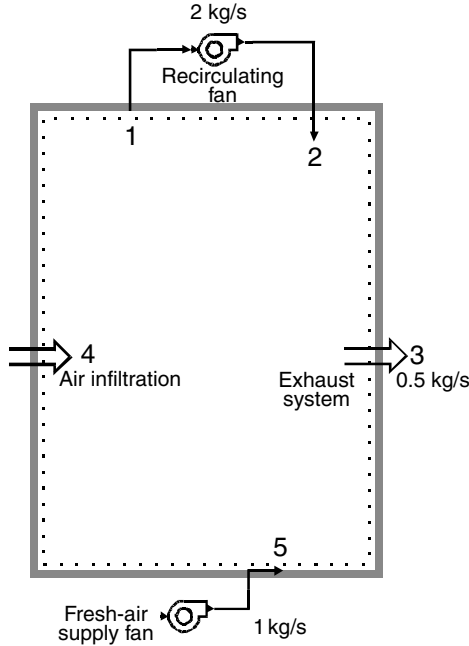


FIGURE 1.5 Example mass conservation balance.

The negative sign implies that choosing the infiltration as inflow was incorrect; instead, the airflow is exfiltration from the room.

A flow quantity often used in HVAC systems is the standard cubic foot per minute (scfm). The term *standard* refers to the volumetric flow rate of a fluid that would occur if the temperature and pressure of the fluid were at some predefined standard condition. In fact, almost all references to volumetric flow rate actually mean standard volumetric flow rate. The definition of the standard volumetric flow rate is:

$$\dot{V}_s \text{ (scfm)} = \dot{m} \text{ (lbm/min)} \times \frac{1}{\rho_s \text{ (lbm/ft}^3\text{)}} \tag{1.16}$$

For airflow, the standard density is usually 0.073 lbm/ft<sup>3</sup>.

**EXAMPLE 1.9** A ventilation system supplies 300 scfm to a conditioned space. Calculate the mass flow rate and the actual volumetric flow rate if the air temperature is 80°F and the actual air pressure is 13.3 psia.

The standard density is 0.073 lbm/ft<sup>3</sup>. When the volumetric flow rate is known in standard cubic feet per minute, the mass flow rate directly follows from the definition of standard cubic feet per minute:

$$\dot{m} = \rho_s \times \dot{V}_s = \frac{0.073 \text{ lbm}}{\text{ft}^3} \times \frac{300 \text{ sf}^3}{\text{min}} = \frac{21.9 \text{ lbm}}{\text{min}}$$

Once the mass flow rate is known, the actual volumetric flow rate in actual cubic feet per minute (acfm) is calculated using the actual density:

$$\dot{V} = \frac{\dot{m}}{\rho}$$

$$\rho = \frac{pM}{R_u T} = \left[ \frac{13.3 \text{ psia}}{(80 + 460)^\circ R} \right] \left( \frac{\text{lbmol} \cdot ^\circ R}{10.732 \text{ psia} \cdot \text{ft}^3} \right) \left( \frac{28.97 \text{ lbm}}{\text{lbmol}} \right)$$

$$\rho = \frac{0.0665 \text{ lbm}}{\text{ft}^3}$$

$$\dot{V} = \left( \frac{21.9 \text{ lbm}}{\text{ft}^3} \right) \left( \frac{\text{ft}^3}{0.0665 \text{ lbm}} \right) = \frac{329.4 \text{ ft}^3}{\text{min}} = 329.4 \text{ acfm}$$

In reality, standard volumetric flow rates are mass flow rates in different units. The only distinction between mass flow rate and standard volumetric flow rate is the standard density.

At this point, the reader should have a good understanding of the mass conservation equation. You should be able to apply it to any control volume and, given all but one of the flow rates, calculate the unknown flow rate. The reader should also have an understanding of standard volumetric flow rates.

### 1.2.2 Conservation of Energy

The energy conservation equation forces a balance on the energy that enters, leaves, and is stored in a control volume. If energy enters a control volume, it is considered positive; if energy leaves a control volume, it is considered negative. Balancing all the possible forms of energy that move into or out of a control volume results in:

$$\sum Q - W_a + \sum_{\text{in}} m(e + pv) - \sum_{\text{out}} m(e + pv) = m_2 e_2 - m_1 e_1 \quad (1.17)$$

The summation sign for the heat transfer term allows the possibility that heat is transferred from more than one source. For example, the sun transfers energy through a window into a room by radiation heat transfer, and energy is transferred by heat conduction through the window to the outdoors. The terms  $\sum_{\text{in}} m(e + pv)$  and  $\sum_{\text{out}} m(e + pv)$  represent energy that is transferred into and out of the control volume by mass movement. The mass can be air through infiltration and ventilation, water flow rate through some kind of irrigation system, or even people moving into and out of a room. As mass moves into and out of a room, it carries a certain amount of energy with it.

The terms  $m_2 e_2$  and  $m_1 e_1$  represent the total amount of energy in the control volume at two different points in time. The term  $W_a$  represents any work that is done on the control volume. These work interactions include work that is done by a blower, the energy necessary to operate an electrical resistance heater, or a fan. Other forms of work may also exist. The energy conservation equation is applicable to *any* process, and it is considered a *basic equation*.

The premise of using the energy conservation equation is that at some initial point in time, five out of the six parameters are measured. At some later point in time, a second measurement is taken. By comparing these measurements, the sixth

parameter can be deduced. For example, you could measure the temperature and weight (mass) of a pot of soup at 2:00 P.M. Then at 3:00 P.M., you could again measure the temperature and mass. From this information, you could calculate how much the mass changed and, assuming you knew the relationship between the internal energy and temperature, you could calculate the total amount of heat lost from the soup using the energy conservation equation [Eq. (1.17)].

The energy conservation equation can be cast into a slightly more usable form by combining the internal energy with the  $pV$  terms and then substituting the enthalpy into Eq. (1.17). This form, which is used in the remainder of this Handbook, is:

$$\sum \dot{Q} - \dot{W}_a + \sum_{\text{in}} \dot{m} \left( h + \frac{V^2}{2} + gz \right) - \sum_{\text{out}} \dot{m} \left( h + \frac{V^2}{2} + gz \right) = \dot{m}_2 e_2 - \dot{m}_1 e_1 \quad (1.18)$$

In Eq. (1.18), the  $V$ s inside the parentheses represent the mass velocity. At some point, there are more variables than there are convenient letters to represent them. Hence, it becomes necessary to reuse some of the letters. In this Handbook, the correct meaning of the letters will always be obvious from the context in which they are used.

The energy conservation equation is oftentimes used in a rate form. The energy conservation equation is basically divided by the time interval  $\Delta t$ , and then  $\Delta t$  is forced to approach zero as was done with the mass conservation equation. The result is the rate form of the energy conservation equation:

$$\sum \dot{Q} - \dot{W}_a + \sum_{\text{in}} \dot{m} \left( h + \frac{W^2}{2} + gz \right) - \sum_{\text{out}} \dot{m} \left( h + \frac{W^2}{2} + gz \right) = \frac{d(me)_{\text{CV}}}{dt} \quad (1.19)$$

### 1.2.3 Methodology for Solving the Conservation Equations

The methodology used in this Handbook for solving conservation equations is very explicit. The steps, if followed, will always lead to a correct solution. Problems usually arise when a haphazard approach is taken without a clear prescription. This section provides the methodology and then a series of solved example problems. The examples were chosen to represent a wide variety of HVAC situations that are useful to the design engineer.

The methodology for solving the conservation equations is:

1. Determine what information needs to be calculated and how precisely and accurately.
2. Sketch the system, including the room, inflows and outflows, heat transfer rates, work interactions, and any other energy source or sink. Figure 1.6 shows an example of a hydronic heating system with the various necessary parameters.

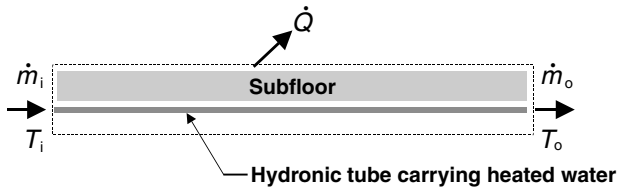


**FIGURE 1.6** An example of a hydronic system simply showing the ins and outs to help describe the methodology.

3. Draw a control volume that includes all the necessary components.
4. Write and then simplify the mass conservation equation so that it is tailored to the specific problem.
5. Write and then simplify the energy conservation equation so that it is tailored to the specific problem.
6. Identify all the known and unknown quantities in the conservation equations.
7. Quantify, if possible, any mass flow rates. Note that other equations may be necessary to calculate infiltration rates, fan flow rates, and so forth.
8. Define any heat transfer rates (e.g., convection, conduction, and radiation heat transfer). Write the appropriate equations that are necessary to calculate the heat transfer rates.
9. Define any work interactions, and then write any equations that are necessary to quantify the work interaction.
10. Apply any state of matter equations to reduce the number of unknowns. These may be useful in calculating pressures, densities, specific volumes, volumes, and temperatures.
11. Obtain property information by employing tabular data, polynomial curve fits, or specific heat equations. The choice depends on the desired level of accuracy.
12. Solve the conservation equations for any remaining unknown quantities. Note that some additional assumptions may be necessary to reduce the number of unknown quantities so that the conservation equations can be solved.

The following examples demonstrate this methodology by using the conservation equations to analyze the thermal conditions in a room. The examples also demonstrate the use of the property tables in the appendix.

**EXAMPLE 1.10** *A room contains four people and a 500-W light fixture. The ventilation system provides 1 kg/s of air at 18°C. Heat is transferred from the room to the surroundings at a rate of 100 W. Calculate the temperature of the air in the room.*

- Step 1.** *The information that is given is provided in the statement of the problem.*
- Step 2.** *A schematic of the system is drawn showing all of the inlets, outlets, work, and heat transfer interactions.*
- Step 3.** *The control volume is also shown in Fig. 1.7.*

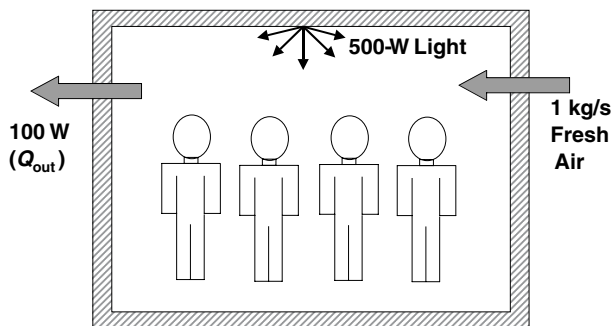


**FIGURE 1.7** Example energy balance in a room.

**Step 4.** Mass conservation equation:

$$\frac{dm_{CV}}{dt} = \sum_{in} \dot{m} - \sum_{out} \dot{m}$$

$$0 = \dot{m}_{vent,in} - \dot{m}_{vent,out}$$

**Step 5.** Energy conservation equation:

$$\sum \dot{Q} - \dot{W}_a + \sum_{in} \dot{m} \left( h + \frac{W^2}{2} + gz \right) - \sum_{out} \dot{m} \left( h + \frac{W^2}{2} + gz \right) = \frac{dE_{CV}}{dt} = 0$$

Again, because the process is steady with respect to time, the time derivative expression in the energy conservation equation is zero.

**Step 6.** Identify all known and unknown parameters. The work and heat transfer rates are known. The major unknown is the room air temperature.

**Step 7.** Identify mass flow rates for the mass conservation equation. The derivative with respect to time in the mass conservation equation is zero because the ventilation rate is assumed constant. The solution of the mass conservation equation becomes fairly trivial:

$$\dot{m}_{in} = \dot{m}_{out} = 1 \text{ kg/s}$$

**Step 8.** Identify heat transfer rates. Each sedentary person is assumed to add 100 W (0.100 kW) of energy through heat transfer to the room air. The heat transfer rate from the room to the outside environment is 100 W.

**Step 9.** Identify any work. No actual work is done.

**Step 10.** Using the equation of state equation(s) is not applicable for this problem.

**Step 11.** Property data from tables and the like—the enthalpies are a function of the air temperature. From air tables, the enthalpy at the inlet temperature of 18°C is 291 kJ/K.

**Step 12.** Solve the conservation equations. The mass conservation equation was solved in step 7. The energy conservation equation reduces to:

$$\dot{Q}_{people} + \dot{Q}_{light} + \dot{Q}_{surr} - \dot{W}_a + \dot{m}_{in} h_{in} - \dot{m}_{out} h_{out} = 0$$

$$\dot{Q}_{people} = 4 \times 0.100 \text{ kW} = 0.400 \text{ kW}$$

$$\dot{Q}_{light} = 0.100 \text{ kW}$$

$$\dot{Q}_{surr} = -0.100 \text{ W}$$

$$\dot{W}_a = 0 \text{ W}$$

$$h_{in} = ?$$

$$h_{out} = ?$$

$$0.400 \text{ kW} + 0.100 \text{ kW} - 0.100 \text{ kW} + 1 \frac{\text{kg}}{\text{s}} (h_{in} - h_{out}) = 0$$

The only unknown in this equation is the exit fluid enthalpy. Substituting the inlet enthalpy from step 11 into the energy equation and solving for the outlet enthalpy results in:

$$\frac{0.500 + 291 \text{ kW}}{1 \text{ kg/s}} = h_{out}$$

$$h_{out} = 291.5 \text{ kJ/kg}$$

Because the air leaving the room is at the same temperature as the air in the room, the room air temperature is found by entering the air tables with the exit enthalpy. The corresponding temperature is 18.5°C.

Of prime importance is learning to apply the fundamental equations to virtually any process. In other words, proficiency at writing the fundamental equation and then zeroing out the terms you don't need (kinetic and potential energies are usually, but not always, good candidates for zeros) is necessary for comprehending the material in the rest of this Handbook.

**EXAMPLE 1.1** The 12 steps to success are not explicitly identified in this example. However, the reader should try to identify these steps.

An interior wall is subjected to convection heat transfer from the room and radiation heat transfer from a radiant panel heater. The radiation heat transfer rate at the wall surface can be approximated by:

$$\dot{Q}_{rad} = h_R A (T_{panel} - T_w)$$

$$h_R = \frac{1.4 \text{ Btu}}{h \cdot ft^2 \cdot ^\circ R}$$

$$T_{panel} = 200^\circ F$$

The convection heat transfer rate at the wall surface can be approximated as:

$$\dot{Q}_{conv} = h_{conv} A (T_{air} - T_w)$$

$$h_{conv} = \frac{2 \text{ Btu}}{h \cdot ft^2 \cdot ^\circ R}$$

$$T_{air} = 70^\circ F$$

The conduction heat transfer rate through the wall can be modeled as:

$$\dot{Q}_{cond} = A \frac{T_w - T_\theta}{R_{cond}}$$

$$R_{cond} = \frac{0.2 \text{ h} \cdot ft^2 \cdot ^\circ R}{\text{Btu}}$$

$$T_\theta = 0^\circ F$$

Figure 1.8 shows the wall with the three heat transfer interactions. The control volume in this case is limited to the inside wall surface. This technique is commonly employed to determine surface temperatures.

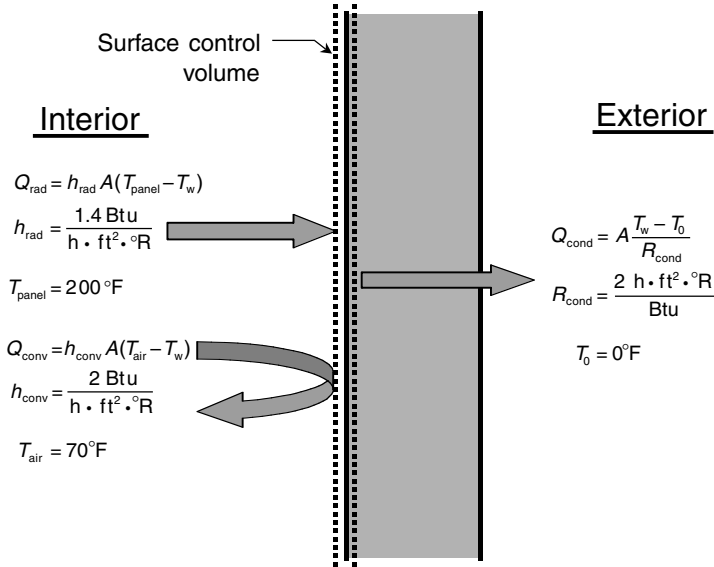


FIGURE 1.8 Surface energy balance on an exterior wall.

The mass conservation equation is unnecessary because mass does not move into or out of the control volume. In fact, when the control volume is just a surface, the mass of the control volume is zero. The energy conservation equation reduces to a balance equation of heat transfer rates:

$$\sum \dot{Q} = 0 = \dot{Q}_{rad} + \dot{Q}_{conv} - \dot{Q}_{cond}$$

$$0 = \underbrace{h_R A (T_{panel} - T_w)}_{\dot{Q}_{rad}} + \underbrace{h_{conv} A (T_{air} - T_w)}_{\dot{Q}_{conv}} - \underbrace{[(A/R_{cond}) (T_w - T_0)]}_{\dot{Q}_{cond}}$$

dividing out the area, and solving for  $T_w$ :

$$T_w = \frac{h_R T_{panel} + h_{conv} T_{air} + R_{cond}^{-1} T_0}{h_{rad} + h_{conv} + R_{cond}^{-1}}$$

$$= \left[ \left( \frac{1.4 \text{ Btu}}{h \cdot \text{ft}^2 \cdot \text{°R}} \right) (200 + 460) \text{°R} + \left( \frac{2 \text{ Btu}}{h \cdot \text{ft}^2 \cdot \text{°R}} \right) (70 + 460) \text{°R} + \left( \frac{2 \text{ Btu}}{h \cdot \text{ft}^2 \cdot \text{°R}} \right) (0 + 460) \text{°R} \right] \times \left[ \left( \frac{1.4 \text{ Btu}}{h \cdot \text{ft}^2 \cdot \text{°R}} \right) + \left( \frac{2 \text{ Btu}}{h \cdot \text{ft}^2 \cdot \text{°R}} \right) + \left( \frac{2 \text{ Btu}}{h \cdot \text{ft}^2 \cdot \text{°R}} \right) \right]^{-1}$$

$$= 537.8 \text{°R}$$

$$= 77.8 \text{°F}$$

Now that the wall surface temperature has been calculated, the individual heat fluxes can be calculated from the definitions at the beginning of the example:

$$\frac{\dot{Q}_{rad}}{A} = \frac{1.4 \text{ Btu}}{h \cdot \text{ft}^2 \cdot ^\circ\text{R}} (660^\circ\text{R} - 537.8^\circ\text{R}) = \frac{171.0 \text{ Btu}}{h \cdot \text{ft}^2}$$

$$\frac{\dot{Q}_{conv}}{A} = \frac{2 \text{ Btu}}{h \cdot \text{ft}^2 \cdot ^\circ\text{R}} (530^\circ\text{R} - 537.8^\circ\text{R}) = \frac{-15.6 \text{ Btu}}{h \cdot \text{ft}^2}$$

$$\frac{\dot{Q}_{cond}}{A} = \frac{0.2 \text{ Btu}}{h \cdot \text{ft}^2 \cdot ^\circ\text{R}} (537.8^\circ\text{R} - 460^\circ\text{R}) = \frac{15.6 \text{ Btu}}{h \cdot \text{ft}^2}$$

**EXAMPLE 1.12** A gas turbine test stand in a laboratory setting provides 200,000 Btu/h of heat to the surrounding air (Fig. 1.9). The maximum outdoor temperature is 100°F. The total heat transfer rate through the structure is approximated as:

$$\dot{Q}_{loss} = \frac{4000 \text{ Btu}}{h \cdot ^\circ\text{R}} \times (T_{outside} - T_{inside})$$

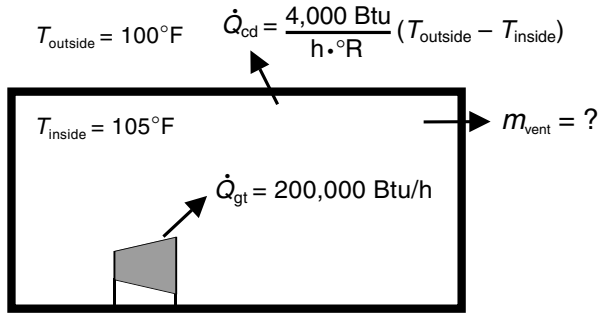


**FIGURE 1.9** Gas turbine laboratory with 200,000 Btu/h internal generation and conduction equal to 4000 Btu/(h · °R) ( $T_{outside} - T_{inside}$ ).

The number of 4000 Btu/h · °R represents the ability of the structure to transfer heat from the inside to the outside. The air infiltration rate is 1 kg/s into the room irrespective of the ventilation system. Determine the ventilation requirement such that the indoor temperature never exceeds the outdoor temperature by 5°F.

The mass conservation equation reduces to a statement saying that the mass into the building is equal to the mass leaving the building. The mass entering the building via the ventilation system is at the outdoor air temperature, and the mass leaving the building via the ventilation system is at the indoor air temperature. Therefore, the energy conservation equation reduces to:

$$\dot{Q}_{turbine} + \dot{Q}_{loss} + \dot{m}_{vent}(h_{outdoor} - h_{indoor}) = 0$$

$$h_{outdoor} - h_{indoor} \approx c_{p,air}(T_{outdoor} - T_{indoor})$$

$$(T_{outdoor} - T_{indoor}) = -5^\circ\text{F}$$

$$\therefore \dot{Q}_{turbine} + \dot{Q}_{loss} + \dot{m}_{vent}[c_{p,air}(-5^\circ\text{F})]$$

The change in enthalpy is calculated using the constant-pressure specific heat for air,  $0.24 \text{ Btu/lbm} \cdot ^\circ\text{R}$ , and the temperature differential is set to the design condition of  $5^\circ\text{F}$ . Substituting these definitions into the energy conservation equation and solving for the ventilation mass flow rate results in:

$$\dot{m}_{\text{vent}} = - \frac{\dot{Q}_{\text{loss}} + \dot{Q}_{\text{turbine}}}{c_{p,\text{air}}(T_{\text{outdoor}} - T_{\text{indoor}})}$$

$$\dot{Q}_{\text{loss}} = \frac{4000 \text{ Btu}}{h \cdot ^\circ\text{R}} (-5^\circ\text{R}) = \frac{-20,000 \text{ Btu}}{h}$$

$$\dot{m}_{\text{vent}} = \left\{ \frac{1}{[0.24 \text{ Btu}/(\text{lbm} \cdot ^\circ\text{R})] \times (-5^\circ\text{R})} \right\} \left[ \left( \frac{-20,000 \text{ Btu}}{h} \right) + \left( \frac{200,000 \text{ Btu}}{h} \right) \right]$$

$$\dot{m}_{\text{vent}} = \frac{150,000 \text{ lbm}}{h}$$

$$\begin{aligned} \dot{V}_S &= \frac{\dot{m}_{\text{vent}}}{\rho_S} = \frac{150,000 \text{ lbm}}{h} \times \frac{\text{ft}^3}{0.073 \text{ lbm}} \times \frac{h}{60 \text{ min}} \\ &= 34,247 \text{ scfm} \end{aligned}$$



---

## CHAPTER 2

---

# CONDUCTION AND CONVECTION HEAT TRANSFER

---

Figure 2.1 illustrates conduction and convection heat transfer, two of the three heat transfer modes. Conduction heat transfer describes the transfer of energy through a solid medium. Convection heat transfer is the transfer of energy between a solid surface and an adjacent fluid. Conduction heat transfer is relevant to heat transfer through walls, ceilings, floors, and other solid objects that experience a temperature gradient. Convection occurs in heat transfer from walls, ceilings, and floors to the surrounding room air; heat transfer from water to the outside pipe surfaces in hydronic heating and cooling; and heat transfer from the heat exchanger in a forced-air furnace to the air; as well as others. Convection can be either *forced* or *natural*. Forced convection occurs when a blower, fan, or pump moves a fluid over a surface.

Natural convection occurs because of the buoyant forces brought about by temperature gradients. The window shown in Fig. 2.1 demonstrates an example of natural convection heat transfer. The cool window surface decreases the temperature of the air that is adjacent to the window glass. Because this volume of air is cooler than the surrounding room air, the air that is adjacent to the window is denser than the room air. This causes the air next to the window to sink relative to the lower-density room air. As the air sinks, additional room air is sucked into the void near the window surface. This new air is then cooled by the window surface and eventually sinks. This continuous process creates a natural circulation path past the window. The heat transfer from the air to the window surface is called *natural convection*.

The reader should keep in mind that conduction and convection heat transfer are two of the essential building blocks required to solve the energy conservation equation, which then leads to thermal comfort calculations. Conduction and convection heat transfer can be as simple as the equations shown in Chap. 1 of this section, or quite complex, involving unsteady, multidimensional calculations.

At the conclusion of this chapter, the reader will be able to calculate steady or unsteady conduction heat transfer through any planar solid medium. The reader will also be able to calculate convection heat transfer from any of the surfaces commonly found in the built environment. Specific use of the data in the appendix should also be understood.

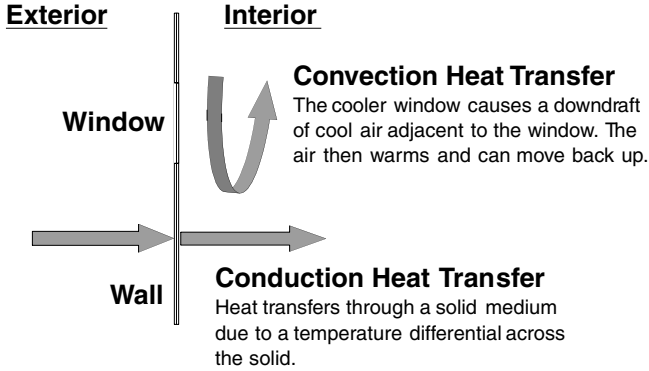


FIGURE 2.1 Examples of conduction and convection heat transfer.

**2.1 FOURIER’S LAW OF HEAT CONDUCTION**

Conduction heat transfer, briefly introduced in Chap. 1 of this section, is defined as the rate at which energy is transported through a solid medium. Experimental data show that conduction is proportional to the temperature difference across the thickness of the solid medium. Mathematically, this is known as Fourier’s law of heat conduction, and is described as:

$$q''_{\text{cond}} \propto \frac{\Delta T}{\Delta x} \tag{2.1}$$

The proportionality constant that relates the conductive heat transfer rate to the ratio of the temperature difference and the thickness is a material property called the *thermal conductivity*,  $k$ . The ratio  $\Delta T/\Delta x$  is the temperature gradient across the wall. In general, the thermal conductivity varies with temperature and the type of solid material. For example, the thermal conductivity of aluminum is 72 W/(m · K), while the thermal conductivity of dry soil is 1 W/(m · K). For preciseness, and to allow for variations in the thermal conductivity of the solid material, the thickness is reduced to zero. The one-dimensional heat conduction equation then becomes the differential equation:

$$q''_{\text{cond},x} = \lim_{\Delta x \rightarrow 0} \left( -k \frac{\Delta T}{\Delta x} \right) = -k \frac{dT}{dx} \tag{2.2}$$

When applied to steady-state situations where the thermal conductivity is independent of temperature, the heat conduction equation is solved using the analogy to an electrical resistance network. The resistors in an electrical network represent the thermal resistances; the voltage differences represent the temperature differences; and the current flows represent the heat transfer rates. The thermal resistances are defined as the thickness divided by the thermal conductivity and are mathematically represented as:

$$R_{\text{th}} = \frac{L}{k} \tag{2.3}$$

Figure 2.2 illustrates a multicomponent wall. This wall is composed of 1/8-in drywall, 4 in of fiberglass insulation, and 1/2-in plywood. The resistive network is shown in the

upper portion of the Fig. 2.2 and includes resistances to heat transfer. Consequently, an equivalent thermal resistance can be calculated for the entire composite medium as:

$$R_{th,eq} = R_{dw} + R_{ins} + R_{ply} = \frac{L_{dw}}{k_{dw}} + \frac{L_{ins}}{k_{ins}} + \frac{L_{ply}}{k_{ply}} \quad (2.4)$$

The heat transfer through this composite surface requires the temperatures at the outside of the plywood and outside of the drywall. With this information, the conduction heat transfer rate is calculated by:

$$q''_{cond} = \frac{T_{dw} - T_{ply}}{R_{th,eq}} \quad (2.5)$$

The conduction-electrical resistance analogy can be used further to calculate the temperature at any point within the composite wall. For example, the temperature between the drywall and the fiberglass is calculated by:

$$q''_{cond} = \frac{T_{dw} - T_{dw-ins}}{(L_{dw}/k_{dw})} \Rightarrow T_{dw-ins} = T_{dw} - q''_{cond} \frac{L_{dw}}{k_{dw}} \quad (2.6)$$

**EXAMPLE 2.1** Given: A composite wall is made of 1/2-in plaster, 3 1/2-in bat of fiberglass insulation (1.5 lb/ft<sup>3</sup>), and 4-in common building brick. The inner surface is 70° F and the outer surface is 32° F.

Find: Calculate the heat loss through the composite-wall-per-unit-surface area. Calculate and compare the R values of each material layer and the complete composite wall.

Solution: The heat transfer rate per unit surface area through the composite wall is calculated by using the concept of thermal resistance. The thermal resistance of each layer in the wall (plaster, insulation, and brick) is:

$$R_{th,p} = \frac{L_p}{k_p}$$

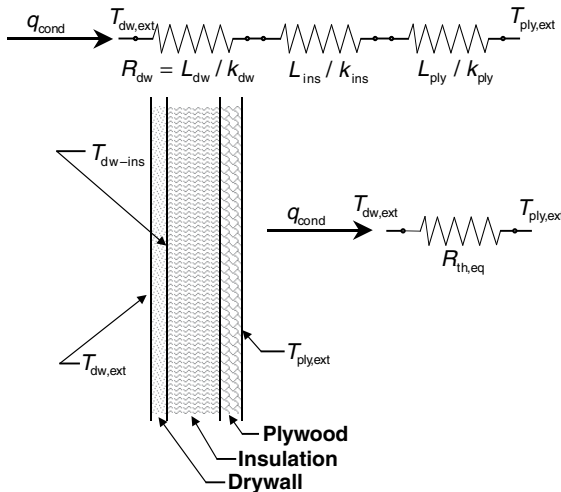


**FIGURE 2.2** Conduction heat transfer can be portrayed as an electrical analog.

$$R_{th,ins} = \frac{L_{ins}}{k_p}$$

$$R_{th,b} = \frac{L_b}{k_b}$$

The thermal conductivity for each material is read from the property table in the appendix. These properties, along with the thermal resistances, are as follows:

$$k_p = \frac{0.162 \text{ Btu}}{h \cdot ft} \Rightarrow R_{th,p} = \frac{L_p}{k_p} = \frac{0.5 \text{ in} \cdot h \cdot ft^2 - \circ R}{0.162 \text{ Btu} \times 12 \text{ in}} = \frac{0.258 h \cdot ft^2 \cdot \circ R}{\text{Btu}}$$

$$k_{ins} = \frac{0.022 \text{ Btu}}{h \cdot ft} \Rightarrow R_{th,ins} = \frac{L_{ins}}{k_{ins}} = \frac{3.5 \text{ in} \cdot h \cdot ft^2 - \circ R}{0.022 \text{ Btu} \times 12 \text{ in}} = \frac{13.284 h \cdot ft^2 \cdot \circ R}{\text{Btu}}$$

$$k_b = \frac{0.399 \text{ Btu}}{h \cdot ft} \Rightarrow R_{th,b} = \frac{L_b}{k_b} = \frac{4.0 \text{ in} \cdot h \cdot ft^2 - \circ R}{0.399 \text{ Btu} \times 12 \text{ in}} = \frac{0.836 h \cdot ft^2 \cdot \circ R}{\text{Btu}}$$

The thermal resistances in units of  $h \cdot ft^2 \cdot \circ R/\text{Btu}$  are actually the R values that are commonly listed for building materials. For example, the R value of the 4-in layer of insulation is 13.3. The total R value can be calculated by adding the individual R values together, as is done in the next step.

The equivalent thermal resistance, or total R value, of the composite wall is:

$$\begin{aligned} R_{th,eq} &= R_{th,p} + R_{th,ins} + R_{th,b} \\ &= \frac{0.258 h \cdot ft^2 \cdot \circ R}{\text{Btu}} + \frac{13.284 h \cdot ft^2 \cdot \circ R}{\text{Btu}} + \frac{0.836 h \cdot ft^2 \cdot \circ R}{\text{Btu}} \\ &= \frac{14.378 h \cdot ft^2 \cdot \circ R}{\text{Btu}} \end{aligned}$$

The heat transfer rate through the wall is then calculated by:

$$\begin{aligned} q''_{wall} &= \frac{T_{in} - T_{out}}{R_{th,eq}} \\ &= (70^\circ F - 32^\circ F) \times \left( \frac{\text{Btu}}{14.378 h \cdot ft^2 \cdot \circ R} \right) \\ &= \frac{2.643 \text{ Btu}}{h \cdot ft^2} \end{aligned}$$

This example illustrates a noteworthy point. Once the R value of a wall is known, then the heat loss through the wall can be calculated by simply measuring the surface temperature on each side of the wall. The heat transfer rate per unit surface area is then the temperature difference ( $^\circ F$ ) divided by the R value.

Using the heat flux to now calculate the temperature of the inside brick surface further extends this example. Because the heat transfer rate is the same anywhere inside the wall, the inside brick surface temperature is calculated by either using the outside temperature and the brick R value, or the inside temperature and the combined R values of the plaster and the insulation:

$$q''_{wall} = \frac{T_{b,in} - T_{out}}{R_{th,b}} = \frac{T_{in} - T_{b,in}}{R_{th,p} + R_{th,ins}}$$

$$\begin{aligned}
 T_{b,in} &= (R_{th,b} \times q''_{wall}) + T_{out} \\
 &= \left( \frac{0.836 \text{ h} \cdot \text{ft}^2 \cdot \text{°R}}{\text{Btu}} \right) \times \left( \frac{2.643 \text{ Btu}}{\text{hr} \cdot \text{ft}^2} \right) + 32\text{°F} \\
 &= 34.21\text{°F}
 \end{aligned}$$

or

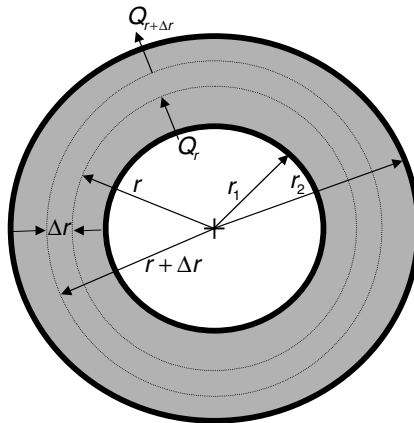
$$\begin{aligned}
 T_{b,in} &= T_{in} - q''_{wall} \times (R_{th,p} + R_{th,ins}) \\
 &= 70\text{°F} - \left( \frac{2.643 \text{ Btu}}{\text{h} \cdot \text{ft}^2} \right) \left( \frac{0.258 \text{ hr} \cdot \text{ft}^2 \cdot \text{°R}}{\text{Btu}} + \frac{13.284 \text{ h} \cdot \text{ft}^2 \cdot \text{°R}}{\text{Btu}} \right) \\
 &= 34.21\text{°F}
 \end{aligned}$$

**2.1.1 Conduction Through Cylindrical Components**

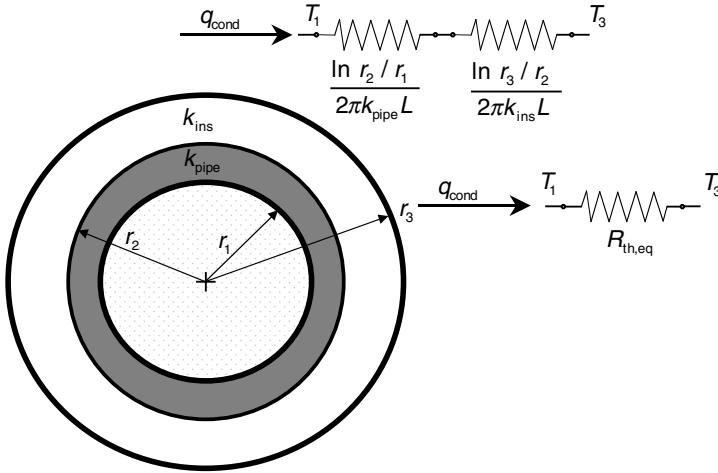
Conduction heat transfer through and from cylindrical components is frequently encountered in heating, ventilating, and air-conditioning (HVAC) problems. A common cylindrical example is heat conduction from an insulated steam pipe. Cylindrical heat transfer is slightly more complex than planar problems because the surface area varies with radius from the center of the cylinder. The heat that is transferred through the cylinder must therefore cross an increasingly larger surface area.

Figure 2.3 shows the cross section of pipe. The inside radius is  $r_1$  and the outside radius is  $r_2$ . The figure also shows a control volume that is a concentric ring of thickness  $\Delta r$ . The radius of the inner ring is  $r$ , and the radius of the outer ring is  $r + \Delta r$ . Because there is no work or mass flow into or out of this control volume, and because it is steady state, the energy conservation equation for this control volume reduces to

$$\dot{Q}_r - \dot{Q}_{r+\Delta r} = 0 \tag{2.7}$$



**FIGURE 2.3** Heat conduction through a cylindrical pipe.



**FIGURE 2.4** Heat conduction through an insulated steam pipe showing the analogous electrical circuit.

This important relationship states that the heat transfer rate at any radius is the same or, stated another way, that the heat transfer rate through the cylinder is independent of  $r$ . At the inner surface, Fourier's law states that:

$$\dot{Q}_r = 2\pi r L \left( -k \frac{\delta T}{\delta r} \right)_r \tag{2.8}$$

The variable  $L$  is the length of the pipe, and the subscript  $r$  on the parentheses indicates that the parenthetic quantity is evaluated at a radius of  $r$ . Because  $L$  is a constant, and if  $k$  is assumed independent of temperature, then Eq. (2.8) is rearranged into a first-order ordinary differential equation:

$$\frac{dT}{dr} = - \frac{\dot{Q}}{2\pi k L r} \tag{2.9}$$

Integrating between any two points along the radius of the cylinder results in a conduction equation as a function of the radii and the temperatures at the two points:

$$\dot{Q} = \frac{2\pi k L}{\ln(r_2/r_1)} (T_1 - T_2) = \frac{T_1 - T_2}{R_{th,eq}} \tag{2.10}$$

Equation (2.10) is in a form that can again be analyzed using the electric analogy. Although a little more complex algebraically, the procedure is the same. Figure 2.4 shows the cross section of an insulated steam pipe. The inside radius  $r_1$  is at temperature  $T_1$ , and the outside radius  $r_3$  is at temperature  $T_3$ . The radius identifying the interface between the steel pipe and the insulation is  $r_2$ , which is at temperature  $T_2$ . The heat conduction equation relating these temperatures and radii to the heat transfer rate and thermal conductivities is:

$$\begin{aligned} \dot{Q} &= \frac{T_1 - T_3}{[\ln(r_2/r_1)/2\pi k_{\text{pipe}}L] + [\ln(r_3/r_2)/2\pi k_{\text{ins}}L]} \\ &= \frac{T_1 - T_2}{[\ln(r_2/r_1)/2\pi k_{\text{pipe}}L]} = \frac{T_2 - T_3}{[\ln(r_3/r_2)/2\pi k_{\text{ins}}L]} \end{aligned} \quad (2.11)$$

Another practical use of cylindrical calculations applies to cylindrically shaped electrical resistance heaters. These heaters, sometimes used as radiative heaters, generate internal heat when a voltage is applied to each end. Figure 2.5 shows the schematic of this heater, as well as the control volume of thickness  $\Delta r$ . The energy conservation equation, again with work and mass flow equal to zero and steady state, reduces to the following:

$$\dot{Q}_r - \dot{Q}_{r+\Delta r} + q'''_{\text{gen}} \times \Delta V = 0, \quad \Delta V = 2\pi L r \Delta r \quad (2.12)$$

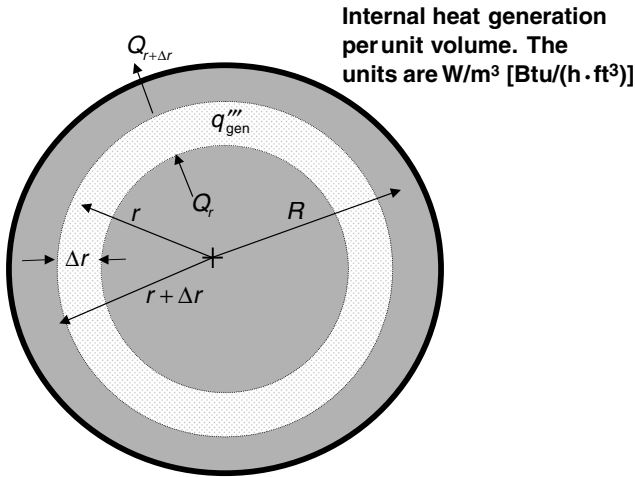


**FIGURE 2.5** Schematic showing heat conduction through an electrically heated cylinder.

Dividing by  $\Delta r$ , letting  $\Delta r$  approach zero, and finally substituting Fourier's law for  $\dot{Q}$ , a second-order ordinary differential equation results that can be solved for the temperature distribution in the cylindrical heater:

$$\frac{d}{dr} \left( r \frac{dT}{dr} \right) = - \frac{r q'''_{\text{gen}}}{k} \quad (2.13)$$

Using appropriate boundary conditions and integrating this equation results in the temperature distribution throughout the cylindrical heater:

$$T(r) = T_s + \frac{q'''_{\text{gen}}}{4k} (R^2 - r^2) \quad (2.14)$$

In this equation,  $R$  is the cylinder radius and  $T_s$  is the cylinder surface temperature. Note that the maximum temperature is at the center of the heater where  $r = 0$ . The centerline, or maximum, temperature can be calculated by:

$$T_{\max} = T_s + \frac{q_{\text{gen}}''' R^2}{4k} \quad (2.15)$$

**EXAMPLE 2.2** Given: A 1-in-diameter cylindrical electrical resistance heater consumes 12,000 Btu/ft<sup>3</sup>. The heater surface temperature is 300°F. The thermal conductivity of the heater material is 0.03 Btu/(h · ft · °F).

Find: Calculate the maximum temperature within the cylindrical heater, graph the temperature distribution within the heater as a function of the radius  $r$ , and calculate the surface heat transfer rate per unit length of the heater.

Solution: This example uses the equation for radial temperature distribution in a cylindrical rod with internal heat generation. The basic equation is:

$$T(r) = T_s + \frac{q_{\text{gen}}'''}{4k} (R^2 - r^2)$$

The maximum temperature is found by setting  $r = 0$  and solving for  $T(0)$ :

$$\begin{aligned} T(0) &= 300^\circ F + \frac{q_{\text{gen}}'''}{4k} R^2 \\ &= 300^\circ F + \left( \frac{12,000 \text{ Btu}}{h \cdot \text{ft}^3} \right) \left( \frac{1}{4} \right) \left( \frac{h \cdot \text{ft} \cdot ^\circ F}{0.03 \text{ Btu}} \right) (0.5 \text{ in})^2 \left( \frac{\text{ft}^2}{144 \text{ in}^2} \right) \\ &= 300^\circ F + 173.6^\circ F \\ &= 473.6^\circ F \end{aligned}$$

The heat transfer rate at the heater surface is calculated by using the basic equation for the heat conduction through a cylindrical rod:

$$\begin{aligned} \frac{\dot{Q}_R}{L} &= 2\pi R \left( -k \frac{\partial T}{\partial r} \right)_R \\ \frac{\partial T}{\partial r} &= \frac{\partial}{\partial r} \left[ T_s + \frac{q_{\text{gen}}'''}{4k} (R^2 - r^2) \right] = -\frac{q_{\text{gen}}'''}{4k} \frac{\partial}{\partial r} (r^2) = -\frac{q_{\text{gen}}''' r}{2k} \\ \frac{\partial T}{\partial r} \Big|_R &= -\frac{q_{\text{gen}}''' R}{2k} \\ \frac{\dot{Q}_R}{L} &= \pi R^2 q_{\text{gen}}''' = \pi (0.5 \text{ in})^2 \left( \frac{\text{ft}^2}{144 \text{ in}^2} \right) \left( \frac{12,000 \text{ Btu}}{h \cdot \text{ft}^3} \right) \\ \frac{\dot{Q}_R}{L} &= \frac{65.5 \text{ Btu}}{h \cdot \text{ft}} \end{aligned}$$

Note that once the heat transfer rate per unit length of the heater is known, then it becomes a simple matter of specifying the heater length to provide the required amount of heat. For example, if a room required 1000 Btu/h of heating, then the heater length would be as follows:

$$L = \left( \frac{1000 \text{ Btu}}{h} \right) \left( \frac{h \cdot \text{ft}}{65.5 \text{ Btu}} \right) = 15.3 \text{ ft}$$

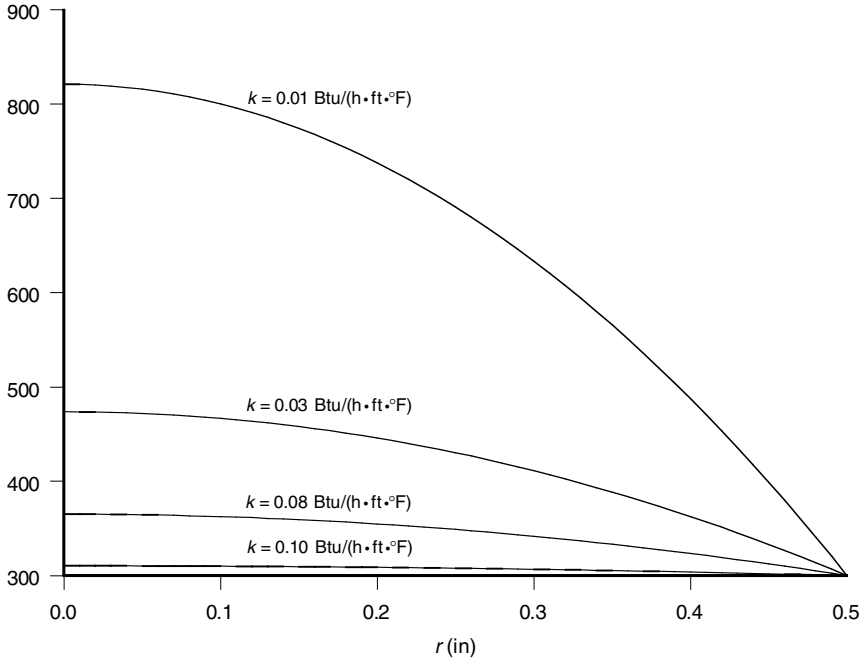


**FIGURE 2.6** Temperature distribution as a function of thermal conductivity.

The temperature distribution through the heater is shown in Fig. 2.6. The temperature distribution is shown for the current example as well as for material thermal conductivities ranging from 0.01 to 0.10 Btu/(h · ft · °F). Noteworthy is that as the thermal conductivity increases, the temperature distribution throughout the heater becomes more uniform.

### 2.1.2 Unsteady, Multidimensional Heat Conduction

Unsteady conduction heat transfer is an important HVAC consideration because setback thermostats play a major role in energy savings. Setback thermostats generally keep the temperatures and the heat transfer rates through room walls in a transient flux. Consequently, transient heat conduction is another integral part of the energy conservation equation and the thermal comfort analysis.

The unsteady, or transient, heat conduction equation is again derived from the energy equation and Fourier's law of heat conduction. This time, though, the unsteady portion of the energy conservation equation cannot be set at zero. This equation is derived in many undergraduate heat transfer textbooks, such as Incropera and DeWitt (1996) and Mills (1995), so the result is only shown here:

$$\rho c \frac{\partial T}{\partial t} = \frac{\partial}{\partial x} \left( k \frac{\partial T}{\partial x} \right) + \frac{\partial}{\partial y} \left( k \frac{\partial T}{\partial y} \right) + \frac{\partial}{\partial z} \left( k \frac{\partial T}{\partial z} \right) \quad (2.16)$$

The left side is the transient portion, and the right side is Fourier's law of heat conduction expressed in three directions. Rarely, if ever, is it important to solve this

complete equation. Rather, the equation is simplified to one- or two-dimensional transient conduction, and even then is generally solved using a numerical procedure.

Complete texts have been written on numerically solving Eq. (2.16). Some texts, such as Carslaw and Jaeger (1959), provide elegant analytical solutions for various applications of the heat conduction equation. With today's modern desktop computers, the heat conduction equation as applied to real engineering problems is usually, if not always, solved by numerical techniques. It is a well-understood technology and, when executed properly, provides solutions as accurate as the historic analytical solutions. The text written by Patankar (1980) provides the most methodical approach to numerical solutions of heat transfer problems. His text fully describes the finite-difference approach to solving the transient, three-dimensional heat conduction equation.

In this Handbook, the transient solutions are almost always carried out numerically. Numerical solutions are discussed to the extent necessary at the end of this chapter. There are, however, two transient conduction problems that are important for HVAC design applications that can be solved analytically. When these methods are used to analyze appropriate engineering problems, the results are usually accurate. The first is the transient temperature in soil and the second is the lumped-capacitance approach.

### 2.1.3 Transient Conduction in Soil

Transient conduction for soil is important in the analysis of slab-on-grade for edge and downward heat loss. The hydronic system, shown schematically in Fig. 2.7, heats the concrete slab with hot water. The slab then radiantly and convectively heats the occupied space and the ground below the slab.

The derivation of the fundamental equation that describes heat transfer from the

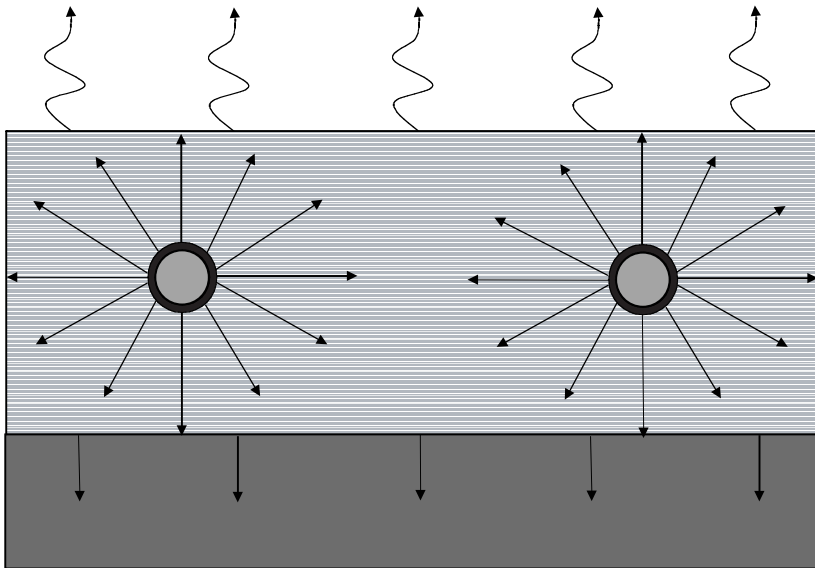


**FIGURE 2.7** Schematic example of a slab-on-grade hydronic system that shows thermal charging of the ground below the slab.

slab to the ground is somewhat complex. It is, however, derived in many of the heat transfer textbooks, such as Incropera and DeWitt (1996), Mills (1995), and Wolf (1983). The governing equation is the transient conduction equation written in one-dimensional form:

$$\frac{\partial T}{\partial t} = \left( \frac{k}{\rho c_p} \right) \frac{\partial^2 T}{\partial x^2} \tag{2.17}$$

The boundary conditions are:

$$\begin{aligned} T(x = 0, t) &= T_s \\ T(x \rightarrow \infty, t) &= T_0 \end{aligned} \tag{2.18}$$

and the initial condition is:

$$T(x, t = 0) = T_0 \tag{2.19}$$

The working equation for the case where the surface temperature is known provides the temperature distribution in the soil at any depth and at any time  $t$ . This governing equation is (refer to Fig. 2.7):

$$\frac{T(x, t) - T_s}{T_i - T_s} = \text{erf} \left( \frac{x}{2\sqrt{\alpha t}} \right) \tag{2.20}$$

The instantaneous heat flux at any time  $t$  into the semi-infinite body from the surface is calculated from the definition of heat conduction:

$$\begin{aligned} \dot{q}_0(t) &= -k \left. \frac{\partial T(t)}{\partial x} \right|_{x=0} \\ &= \frac{-kA(T_0 - T_s)}{\sqrt{\pi\alpha t}} \end{aligned} \tag{2.21}$$

where  $\alpha = k/\rho c_p$ . The total amount of heat that has been transferred to the semi-infinite body over a particular length of time can be calculated by (Wolf, 1983):

$$\dot{Q}_0 = \frac{-2kA(T_i - T_s)}{\sqrt{\pi\alpha t}} \tag{2.22}$$

The temperature distribution equation for the case where the convection heat transfer coefficient is known at the surface is (Wolf, 1983):

$$\frac{T(x, t) - T_\infty}{T_i - T_\infty} = \text{erf} \left( \frac{x}{2\sqrt{\alpha t}} \right) + \exp \left( \frac{hx}{k} + \frac{h^2\alpha t}{k^2} \right) \left[ 1 - \text{erf} \left( \frac{x}{2\sqrt{\alpha t}} + \frac{h\sqrt{\alpha t}}{k} \right) \right] \tag{2.23}$$

The heat transfer rate to the soil is calculated from the convection heat transfer equation.

$$\dot{q}''(t) = h[T_\infty - T_s(t)] \tag{2.24}$$

The basis behind these equations is that no matter how much heat is transferred to the soil below the slab, somewhere below the slab the soil temperature is unaffected. For example, assume you dig a hole into the ground until you are far below the frost point. If you measure the temperature at every inch, you will end up with a description of how the soil temperature varies within the first few feet of the soil surface. After you dig deep enough, the soil temperature will reach a constant temperature that depends on the annual average climate. Define this temperature and depth as the *constant* point (the variable  $T_i$  is the constant temperature at this point in the preceding equations).

Now, place a heated concrete slab on the soil surface and energize the heating system. The temperature of the ground directly under the slab will begin to increase, but the soil temperature at some distance below the slab will remain the same. As time marches on, the concrete slab will affect the temperature further into the soil. The depth of the temperature effect is called the *penetration depth*. After a very long time, the effect of the heated concrete slab will extend past the constant point. But somewhere, no matter how long you wait, there exists a point where the slab has no effect on the soil temperature. This point is called the *maximum penetration depth* of the slab.

The slab loses more energy to the soil when the soil is at its normal temperature. The longer the slab is energized, the lower the energy loss—to a point. Once the maximum penetration depth is reached, the heat loss from the concrete slab becomes constant, except perhaps in the case of edge losses at ground level.

Heat loss of a room is largely dependent on the size of the room. For a small building, the dominant loss is at the intersection of the concrete slab and the earth. For larger structures, the dominant loss is due to infiltration. The infiltration surface area of the walls is much larger than the floor surface area in these larger structures.

**EXAMPLE 2.3** Calculate the heat transfer rate from a slab first energized at 294 K (529.2°R) with the soil at 272 K (489.6°R), and then the heat transfer rate at a depth of 5 ft after the slab has been energized for 4 h and the soil is 280 K (540°R).

$$h = 5.64 \frac{W}{m^2 \cdot K}$$

$$\rho = 2050 \frac{kg}{m^3}$$

$$c_p = 1840 \frac{J}{kg \cdot K}$$

$$\alpha = \frac{k}{\rho c_p} = 1.5 \times 10^{-6} \frac{m^2}{sec}$$

$$q''_0(t) = h[T_\infty - T_s(t)] = 5.64 \frac{W}{m^2 \cdot K} [272 - 294]$$

$$q''_0(t) = 125.6 \frac{W}{m^2} \frac{280 - 294}{\quad}$$

$$q''_0 = \frac{-2k(T_i - T_s)}{\sqrt{\pi \alpha t}} = -2 \times 0.52 \frac{W}{m \cdot K} \left[ \sqrt{\pi \left( 1.5 \times 10^{-6} \frac{m^2}{s} \right) \left( 4 h \times 3600 \frac{s}{h} \right)} \right]$$

$$q''_0 = 5.59 \frac{W}{m^2}$$

### 2.1.4 Lumped-Capacitance Approach

The lumped-capacitance method provides a method to calculate the transient temperature of a solid object. The *major assumption* is that the object around which the control volume is drawn remains at a uniform temperature. What this means is that the entire object is at exactly the same temperature. When the temperature of a portion of the object increases, or decreases, the rest of it must change *at the same time*.

Note that when using this method, this assumption should always be validated, or errors of several hundred percent could result. The method is only as accurate as this assumption.

Fortunately, a technique exists to test the validity of the uniform assumption. Figure 2.8 illustrates an aluminum sphere that is initially at a temperature of 20°C. The sphere is plunged into a 10°C atmosphere. If the sphere is small, and because the thermal conductivity of aluminum is fairly high, the entire sphere will change tem-

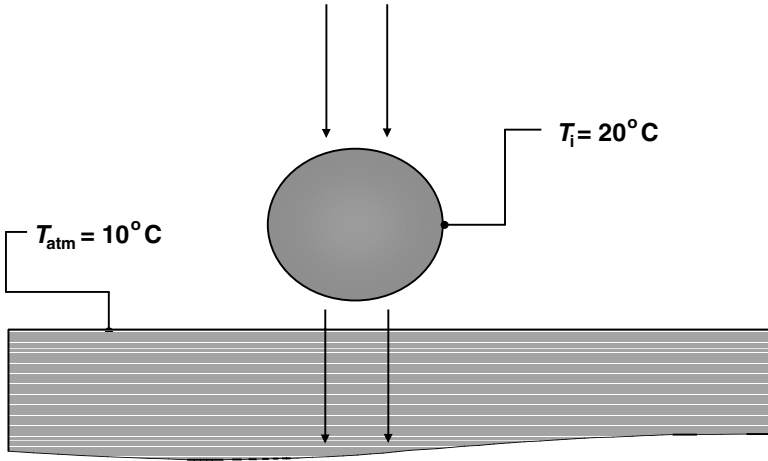


**FIGURE 2.8** A sphere demonstrating the lumped-capacitance method.

perature at approximately the same rate until the sphere temperature equals the surrounding air temperature. In other words, the sphere changes temperature uniformly from the initial to the final temperature.

This example suggests that the lumped-capacitance method can be readily applied to systems that are small and have a high thermal conductivity. The relationship between size and thermal conductivity is the *internal thermal resistance*.

The *external thermal resistance* also plays a role in an object's temperature uniformity. The external thermal resistance is a measure of how fast energy can be connected between the solid object and the surrounding fluid. The external thermal resistance is expressed as:

$$R_{\text{th,ext}} = \frac{1}{A_{\text{surf}} h_{\text{surf}}} \quad (2.25)$$

The internal resistance depends on the object geometry and, for a wall of constant composition, is written as:

$$R_{\text{th,int}} = \frac{L}{k_{\text{solid}} A_{\text{surf}}} \quad (2.26)$$

Calculating the Biot number,  $Bi$ , tests the validity of the lumped-capacitance method. The Biot number is the ratio between the internal and external thermal resistances, and is mathematically defined as:

$$Bi = \frac{R_{\text{th,int}}}{R_{\text{th,ext}}} = \frac{h_{\text{surf}} L}{k_{\text{solid}}} \quad (2.27)$$

When  $Bi$  is less than or equal to 0.1, the lumped-capacitance method can be applied with little loss in accuracy.

The lumped-capacitance method follows directly from the energy conservation equation. For a plate with the conditions that the control volume is drawn around the solid surfaces so that mass neither enters nor leaves the control volume, that kinetic and potential energy are negligible, and that work is not present, the energy conservation equation reduces to:

$$\dot{Q}_{\text{surf}} = \frac{d(me)}{dt} = \rho V \frac{du}{dt} = \rho cLA \frac{dT}{dt} \quad (2.28)$$

Dividing by the surface area and recognizing that the surface heat transfer rate must be equal to convection from the surface, Eq. (2.28) is rewritten as:

$$\frac{dT}{dt} = \frac{h(T_0 - T)}{\rho cL} \quad (2.29)$$

Once again, a first-order, ordinary differential equation results, whose solution is:

$$\frac{T(t) - T_0}{T_i - T_0} = \exp\left(\frac{-ht}{\rho cL}\right) \quad (2.30)$$

Equation (2.30) results in the transient time response of a component whose spatial temperature distribution remains uniform.

**EXAMPLE 2.4** Given: *A 100-mm copper plate is well insulated on both sides. The copper temperature is 400 K. At some point in time, the insulation from one of the surfaces is removed. The resulting heat transfer coefficient is 20 W/(m<sup>2</sup> · K), and the ambient temperature is 280 K (504°R).*

Find: *Calculate the time required for the aluminum plate to reach 300 K (540°R).*

Solution: *The first task is to ensure that the lumped-capacitance method is appropriate for this problem. From the appendix, the relevant properties are:*

$$h = 20 \frac{W}{m^2 \cdot K} \quad c = 385 \frac{J}{kg \cdot K} \quad k = 401 \frac{W}{m \cdot K}$$

$$\rho = 8933 \frac{kg}{m^3} \quad L = 100 \cdot mm$$

$$Bi = \frac{h \cdot L}{k} \quad Bi = 4.988 \cdot 10^{-3} < 0.1 \text{ (Assume that lumped-capacitance method is applicable)}$$

$$\frac{dT}{dt} = \frac{h(T_0 - T)}{\rho cL} \quad \text{Solve for } t \text{ assuming } t_0 = 0$$

$$t = \ln\left(\frac{300 - 280}{400 - 280}\right) \cdot \frac{\rho \cdot c \cdot L}{-h}$$

$$t = 3.081 \cdot 10^4 \text{ s} \quad \text{or} \quad t = 8.559 \cdot h$$

### 2.1.5 Combining Building Materials into a Wall, Floor, or Ceiling

The information covered in the preceding sections provides the background for calculating the heat transfer rate through walls, floors, ceilings, and other types of build-

ing partitions. The resistance method is generally the method of choice. This method can be used to incorporate the effect of thermal bridging, which can effectively reduce the overall insulating effect by up to 20 percent. Walls are considered composite structures that are made up of one or more materials. For example, an outside wall in a house will be made up of at least four components: sheetrock, insulation, outer wall, and siding. The thermal conductivity of these materials varies from approximately 0.03 Btu/(h · ft · °F) for insulating materials to several hundred for metals. The subject of this section is to investigate how composite walls made from materials with different thermal conductivities are analyzed.

Figure 2.9 illustrates a composite wall that is composed of sheetrock, insulation, an exterior plywood wall, and exterior brick siding. The thermal conductivity of each material is shown in the figure, along with each component's thickness. The inside and outside temperatures are also shown in the figure. The electric analogy is applicable in this case. The heat transfer rate through the wall is related to the temperatures and the composite properties by:

$$q_w'' = \frac{T_R - T_{wO}}{R_{th,eq}} \tag{2.31}$$

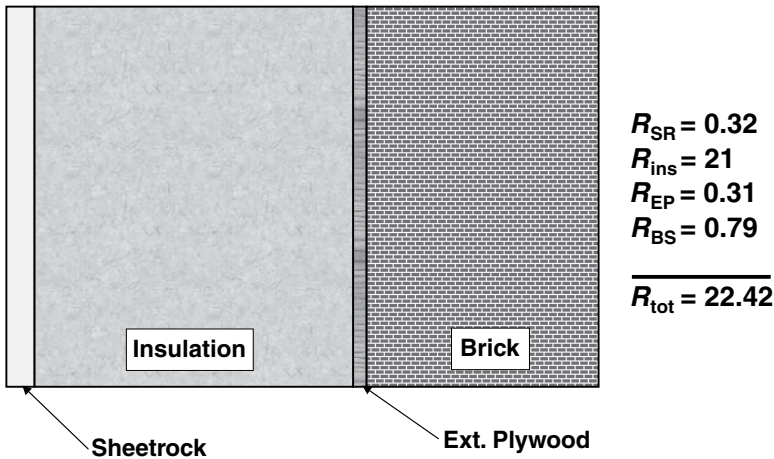


**FIGURE 2.9** A cross section of a composite building wall showing four different materials and the wall structure.

The equivalent thermal resistance is calculated using Eq. (2.31):

$$R_{th,eq} = \frac{L_{dw}}{k_{dw}} + \frac{L_{ins}}{k_{ins}} + \frac{L_{ply}}{k_{ply}} + \frac{L_{br}}{k_{br}} \tag{2.32}$$

Note from Eq. (2.31) that there are two ways to reduce the heat transfer from the inside to the outside of the wall. The first is to reduce the temperature differential across the wall and the second is to increase the thermal resistance. Usually, one has little control over the temperature differential. However, part of the design process is the specification of materials and sizes. Note from Eq. (2.32) that decreasing component thermal conductivity and increasing component thickness increases the equivalent thermal resistance.

The more complicated case considers the effect of thermal bridging through the wall. Thermal bridging is caused by some intermediate component, such as a wall stud, that exhibits a different thermal resistance than the rest of the wall. This situation is illustrated in Fig. 2.10 by an electric analogy. The parallel resistances represent the wall studs and the layers of insulation. The resistor to the left represents the thermal resistance of the inside drywall, and the resistor to the right represents the thermal resistance of the exterior plywood layer. Whereas series of thermal resistances simply add together to obtain the equivalent thermal resistance, parallel resistances are a little more complicated. The equivalent thermal resistance for  $N$  parallel resistors  $R_p$  is written as:

$$R_p = \left[ \frac{A_1}{R_1} + \frac{A_2}{R_2} + \frac{A_3}{R_3} + \dots + \frac{A_N}{R_N} \right]^{-1} \times \sum_{i=1}^N A_i \quad (2.33)$$

This equation can be simplified by recognizing that the insulation layers shown in Fig. 2.10 all exhibit the same thermal resistance, and the wall studs all exhibit the

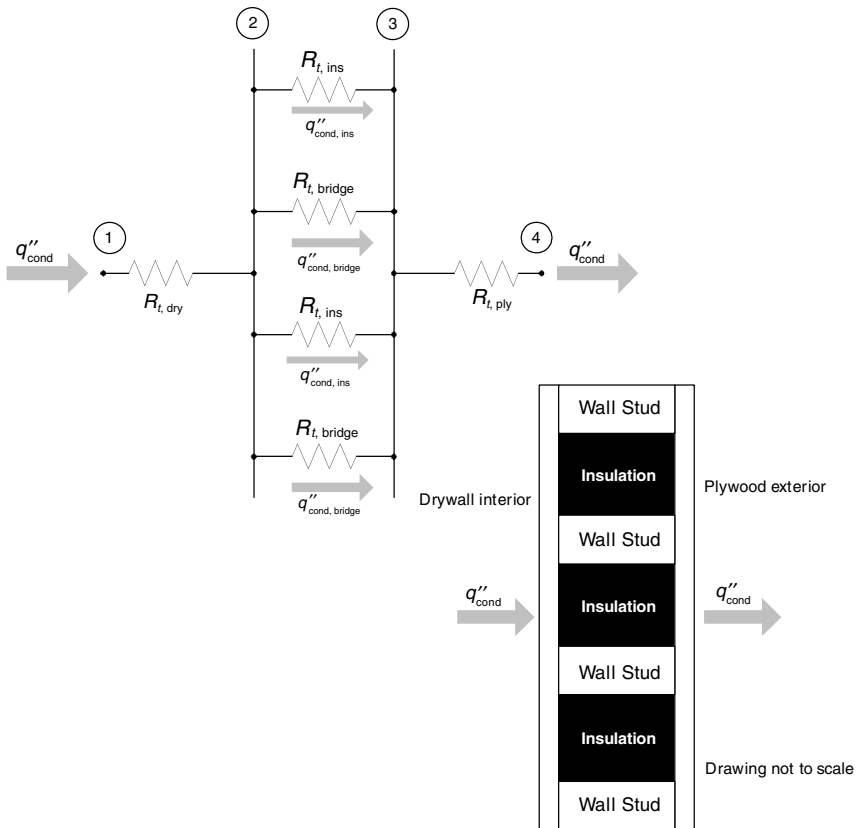


FIGURE 2.10 Resistance analogy for thermal bridging analysis.

same thermal resistance. Additionally, if there are  $N$  wall studs, then there are  $(N - 1)$  insulation layers. Equation (2.33) simplifies to:

$$\begin{aligned}
 R_p &= \left[ \frac{A_{\text{bridge}}N}{R_{t,\text{bridge}}} + \frac{A_{\text{ins}}(N-1)}{R_{t,\text{ins}}} \right]^{-1} [N \times A_{\text{bridge}} + (N-1)A_{\text{ins}}] \\
 &= \left[ \frac{R_{t,\text{ins}}A_{\text{bridge}}N + R_{t,\text{bridge}}A_{\text{ins}}(N-1)}{R_{t,\text{ins}}R_{t,\text{bridge}}} \right]^{-1} [N \times A_{\text{bridge}} + (N-1)A_{\text{ins}}] \quad (2.34) \\
 &= \frac{R_{t,\text{ins}}R_{t,\text{bridge}}[N \times A_{\text{bridge}} + (N-1)A_{\text{ins}}]}{R_{t,\text{ins}}A_{\text{bridge}}N + R_{t,\text{bridge}}A_{\text{ins}}(N-1)}
 \end{aligned}$$

Finally, the total thermal resistance from the inside surface of the drywall to the outside surface of the plywood is:

$$R_{\text{eq}} = R_{t,\text{dry}} + \frac{R_{t,\text{ins}}R_{t,\text{bridge}}[N \times A_{\text{bridge}} + (N-1)A_{\text{ins}}]}{R_{t,\text{ins}}A_{\text{bridge}}N + R_{t,\text{bridge}}A_{\text{ins}}(N-1)} + R_{r,\text{ply}} \quad (2.35)$$

In Fig. 2.10, the resistance of each component is as follows:

- Drywall (½ in): 0.32 (h · ft² · °F)/Btu
- Insulation (5.5 in): 21 (h · ft² · °F)/Btu
- Exterior plywood (¼ in): 0.31 (h · ft² · °F)/Btu
- Wall studs (2 × 4 in): 1.0 (h · ft² · °F)/Btu
- Number of wall studs ( $N$ ): 10
- Wall stud width: 2 in
- Insulation layer width: 14 in

For this particular case, the equivalent thermal resistance for the parallel section of the wall is calculated as:

$$\begin{aligned}
 R_p &= \left\{ \underbrace{\left( \frac{21 \text{ h} \cdot \text{ft}^2 \cdot \text{°R}}{\text{Btu}} \right)}_{R_{t,\text{ins}}} \underbrace{\left( \frac{1.0 \text{ h} \cdot \text{ft}^2 \cdot \text{°R}}{\text{Btu}} \right)}_{R_{t,\text{bridge}}} \left[ 10 \times \underbrace{\left( 8 \text{ ft} \times \frac{2}{12} \text{ ft} \right)}_{A_{\text{bridge}}} + (10-1) \underbrace{\left( 8 \text{ ft} \times \frac{14}{12} \text{ ft} \right)}_{A_{\text{ins}}} \right] \right\} \\
 &\times \left[ \underbrace{\left( \frac{21 \text{ h} \cdot \text{ft}^2 \cdot \text{°R}}{\text{Btu}} \right)}_{R_{t,\text{ins}}} \underbrace{\left( 8 \text{ ft} \times \frac{2}{12} \text{ ft} \right)}_{A_{\text{bridge}}} \times 10 + \underbrace{\left( \frac{1.0 \text{ h} \cdot \text{ft}^2 \cdot \text{°R}}{\text{Btu}} \right)}_{R_{t,\text{bridge}}} \underbrace{\left( 8 \text{ ft} \times \frac{14}{12} \text{ ft} \right)}_{A_{\text{ins}}} (10-1) \right]^{-1} \quad (2.36) \\
 &= \frac{2044 \text{ ft}^2 (\text{h} \cdot \text{ft}^2 \cdot \text{°R}/\text{Btu})^2}{345.3 \text{ ft}^2 (\text{h} \cdot \text{ft}^2 \cdot \text{°R}/\text{Btu})} \\
 &= \frac{5.92 \text{ h} \cdot \text{ft}^2 \cdot \text{°R}}{\text{Btu}}
 \end{aligned}$$

The total equivalent thermal resistance, which includes the effect of the drywall and plywood, is:

$$R_{eq} = \frac{0.32 \text{ h} \cdot \text{ft}^2 \cdot \text{°R}}{\text{Btu}} + \frac{5.92 \text{ h} \cdot \text{ft}^2 \cdot \text{°R}}{\text{Btu}} + \frac{0.31 \text{ h} \cdot \text{ft}^2 \cdot \text{°R}}{\text{Btu}} \quad (2.37)$$

$$= \frac{6.54 \text{ h} \cdot \text{ft}^2 \cdot \text{°R}}{\text{Btu}}$$

For the case where the interior surface temperature is 70°F and the exterior surface temperature is 10°F, the heat transfer rate across the wall is:

$$q''_{cond} = \frac{T_1 - T_4}{R_{eq}} = (70\text{°F} - 20\text{°F}) \times \left[ \frac{\text{Btu}}{6.54 \text{ h} \cdot \text{ft}^2 \cdot \text{°R}} \right] \quad (2.38)$$

$$= \frac{7.65 \text{ Btu}}{\text{h} \cdot \text{ft}^2}$$

The total surface area of the wall is:

$$A_{total} = 8 \text{ ft} \times [(10 \times 2 \text{ in}) + (10 - 1) \times (14 \text{ in})] \quad (2.39)$$

$$= 97.3 \text{ ft}^2$$

Then the total heat transfer rate through the wall is:

$$\dot{Q}_{cond} = A_{total} q''_{cond} = (97.3 \text{ ft}^2) \left( \frac{7.65 \text{ Btu}}{\text{h} \cdot \text{ft}^2} \right) = \frac{744.3 \text{ Btu}}{\text{h}} \quad (218.1 \text{ W}) \quad (2.40)$$

An interesting parametric study is to investigate how the heat transfer rate varies through the wall with the thermal resistance of the bridging material. For example, one may wish to use metal studs instead of wooden studs. Figure 2.11 illustrates this variation. When the bridge thermal resistance is small, the heat transfer rate is large. The reason for this is that the bridge behaves as a short circuit, allowing heat to pass

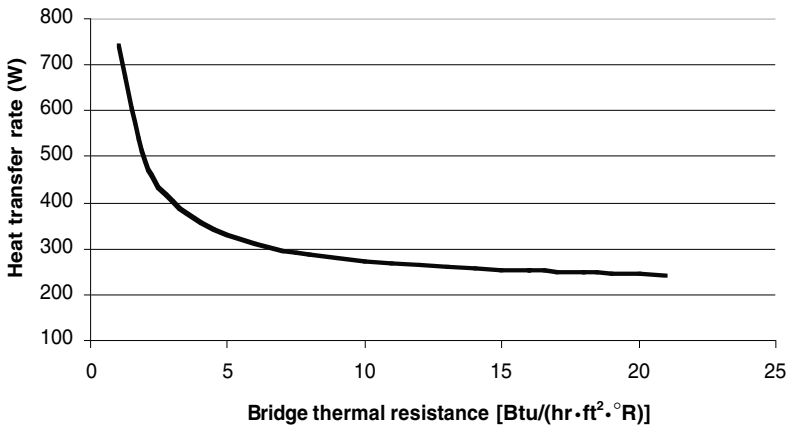


FIGURE 2.11 Heat transfer rate as a function of thermal bridging resistance.

from the inside surface to the exterior surface. When the bridge thermal resistance is small, the insulation itself can become virtually ineffective. As the bridge thermal resistance increases, the insulation becomes the controlling factor. As the thermal resistance of the bridging material increases, it behaves more and more like an open circuit, preventing heat from transferring except through the insulation.

The equivalent thermal resistance is directly related to the  $R$  value of the wall. An  $R$  value of 19 means that the equivalent thermal resistance is  $19 \text{ h} \cdot \text{ft}^2 \cdot ^\circ\text{R}/\text{Btu}$ . Hence, if one wants to calculate the heat transfer through an  $R$ -19 wall when the indoor temperature is  $70^\circ\text{F}$  and the outdoor temperature is  $20^\circ\text{F}$ , the temperature difference is divided by the  $R$  value, resulting in  $2.63 \text{ Btu}/(\text{h} \cdot \text{ft}^2)$  in this case.

## 2.2 NEWTON'S LAW OF COOLING

---

Newton's law of cooling states that the temperature difference between a surface and the surrounding fluid (air in most cases) is directly proportional to the heat transfer rate from the surface to the fluid. This proportionality is written as:

$$q_s'' = h(T_s - T_\infty) \quad (2.41)$$

The proportionality constant is the heat transfer coefficient,  $h$ .

The heat transfer coefficient is a function of many parameters. The fluid velocity, fluid properties, and the orientation of the surface to the fluid are some of the more important parameters. The heat transfer coefficient is developed from large databases of temperature and heat transfer data. For example, one may record the heat transfer rate and the temperature difference between a solid surface and the surrounding flowing fluid. Data would be recorded over a large range of operating parameters by varying the fluid velocity and temperature, and possibly even the fluid itself. Then the data would be inspected to determine the heat transfer coefficient that maximizes the accuracy of Eq. (2.41).

The heat transfer coefficient also depends on whether the flow is forced or free. The distinction between these two modes of convection heat transfer comes from the relative magnitude of the fluid buoyant forces. In the case of room air, the air-flow creates forced convection in the vicinity of an air inlet diffuser. Near a cold window, though, the flow field is driven by the buoyant forces that are created by the temperature gradient in the air around the window. It turns out that the determination of the heat transfer coefficient is drastically different for buoyant and forced flow fields. Fortunately, this is not a new area and many correlations are available for just about every conceivable configuration used in the built environment. The rest of this section provides the methods and correlations that are necessary to calculate the heat transfer coefficient for just about any case encountered by the HVAC engineer. The end of this section includes a series of examples of typical HVAC situations.

### 2.2.1 The Reynolds, Prandtl, Grashof, and Rayleigh Numbers

The heat transfer coefficient has historically been found to be a function of two dimensionless groups: the Reynolds ( $Re$ ) and Prandtl ( $Pr$ ) numbers for forced convection, and the Grashof ( $Gr$ ) and Rayleigh ( $Ra$ ) numbers for free convection. The Reynolds number,  $Re$ , is defined as:

$$Re = \frac{\rho \bar{V} L}{\mu} \quad (2.42)$$

The velocity  $\bar{V}$  is the average velocity of the fluid over the surface, the length  $L$  is a characteristic length, and the properties  $\rho$  and  $\mu$  are the fluid density and viscosity. The characteristic length  $L$  depends on the shape and orientation of the solid and is provided as part of the correlation between the  $Re$  and the heat transfer coefficient.

The Prandtl number,  $Pr$ , is defined as:

$$Pr = \frac{c_p \mu}{k} \quad (2.43)$$

The properties  $c_p$ ,  $\mu$ , and  $k$  are the fluid specific heat, fluid dynamic viscosity, and the thermal conductivity.

The Grashof number,  $Gr$ , is defined as:

$$Gr = \frac{L^3 \rho^2 \beta g \Delta T}{\mu^2} \quad (2.44)$$

The numerator of Eq. (2.44) represents the buoyant force, and the denominator is indicative of the fluid viscous forces. The variable  $\beta$  is the fluid volume expansivity, and for ideal gases is  $1/T$ .

The Rayleigh number,  $Ra$ , is a combination of the Grashof and Prandtl numbers and is defined as:

$$Ra = Gr \times Pr = \frac{L^3 \rho \beta g \Delta T}{\mu \alpha} \quad (2.45)$$

The Rayleigh number represents the ratio between the buoyancy effects to the viscous and thermal diffusion effects.

**EXAMPLE 2.6** Calculate  $Re$ ,  $Ra$ ,  $Pr$ , and  $Gr$  of flow over a floor. Calculate the ratio between  $Ra$  and  $Gr$  (this should equal  $Pr$ ). The surface temperature is  $60^\circ F$ , and the air temperature is  $70^\circ F$ . The air velocity is  $5 \text{ ft/s}$ , and the floor is  $20 \text{ ft}^2$ .

Known:

$$T_s = 520^\circ R \quad T_{air} = 530^\circ R \quad T_b = \frac{T_s + T_{air}}{2} \quad T_b = 525^\circ R$$

Use  $T_b$  for determining properties.

$$\rho = 1.1728 \frac{\text{kg}}{\text{m}^3} \quad \mu = 18.1626 \cdot \frac{\text{N}}{\text{m}^2} \cdot \text{s}$$

$$\rho = 0.073 \cdot \frac{\text{lb}}{\text{ft}^3} \quad \mu = 1.872 \cdot 10^{-8} \frac{\text{lb}}{\text{ft} \cdot \text{s}} \quad L = 20 \text{ ft}$$

$$k = 0.025 \cdot \frac{\text{W}}{\text{m} \cdot \text{K}} \quad c_p = 1011.9 \frac{\text{J}}{\text{kg} \cdot \text{K}} \quad g = 32.174 \frac{\text{ft}}{\text{s}^2}$$

$$k = 0.181 \frac{\text{lb} \cdot \text{ft}}{\text{s}^3 \cdot \text{K}} \quad c_p = 1.089 \cdot 10^4 \frac{\text{ft}^2}{\text{s}^2 \cdot \text{K}} \quad V_i = 5 \cdot \frac{\text{ft}}{\text{s}}$$

Solution:

$$\beta = \frac{1}{T_{air}} \quad \Delta T = T_{air} - T_s \quad \alpha = \frac{k}{\rho \cdot c_p}$$

$$Re = \frac{\rho \cdot V_l \cdot L}{\mu} \qquad Gr = \frac{L^3 \cdot \rho^2 \cdot \beta \cdot g \cdot \Delta T}{\mu^2}$$

$$Ra = \frac{L^3 \cdot \rho \cdot \beta \cdot g \cdot \Delta T}{\mu \cdot \alpha} \qquad Pr = \frac{c_p \cdot \mu}{k}$$

Answers:

$$Re = 3.91 \cdot 10^8 \qquad Gr = 7.426 \cdot 10^{16}$$

$$Ra = 8.375 \cdot 10^{13} \qquad Pr = 1.128 \cdot 10^{-3}$$

$$\frac{Ra}{Gr} = 1.128 \cdot 10^{-3} \quad (\text{same as } Pr)$$

### 2.2.2 The Nusselt Number and Correlations for the Heat Transfer Coefficient

Common practice is to nondimensionalize the heat transfer coefficient. This is accomplished by defining the Nusselt number, Nu, as:

$$Nu = \frac{hL}{k} \tag{2.46}$$

Like the Reynolds number, the characteristic length  $L$  depends on the geometry and orientation of the solid surface. The thermal conductivity is that of the fluid.

Many correlations are used to calculate Nu. These correlations include the Re, Pr, Gr, and Ra. Even though these correlations depend on the geometry and orientation of the solid, they all have similar form. This Handbook will only discuss average Nusselt correlations pertinent to the HVAC industry. There are many textbooks that describe Nu in great detail, and reading them is recommended to gain a more thorough understanding of the Nusselt correlations.

As with the heat transfer coefficient, Nu varies for buoyant/free and forced flow fields. Table 2.1 will help in deciding which form of the Nusselt equation to use.

### 2.2.3 Examples Using Specific Heat Transfer Coefficients for Floors, Ceilings, and Walls

This section is devoted to the actual calculation of the heat transfer coefficient for free and forced convection to and from walls, floors, ceilings, and windows.

**EXAMPLE 2.7** *A radiantly heated 15-ft<sup>2</sup> floor is at 80°F, and the room air temperature is 70°F. Calculate the heat transfer rate by convection from the floor to the room air if the air is moving at 3 ft/s.*

Known:

$$T_s = (80 + 460)^\circ R \qquad T_{air} = (70 + 460)^\circ R \qquad T_b = \frac{T_s + T_{air}}{2} \qquad T_b = 535^\circ R$$

$$\rho = 1.15 \frac{kg}{m^3} \qquad \mu = 18.412 \cdot 10^{-6} \cdot \frac{N}{m^2} \cdot s \qquad L = 15 \text{ ft}$$

$$\rho = 0.072 \frac{lb}{ft^3} \qquad \mu = 1.237 \cdot 10^{-5} \frac{lb}{ft \cdot s} \qquad g = 32.174 \frac{ft}{s^2}$$

$$k = 0.0254 \frac{W}{m \cdot K} \qquad c_p = 1012.4 \frac{J}{kg \cdot K} \qquad V_l = 3 \cdot \frac{ft}{s}$$

**TABLE 2.1** Various Nusselt Number Correlations Appropriate to the Built Environment

Free convection		
Physical condition	Flow regime	Correlation
Over a vertical plane surface	$0 < Ra < 10^9$	$Nu = 0.68 + 0.670 Ra^{1/4} \left[ 1 + \left( \frac{0.492}{Pr} \right)^{9/16} \right]^{-4/9}$
	$10^9 < Ra$	$Nu = 0.825 + 0.387 Ra^{1/6} \left[ 1 + \left( \frac{0.429}{Pr} \right)^{9/16} \right]^{8/27}$
Around horizontal plates	$T_{\text{floor}} > T_{\text{air}}; T_{\text{ceiling}} < T_{\text{air}};$ $3.6 \times 10^4 < Ra_{Lc} < 10^7$	$Nu = 0.54 Ra^{1/4}$
	$10^7 < Ra_{Lc} < 3 \times 10^{10}$	$Nu = 0.15 Ra^{1/3}$
	$T_{\text{floor}} < T_{\text{air}}; T_{\text{ceiling}} > T_{\text{air}};$ $3 \times 10^5 < Ra_{Lc} < 10^{10}$	$Nu = 0.27 Ra^{1/4}$
Forced convection (internal)		
Fully developed laminar flow in long tubes with uniform heat flux	$Pr > 0.6$	$\bar{Nu}_D = 4.36$
Fully developed laminar flow in long tubes with uniform wall temperature	$Pr > 0.6$	$\bar{Nu}_D = 3.66$
Laminar flow in tubes and ducts of intermediate length with uniform wall temperature	$\left( \frac{Re_{D_H} Pr D_H}{L} \right)^{0.33} \left( \frac{\mu_b}{\mu_s} \right)^{0.14} > 2$ $0.004 < \left( \frac{\mu_b}{\mu_s} \right) < 10$ $0.5 < Pr < 16,000$	$\bar{Nu}_{D_H} = 1.86 \left( \frac{Re_{D_H} Pr D_H}{L} \right)^{0.33} \left( \frac{\mu_b}{\mu_s} \right)^{0.14}$
Laminar flow in short tubes and ducts with uniform wall temperature	$100 < \left( \frac{Re_{D_H} Pr D_H}{L} \right) < 1500$ $Pr > 0.7$	$\bar{Nu}_{D_H} = 3.66 + \left[ \frac{0.0668 Re_{D_H} Pr D}{L} \right] \left( \frac{\mu_b}{\mu_s} \right)^{0.14}$ $\left[ 1 + 0.045 \left( \frac{Re_{D_H} Pr D}{L} \right)^{0.66} \right]$
Fully developed turbulent flow through smooth, long tubes and ducts	$6,000 < Re_{D_H} < 10^7$ $0.7 < Pr < 10,000$ $\frac{L}{D_H} > 60$	$\bar{Nu}_{D_H} = 0.027 Re_{D_H}^{0.8} Pr^{0.33} \left( \frac{\mu_b}{\mu_s} \right)^{0.14}$
Forced convection (external)		
Uniform wall temperature	$0.5 < Pr < 10$	$Nu_L = 0.332 Re_L^{1/2} Pr^{1/3}$
Uniform wall temperature	$Pr > 10$	$Nu_L = 0.339 Re_L^{1/2} Pr^{1/3}$
Uniform heat flux	$Pr \geq 0.464$	$Nu_L = 0.450 Re_L^{1/2} Pr^{1/3}$

**NOTE:** The average of  $T_s$  and  $T_{air}$  is used to determine the properties for the calculations of the Reynolds, Prandtl, Rayleigh, and Grashof numbers, except where the subscript “s” refers to surface properties, and the subscript “b” refers to boundary properties.  $T_{film} = (T_s + T_{air})/2$ .

\* For the derivations, and a better understanding of these Nusselt number correlations, refer to the *Principles of Heat Transfer* by Kreith and Bohn, Fifth Edition.

$$k = 0.184 \frac{\text{lb} \cdot \text{ft}}{\text{s}^3} \cdot \text{K} \quad c_p = 1.09 \cdot 10^4 \frac{\text{ft}^2}{\text{s}^2 \cdot \text{K}}$$

Solution:

$$\beta = \frac{1}{T_{air}} \quad \Delta T = T_s - T_{air} \quad \alpha = \frac{k}{\rho \cdot c_p}$$

$$Re = \frac{\rho \cdot V_l \cdot L}{\mu} \quad Re = 2.611 \cdot 10^5$$

$$Gr = \frac{L^3 \cdot \rho^2 \cdot \beta \cdot g \cdot \Delta T}{\mu^2} \quad Gr = 6.898 \cdot 10^{10}$$

$$Ra = \frac{L^3 \cdot \rho \cdot \beta \cdot g \cdot \Delta T}{\mu \cdot \alpha} \quad Ra = 5.063 \cdot 10^{10}$$

$$Pr = \frac{c_p \cdot \mu}{k} \quad Pr = 0.734$$

$$Nu = 0.15 \cdot Ra^{(1/3)} \quad Nu = 554.898$$

$$h = \frac{Nu \cdot k}{L} \quad h = 6.796 \frac{\text{lb}}{\text{s}^3 \cdot \text{K}}$$

Answers:

$$q = h \cdot (T_s - T_{air})$$

$$q = 37.758 \frac{\text{lb}}{\text{s}^3} \quad q = 5.429 \frac{\text{Btu}}{\text{h} \cdot \text{ft}^2}$$

**EXAMPLE 2.8** A baseboard heating system is located 2 ft below a window. The air temperature directly surrounding the baseboard heater is 85°F. The window inside surface temperature is 40°F. Calculate the heat transfer rate from the heated air to the window surface if the air is moving at 3 ft/s.

Known:

$$T_s = (40 + 460)^\circ R \quad T_{air} = (85 + 460)^\circ R \quad T_b = \frac{T_s + T_{air}}{2} \quad T_b = 522.5^\circ R$$

$$\rho = 1.177 \frac{\text{kg}}{\text{m}^3} \quad \mu = (18.122 \cdot 10^{-6}) \frac{\text{N}}{\text{m}^2} \cdot \text{s} \quad L = 2 \text{ ft}$$

$$\rho = 0.073 \frac{\text{lb}}{\text{ft}^3} \quad \mu = 1.218 \cdot 10^{-5} \frac{\text{lb}}{\text{ft} \cdot \text{s}} \quad g = 32.174 \frac{\text{ft}}{\text{s}^2}$$

$$k = 0.0249 \frac{\text{W}}{\text{m} \cdot \text{K}} \quad c_p = 1012 \cdot \frac{\text{J}}{\text{kg} \cdot \text{K}} \quad V_l = 3 \frac{\text{ft}}{\text{s}}$$

$$k = 0.18 \frac{\text{lb} \cdot \text{ft}}{\text{s}^3 \cdot \text{K}} \quad c_p = 1.089 \cdot 10^4 \frac{\text{ft}^2}{\text{s}^2 \cdot \text{K}}$$

Solution: Recognize this as a forced convection (external) problem with uniform heat flux.

2.52

HEAT TRANSFER AND THERMODYNAMICS

$$\beta = \frac{1}{T_{air}} \quad \Delta T = T_{air} - T_s \quad \alpha = \frac{k}{\rho \cdot c_p}$$

$$Re = \frac{\rho \cdot V_l \cdot L}{\mu} \quad Re = 3.62 \cdot 10^4$$

$$Gr = \frac{L^3 \cdot \rho^2 \cdot \beta \cdot g \cdot \Delta T}{\mu^2} \quad Gr = 7.737 \cdot 10^8$$

$$Ra = \frac{L^3 \cdot \rho \cdot \beta \cdot g \cdot \Delta T}{\mu \cdot \alpha} \quad Ra = 5.699 \cdot 10^8$$

$$Pr = \frac{c_p \cdot \mu}{k} \quad Pr = 0.737$$

$$Nu = 0.450 \cdot Re^{(1/2)} \cdot Pr^{(1/3)} \quad Nu = 77.324$$

$$h = \frac{Nu \cdot k}{L} \quad h = 6.963 \frac{lb}{s^3 \cdot K}$$

Answers:

$$q = h \cdot (T_s - T_{air}) \quad q = -174.082 \frac{lb}{s^3}$$

$$q = -25.031 \frac{Btu}{h \cdot ft^2} \quad \text{Lost to the window}$$

**EXAMPLE 2.9** Repeat the foregoing example with (1) an air temperature of 90°F, which is typical of a heat pump, and (2) 120°F, which is typical of a forced-air furnace.

**Part 1:**

Known:

$$\rho = 1.15 \frac{kg}{m^3} \quad \mu = (18.8 \cdot 10^{-6}) \cdot \frac{N}{m^2} \cdot s \quad L = 2 \text{ ft}$$

$$\rho = 0.072 \frac{lb}{ft^3} \quad \mu = 1.263 \cdot 10^{-5} \frac{lb}{ft \cdot s} \quad g = 32.174 \frac{ft}{s^2}$$

$$T_s = (40 + 460)^\circ R \quad T_{air} = (90 + 460)^\circ R \quad V_l = 3 \frac{ft}{s}$$

$$k = 0.0256 \frac{W}{m \cdot K} \quad c_p = 1013 \cdot \frac{J}{kg \cdot K}$$

$$k = 0.185 \frac{lb \cdot ft}{s^3 \cdot K} \quad c_p = 1.09 \cdot 10^4 \frac{ft^2}{s^2 \cdot K}$$

Solution: *Recognize this as a forced convection (external) problem with uniform heat flux.*

$$\beta = \frac{1}{T_{air}} \quad \Delta T = T_{air} - T_s \quad \alpha = \frac{k}{\rho \cdot c_p}$$

$$Re = \frac{\rho \cdot V_1 \cdot L}{\mu} \quad Re = 3.41 \cdot 10^4$$

$$Gr = \frac{L^3 \cdot \rho^2 \cdot \beta \cdot g \cdot \Delta T}{\mu^2} \quad Gr = 7.557 \cdot 10^8$$

$$Ra = \frac{L^3 \cdot \rho \cdot \beta \cdot g \cdot \Delta T}{\mu \cdot \alpha} \quad Ra = 5.622 \cdot 10^8$$

$$Pr = \frac{c_p \cdot \mu}{k} \quad Pr = 0.744$$

$$Nu = 0.450 \cdot Re^{(1/2)} \cdot Pr^{(1/3)} \quad Nu = 75.292$$

$$h = \frac{Nu \cdot k}{L} \quad h = 6.971 \frac{lb}{s^3 \cdot K}$$

Answers:

$$q = h \cdot (T_s - T_{air}) \quad q = -193.635 \text{ lb}\lambda s^3$$

$$q = -27.842 \frac{Btu}{h \cdot ft^2} \quad \text{Lost to the window}$$

**Part 2:**

Known:

$$T_s = (40 + 460)^\circ R \quad T_{air} = (120 + 460)^\circ R \quad T_b = \frac{T_s + T_{air}}{2} \quad T_b = 540^\circ R$$

$$\rho = 1.1388 \frac{kg}{m^3} \quad \mu = (18.5491 \cdot 10^{-6}) \cdot \frac{N}{m^2} \cdot s$$

$$\rho = 0.071 \frac{lb}{ft^3} \quad \mu = 1.246 \cdot 10^{-5} \frac{lb}{ft \cdot s} \quad L = 2 \text{ ft}$$

$$k = 0.0256 \frac{W}{m \cdot K} \quad c_p = 1013 \frac{J}{kg \cdot K} \quad g = 32.174 \frac{ft}{s^2}$$

$$k = 0.185 \frac{lb \cdot ft}{s^3 \cdot K} \quad c_p = 1.09 \cdot 10^4 \frac{ft^2}{s^2 \cdot K} \quad V_1 = 3 \frac{ft}{s}$$

Solution: *Recognize this as a forced-convection (external) problem with uniform heat flux.*

$$\beta = \frac{1}{T_{air}} \quad \Delta T = T_{air} - T_s \quad \alpha = \frac{k}{\rho \cdot c_p}$$

2.54

HEAT TRANSFER AND THERMODYNAMICS

$$Re = \frac{\rho \cdot V_1 \cdot L}{\mu} \quad Re = 3.422 \cdot 10^4$$

$$Gr = \frac{L^3 \cdot \rho^2 \cdot \beta \cdot g \cdot \Delta T}{\mu^2} \quad Gr = 1.155 \cdot 10^9$$

$$Ra = \frac{L^3 \cdot \rho \cdot \beta \cdot g \cdot \Delta T}{\mu \cdot \alpha} \quad Ra = 8.475 \cdot 10^8$$

$$Pr = \frac{c_p \cdot \mu}{k} \quad Pr = 0.734$$

$$Nu = 0.450 \cdot Re^{(1/2)} \cdot Pr^{(1/3)} \quad Nu = 75.085$$

$$h = \frac{Nu \cdot k}{L} \quad h = 6.952 \frac{lb}{s^3 \cdot K}$$

Answers:

$$q = h \cdot (T_s - T_{air}) \quad q = -308.964 \frac{lb}{s^3}$$

$$q = -44.425 \frac{Btu}{h \cdot ft^2} \quad \text{Lost to the window}$$

**EXAMPLE 2.10** *The inside surface temperature of a window is 40°F. The air temperature 2 ft below is 70°F. Calculate the heat transfer rate by convection from the room air to the window if the air is moving 3 ft/s.*

Known:

$$T_s = (40 + 460)^\circ R \quad T_{air} = (70 + 460)^\circ R \quad T_b = \frac{T_s + T_{air}}{2} \quad T_b = 515^\circ R$$

$$\rho = 1.1958 \frac{kg}{m^3} \quad \mu = (17.957 \cdot 10^{-6}) \cdot \frac{N}{m^2} \cdot s$$

$$\rho = 0.075 \frac{lb}{ft^3} \quad \mu = 1.207 \cdot 10^{-5} \frac{lb}{ft \cdot s} \quad L = 2 \text{ ft}$$

$$k = 0.0246 \frac{W}{m \cdot K} \quad c_p = 1011.6 \frac{J}{kg \cdot K} \quad g = 32.174 \frac{ft}{s^2}$$

$$k = 0.178 \frac{lb \cdot ft}{s^3 \cdot K} \quad c_p = 1.09 \cdot 10^4 \frac{ft^2}{s^2 \cdot K} \quad V_1 = 3 \frac{ft}{s}$$

**Solution:** *Recognize this as a forced-convection (external) problem with uniform heat flux.*

$$\beta = \frac{1}{T_{air}} \quad \Delta T = T_{air} - T_s \quad \alpha = \frac{k}{\rho \cdot c_p}$$

$$Re = \frac{\rho \cdot V_1 \cdot L}{\mu} \quad Re = 3.712 \cdot 10^4$$

$$Gr = \frac{L^3 \cdot \rho^2 \cdot \beta \cdot g \cdot \Delta T}{\mu^2} \quad Gr = 5.576 \cdot 10^8$$

$$Ra = \frac{L^3 \cdot \rho \cdot \beta \cdot g \cdot \Delta T}{\mu \cdot \alpha} \quad Ra = 4.118 \cdot 10^8$$

$$Pr = \frac{c_p \cdot \mu}{k} \quad Pr = 0.738$$

$$Nu = 0.450 \cdot Re^{(1/2)} \cdot Pr^{(1/3)} \quad Nu = 78.364$$

$$h = \frac{Nu \cdot k}{L} \quad h = 6.972 \frac{lb}{s^3 \cdot K}$$

Answers:

$$q = h \cdot (T_s - T_{air}) \quad q = -116.198 \frac{lb}{s^3}$$

$$q = -16.708 \frac{Btu}{h \cdot ft^2} \quad \text{Lost to the window}$$



---

## CHAPTER 3

---

# RADIATION HEAT TRANSFER

---

Radiation heat transfer is the subject of many complete books. The goal of this chapter is to provide a working foundation that can then be used to analyze the thermal comfort delivery characteristics of radiant heating and cooling systems. One must realize, though, that even the walls and windows affect the radiation field in the built environment. It is not enough to analyze the radiant heating or cooling system without also analyzing all the surfaces in the room. To accomplish this complete analysis, one should look at the entire radiation spectrum. All radiation acts the same, with the only distinguishing feature being the frequency or wavelength.

For the purposes of this Handbook, radiation will be viewed as rays of intensity traveling through the medium (usually air). When the medium is nonparticipating, the radiation intensity propagates through the medium at the speed of light ( $c = 9.83517 \times 10^8$  ft/s). The term *nonparticipating* means that the medium does not affect the beam of radiant intensity. The strength of a radiant intensity beam traveling through a nonparticipating medium like air does not increase or decrease. In most cases, the mediums within the built environment are nonparticipating. The only exception is when the air has a high moisture content. This exception is minor in most cases, but it will be explored later in this chapter.

Figure 3.1 shows how every surface emits intensity beams in all directions. Only when the intensity beams intercept a solid object (or participating medium) does the intensity convert to thermal energy. In Fig. 3.1, the person standing in the middle of the room intercepts intensity beams from every direction. Consideration of all of these intensity beams is necessary to determine the *incident* radiation on the person. Later in this chapter, we will investigate how much of this radiation the person actually “feels.”

For now, it is important for the reader to understand that when surfaces enclose a nonparticipating medium, radiation heat transfer is fundamentally a process in which intensity beams are created by the surfaces through a mechanism called *emission*. These beams propagate through the medium until they are intercepted by another surface. At that point, the beams are either absorbed or reflected by the intercepting surface. The beams that are absorbed are converted into thermal energy. The goal of this chapter is to develop an understanding of how these beams propagate and what properties control emission, absorption, reflection, and propagation of these beams.

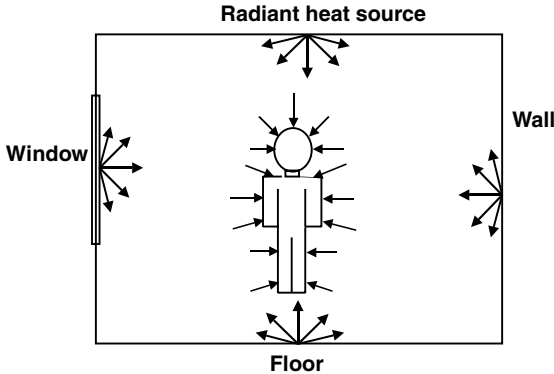


FIGURE 3.1 Radiation intensity field.

**3.1 WAVELENGTHS, MICRONS, AND THE ELECTROMAGNETIC SPECTRUM**

Radiation in its broadest sense includes energy transmission at all wavelengths. Only a small fraction of these wavelengths are thermal radiation. Other radiation wavelengths include x-rays and radio waves. Although these are important in some fields of study, they do not contribute to thermal radiation.

Figure 3.2 illustrates the part of the radiation spectrum that includes thermal radiation. The wavelengths are measured in microns ( $\mu\text{m}$ ). There are a million microns in a meter, or  $1 \mu\text{m} = 10^{-6} \text{ m}$ . The thermal energy range exists between 0.1 and  $100 \mu\text{m}$ . The shorter-wavelength radiation beams carry more energy and can partially travel through a solid. This is how x-rays can take a picture of something inside a structure. The x-rays are short enough to pass through a person’s skin but not short enough to pass through bones. Beams in the thermal radiation region are generally long enough so that the entire radiation interaction is at the surface of the solid. Windows are an exception that will be discussed later.

The visible part of the radiation spectrum lies in the range between 0.4 and  $0.7 \mu\text{m}$ . Coincidentally, this is the range within which the sun emits maximum radiation. Note that although many people think of radiation as light, we can only see a small portion of the thermal radiation spectrum.

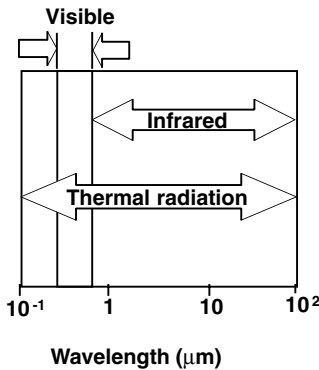


FIGURE 3.2 Radiation spectrum.

**3.2 RADIATIVE PROPAGATION AND INTENSITY—THE BASIC BUILDING BLOCK OF RADIATIVE HEAT TRANSFER**

The intensity,  $I$ , is defined as the amount of radiant flux per steradian of solid angle per unit of projected area in the direction of propagation. This definition is best understood by referring to Fig. 3.3,

which shows a small surface area that is emitting radiation in a specific direction at a specific wavelength. The unit normal from the surface is designated as  $\hat{n}$ . The direction of the intensity is measured from the unit normal and from the  $x$  axis. The angle from the unit normal is called the *zenith angle* and is designated by the variable  $\theta$ . The angle from the  $x$  axis is called the *azimuth angle* and is designated by the parameter  $\phi$ . The wavelength about which the intensity is propagating is designated by the variable  $\lambda$ . The location of the center of the small surface area is at a position relative to some arbitrary origin (e.g., the corner of a room or the center of the earth) and is designated by the vector  $\mathbf{r}$ . From these variables, the intensity can then be defined as a function of direction, wavelength, and position:  $I_\lambda(\mathbf{r},\theta,\phi)$ .

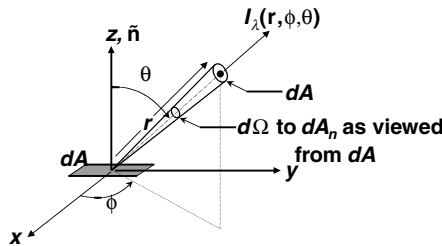


FIGURE 3.3 Definition of radiation intensity.

The solid angle can be thought of as a cone that is viewed from the center of the small area in Fig. 3.3. The small solid angle  $d\Omega$  is said to *subtend* a surface in the direction of intensity propagation. In this case, that area is the normal area  $dA_n$ . By definition, the solid angle is defined in terms of the subtended angle and the distance between the two surfaces:

$$d\Omega = \frac{dA_n}{r^2} \tag{3.1}$$

The solid angle is analogous to a planar angle. The difference is that although the planar angle is defined as the arc length over the radius, a solid angle is defined as the surface area over the square of the radius. The solid angle is measured in units of steradians (sr) just as a planar angle is measured in terms of radians (rad).

Figure 3.4 defines the solid angle in terms of the zenith and azimuth angles. The subtended surface  $dA_n$  exists on the surface of a sphere with a radius  $r$ . In the figure,

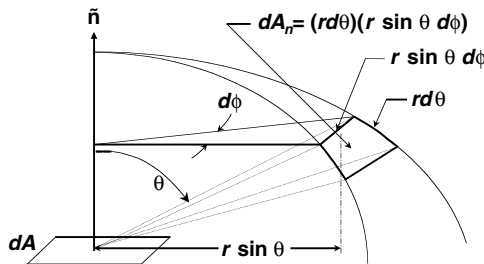


FIGURE 3.4 Definition of solid angle.

only enough of the sphere is shown to carve out the area  $dA_n$ . Because the area is small, it can be approximated as a rectangle. By using geometric relationships, the area is defined in equation form as:

$$dA_n = (r d\theta)(r \sin \theta d\phi) = r^2 \sin \theta d\theta d\phi \quad (3.2)$$

The differential solid angle then becomes:

$$d\Omega = \frac{r^2 \sin \theta d\theta d\phi}{r^2} = \sin \theta d\theta d\phi \quad (3.3)$$

**EXAMPLE 3.1** Calculate the solid angle for a hemisphere and a sphere.

By referring to Fig. 3.4, a hemisphere can be created by moving the surface  $dA_n$  around so that a bubble is traced. This is comparable to letting  $\theta$  sweep from  $0^\circ$  to  $90^\circ$  ( $0$  to  $\pi/2$  rad), and letting  $\phi$  sweep from  $0^\circ$  to  $360^\circ$  ( $0$  to  $2\pi$  rad). In mathematical terms, the solid angle is integrated over these angular limits:

$$\begin{aligned} \Omega_h &= \int_0^{2\pi} \int_0^{\pi/2} d\Omega = \int_0^{2\pi} \int_0^{\pi/2} \sin \theta d\theta d\phi \\ &= (2\pi - 0) \int_0^{\pi/2} \sin \theta d\theta \\ &= -2\pi [\cos \theta]_0^{\pi/2} \\ &= -2\pi [\cos (\pi/2) - \cos (0)] \\ &= -2\pi [0 - 1] \\ &= 2\pi \end{aligned}$$

To find the solid angle for an entire sphere, the “sweep” limits on  $\theta$  are extended to  $180^\circ$ :

$$\begin{aligned} \Omega_s &= \int_0^{2\pi} \int_0^\pi d\Omega = \int_0^{2\pi} \int_0^\pi \sin \theta d\theta d\phi \\ &= (2\pi - 0) \int_0^\pi \sin \theta d\theta \\ &= -2\pi [\cos \theta]_0^\pi \\ &= -2\pi [\cos (\pi) - \cos (0)] \\ &= -2\pi [(-1) - 1] \\ &= 4\pi \end{aligned}$$

The solid angle will take on significance later in this chapter during the discussion of the radiant heat flux absorbed and/or emitted by a surface. It will also become important in Sec. 3 during the discussion of the mean radiant temperature.

**EXAMPLE 3.2** A window in a room intercepts the radiation intensity leaving a small ceiling panel. Assume each surface can be treated “small.” The area of the panel is  $1 \text{ ft}^2$ ,

and the area of the window is  $3 \text{ ft}^2$ . The distance from the center of the panel to the center of the window is  $14 \text{ ft}$ . The angle from the unit normal of the panel to the center of the window is  $40^\circ$ . Calculate the solid angle subtended by the window as seen from the radiant panel. Show how the solid angle changes as the window is repositioned at different heights along the wall.

Figure 3.5 shows the configuration. Because each surface can be treated as small, the solid angle subtended by the window as seen from the panel can be approximated by:

$$\Omega_{p-w} = \frac{dA_{n,w}}{r^2}$$

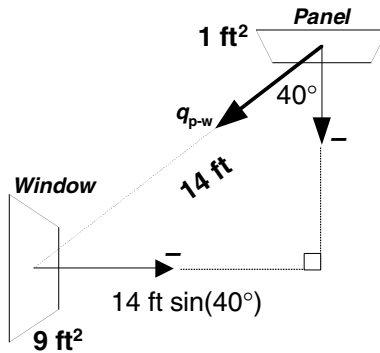


FIGURE 3.5 Configuration for Example 3.2.

The projected area of the window normal to the line drawn from the center of the panel to the center of the window is calculated by (refer to Fig. 3.6):

$$\begin{aligned} dA_{n,w} &= A_w \times \cos(\pi/2 - \theta) \\ &= 9 \text{ ft}^2 \cos(90^\circ - 40^\circ) \\ &= 51.4 \text{ ft}^2 \end{aligned}$$

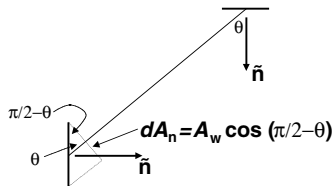


FIGURE 3.6 Geometry for Example 3.2.

The solid angle is then:

$$\Omega_{p-w} = \frac{51.4 \text{ ft}^2}{(14 \text{ ft})^2} = 0.262 \text{ sr}$$

The next question is how does this solid angle change as the window is vertically repositioned along the wall. By referring to Fig. 3.5, the horizontal distance from the window to the center of the panel remains constant at  $14 \text{ ft} \times \sin(40^\circ) = 9.0 \text{ ft}$ . Changing the angle  $\theta$  changes the distance  $r$  in the following fashion:

$$r = \frac{9.0 \text{ ft}}{\sin(\theta)}$$

Substituting into the solid-angle equation:

$$\Omega_{p-w} = \frac{A_w \cos(90^\circ - \theta)}{(9 \text{ ft})^2} \sin^2(\theta)$$

Figure 3.7 illustrates the variation in the projected normal surface area as well as the solid angle with  $\theta$ . Of interest is the variation in the solid angle. Because the solid angle represents the cone by which radiation will pass from the panel to the window, the figure shows that there is a region where the window should be placed to minimize the solid angle. For  $\theta < 20^\circ$ , the solid angle is small. As  $\theta$  increases above  $20^\circ$ , the solid angle increases by several factors. This example shows that the window-versus-panel positioning can play an important role in optimizing panel efficiency.

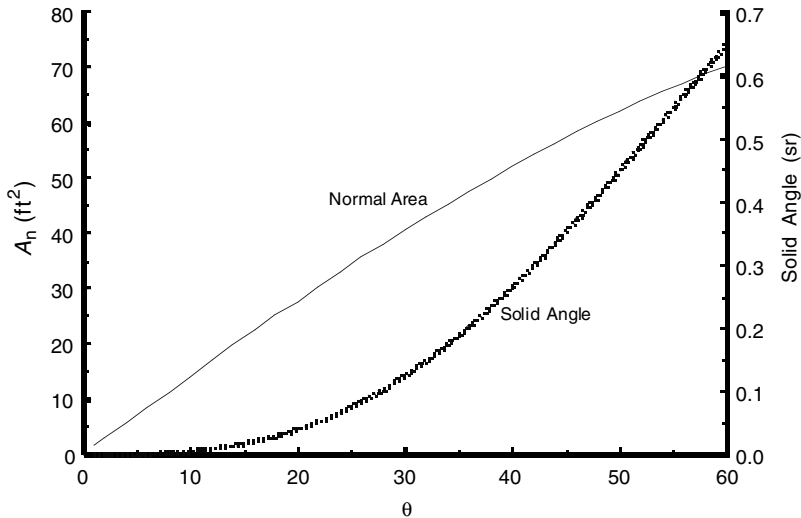


FIGURE 3.7 Variation in  $A_n$  and  $\Omega_{p-w}$  with  $\theta$ .

Now that the solid angle has been defined, we return to the definition of the radiation intensity: the amount of radiant flux per steradian of solid angle per unit of projected area in the direction of propagation per wavelength about  $\lambda$ . Figure 3.8 illustrates the relationship between the radiant energy, the projected area in the direction of propagation, and the solid angle. The radiant heat transfer rate  $Q_r$  is shown leaving the small area  $dA$  and propagating in a direction  $\theta$ . The projected area

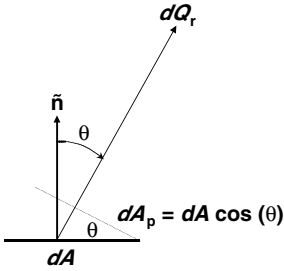


FIGURE 3.8 Radiant energy.

in the direction of propagation is  $dA_p$ . At some point in space, the radiation is intercepted by some other solid small area that is subtended by the solid angle. The unit normal vector for the surface  $dA$  is shown as the arrow pointing up. Directions are measured relative to the unit normal. In this case, the angle between the unit normal and the direction of propagation is denoted by the zenith angle  $\theta$ . As before, the azimuth angle  $\phi$  sweeps around the unit normal. The origin ( $\phi = 0$  rad) is arbitrary but is usually measured from the  $x$  axis.

By definition, the intensity propagating through the medium in the direction  $\theta$  is:

$$I_\lambda(\theta, \phi, r) = \frac{\text{Radiation heat transfer rate}}{(\text{Unit projected area})(\text{Unit solid angle})(\text{Unit wavelength})}$$

$$= \frac{Q_r}{dA_p d\Omega d\lambda} \tag{3.4}$$

The projected area is defined as:

$$dA_p = dA \times \cos \theta \tag{3.5}$$

Substituting the definition of the solid angle as well as the projected area in the direction of propagation results in:

$$q_r = I_\lambda(\theta, \phi, r) \cos \theta \sin \theta \, d\theta d\phi \tag{3.6}$$

The total radiant heat flux from a surface can now be calculated by integrating over the hemisphere, as shown in the following example. If the intensity is equal in all directions, then the surface is said to be diffuse.

**EXAMPLE 3.3** *A window in a room intercepts the radiation intensity leaving a small ceiling panel. Assume that each surface can be treated as “small.” The area of the panel is 1 ft<sup>2</sup> and the area of the window is 3 ft<sup>2</sup>. The radiant energy leaving the panel is 100 W and is equal in all directions. The distance from the center of the panel to the center of the window is 14 ft. The angle from the unit normal of the panel to the center of the window is 40°. Calculate the radiant energy that leaves the panel and is intercepted by the window.*

*Because the radiant energy leaving the panel is equal in all directions, the radiation intensity leaving the panel is calculated from the intensity definition:*

$$\dot{Q}_{\text{panel}} = A_{\text{panel}} \int_0^{2\pi} \int_0^{\pi/2} I(\theta, \phi) \cos \theta \sin \theta \, d\theta d\phi$$

$$= A_{\text{panel}} I_{\text{panel}} \int_0^{2\pi} \int_0^{\pi/2} \cos \theta \sin \theta \, d\theta d\phi$$

$$\begin{aligned}
 &= A_{panel} I_{panel} 2\pi \int_0^{\pi/2} \cos \theta \sin \theta \, d\theta \\
 &= A_{panel} I_{panel} \pi
 \end{aligned}$$

The radiant intensity leaving the panel is calculated by rearranging the foregoing relationship:

$$\begin{aligned}
 I_{panel} &= \frac{\dot{Q}_{panel}}{\pi A_{panel}} \\
 &= \frac{100 \text{ W}}{\pi (1 \text{ ft}^2)} \\
 &= \frac{31.83 \text{ W}}{\text{sr} \cdot \text{ft}^2}
 \end{aligned}$$

An alternative definition for the intensity is used that is valid only for small areas:

$$I = \frac{d\dot{Q}_r}{dA_p d\Omega} \approx \frac{\dot{Q}_{p-w} \times r^2}{A_{panel} \cos(\theta_{panel}) A_{window} \cos(\theta_{window})}$$

This definition is tailored for this example, but it basically defines the radiant intensity as the radiant energy that leaves the panel through an area projected in the direction of propagation that then passes through a second area perpendicular to the direction of propagation (the projected area of the window). Note, though, that this definition is compatible with the exact intensity definition only for small areas.

The heat that is transferred from the panel to the window is now calculated by rearranging the foregoing equation:

$$\begin{aligned}
 \dot{Q}_{p-w} &= \frac{I_{panel} A_{panel} A_{window} \cos(\theta_{panel}) \cos(\theta_{window})}{r^2} \\
 &= \frac{31.83 \text{ W}}{\text{ft}^2} (81 \text{ ft}^2 \times 1 \text{ ft}^2) \cos(40^\circ) \cos(50^\circ) \frac{1}{(14 \text{ ft})^2} \\
 &= 6.47 \text{ W}
 \end{aligned}$$

Consequently, only 6.47 percent of the radiant energy leaving the panel is intercepted by the window.

### 3.3 EMISSION AND RADIATION LAWS

Radiative emissive power of a surface is denoted by the symbol  $E$ . The maximum emissive power that can be emitted from any surface is called the *blackbody* emission ( $E_b$ ). The blackbody emission from any surface is calculated using the Stefan-Boltzmann constant:

$$E_b = \left[ \frac{0.1714 \times 10^{-8} \text{ Btu}}{\text{h} \cdot \text{ft}^2 \cdot ^\circ\text{R}^4} \right] T^4 \tag{3.7}$$

Stefan-Boltzmann  
 constant,  $\sigma$

The Stefan-Boltzmann constant  $\sigma$  is derived from fundamental concepts. The temperature must be in units of  $^{\circ}\text{R}$ , not  $^{\circ}\text{F}$ .

### 3.3.1 Planck's Law

The emissive power also varies with wavelength. The spectral emissive power is denoted by the variable  $E_{b\lambda}$ , and is calculated from Planck's law (Planck, 1959):

$$E_{b\lambda} = \frac{c_1 \lambda^{-5}}{\exp(c_2/\lambda T) - 1} \quad (3.8)$$

The constants  $c_1$  and  $c_2$  are  $1.1870 \times 10^8 \text{ Btu}/(\mu\text{m}^4 \cdot \text{hr} \cdot \text{ft}^2)$  and  $2.5896 \times 10^4 \mu\text{m} \cdot ^{\circ}\text{R}$ , respectively. Figure 3.9 demonstrates how the emissive power from a blackbody varies with temperature and with wavelength.

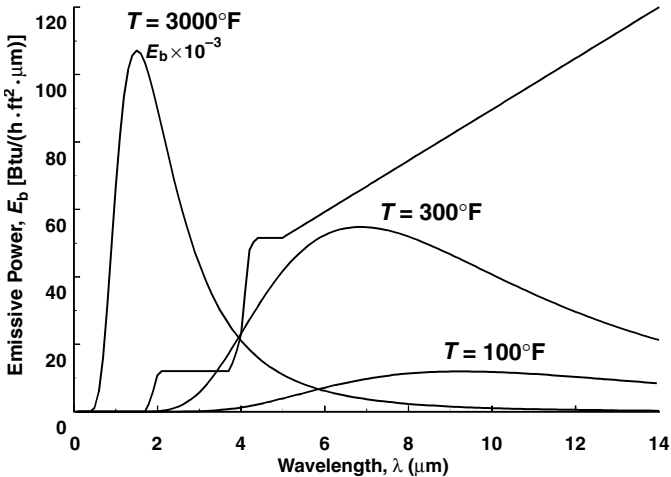


FIGURE 3.9 Emissive power from a blackbody.

### 3.3.2 Wien's Displacement Law

Wien's displacement law provides the relationship between the maximum emissive power of a blackbody at a specific temperature and the wavelength at which the maximum occurs. This relationship is:

$$\lambda_{\max} T = 5215.6 \mu\text{m} \cdot ^{\circ}\text{R} \quad (3.9)$$

For example, if the sun is approximated as a blackbody at  $8500^{\circ}\text{R}$  ( $4722.2 \text{ K}$ ), then the wavelength where the sun's emissive power is a maximum is  $\lambda_{\max} = 5215.6 \mu\text{m} \cdot ^{\circ}\text{R}/8500^{\circ}\text{R} = 0.61 \mu\text{m}$ .

### 3.3.3 Blackbody Fractions

Blackbody fractions are used to determine the magnitude of the emissive power over a specific wavelength band. The prime application for these functions is the determination of how much radiation passes through window glass from a source at a specific temperature. Window glass is transparent between the wavelengths of 0 and about 4  $\mu\text{m}$ . Above 4  $\mu\text{m}$ , window glass is opaque to radiation. In other words, above 4  $\mu\text{m}$  the window may as well be a solid wall as far as radiation heat transfer is concerned.

At this point, we have investigated how the emissive power varies as a function of wavelength and the source temperature. Figure 3.9 illustrates this variation. Figure 3.10 shows a window that has the sun on the outside and a radiant heating panel on the inside. The sun is approximated as a blackbody at about 8500°R (4722.2 K). The radiant panel is approximated as a blackbody at 300°F (760°R or 422.2 K).

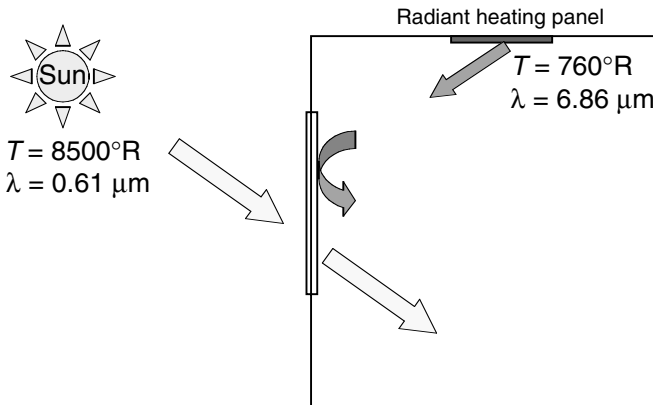


**FIGURE 3.10** Impact of solar heat gain through a window.

Equation (3.9) shows that the wavelength where the emissive power is maximum for each radiant source is 0.61  $\mu\text{m}$  for the sun and 6.86  $\mu\text{m}$  for the radiant panel. This suggests the idea that most of the sun's emissive power passes through the window (0.61  $\mu\text{m}$  < 4  $\mu\text{m}$ ) and that the window will block the energy from the radiant panel (6.86  $\mu\text{m}$  > 4  $\mu\text{m}$ ). The blackbody fractions give us a way to verify this suspicion.

The blackbody fractions are defined as:

$$F_{0-\lambda T} = \frac{1}{\sigma T^4} \int_0^{\lambda} E_{b\lambda}(T) d\lambda \quad (3.10)$$

The fraction  $F$  represents the total emissive power from a source at a specific temperature that is emitted between the wavelengths of 0  $\mu\text{m}$  and  $\lambda$ . Unfortunately, the integral is very difficult to evaluate. Fortunately, there are ways to analyze it, and the results of those methods are presented in Table 3.1. The values in Table 3.1 were generated from the following series approximation (Chang and Rhee, 1984):

$$F_{0-\lambda T} = \frac{15}{\pi^4} \sum_{n=1}^{\infty} \left[ \frac{e^{-n\zeta}}{n} \left( \zeta^3 + \frac{3\zeta^2}{n} + \frac{6\zeta}{n^2} + \frac{6}{n^3} \right) \right], \quad \zeta = \frac{c_2}{\lambda T} \quad (3.11)$$

Equation (3.11) is presented here because it is convenient to use in computer calculations.

**TABLE 3.1** Blackbody Fractions Created by Using Eq. (3.11)

Wavelength · temperature (λT)			Wavelength · temperature (λT)		
μm · K	μm · °R	Blackbody fraction	μm · K	μm · °R	Blackbody fraction
500	900	1.30E-09	2,600	4,680	0.18312
550	990	1.35E-08	2,650	4,770	0.19419
600	1,080	9.29E-08	2,700	4,860	0.20536
650	1,170	4.67E-07	2,750	4,950	0.2166
700	1,260	1.84E-06	2,800	5,040	0.22789
750	1,350	5.95E-06	2,850	5,130	0.23922
800	1,440	1.64E-05	2,900	5,220	0.25056
850	1,530	3.99E-05	2,950	5,310	0.26191
900	1,620	8.70E-05	3,000	5,400	0.27323
950	1,710	0.00017	3,050	5,490	0.28453
1,000	1,800	0.00032	3,100	5,580	0.29578
1,050	1,890	0.00056	3,150	5,670	0.30697
1,100	1,980	0.00091	3,200	5,760	0.3181
1,150	2,070	0.00142	3,250	5,850	0.32915
1,200	2,160	0.00213	3,300	5,940	0.34011
1,250	2,250	0.00308	3,350	6,030	0.35097
1,300	2,340	0.00432	3,400	6,120	0.36173
1,350	2,430	0.00587	3,450	6,210	0.37238
1,400	2,520	0.00779	3,500	6,300	0.38291
1,450	2,610	0.01011	3,550	6,390	0.39332
1,500	2,700	0.01285	3,600	6,480	0.4036
1,550	2,790	0.01605	3,650	6,570	0.41375
1,600	2,880	0.01972	3,700	6,660	0.42377
1,650	2,970	0.02388	3,750	6,750	0.43364
1,700	3,060	0.02854	3,800	6,840	0.44338
1,750	3,150	0.03369	3,850	6,930	0.45297
1,800	3,240	0.03934	3,900	7,020	0.46241
1,850	3,330	0.04549	3,950	7,110	0.47172
1,900	3,420	0.05211	4,000	7,200	0.48087
1,950	3,510	0.0592	4,050	7,290	0.48987
2,000	3,600	0.06673	4,100	7,380	0.49873
2,050	3,690	0.07469	4,150	7,470	0.50744
2,100	3,780	0.08306	4,200	7,560	0.516
2,150	3,870	0.0918	4,250	7,650	0.52442
2,200	3,960	0.10089	4,300	7,740	0.53269
2,250	4,050	0.11031	4,350	7,830	0.54081
2,300	4,140	0.12003	4,400	7,920	0.54878
2,350	4,230	0.13002	4,450	8,010	0.55662
2,400	4,320	0.14026	4,500	8,100	0.56431
2,450	4,410	0.15071	4,550	8,190	0.57186
2,500	4,500	0.16136	4,600	8,280	0.57927
2,550	4,590	0.17217	4,650	8,370	0.58654

**TABLE 3.1** Blackbody Fractions Created by Using Eq. (3.11) (Continued)

Wavelength · temperature ( $\lambda T$ )			Wavelength · temperature ( $\lambda T$ )		
$\mu\text{m} \cdot \text{K}$	$\mu\text{m} \cdot ^\circ\text{R}$	Blackbody fraction	$\mu\text{m} \cdot \text{K}$	$\mu\text{m} \cdot ^\circ\text{R}$	Blackbody fraction
4,700	8,460	0.59367	7,200	12,960	0.81918
4,750	8,550	0.60067	7,250	13,050	0.82183
4,800	8,640	0.60754	7,300	13,140	0.82443
4,850	8,730	0.61428	7,350	13,230	0.82699
4,900	8,820	0.62089	7,400	13,320	0.82949
4,950	8,910	0.62737	7,450	13,410	0.83195
5,000	9,000	0.63373	7,500	13,500	0.83437
5,050	9,090	0.63996	7,550	13,590	0.83674
5,100	9,180	0.64608	7,600	13,680	0.83907
5,150	9,270	0.65207	7,650	13,770	0.84135
5,200	9,360	0.65795	7,700	13,860	0.8436
5,250	9,450	0.66371	7,750	13,950	0.8458
5,300	9,540	0.66937	7,800	14,040	0.84797
5,350	9,630	0.67491	7,850	14,130	0.8501
5,400	9,720	0.68034	7,900	14,220	0.85219
5,450	9,810	0.68566	7,950	14,310	0.85424
5,500	9,900	0.69089	8,000	14,400	0.85625
5,550	9,990	0.696	8,050	14,490	0.85823
5,600	10,080	0.70102	8,100	14,580	0.86018
5,650	10,170	0.70594	8,150	14,670	0.86209
5,700	10,260	0.71077	8,200	14,760	0.86397
5,750	10,350	0.7155	8,250	14,850	0.86581
5,800	10,440	0.72013	8,300	14,940	0.86762
5,850	10,530	0.72468	8,350	15,030	0.86941
5,900	10,620	0.72914	8,400	15,120	0.87116
5,950	10,710	0.73351	8,450	15,210	0.87288
6,000	10,800	0.73779	8,500	15,300	0.87457
6,050	10,890	0.74199	8,550	15,390	0.87623
6,100	10,980	0.74611	8,600	15,480	0.87787
6,150	11,070	0.75015	8,650	15,570	0.87947
6,200	11,160	0.75411	8,700	15,660	0.88105
6,250	11,250	0.758	8,750	15,750	0.88261
6,300	11,340	0.76181	8,800	15,840	0.88413
6,350	11,430	0.76554	8,850	15,930	0.88563
6,400	11,520	0.76921	8,900	16,020	0.88711
6,450	11,610	0.7728	8,950	16,110	0.88856
6,500	11,700	0.77632	9,000	16,200	0.88999
6,550	11,790	0.77978	9,050	16,290	0.89139
6,600	11,880	0.78317	9,100	16,380	0.89278
6,650	11,970	0.7865	9,150	16,470	0.89413
6,700	12,060	0.78976	9,200	16,560	0.89547
6,750	12,150	0.79296	9,250	16,650	0.89679
6,800	12,240	0.7961	9,300	16,740	0.89808
6,850	12,330	0.79918	9,350	16,830	0.89935
6,900	12,420	0.8022	9,400	16,920	0.9006
6,950	12,510	0.80517	9,450	17,010	0.90183
7,000	12,600	0.80808	9,500	17,100	0.90305
7,050	12,690	0.81093	9,550	17,190	0.90424
7,100	12,780	0.81374	9,600	17,280	0.90541
7,150	12,870	0.81649	9,650	17,370	0.90657

**TABLE 3.1** Blackbody Fractions Created by Using Eq. (3.11) (Continued)

Wavelength · temperature ( $\lambda T$ )			Wavelength · temperature ( $\lambda T$ )		
$\mu\text{m} \cdot \text{K}$	$\mu\text{m} \cdot ^\circ\text{R}$	Blackbody fraction	$\mu\text{m} \cdot \text{K}$	$\mu\text{m} \cdot ^\circ\text{R}$	Blackbody fraction
9,700	17,460	0.9077	12,200	21,960	0.94728
9,750	17,550	0.90882	12,250	22,050	0.94782
9,800	17,640	0.90992	12,300	22,140	0.94835
9,850	17,730	0.91101	12,350	22,230	0.94888
9,900	17,820	0.91207	12,400	22,320	0.94939
9,950	17,910	0.91312	12,450	22,410	0.9499
10,000	18,000	0.91416	12,500	22,500	0.95041
10,050	18,090	0.91518	12,550	22,590	0.9509
10,100	18,180	0.91618	12,600	22,680	0.95139
10,150	18,270	0.91717	12,650	22,770	0.95188
10,200	18,360	0.91814	12,700	22,860	0.95236
10,250	18,450	0.91909	12,750	22,950	0.95283
10,300	18,540	0.92004	12,800	23,040	0.95329
10,350	18,630	0.92097	12,850	23,130	0.95375
10,400	18,720	0.92188	12,900	23,220	0.9542
10,450	18,810	0.92278	12,950	23,310	0.95465
10,500	18,900	0.92367	13,000	23,400	0.95509
10,550	18,990	0.92454	13,050	23,490	0.95553
10,600	19,080	0.9254	13,100	23,580	0.95596
10,650	19,170	0.92625	13,150	23,670	0.95639
10,700	19,260	0.92709	13,200	23,760	0.95681
10,750	19,350	0.92791	13,250	23,850	0.95722
10,800	19,440	0.92872	13,300	23,940	0.95763
10,850	19,530	0.92952	13,350	24,030	0.95803
10,900	19,620	0.93031	13,400	24,120	0.95843
10,950	19,710	0.93108	13,450	24,210	0.95883
11,000	19,800	0.93185	13,500	24,300	0.95921
11,050	19,890	0.9326	13,550	24,390	0.9596
11,100	19,980	0.93334	13,600	24,480	0.95998
11,150	20,070	0.93408	13,650	24,570	0.96035
11,200	20,160	0.9348	13,700	24,660	0.96072
11,250	20,250	0.93551	13,750	24,750	0.96109
11,300	20,340	0.93621	13,800	24,840	0.96145
11,350	20,430	0.9369	13,850	24,930	0.96181
11,400	20,520	0.93758	13,900	25,020	0.96216
11,450	20,610	0.93825	13,950	25,110	0.96251
11,500	20,700	0.93892	14,000	25,200	0.96285
11,550	20,790	0.93957	14,050	25,290	0.96319
11,600	20,880	0.94021	14,100	25,380	0.96353
11,650	20,970	0.94085	14,150	25,470	0.96386
11,700	21,060	0.94147	14,200	25,560	0.96419
11,750	21,150	0.94209	14,250	25,650	0.96451
11,800	21,240	0.9427	14,300	25,740	0.96483
11,850	21,330	0.9433	14,350	25,830	0.96515
11,900	21,420	0.94389	14,400	25,920	0.96546
11,950	21,510	0.94448	14,450	26,010	0.96577
12,000	21,600	0.94505	14,500	26,100	0.96607
12,050	21,690	0.94562	14,550	26,190	0.96637
12,100	21,780	0.94618	14,600	26,280	0.96667
12,150	21,870	0.94674	14,650	26,370	0.96697

**TABLE 3.1** Blackbody Fractions Created by Using Eq. (3.11) (Continued)

Wavelength · temperature ( $\lambda T$ )			Wavelength · temperature ( $\lambda T$ )		
$\mu\text{m} \cdot \text{K}$	$\mu\text{m} \cdot ^\circ\text{R}$	Blackbody fraction	$\mu\text{m} \cdot \text{K}$	$\mu\text{m} \cdot ^\circ\text{R}$	Blackbody fraction
14,700	26,460	0.96726	17,200	30,960	0.97834
14,750	26,550	0.96754	17,250	31,050	0.9785
14,800	26,640	0.96783	17,300	31,140	0.97867
14,850	26,730	0.96811	17,350	31,230	0.97883
14,900	26,820	0.96839	17,400	31,320	0.97899
14,950	26,910	0.96866	17,450	31,410	0.97915
15,000	27,000	0.96893	17,500	31,500	0.97931
15,050	27,090	0.9692	17,550	31,590	0.97947
15,100	27,180	0.96947	17,600	31,680	0.97962
15,150	27,270	0.96973	17,650	31,770	0.97978
15,200	27,360	0.96999	17,700	31,860	0.97993
15,250	27,450	0.97025	17,750	31,950	0.98008
15,300	27,540	0.9705	17,800	32,040	0.98023
15,350	27,630	0.97075	17,850	32,130	0.98038
15,400	27,720	0.971	17,900	32,220	0.98052
15,450	27,810	0.97124	17,950	32,310	0.98067
15,500	27,900	0.97149	18,000	32,400	0.98081
15,550	27,990	0.97172	18,050	32,490	0.98095
15,600	28,080	0.97196	18,100	32,580	0.98109
15,650	28,170	0.9722	18,150	32,670	0.98123
15,700	28,260	0.97243	18,200	32,760	0.98137
15,750	28,350	0.97266	18,250	32,850	0.98151
15,800	28,440	0.97288	18,300	32,940	0.98164
15,850	28,530	0.97311	18,350	33,030	0.98177
15,900	28,620	0.97333	18,400	33,120	0.98191
15,950	28,710	0.97355	18,450	33,210	0.98204
16,000	28,800	0.97377	18,500	33,300	0.98217
16,050	28,890	0.97398	18,550	33,390	0.9823
16,100	28,980	0.97419	18,600	33,480	0.98242
16,150	29,070	0.9744	18,650	33,570	0.98255
16,200	29,160	0.97461	18,700	33,660	0.98268
16,250	29,250	0.97482	18,750	33,750	0.9828
16,300	29,340	0.97502	18,800	33,840	0.98292
16,350	29,430	0.97522	18,850	33,930	0.98304
16,400	29,520	0.97542	18,900	34,020	0.98316
16,450	29,610	0.97562	18,950	34,110	0.98328
16,500	29,700	0.97581	19,000	34,200	0.9834
16,550	29,790	0.97601	19,050	34,290	0.98352
16,600	29,880	0.9762	19,100	34,380	0.98364
16,650	29,970	0.97638	19,150	34,470	0.98375
16,700	30,060	0.97657	19,200	34,560	0.98386
16,750	30,150	0.97676	19,250	34,650	0.98398
16,800	30,240	0.97694	19,300	34,740	0.98409
16,850	30,330	0.97712	19,350	34,830	0.9842
16,900	30,420	0.9773	19,400	34,920	0.98431
16,950	30,510	0.97748	19,450	35,010	0.98442
17,000	30,600	0.97765	19,500	35,100	0.98453
17,050	30,690	0.97783	19,550	35,190	0.98463
17,100	30,780	0.978	19,600	35,280	0.98474
17,150	30,870	0.97817	19,650	35,370	0.98484

**TABLE 3.1** Blackbody Fractions Created by Using Eq. (3.11) (Continued)

Wavelength · temperature ( $\lambda T$ )			Wavelength · temperature ( $\lambda T$ )		
$\mu\text{m} \cdot \text{K}$	$\mu\text{m} \cdot ^\circ\text{R}$	Blackbody fraction	$\mu\text{m} \cdot \text{K}$	$\mu\text{m} \cdot ^\circ\text{R}$	Blackbody fraction
19,700	35,460	0.98495	22,200	39,960	0.98912
19,750	35,550	0.98505	22,250	40,050	0.98919
19,800	35,640	0.98515	22,300	40,140	0.98926
19,850	35,730	0.98525	22,350	40,230	0.98932
19,900	35,820	0.98535	22,400	40,320	0.98939
19,950	35,910	0.98545	22,450	40,410	0.98945
20,000	36,000	0.98555	22,500	40,500	0.98951
20,050	36,090	0.98565	22,550	40,590	0.98958
20,100	36,180	0.98574	22,600	40,680	0.98964
20,150	36,270	0.98584	22,650	40,770	0.9897
20,200	36,360	0.98593	22,700	40,860	0.98977
20,250	36,450	0.98603	22,750	40,950	0.98983
20,300	36,540	0.98612	22,800	41,040	0.98989
20,350	36,630	0.98621	22,850	41,130	0.98995
20,400	36,720	0.9863	22,900	41,220	0.99001
20,450	36,810	0.98639	22,950	41,310	0.99007
20,500	36,900	0.98648	23,000	41,400	0.99013
20,550	36,990	0.98657	23,050	41,490	0.99019
20,600	37,080	0.98666	23,100	41,580	0.99024
20,650	37,170	0.98675	23,150	41,670	0.9903
20,700	37,260	0.98684	23,200	41,760	0.99036
20,750	37,350	0.98692	23,250	41,850	0.99042
20,800	37,440	0.98701	23,300	41,940	0.99047
20,850	37,530	0.98709	23,350	42,030	0.99053
20,900	37,620	0.98718	23,400	42,120	0.99058
20,950	37,710	0.98726	23,450	42,210	0.99064
21,000	37,800	0.98734	23,500	42,300	0.99069
21,050	37,890	0.98742	23,550	42,390	0.99075
21,100	37,980	0.9875	23,600	42,480	0.9908
21,150	38,070	0.98758	23,650	42,570	0.99085
21,200	38,160	0.98766	23,700	42,660	0.99091
21,250	38,250	0.98774	23,750	42,750	0.99096
21,300	38,340	0.98782	23,800	42,840	0.99101
21,350	38,430	0.9879	23,850	42,930	0.99106
21,400	38,520	0.98798	23,900	43,020	0.99111
21,450	38,610	0.98805	23,950	43,110	0.99117
21,500	38,700	0.98813	24,000	43,200	0.99122
21,550	38,790	0.9882	24,050	43,290	0.99127
21,600	38,880	0.98828	24,100	43,380	0.99132
21,650	38,970	0.98835	24,150	43,470	0.99137
21,700	39,060	0.98842	24,200	43,560	0.99141
21,750	39,150	0.9885	24,250	43,650	0.99146
21,800	39,240	0.98857	24,300	43,740	0.99151
21,850	39,330	0.98864	24,350	43,830	0.99156
21,900	39,420	0.98871	24,400	43,920	0.99161
21,950	39,510	0.98878	24,450	44,010	0.99165
22,000	39,600	0.98885	24,500	44,100	0.9917
22,050	39,690	0.98892	24,550	44,190	0.99175
22,100	39,780	0.98899	24,600	44,280	0.99179
22,150	39,870	0.98905	24,650	44,370	0.99184

**TABLE 3.1** Blackbody Fractions Created by Using Eq. (3.11) (Continued)

Wavelength · temperature ( $\lambda T$ )			Wavelength · temperature ( $\lambda T$ )		
$\mu\text{m} \cdot \text{K}$	$\mu\text{m} \cdot ^\circ\text{R}$	Blackbody fraction	$\mu\text{m} \cdot \text{K}$	$\mu\text{m} \cdot ^\circ\text{R}$	Blackbody fraction
24,700	44,460	0.99188	27,200	48,960	0.99378
24,750	44,550	0.99193	27,250	49,050	0.99381
24,800	44,640	0.99197	27,300	49,140	0.99384
24,850	44,730	0.99202	27,350	49,230	0.99388
24,900	44,820	0.99206	27,400	49,320	0.99391
24,950	44,910	0.99211	27,450	49,410	0.99394
25,000	45,000	0.99215	27,500	49,500	0.99397
25,050	45,090	0.99219	27,550	49,590	0.994
25,100	45,180	0.99224	27,600	49,680	0.99403
25,150	45,270	0.99228	27,650	49,770	0.99406
25,200	45,360	0.99232	27,700	49,860	0.99409
25,250	45,450	0.99236	27,750	49,950	0.99412
25,300	45,540	0.9924	27,800	50,040	0.99415
25,350	45,630	0.99245	27,850	50,130	0.99418
25,400	45,720	0.99249	27,900	50,220	0.9942
25,450	45,810	0.99253	27,950	50,310	0.99423
25,500	45,900	0.99257	28,000	50,400	0.99426
25,550	45,990	0.99261	28,050	50,490	0.99429
25,600	46,080	0.99265	28,100	50,580	0.99432
25,650	46,170	0.99269	28,150	50,670	0.99435
25,700	46,260	0.99273	28,200	50,760	0.99437
25,750	46,350	0.99277	28,250	50,850	0.9944
25,800	46,440	0.9928	28,300	50,940	0.99443
25,850	46,530	0.99284	28,350	51,030	0.99446
25,900	46,620	0.99288	28,400	51,120	0.99448
25,950	46,710	0.99292	28,450	51,210	0.99451
26,000	46,800	0.99296	28,500	51,300	0.99454
26,050	46,890	0.99299	28,550	51,390	0.99456
26,100	46,980	0.99303	28,600	51,480	0.99459
26,150	47,070	0.99307	28,650	51,570	0.99461
26,200	47,160	0.9931	28,700	51,660	0.99464
26,250	47,250	0.99314	28,750	51,750	0.99467
26,300	47,340	0.99318	28,800	51,840	0.99469
26,350	47,430	0.99321	28,850	51,930	0.99472
26,400	47,520	0.99325	28,900	52,020	0.99474
26,450	47,610	0.99328	28,950	52,110	0.99477
26,500	47,700	0.99332	29,000	52,200	0.99479
26,550	47,790	0.99335	29,050	52,290	0.99482
26,600	47,880	0.99339	29,100	52,380	0.99484
26,650	47,970	0.99342	29,150	52,470	0.99487
26,700	48,060	0.99345	29,200	52,560	0.99489
26,750	48,150	0.99349	29,250	52,650	0.99492
26,800	48,240	0.99352	29,300	52,740	0.99494
26,850	48,330	0.99356	29,350	52,830	0.99496
26,900	48,420	0.99359	29,400	52,920	0.99499
26,950	48,510	0.99362	29,450	53,010	0.99501
27,000	48,600	0.99365	29,500	53,100	0.99503
27,050	48,690	0.99369	29,550	53,190	0.99506
27,100	48,780	0.99372	29,600	53,280	0.99508
27,150	48,870	0.99375	29,650	53,370	0.9951

**TABLE 3.1** Blackbody Fractions Created by Using Eq. (3.11) (Continued)

Wavelength · temperature ( $\lambda T$ )			Wavelength · temperature ( $\lambda T$ )		
$\mu\text{m} \cdot \text{K}$	$\mu\text{m} \cdot ^\circ\text{R}$	Blackbody fraction	$\mu\text{m} \cdot \text{K}$	$\mu\text{m} \cdot ^\circ\text{R}$	Blackbody fraction
29,700	53,460	0.99513	32,200	57,960	0.9961
29,750	53,550	0.99515	32,250	58,050	0.99612
29,800	53,640	0.99517	32,300	58,140	0.99614
29,850	53,730	0.99519	32,350	58,230	0.99615
29,900	53,820	0.99522	32,400	58,320	0.99617
29,950	53,910	0.99524	32,450	58,410	0.99618
30,000	54,000	0.99526	32,500	58,500	0.9962
30,050	54,090	0.99528	32,550	58,590	0.99622
30,100	54,180	0.9953	32,600	58,680	0.99623
30,150	54,270	0.99532	32,650	58,770	0.99625
30,200	54,360	0.99535	32,700	58,860	0.99626
30,250	54,450	0.99537	32,750	58,950	0.99628
30,300	54,540	0.99539	32,800	59,040	0.9963
30,350	54,630	0.99541	32,850	59,130	0.99631
30,400	54,720	0.99543	32,900	59,220	0.99633
30,450	54,810	0.99545	32,950	59,310	0.99634
30,500	54,900	0.99547	33,000	59,400	0.99636
30,550	54,990	0.99549	33,050	59,490	0.99637
30,600	55,080	0.99551	33,100	59,580	0.99639
30,650	55,170	0.99553	33,150	59,670	0.9964
30,700	55,260	0.99555	33,200	59,760	0.99642
30,750	55,350	0.99557	33,250	59,850	0.99643
30,800	55,440	0.99559	33,300	59,940	0.99645
30,850	55,530	0.99561	33,350	60,030	0.99646
30,900	55,620	0.99563	33,400	60,120	0.99648
30,950	55,710	0.99565	33,450	60,210	0.99649
31,000	55,800	0.99567	33,500	60,300	0.99651
31,050	55,890	0.99569	33,550	60,390	0.99652
31,100	55,980	0.99571	33,600	60,480	0.99653
31,150	56,070	0.99573	33,650	60,570	0.99655
31,200	56,160	0.99575	33,700	60,660	0.99656
31,250	56,250	0.99577	33,750	60,750	0.99658
31,300	56,340	0.99578	33,800	60,840	0.99659
31,350	56,430	0.9958	33,850	60,930	0.9966
31,400	56,520	0.99582	33,900	61,020	0.99662
31,450	56,610	0.99584	33,950	61,110	0.99663
31,500	56,700	0.99586	34,000	61,200	0.99665
31,550	56,790	0.99588	34,050	61,290	0.99666
31,600	56,880	0.99589	34,100	61,380	0.99667
31,650	56,970	0.99591	34,150	61,470	0.99669
31,700	57,060	0.99593	34,200	61,560	0.9967
31,750	57,150	0.99595	34,250	61,650	0.99671
31,800	57,240	0.99597	34,300	61,740	0.99673
31,850	57,330	0.99598	34,350	61,830	0.99674
31,900	57,420	0.996	34,400	61,920	0.99675
31,950	57,510	0.99602	34,450	62,010	0.99676
32,000	57,600	0.99603	34,500	62,100	0.99678
32,050	57,690	0.99605	34,550	62,190	0.99679
32,100	57,780	0.99607	34,600	62,280	0.9968
32,150	57,870	0.99609	34,650	62,370	0.99682

**TABLE 3.1** Blackbody Fractions Created by Using Eq. (3.11) (Continued)

Wavelength · temperature ( $\lambda T$ )			Wavelength · temperature ( $\lambda T$ )		
$\mu\text{m} \cdot \text{K}$	$\mu\text{m} \cdot ^\circ\text{R}$	Blackbody fraction	$\mu\text{m} \cdot \text{K}$	$\mu\text{m} \cdot ^\circ\text{R}$	Blackbody fraction
34,700	62,460	0.99683	37,200	66,960	0.99738
34,750	62,550	0.99684	37,250	67,050	0.99739
34,800	62,640	0.99685	37,300	67,140	0.9974
34,850	62,730	0.99687	37,350	67,230	0.99741
34,900	62,820	0.99688	37,400	67,320	0.99742
34,950	62,910	0.99689	37,450	67,410	0.99743
35,000	63,000	0.9969	37,500	67,500	0.99744
35,050	63,090	0.99691	37,550	67,590	0.99744
35,100	63,180	0.99693	37,600	67,680	0.99745
35,150	63,270	0.99694	37,650	67,770	0.99746
35,200	63,360	0.99695	37,700	67,860	0.99747
35,250	63,450	0.99696	37,750	67,950	0.99748
35,300	63,540	0.99697	37,800	68,040	0.99749
35,350	63,630	0.99699	37,850	68,130	0.9975
35,400	63,720	0.997	37,900	68,220	0.99751
35,450	63,810	0.99701	37,950	68,310	0.99752
35,500	63,900	0.99702	38,000	68,400	0.99753
35,550	63,990	0.99703	38,050	68,490	0.99753
35,600	64,080	0.99704	38,100	68,580	0.99754
35,650	64,170	0.99706	38,150	68,670	0.99755
35,700	64,260	0.99707	38,200	68,760	0.99756
35,750	64,350	0.99708	38,250	68,850	0.99757
35,800	64,440	0.99709	38,300	68,940	0.99758
35,850	64,530	0.9971	38,350	69,030	0.99759
35,900	64,620	0.99711	38,400	69,120	0.9976
35,950	64,710	0.99712	38,450	69,210	0.9976
36,000	64,800	0.99713	38,500	69,300	0.99761
36,050	64,890	0.99714	38,550	69,390	0.99762
36,100	64,980	0.99715	38,600	69,480	0.99763
36,150	65,070	0.99717	38,650	69,570	0.99764
36,200	65,160	0.99718	38,700	69,660	0.99765
36,250	65,250	0.99719	38,750	69,750	0.99765
36,300	65,340	0.9972	38,800	69,840	0.99766
36,350	65,430	0.99721	38,850	69,930	0.99767
36,400	65,520	0.99722	38,900	70,020	0.99768
36,450	65,610	0.99723	38,950	70,110	0.99769
36,500	65,700	0.99724	39,000	70,200	0.99769
36,550	65,790	0.99725	39,050	70,290	0.9977
36,600	65,880	0.99726	39,100	70,380	0.99771
36,650	65,970	0.99727	39,150	70,470	0.99772
36,700	66,060	0.99728	39,200	70,560	0.99773
36,750	66,150	0.99729	39,250	70,650	0.99773
36,800	66,240	0.9973	39,300	70,740	0.99774
36,850	66,330	0.99731	39,350	70,830	0.99775
36,900	66,420	0.99732	39,400	70,920	0.99776
36,950	66,510	0.99733	39,450	71,010	0.99776
37,000	66,600	0.99734	39,500	71,100	0.99777
37,050	66,690	0.99735	39,550	71,190	0.99778
37,100	66,780	0.99736	39,600	71,280	0.99779
37,150	66,870	0.99737	39,650	71,370	0.99779

**TABLE 3.1** Blackbody Fractions Created by Using Eq. (3.11) (Continued)

Wavelength · temperature ( $\lambda T$ )			Wavelength · temperature ( $\lambda T$ )		
$\mu\text{m} \cdot \text{K}$	$\mu\text{m} \cdot ^\circ\text{R}$	Blackbody fraction	$\mu\text{m} \cdot \text{K}$	$\mu\text{m} \cdot ^\circ\text{R}$	Blackbody fraction
39,700	71,460	0.9978	42,200	75,960	0.99813
39,750	71,550	0.99781	42,250	76,050	0.99814
39,800	71,640	0.99782	42,300	76,140	0.99815
39,850	71,730	0.99782	42,350	76,230	0.99815
39,900	71,820	0.99783	42,400	76,320	0.99816
39,950	71,910	0.99784	42,450	76,410	0.99816
40,000	72,000	0.99785	42,500	76,500	0.99817
40,050	72,090	0.99785	42,550	76,590	0.99817
40,100	72,180	0.99786	42,600	76,680	0.99818
40,150	72,270	0.99787	42,650	76,770	0.99819
40,200	72,360	0.99787	42,700	76,860	0.99819
40,250	72,450	0.99788	42,750	76,950	0.9982
40,300	72,540	0.99789	42,800	77,040	0.9982
40,350	72,630	0.9979	42,850	77,130	0.99821
40,400	72,720	0.9979	42,900	77,220	0.99821
40,450	72,810	0.99791	42,950	77,310	0.99822
40,500	72,900	0.99792	43,000	77,400	0.99822
40,550	72,990	0.99792	43,050	77,490	0.99823
40,600	73,080	0.99793	43,100	77,580	0.99823
40,650	73,170	0.99794	43,150	77,670	0.99824
40,700	73,260	0.99794	43,200	77,760	0.99825
40,750	73,350	0.99795	43,250	77,850	0.99825
40,800	73,440	0.99796	43,300	77,940	0.99826
40,850	73,530	0.99796	43,350	78,030	0.99826
40,900	73,620	0.99797	43,400	78,120	0.99827
40,950	73,710	0.99798	43,450	78,210	0.99827
41,000	73,800	0.99798	43,500	78,300	0.99828
41,050	73,890	0.99799	43,550	78,390	0.99828
41,100	73,980	0.998	43,600	78,480	0.99829
41,150	74,070	0.998	43,650	78,570	0.99829
41,200	74,160	0.99801	43,700	78,660	0.9983
41,250	74,250	0.99802	43,750	78,750	0.9983
41,300	74,340	0.99802	43,800	78,840	0.99831
41,350	74,430	0.99803	43,850	78,930	0.99831
41,400	74,520	0.99804	43,900	79,020	0.99832
41,450	74,610	0.99804	43,950	79,110	0.99832
41,500	74,700	0.99805	44,000	79,200	0.99833
41,550	74,790	0.99805	44,050	79,290	0.99833
41,600	74,880	0.99806	44,100	79,380	0.99834
41,650	74,970	0.99807	44,150	79,470	0.99834
41,700	75,060	0.99807	44,200	79,560	0.99835
41,750	75,150	0.99808	44,250	79,650	0.99835
41,800	75,240	0.99809	44,300	79,740	0.99836
41,850	75,330	0.99809	44,350	79,830	0.99836
41,900	75,420	0.9981	44,400	79,920	0.99837
41,950	75,510	0.9981	44,450	80,010	0.99837
42,000	75,600	0.99811	44,500	80,100	0.99838
42,050	75,690	0.99812	44,550	80,190	0.99838
42,100	75,780	0.99812	44,600	80,280	0.99839
42,150	75,870	0.99813	44,650	80,370	0.99839

**TABLE 3.1** Blackbody Fractions Created by Using Eq. (3.11) (Continued)

Wavelength · temperature ( $\lambda T$ )			Wavelength · temperature ( $\lambda T$ )		
$\mu\text{m} \cdot \text{K}$	$\mu\text{m} \cdot ^\circ\text{R}$	Blackbody fraction	$\mu\text{m} \cdot \text{K}$	$\mu\text{m} \cdot ^\circ\text{R}$	Blackbody fraction
44,700	80,460	0.9984	47,200	84,960	0.99861
44,750	80,550	0.9984	47,250	85,050	0.99861
44,800	80,640	0.9984	47,300	85,140	0.99861
44,850	80,730	0.99841	47,350	85,230	0.99862
44,900	80,820	0.99841	47,400	85,320	0.99862
44,950	80,910	0.99842	47,450	85,410	0.99862
45,000	81,000	0.99842	47,500	85,500	0.99863
45,050	81,090	0.99843	47,550	85,590	0.99863
45,100	81,180	0.99843	47,600	85,680	0.99864
45,150	81,270	0.99844	47,650	85,770	0.99864
45,200	81,360	0.99844	47,700	85,860	0.99864
45,250	81,450	0.99845	47,750	85,950	0.99865
45,300	81,540	0.99845	47,800	86,040	0.99865
45,350	81,630	0.99845	47,850	86,130	0.99865
45,400	81,720	0.99846	47,900	86,220	0.99866
45,450	81,810	0.99846	47,950	86,310	0.99866
45,500	81,900	0.99847	48,000	86,400	0.99866
45,550	81,990	0.99847	48,050	86,490	0.99867
45,600	82,080	0.99848	48,100	86,580	0.99867
45,650	82,170	0.99848	48,150	86,670	0.99867
45,700	82,260	0.99849	48,200	86,760	0.99868
45,750	82,350	0.99849	48,250	86,850	0.99868
45,800	82,440	0.99849	48,300	86,940	0.99868
45,850	82,530	0.9985	48,350	87,030	0.99869
45,900	82,620	0.9985	48,400	87,120	0.99869
45,950	82,710	0.99851	48,450	87,210	0.99869
46,000	82,800	0.99851	48,500	87,300	0.9987
46,050	82,890	0.99851	48,550	87,390	0.9987
46,100	82,980	0.99852	48,600	87,480	0.9987
46,150	83,070	0.99852	48,650	87,570	0.99871
46,200	83,160	0.99853	48,700	87,660	0.99871
46,250	83,250	0.99853	48,750	87,750	0.99871
46,300	83,340	0.99854	48,800	87,840	0.99872
46,350	83,430	0.99854	48,850	87,930	0.99872
46,400	83,520	0.99854	48,900	88,020	0.99872
46,450	83,610	0.99855	48,950	88,110	0.99873
46,500	83,700	0.99855	49,000	88,200	0.99873
46,550	83,790	0.99856	49,050	88,290	0.99873
46,600	83,880	0.99856	49,100	88,380	0.99874
46,650	83,970	0.99856	49,150	88,470	0.99874
46,700	84,060	0.99857	49,200	88,560	0.99874
46,750	84,150	0.99857	49,250	88,650	0.99875
46,800	84,240	0.99857	49,300	88,740	0.99875
46,850	84,330	0.99858	49,350	88,830	0.99875
46,900	84,420	0.99858	49,400	88,920	0.99876
46,950	84,510	0.99859	49,450	89,010	0.99876
47,000	84,600	0.99859	49,500	89,100	0.99876
47,050	84,690	0.99859	49,550	89,190	0.99877
47,100	84,780	0.9986	49,600	89,280	0.99877
47,150	84,870	0.9986	49,650	89,370	0.99877

**TABLE 3.1** Blackbody Fractions Created by Using Eq. (3.11) (Continued)

Wavelength · temperature ( $\lambda T$ )			Wavelength · temperature ( $\lambda T$ )		
$\mu\text{m} \cdot \text{K}$	$\mu\text{m} \cdot ^\circ\text{R}$	Blackbody fraction	$\mu\text{m} \cdot \text{K}$	$\mu\text{m} \cdot ^\circ\text{R}$	Blackbody fraction
49,700	89,460	0.99878	52,200	93,960	0.99891
49,750	89,550	0.99878	52,250	94,050	0.99892
49,800	89,640	0.99878	52,300	94,140	0.99892
49,850	89,730	0.99878	52,350	94,230	0.99892
49,900	89,820	0.99879	52,400	94,320	0.99892
49,950	89,910	0.99879	52,450	94,410	0.99893
50,000	90,000	0.99879	52,500	94,500	0.99893
50,050	90,090	0.99888	52,550	94,590	0.99893
50,100	90,180	0.99888	52,600	94,680	0.99893
50,150	90,270	0.99888	52,650	94,770	0.99894
50,200	90,360	0.99881	52,700	94,860	0.99894
50,250	90,450	0.99881	52,750	94,950	0.99894
50,300	90,540	0.99881	52,800	95,040	0.99894
50,350	90,630	0.99881	52,850	95,130	0.99895
50,400	90,720	0.99882	52,900	95,220	0.99895
50,450	90,810	0.99882	52,950	95,310	0.99895
50,500	90,900	0.99882	53,000	95,400	0.99895
50,550	90,990	0.99883	53,050	95,490	0.99896
50,600	91,080	0.99883	53,100	95,580	0.99896
50,650	91,170	0.99883	53,150	95,670	0.99896
50,700	91,260	0.99883	53,200	95,760	0.99896
50,750	91,350	0.99884	53,250	95,850	0.99896
50,800	91,440	0.99884	53,300	95,940	0.99897
50,850	91,530	0.99884	53,350	96,030	0.99897
50,900	91,620	0.99885	53,400	96,120	0.99897
50,950	91,710	0.99885	53,450	96,210	0.99897
51,000	91,800	0.99885	53,500	96,300	0.99898
51,050	91,890	0.99885	53,550	96,390	0.99898
51,100	91,980	0.99886	53,600	96,480	0.99898
51,150	92,070	0.99886	53,650	96,570	0.99898
51,200	92,160	0.99886	53,700	96,660	0.99899
51,250	92,250	0.99886	53,750	96,750	0.99899
51,300	92,340	0.99887	53,800	96,840	0.99899
51,350	92,430	0.99887	53,850	96,930	0.99899
51,400	92,520	0.99887	53,900	97,020	0.99899
51,450	92,610	0.99888	53,950	97,110	0.999
51,500	92,700	0.99888	54,000	97,200	0.999
51,550	92,790	0.99888	54,050	97,290	0.999
51,600	92,880	0.99888	54,100	97,380	0.999
51,650	92,970	0.99889	54,150	97,470	0.99901
51,700	93,060	0.99889	54,200	97,560	0.99901
51,750	93,150	0.99889	54,250	97,650	0.99901
51,800	93,240	0.99889	54,300	97,740	0.99901
51,850	93,330	0.9989	54,350	97,830	0.99901
51,900	93,420	0.9989	54,400	97,920	0.99902
51,950	93,510	0.9989	54,450	98,010	0.99902
52,000	93,600	0.9989	54,500	98,100	0.99902
52,050	93,690	0.99891	54,550	98,190	0.99902
52,100	93,780	0.99891	54,600	98,280	0.99902
52,150	93,870	0.99891	54,650	98,370	0.99903

**TABLE 3.1** Blackbody Fractions Created by Using Eq. (3.11) (Continued)

Wavelength · temperature ( $\lambda T$ )			Wavelength · temperature ( $\lambda T$ )		
$\mu\text{m} \cdot \text{K}$	$\mu\text{m} \cdot ^\circ\text{R}$	Blackbody fraction	$\mu\text{m} \cdot \text{K}$	$\mu\text{m} \cdot ^\circ\text{R}$	Blackbody fraction
54,700	98,460	0.99903	57,200	102,960	0.99912
54,750	98,550	0.99903	57,250	103,050	0.99913
54,800	98,640	0.99903	57,300	103,140	0.99913
54,850	98,730	0.99903	57,350	103,230	0.99913
54,900	98,820	0.99904	57,400	103,320	0.99913
54,950	98,910	0.99904	57,450	103,410	0.99913
55,000	99,000	0.99904	57,500	103,500	0.99913
55,050	99,090	0.99904	57,550	103,590	0.99914
55,100	99,180	0.99904	57,600	103,680	0.99914
55,150	99,270	0.99905	57,650	103,770	0.99914
55,200	99,360	0.99905	57,700	103,860	0.99914
55,250	99,450	0.99905	57,750	103,950	0.99914
55,300	99,540	0.99905	57,800	104,040	0.99914
55,350	99,630	0.99905	57,850	104,130	0.99915
55,400	99,720	0.99906	57,900	104,220	0.99915
55,450	99,810	0.99906	57,950	104,310	0.99915
55,500	99,900	0.99906	58,000	104,400	0.99915
55,550	99,990	0.99906	58,050	104,490	0.99915
55,600	100,080	0.99906	58,100	104,580	0.99915
55,650	100,170	0.99907	58,150	104,670	0.99916
55,700	100,260	0.99907	58,200	104,760	0.99916
55,750	100,350	0.99907	58,250	104,850	0.99916
55,800	100,440	0.99907	58,300	104,940	0.99916
55,850	100,530	0.99907	58,350	105,030	0.99916
55,900	100,620	0.99908	58,400	105,120	0.99916
55,950	100,710	0.99908	58,450	105,210	0.99916
56,000	100,800	0.99908	58,500	105,300	0.99917
56,050	100,890	0.99908	58,550	105,390	0.99917
56,100	100,980	0.99908	58,600	105,480	0.99917
56,150	101,070	0.99909	58,650	105,570	0.99917
56,200	101,160	0.99909	58,700	105,660	0.99917
56,250	101,250	0.99909	58,750	105,750	0.99917
56,300	101,340	0.99909	58,800	105,840	0.99918
56,350	101,430	0.99909	58,850	105,930	0.99918
56,400	101,520	0.99909	58,900	106,020	0.99918
56,450	101,610	0.9991	58,950	106,110	0.99918
56,500	101,700	0.9991	59,000	106,200	0.99918
56,550	101,790	0.9991	59,050	106,290	0.99918
56,600	101,880	0.9991	59,100	106,380	0.99919
56,650	101,970	0.9991	59,150	106,470	0.99919
56,700	102,060	0.99911	59,200	106,560	0.99919
56,750	102,150	0.99911	59,250	106,650	0.99919
56,800	102,240	0.99911	59,300	106,740	0.99919
56,850	102,330	0.99911	59,350	106,830	0.99919
56,900	102,420	0.99911	59,400	106,920	0.99919
56,950	102,510	0.99911	59,450	107,010	0.9992
57,000	102,600	0.99912	59,500	107,100	0.9992
57,050	102,690	0.99912	59,550	107,190	0.9992
57,100	102,780	0.99912	59,600	107,280	0.9992
57,150	102,870	0.99912	59,650	107,370	0.9992

**TABLE 3.1** Blackbody Fractions Created by Using Eq. (3.11) (Continued)

Wavelength · temperature ( $\lambda T$ )			Wavelength · temperature ( $\lambda T$ )		
$\mu\text{m} \cdot \text{K}$	$\mu\text{m} \cdot ^\circ\text{R}$	Blackbody fraction	$\mu\text{m} \cdot \text{K}$	$\mu\text{m} \cdot ^\circ\text{R}$	Blackbody fraction
59,700	107,460	0.9992	62,200	111,960	0.99927
59,750	107,550	0.9992	62,250	112,050	0.99927
59,800	107,640	0.99921	62,300	112,140	0.99927
59,850	107,730	0.99921	62,350	112,230	0.99927
59,900	107,820	0.99921	62,400	112,320	0.99927
59,950	107,910	0.99921	62,450	112,410	0.99928
60,000	108,000	0.99921	62,500	112,500	0.99928
60,050	108,090	0.99921	62,550	112,590	0.99928
60,100	108,180	0.99921	62,600	112,680	0.99928
60,150	108,270	0.99922	62,650	112,770	0.99928
60,200	108,360	0.99922	62,700	112,860	0.99928
60,250	108,450	0.99922	62,750	112,950	0.99928
60,300	108,540	0.99922	62,800	113,040	0.99928
60,350	108,630	0.99922	62,850	113,130	0.99929
60,400	108,720	0.99922	62,900	113,220	0.99929
60,450	108,810	0.99922	62,950	113,310	0.99929
60,500	108,900	0.99923	63,000	113,400	0.99929
60,550	108,990	0.99923	63,050	113,490	0.99929
60,600	109,080	0.99923	63,100	113,580	0.99929
60,650	109,170	0.99923	63,150	113,670	0.99929
60,700	109,260	0.99923	63,200	113,760	0.99929
60,750	109,350	0.99923	63,250	113,850	0.99929
60,800	109,440	0.99923	63,300	113,940	0.9993
60,850	109,530	0.99923	63,350	114,030	0.9993
60,900	109,620	0.99924	63,400	114,120	0.9993
60,950	109,710	0.99924	63,450	114,210	0.9993
61,000	109,800	0.99924	63,500	114,300	0.9993
61,050	109,890	0.99924	63,550	114,390	0.9993
61,100	109,980	0.99924	63,600	114,480	0.9993
61,150	110,070	0.99924	63,650	114,570	0.9993
61,200	110,160	0.99924	63,700	114,660	0.9993
61,250	110,250	0.99925	63,750	114,750	0.99931
61,300	110,340	0.99925	63,800	114,840	0.99931
61,350	110,430	0.99925	63,850	114,930	0.99931
61,400	110,520	0.99925	63,900	115,020	0.99931
61,450	110,610	0.99925	63,950	115,110	0.99931
61,500	110,700	0.99925	64,000	115,200	0.99931
61,550	110,790	0.99925	64,050	115,290	0.99931
61,600	110,880	0.99925	64,100	115,380	0.99931
61,650	110,970	0.99926	64,150	115,470	0.99931
61,700	111,060	0.99926	64,200	115,560	0.99932
61,750	111,150	0.99926	64,250	115,650	0.99932
61,800	111,240	0.99926	64,300	115,740	0.99932
61,850	111,330	0.99926	64,350	115,830	0.99932
61,900	111,420	0.99926	64,400	115,920	0.99932
61,950	111,510	0.99926	64,450	116,010	0.99932
62,000	111,600	0.99926	64,500	116,100	0.99932
62,050	111,690	0.99927	64,550	116,190	0.99932
62,100	111,780	0.99927	64,600	116,280	0.99932
62,150	111,870	0.99927	64,650	116,370	0.99933

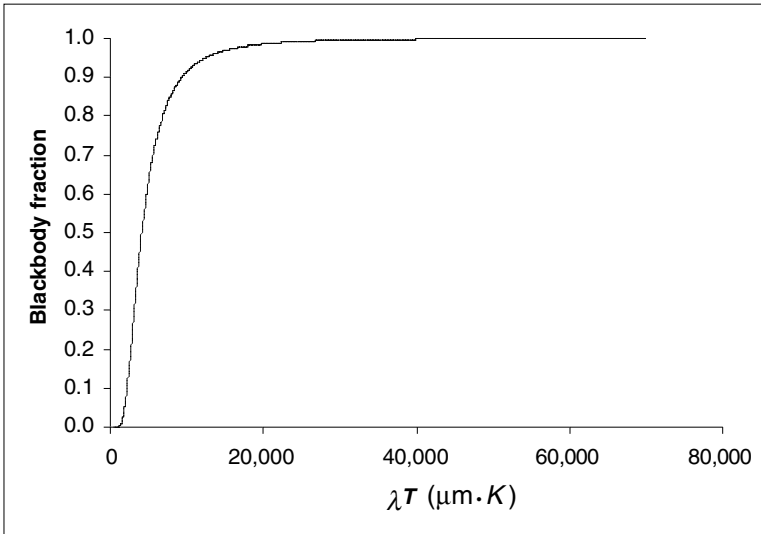
**TABLE 3.1** Blackbody Fractions Created by Using Eq. (3.11) (Continued)

Wavelength · temperature ( $\lambda T$ )			Wavelength · temperature ( $\lambda T$ )		
$\mu\text{m} \cdot \text{K}$	$\mu\text{m} \cdot ^\circ\text{R}$	Blackbody fraction	$\mu\text{m} \cdot \text{K}$	$\mu\text{m} \cdot ^\circ\text{R}$	Blackbody fraction
64,700	116,460	0.99933	67,150	120,870	0.99937
64,750	116,550	0.99933	67,200	120,960	0.99937
64,800	116,640	0.99933	67,250	121,050	0.99938
64,850	116,730	0.99933	67,300	121,140	0.99938
64,900	116,820	0.99933	67,350	121,230	0.99938
64,950	116,910	0.99933	67,400	121,320	0.99938
65,000	117,000	0.99933	67,450	121,410	0.99938
65,050	117,090	0.99933	67,500	121,500	0.99938
65,100	117,180	0.99933	67,550	121,590	0.99938
65,150	117,270	0.99934	67,600	121,680	0.99938
65,200	117,360	0.99934	67,650	121,770	0.99938
65,250	117,450	0.99934	67,700	121,860	0.99938
65,300	117,540	0.99934	67,750	121,950	0.99938
65,350	117,630	0.99934	67,800	122,040	0.99938
65,400	117,720	0.99934	67,850	122,130	0.99939
65,450	117,810	0.99934	67,900	122,220	0.99939
65,500	117,900	0.99934	67,950	122,310	0.99939
65,550	117,990	0.99934	68,000	122,400	0.99939
65,600	118,080	0.99934	68,050	122,490	0.99939
65,650	118,170	0.99935	68,100	122,580	0.99939
65,700	118,260	0.99935	68,150	122,670	0.99939
65,750	118,350	0.99935	68,200	122,760	0.99939
65,800	118,440	0.99935	68,250	122,850	0.99939
65,850	118,530	0.99935	68,300	122,940	0.99939
65,900	118,620	0.99935	68,350	123,030	0.99939
65,950	118,710	0.99935	68,400	123,120	0.99939
66,000	118,800	0.99935	68,450	123,210	0.9994
66,050	118,890	0.99935	68,500	123,300	0.9994
66,100	118,980	0.99935	68,550	123,390	0.9994
66,150	119,070	0.99936	68,600	123,480	0.9994
66,200	119,160	0.99936	68,650	123,570	0.9994
66,250	119,250	0.99936	68,700	123,660	0.9994
66,300	119,340	0.99936	68,750	123,750	0.9994
66,350	119,430	0.99936	68,800	123,840	0.9994
66,400	119,520	0.99936	68,850	123,930	0.9994
66,450	119,610	0.99936	68,900	124,020	0.9994
66,500	119,700	0.99936	68,950	124,110	0.9994
66,550	119,790	0.99936	69,000	124,200	0.9994
66,600	119,880	0.99936	69,050	124,290	0.99941
66,650	119,970	0.99936	69,100	124,380	0.99941
66,700	120,060	0.99937	69,150	124,470	0.99941
66,750	120,150	0.99937	69,200	124,560	0.99941
66,800	120,240	0.99937	69,250	124,650	0.99941
66,850	120,330	0.99937	69,300	124,740	0.99941
66,900	120,420	0.99937	69,350	124,830	0.99941
66,950	120,510	0.99937	69,400	124,920	0.99941
67,000	120,600	0.99937	69,450	125,010	0.99941
67,050	120,690	0.99937	69,500	125,100	0.99941
67,100	120,780	0.99937	69,550	125,190	0.99941

**TABLE 3.1** Blackbody Fractions Created by Using Eq. (3.11) (Continued)

Wavelength · temperature ( $\lambda T$ )			Wavelength · temperature ( $\lambda T$ )		
$\mu\text{m} \cdot \text{K}$	$\mu\text{m} \cdot ^\circ\text{R}$	Blackbody fraction	$\mu\text{m} \cdot \text{K}$	$\mu\text{m} \cdot ^\circ\text{R}$	Blackbody fraction
69,600	125,280	0.99941	69,800	125,640	0.99942
69,650	125,370	0.99941	69,850	125,730	0.99942
69,700	125,460	0.99942	69,900	125,820	0.99942
69,750	125,550	0.99942	69,950	125,910	0.99942

## Graphical Representation of Tabulated Data



For the example in Fig. 3.10, the fraction of the sun's energy that passes through the window within the wavelength band of 0 to 4  $\mu\text{m}$  is calculated from the blackbody fractions. Between any two wavelengths, the emissive power fraction is calculated by:

$$E_{b,\lambda_1-\lambda_2}(T) = \sigma T^4 [F_{0-\lambda_2 T} - F_{0-\lambda_1 T}] \quad (3.12)$$

For the sun,  $\lambda_2 T = 4 \mu\text{m} \times 8500^\circ\text{R} = 34,000 \mu\text{m} \cdot ^\circ\text{R}$ . From Table 3.1, the blackbody fraction that corresponds to  $34,000 \mu\text{m} \cdot ^\circ\text{R}$  is  $F_{0-\lambda_2 T} = 0.98314$ . This means that 98.314 percent of the sun's emissive energy passes through the window. Conversely, the window filters only 1.686 percent of the sun's radiative energy. For the radiant heating panel,  $\lambda_2 T = 4 \mu\text{m} \times 760^\circ\text{R} = 3040 \mu\text{m} \cdot ^\circ\text{R}$  and from Table 3.1, the blackbody fraction corresponding to  $3040 \mu\text{m} \cdot ^\circ\text{R}$  is  $F_{0-\lambda_2 T} = 0.02746$ . This means that only 2.746 percent of the energy emitted from the radiant heating panel passes through the window.

Another useful equation that utilizes blackbody fractions determines the amount of emissive power for a specific wavelength and beyond. This equation is:

$$E_{b\lambda-\infty}(T) = \sigma T^4 [1 - F_{0-\lambda T}] \quad (3.13)$$

An example of Eq. (3.13) is the determination of how much radiation is emitted from a lightbulb above the visible spectrum. Approximate the lightbulb as a blackbody at 5400°R (3000 K). The upper limit of the visible spectrum is 0.7  $\mu\text{m}$ . Therefore, from Table 3.1, the fraction of energy emitted from the lightbulb above 0.7  $\mu\text{m}$  is ( $\lambda T = 3780 \mu\text{m} \cdot ^\circ\text{R}$ ) 91.694 percent. The unfortunate side to this calculation is that less than 10 percent of the energy put into a lightbulb is used to produce the desired result—visible radiation, or light. These calculations have led to the development of energy-efficient lighting, which emits a higher percentage of visible radiation (light) and a lesser percentage of thermal radiation in nonvisible radiation spectra.

### 3.4 RADIATION PROPERTIES

The preceding sections of this chapter treat all surfaces as if they are blackbodies. This also implies that they emit at their maximum capabilities, or at a rate of  $\sigma T^4$ . Measurements and experiments show that this is rarely true. Walls, furniture, and carpeting, as well as most other surfaces, emit radiant energy at a rate less than the blackbody calculation.

To confuse the issue, radiation properties can vary with direction and wavelength. To maintain order, the properties are separated into four categories: (1) spectral, directional; (2) spectral, hemispherical; (3) total, directional; and (4) hemispherical, total.

The terms *directional* and *hemispherical* refer to property variation with direction, namely the angles  $\theta$  and  $\phi$ . One of the more frequent occurrences of this variation is visible on a hot day when driving down a blacktop road. In the distance, sometimes it appears as if water is standing on the road. In reality, the emissivity ( $\epsilon$ ) of the road surface becomes very low at the particular viewing angle. As the driver approaches this reflective spot, the viewing angle changes, followed by the emissivity. Hence, the directional properties describe variation with  $\theta$  and  $\phi$ , whereas the hemispherical properties are averaged over the entire viewing hemisphere.

The terms *spectral* and *total* refer to property variation with wavelength. Earlier in this chapter, the transmissivity ( $\tau$ ) of the window varied with wavelength: completely transparent up to 4  $\mu\text{m}$  and completely opaque above 4  $\mu\text{m}$ . This variation is referred to as the *spectral property*. The *total property* is the integrated average over all wavelengths.

Finally, the *total, hemispherical property* is averaged over all directions and wavelengths. This property value is the one most often cited in tables. Sometimes, though, it can be completely misleading, such as in the case of the window.

This portion of the Handbook discusses the surface properties that can be used to obtain realistic emission rates from real surfaces. These properties are the surface emissivity ( $\epsilon$ ), the surface absorptivity ( $\alpha$ ), the surface transmissivity ( $\tau$ ), and the surface reflectivity ( $\rho$ ). When radiation is incident upon a surface, that radiation is either absorbed, transmitted, or reflected by the surface. In mathematical terms:

$$\rho + \alpha + \tau = 1 \quad (3.14)$$

This is a very important correlation and will be used in subsequent sections.

### 3.4.1 Emissivity

The emissivity ( $\epsilon$ ) of a surface is the measure of how well that surface emits relative to a blackbody. By definition, the emissivity must be between zero and one. Mathematically, the spectral, directional emissivity is defined as:

$$\epsilon_\lambda (\theta, \phi, T) = \frac{E_\lambda (\theta, \phi, T)}{E_{b\lambda} (\theta, T)} \quad (3.15)$$

By definition, this is the most basic emissivity because it depends on direction, wavelength, and surface temperature. It will rarely be used in this text, except to calculate the rest of the emissivities.

The *directional, total emissivity* is averaged over all wavelengths. This emissivity is defined as:

$$\epsilon(\theta, \phi, T) = \int_0^\infty \epsilon_\lambda (\theta, \phi, T) d\lambda \quad (3.16)$$

Substituting Eq. (3.15) into this equation and carrying out the integral results in the expression for the directional, total emissivity in terms of the *directional, spectral emissivity*:

$$\epsilon(\theta, \phi, T) = \frac{\int_0^\infty \epsilon_\lambda (\theta, \phi, T) E_{b\lambda}(T) d\lambda}{\sigma T^4} \quad (3.17)$$

This equation applies to the total emissivity of a surface as viewed from the direction  $\theta$ .

The *hemispherical, spectral emissivity* has more application in the built environment. Two of these applications are the aforementioned window and surfaces where the radiation properties vary substantially with wavelength. Mathematically, the hemispherical, spectral emissivity is defined in terms of the directional, spectral emissivity as:

$$\epsilon_\lambda = \frac{E_\lambda (T)}{E_{b\lambda} (T)} = \frac{1}{\pi} \int_\Omega \epsilon_\lambda (\theta, \phi, T) d\Omega = \frac{1}{\pi} \int_0^{2\pi} \int_0^{\pi/2} \epsilon_\lambda (\theta, \phi, T) d\theta d\phi \quad (3.18)$$

The integral is over the solid angle that describes the hemisphere ( $0 < \phi < 2\pi$  and  $0 < \theta < \pi/2$ ). The spectral blackbody emissive power is mathematically described as:

$$E_{b\lambda} (T) = \frac{c_1 \lambda^{-5}}{\exp (c_2/\lambda T) - 1} \quad (3.19)$$

The *hemispherical, total emissivity* of a surface is defined as the integral of hemispherical, spectral emissivity over all wavelengths. Mathematically, hemispherical, total emissivity is:

$$\epsilon = \frac{E(T)}{E_b(T)} = \frac{\int_0^\infty \epsilon_\lambda E_{b\lambda} (T) d\lambda}{\sigma T^4} \quad (3.20)$$

Equation (3.20) is one of the important properties that will be used throughout the rest of this book. Figure 3.11 demonstrates the utility of this equation. The figure shows the blackbody and real emission from a surface at 300°F. The line designated as the blackbody emission line is the emission calculated from Eq. (3.19). The area under this curve is  $\sigma T^4$ . The other line is the real emission from the surface which has a hemispherical, spectral emissivity that is 0.8 between 0 and 5  $\mu\text{m}$  and is 0.4 above 5  $\mu\text{m}$ . The area under this lower curve represents the emission from the real surface and is exactly equal to the numerator in Eq. (3.20). The ratio of the areas under each of these curves is the hemispherical, total emissivity.

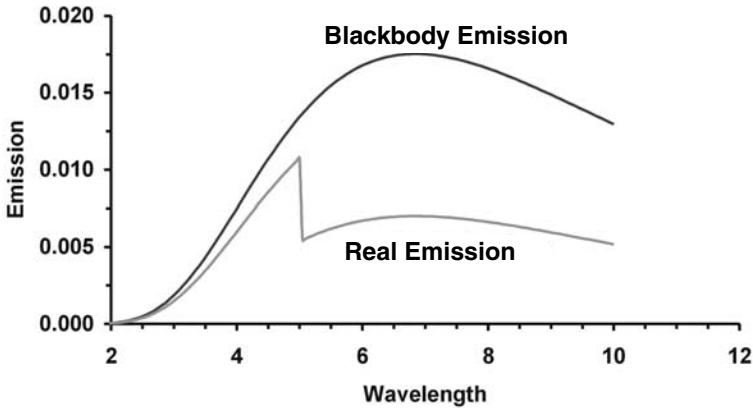


FIGURE 3.11 Equation showing emissivity and wavelength.

Oftentimes, the necessity arises where the spectral emissivity is known but not the total emissivity. The total emissivity is a function of the surface temperature. As the surface temperature changes, so does the total emissivity, even though the spectral emissivity remains constant. The accepted procedure for calculating the total emissivity from spectral data is to approximate the spectral emissivity as a series of wavelength bands, each of which contains a constant emissivity over that band. The constant “banded” emissivities are then averaged by (Siegel and Howell, 1992):

$$\begin{aligned} \varepsilon = & \underbrace{(F_{0-(\lambda_1 + \Delta\lambda_1)T} - 0)\varepsilon_{\lambda_1}}_{\lambda_1 = 0} + \underbrace{(F_{0-(\lambda_2 + \Delta\lambda_2)T} - F_{0-\lambda_2T})\varepsilon_{\lambda_2}}_{\lambda_2 = \lambda_1 + \Delta\lambda_1} \quad (3.21) \\ & + \underbrace{(F_{0-(\lambda_3 + \Delta\lambda_3)T} - F_{0-\lambda_3T})\varepsilon_{\lambda_3}}_{\lambda_3 = \lambda_2 + \Delta\lambda_2} + \dots + \underbrace{(1 - F_{0-\lambda_nT})\varepsilon_{\lambda_n}}_{\lambda_n = \lambda_{n-1} + \Delta\lambda_{n-1}} \end{aligned}$$

The variable  $n$  is the number of wavelength bands in the spectral approximation of the emissivity.

**EXAMPLE 3.4** *The measured spectral emissivity of a surface is shown in Fig. 3.12. Calculate the approximate total emissivity at 85°F (representative of a floor radiant heating system) and at 1000°F (representative of a high-temperature heating system). The solid lines in Fig. 3.12 show three wavelength bands that approximate the real emissivity. The first band, extending from 0 to 3.5  $\mu\text{m}$ , has an emissivity of 0.2; the second band, extending from 3.5 to 7  $\mu\text{m}$ , has an emissivity of 0.7; and the third band,*

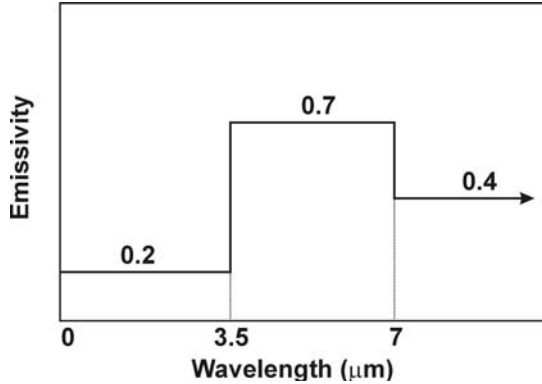


FIGURE 3.12 Emissivity variation for Example 3.4.

extending to infinity from 7 μm, exhibits an emissivity of 0.4. The blackbody fractions for the two temperatures and wavelengths are:

$\lambda$	85° F	1000° F
3.5 μm	0.00061	0.23670
7.0 μm	0.08641	0.70864

At 85° F, Eq. (3.20) becomes:

$$\begin{aligned} \epsilon &= \underbrace{(0.00061) \times 0.2}_{\substack{\lambda_1 = 0 \mu\text{m}; \\ \Delta\lambda_1 = 3.5 \mu\text{m}}} + \underbrace{(0.08641 - 0.00061) \times 0.7}_{\substack{\lambda_2 = 3.5 \mu\text{m}; \Delta\lambda_2 = 2.5 \mu\text{m}}} + \underbrace{(1 - 0.08641) \times 0.4}_{\lambda_n = 7.0 \mu\text{m}} \\ &= 0.00012 \quad + \quad 0.06006 \quad + \quad 0.36544 \\ &= 0.4256 \end{aligned}$$

At 1000° F, Eq. (3.20) results in:

$$\begin{aligned} \epsilon &= \underbrace{(0.2367) \times 0.2}_{\substack{\lambda_1 = 0 \mu\text{m}; \\ \Delta\lambda_1 = 3.5 \mu\text{m}}} + \underbrace{(0.70864 - 0.2367) \times 0.7}_{\substack{\lambda_2 = 3.5 \mu\text{m}; \Delta\lambda_2 = 2.5 \mu\text{m}}} + \underbrace{(1 - 0.70864) \times 0.4}_{\lambda_n = 7.0 \mu\text{m}} \\ &= 0.0473 \quad + \quad 0.3304 \quad + \quad 0.1165 \\ &= 0.4942 \end{aligned}$$

The interesting characteristic of this example is the large change in the hemispherical, total emissivity with temperature. The conclusion is that hotter surfaces are dominated by emissivities at shorter wavelengths, whereas cooler surfaces are dominated by emissivities at longer wavelengths.

### 3.4.2 Absorptivity

The absorptivity ( $\alpha$ ) of a surface is defined as the fraction of the energy incident on a surface that is actually absorbed by that surface. This definition implies that not all

radiant energy is absorbed by a surface. As with the emissivity, there are four separate definitions of absorptivity. The *spectral, directional absorptivity* is:

$$\alpha_{\lambda}(\theta, \phi, T) = \frac{q_{a\lambda}(\theta, \phi, T)}{q_{i\lambda}(\theta, \phi)} \quad (3.22)$$

The numerator is the radiant energy that is absorbed by the surface, and the denominator is the radiant energy that is incident on the surface. When the absorptivity is one, then the surface absorbs all the radiant energy that is incident on that surface. In other words, it absorbs all that it can get. The definition of the incident radiant energy from a particular direction at a particular wavelength is:

$$q_{i\lambda}(\theta, \phi) = I_{i\lambda}(\theta, \phi) \cos \theta \sin \phi d\theta d\phi d\lambda \quad (3.23)$$

As an aside, note that the incident radiant energy and ultimately the quantity of radiant energy absorbed by a surface is a function of the spectral, directional radiant intensity.

The *directional, total absorptivity* is defined as the ratio between the amount of radiant energy over all wavelengths that is absorbed by a surface, and the radiant energy over all wavelengths that is incident on the surface. Mathematically, the directional, total absorptivity is:

$$\alpha(\theta, \phi, T) = \frac{q_a(\theta, \phi, T)}{q_i(\theta, \phi)} = \frac{\int_0^{\infty} \alpha_{\lambda}(\theta, \phi, T) I_{i\lambda}(\theta, \phi) d\lambda}{\int_0^{\infty} I_{i\lambda}(\theta, \phi) d\lambda} \quad (3.24)$$

The *hemispherical, spectral absorptivity* is defined as the ratio between the amount of radiant energy at a particular wavelength but over all directions that is absorbed by a surface, and the radiant energy at a particular wavelength but over directions that is incident on the surface. Mathematically, the hemispherical, spectral absorptivity is:

$$\alpha_{\lambda}(T) = \frac{q_{a\lambda}}{q_{i\lambda}} = \frac{\int_0^{2\pi} \int_0^{\pi/2} \alpha_{\lambda}(\theta, \phi, T) I_{i\lambda}(\theta, \phi) d\theta d\phi}{\int_0^{2\pi} \int_0^{\pi/2} I_{i\lambda}(\theta, \phi) d\theta d\phi} \quad (3.25)$$

Finally, the *total, hemispherical absorptivity* is the ratio between all the radiant energy that is absorbed by a surface, and all the radiant energy incident on that surface:

$$\alpha(T) = \frac{q_a}{q_i} = \frac{\int_0^{\infty} \left[ \int_0^{2\pi} \int_0^{\pi/2} \alpha_{\lambda}(\theta, \phi, T) I_{i\lambda}(\theta, \phi) d\theta d\phi \right] d\lambda}{\int_0^{\infty} \int_0^{2\pi} \int_0^{\pi/2} I_{i\lambda}(\theta, \phi) d\theta d\phi d\lambda} \quad (3.26)$$

### 3.4.3 Transmissivity

The *transmissivity* ( $\tau$ ) of a surface is defined as the fraction of the energy incident on a surface that is transmitted through the surface. As with the absorptivity, there are four separate definitions of transmissivity. The *spectral, directional transmissivity* is:

$$\tau_{\lambda}(\theta, \phi, T) = \frac{q_{\tau\lambda}(\theta, \phi, T)}{q_{i\lambda}(\theta, \phi)} \quad (3.27)$$

The numerator is the radiant energy that is transmitted by the surface, and the denominator is the radiant energy that is incident on the surface. When the transmissivity is one, then the surface transmits all the radiant energy that is incident on that surface.

The *directional, total transmissivity* is defined as the ratio between the amount of radiant energy over all wavelengths that is transmitted by a surface, and the radiant energy over all wavelengths that is incident on the surface. Mathematically, the directional, total transmissivity is:

$$\tau(\theta, \phi, T) = \frac{q_{\tau}(\theta, \phi, T)}{q_i(\theta, \phi)} = \frac{\int_0^{\infty} \tau_{\lambda}(\theta, \phi, T) I_{i\lambda}(\theta, \phi) d\lambda}{\int_0^{\infty} I_{i\lambda}(\theta, \phi) d\lambda} \quad (3.28)$$

The *hemispherical, spectral transmissivity* is defined as the ratio between the amount of radiant energy at a particular wavelength but over all directions that is transmitted by a surface, and the radiant energy at a particular wavelength but over directions that is incident on the surface. Mathematically, the hemispherical, spectral transmissivity is:

$$\tau_{\lambda}(T) = \frac{q_{\tau\lambda}}{q_{i\lambda}} = \frac{\int_0^{2\pi} \int_0^{\pi/2} \tau_{\lambda}(\theta, \phi, T) I_{i\lambda}(\theta, \phi) d\theta d\phi}{\int_0^{2\pi} \int_0^{\pi/2} I_{i\lambda}(\theta, \phi) d\theta d\phi} \quad (3.29)$$

Finally, the *total, hemispherical transmissivity* is the ratio between all the radiant energy that is transmitted by a surface, and all the radiant energy incident on that surface:

$$\tau(T) = \frac{q_{\tau}}{q_i} = \frac{\int_0^{\infty} \left[ \int_0^{2\pi} \int_0^{\pi/2} \tau_{\lambda}(\theta, \phi, T) I_{i\lambda}(\theta, \phi) d\theta d\phi \right] d\lambda}{\int_0^{\infty} \int_0^{2\pi} \int_0^{\pi/2} I_{i\lambda}(\theta, \phi) d\theta d\phi d\lambda} \quad (3.30)$$

### 3.4.4 Reflectivity

The *reflectivity* ( $\rho$ ) of a surface is defined as the fraction of the energy incident on a surface that is reflected off the surface. As with the absorptivity and transmissivity, there are four separate definitions of reflectivity. The *spectral, directional reflectivity* is:

$$\rho_\lambda(\theta, \phi, T) = \frac{q_{\rho\lambda}(\theta, \phi, T)}{q_{i\lambda}(\theta, \phi)} \quad (3.31)$$

The numerator is the radiant energy that is reflected by the surface, and the denominator is the radiant energy that is incident on the surface. When the reflectivity is one, then the surface reflects all the radiant energy that is incident on that surface.

The *directional, total reflectivity* is defined as the ratio between the amount of radiant energy over all wavelengths that is reflected by a surface, and the radiant energy over all wavelengths that is incident on the surface. Mathematically, the directional, total reflectivity is:

$$\rho(\theta, \phi, T) = \frac{q_p(\theta, \phi, T)}{q_i(\theta, \phi)} = \frac{\int_0^\infty \rho_\lambda(\theta, \phi, T) I_{i\lambda}(\theta, \phi) d\lambda}{\int_0^\infty I_{i\lambda}(\theta, \phi) d\lambda} \quad (3.32)$$

The *hemispherical, spectral reflectivity* is defined as the ratio between the amount of radiant energy at a particular wavelength but over all directions that is reflected by a surface, and the radiant energy at a particular wavelength but over directions that is incident on the surface. Mathematically, the hemispherical, spectral reflectivity is:

$$\rho_\lambda(T) = \frac{q_{\rho\lambda}}{q_{i\lambda}} = \frac{\int_0^{2\pi} \int_0^{\pi/2} \rho_\lambda(\theta, \phi, T) I_{i\lambda}(\theta, \phi) d\theta d\phi}{\int_0^{2\pi} \int_0^{\pi/2} I_{i\lambda}(\theta, \phi) d\theta d\phi} \quad (3.33)$$

Finally, the *total, hemispherical reflectivity* is the ratio between all the radiant energy that is reflected by a surface, and all the radiant energy incident on that surface:

$$\tau(T) = \frac{q_p}{q_i} = \frac{\int_0^\infty \left[ \int_0^{2\pi} \int_0^{\pi/2} \rho_\lambda(\theta, \phi, T) I_{i\lambda}(\theta, \phi) d\theta d\phi \right] d\lambda}{\int_0^\infty \int_0^{2\pi} \int_0^{\pi/2} I_{i\lambda}(\theta, \phi) d\theta d\phi d\lambda}$$

### 3.4.5 Kirchhoff's Law

Kirchhoff's law basically states that the emissivity and the absorptivity are equal. This is only exactly true for the most fundamental case level. In this case, the spectral, directional emissivity is exactly equal to the spectral, directional absorptivity:

$$\epsilon_\lambda(\theta, \phi, T) = \alpha_\lambda(\theta, \phi, T) \quad (3.34)$$

To go beyond this statement requires certain conditions. The following paragraphs explain these conditions.

In the case of directional total properties, Eqs. (3.17) and (3.24) must be equal in order for Kirchoff's law to be valid. In other words:

$$\epsilon(\theta, \phi, T) = \frac{\int_0^\infty \epsilon_\lambda(\theta, \phi, T) E_{\lambda b}(T) d\lambda}{\sigma T^4} = \frac{\int_0^\infty \alpha_\lambda(\theta, \phi, T) I_{i\lambda}(\theta, \phi) d\lambda}{\int_0^\infty I_{i\lambda}(\theta, \phi) d\lambda} = \alpha(\theta, \phi, T) \quad (3.35)$$

The restriction is that the incident radiation must have a spectral distribution proportional to the incident radiation from a blackbody at the same temperature. This provides the relationship:

$$I_{i\lambda}(\theta, \phi) = K(\theta, \phi) I_{b\lambda}(T) = \frac{K(\theta, \phi) E_{b\lambda}(T)}{\pi} \quad (3.36)$$

Substituting Eq. (3.36) into Eq. (3.35) results in

$$\epsilon(\theta, \phi, T) = \frac{\int_0^\infty \epsilon_\lambda(\theta, \phi, T) E_{\lambda b}(T) d\lambda}{\sigma T^4} = \frac{\int_0^\infty \alpha_\lambda(\theta, \phi, T) E_{b\lambda}(T) d\lambda}{\int_0^\infty E_{b\lambda}(T) d\lambda [= \sigma T^4]} = \alpha(\theta, \phi, T) \quad (3.37)$$

Because the directional, spectral properties are equal, then so are directional, total properties.

Kirchoff's law can continue to be applied to the other cases in a similar fashion. The restrictions for each are listed as follows:

1. *Hemispherical, spectral.* Incident radiation must be independent of angle.
2. *Hemispherical, total.* Incident radiation must be independent of angle and incident radiation must have a spectral distribution similar to a blackbody; or incident radiation is independent of angle and the directional spectral properties are independent of wavelength.

**EXAMPLE 3.5** Consider a solar collector that has a spectral, hemispherical emissivity of 0.85 between 0 and 2 μm and is 0.4 above 2 μm. Calculate the hemispherical, total absorptivity for incident radiation from the sun at 8500°R (4722.2 K).

The sun's radiation is generally diffuse. Diffuse means that the incident radiation comes equally from all directions. Because the incident radiation is diffuse, Kirchoff's law is satisfied for the hemispherical, spectral case that requires that the incident radiation is independent of direction.

Imposing Kirchoff's law:  $\epsilon_\lambda(T) = \alpha_\lambda(T)$

From Eq. (3.26):

$$\alpha(T) = \frac{\int_0^\infty \left[ \int_0^{2\pi} \int_0^{2\pi} \alpha_\lambda(\theta, \phi, T) I_{i\lambda}(\theta, \phi) d\theta d\phi \right] d\lambda}{\int_0^\infty \int_0^{2\pi} \int_0^{2\pi} I_{i\lambda}(\theta, \phi) d\theta d\phi d\lambda}$$

$$= \frac{\int_0^\infty \alpha_\lambda(T_i) I_{ib\lambda}(T_i) d\lambda}{\int_0^\infty I_{ib\lambda}(T_i) d\lambda} = \frac{\int_0^\infty \epsilon_\lambda(T_i) E_{b\lambda}(T_i) d\lambda}{\sigma T_i^4}$$

The first simplification (from the first ratio to the second ratio) is possible because nothing is a function of direction. The blackbody intensities are substituted because the solar source is approximated as a blackbody at 8500°R (4722.2 K). The second simplification is made because the hemispherical, spectral properties satisfy Kirchhoff's law and, therefore, are equal. The blackbody intensities are replaced by the definition relating the blackbody intensity to the blackbody emissive power [ $\pi I_{b\lambda}(T) = E_{b\lambda}(T)$ ].

The total, hemispherical absorptivity is now calculated by using Eq. (3.21):

$$\begin{aligned} \alpha(T_i) &= 0.85F_{0-2\mu\text{m} \times 8500^\circ\text{R}} + 0.4(1 - F_{0-2\mu\text{m} \times 8500^\circ\text{R}}) \\ &= 0.85 \times 0.8868 + 0.4(1 - 0.8868) \\ &= 0.7538 + 0.0453 \\ &= 0.799 \end{aligned}$$

Note that if the temperature source were decreased, the total absorptivity would be weighted toward the longer wavelengths, and the absorptivity would be closer to 0.4 instead of 0.85.

### 3.5 CALCULATION TECHNIQUES

Up until this point, all of the radiation calculations have been to or from one surface independent of surrounding surfaces. The focus of this section is to implement the property definitions and other radiation definitions so that we can explore the interaction between two or more surfaces. This portion of the Handbook starts with the familiar view factor method (which is applied by using the radiative resistance network technique), and it concludes with a much more general approach to radiation calculations—the radiative transfer equation. Although this method is general, it is almost impossible to implement without a computer solution. Fortunately, one has been provided on the CD-ROM included with this Handbook.

#### 3.5.1 View Factor Calculations

View factors, or radiation shape factors, have been used for decades to complete radiation calculations. The basic definition of a *view factor* is the fraction of radiative energy leaving one surface that reaches a second surface. Figure 3.13 demonstrates this definition. In the diagram, assume for simplicity that the two surfaces are black and that a person standing on either surface can see the entire other surface. The small area  $dA_1$  emits radiative energy with an intensity  $I_1$ . The flux leaving surface  $dA_1$  that reaches  $dA_2$  is:

$$dq_{dA_1 \rightarrow dA_2} = I_{b1} \cos \theta_1 \frac{dA_2 \cos \theta_2}{r^2} = E_{b1} \cos \theta_1 \frac{dA_2 \cos \theta_2}{\pi r^2} \tag{3.38}$$

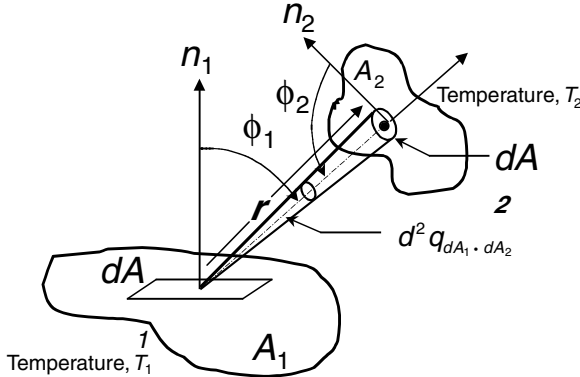


FIGURE 3.13 Boundary radiation exchange.

Equation (3.38) truly represents the quantity of radiative energy that leaves surface  $dA_1$  and that is intercepted by  $dA_2$ . In addition, the total energy flux that leaves  $dA_1$  is  $E_{b1}$ . Then the fraction of the radiative energy leaving surface  $dA_1$  that is intercepted by surface  $dA_2$  is the ratio:

$$dF_{dA_1 \rightarrow dA_2} = \frac{dq_{dA_1 \rightarrow dA_2}}{E_{b1}} = \cos \theta_1 \cos \theta_2 \frac{dA_2}{\pi r^2} \quad (3.39)$$

This result is the differential form of the view/interchange factor. To get the complete view factor between two large surfaces, Eq. (3.39) needs to be integrated over both complete surfaces (not a trivial task). However, there are several sources available where these integrations have already been completed. Most heat transfer textbooks include several popular view factor relationships. Table 3.2 lists several view factor relationships that are commonly found in the built environment.

There are several view factor relationships that preclude the necessity of a large database of view factors. Refer to Fig. 3.13, and consider the same definition, but now reverse roles of the two areas. Area  $dA_2$  now emits and area  $dA_1$  intercepts the emitted energy. Equation (3.39) is rewritten for this case as:

$$dF_{dA_2 \rightarrow dA_1} = \cos \theta_1 \cos \theta_2 \frac{dA_1}{\pi r^2} \quad (3.40)$$

Rearranging Eqs. (3.39) and (3.40) results in:

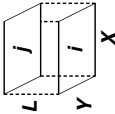
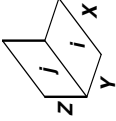
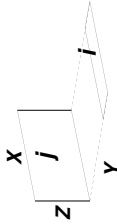
$$dA_1 dF_{dA_1 \rightarrow dA_2} = dA_2 dF_{dA_2 \rightarrow dA_1} \quad (3.41)$$

This relationship is referred to as the *reciprocity relationship for small areas*.

To apply this technique to large, finite areas, Eq. (3.38) must be integrated over both areas. The result of this integration is:

$$F_{12} = \frac{Q_{A_1 \rightarrow A_2}}{E_{b1} A_1} = \frac{1}{A_1} \int_{A_1} \int_{A_2} \frac{\cos \theta_1 \cos \theta_2}{\pi r^2} dA_1 dA_2 \quad (3.42)$$

TABLE 3.2 Various Radiation View Factors

Geometry	Equations
<p>Aligned parallel plates</p> 	$\bar{X} = \frac{X}{L}, \bar{Y} = \frac{Y}{L}$ $F_{ij} = \frac{2}{\pi \bar{X} \bar{Y}} \ln \frac{(1 + \bar{X}^2)(1 + \bar{Y}^2)^{1/2}}{1 + \bar{X}^2 + \bar{Y}^2} + \bar{X}(1 + \bar{Y}^2)^{1/2} \tan^{-1} \frac{\bar{X}}{(1 + \bar{Y}^2)^{1/2}} + \bar{Y}(1 + \bar{X}^2)^{1/2} \tan^{-1} \frac{\bar{Y}}{(1 + \bar{X}^2)^{1/2}} - \bar{X} \tan^{-1} \bar{X} - \bar{Y} \tan^{-1} \bar{Y}$
<p>Aligned perpendicular plates</p> 	$H = \frac{Z}{X}, W = \frac{Y}{X}$ $F_{ij} = \frac{1}{\pi W} W \tan^{-1} \frac{1}{W} + H \tan^{-1} \frac{1}{H} - (H^2 + W^2)^{1/2} \tan^{-1} \frac{1}{(H^2 + W^2)^{1/2}} + \frac{1}{4} \ln \frac{(1 + W^2)(1 + H^2)}{1 + W^2 + H^2} + \frac{W^2(1 + W^2 + H^2)}{(1 + W^2)(W^2 + H^2)} \leftrightarrow \frac{H^2(1 + W^2 + H^2)}{(1 + H^2)(W^2 + H^2)}$
<p>Perpendicular strip</p> 	$\bar{X} = \frac{Z}{X}, \bar{Y} = \frac{Y}{X}$ $F_{ij} = \frac{1}{\pi} \tan^{-1} \frac{1}{\bar{Y}} + \frac{\bar{Y}}{2} \ln \frac{\bar{Y}^2(\bar{X}^2 + \bar{Y}^2 + 1)}{(\bar{Y}^2 + 1)(\bar{X}^2 + \bar{Y}^2)} - \sqrt{\bar{X}^2 + \bar{Y}^2} \tan^{-1} \frac{1}{\sqrt{\bar{X}^2 + \bar{Y}^2}}$

As before, the reciprocity relationship is:

$$A_1 F_{12} = A_2 F_{21} \tag{3.43}$$

The net radiative exchange between two surfaces can now be calculated in terms of the view factors and the blackbody emission from each of the surfaces:

$$Q_{1 \leftrightarrow 2} = Q_{A_1 \rightarrow A_2} - Q_{A_2 \rightarrow A_1} = A_1 F_{12} (E_{b1} - E_{b2}) = A_2 F_{21} (E_{b1} - E_{b2}) \tag{3.44}$$

### 3.5.2 Radiative Resistance Network Approach to Radiative Heat Transfer Calculations

One can utilize the radiative resistance network method to calculate the radiative heat transfer. This method is based on the net radiation heat transfer equation. This equation can be modeled similar to equations used in electrical circuit analysis. This section describes how to accomplish modeling the radiation heat transfer equation as an electrical circuit. Radiation between nonblackbodies will be discussed here, and later simplifications will be introduced that will allow for analysis of blackbodies.

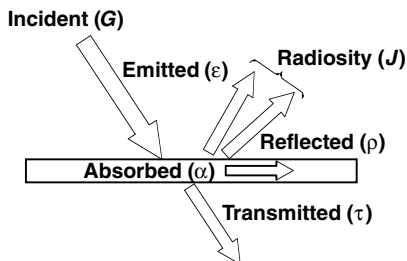


FIGURE 3.14 Radiation energy balance.

Because only blackbodies are perfect emitters and absorbers, when looking at nonblackbodies, the portion of the incident radiation that is emitted as well as reflected by the surface must be considered. Figure 3.14 illustrates what happens to radiation that is incident upon a surface. The combination of the reflected portion and the emitted

portion is referred to as the *radiosity* ( $J$ ). In mathematical terms, radiosity is defined as:

$$J = \epsilon E_b + \rho G \tag{3.45}$$

$E_b$  = blackbody emission

$\epsilon$  = surface emissivity

$\rho$  = surface reflectivity

$G$  = incident radiation

In most cases, except when dealing with windows, the surfaces considered in heating, ventilating, and air-conditioning (HVAC) applications will be opaque. When a surface is opaque, it can be said that the transmissivity of that surface is 0 ( $\tau = 0$ ). If the transmissivity is zero, then the summation of the absorptivity and the reflectivity is equal to 1 ( $\alpha + \rho = 1$ ). Using Kirchoff's law,  $\rho = 1 - \alpha = 1 - \epsilon$ , the radiosity equation can be rewritten as:

$$J = \epsilon E_b + (1 - \epsilon)G \tag{3.46}$$

This equation can be rewritten in the form:

$$G = \frac{J - \epsilon E_b}{(1 - \epsilon)} \quad (3.47)$$

To find the net radiation leaving a surface, the difference between the incident radiation ( $G$ ) and the radiosity must be found:

$$\frac{q}{A} = J - G \quad (3.48)$$

Substituting Eq. (3.47) into this equation yields:

$$\frac{q}{A} = J - \frac{J - \epsilon E_b}{(1 - \epsilon)} \quad (3.49)$$

Rearranging this equation

$$q = \frac{E_b - J}{\left(\frac{1 - \epsilon}{\epsilon A}\right)} \quad (3.50)$$

This is the form of the equation that is most useful and that can be used in a form analogous to the electrical resistance method. A useful way to think of this equation is:

$$\text{Flow} = \frac{\text{potential}}{\text{resistance}} \quad (3.51)$$

In Eq. (3.50),  $q$  represents the flow,  $E_b - J$  represents the potential, and  $(1 - \epsilon)/\epsilon A$  is the resistance (surface resistance). Figure 3.15 shows how this can be represented schematically.

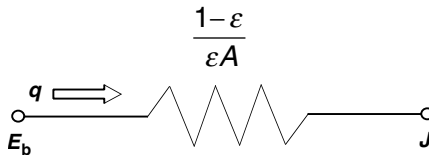


FIGURE 3.15 Radiation network.

Now that the equation for the net radiant heat exchange from a surface is in the needed form, the net radiant heat exchange between two surfaces must now be considered:

$$q_{1 \rightarrow 2}: J_1 A_1 F_{12}$$

$$q_{2 \rightarrow 1}: J_2 A_2 F_{21}$$

The net radiant heat exchange between these two surfaces can be represented as:

$$q_{12} = J_1 A_1 F_{12} - J_2 A_2 F_{21} \quad (3.52)$$

Using reciprocity, this equation can now be rewritten as:

$$q_{12} = (J_1 - J_2)A_2F_{12} \tag{3.53}$$

To get it in network circuit form, this equation is rewritten as:

$$q_{12} = \left( \frac{J_1 - J_2}{\frac{1}{A_2F_{12}}} \right) \tag{3.54}$$

In Eq. (3.54),  $q_{12}$  represents the flow,  $(J_1 - J_2)$  represents the potential, and  $1/A_2F_{12}$  represents the spatial resistance. Refer to Fig. 3.15 to see how to represent this schematically.

To illustrate how these equations that have been developed can be used, an example problem will now be worked.

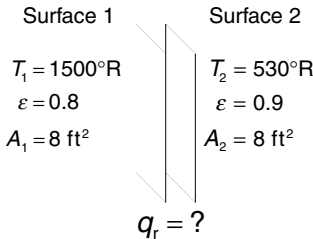


FIGURE 3.16 Surfaces in Example 3.6.

**EXAMPLE 3.6** Two surfaces facing each other, as shown in Fig. 3.16 have interaction only between the two of them. Surface 1 has an emissivity of 0.8, a surface temperature of 1500°R (833.3 K), and each surface has a surface area of 8 ft<sup>2</sup>. Surface 2 has an emissivity of 0.9 and a surface temperature of 530°R (294.4 K). Both surfaces are opaque. What is the net radiative heat transfer from surface 1 to surface 2?

The first step is to set up the resistance network. Each wall is represented by a

resistor as well as the medium between the two. The resistance network for this example can be seen in Fig. 3.17.

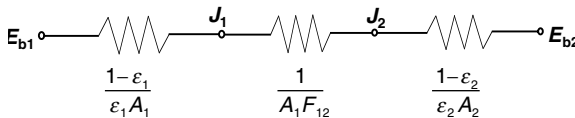


FIGURE 3.17 Radiation network for Example 3.6.

When working with thermal resistance networks, the radiant heat transfer can be calculated as:

$$q = \frac{\Delta E_b}{\sum R}$$

$E_b$  represents the blackbody emittance,  $R$  is the resistance, and  $q$  is the radiant heat transfer. In this example this equation would have the form:

$$q = \frac{E_{b1} - E_{b2}}{\frac{1-\varepsilon_1}{\varepsilon_1 A_1} + \frac{1}{A_1 F_{12}} + \frac{1-\varepsilon_2}{\varepsilon_2 A_2}}$$

Substituting in  $E_b = \sigma T^4$

$$q = \frac{\sigma(T_1^4 - T_2^4)}{\frac{1 - \epsilon_1}{\epsilon_1 A_1} + \frac{1}{A_1 F_{12}} + \frac{1 - \epsilon_2}{\epsilon_2 A_2}}$$

Substituting the numbers from the example:

$$q = \frac{\left(0.1714 \times 10^{-8} \frac{\text{Btu}}{\text{h} \times \text{ft}^2 \times \text{R}^4}\right) [(1500^\circ\text{R})^4 - (530^\circ\text{R})^4]}{\frac{1 - 0.8}{0.8 \times 8 \text{ ft}^2} + \frac{1}{1.0 \times 8 \text{ ft}^2} + \frac{1 - 0.9}{0.9 \times 8 \text{ ft}^2}}$$

Notice that the Stefan-Boltzmann constant ( $\sigma$ ) is:

$$\sigma = 0.1714 \times 10^{-8} \frac{\text{Btu}}{\text{h} \times \text{ft}^2 \times \text{R}^4}$$

Also, note that for this example, because the two plates only “see” one another, the view factor is 1. The result of this calculation is:

$$q = 50,205.3 \text{ Btu/h}$$

This example is an idealized situation; in practical applications this example would be a three-“surface” calculation (the two surfaces and the surroundings). The setup of a nodal network for a problem with more than one other surface will be discussed in the following paragraphs.

Consider the setup in the previous example. As was mentioned in the previous paragraph, this system would be a three-surface system. In this system there would be heat transfer occurring between the two plates as well as between each of the plates and the surroundings. To see how this system would be represented by using a resistance network, refer to Fig. 3.18. At each node a set of equations can be generated to describe the heat transfer that is occurring. At each node the summation of the radiative heat transfer is equal to zero. Knowing this, these equations can be used to generate a set of equations that then can be used to solve for the unknown values. Once these values are known, equations for the radiative heat transfer can be established in the form of Eq. (3.54) to solve for the net radiative heat transfer rate.

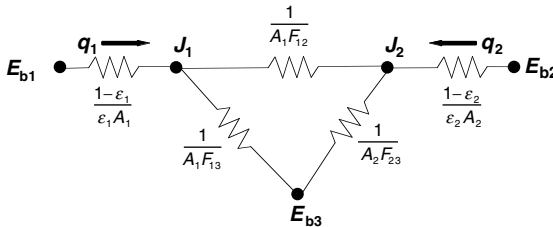


FIGURE 3.18 Three-surface radiation network.

In general the following steps can be used when using resistance networks.

- Step 1.** Represent the system with a resistance network.
- Step 2.** Calculate all necessary view factors.
- Step 3.** Write the nodal equation for each junction.
- Step 4.** Calculate needed emissive powers and resistances.
- Step 5.** Using the equations written in step 3, solve for unknown radiosities.
- Step 6.** Solve for the radiative heat transfer between surfaces of interest.

This six-step method will be demonstrated in the following example.

**EXAMPLE 3.7** *Two parallel plates 1.5 ft wide and 3 ft long are positioned 1.5 ft apart. The temperature of plate 1 is 2300°R (1277.8 K) and the temperature of plate 2 is 1400°R (777.8 K). The emissivities for plates 1 and 2 are 0.2 and 0.5, respectively. The plates are in a large room with a wall temperature of 550°R (305.6 K). Find the net radiative heat transfer rate to both of the plates and to the surroundings.*

Known:

$$A_1 = A_2 = 1.5 \text{ ft} \times 3 \text{ ft} = 4.5 \text{ ft}^2$$

$$T_1 = 2300^\circ\text{R} \text{ (1277.8 K)} \quad T_2 = 1400^\circ\text{R} \text{ (777.8 K)}$$

$$\epsilon_1 = 0.2 \quad \epsilon_2 = 0.5$$

Assumptions: *Because the room is a large room, it can be approximated as a blackbody. Notice the effect this assumption has at node 3 in the resistance network sketch. Blackbodies have no surface resistances.*

**Step 1.** *Represent the system with a resistance network. See Fig. 3.18.*

**Step 2.** *Calculate all necessary view factors. Use the equation from Table 3.2 for aligned parallel plates:*

$$\bar{X} = \frac{X}{L}, \quad \bar{Y} = \frac{Y}{L}$$

$$F_{ij} = \frac{2}{\pi \bar{X}\bar{Y}} \left\{ \ln \left[ \frac{(1 + \bar{X}^2)(1 + \bar{Y}^2)}{1 + \bar{X}^2 + \bar{Y}^2} \right]^{1/2} + \bar{X}(1 + \bar{Y}^2)^{1/2} \tan^{-1} \frac{\bar{X}}{(1 + \bar{Y}^2)^{1/2}} \right. \\ \left. + \bar{Y}(1 + \bar{X}^2)^{1/2} \tan^{-1} \frac{\bar{Y}}{(1 + \bar{X}^2)^{1/2}} - \bar{X} \tan^{-1} \bar{X} - \bar{Y} \tan^{-1} \bar{Y} \right\} = 0.25$$

Use the summation rule:

$$F_{12} + F_{13} = 1.0$$

$$\Rightarrow F_{13} = 0.75$$

$$F_{23} + F_{21} = 1.0$$

$$\Rightarrow F_{23} = 0.75$$

**Step 3.** Write the nodal equation for each junction.

At  $J_1$ :

$$\frac{E_{b1} - J_1}{\frac{1 - \epsilon_1}{\epsilon_1 A_1}} + \frac{J_2 - J_1}{\frac{1}{A_1 F_{12}}} + \frac{E_{b3} - J_1}{\frac{1}{A_1 F_{13}}} = 0$$

At  $J_2$ :

$$\frac{J_1 - J_2}{\frac{1}{A_1 F_{12}}} + \frac{E_{b3} - J_2}{\frac{1}{A_2 F_{23}}} + \frac{E_{b2} - J_2}{\frac{1 - \epsilon_2}{\epsilon_2 A_2}} = 0$$

**Step 4.** Calculate needed emissive powers and resistances.

Emissive powers:

$$E_{b1} = \sigma T_1^4 = 47,964.7 \frac{\text{Btu}}{\text{h} \times \text{ft}^2}$$

$$E_{b2} = \sigma T_2^4 = 6584.5 \frac{\text{Btu}}{\text{h} \times \text{ft}^2}$$

$$E_{b3} = \sigma T_3^4 = 156.84 \frac{\text{Btu}}{\text{h} \times \text{ft}^2}$$

Surface resistances:

$$\frac{1 - \epsilon_1}{\epsilon_1 A_1} = 0.889$$

$$\frac{1 - \epsilon_2}{\epsilon_2 A_2} = 0.222$$

Spatial resistances:

$$\frac{1}{A_1 F_{12}} = 0.889$$

$$\frac{1}{A_1 F_{13}} = 0.296$$

$$\frac{1}{A_2 F_{23}} = 0.296$$

**Step 5.** Using the equations written in step 3, solve for unknown radiosities.

$$J_1 = 10,580.6 \frac{\text{Btu}}{\text{h} \times \text{ft}^2}$$

$$J_2 = 4676.8 \frac{\text{Btu}}{\text{h} \times \text{ft}^2}$$

**Step 6.** Calculate the net radiative heat transfer from surfaces of interest.

$$q_1 = \frac{E_{b1} - J_1}{\frac{1 - \epsilon_1}{\epsilon_1 A_1}} = 42,051.9 \frac{Btu}{h}$$

$$q_2 = \frac{E_{b2} - J_2}{\frac{1 - \epsilon_2}{\epsilon_2 A_2}} = 8593.2 \frac{Btu}{h}$$

$$q_3 = q_1 + q_2 = 50,645.1 \frac{Btu}{h}$$

**3.5.3 Thermal Circuit Method**

Three simplified thermal circuit models are used to evaluate radiant transport: (1) binary star model, (2) rad-air model, and (3) the air index model. Each of these methods are discussed in the following paragraphs.

**3.5.3.1 Binary Star Model.** The binary star model is based on the assumption that convective and radiative heat transfer take place independently of each other and that energy conversion only occurs at solid surfaces. Various values can be assigned to convective coefficients and emissivities at each surface, and room size can also be varied as long as the room shape remains rectangular. However, the given surface must be treated as isothermal. The binary star model is presented in Fig. 3.19. Radiant and convective heat inputs occur at the nodes  $T_{rs}$  and  $T_{av}$ , respectively. The radiant and convective heat sources are resisted at the inside surface by a radiative conductance ( $S_1$ ) and a convective conductance ( $C_1$ ), respectively. Heat is lost to the outdoors by air infiltration ( $V$ ) and conduction through the wall ( $F_1$ ).

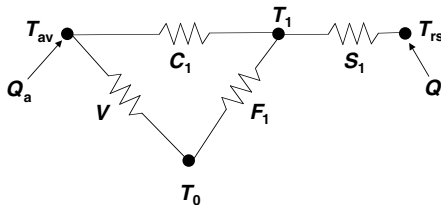


**FIGURE 3.19** Binary star model.

This model is based on the assumption that the enclosure has similar surfaces with equivalent boundary conditions. Therefore, only a single temperature  $T_1$  has to be considered. Equations for  $T_{rs}$ ,  $C_1$ , and  $S_1$  are given by Davies (1990). The comfort temperature  $T_c$  is linked to  $T_{av}$  and  $T_{rs}$  by very small conductances, as shown in Fig. 3.20.

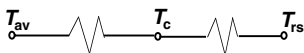


**FIGURE 3.20** Link to comfort temperature.

**3.5.3.2 Rad-Air Model.** The rad-air model incorporates both radiant and convective exchange into a general global room temperature  $T_{ra}$  (radiant air temper-

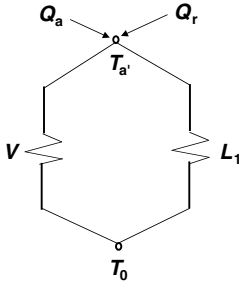


FIGURE 3.21 Air index model.

ature). Figure 3.21 presents the rad-air model. The variables  $T_{av}$ ,  $T_1$ ,  $V$ ,  $F_1$ , and  $Q_a$  have the same meanings as in the binary star model, but the radiant star temperature ( $T_{rs}$ ) is replaced by the radiant air temperature ( $T_{ra}$ ). The radiant input  $Q_r$  is replaced by the augmented radiant input  $Q_r(1 + C_1/S_1)$  at  $T_{ra}$  and output  $Q_r(C_1/S_1)$  at  $T_{av}$ . By letting the conductance between  $T_{av}$  and  $T_{ra}$  be:

$$X = (S_1 + C_1)C_1/S_1 \quad (3.55)$$

and by letting the conductance between  $T_{ra}$  and  $T_1$  be  $S_1 + C_1$ , the total conductance between  $T_1$  and  $T_{av}$  is equivalent to the convective conductance  $C_1$  as found in the binary star model. Heat inputs in the rad-air model produce the same temperatures,  $T_1$  and  $T_{av}$ , found in the binary star model; furthermore,  $T_{rs}$  can be calculated from the rad-air model by:

$$T_{rs} = T_{ra}(S_1 + C_1)/S_1 - T_{av}(C_1/S_1) \quad (3.56)$$

Using this relationship and solving for  $T_{ra}$ :

$$T_{ra} = \frac{S_1 T_{rs} + C_1 T_{av}}{S_1 + C_1} \quad (3.57)$$

The variable  $T_{ra}$  appears to be the weighted mean of the radiant star and average air temperatures.

The variable  $T_{ra}$  is a combination of convective and radiant transport. Therefore, the comfort temperature  $T_c$  cannot be directly incorporated into the rad-air model. The rad-air model allows room temperature to be expressed as a function of the indoor air temperature and the long-wave radiant field. When surface emissivities are high, results between the binary star and rad-air models compare closely (Davies, 1990).

**3.5.3.3 Air Index Model.** Figure 3.21 illustrates the air index model. If the conductance  $X$  from the rad-air model is assumed to be very large (infinite),  $T_1$  and  $T_{av}$  combine to form the air index node  $T_a'$ , which is equivalent to the comfort temperature  $T_c$ . Radiant and convective heat inputs occur at node  $T_a'$ , and all heat loss occurs through ventilation and conduction ( $V$  and  $L_1$ ) where  $L_1$  is the combination of  $F_1$  and  $S_1 + C_1$  in "parallel":

$$\frac{1}{L_1} = \frac{1}{S_1 + C_1} + \frac{1}{F_1} \quad (3.58)$$

The air index model is in widespread use for plant sizing applications. Although the air index model is not well founded, it is a simple model and produces adequate results for well-insulated rooms with small ventilation loss and little solar gain.

The thermal circuits for the binary star model, the rad-air model, and the air index model can be expanded into circuit diagrams representing multisurface enclosures. These circuit diagrams are presented in Fig. 3.22. The thermal circuit diagrams are easy

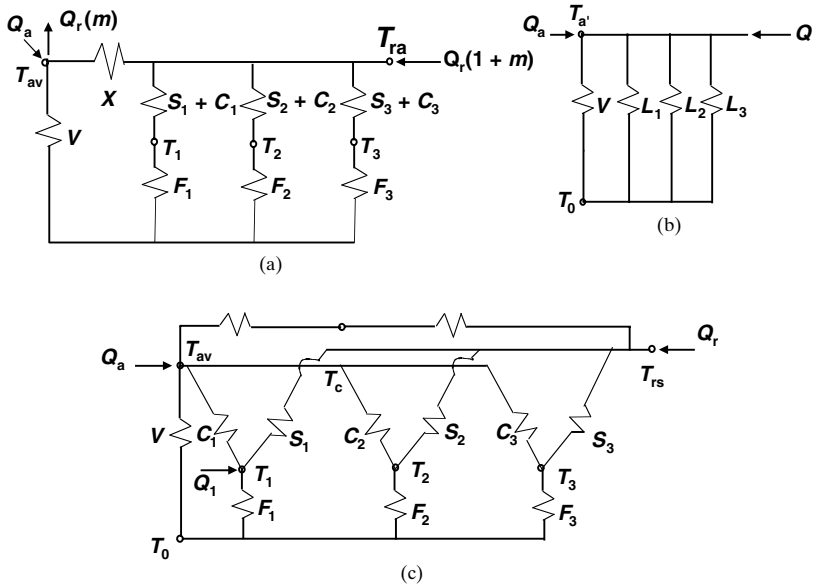


**FIGURE 3.22** Circuit diagrams representing multisurface enclosures. (a) Rad-air model. (b) Air index model. (c) Binary star model.

to create. However, the diagrams presented in Fig. 3.22 are only valid for rectangular enclosures. Computer programs can be written to calculate heat transfer and surface temperatures for a multisurface enclosure, allowing the designer to choose room size, surface emissivity, and the convective heat transfer coefficient at each surface.

The binary star and rad-air models produce more accurate results than the air index model because the air index model neglects conductance between  $T_{av}$  and  $T_{ra}$ . However, the solution for the air index model is easiest to set up (Khan et al., 1990).

### 3.5.4 MRT Correction Method

Walton (1980) proposed an algorithm for improving the accuracy of Blast's Gauss Seidel iteration by using the mean radiant temperature (MRT) method developed by Davies (1980). According to the MRT method, radiant heat transfer within an enclosure is modeled in two steps. First, it is assumed that each actual radiating surface  $i$  in the enclosure is paralleled by a single fictitious surface  $f$  that replaces the remaining actual surfaces within the enclosure. Second, each fictitious surface is assumed to have a surface area, emissivity, and temperature that create the same heat transfer with surface  $i$  as would the remaining actual surfaces. The temperature of each fictitious surface  $f$  is the mean radiant temperature  $T_{fi}$  seen by each corresponding surface  $i$  and is defined by an average of all temperatures inside the enclosure weighted by the product of area and emissivity:

$$T_{fi} = \frac{\sum_{j \neq i}^n A_j \epsilon_j T_j}{\sum_{j \neq i}^n A_j \epsilon_j} \tag{3.59}$$

The emissivity  $\epsilon_{f_i}$  of the fictitious surface is an area weighted average defined by:

$$\epsilon_{f_i} = \frac{\sum_{j \neq i}^n A_j \epsilon_j}{\sum_{j \neq i}^n A_j} \quad (3.60)$$

and the area of the fictitious surface  $A_{f_i}$  is the sum of the surrounding surface areas defined by:

$$A_{f_i} = \sum_{j \neq i}^n A_j \quad (3.61)$$

The ‘‘MRT/balance’’ equation for the radiant heat transfer in an enclosure, expressed as a function of the MRT, is:

$$q_{\text{rad},i,\text{MRT/bal}} = 4\sigma F_{if}(T_i^4 - T_{f_i}^4) + q_{\text{int}_i} + q_{\text{sol}_i} + q_{\text{bal}_i}, \quad i = 1 \rightarrow n \quad (3.62)$$

The first term on the right side of Eq. (3.62) represents the radiative heat flux calculated by the basic MRT method, and the last term represents a necessary quantity of energy to satisfy energy conservation. The remaining two terms represent the radiant flux from internal sources and the solar radiant flux.

The radiant interchange factor  $F_{if}$  is an estimated view factor between surface  $i$  and its corresponding fictitious surface  $f$ , and it is a function of emissivity ( $\epsilon_{f_i}, \epsilon_i$ ) and area ( $A_{f_i}, A_i$ ) of surface  $i$  and  $f$ . Without the radiation balance term  $q_{\text{bal},i}$  in Eq. (3.62), the MRT method does not satisfy the fundamental energy conservation equation. Equations for  $q_{\text{bal},i}$  and  $F_{if}$  are described by Steinman et al. (1989).

In the MRT method, the radiative heat flux is linearized by the approximation:

$$(T_i^4 - T_{f_i}^4) = 4T_{\text{avg},i}^3(T_i - T_{f_i}) \quad (3.63)$$

Substituting Eq. (3.63) into (3.62) gives the final form for the ‘‘MRT/balance’’ equation:

$$q_{\text{rad},i,\text{MRT/bal}} = 4\sigma F_{if} T_{\text{avg},i}^3(T_i - T_{f_i}) + q_{\text{int}_i} + q_{\text{sol}_i} + q_{\text{bal}_i} \quad (3.64)$$

The variable  $T_{\text{avg}}$  is an average of  $T_i$  and  $T_{f_i}$  and is treated as a constant at each iteration, thereby linearizing the ‘‘MRT/balance’’ equation. Computational speed using the MRT method is greatly enhanced compared with using the exact solution (Steinman et al., 1989). However, the MRT method is based on many assumptions and may not produce accurate answers for complex geometries or enclosures with diverse surface temperatures. The loss of accuracy partially occurs from the equality of Eq. (3.63) never being satisfied, even in the converged solution.

A correction component has since been developed for the MRT method, which accounts for the loss in accuracy from estimating  $F_{if}$  (Steinman et al., 1989). An MRT correction component has been developed for two situations:

**Case 1.** Variation of all surface emittances.

**Case 2.** Variation of one surface emittance with other surface emittances held constant.

Each of the cases is discussed in the following paragraphs.

**3.5.4.1 Case 1: Variation of All Surface Emittances.** In case 1, a correction component is developed for an enclosure where all surface emittances are varied from 0.0 to 1.0. The correction component for case 1 is:

$$q_{ci_{\epsilon_i}} = Q_{ci_{\epsilon_i}} \div A_i \tag{3.65}$$

for any emissivity  $\epsilon_i$ . The correction component  $q_{ci_{\epsilon_i}}$  is included in  $q_{rad,i,MRT/bal}$  to give the “MRT correction/balance” equation:

$$q_{rad,i,MRTcor/bal} = 4\sigma F_{if} T_{avg}^3 (T_i - T_{fi}) + q_{int_i} + q_{sol_i} + q_{bal_i} + q_{ci_{\epsilon_i}} \tag{3.66}$$

The correction component  $q_{ci_{\epsilon_i}}$  is also included in  $q_{bal_i}$ . The equation to give the  $q_{bal_i}$ , and the steps leading to Eq. (3.65) are explained by Steinman et al. (1989).

Figure 3.23 compares the exact solution with the solution produced by the “MRT/balance” equation and the “MRT correction/balance” equation using a curve of surface emittance ( $E_i$ ) versus the net surface radiation ( $Q_{rad,i}$ ). These results show that the MRT correction method gives a better approximation to the exact solution.

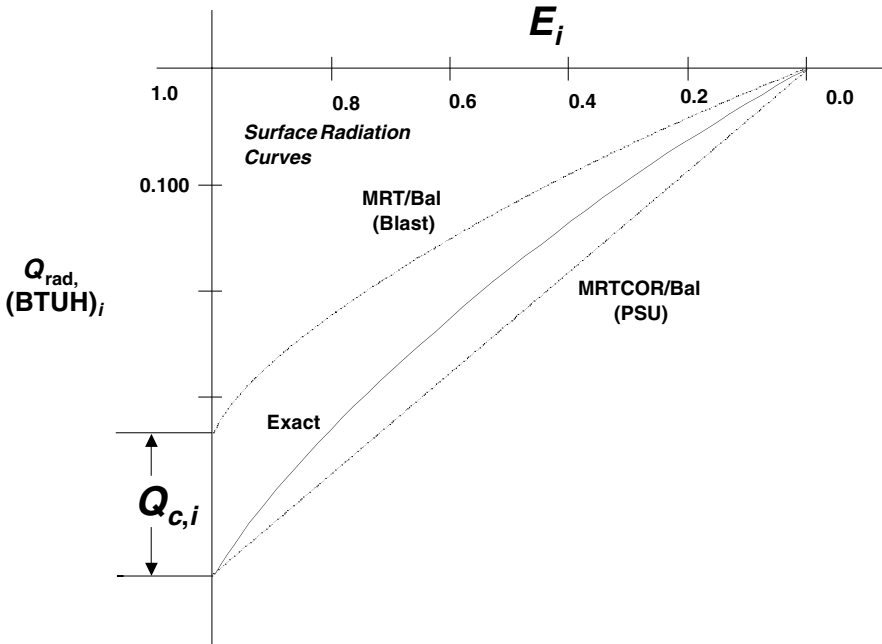


**FIGURE 3.23** Comparison of the various MRT methods to the exact solution.

**3.5.4.2 Case 2: Variation of One Surface Emittance with Other Surface Emittances Held Constant.** For case 2, a correction component  $Q_{ci}$  is developed for an enclosure where all surface emittances are held constant except one surface designated by  $a$ . If  $n$  is the total number of surfaces within the enclosure, surface  $a$  represents the single surface where emissivity is varied from 0.0 to 1.0, and surface  $i$  ( $i = 1, n; i \neq a$ ) represents the remaining surfaces of constant emissivity. Six curves are generated for six different values of  $\epsilon_i$ , holding  $\epsilon_i$  constant for each curve as  $\epsilon_a$  is varied

from 0.0 to 1.0. Figure 3.24 illustrates the actual arithmetic difference between the “MRT/balance” solution and the exact solution. This difference has been graphed at constant wall emittance ( $\epsilon_i$ ) values of 0.0, 0.2, 0.4, 0.6, 0.8, and 1.0 with surface  $a$  being the floor. The curves tend to reach a maximum value of  $Q_{ci}$  between floor emittances of 0.0 and 1.0.

The numerical solution for case 2 attempts to develop  $Q_{ci}$  error curves characteristic of the actual error curves shown in Fig. 3.24. Development of the MRT correction curves in Fig. 3.25 begins by plotting one known point on each curve (at  $\epsilon_i = \epsilon_a$ ) using Eq. (3.66) from case 1.

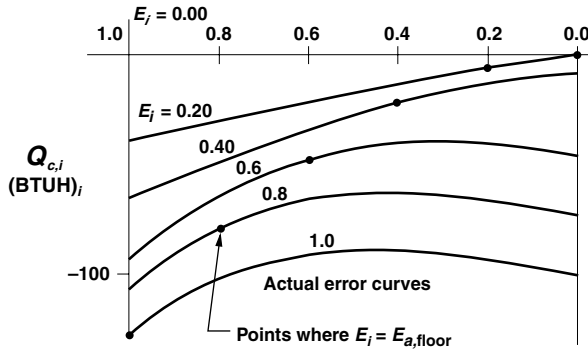


FIGURE 3.24 MRT correction curves.

The curves being developed must follow the nonlinear characteristics of the actual error curves shown in Fig. 3.25. Therefore, two endpoints and one midpoint are calculated for each curve. These three points are necessary to utilize nonlinear curve fitting techniques. The endpoints at ( $\epsilon_a = 1.0, \epsilon_i < 1.0$ ) are determined by extrapolation from the corresponding known points at  $\epsilon_i = \epsilon_a$ . Because the endpoint  $Q_{ci}$  at ( $\epsilon_a = 1.0, \epsilon_i = 1.0$ ) is determined directly rather than by extrapolation, three points for the curve of constant  $\epsilon_i = 1.0$  are determined first. The midpoint  $Q_{ci}$  at  $\epsilon_a = 0.4$  and the endpoint  $Q_{ci}$  at  $\epsilon_a = 0.0$  are calculated for the curve of constant  $\epsilon_i = 1.0$ .

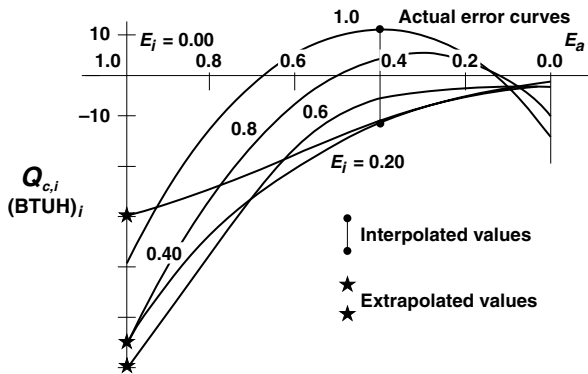


FIGURE 3.25 Developing MRT correction curve approximations.

The following equation is used to calculate the endpoint  $Q_{ci}$  at  $\varepsilon_a = 0.0$  and  $\varepsilon_i = 1.0$ :

$$Q_{ci} = \sigma A_i \left\{ T_{fi}^4 - \left[ \sum_{\substack{j \neq a \\ j \neq i}} \sigma T_j^4 F_{ij} + (\sigma T_k^4 F_{ak}) F_{ia} \right] \right\} \quad (3.67)$$

The following equation is used to calculate the midpoint  $Q_{ci}$  at  $\varepsilon_a = 0.4$  and  $\varepsilon_i = 1.0$ :

$$Q_{ci} = A_i (q_{\text{rad}, \text{exact}} - q_{\text{rad}, \text{MRT}}) \quad (3.68)$$

where:

$$q_{\text{rad}, \text{exact}} = \sigma T_i^4 - \sum_{j=1}^n \sigma T_i^4 F_{ij} - \left[ \varepsilon_a \sigma T_a^4 + (1 - \varepsilon_a) \sum_{k \neq a} \sigma T_k^4 F_{ak} \right] F_{ak} \quad (3.69)$$

and

$$q_{\text{rad}, \text{MRT}} = \sigma F_{ij} (T_i^4 - T_{fi}^4) \quad (3.70)$$

Equations (3.67) through (3.70) and the steps leading to these equations are explained by Steinman et al. (1989). Now, three points are known for the correction curve and  $\varepsilon_i = 1.0$ , and the midpoints and endpoints for the remaining five curves for  $\varepsilon_i < 1.0$  are determined by interpolation. Curves through each set of points are approximated by using curve fitting techniques. Simulation tests provided by Steinman et al. (1989) show that the MRT correction method shows improvement in the solution accuracy over the MRT method.

The correction component used in the MRT correction method produces results that are more accurate than the MRT method. The MRT correction method produces results within 1.4 percent of the exact solution for an L-shaped room (complex geometry), whereas results of the MRT method for an L-shaped room produced inaccuracies over 100 percent (Steinman et al., 1989). However, like the MRT method, the MRT correction method contains inaccuracies from the inequality of Eq. (3.63) used to linearize the radiative heat flux. In addition, the correction terms have not been proven for geometries and temperature conditions other than for those cases for which it was developed.

### 3.5.5 SIMPLIFIED RADIANT TRANSPORT FUNCTION

Radiant transport functions are complex, diverse, and different for each building because of transparency conditions in rooms. Nakamura (1989) developed a simplified radiant transport function that has been developed to overcome these difficulties and to obtain a systematic understanding of the entire system (Nakamura, 1989).

The *simplified radiant transport function* is defined as the radiant intensity at any point and in any direction, when radiant energy of amount 1 is emitted at a point and in a certain direction within an enclosure (Nakamura, 1989). The simplified radiant transport function at  $(\mathbf{p}, \mathbf{s})$  (point  $\mathbf{p}$  and direction  $\mathbf{s}$  at the surface) for emission at  $(\xi, \eta)$  (point  $\xi$  and direction  $\eta$  at the surface) is expressed as  $R(\xi, \eta; \mathbf{p}, \mathbf{s})$ . An enclosure containing radiant transfer through a nonparticipating medium is shown in Fig. 3.26. With a nonparticipating medium in the enclosure of Fig. 3.26, the incoming radiant intensity is equal to the outgoing radiant intensity.

$$I_0(\mathbf{p}, \mathbf{s}') = I_0(\mathbf{p}', \mathbf{s}') \quad (3.71)$$

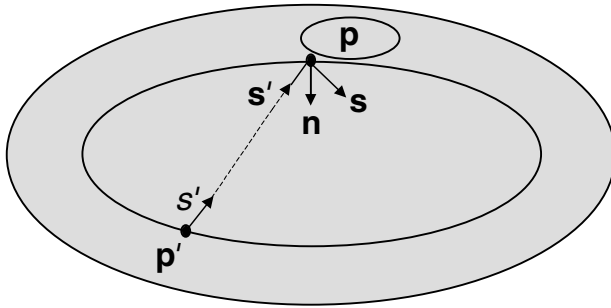


FIGURE 3.26 Schematic of the radiant transport function.

The radiant intensity for an area element on the boundary surface of the enclosure is:

$$I^*(\mathbf{p}, \mathbf{s}) = I_d(\mathbf{p}, \mathbf{s}) + \pi \int_{\Omega} r(\mathbf{p}, \mathbf{s}', \mathbf{s}) I^*(\mathbf{p}, \mathbf{s}') dF(\mathbf{p}, \mathbf{s}') \quad (3.72)$$

By introducing the Dirac delta function and by definition of the simplified radiant transport function, the basic equation for the simplified radiant transport function in an enclosure with radiant transfer through a nonparticipating medium is:

$$R(\boldsymbol{\varepsilon}, \boldsymbol{\eta} : \mathbf{p}, \mathbf{s}) = \delta(\mathbf{p} - \boldsymbol{\varepsilon}, \mathbf{s} - \boldsymbol{\eta}) + \pi \int_{\Omega} r(\mathbf{p}, \mathbf{s}', \mathbf{s}) R(\boldsymbol{\varepsilon}, \boldsymbol{\eta} : \mathbf{p}', \mathbf{s}') dF(\mathbf{p}, \mathbf{s}') \quad (3.73)$$

The simplified radiant transport function can be extended to the case of diffuse reflection and emission at the surface. In addition, an equation can be derived for an enclosure with an absorbing and emitting medium (Nakamura, 1989). Conduction and convection can be incorporated into the simplified radiant transport function and applied to enclosures of complex geometry. The simplified radiant transport function for an enclosure with a nonparticipating medium is a *Fredholm integral equation of the second kind*. Some solutions for the Fredholm integral equation of the second kind can be found by successive substitution and successive approximation of the temperature distribution and/or radiant intensity on the surfaces (Nakamura, 1989).

### 3.5.6 SUMMARY

Each of the methods described in this section was used to analyze radiant heat exchange within occupied spaces. However, each method includes constraints and, in some cases, oversimplifications. If the user does not fully understand and satisfy these constraints, analysis errors can be very large. The next section discusses the radiative transfer equation, which eliminates many of the assumptions and, hence, pitfalls of the simplified methods described in this section.

## 3.6 THE RADIATIVE TRANSFER EQUATION— THE MOST GENERAL APPROACH

This portion covers the radiative transfer equation and various techniques for solving the radiative transfer equations (RTE). The RTE is the most general technique

for modeling and predicting radiative heat transfer in an enclosed space. Solving this equation does not require knowledge of view factors. In fact, view factors can be calculated by solving the radiative heat transfer. There is a drawback to this equation: it is very difficult to solve without the use of a computer simulation. Several computer solution techniques have been developed over the last several decades.

The RTE solves directly for the radiant intensity at each point in the enclosed space, at each wavelength, and in each direction. Once the intensity “field” is known, the local radiant heat fluxes can be calculated by integrating the intensity over the solid angle. This process sounds very complex, and indeed it is. The reader needs to be patient at this point, because a computer solution for the RTE will be explained in the following sections.

The general form of the RTE (Viskanta and Mengüç, 1987; Siegel and Howell, 1981; Özisik, 1977) is given by:

$$\begin{aligned}
 (\nabla \cdot \vec{\Omega})I_{\lambda}(\vec{r}, \vec{\Omega}) = & \mu \frac{\partial I_{\lambda}}{\partial x} + \xi \frac{\partial I_{\lambda}}{\partial y} + \eta \frac{\partial I_{\lambda}}{\partial z} = -(\kappa_{\lambda} + \sigma_{s\lambda})I_{\lambda} + \kappa_{\lambda}I_{b\lambda} \\
 & + \frac{\sigma_{s\lambda}}{4\pi} \int_{\Omega'} \Phi(\Omega' \rightarrow \Omega)I_{\lambda}(\Omega')d\Omega'
 \end{aligned}
 \tag{3.74}$$

The intensities and properties in Eq. (3.74) have the subscript  $\lambda$  to designate that each quantity is a function of wavelength. The first term in the equation represents the spatial distribution of the radiant intensity. The variables  $\mu$ ,  $\xi$ , and  $\eta$  are the directional cosines that describe the direction of the radiant intensity. The variables  $\kappa$  and  $\sigma$  represent the medium absorption coefficient and the medium scattering coefficient.

The absorption coefficient can be as small as zero and as unbounded at the upper end. The higher the absorption coefficient, the “thicker” the medium behaves toward radiation. As a medium becomes thicker, it “participates” in the radiation exchange process. The participating medium can either increase or decrease the intensity magnitude. As we will soon see, the increase or decrease in the intensity magnitude depends on the absorption coefficient, the medium temperature, the temperature of the surrounding surfaces, and the magnitude of the intensity. The absorption coefficient can normally be assumed to be negligible except in the case of very high humidity cases. These cases are discussed in more detail later in the book.

The scattering coefficient is probably one of the least understood parameters in the radiant heat transfer field. The scattering coefficient describes how the intensity in a specific direction is scattered into a different direction. The intensity from a different direction can also be scattered into the direction of concern. Although the scattering coefficient is important in industrial processes such as glass making, it has little relevance in the built environment and can be assumed to be zero with little concern.

For the special case of a typical occupied room in which the absorption and scattering coefficients can be assumed zero, the equation reduces to the form:

$$\mu \frac{\partial I}{\partial x} + \xi \frac{\partial I}{\partial y} + \eta \frac{\partial I}{\partial z} = 0
 \tag{3.75}$$

The boundary conditions for Eq. (3.75) are developed by considering the energy emitted by the boundary and the incident radiant energy reflected by the boundary. If the boundary is considered to be a diffuse emitter and absorber and the incident

radiation is transmitted through the boundary surface, the boundary conditions are written as:

$$\begin{aligned} I_{\lambda, \text{bound}} &= \varepsilon_{\lambda} I_{b,\lambda} + \frac{\rho_{\lambda}}{\pi} \int_{n \cdot \Omega' < 0} |n \cdot \Omega'| I_{\lambda}(\Omega') d\Omega' \\ &= \varepsilon_{\lambda} I_{b,\lambda} + \frac{(1 - \varepsilon_{\lambda} - \tau_{\lambda})}{\pi} \int_{n \cdot \Omega' < 0} |n \cdot \Omega'| I_{\lambda}(\Omega') d\Omega' \end{aligned} \quad (3.76)$$

To solve this nonlinear equation, there are several solution methods discussed in the following paragraphs.

### 3.7 SOLUTION TECHNIQUES FOR THE RTE

There are many methods to solve the RTE. The choice of a solution method is a careful balance between accurate results and low computational time. The three methods presented here are well documented by other sources. The first two descriptions briefly describe well-known solution methods that, to the authors' knowledge, are not used by the HVAC community. The discrete ordinates method is used by the Building Comfort Analysis Program methodology (Jones and Chapman, 1994; Chapman and Zhang, 1995, 1996; Chapman et al., 1997) and is, therefore, described in more detail.

#### 3.7.1 SPHERICAL HARMONICS METHOD

This method turns the RTE into simple partial differential equations that can be solved similar to conservation equations (Modest, 1993). The  $P_1$  approximation is not very accurate near boundaries or for large temperature gradients in the medium. Although the  $P_3$  approximation yields more accurate results, the computational time is increased (Viskanta and Ramadhyani, 1988; Viskanta and Mengüç, 1987; Khalil, 1982).

#### 3.7.2 MONTE CARLO METHOD

The Monte Carlo method is not strictly a radiative heat transfer solution method; rather, it is a statistical method to trace the history of a package of radiant energy as it travels from the point of emission to the point of absorption (Modest, 1993). The Monte Carlo method is usually used with the zone method. The zone method divides the enclosure into a finite number of isothermal surface area zones. The area of the surface must be small enough to justify the approximation of isothermal.

A beam of radiation from a point source on the surface is emitted in a random solid angle and traced until it hits a surface. A statistical method, such as Monte Carlo, is used to determine if the beam is absorbed or reflected. For the Monte Carlo method to yield accurate results, at least 1000 packages of energy per surface must be emitted. The main disadvantage of the Monte Carlo method is that it inherently includes statistical error (Modest, 1993) and can be computationally intensive.

#### 3.7.3 DISCRETE ORDINATES MODELING

The discrete ordinates method was first applied to neutron transport theory and is described by Carlson and Lathrop (1963). The discrete ordinates method is used by

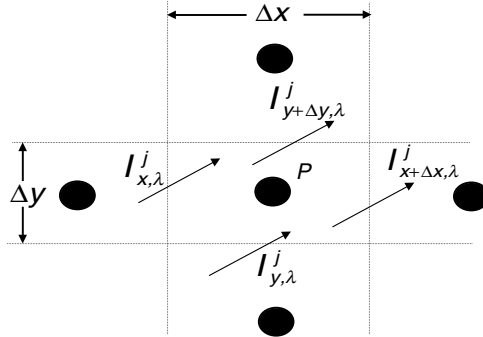


FIGURE 3.27 Integrating the RTE.

the BCAP methodology (Jones and Chapman, 1994; Chapman and Zhang, 1995, 1996; Chapman et al., 1997), considers discrete directions and nodes on the surface, and calculates the radiant intensity at each point and direction. The enclosure space is divided into control volumes as shown in Fig. 3.27. Increasing the number of control volumes increases accuracy. Equation (3.75) is integrated over each three-dimensional control volume. The resulting equation for a gray surface in a discrete direction,  $j$  is:

$$\int_z^{z+\Delta z} \int_y^{y+\Delta y} \int_x^{x+\Delta x} \left[ \mu \frac{\partial I^j}{\partial x} + \xi \frac{\partial I^j}{\partial y} + \eta \frac{\partial I^j}{\partial z} \right] dx dy dz = 0 \quad (3.77)$$

The order of the discrete ordinates method designates the number of directions for  $j$  as well as the particular directions. Higher orders of approximation have more prescribed directions and can increase the accuracy of the results. However, the larger order approximations require more computational time.

The intensity along one side of the control volume is assumed to be independent of the other two directions. For example, the intensity along the  $x$  interface is not affected by the  $y$  and  $z$  direction (Patankar, 1980). Equation (3.77) then becomes:

$$\mu^j \Delta z \Delta y (I_{x+\Delta x}^j - I_x^j) + \xi^j \Delta z \Delta x (I_{y+\Delta y}^j - I_y^j) + \eta^j \Delta x \Delta y (I_{z+\Delta z}^j - I_z^j) = 0 \quad (3.78)$$

This equation contains six interface intensities. By assuming that the intensity profile across the control volume is linear, the intensity at the center of the control volume, point  $p$ , is (Truelove, 1988; Fiveland, 1988):

$$I_p^j = \alpha I_{x+\Delta x}^j + (1 - \alpha) I_x^j = \alpha I_{y+\Delta y}^j + (1 - \alpha) I_y^j = \alpha I_{z+\Delta z}^j + (1 - \alpha) I_z^j \quad (3.79)$$

The interpolation factor  $\alpha$  is set equal to one to avoid negative intensities that are physically impossible and yield unstable solutions. Some researchers chose values of  $\alpha$  less than one with the idea that the solution will be more accurate. However, whenever  $\alpha < 1$ , some consideration must be given to handling negative intensities, which are physically impossible. Fiveland (1984, 1988) reports that  $\alpha = 1$  will always provide positive intensities. Substituting Eq. (3.79) into Eq. (3.78) yields:

$$I_p^j = \frac{\mu^j \Delta z \Delta y I_x^j + \xi^j \Delta z \Delta x I_y^j + \eta^j \Delta x \Delta y I_z^j}{\mu^j \Delta z \Delta y + \xi^j \Delta z \Delta x + \eta^j \Delta x \Delta y} \quad (3.80)$$

Equation (3.80) is written for all the discrete directions for each control volume. For the  $S_4$  approximation, there are 24 discrete directions. The values for  $\mu^j$ ,  $\xi^j$ , and  $\eta^j$

must satisfy the integral of the solid angle over all the directions, the half-range flux, and the diffusion theory (Truelove, 1987, 1988). Table 3.3 gives the values for  $\mu^i$ ,  $\xi^j$ , and  $\eta^j$  for the first quadrant that satisfy these conditions. A complete table of values satisfying these conditions is tabulated and available from Fiveland (1988) and Chapman (1992).

**TABLE 3.3** First-Quadrant Values for Directional Cosines and Weighting Factor

Ordinate direction	$\mu^i$	$\xi^j$	$\eta^j$	$w^j$
1	0.2959	0.9082	0.2959	0.5236
2	0.9082	0.9082	0.2959	0.5236
3	0.2959	0.2959	0.9082	0.5236

The values for  $\Delta x$ ,  $\Delta y$ , and  $\Delta z$  are determined by the size of the control volume. The values for  $I_x^i$ ,  $I_y^j$ , and  $I_z^k$  are known from the previous iteration. Initially, the intensities are set to guessed values. The solution is iterative around a loop from  $p = 1$  to  $p$  equals the total number of control volumes until the solution converges.

Once the radiant intensity is known, the incident radiative heat flux on a surface can be written as (Siegel and Howell, 1981):

$$q_{\text{rad}} = \int_{\Omega'} \mathbf{n} \cdot \Omega' I(\Omega') d\Omega' \tag{3.81}$$

For a radiant heat flux in the  $x$  direction, Eq. (3.81) is approximated by using a quadrature (Fiveland, 1988) and becomes:

$$q_{\text{rad}} = \sum_j \mu^j I^j w^j \tag{3.82}$$

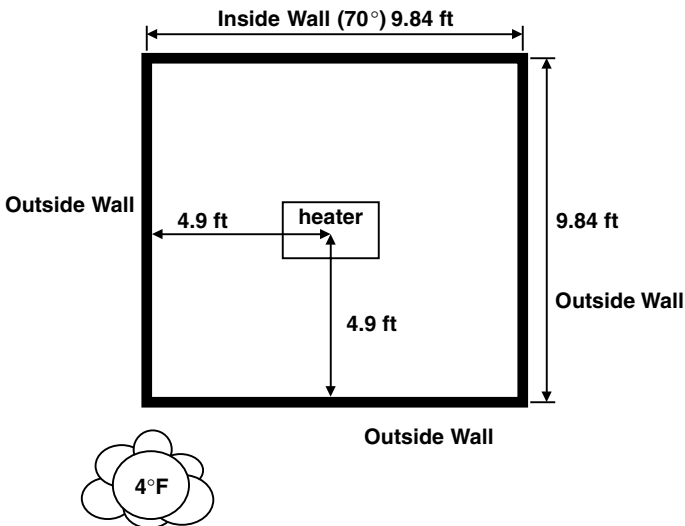


**FIGURE 3.28** Configuration for Example 3.8.

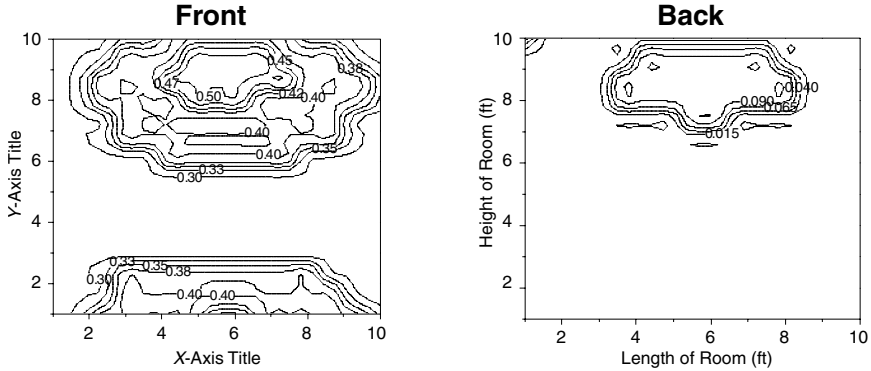


**FIGURE 3.29** Results from Example 3.8.

The values for  $w^i$  are given in Table 3.3. A complete list of the values is available in Fiveland (1988) and Chapman (1992). This value for  $w^i$  can be used to solve Eq. (3.82).

The discrete ordinates method has been studied and found to be accurate by Fiveland (1987, 1988), Fiveland and Jamaluddin (1989), Truelove (1987, 1988), Jamaluddin and Smith (1988), Sanchez and Smith (1992), and Yücel (1989). The  $S_4$  approximation has been found to be a reasonable compromise between accurate results and a low computational time (Fiveland, 1988; Jamaluddin, 1988). In addition, Fiveland (1984) reported the discrete ordinates method gave more accurate and faster solutions than the  $P_3$  and zonal solutions. For these reasons, it is used extensively in the calculations throughout the rest of this Handbook. It is a very general technique that requires little information about the room.

**EXAMPLE 3.8** Use the discrete ordinates method on the accompanying disk to calculate the wall radiant heat flux distribution on an exterior wall and an interior wall of a room. The room has three sides exposed to outside conditions, which are  $-4^\circ\text{F}$ . The remaining wall is an interior with an adjacent temperature of  $69.8^\circ\text{F}$ . This room configuration, shown in Fig. 3.28, was chosen for its simplicity. There are no windows or doors in this room. The room is a 10-ft cube.

The discrete ordinates model was used to generate the contour plots in Fig. 3.29. The  $x$  and  $y$  axis are the length and height of the room, respectively. The variations in the heat flux on both of the walls can be seen in these plots. The lines represent lines of constant heat flux, and the numbers on the line are the heat flux in  $\text{Btu/h}$ . The front wall, the plot on the right hand side of Fig. 3.29, is an exterior wall and the back wall; the plot on the left hand side of Fig. 3.29, is an interior wall. There is a noticeable difference between the two walls, which is due to the difference in adjoining temperatures. The front wall has a larger temperature difference across it than the back wall. This larger temperature difference causes the increased heat flux on this wall.



---

# CHAPTER 4

---

## MULTIMODAL HEAT TRANSFER

---

Multimodal heat transfer is the integration of convection, conduction, and radiation heat transfer into a complete heat transfer analysis system. Although the fundamental concepts of each heat transfer mode were covered in Chaps. 2 and 3, this chapter discusses techniques to analyze combined heat transfer cases.

Radiant systems necessarily include the effect of all three heat transfer modes. Figure 4.1 demonstrates all three modes of heat transfer in a radiantly heated room. *Radiation heat transfer* exists between all the surfaces of a room. Radiation is especially evident from the radiant panel to the other room surfaces. *Convection heat transfer* occurs between the room surfaces and the enclosed room air. *Conduction heat transfer* occurs through the walls to the outside environment. The focus of this chapter is to discuss methods that can be used to solve the multimodal heat transfer problem.

### 4.1 SOLUTION TECHNIQUES

---

Figure 4.2 shows a wall segment experiencing radiation, convection, and conduction heat transfer. The inside surface of the wall emits radiant energy, absorbs radiant energy incident on the surface, convects energy to or from the room air, and conducts energy from the inside wall surface to the outside wall surface. The energy balance on the inside wall surface is:

$$\alpha G - \varepsilon E_b + q_{\text{conv}} - q_{\text{cond}} = 0 \quad (4.1)$$

All incoming energy into the surface is considered positive and all outgoing energy is considered negative. Equation (4.1) can be written in terms of the surface temperature by inserting the definitions of each heat transfer mode. The equation becomes:

$$\alpha G - \varepsilon \sigma T_s^4 + h(T_{\text{air}} - T_s) - \frac{T_s - T_o}{R_{\text{th}}} = 0 \quad (4.2)$$

The term  $R_{\text{th}}$  is the wall thermal resistance and  $T_o$  is the outside temperature. The term  $G$  is the incident radiative heat flux from the other surfaces in the room.

If the wall properties, convection coefficient, air temperature, and incident radiation are known or can be calculated, then the wall surface temperature can be calculated from Eq. (4.2). Of course, Eq. (4.2) must be applied to each surface individually.

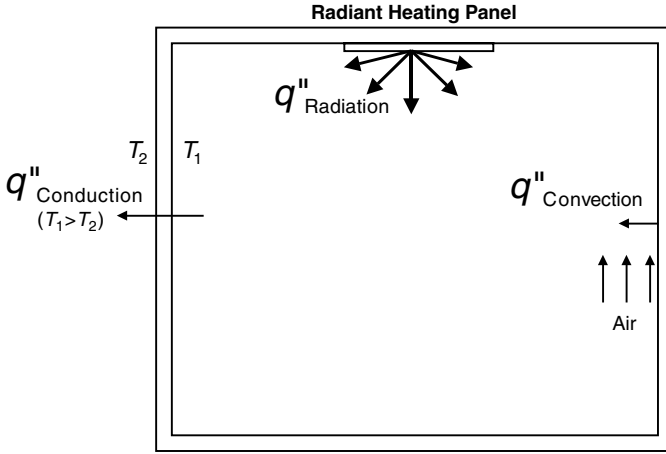


FIGURE 4.1 Radiantly heated room demonstrating multimodal heat transfer.

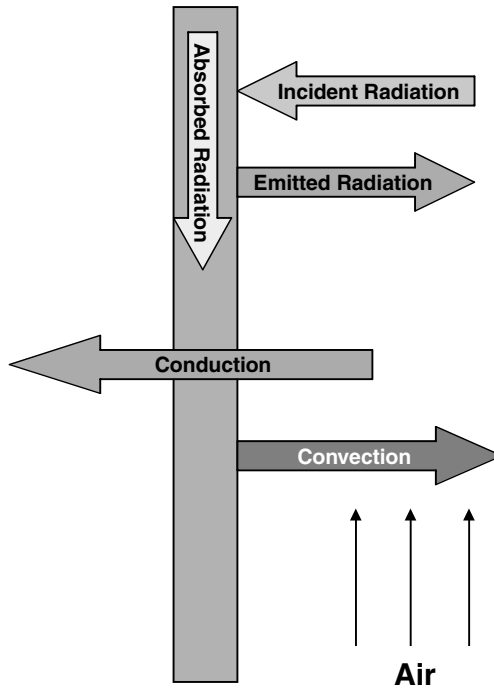


FIGURE 4.2 Surface energy balance with radiation, convection, and conduction heat transfer.

The savvy reader will realize that the incident radiation depends on the other wall surface temperatures. Consider the two surfaces in Fig. 4.3. The air temperature between the two surfaces is 70°F (21.4°C), and the outside surface temperature is 20°F (-6.3°C). The  $R$  value of surface 1 is 19 and the  $R$  value of surface 2 is 10. The goal is to determine the temperature of each inside wall surface. If conditions are such that Kirchhoff’s law applies, then each surface’s emissivity equals the absorptivity. Now apply Eq. (4.2) to surface 2. To do so, you must assume a value for the incident radiation. In this made-up case, we need to assume a temperature for surface 2 and then calculate the emission from that surface. Once this is done, we are free to calculate the temperature of surface 1. Now we repeat the process for surface 2. As before, the incident radiation for this surface is the emission from surface 1. We now have a temperature at which to calculate the emission. We do this and then proceed to calculate the temperature of surface 2. It will most undoubtedly be different from the temperature we assumed earlier in the process. Hence, this is an iterative process.

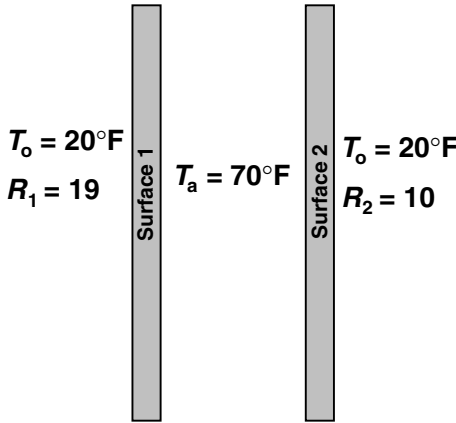


FIGURE 4.3 Schematic of the room used in the example problem.

The preceding example is a simple demonstration of how complex multimodal heat transfer analysis can become. But we are not yet done. To make it more complete, one needs to consider the energy balance of the air enclosed in the room. This energy balance is:

$$\sum_{i=1}^n h(T_{si} - T_{air}) = 0 \tag{4.3}$$

Heat transfer from each surface to the air enclosed by those surfaces

This equation shows that the air temperature needs to be known to calculate the surface temperatures, but then the surface temperatures need to be known to calculate the air temperature. This appears to be a situation of “which comes first, the chicken or the egg?”

It turns out that it does not matter as long as one proceeds in a methodical manner. The general procedure suggested here is the following:

1. Guess all unknown temperatures except one.
2. Calculate the one unknown temperature from the governing equations, either Eq. (4.2) or Eq. (4.3).
3. Use this calculated temperature to recalculate one by one the previously guessed temperatures.
4. Compare each calculated temperature with the previously guessed value.
5. Keep calculating until the calculated values equal the previous values within some preset error tolerance.

This general methodology is demonstrated in the following example.

**EXAMPLE 4.1** Figure 4.4 illustrates a cubic room with 8-ft dimensions and the ceiling as a radiant heating panel. The air is stagnant, and the outside temperature is 20°F (−6.3°C). The energy input into the ceiling is 400 W. In this example, the entire ceiling is treated as a radiant heater to simplify the calculations. The reader should note that in a practical case, the radiant heater would not extend to the walls. The convection coefficients from each outside surface to the ambient is 10 Btu/(h · ft<sup>2</sup> · °F). Calculate the temperature of each inside and outside surface, and the air temperature. View factors are used for the radiation calculations so that the methodology can be better demonstrated. Heat transfer correlations from Chap. 3 are used for each of the inside surfaces. The R value of each surface is 19.

$$L = 8 \text{ ft}$$

$$W = 8 \text{ ft}$$

$$F_{ij} = 0$$

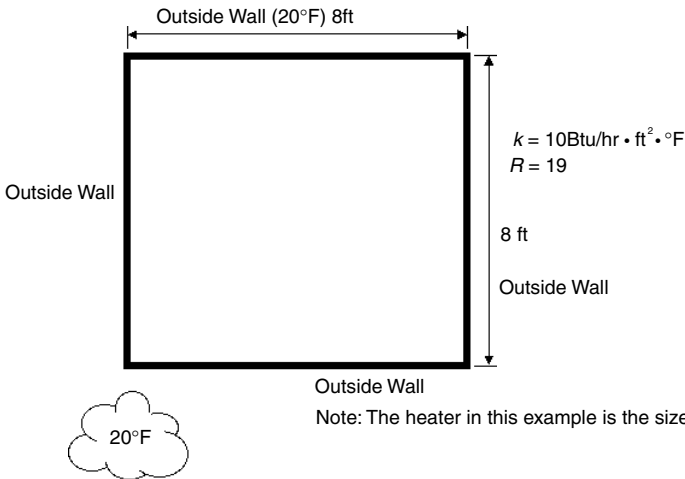


**FIGURE 4.4** Room geometry for Example 4.1.

$$\varepsilon_l = 0$$

$$R_w = 19 \cdot \frac{h \cdot ft^2 \cdot {}^\circ R}{Btu}$$

$$h_i = 5 \cdot \frac{Btu}{h \cdot ft^2 \cdot {}^\circ R}$$

$$\varepsilon_2 = \varepsilon_l$$

$$R_l = R_w$$

$$h_l = h_i$$

$$h_2 = h_i$$

$$\varepsilon_3 = \varepsilon_l$$

$$R_2 = R_w$$

$$h_3 = h_i$$

$$h_4 = h_i$$

$$h_e = 10 \cdot \frac{Btu}{h \cdot ft^2 \cdot {}^\circ R}$$

$$\varepsilon_4 = \varepsilon_i$$

$$R_3 = R_w$$

$$h_5 = h_i$$

$$h_6 = h_i$$

$$Q_{heater} = 400 \cdot \frac{Btu}{h}$$

$$R_4 = R_w$$

$$\varepsilon_5 = \varepsilon_l$$

$$\sigma = 0.171410^{-8} \cdot \frac{Btu}{h \cdot ft^2 \cdot {}^\circ R^4}$$

$$A = L \cdot W$$

$$A_l = A$$

$$R_5 = R_w$$

$$\varepsilon_6 = \varepsilon_l$$

$$A_2 = A_l$$

$$A_3 = A_l$$

$$R_6 = R_w$$

$$A_4 = A_I$$

$$A_5 = A_I$$

$$A_6 = A_I$$

Equations:

$$\dot{Q}_{conv_{1i}} = h_i A_1 (T_{air} - T_{1i})$$

$$\dot{Q}_{conv_{2i}} = h_i A_2 (T_{air} - T_{2i})$$

$$\dot{Q}_{conv_{3i}} = h_i A_3 (T_{air} - T_{3i})$$

$$\dot{Q}_{conv_{4i}} = h_i A_4 (T_{air} - T_{4i})$$

$$\dot{Q}_{conv_{5i}} = h_i A_5 (T_{air} - T_{5i})$$

$$\dot{Q}_{conv_{6i}} = h_i A_6 (T_{air} - T_{6i})$$

$$\dot{Q}_{conv_{1e}} = h_e A_1 (T_{1e} - T_o)$$

$$\dot{Q}_{conv_{2e}} = h_e A_2 (T_{2e} - T_o)$$

$$\dot{Q}_{conv_{3e}} = h_e A_3 (T_{3e} - T_o)$$

$$\dot{Q}_{conv_{4e}} = h_e A_4 (T_{4e} - T_o)$$

$$\dot{Q}_{conv_{5e}} = h_e A_5 (T_{5e} - T_o)$$

$$\dot{Q}_{conv_{6e}} = h_e A_6 (T_{6e} - T_o)$$

Wall 1 energy balance (inside surface):

$$\dot{Q}_{conv_1} + \dot{Q}_{rad_1} = \dot{Q}_{cond_1}$$

$$\dot{Q}_{conv_2} + \dot{Q}_{rad_2} = \dot{Q}_{cond_2}$$

$$\dot{Q}_{conv_3} + \dot{Q}_{rad_3} = \dot{Q}_{cond_3}$$

$$\dot{Q}_{conv_4} + \dot{Q}_{rad_4} = \dot{Q}_{cond_4}$$

$$\dot{Q}_{conv_5} + \dot{Q}_{rad_5} = \dot{Q}_{cond_5}$$

$$\dot{Q}_{conv_6} + \dot{Q}_{rad_6} = \dot{Q}_{cond_6}$$

$$\dot{Q}_{cond_1} = \frac{T_{1i} - T_{1e}}{R_1}$$

$$\dot{Q}_{cond_2} = \frac{T_{2i} - T_{2e}}{R_2}$$

$$\dot{Q}_{cond_3} = \frac{T_{3i} - T_{3e}}{R_3}$$

$$\dot{Q}_{cond_4} = \frac{T_{4i} - T_{4e}}{R_4}$$

$$\dot{Q}_{cond_5} = \frac{T_{5i} - T_{5e}}{R_5}$$

$$\dot{Q}_{cond_6} = \frac{T_{6i} - T_{6e}}{R_6}$$

$$Q_{conv_1}(T_{li}, T_{air}) = h \cdot A \cdot (T_{air} - T_{li})$$

$$Q_{rad_1}(T_k, T_{li}) = \sum_{k=1}^6 F_{k1} \cdot A_1 \cdot \sigma \cdot (T_k^d - T_{li}^d) \epsilon_1$$

$$Q_{conv_2}(T_{2i}, T_{air}) = h \cdot A \cdot (T_{air} - T_{2i})$$

$$Q_{rad_2}(T_k, T_{2i}) = \sum_{k=1}^6 F_{k2} \cdot A_2 \cdot \sigma \cdot (T_k^d - T_{2i}^d) \epsilon_2$$

$$Q_{conv_3}(T_{3i}, T_{air}) = h \cdot A \cdot (T_{air} - T_{3i})$$

$$Q_{rad_3}(T_k, T_{3i}) = \sum_{k=1}^6 F_{k3} \cdot A_3 \cdot \sigma \cdot (T_k^d - T_{3i}^d) \epsilon_3$$

$$Q_{conv_4}(T_{4i}, T_{air}) = h \cdot A \cdot (T_{air} - T_{4i})$$

$$Q_{rad_4}(T_k, T_{4i}) = \sum_{k=1}^6 F_{k4} \cdot A_4 \cdot \sigma \cdot (T_k^d - T_{4i}^d) \epsilon_4$$

$$Q_{conv_5}(T_{5i}, T_{air}) = h \cdot A \cdot (T_{air} - T_{5i})$$

$$Q_{rad_5}(T_k, T_{5i}) = \sum_{k=1}^6 F_{k5} \cdot A_5 \cdot \sigma \cdot (T_k^d - T_{5i}^d) \epsilon_5$$

$$Q_{conv_6}(T_{6i}, T_{air}) = h \cdot A \cdot (T_{air} - T_{6i})$$

$$Q_{rad_6}(T_k, T_{6i}) = \sum_{k=1}^6 F_{k6} \cdot A_6 \cdot \sigma \cdot (T_k^d - T_{6i}^d) \epsilon_6$$

Guess:

$$T_1 = 500^\circ R$$

$$T_2 = 500^\circ R$$

$$T_3 = 500^\circ R$$

$$T_4 = 500^\circ R$$

$$T_5 = 500^\circ R$$

$$T_6 = 550^\circ R$$

$$T_{air} = 535^\circ R$$

$$T_0 = 456^\circ R$$

Given:

$$h_i \cdot A_1 \cdot (T_{air} - T_1) + \varepsilon \cdot (\sigma \cdot A_1) \left\{ \sum_{j=1}^6 F_{ij} \cdot [(T_j^f - T_1^f)] \right\} = \frac{(T_1 - T_0) \cdot A_1}{\left( R_w + \frac{I}{h_c} \right)}$$

When this equation is expanded, you can see just how involved this type of problem can be, and how the use of computers can easily reduce the amount of work required to solve them.

$$\begin{aligned} h_1 \cdot A_1 \cdot (T_{air} - T_1) + F_{21} \cdot A_1 \cdot \varepsilon_1 \cdot \sigma \cdot (T_2^f - T_1^f) + F_{31} \cdot A_1 \cdot \varepsilon_1 \cdot \sigma \cdot (T_3^f - T_1^f) \\ + F_{41} \cdot A_1 \cdot \varepsilon_1 \cdot \sigma \cdot (T_4^f - T_1^f) + F_{51} \cdot A_1 \cdot \varepsilon_1 \cdot \sigma \cdot (T_5^f - T_1^f) \\ + F_{61} \cdot A_1 \cdot \varepsilon_1 \cdot \sigma \cdot (T_6^f - T_1^f) = \frac{T_1 - T_0}{R_1 + \frac{I}{h_e \cdot A_1}} \end{aligned}$$

$$h_i \cdot A_2 \cdot (T_{air} - T_2) + \varepsilon \cdot (\sigma \cdot A_2) \cdot \left\{ \sum_{j=1}^6 F_{ij} \cdot [(T_j^f - T_2^f)] \right\} = \frac{(T_2 - T_0) \cdot A_2}{\left( R_w + \frac{I}{h_c} \right)}$$

$$h_i \cdot A_3 \cdot (T_{air} - T_3) + \varepsilon \cdot (\sigma \cdot A_3) \cdot \left\{ \sum_{j=1}^6 F_{ij} \cdot [(T_j^f - T_3^f)] \right\} = \frac{(T_3 - T_0) \cdot A_3}{\left( R_w + \frac{I}{h_c} \right)}$$

$$h_i \cdot A_4 \cdot (T_{air} - T_4) + \varepsilon \cdot (\sigma \cdot A_4) \cdot \left\{ \sum_{j=1}^6 F_{ij} \cdot [(T_j^f - T_4^f)] \right\} = \frac{(T_4 - T_0) \cdot A_4}{\left( R_w + \frac{I}{h_c} \right)}$$

$$h_i \cdot A_5 \cdot (T_{air} - T_5) + \varepsilon \cdot (\sigma \cdot A_5) \cdot \left\{ \sum_{j=1}^6 F_{ij} \cdot [(T_j^f - T_5^f)] \right\} = \frac{(T_5 - T_0) \cdot A_5}{\left( R_w + \frac{I}{h_c} \right)}$$

$$\left( h_i \cdot A_6 \cdot (T_{air} - T_6) + \varepsilon \cdot (\sigma \cdot A_6) \cdot \left\{ \sum_{j=1}^6 F_{ij} \cdot [(T_j^f - T_6^f)] \right\} \right) + Q_{heater} = 0$$

$$\sum_{j=1}^6 h_i \cdot A_j \cdot (T_{air} - T_j) = 0$$

Find:  $(T_1, T_2, T_3, T_4, T_5, T_6, T_{air})$

$$T_1 = 537.14^\circ R$$

$$T_2 = 537.14^\circ R$$

$$T_3 = 537.14^\circ R$$

$$T_4 = 537.14^\circ R$$

$$T_5 = 537.14^\circ R$$

$$T_6 = 541.707^\circ R$$

$$T_{air} = 541.38^\circ R$$

Although this problem simplifies the situation in that all  $R$  values will not be the same and the view factors would normally be more complicated, the problem is still very difficult to solve. When realistic room specifications are used, such as differing  $R$  values and varying view factors, this problem becomes much more involved, tedious, and difficult to solve by hand. In a problem like this, there could be 30 or more view factors to calculate, before even attempting the equations. The use of a program such as BCAP or ABOVE™ greatly simplifies this drawn-out process.



---

# CHAPTER 5

---

## PSYCHROMETRICS AND MIXTURES

---

A chapter on psychrometrics and mixtures is included in this Handbook for two reasons: (1) Psychrometrics are important for determining the dew point temperature and condensation issues that are associated with radiant cooling, and (2) mixtures are important for determining the airborne concentrations of contaminants such as carbon dioxide (CO<sub>2</sub>) and carbon monoxide (CO). Air by its very nature is a mixture of several gases. Dry air is commonly modeled as a combination of oxygen (O<sub>2</sub>), nitrogen (N<sub>2</sub>), argon (Ar), and CO<sub>2</sub>. On a volumetric basis, dry air contains 20.95 percent O<sub>2</sub>, 78.09 percent N<sub>2</sub>, 0.93 percent Ar, and 0.03 percent CO<sub>2</sub> (Van Wylen and Sonntag, 1978). The analysis becomes slightly more complicated when the air contains water vapor.

The goal of this chapter is to give the reader the necessary tools to calculate volume fractions of contaminants and dew point temperatures in the occupied space. The last part of the chapter discusses some consequences of heating and cooling humid air, concentrating on how much the air must be dehumidified or humidified.

### 5.1 GAS MIXTURES

---

The primary measurement of the concentration of one gas species in a gas mixture is the mole fractions ( $y_i$ ). By definition, the mole fraction of a gas species in a mixture of gases is:

$$y_i = \frac{N_i}{N_m} \quad (5.1)$$

The variable  $N_i$  is the number of moles of species  $i$  in the mixture and  $N_m$  is the total number of moles of gas in the mixture. Consider a container that has a mixture of CO<sub>2</sub> and O<sub>2</sub>. In the mixture, there is 1 mol of CO<sub>2</sub> and 0.5 mol of O<sub>2</sub>. By using Eq. (5.1), the mole fractions of each specie is:

$$y_{O_2} = \frac{0.5 \text{ mol}}{1 \text{ mol} + 0.5 \text{ mol}} = 0.333 = 33.3 \text{ percent} \quad (5.2)$$

$$y_{N_2} = \frac{1 \text{ mol}}{1 \text{ mol} + 0.5 \text{ mol}} = 0.66 = 66.7 \text{ percent}$$

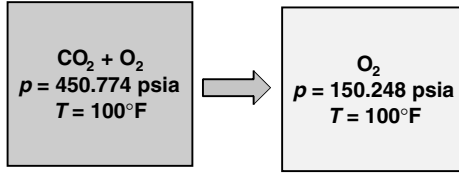


FIGURE 5.1 Gas mixture in a 2-ft<sup>3</sup> container.

Figure 5.1 illustrates the gases in the previous example in a 2-ft<sup>3</sup> container. The temperature of the mixture is 100°F and the pressure is 450.774 psia. Assume for a moment that we can extract all of the CO<sub>2</sub> with a special syringe so that only the O<sub>2</sub> molecules remain in the container. What would change? The gas temperature and the volume of the container would stay the same. We can use the ideal gas law to calculate the pressure without the CO<sub>2</sub> molecules. Doing so, we find that the pressure of just the oxygen is:

$$p_{\text{O}_2} = \frac{N_{\text{O}_2} R_u T}{V} = \frac{(0.5 \text{ mol})(560^\circ\text{R})}{20 \text{ ft}^3} \left( \frac{10.732 \text{ psia} \cdot \text{ft}^3}{\text{mol} \cdot ^\circ\text{R}} \right) = 150.248 \text{ psia} \quad (5.3)$$

Now we return the CO<sub>2</sub> molecules to the container and remove the O<sub>2</sub> molecules. The pressure of just the N<sub>2</sub> is:

$$p_{\text{N}_2} = \frac{N_{\text{N}_2} R_u T}{V} = \frac{(1 \text{ mol})(560^\circ\text{R})}{20 \text{ ft}^3} \left( \frac{10.732 \text{ psia} \cdot \text{ft}^3}{\text{mol} \cdot ^\circ\text{R}} \right) = 300.496 \text{ psia} \quad (5.4)$$

These pressures are called the *partial pressures of the gas species in the gas mixture*. By definition, they are the pressures that would exist if all of the other gases were removed from the mixture, keeping the temperature and volume the same. Note that the sum of these two partial pressures equals the total mixture pressure. This equivalency is more than a coincidence. It turns out that the partial pressures are related to the total mixture pressure through the mole fractions by:

$$\left. \begin{aligned} p_{\text{O}_2} &= y_{\text{O}_2} \times p_m \\ p_{\text{CO}_2} &= y_{\text{CO}_2} \times p_m \end{aligned} \right\} y_i = \frac{p_i}{p_m} = \frac{N_i}{N_m} \quad (5.5)$$

It can become tedious conducting calculations using mixture concentrations. Often we are only interested in the overall mixture properties. In this case, the effective mixture molecular weight is defined as:

$$M_m = \sum_{i=1}^n y_i M_i \quad (5.6)$$

For the mixture in Fig. 5.1, the effective molecular weight is:

$$M_m = \left( \frac{0.5}{1.5} \right)_{\text{O}_2} \frac{32 \text{ lbm}}{\text{mol}} + \left( \frac{1}{1.5} \right)_{\text{CO}_2} \frac{44 \text{ lbm}}{\text{mol}} = \frac{40 \text{ lbm}}{\text{mol}} \quad (5.7)$$

The effective molecular weight can then be used in the ideal gas law to treat the mixture as a pure substance.

Other thermodynamic mixture properties can be calculated in a similar manner as the mixture molecular weight. In general, any thermodynamic property of a mixture of ideal gases can be calculated by:

$$x_i = \frac{1}{M_m} \sum_{i=1}^n y_i \bar{x}_i \tag{5.8}$$

The variable  $\bar{x}_i$  is the molar property (per mole)  $x$  of substance  $i$ . The mixture molecular weight is used to convert the molar property into mass units.

**EXAMPLE 5.1** *A mixture of 50 percent CO<sub>2</sub> and 50 percent H<sub>2</sub> by volume is contained in a 2-ft<sup>3</sup> container at a pressure of 100 psia. The container is heated from 100°F to 200°F. Calculate the heat that is transferred to the container, the mass of each gas, and the pressure of the mixture after the container has been heated to 200°F.*

**Solution:** *The best way to approach a mixture problem is to create the following table:*

Specie	M <sub>i</sub>	m <sub>i</sub>	y <sub>i</sub>	y <sub>i</sub> M <sub>i</sub>	N <sub>i</sub>	$\bar{c}_{v,i}$	y <sub>i</sub> $\bar{c}_{v,i}$	x <sub>i</sub>
H <sub>2</sub>	2	—	0.5	1.0	—	4.88	2.44	—
CO <sub>2</sub>	44	—	0.5	22.0	—	6.95	3.48	—
Totals	—	—	1.0	32.0	—	—	5.92	—

The units on the molecular weights are lbm/mol and on the specific heat are Btu/(mol · °F). The specific heats were included because the heat transferred to the tank will eventually have to be calculated. The second column in the table contains the molecular weight of each gas specie. These are obtained from the appendix. The third column contains the mass of each specie, which at this point is unknown. The fourth and fifth columns contain the mole fraction of each specie and the product of the mole fraction and the molecular weight. The sum of the fifth column is the definition of the effective mixture weight and, in this example, is 32 lbm/mol. The sixth column will contain the moles of each specie, and the last two columns contain the specific heat information. The seventh column uses Eq. (5.8) to calculate the effective specific heat of the mixture. The last column is the mass fraction of each specie. The mass fraction is defined as the ratio of the gas mass to the total mixture mass (m<sub>i</sub>/m<sub>m</sub>).

At this point, the mixture temperature, volume, pressure, and molecular weight are known. The ideal gas equation is used to calculate the total number of moles in the mixture:

$$N_m = \frac{p_{m,l}V}{R_u T} = \frac{(100 \text{ psia})(2 \text{ ft}^3)}{(100 + 460)^\circ R} \frac{\text{mol} \cdot ^\circ R}{10.732 \text{ psia} \cdot \text{ft}^3} = 0.0333 \text{ mol}$$

The number of moles of each gas is then calculated by using the mole fractions:

$$N_{H_2} = y_{H_2} \times N_m = 0.5 \times 0.0333 \text{ mol} = 0.01665 \text{ mol } H_2$$

$$N_{CO_2} = y_{CO_2} \times N_m = 0.5 \times 0.0333 \text{ mol} = 0.01665 \text{ mol } CO_2$$

The mass of each gas is then calculated by using the definition of the molecular weight:

$$m_{H_2} = N_{H_2} \times M_{H_2} = 0.01665 \text{ mol } H_2 \times \frac{2 \text{ lbm}}{\text{mol}} = 0.0333 \text{ lbm } H_2$$

$$m_{CO_2} = N_{CO_2} \times M_{CO_2} = 0.01665 \text{ mol } CO_2 \times \frac{44 \text{ lbm}}{\text{mol}} = 0.7326 \text{ lbm } CO_2$$

$$m_m = 0.7326 \text{ lbm } CO_2 + 0.0333 \text{ lbm } H_2 = 0.7659 \text{ lbm mixture}$$

Of interest is the comparison between the masses of  $H_2$  and  $CO_2$ . Even though the number of moles of each gas is the same, the mass of each gas differs by a large amount. This is true because of the large difference in the molecular weights. The mass fractions are calculated by taking the ratio of the mass of each gas to the total mixture mass. Our table is now complete:

Specie	$M_i$	$m_i$	$y_i$	$y_i M_i$	$N_i$	$\bar{c}_{v,i}$	$y_i \bar{c}_{v,i}$	$x_i$
$H_2$	2	0.0333	0.5	1.0	0.01665	4.88	2.44	0.043
$CO_2$	44	0.7326	0.5	22.0	0.01665	6.95	3.48	0.957
Totals	—	0.7659	1.0	32.0	0.0333	—	5.92	1.000

The first law of thermodynamics is used to calculate the heat that is transferred to the container and the final pressure of the gas mixture. For this particular case, the first law of thermodynamics reduces to:

$$Q = m(u_2 - u_1) \approx m_m c_{v,m} (T_2 - T_1)$$

From the table, the mixture specific heat is 5.92 Btu/(mol · °F). Dividing this by the effective mixture molecular weight results in the mass-based specific heat:

$$c_{v,m} = \frac{\bar{c}_{v,m}}{M_m} = \left( \frac{5.92 \text{ Btu}}{\text{mol} \cdot ^\circ F} \right) \left( \frac{\text{mol}}{32 \text{ lbm}} \right) = \frac{0.185 \text{ Btu}}{\text{lbm} \cdot ^\circ F}$$

The heat transferred to the container is then calculated by:

$$Q = 0.7659 \text{ lbm} \left( \frac{0.185 \text{ Btu}}{\text{lbm} \cdot ^\circ F} \right) (200^\circ F - 100^\circ F) = 14.17 \text{ Btu}$$

Finally, the pressure of the gases at 200°F is calculated from the ideal gas law as:

$$p_{m,2} = \frac{N_m R_u T_2}{V} = \frac{(0.0333 \text{ mol})(660^\circ R)}{2 \text{ ft}^3} \left( \frac{10.732 \text{ psia} \cdot \text{ft}^3}{\text{mol} \cdot ^\circ R} \right) = 117.93 \text{ psia}$$

The goal of this example is to give the reader a working knowledge of ideal gas mixtures and the ability to carry out an analysis. Although the field of gas mixtures can be very complex, this is the extent necessary for this Handbook. The remaining sections of this chapter apply the ideal gas mixture concepts to humid air.

## 5.2 PSYCHROMETRICS AND HUMID AIR

Mixtures of air and water vapor represent a special case of ideal gas mixtures. The term *psychrometrics* refers to the analysis and study of air/water vapor mixtures. The remaining sections of this chapter are devoted to this analysis, with the goal that the reader will obtain a working knowledge of how to determine the dew point of humid air and how much water would need to be removed (condensed) to lower the dew point to a certain level.

### 5.2.1 HUMIDITY RATIO

The humidity ratio is one of several measures of air humidity. The definition of the humidity ratio is the mass of the water vapor in a specific volume of humid air divided by the mass of the dry air in that same volume. In equation form, the humidity ratio is expressed as:

$$\omega = \frac{m_v}{m_a} \quad (5.9)$$

The air and water vapor in a humid air mixture can always be treated as ideal gases in normal HVAC temperature and pressure ranges. The masses in Eq. (5.9) can then be expressed in terms of the temperature, the partial pressures of the air and water vapor, and the molecular weights:

$$\omega = \left( \frac{p_v VM_v}{R_u T} \right) \left( \frac{R_u T}{p_a VM_a} \right) = 0.622 \frac{p_v}{p_a} = 0.622 \frac{p_v}{p - p_v} \quad (5.10)$$

By knowing the partial pressure of the water vapor and the total pressure of the humid air, the humidity ratio can be calculated. Specifically of interest is that the humidity ratio does not vary with the temperature as long as the mass of the vapor remains constant. However, at this point, information is missing in order to carry out this calculation.

### 5.2.2 RELATIVE HUMIDITY

The relative humidity is defined as the mole ratio of the water vapor mole fraction in the mixture to the saturated mole fraction that would exist at the same temperature and pressure. In equation form, the relative humidity is expressed as:

$$\phi = \frac{N_v}{N_{v,\text{sat}}} = \frac{p_v}{p_{v,\text{sat}}} \quad (5.11)$$

The relative humidity is graphically shown in Fig. 5.2. This figure shows the relationship between the water vapor temperature, the water vapor partial pressure in the humid air mixture, and the water vapor entropy. The dome-shaped curve in the figure is called the *saturation dome*. The pinnacle of the dome is called the critical temperature. The standard definition of the *critical temperature* is the maximum temperature above which no matter how large the pressure, the vapor cannot be forced to condense. The portion of the curve to the right of the critical temperature is referred to as the *saturated vapor line* and the line to the left of the critical temperature is referred to as the *saturated liquid line*. Lines of constant pressure are also shown in the figure and extend up and to the right from the saturated vapor line.

To the right of the saturated vapor line, the water in the humid air mixture is entirely in vapor form. Starting at point A in the figure, if the temperature is decreased at constant pressure until the temperature reaches point B, the water will just begin to condense at point B. Further decreases in temperature will cause all the water to condense at the saturated liquid line.

By referring to Eq. (5.11), the saturation pressure in the denominator refers to the water vapor saturation pressure at the temperature of the humid air mixture. In the figure, the humid air temperature is at  $T_A$ . The saturation vapor pressure corresponding to that temperature is  $p_{v,\text{sat}}(T_A)$ ; therefore, the relative humidity is proportional to the inverse of the horizontal distance between the saturation pressure and

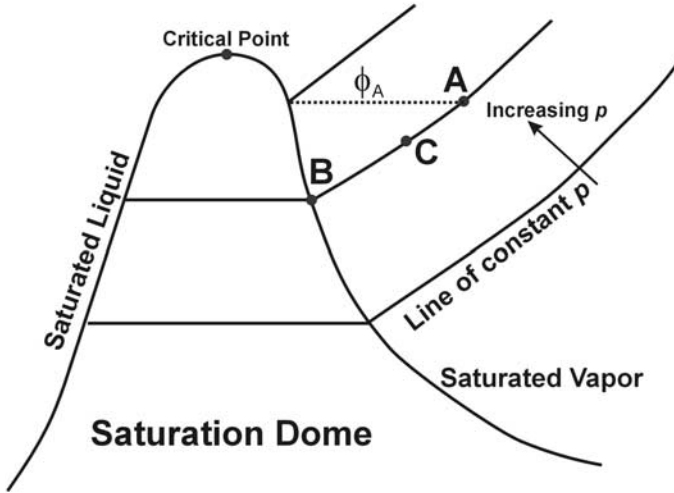


FIGURE 5.2 Graphical representation of relative humidity.

the partial pressure of the water vapor within the mixture (the distance shown as  $\phi_A$  in the figure). Now let the mixture temperature be reduced to  $T_C$ . The water vapor partial pressure remains the same, but the saturation pressure decreases with the temperature. Now the relative humidity of the humid air is represented by the inverse of the distance between the partial pressure and the new saturation pressure, which is greater than  $\phi_A$ .

Because the distance is inversely proportional to the relative humidity, as the temperature continues to decrease, the relative humidity continues to increase until it reaches 100 percent at point B. The lesson here is that the relative humidity varies as a function of temperature. Remember that the humidity ratio was independent of the temperature.

### 5.2.3 DEW POINT TEMPERATURE

By referring again to Fig. 5.2, the temperature at point B is where water just begins to condense from the humid air mixture. This temperature is called the *dew point temperature*. The significance of the dew point temperature is that condensation will occur on any surface that is equal to or less than the dew point temperature. A good example of this is a bathroom mirror during or after someone has taken a shower. The air in the bathroom becomes more humid from the shower. If the air becomes humid enough, then the mirror and walls in the bathroom can be below the dew point temperature. Hence, water from the air condenses on the mirror and walls. As an aside, radiant panels can be used to raise the surface temperature of the mirror and reduce or eliminate fogging.

The dew point temperature is important for radiant cooling applications. If temperature of the room air is reduced to the point where the relative humidity is near 100 percent, then the possibility exists for condensation on the walls. In addition, the radiant cooler surface can reach temperatures that are less than the air dew point temperature. Again, the result is condensation on the radiant cooler.

### 5.2.4 THE PSYCHROMETRIC CHART

The psychrometric chart is illustrated in Fig. 5.3. The chart provides a convenient method to quickly determine the relative humidity, humidity ratio, and dew point temperature for a humid air mixture.

**EXAMPLE 5.2** *Humid air at 70°F exhibits a wet-bulb temperature of 60°F. Determine the relative humidity, humidity ratio, and dew point temperature using the psychrometric chart.*

$$\text{Relative humidity} = 55 \text{ percent}$$

$$\text{Humidity ratio} = 0.00875$$

$$\text{Dew point} = 53.5^\circ\text{F}$$

### 5.2.5 HEATING AND COOLING HUMID AIR

This portion of the chapter utilizes the concepts of psychrometrics to solve two cooling design problems. Before doing that, the mixture concepts are incorporated into the energy conservation equation.

As an example, we will consider the cooling of warm humid air by the air-conditioning system shown in Fig. 5.4. In this figure, warm humid air enters the air conditioner. Heat is transferred from the air to cool and dehumidify the air. Once the humid air is cooled below the dew point temperature, water condenses and drains through the bottom of the air-conditioning unit. The steady-state form of the energy conservation for this application is:

$$\dot{Q} + \sum_{\text{in}} \dot{m}h = \sum_{\text{out}} \dot{m}h = 0 \quad (5.12)$$

The potential and kinetic energy effects have been neglected as have any power terms. When water vapor and air need to be considered separately, as they do in this cooling application, Eq. (5.12) is modified to treat the incoming water and air vapor as two separate streams by using the summation signs. Simply put, the inlet and outlet streams are rewritten as:

$$\sum \dot{m}h = \dot{m}_v h_v + \dot{m}_a h_a \quad (5.13)$$

Substituting Eq. (5.13) into Eq. (5.12) results in:

$$\dot{Q} = (\dot{m}_{a,\text{out}} h_{a,\text{out}} + \dot{m}_{v,\text{out}} h_{v,\text{out}} + \dot{m}_{l,\text{out}} h_{l,\text{out}}) - (\dot{m}_{a,\text{in}} h_{a,\text{in}} + \dot{m}_{v,\text{in}} h_{v,\text{in}}) \quad (5.14)$$

At this point, the definition of the humidity ratio is used to simplify the equation. In addition, the inlet mass flow rate of air is assumed to be the same as the outlet mass flow rate. Applying this assumption and definition results in:

$$\frac{\dot{Q}}{\dot{m}_a} = (h_{a,\text{out}} - h_{a,\text{in}}) + \omega_{\text{out}}(h_{v,\text{out}} - h_l) + \omega_{\text{in}}(h_l - h_{v,\text{in}}) \quad (5.15)$$

At this point, the enthalpies need to be evaluated in any of the ways that are explained in Chap. 1.

**EXAMPLE 5.3** *A long channel is constructed to measure the relative humidity of air. The channel, shown in Fig. 5.5, is long enough so that the exiting air is completely sat-*

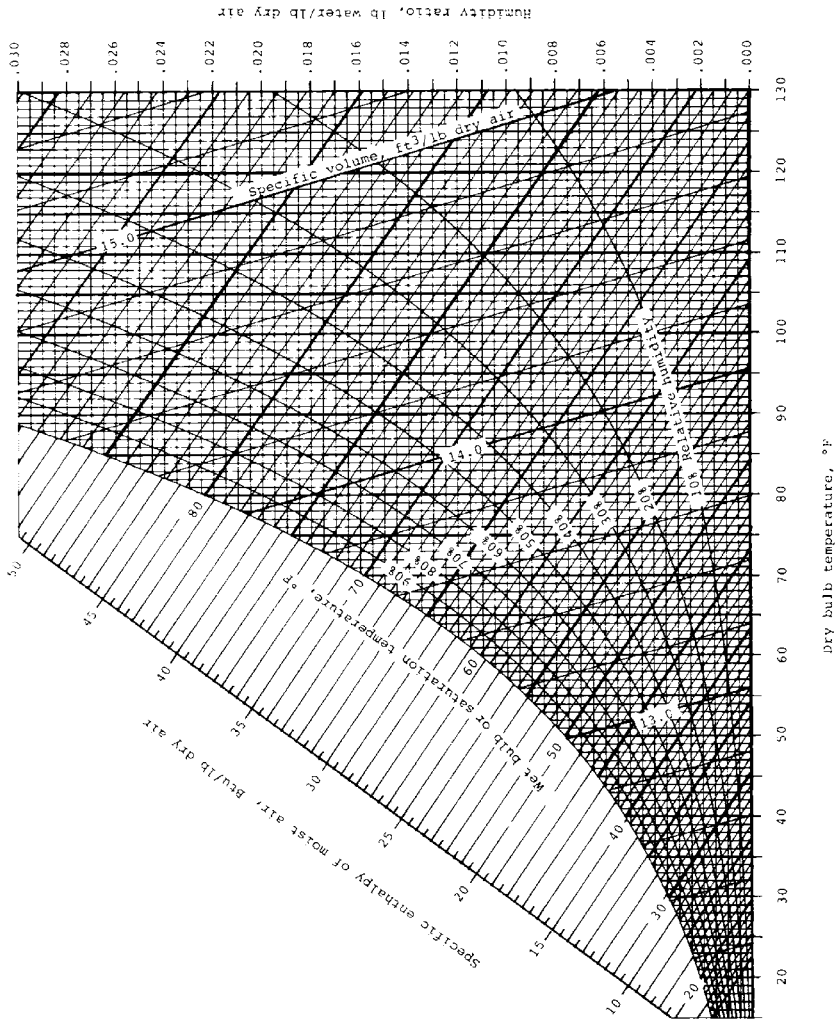


FIGURE 5.3 Psychrometric chart.

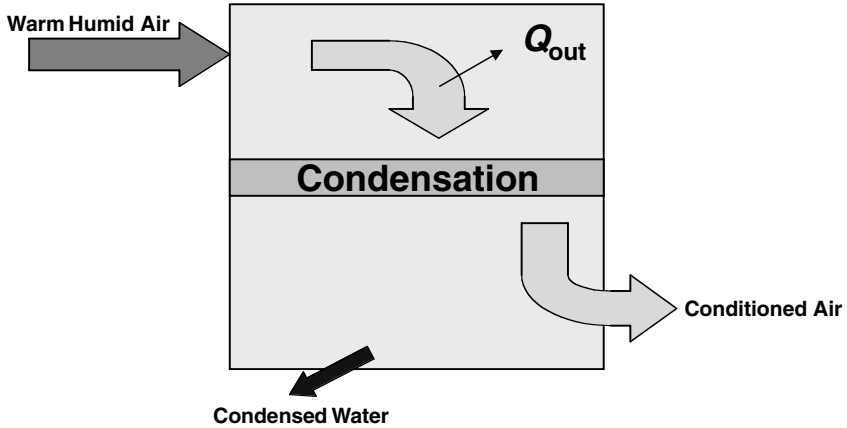


FIGURE 5.4 Air-conditioning system.

urated with water vapor, that is,  $\phi_{exit} = 100$  percent, through evaporation. The water level is maintained by makeup water, which is at the same temperature as the air exit dry-bulb temperature. The inlet dry-bulb temperature is  $70^\circ\text{F}$ , the exit dry-bulb temperature is  $60^\circ\text{F}$ , and the atmospheric pressure is  $14.7$  psia.

Find: Determine the relative humidity of the inlet air stream.

Solution: Identifying the inlet as point 1 and the exit as point 2, the energy conservation equation for this process is:

$$\omega_1 = \frac{(h_{a,1} - h_{a,2}) - \omega_2(h_{v,2} - h_{l,2})}{(h_{l,2} - h_{v,1})}$$

By definition, the second parenthetic quantity in the numerator is the liquid and vapor saturation enthalpies at temperature  $T_2 = 60^\circ\text{F}$ . Hence, from the water saturation tables:

$$h_{v,2} = h_{g,2} = 1087.7 \text{ Btu/lbm}$$

$$h_{l,2} = h_{f,2} = 28.08 \text{ Btu/lbm}$$

$$h_{v,1} = h_{g,1} = 1092.0 \text{ Btu/lbm}$$

$$p_{v,2} = p_{sat,2} = 0.2563 \text{ psia}$$

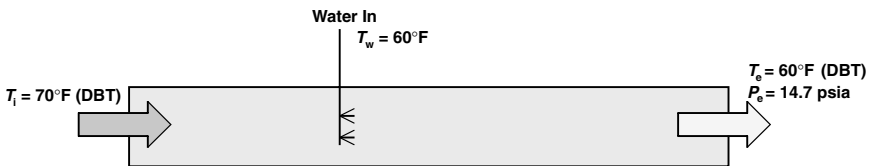


FIGURE 5.5 Channel used for Example 5.3.

The partial pressure of the water vapor in the humid air mixture was also extracted from the water saturation tables. Because the relative humidity is 100 percent, the vapor partial pressure at the exit equals the saturation pressure at the exit temperature. The humidity ratio at point 2 is found by using Eq. (5.10):

$$\omega_2 = 0.622 \frac{P_{v,2}}{p - P_{v,2}} = 0.622 \times \left( \frac{0.2563}{14.7 - 0.2563} \right) = 0.01104 \text{ lbm vapor/lbm air}$$

The only remaining terms are the air enthalpies. These are approximated by using the temperature difference and the specific heat of air, 0.24 Btu/(lbm · °F). With all of this information, the humidity ratio at the inlet is calculated by:

$$\begin{aligned} \omega_1 &= \frac{[0.24 \text{ Btu}/(\text{lbm} \cdot ^\circ\text{F})](70^\circ\text{F} - 60^\circ\text{F}) - 0.01104(1087.7 - 28.08) \text{ Btu}/\text{lbm}}{(28.08 - 1092) \text{ Btu}/\text{lbm}} \\ &= 0.00874 \text{ lbm vapor/lbm air} \end{aligned}$$

To calculate the relative humidity of the incoming air, the partial pressure of the water vapor in the incoming air stream needs to be calculated:

$$\omega_1 = 0.622 \frac{P_{v,1}}{p - P_{v,1}} \rightarrow P_{v,1} = \frac{\omega_1 p}{\omega_1 + 0.622} = 0.204 \text{ psia}$$

From the tables:

$$P_{\text{sat},1} = 0.3632 \text{ psia}$$

and

$$\phi_1 = \frac{P_{v,1}}{P_{g,1}} = \frac{0.204}{0.3632} = 0.561 = 56.1 \text{ percent}$$

Note: This is obviously not a practical way to measure the relative humidity of humid air. A more practical approach is to use the dry- and wet-bulb air temperatures. It just so happens that the wet-bulb temperature is very close to the saturation temperature of the humid air mixture and can be used interchangeably. In this example, the wet-bulb temperature would have been used in place of the exit temperature, and the dry-bulb temperature would have been used in place of the inlet temperature.

**EXAMPLE 5.4** An air-conditioning system receives humid air at a relative humidity of 80 percent, a temperature of 85°F, and a pressure of 15.5 psia. The humid air passes over the cooling coils and exits the system at 60°F, 14.5 psia, and 100 percent relative humidity. The airflow through the system is 500 scfm.

Find: Calculate the total cooling load on the air-conditioning coil.

Solution: The air-conditioning system is illustrated in Fig. 5.6. The conservation of energy and mass conservation equations are required to solve this problem. The mass conservation equation can be written for the water vapor and liquid water as:

$$\dot{m}_{v,1} = \dot{m}_{v,2} + \dot{m}_l$$

The energy conservation equation reduces to:

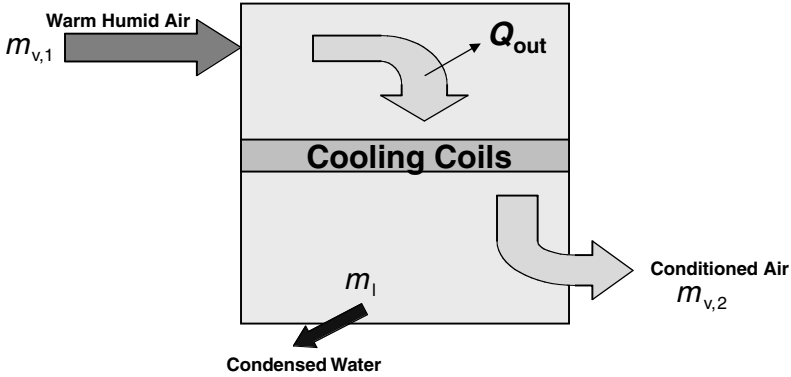


FIGURE 5.6 Air-conditioning system used in Example 5.4.

$$\frac{\dot{Q}}{\dot{m}_a} = c_{p,a}(T_2 - T_1) + \omega_2 (h_{v,2} - h_l) + \omega_l (h_l - h_{v,1})$$

From the water saturation tables, the saturation pressures and enthalpies of the water vapor at the inlet and exit are:

Property	Inlet 1	Inlet 2
$p_{sat}$ (psia)	0.6988	0.2563
$h_v$ (Btu/lbm)	1,100.7	1087.7
$h_l$ (Btu/lbm)	—	28.08

The partial pressures and then the humidity ratios are found by:

$$p_{v,1} = \phi_1 \times p_{sat,1} = 0.559 \text{ psia} \rightarrow \omega_1 = 0.622 \times \left( \frac{0.559}{15.5 - 0.559} \right) = 0.02494$$

$$p_{v,2} = \phi_2 \times p_{sat,2} = 0.256 \text{ psia} \rightarrow \omega_2 = 0.622 \times \left( \frac{0.256}{14.5 - 0.256} \right) = 0.01046$$

The water condensation rate is then calculated from the airflow rate and the humidity ratios:

$$\begin{aligned} \dot{m}_l &= \dot{m}_a (\omega_1 - \omega_2) = \left( \frac{500 \text{ ft}^3}{\text{min}} \right) \left( \frac{0.073 \text{ lbm}}{\text{ft}^3} \right) (0.02494 - 0.01046) \\ & \qquad \qquad \qquad \text{standard air density} \\ &= \frac{0.529 \text{ lbm}}{\text{min}} \end{aligned}$$

$$\begin{aligned} \dot{V}_l &= \frac{\dot{m}_l}{\rho_l} = \left( \frac{0.529 \text{ lbm}}{\text{min}} \right) \left( \frac{\text{ft}^3}{62.4 \text{ lbm}} \right) \left( \frac{7.4805 \text{ gal}}{\text{ft}^3} \right) \left( \frac{60 \text{ min}}{\text{h}} \right) \\ &= 3.8 \text{ gph of condensate} \end{aligned}$$

The air-conditioning heat load is calculated from the energy conservation equation:

$$\begin{aligned}\dot{Q}_{ac} &= \dot{m}_a \left[ \left( \frac{0.24 \text{ Btu}}{\text{lbm} \cdot ^\circ\text{F}} \right) (60^\circ\text{F} - 90^\circ\text{F}) + 0.01046(1087.7 - 28.08) \frac{\text{Btu}}{\text{lbm}} \right. \\ &\quad \left. + 0.02494(28.08 - 1100.7) \frac{\text{Btu}}{\text{lbm}} \right] \\ &= \frac{-50,070 \text{ Btu}}{h} \times \left( \frac{\text{ton}}{12,000 \text{ Btu/h}} \right) \\ &= 4.2 \text{ tons of cooling}\end{aligned}$$

Of special interest in this example are the relative amounts of cooling that are necessary to actually cool the air versus the amount needed to remove the water. Only the first term in the equation, the portion with the specific heat, is required to cool the air. The remainder is used to remove the water from the humid air. Hence, the "cooling" portion of the energy is:

$$\begin{aligned}\dot{Q}_{cooling} &= \left( \frac{0.608 \text{ lbm}}{s} \right) \left( \frac{0.24 \text{ Btu}}{\text{lbm} \cdot ^\circ\text{F}} \right) (60 - 90)^\circ\text{F} \\ &= \frac{15,759 \text{ Btu}}{h}\end{aligned}$$

or

$$\frac{15,759}{50,070} \times 100\%$$

which is 31 percent.

The moral of the story is that about 70 percent of cooling energy is used to remove water from the humid air in this example. This provides an idea of the potential energy savings by using dessicants to remove moisture from humid air and then by using radiant cooling panels to create a thermally comfortable environment.

---

# CHAPTER 6

---

## FLUID MECHANICS

---

Fluid mechanics is important in the study and understanding of radiant heat transfer for hydronic systems. Fluid mechanics describes the relationship between pressure drops and flow rates through the water conduits of a hydronic system. These same principles can also be applied to airflow through ventilation ducts. This relationship is important to determine pipe diameters, the effect of different tubing materials, and the size of the required pump.

The focus of this chapter is to investigate the background information that is necessary to predict the pressure drop, flow rate, and pumping power required for a given piping system. To accomplish this task, we will introduce Bernoulli's equation, major and minor head loss terms, and the friction factor.

### 6.1 BERNOULLI'S EQUATION

---

One of the better known relationships in the field of fluid dynamics is Bernoulli's equation. This equation is derived from the conservation of energy equation and relates fluid velocity and pressure. Bernoulli's equation is expressed as:

$$\frac{p}{\rho} + \frac{V^2}{2} + gz = \text{constant} \quad (6.1)$$

The conditions for using this equation are steady, incompressible flow along a streamline without the effects of friction. After studying Eq. (6.1), the effects of friction and pipe losses will be introduced.

The best application of Bernoulli's equation is to calculate the effect of elevation change. For example, if water is raised from a low level to a high level in a constant-diameter pipe, Bernoulli's equation relates the pressure change to the elevation change. Applying Bernoulli's equation between two points in a pipe is:

$$\frac{p_1}{\rho} + \frac{V_1^2}{2} + gz_1 = \frac{p_2}{\rho} + \frac{V_2^2}{2} + gz_2 \quad (6.2)$$

This procedure is illustrated in the following example.

**EXAMPLE 6.1** *Water flowing at the rate of 20 gpm in a 1-in-diameter pipe is raised from an elevation of 0 to 30 ft. If the pressure at the lower elevation is 20 psig, calculate the pressure at the higher elevation.*

2.136

HEAT TRANSFER AND THERMODYNAMICS

Known:

$$\begin{aligned}
 Q &= 20 \frac{\text{gal}}{\text{min}} & P_1 &= 20 \text{ psi} & \rho &= 999 \frac{\text{kg}}{\text{m}^3} \\
 Q &= 0.045 \frac{\text{ft}^3}{\text{s}} & P_1 &= 9.266 \cdot 10^4 \frac{\text{lb}}{\text{ft} \cdot \text{s}^2} & \rho &= 62.366 \frac{\text{lb}}{\text{ft}^3} \\
 Z_1 &= 0 \text{ ft} & D &= 1 \text{ in} & g &= 32.174 \frac{\text{ft}}{\text{s}^2} \\
 Z_2 &= 20 \text{ ft} & D &= 0.083 \text{ ft} & A &= \pi \cdot \left(\frac{D}{2}\right)^2
 \end{aligned}$$

Solution:

$$\begin{aligned}
 V_1 &= \frac{Q}{A} & V_2 &= \frac{Q}{A} \\
 C &= \frac{P_1}{\rho} + \frac{(V_1)^2}{2} + g \cdot Z_1 & C &= 1.519 \cdot 10^3 \frac{\text{ft}^2}{\text{s}^2} \\
 P_2 &= \left[ C - g \cdot Z_2 - \frac{(V_2)^2}{2} \right] \cdot \rho
 \end{aligned}$$

Answer:  $P_2 = 11.338 \text{ psi}$

**EXAMPLE 6.2** Water flowing at the rate of 20 gpm in a 1-in pipe at 30 psig enters a 0.50-in section of pipe. If the elevation change is zero, calculate the velocity and pressure in the smaller-diameter pipe.

Known:

$$\begin{aligned}
 Q &= 20 \frac{\text{gal}}{\text{min}} & P_1 &= 20 \cdot \text{psi} & \rho &= 999 \frac{\text{kg}}{\text{m}^3} & g &= 32.174 \frac{\text{ft}}{\text{s}^2} \\
 Q &= 0.045 \frac{\text{ft}^3}{\text{s}} & P_1 &= 9.266 \cdot 10^4 \frac{\text{lb}}{\text{ft} \cdot \text{s}^2} & \rho &= 62.366 \frac{\text{lb}}{\text{ft}^3} \\
 Z_1 &= 0 \text{ ft} & D_1 &= 1.0 \text{ in} & D_1 &= 0.083 \text{ ft} \\
 Z_2 &= 20 \text{ ft} & D_2 &= 0.5 \text{ in} & D_2 &= 0.042 \text{ ft} \\
 & & A_1 &= \pi \cdot \left(\frac{D_1}{2}\right)^2 & A_2 &= \pi \cdot \left(\frac{D_2}{2}\right)^2
 \end{aligned}$$

Solution: *Continuity:*

$$\begin{aligned}
 0 &= -\rho \cdot V_1 \cdot A_1 + \rho \cdot V_2 \cdot A_2 \\
 V_1 &= \frac{Q}{A_1} & V_2 &= \frac{Q}{A_2}
 \end{aligned}$$

$$C = \frac{P_1}{\rho} + \frac{(V_1)^2}{2} + g \cdot Z_1 \qquad C = 1.519 \cdot \theta^3 \frac{ft^2}{s^2}$$

$$P_2 = \left[ C - g \cdot Z_2 - \frac{(V_2)^2}{2} \right] \cdot \rho$$

Answers:  $V_2 = 32.68 \frac{ft}{s}$   $P_2 = 4.599 psi$

## 6.2 PIPE FLOW CALCULATIONS

Pipe flow calculations build on Bernoulli’s equation, but they remove the restriction of frictionless flow. The introduced term is the *head loss* that takes into consideration viscous pipe losses, losses due to valves and bends in the pipe, and other effects. Bernoulli’s equation is modified as:

$$\left( \frac{p_1}{\rho} + \alpha_1 \frac{\bar{V}_1^2}{2} + gz_1 \right) - \left( \frac{p_2}{\rho} + \alpha_2 \frac{\bar{V}_2^2}{2} + gz_2 \right) = h_{lr} \qquad (6.3)$$

The parameter  $h_{lr}$  is the head loss term. The  $\alpha$  terms are “velocity profile” corrections. These can be assumed to be one with little loss in accuracy. The only other difference between Eqs. (6.3) and (6.4) is that the velocity terms have lines over them. These lines designate that the velocities are average velocities over the cross section of the pipe. The average velocity is defined as:

$$\bar{V} = \frac{\dot{m}}{\rho A} = \frac{\dot{V}}{A} \qquad (6.4)$$

### 6.2.1 Major Head Losses

The total head loss term is separated into two components: (1) the major-friction loss term and (2) the minor loss term. By definition, the major head loss is the pressure loss through a horizontal constant-area pipe at steady flow. This condition is illustrated in Fig. 6.1. In equation form, this definition is:

$$\frac{\Delta p}{\rho} = \frac{p_1 - p_2}{\rho} = h_l \qquad (6.5)$$



**FIGURE 6.1** Pressure loss in a horizontal constant area pipe with steady flow.

Experimental studies show that the major-frictional head loss in a pipe is a function of the pipe roughness, the Reynolds number ( $Re$ ), and the length-to-diameter ratio of the pipe. In equation form, this relationship is:

$$h_f = f \frac{L\bar{V}^2}{D} \quad , \quad f = f\left(Re, \frac{e}{D}\right) \tag{6.6}$$

The parameter  $e$  is the pipe roughness. Figure 6.2 illustrates the roughness of various pipe materials. For example, drawn tubing is 0.000005 ft and the relative roughness of 10-in drawn tubing is 0.000006. The parameter  $f$  is called the friction factor and is a function of  $Re$  and the relative roughness  $e/D$ .

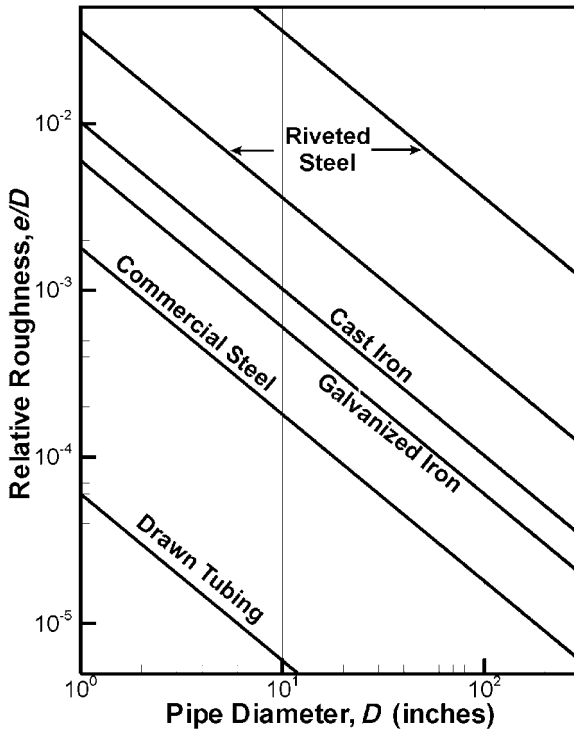


FIGURE 6.2 Relative roughness of various pipe materials.

The friction factor has been the subject of numerous studies. Arguably the best set of experimental data was collected and analyzed by Moody (1944). Figure 6.3 demonstrates the results of his experiments in the form of a Moody chart. This chart shows the relationship between  $Re$  on the  $x$  axis, the friction factor on the  $y$  axis, and the relative roughness shown as lines on the chart.

**EXAMPLE 6.3** Determine the friction factor for a 2-gpm flow rate through 0.50-inch diameter drawn tubing. The water flowing through the pipe is 70°F. If the pipe is horizontal, calculate the pressure drop along a 500-ft section of pipe. Compare this pressure drop with the pressure drop that would occur in typical hydronic conduit.

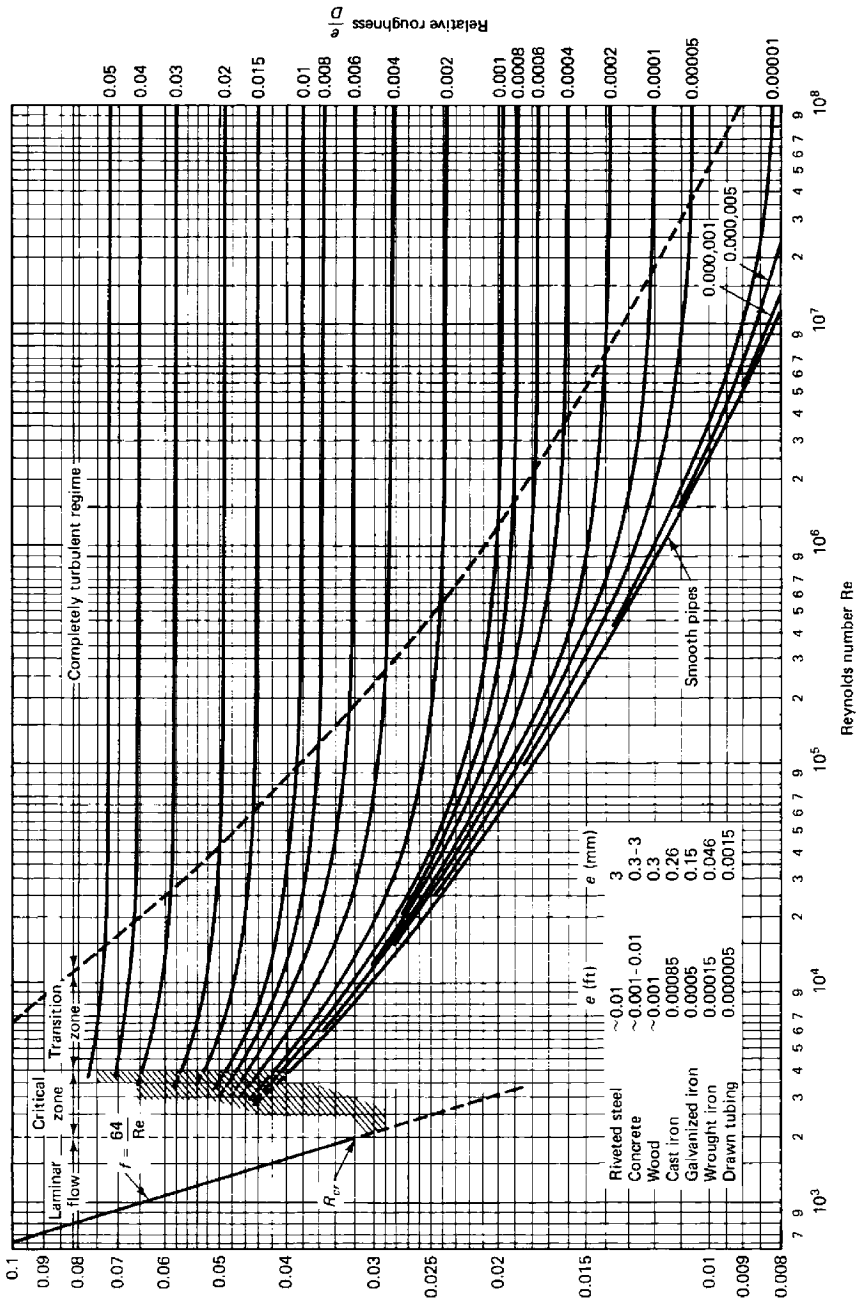


FIGURE 6.3 Moody friction factor diagram.

2.140

HEAT TRANSFER AND THERMODYNAMICS

Known:

$$Q = 2 \frac{\text{gal}}{\text{min}} \quad P_1 = 20 \text{ psi} \quad \rho = 997 \frac{\text{kg}}{\text{m}^3} \quad \mu = (968 \cdot 10^{-6}) \cdot \frac{\text{N}}{\text{m}^2 \cdot \text{s}}$$

$$Q = 4.456 \cdot 10^{-3} \frac{\text{ft}^3}{\text{s}} \quad P_1 = 9.266 \cdot 10^4 \frac{\text{lb}}{\text{ft} \cdot \text{s}^2} \quad \rho = 62.241 \frac{\text{lb}}{\text{ft}^3} \quad \mu = 6.505 \cdot 10^{-4} \frac{\text{lb}}{\text{ft} \cdot \text{s}}$$

$$D_i = 0.5 \text{ in} \quad e = 0.000005 \quad g = 32.174 \frac{\text{ft}}{\text{s}^2} \quad L = 500 \text{ ft}$$

$$\frac{e}{D_i} = 0.00012 \frac{1}{\text{ft}} \quad D_f = \frac{0.5}{12} \text{ ft} \quad A = \pi \cdot \left(\frac{D_f}{2}\right)^2 \quad V_1 = \frac{Q}{A}$$

Solution:

$$Re = \frac{V_1 \cdot D_f \cdot \rho}{\mu} \quad Re = 1.303 \cdot 10^4$$

From Moody chart:

$$f = 0.017 \quad h_f = f \cdot \frac{L}{D_f} \cdot \frac{(V_1)^2}{2}$$

Answers:

$$h_f = 1.089 \cdot 10^3 \frac{\text{ft}^2}{\text{s}^2} \quad \frac{h_f}{g} = 33.857 \text{ ft}$$

$$P_0 = h_f \cdot \rho \cdot Q \quad P_0 = 0.017 \text{ hp}$$

**EXAMPLE 6.4** Calculate the pressure loss in a pipe that has a 20-ft vertical rise over 100 ft. The pipe flow rate is 30 gpm, the diameter is 0.50 in, and the water temperature is 90°F.

Known:

$$Q = 30 \frac{\text{gal}}{\text{min}} \quad \rho = 995 \frac{\text{kg}}{\text{m}^3} \quad g = 32.174 \frac{\text{ft}}{\text{s}^2}$$

$$Q = 0.067 \frac{\text{ft}^3}{\text{s}} \quad \rho = 62.116 \frac{\text{lb}}{\text{ft}^3}$$

$$Z_1 = 0 \text{ ft} \quad D_1 = 0.5 \text{ in} \quad D_1 = 0.042 \text{ ft}$$

$$Z_2 = 20 \text{ ft} \quad A_1 = \pi \cdot \left(\frac{D_1}{2}\right)^2$$

Solution: Because  $V_1 = V_2$  and  $Z_1 = 0$ , Bernoulli's equation reduces to:

$$\frac{P_1}{\rho} = \frac{P_2}{\rho} + g \cdot Z_2$$

$$\frac{P_1}{\rho} - \frac{P_2}{\rho} = g \cdot Z_2$$

$$\Delta P = \rho \cdot g \cdot Z_2$$

Answers:

$$\Delta P = 3.997 \cdot 10^4 \frac{lb}{ft \cdot s^2} \quad \Delta P = 8.627 \text{ psi}$$

**6.2.2 Minor Losses**

Minor losses, which can sometimes be quite large, are due to anything other than straight sections of pipe. Examples are valves, entrances and exits, pipe elbows, expansions and contractions, and fittings. There are two ways to calculate the effect of minor losses. The first is to introduce a *K* value and the second is to designate an equivalent length of pipe, which is then used in Eq. (6.6). Each of these methods is related to the minor head loss term by:

$$h_m = K \frac{\bar{V}^2}{2} = f \frac{L_{eq}}{D} \frac{\bar{V}^2}{2} \tag{6.7}$$

Both methods are frequently used and are discussed in the following paragraphs.

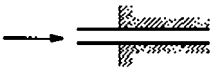
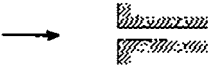
Table 6.1 illustrates three common inlets and exits from a piping system and their associated loss coefficients. These become important in the case of a surge tank or pressure volume in a piping system. As shown in the table, the well-rounded entrance exhibits the lowest loss coefficient, whereas the loss term at an exit is independent of the configuration. Figures 6.4 and 6.5 illustrate the effect of pipe elbows and miter pipe bends. Table 6.2 provides several loss terms for valves and fittings. All these data are from the “Crane Industrial Products Group Technical Paper No. 410.”

**6.2.3 Pipe Solution Techniques**

There are four separate cases of pipe system problems that may be encountered. These cases are all functions of the pressure loss equation:

$$\Delta p = f(L/D, \dot{V}, e/D) \tag{6.8}$$

**TABLE 6.1** Inlet and Exit Head Loss Terms

Entrance type		Minor loss coefficient, <i>K</i> *								
Reentrant		0.78								
Square-edged		0.5								
Rounded		<table border="1" style="display: inline-table; vertical-align: middle;"> <tr> <td><i>r/D</i></td> <td>0.02</td> <td>0.06</td> <td>≥0.15</td> </tr> <tr> <td><i>K</i></td> <td>0.28</td> <td>0.15</td> <td>0.04</td> </tr> </table>	<i>r/D</i>	0.02	0.06	≥0.15	<i>K</i>	0.28	0.15	0.04
<i>r/D</i>	0.02	0.06	≥0.15							
<i>K</i>	0.28	0.15	0.04							

\* Based on  $h_m = K(\bar{V}^2/2)$ , where  $\bar{V}$  is the mean velocity in the pipe.

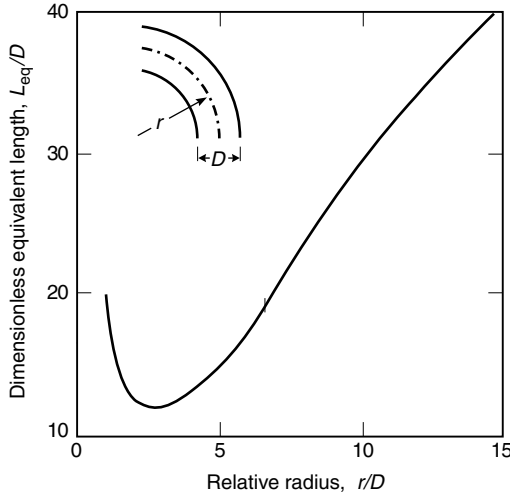


FIGURE 6.4 Head loss due to pipe elbows.

Of the four variable groups in Eq. (6.8), three need to be specified with the fourth calculated. Each situation requires a slightly different solution procedure. Each case is illustrated in the following examples. Each example uses water at 90°F and smooth drawn pipes.

**EXAMPLE 6.5** *Flow = 20 gpm,  $D = 1.5$  in,  $L = 100$  ft. For the case in which the pressure loss is the unknown, one first obtains the friction factor from the Moody chart*

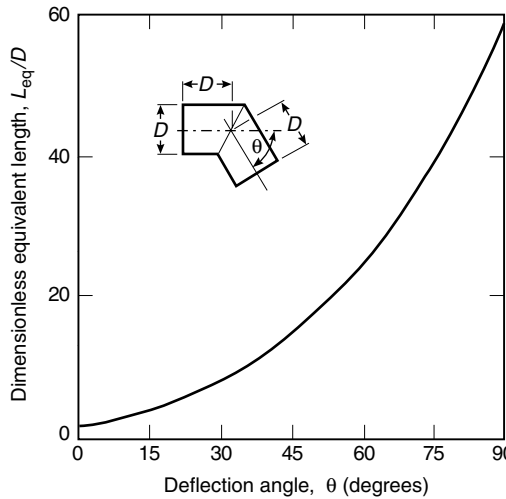


FIGURE 6.5 Head loss due to mitered pipe bends.

**TABLE 6.2** Loss Terms for Valves and Fittings

Fitting type	Equivalent length,* $L_e/D$
Valves (fully open)	
Gate valve	8
Globe valve	340
Angle valve	150
Ball valve	3
Lift check valve	
Globe lift	600
Angle lift	55
Foot valve with strainer	
Poppet disk	420
Hinged disk	75
Standard elbow	
90°	30
45°	16
Return bend, close pattern	50
Standard tee	
Flow through run	20
Flow through branch	60

\*Based on  $h_{L_e} = f \frac{L_e}{D} \frac{\bar{V}_2^2}{2}$ .

using  $Re$  and the relative roughness. The head loss is then calculated. The pressure loss is calculated by using Eq. (6.5).

Known:

$$Q = 20 \frac{\text{gal}}{\text{min}} \quad P_1 = 20 \text{ psi} \quad \rho = 995 \frac{\text{kg}}{\text{m}^3} \quad \mu = (760 \cdot 10^{-6}) \cdot \frac{\text{N}}{\text{m}^2} \cdot \text{s}$$

$$Q = 0.045 \frac{\text{ft}^3}{\text{s}} \quad P_1 = 9.266 \cdot 10^4 \frac{\text{lb}}{\text{ft} \cdot \text{s}^2} \quad \rho = 62.116 \frac{\text{lb}}{\text{ft}^3} \quad \mu = 5.108 \cdot 10^{-4} \frac{\text{lb}}{\text{ft} \cdot \text{s}}$$

$$D_i = 1.5 \text{ in} \quad e = 0.000005 \quad g = 32.174 \frac{\text{ft}}{\text{s}^2} \quad L = 100 \text{ ft}$$

$$\frac{e}{D_i} = 4 \cdot 10^{-5} \frac{1}{\text{ft}} \quad D_f = \frac{1.5}{12} \cdot \text{ft} \quad A = \pi \cdot \left(\frac{D_f}{2}\right)^2 \quad V_1 = \frac{Q}{A}$$

Solution:

$$Re = \frac{V_1 \cdot D_f \cdot \rho}{\mu} \quad Re = 5.52 \cdot 10^4$$

From Moody chart:

$$f = 0.016$$

$$h_f = f \cdot \frac{L}{D_f} \cdot \frac{(V_1)^2}{2}$$

$$h_f = 84.383 \frac{ft^2}{s^2} \quad \frac{h_f}{g} = 2.623 ft$$

$$\Delta P = h_f \cdot \rho$$

Answers:

$$\Delta P = 1.131 psi$$

**EXAMPLE 6.6**  $\Delta p = 10 psi$ ,  $Q = 30 gpm$ ,  $D = 1 in$ ,  $L = ?$  Calculate the total head loss from main equation. Get  $f$  from the Moody chart by using  $Re$  and  $e/D$ . Calculate  $L$  from head loss.

Known:

$$Q = 30 \frac{gal}{min} \quad \Delta P = 10 psi \quad \rho = 997 \frac{kg}{m^3} \quad \mu = (968 \cdot 10^{-6}) \cdot \frac{N}{m^2} \cdot s$$

$$Q = 0.067 \frac{ft^3}{s} \quad \Delta P = 4.633 \cdot 10^4 \frac{lb}{ft \cdot s^2} \quad \rho = 62.241 \frac{lb}{ft^3} \quad \mu = 6.505 \cdot 10^{-4} \frac{lb}{ft \cdot s}$$

$$D_i = 1 in \quad e = 0.000005 \quad g = 32.174 \frac{ft}{s^2}$$

$$\frac{e}{D_i} = 6 \cdot 10^{-5} \frac{1}{ft} \quad D_f = \frac{1}{12} ft \quad A = \pi \cdot \left(\frac{D_f}{2}\right)^2 \quad V_1 = \frac{Q}{A}$$

Solution:

$$h_f = \frac{\Delta P}{\rho} \quad h_f = 744.379 \frac{ft^2}{s^2} \quad \frac{h_f}{g} = 23.136 ft$$

$$Re = \frac{V_1 \cdot D_f \cdot \rho}{\mu} \quad Re = 9.772 \cdot 10^4$$

From Moody chart:

$$f = 0.016 \quad L = \frac{(h_f \cdot D_f \cdot 2)}{f \cdot (V_1)^2}$$

Answers:

$$L = 51.63 ft$$

**EXAMPLE 6.7**  $\Delta p = 10 psi$ ,  $L = 20 ft$ ,  $D = 1 in$ ,  $Q = ?$  This situation requires an iterative method, because the calculation of  $f$  requires knowledge of the flow rate. Calculate head loss from the basic equation, guess a high  $Re$  number, and then get  $f$  from the Moody chart for the appropriate  $e/D$ . Then calculate the velocity and a new head loss from these estimated values. Correct  $Re$  until the two head losses are within 1 percent of each other. Finally, calculate the flow rate.

Known:

$$\Delta P = 10 psi \quad \rho = 997 \frac{kg}{m^3} \quad \mu = (968 \cdot 10^{-6}) \cdot \frac{N}{m^2} \cdot s$$

$$\Delta P = 4.633 \cdot 10^4 \frac{\text{lb}}{\text{ft} \cdot \text{s}^2} \quad \rho = 62.241 \frac{\text{lb}}{\text{ft}^3} \quad \mu = 6.505 \cdot 10^{-4} \frac{\text{lb}}{\text{ft} \cdot \text{s}}$$

$$D_i = 1 \text{ in} \quad e = 0.000005 \quad g = 32.174 \frac{\text{ft}}{\text{s}^2}$$

$$\frac{e}{D_i} = 6 \cdot 10^{-5} \frac{1}{\text{ft}} \quad D_f = \frac{1}{12} \text{ ft} \quad L = 20 \text{ ft}$$

Solution:

$$h_l = \frac{\Delta P}{\rho} \quad \frac{h_l}{g} = 23.136 \text{ ft}$$

Guess:

$$Re = 5 \cdot 10^5$$

From Moody chart:

$$f = 0.013$$

$$V_l = \frac{(Re \cdot \mu)}{D_f \cdot \rho} \quad V_l = 62.706 \frac{\text{ft}}{\text{s}}$$

$$h_l = f \cdot \frac{L}{D_f} \cdot \frac{(V_l)^2}{2} \quad \frac{h_l}{g} = 190.652 \text{ ft} \quad 23.136 < 190.652 \quad \text{Guess lower } Re.$$

Guess:

$$Re = 1.5 \cdot 10^5$$

From Moody chart:

$$f = 0.0165$$

$$V_l = \frac{(Re \cdot \mu)}{D_f \cdot \rho} \quad V_l = 18.812 \frac{\text{ft}}{\text{s}}$$

$$h_l = f \cdot \frac{L}{D_f} \cdot \frac{(V_l)^2}{2} \quad \frac{h_l}{g} = 21.778 \text{ ft} \quad 23.136 > 21.778 \quad \text{Guess higher } Re.$$

Guess:

$$Re = 1.55 \cdot 10^5$$

From Moody chart:

$$f = 0.0164$$

$$V_l = \frac{(Re \cdot \mu)}{D_f \cdot \rho} \quad V_l = 19.439 \frac{\text{ft}}{\text{s}} \quad \frac{(23.136 - 23.113)}{23.136} = 0.099\%$$

$$h_l = f \cdot \frac{L}{D_f} \cdot \frac{(V_l)^2}{2} \quad \frac{h_l}{g} = 23.113 \text{ ft} \quad \text{Close enough!}$$

Answer:

$$V_1 = 19.439 \frac{\text{ft}}{\text{s}} \quad A = \pi \cdot \left(\frac{D_f}{2}\right)^2$$

$$Q = V_1 \cdot A \quad Q = 0.106 \frac{\text{ft}^3}{\text{s}} \quad Q = 47.586 \frac{\text{gal}}{\text{min}}$$

**EXAMPLE 6.8**  $\Delta p = 10 \text{ psi}$ ,  $L = 20 \text{ ft}$ ,  $Q = 40 \text{ gpm}$ ,  $D = ?$  Obviously, if the flow rate is known, along with the maximum allowable pressure loss and pipe length, the designer wishes to determine the smallest diameter to keep costs low. This situation requires an iterative solution that starts with a guessed  $D$ . From this diameter,  $e/D$  can be calculated, and then velocity can be found from the area and flow. Next,  $f$  can be found from the Moody diagram after calculating  $Re$ . With this  $f$ , the head loss can be calculated. Use the main equation to calculate the pressure loss and compare with the maximum allowable pressure drop.

Known:

$$Q = 40 \frac{\text{gal}}{\text{min}} \quad \Delta P = 10 \text{ psi} \quad \rho = 997 \frac{\text{kg}}{\text{m}^3} \quad \mu = (968 \cdot 10^{-6}) \cdot \frac{\text{N}}{\text{m}^2} \cdot \text{s}$$

$$Q = 0.089 \frac{\text{ft}^3}{\text{s}} \quad \Delta P = 4.633 \cdot 10^4 \frac{\text{lb}}{\text{ft} \cdot \text{s}^2} \quad \rho = 62.241 \frac{\text{lb}}{\text{ft}^3} \quad \mu = 6.505 \cdot 10^{-4} \frac{\text{lb}}{\text{ft} \cdot \text{s}}$$

$$e = 0.000005 \quad g = 32.174 \frac{\text{ft}}{\text{s}^2} \quad L = 20 \text{ ft}$$

Solution: *Guess:*

$$D_i = 1 \text{ in}$$

$$D_f = \frac{D_i}{12 \frac{\text{in}}{\text{ft}}} \quad D_f = 0.083 \text{ ft} \quad \frac{e}{D_i} = 6 \cdot 10^{-5} \frac{1}{\text{ft}}$$

$$A = \pi \cdot \left(\frac{D_f}{2}\right)^2 \quad A = 5.454 \cdot 10^{-3} \text{ ft}^2$$

$$V_1 = \frac{Q}{A} \quad V_1 = 16.34 \frac{\text{ft}}{\text{s}}$$

$$Re = \frac{(\rho \cdot V_1 \cdot D_f)}{\mu} \quad Re = 1.303 \cdot 10^5$$

From Moody chart:

$$f = 0.017$$

$$h_1 = f \cdot \frac{L}{D_f} \cdot \frac{V_1^2}{2} \quad h_1 = 544.665 \frac{\text{ft}^2}{\text{s}^2}$$

$$\Delta P = h_1 \cdot \rho \quad \Delta P = 3.39 \cdot 10^4 \frac{\text{lb}}{\text{ft} \cdot \text{s}^2} \quad \Delta P = 7.317 \text{ psi} \quad 7.317 < 10 \quad \text{Pick smaller diameter.}$$

Guess:

$$D_i = 0.75 \text{ in}$$

$$D_f = \frac{D_i}{12} \frac{\text{in}}{\text{ft}} \quad D_f = 0.062 \text{ ft} \quad \frac{e}{D_i} = 8 \cdot 10^{-5} \frac{1}{\text{ft}}$$

$$A = \pi \cdot \left( \frac{D_f}{2} \right)^2 \quad A = 3.068 \cdot 10^{-3} \text{ ft}^2$$

$$V_I = \frac{Q}{A} \quad V_I = 29.049 \frac{\text{ft}}{\text{s}}$$

$$Re = \frac{(\rho \cdot V_I \cdot D_f)}{\mu} \quad Re = 1.737 \cdot 10^5$$

From Moody chart:

$$f = 0.016$$

$$h_f = f \cdot \frac{L}{D_f} \cdot \frac{V_I^2}{2} \quad h_f = 2.16 \cdot 10^3 \frac{\text{ft}^2}{\text{s}^2}$$

$$\Delta P = h_f \cdot \rho \quad \Delta P = 1.345 \cdot 10^5 \frac{\text{lb}}{\text{ft} \cdot \text{s}^2} \quad \Delta P = 29.02 \text{ psi} \quad 29.02 > 10 \text{ Pick larger diameter.}$$

Guess:

$$D_i = 0.94 \text{ in}$$

$$D_f = \frac{D_i}{12} \frac{\text{in}}{\text{ft}} \quad D_f = 0.078 \text{ ft} \quad \frac{e}{D_i} = 6.383 \cdot 10^{-5} \frac{1}{\text{ft}}$$

$$A = \pi \cdot \left( \frac{D_f}{2} \right)^2 \quad A = 4.819 \cdot 10^{-3} \text{ ft}^2$$

$$V_I = \frac{Q}{A} \quad V_I = 18.492 \frac{\text{ft}}{\text{s}}$$

$$Re = \frac{(\rho \cdot V_I \cdot D_f)}{\mu} \quad Re = 1.386 \cdot 10^5$$

From Moody chart:

$$f = 0.017$$

$$h_f = f \cdot \frac{L}{D_f} \cdot \frac{V_I^2}{2} \quad h_f = 742.147 \frac{\text{ft}^2}{\text{s}^2}$$

$$\Delta P = h_f \cdot \rho \quad \Delta P = 4.619 \cdot 10^4 \frac{lb}{ft \cdot s^2} \quad \Delta P = 9.97 \text{ psi}$$

$$\frac{(10 - 9.97)}{10} = 0.3\% \quad \text{Close enough!}$$

**6.2.4 Pump Power Calculations**

The head loss equation can be modified to include the power necessary to operate a pump. This modification is derived from the fundamental energy conservation equation and is expressed as:

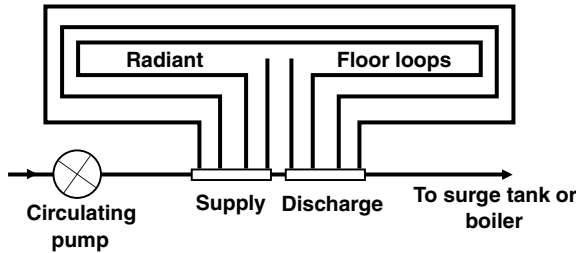


**FIGURE 6.6** Hydronic piping system using a manifold of four pipes.

$$\left( \frac{p_1}{\rho} + \alpha_1 \frac{\bar{V}_1^2}{2} + gz_1 \right) - \left( \frac{p_2}{\rho} + \alpha_2 \frac{\bar{V}_2^2}{2} + gz_2 \right) = h_1 + h_m + h_p \quad (6.9)$$

The pump head term  $h_p$  is negative because the power is into the pump. Use of Eq. (6.9) is demonstrated in the following example.

**EXAMPLE 6.9** *The level of a surge tank is 20 ft above the suction of a pump. The pump discharges 20 gpm of water into a single-path pipe system that comprises 200 ft of drawn tubing. The water is 80°F. The pipe system includes one gate valve, and the pipe is 0.50 in in diameter. The pipe system discharges into a second surge tank that is 40 ft above the pump discharge and is sealed at a pressure of 10 psig. Calculate the pump head and pump power necessary to accomplish this task. Figure 6.6 shows this schematically.*

Known:

$$Q = 20 \frac{\text{gal}}{\text{min}} \quad D = 0.5 \text{ in} \quad \rho = 999 \frac{\text{kg}}{\text{m}^3}$$

$$Q = 0.045 \frac{\text{ft}^3}{\text{s}} \quad D = 0.042 \text{ ft} \quad \rho = 62.366 \frac{\text{lb}}{\text{ft}^3}$$

$$Z_1 = 20 \text{ ft} \quad A = \pi \cdot \left( \frac{D}{2} \right)^2 \quad g = 32.174 \frac{\text{ft}}{\text{s}^2}$$

$$Z_2 = 40 \text{ ft} \quad V_1 = 0 \frac{\text{ft}}{\text{s}} \quad V_2 = 0 \frac{\text{ft}}{\text{s}}$$

Solution:

$$P_1 = \rho g Z_1 = 8.662 \text{ psig}$$

$$P_2 = 10 \text{ psi} + \rho \cdot g \cdot Z_2 = 27.324 \text{ psig}$$

$$\text{Power} = \Delta P \cdot Q = 0.218 \text{ hp}$$



**S · E · C · T · I · O · N · 3**

# **THERMAL COMFORT**



---

# CHAPTER 1

---

## WHAT IS THERMAL COMFORT?

---

American Society of Heating Refrigerating and Air-Conditioning Engineers (ASHRAE) Standard 55 (1992) defines *thermal comfort* as “the condition of mind that expresses satisfaction with the thermal environment.” This definition loosely translates to the question of whether the occupant feels too hot, too cold, or just right. The next step is to determine if the room is thermally comfortable. The simplest way is to ask all the occupants if they are satisfied with their thermal environment. However, this method may result in numerous thermostat adjustments and, as a worst case, reinstallation of the entire heating or cooling system. The ultimate goal is to predict the thermal comfort in a room without resorting to a polling system.

The six primary variables used to predict thermal comfort are activity level, clothing insulation value, air velocity, humidity, air temperature, and mean radiant temperature (Fanger, 1967). For most design situations, the room usage dictates the activity level and clothing insulation value. For example, an office situation implies sedentary activity with business attire. In contrast, an exercise room implies a high activity level with shorts and a T-shirt. In addition, the humidity depends on the heating or cooling system, generically referred to as a thermal distribution system, for the entire building, which may not be controlled at the room level. Usually, the air velocity is maintained at a level that avoids a draft yet provides the necessary fresh air for the occupants.

In an individual room, the dry-bulb air and mean radiant temperatures are two variables that the design engineer may control on an individual room level. The dry-bulb air temperature measures the temperature of the air in the room. The mean radiant temperature is a measure of the radiant energy exchange. In most design situations, only the air temperature is used, whereas the MRT is ignored. This chapter focuses on defining thermal comfort and establishing its general relationship between air and mean radiant temperatures.

### 1.1 OCCUPANT PERCEPTION

---

An occupant’s thermal comfort depends on the continuous generation and exchange of heat with the surrounding environment. First, the body internally generates heat due to physical activity. The amount of metabolic heat generation depends on the activity level and size of the person. For example, an average-sized

male seated quietly produces 108 W (368 Btu/h) of body heat. Compared with walking on level ground at 1.34 m/s (3.0 mph), the same man generates 270 W (920 Btu/h) (ASHRAE, 1997). Figure 1.1 shows metabolic heat generation rates for sample activities. ASHRAE 1997 *Fundamentals Handbook* gives additional activities and explains how to adjust these levels for a specific body height and mass. However, these charts and calculations do not account for the individual person's characteristics and surrounding conditions, which also affect the amount of heat generation for a given activity. Another part of metabolic heat generation is the effect of shivering. Shivering is the body's method of raising the activity level to increase the internal heat generation, thereby reducing the body's heat deficit. The amount of heat generated by shivering depends on how cold the body perceives itself to be.

There are several ways the body loses or gains heat. The first three to be discussed are perspiration, evaporation, and respiration. Sweating causes perspiration or, for calculation purposes water, to build up on the skin surface. The evaporation of this water results in a body energy loss. Even when the body is not sweating to regulate its temperature, water is diffusing through the skin surface into the environment, resulting in body energy loss. In addition, the body also loses water and energy through respiration.

The other two methods of interacting with the environment are convection and radiation. The convective exchange can be driven by either the natural air movement or by an external source (e.g., the wind or a fan). The convective heat exchange rate depends on the activity, wind speed, and temperature difference between the skin and surrounding air. Since air does not affect radiative heat trans-

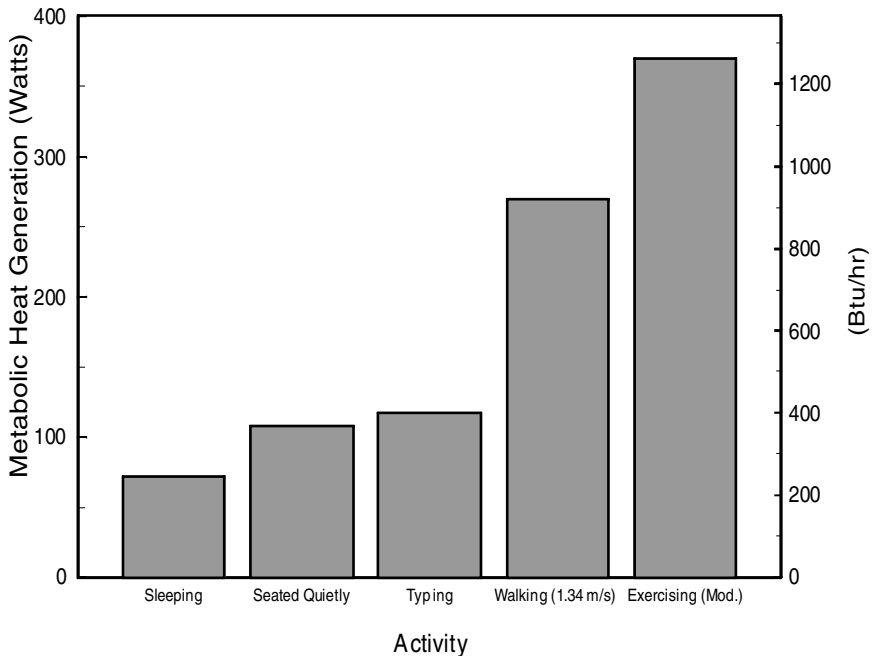


**FIGURE 1.1** Sample metabolic heat generation rates for various activities.

fer, the radiation exchange rate depends primarily on the position of the occupant and the temperature difference between the occupant and surrounding objects along with the emissivity and area of both participating surfaces. As with all heat transfer, both convection and radiation have a net heat transfer from warm to cold, which depends on the geometric relationship between the occupant and surroundings. For example, if the air temperature is below the skin temperature, the occupant will lose energy to the air by convection. Likewise, if the surrounding enclosure's temperature is above the skin temperature, the occupant will gain energy from the surroundings by radiation. Any combination of these two can occur (e.g., losing energy by convection while gaining energy by radiation or gaining from both radiation and convection).

Each of these energy losses and gains relates to one or more of the variables of thermal comfort. Table 1.1 lists the energy gain or loss mechanism in the left column with the typically related variable(s) of thermal comfort in the right column. This table provides the first glimpse at the complicated nature of determining an occupant's thermal comfort.

Energy exchange has two different states: steady state (when the energy net gain is constant) and transient (when the energy net gain is changing). Figure 1.2 visually displays the difference between steady state and transient energy exchange. Both graphs show time increasing on the horizontal axis from left to right and the system energy increasing on the vertical axis from bottom to top. The graph on the left in the figure shows a horizontal line signifying constant system energy or steady state for each time segment. The graph on the right in the figure representing the transient state shows a line slanting upward, signifying an increase in the amount of system energy as time marches forward.

**TABLE 1.1** Relationship of Occupant Energy Exchanges with Variables of Thermal Comfort

Process	Related thermal comfort variable
Metabolic heat generation	activity level
Evaporation through sweating	air temperature humidity air velocity activity level clothing insulation
Diffusion through skin	air temperature humidity air velocity clothing insulation
Respiratory heat loss	air temperature humidity activity level
Convection	air temperature air velocity activity level clothing insulation
Radiation	mean radiant temperature clothing insulation

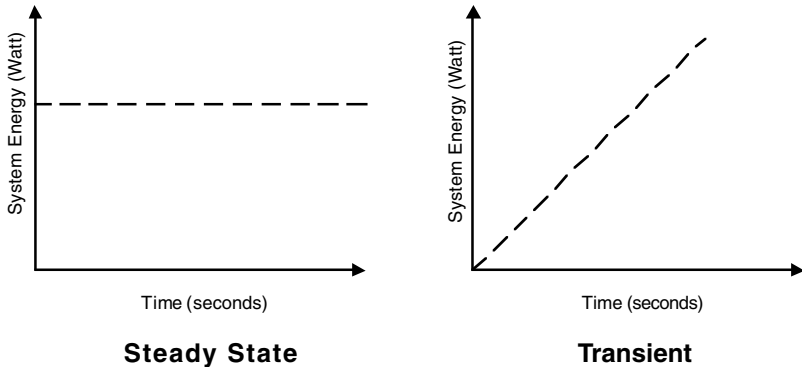


**FIGURE 1.2** Difference between steady state and transient energy exchange.

Thermal comfort requires a balance between the amount of energy gained and lost by a person. The person is at steady state because the energy of the person is not changing. This does not mean the rate of a person's energy gain is not changing. Instead, it means that if the amount of energy gained is increasing, the amount of energy lost by the person is increasing equally. Although normally considered in a negative context, a transient situation could be desirable for a brief period of time. For instance, standing in front of a warm fireplace is often welcome after a person is exposed for a long period of time to cold winter temperatures. At some point, the additional energy provided by the fire will become unwanted, and the person will move.

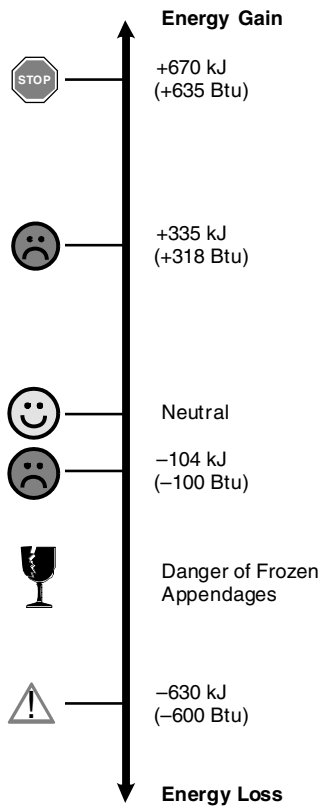


**FIGURE 1.3** Approximate levels of body internal energy.

A person can also be thermally uncomfortable at steady state. If the person has gained too much energy at an earlier time and was unable to lose the heat, thermal comfort has not been achieved although at steady state.

Using the steady-state balance of energy gains and losses, physically dangerous conditions can be predicted. Chapter 2 discusses the methods used to calculate an occupant's energy gain or loss in detail. Figure 1.3 shows approximate body response based on body energy gain. Body energy increases toward the top of the line and decreases toward the bottom of the line. A neutral or thermally comfortable sensation is shown in the center with the smiling occupant. The values given are averages

and subject to a wide variation based on individual differences. This information is given for the readers' personal edification because most HVAC systems do not go to these extremes.

For hot and humid environments, a body energy gain of 335 kJ (318 Btu) or a raise in body temperature of 1.4°C (2.5°F) is the average voluntary limit for an average-sized man. At this point, the average-sized man, represented by the frowning face near the top, will move unless a life-or-death reason forces for him to stay. An energy gain of 670 kJ (635 Btu) or an increase in body temperature of 2.8°C (5°F) causes collapse displayed by the Stop sign. To the other extreme, for cold environments,

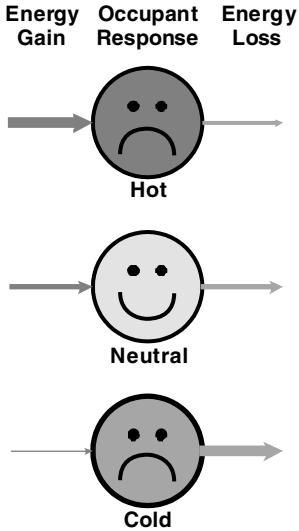


**FIGURE 1.4** Occupant responses to energy gain and loss imbalance given initially neutral condition.

able. The reverse case is shown at the bottom of the figure. This occupant has a heat loss larger than the energy gain and feels cold.

Historically, heating and air-conditioning design philosophies have focused on obtaining a specific indoor air temperature for a given outdoor design air temperature. This technique is referred to as an “envelope” calculation. If the design air temperature was achieved in a room, then the occupants were considered thermally comfortable. This approach does not differentiate convective energy from radiant energy exchange. Therefore, the design air temperature may not accurately represent the occupant's thermal comfort.

One of the most common examples of the air temperature misrepresenting the occupant's thermal comfort is standing outside on a cool, calm day. As shown in Fig. 1.5, the air is a chilly 10°C (50°F). Without any unusual weather patterns, the outdoor surroundings are approximately equal to the air temperature. The occupant loses energy by (1) convection to the cooler air shown by the thin wavy lines around the “air cloud” and (2) radiation to the cooler surrounding surfaces shown by the thin horizontal lines from the occupant's right to the tree.

With the sun shining, the occupant receives additional energy from the sun via radiant energy shown by the thick straight lines directed to the occupant's left. The occupant feels thermally comfortable due to the energy balance between energy lost

ments, a body energy loss of 104 kJ (100 Btu) causes mild discomfort, represented by the frowning face near the bottom. A body energy loss of 630 kJ (600 Btu) or a body temperature drop of 2.6°C (4.7°F) causes extreme discomfort shown by the exclamation sign (ASHRAE, 1997). Body appendages may freeze while progressing from mild discomfort to extreme discomfort. In the progression from neutral to extreme discomfort, the person's body will begin to shiver and may also fidget. These are reactions of the body to generate more energy and lower the deficit.

The thermal condition perceived by the occupant depends on the balance between the energy gains and losses. The smiling occupant in the center of Fig. 1.4 is thermally neutral. The energy gained equals the energy lost, resulting in a neutral sensation. The frowning occupant at the top of Fig. 1.4 has a energy gain greater than the energy loss. The occupant feels hot and thermally uncomfortable.

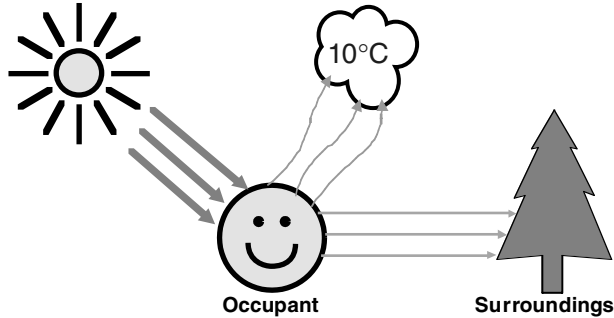


**FIGURE 1.5** Simplified energy exchange diagram for a sunny day.

to the air and surroundings and the slowing of energy loss by the sun plus internal heat generation. The mean radiant temperature would be above the air temperature of  $10^{\circ}\text{C}$  ( $50^{\circ}\text{F}$ ).

When a cloud covers the sunshine and blocks some of the radiant energy from the sun as shown in Fig. 1.6, the occupant's energy gain decreases. The occupant is still losing energy to the air and surroundings. In this situation, the amount of energy lost to the air and surroundings is greater than the energy gained from the sun. Due to the energy imbalance, the occupant begins feeling chilled. Although the mean radiant temperature may be above the air temperature, the occupant is still thermally uncomfortable, due to a net energy loss.

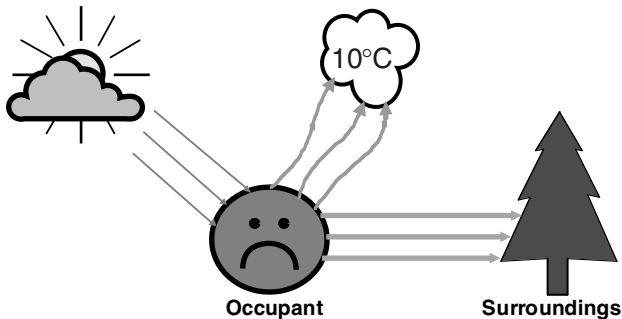


**FIGURE 1.6** Simplified energy exchange diagram for a cloudy day.

Another example of air temperature not accurately representing thermal comfort is a nonuniform radiation field in a room heated by a convective or forced-air heating system with a large window. The top view of such room is shown in Fig. 1.7. The outside air temperature is  $-18^{\circ}\text{C}$  ( $0^{\circ}\text{F}$ ), and the inside air is maintained uniformly at  $20^{\circ}\text{C}$  ( $68^{\circ}\text{F}$ ). If the window  $R$  value is 2, then the inside window surface temperature will be  $8.8^{\circ}\text{C}$  ( $48^{\circ}\text{F}$ ). The radiative heat transfer experienced by the person seated on the couch in front of the window is due to two components: (1) the radiative flux emitted by the person shown by an arrow leaving the couch area and (2) the radiative flux incident on the person shown by the arrow pointing toward the couch area.

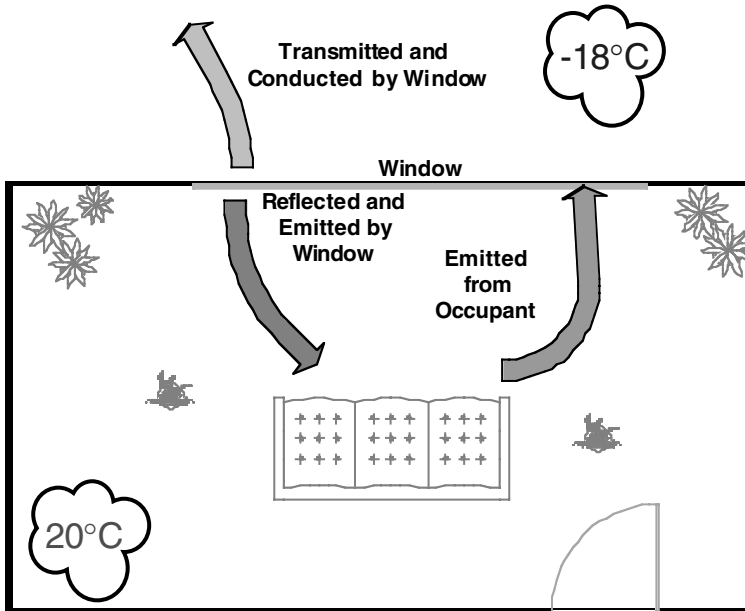


FIGURE 1.7 Nonuniform radiant field in a room.

The incident flux on the person comes from the radiation that is emitted and reflected by the relatively cool window surface. For a previously neutral occupant, moving to the window area would create a sense of thermal discomfort due to a net radiative transmission through the window and a net radiative heat loss to the cool window surface.

The radiative transmission loss depends on the window transmissivity. Generally, window glass is transparent below wavelengths of  $\lambda = 2 \mu\text{m}$  and opaque above  $\lambda = 4 \mu\text{m}$ . For normal indoor wall temperatures of 24°C (75°F), about 2 percent of the radiation is transmitted through the window (Siegel and Howell, 1981). The remaining 98 percent is either absorbed by the window or reflected into the room. This is not to be confused with radiation from the sun, which radiates at 5507°C (9944°F). At this temperature, almost 95 percent of the radiant energy will pass through the window (Siegel and Howell, 1981). This is the fundamental concept behind the greenhouse effect.

The second loss for the occupant, a radiative heat loss to the window surface, is due to radiation absorption by the relatively cool window surface. The absorbed portion is either conducted to the outdoors through the window or re-emitted into the room at the window surface temperature. Since the radiant emission directed from the cooler window toward the occupant is less than the emission from the occupant toward the window, the previously neutral occupant experiences a net radiative heat loss. The heat loss leads to an uncomfortable cool feeling. Despite the surrounding air temperature of 20°C (68°F), the net radiative losses result in a local mean radiant temperature, which represents the radiant energy exchange, below the air temperature of 20°C (68°F). The mean radiant temperature is defined and discussed in detail in Chapter 3.

In this example, the occupant could be made thermally comfortable by offsetting the net radiant energy loss to the environment with a corresponding energy gain. The gain could come from an additional forced-air heater (i.e., wall furnace or cord-connect portable) or a radiant heater.

These examples show air temperature alone is not an accurate thermal comfort indicator. Instead, Fanger (1967) suggests using the operative temperature to measure local thermal comfort. The *operative temperature* is defined as “the temperature of a uniform isothermal black enclosure in which the occupant exchanges the same amount of heat by radiation and convection as in the actual nonuniform environment” (Fanger, 1967). It is approximately the average of the air and mean radiant temperature for typical indoor applications and is indicative of the temperature the occupant feels. Figure 1.8 gives a pictorial representation of the air, operative, and mean radiant temperatures. The air temperature is the temperature of the surrounding air represented by the cloud. The mean radiant temperature, represented in this figure by the sun, indicates the temperature of the surrounding surfaces. However, the radiation field includes all objects in the surroundings (e.g., walls, windows, furniture, and buildings). Combining the impact of dry-bulb air and mean radiant temperature provides the operative temperature that the occupant perceives. The temperatures are represented in the picture as tagged to one point. In reality, they are distributed around the environment and come simultaneously from many different directions.

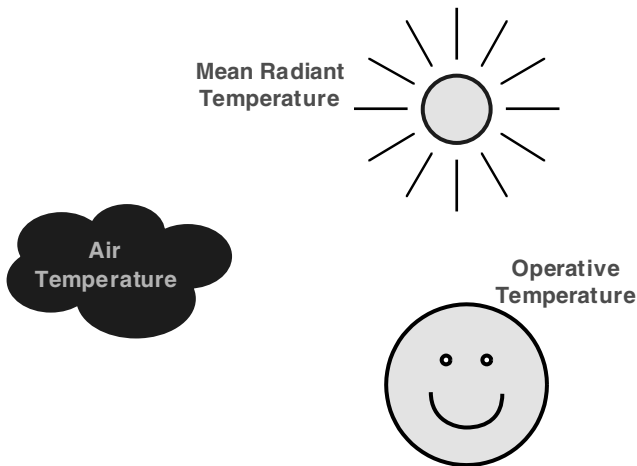


**FIGURE 1.8** Pictorial representation of air, mean radiant, and operative temperatures.

Lastly, note that in positioning a forced-air or radiant heater, radiant asymmetry needs to be considered. Radiant asymmetry can cause thermal discomfort regardless of the mean radiant and air temperatures. For example, consider a person standing outside on a cold winter day. Then give the person a campfire for warmth as shown in Fig. 1.9. The person would tend naturally to creep closer to the fire to offset the cold from the air. The warmth of the fire would warm the left half of the person. However, the right side would continue to feel cold. The person

might creep toward the fire again to try to offset the feeling. To confuse matters, the net energy gain from the fire could exactly equal the heat loss to the cold air. However, the person is thermally uncomfortable due to radiant asymmetry.

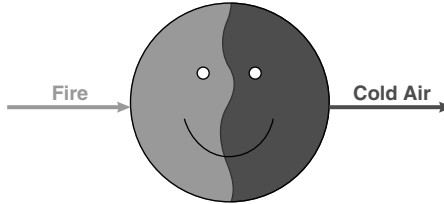


**FIGURE 1.9** Role of radiant asymmetry in thermal comfort.

## 1.2 EFFECTS OF THERMAL DISTRIBUTION SYSTEMS

Gan and Croome (1994) reported that almost 40 percent of the world's nonrenewable energy is used to achieve thermal comfort in buildings. Thermal distribution systems can use one or both of two different modes of heat transfer, convection and radiation, to deliver thermal comfort to an occupant.

### 1.2.1 Heating

Figure 1.10 illustrates the difference in heating modes. The forced-air system on the left uses primarily convection to deliver the heat energy to the room as illustrated by the thick arrow labeled  $Q_{\text{conv}}$  at the upper right of the occupant. Energy is transferred by warm air circulating around the room warming surfaces. A forced-air system heats the room air first. Then the air circulates to the occupant and other surfaces. The room air will be warmer than the room wall and object surfaces, since

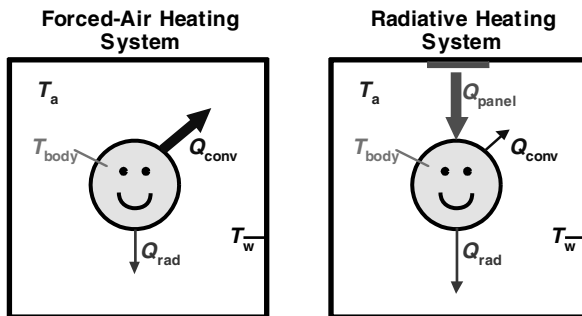


**FIGURE 1.10** Heating system differences.

moving air is the primary mode of energy transfer. The simplified net energy balance corresponding with both sides of Fig. 1.10 is:

$$Q_{\text{net}} = Q_{\text{rad}} + Q_{\text{conv}} \quad (1.1)$$

An example of a forced-air heating system is an office with ceiling vents gently blowing warm air into the room. Although the air feels warm and the occupant is comfortable, some surfaces in the room may feel cooler to the touch.

The reader should note the human body is constantly generating heat (i.e., it never needs to be warmed to maintain comfort at steady state). The sensation of feeling cool indicates too much energy loss by the body. A forced-air heating system reduces the body energy lost through convection by elevating the air temperature and reducing the temperature difference. Equation (1.2) shows the basic equation to calculate convection heat transfer  $Q$  from the body at temperature  $T_{\text{body}}$  to the air at temperature  $T_{\text{air}}$  (Incropera and DeWitt, 1990):

$$Q_{\text{conv}} = h_c A (T_{\text{body}} - T_{\text{air}}) \quad (1.2)$$

For the same convective coefficient  $h_c$  and area  $A$ , as the difference between the body and air temperature decreases so does the amount of convective heat transfer.

The radiant system on the right-hand side transfers heat by electromagnetic waves, which is absorbed by the room surfaces, not the air. The room surfaces receive the energy first and then transfer energy to the surrounding air, reducing the amount of energy lost by the occupant. The net amount of energy transferred from the occupant for the radiant heating system is:

$$Q_{\text{net}} = Q_{\text{rad}} + Q_{\text{conv}} + Q_{\text{panel}} \quad (1.3)$$

The only difference between Eqs. (1.3) and (1.1) is the  $Q_{\text{panel}}$  term. For the two heating systems  $Q_{\text{net}}$  could be equal for both types of systems, and the individual terms would be adjusted. An example of radiant heating is standing in front of a fireplace. Although the air is slightly cool, the occupant feels warm and comfortable on at least one side of the body due to the radiant energy provided by the fire. It should be noted, if the radiant asymmetry created by the warm fire on one side and cold air on the other is too great, the occupant will not be thermally comfortable regardless of how the temperatures are adjusted.

When considering an occupant's thermal comfort, it is important to consider how the thermal distribution system interacts with the room. Radiant and forced-air systems have different relationships with the air temperature and the occupant's thermal comfort. Consider two identical rooms, one heated by a force-air system and the other by a radiant system. Both heating systems deliver the same amount of thermal comfort and have approximately the same operative temperature.

The forced-air heating system provides a warm air temperature to the room, which then heats the surfaces raising their temperature. The room air temperature will be warmer than the wall surface temperatures. The surface temperatures in the room affect radiant heat transfer in the room, indicated by the mean radiant temperature. Therefore, for a forced-air heating system on the left of Fig. 1.11, the air temperature represented by the cloud will be greater than the mean radiant temperature represented by the sun. By definition, the operative temperature, shown as the smiling occupant, is always between the air and mean radiant temperature regardless of the system.

The radiant heating system directly delivers energy from a surface to the occupant and other room objects to the walls, which then warm the air by natural con-

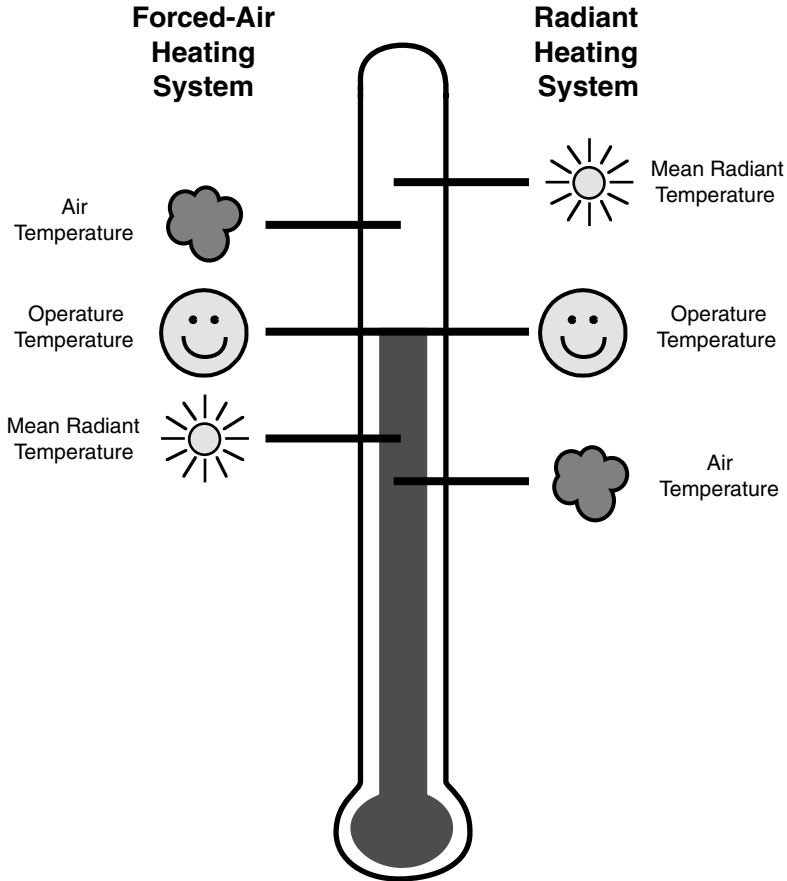


**FIGURE 1.11** Relative temperature relationships for two different heating systems.

vection. The radiantly heated room will have some surface temperatures greater than the air temperature, translating into a mean radiant temperature above the air temperature shown in Fig. 1.11 on the right side of the thermometer. Although the forced-air and radiant heating systems have different air and mean radiant temperatures, the operative temperature may be approximately the same. The key to providing equivalent thermal comfort with both heating systems is considering the modes of heat transfer.

## 1.2.2 Cooling

Cooling is commonly thought as the opposite of heating. Instead of adding energy to the room, the cooling system removes energy from the room, either by convection or radiation. As with heating, the method of removing the energy affects the occupant's thermal comfort. Figure 1.12 shows the difference in cooling systems and follows the form used to compare the heating systems. A forced-air cooling system provides cool

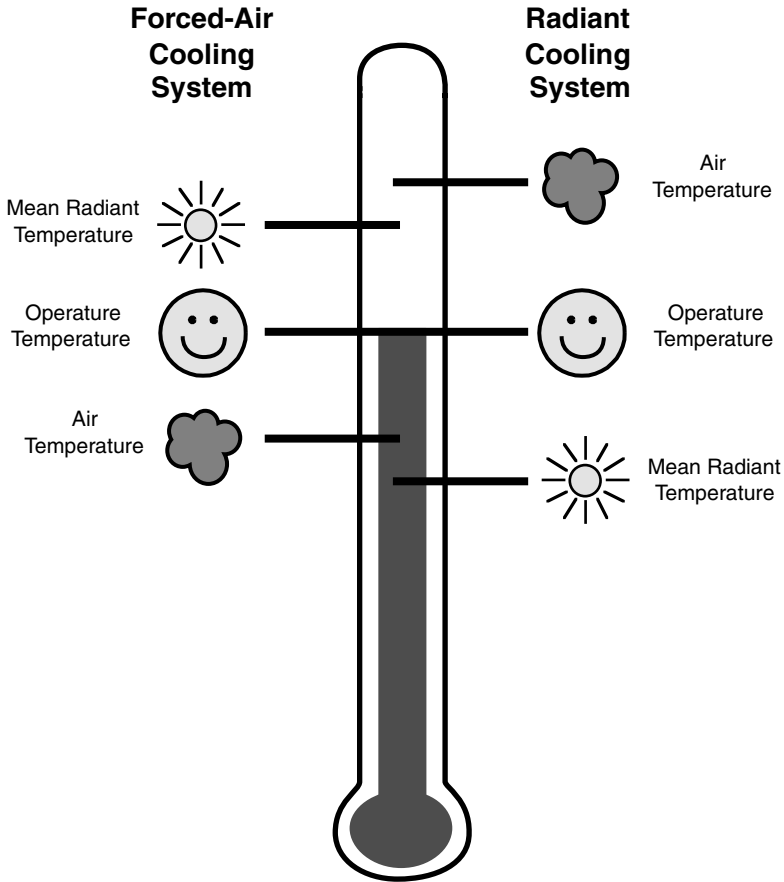


**FIGURE 1.12** Relative temperature relationships for two different cooling systems.

air into the room. The cool air circulates around the occupant and wall surfaces and carries heat away. An example of a forced-air cooling system would be a window air conditioner gently blowing cool air into a room.

A radiant cooling system provides a cool surface with which the warmer occupant exchanges radiant energy at a net energy loss. This is the same principle discussed in the example with an occupant in front of a cold window. The occupant will experience a net radiant heat loss to the cooler surface. In the case with the warm room and cool window, this is undesirable because the occupant wanted to gain energy to feel warm. However, for the purposes of radiant cooling, energy loss to the cold surface is desirable. A simplified schematic of a radiant cooling surface is shown in Fig. 1.13. The cool radiant surface could be provided by a surface with cooling coils. Cold water or some other fluid from a supply source maintains a cool temperature to absorb heat and carry the heat back to a reservoir to be cooled again or discarded.

As with heating, determining an occupant's thermal comfort relies on knowing what type of system is used. Referring to Fig. 1.12, which shows the relative temper-

ature relationships for a forced-air and radiant cooling system, the forced-air cooling system shown on the left side of the thermometer provides cool air to remove energy from the surfaces. The air temperature will be below the mean radiant temperature. The radiant cooling system shown on the right side of the thermometer absorbs radiant energy from the room surfaces, lowering the mean radiant temperature. For a radiant cooling system, the mean radiant temperature will be below the air temperature. Again, both systems provide the same operative temperature and level of thermal comfort. However, the heat transfer in each room has distinctly different characteristics. One of the main differences between a forced-air and radiant cooling system is the constraint of the dew point temperature. The radiant system has to be controlled so that the panel surface temperature remains above the dew point temperature.

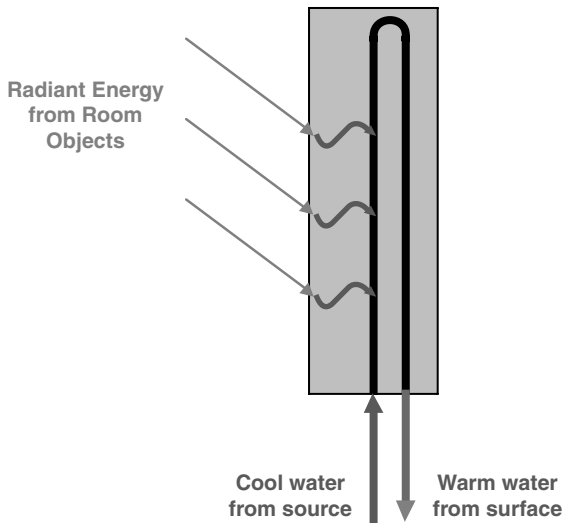


**FIGURE 1.13** Simplified radiant cooling surface schematic.

### 1.2.3 Other Considerations

Besides the mean radiant and air temperatures, there are four other factors of thermal comfort: activity level, clothing insulation value, air velocity, and humidity. A forced-air system almost intrinsically handles air humidity. With a radiant system, the air humidity must be regulated by a component not clearly defined as part of the heating system. The regulation of air humidity becomes very important for radiant cooling systems. Since the surface of a radiant cooler is colder than the air and other surfaces, it is susceptible to condensation, which creates biological growth (e.g., mildew and mold) and at the extreme “rain” in the room.

Another consideration is providing fresh air to the occupants. Again, the forced-air system naturally incorporates this into its system. The radiant heater has no need to move air, and again, an additional mechanism must be added to provide the occupants with the required fresh air.

## WHAT IS THERMAL COMFORT?

---

# CHAPTER 2

---

# THERMAL COMFORT MODELS

---

Many studies and models have been made in an effort to determine the complex nature of thermal comfort. This chapter briefly explains several studies and models. These descriptions are brief explanations for the in-depth material. The ASHRAE handbooks and referenced studies provide additional detailed information on all the material discussed in this chapter.

## **2.1 ROHLES-NEVIN STUDIES**

---

In 1971, Rohles and Nevins exposed 1600 students to 160 temperature-humidity conditions in an environmental test chamber at Kansas State University. For each temperature-humidity condition, five males and five females involved in sedentary activity were tested for 3 h. The subjects wore identical clothing with insulation values of  $0.9m^2K/W$  (0.6 clo). After being in the chamber for 1 h, subjects recorded their thermal sensation on a comfort ballot, and sensations were recorded at half-hour intervals for the remainder of the testing period. The comfort ballot contained a numerical scale consisting of integers ranging from 1 (cold) to 7 (hot). The Rohles-Nevins study is the largest study analyzing thermal comfort and serves as a model for many comfort research projects.

## **2.2 THE FANGER MODEL**

---

Fanger (1967) developed a thermal comfort equation that consists of the following six variables: air temperature, humidity, mean radiant temperature, relative air velocity, activity level, and insulation value of the clothing.

Fanger's model is based on the linear relationships of mean skin temperature and evaporative heat loss required for comfort at different activity levels.

### **2.2.1 Thermal Comfort Equation**

Fanger assumes long exposures to a constant thermal environment with constant metabolic rate (i.e., steady state) results in a heat balance between heat production and heat dissipation by the human body. Fanger's comfort equation (1970) is a result

of this heat balance illustrated by Fig. 2.1 and the general expression with all quantities in watts:

$$H - (E_d + E_{sw}) - (E_{re} + L) = K = R + C \quad (2.1)$$

The double equality of Eq. (2.1) represents a steady-state balance between the

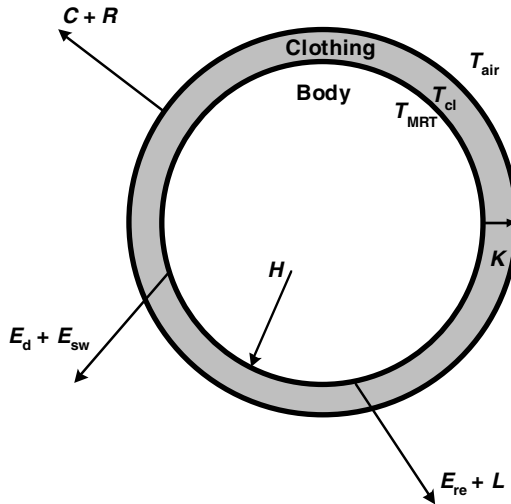


FIGURE 2.1 Fanger one-node model (1970).

net gain of energy of the body, the amount of energy conducted from the body to the clothing, and the energy dissipated to the surrounding environment. The terms on the far left side of Eq. (2.1) represent internal heat production ( $H$ ), the heat lost due to evaporation from the skin ( $E_d + E_{sw}$ ) by diffusion and sweat evaporation, respectively, and the heat lost by latent and dry respiration ( $E_{re} + L$ ). The middle term ( $K$ ) is the heat conducted through the clothing. The far right side ( $R + C$ ) represents the radiation and convection heat transferred from the outer surface of the clothing and unclothed parts of the body to the surrounding environment.

Fanger's model treats the heat balance of the body as steady state. The thermal load is defined as the metabolic heat generation less the amount of heat that would be dissipated in the actual environment if the body were at comfort conditions. It is a measure of the thermal regulatory effort required of the body to maintain thermal comfort. Figure 2.2 indicates the conditions of imbalance between actual and ideal. The face represents the entire person, and the shaded area surrounding the face represents the person's clothing. The equalities of Eq. (2.1) must be satisfied for the condition of thermal comfort to occur as shown by the center face labeled Neutral. If the ideal heat loss on the far left is less than the heat dissipation indicated by the other two equalities as on the far left, the person feels cold as indicated by the thermally uncomfortable person. Conversely, if the ideal heat loss is greater than the heat dissipation, the person feels hot as shown by the person on the far right.

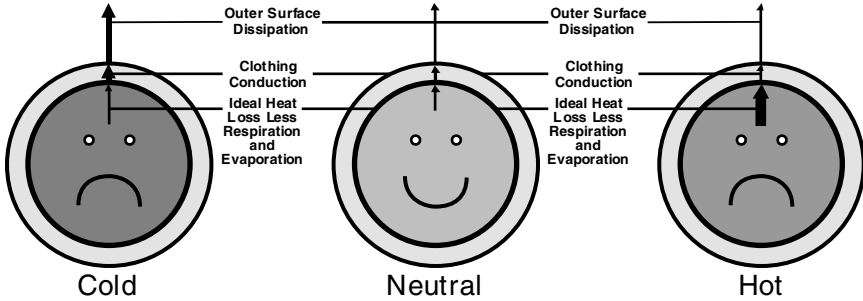


FIGURE 2.2 Illustration of Fanger’s one-node equality equation.

Fanger (1970) and ASHRAE (1997) thoroughly developed the calculation of each term in Eq. 2.1. The scope of this Handbook focuses on practical applications. With the advancement of computers, the calculations have been automated, and it is no longer practical and efficient to perform them by hand. This information is presented to illustrate the complex and intertwined relationship of all the variables of thermal comfort and to give a greater appreciation for the computer models available today.

First, the internal heat production is a function of metabolic rate ( $M$ ) and external mechanical work ( $W$ ). Metabolic rates per unit body surface area for sample activities are given in the second column of Table 2.1. More complete tables are available from Fanger (1970) and ASHRAE (1997). ASHRAE (1997) provides a relationship between body surface area and body mass and height to surface area as measured by Dubois.

TABLE 2.1 Sample Metabolic Rates (Fanger, 1970)

Activity	Metabolic rate (W/m <sup>2</sup> )
Seated quietly	58
Miscellaneous office work	58–70
Walking at 3.2 km/h on the level	116
Walking at 4.8 km/h on the level	151
Playing tennis	268
Playing basketball	442

Walking even at a slow rate generates approximately twice the energy as sitting. Most activities convert all of the metabolic energy to internal heat production. There the internal heat production, represented by the first term in Eq. (2.1), can be assumed to be metabolic rate.

The heat loss by diffusion ( $E_d$  in watts) through the skin is a function of the activity level and the vapor pressure of the ambient air. Fanger performed a linear curve fit between the temperature of the water vapor in the skin and the saturation pressure for skin temperatures between 27°C (81°F) and 37°C (99°F) to linearize the equation (Fanger, 1970). Therefore, that equation is only valid for that range.

The heat loss due to evaporation of sweat ( $\bar{E}_{sw}$  in watts) is estimated from a regression analysis from experimental data for people experiencing thermal comfort and uses the internal energy gain (Fanger, 1970).

To analyze the respiration heat loss, the exhaled air is divided into two parts: water and dry air. The latent respiration heat loss is due to the water vapor in the exhaled air. By relating breathing rate to activity level and approximating water vapor energy, Fanger (1970) developed a simplified expression for latent respiration heat loss.

The other heat loss from exhaled air is due to the temperature difference between the ambient air and the respired air. Again, the expression relates breathing rate to activity level. In addition, the exhaled air is assumed to be at a constant temperature of 34°C (93.2°F). This equation depends on the heat conducted through the clothing, which is a function of the thermal resistance of clothing. ASHRAE (1997) quantitates resistances for various types of clothing, which have been determined experimentally. Sample values are given in the second column of Table 2.2.

**TABLE 2.2** Sample Clothing Insulation Values and Radiation Correction Factors (ASHRAE, 1997)

Clothing	$I_{clo} \left( \frac{m^2 \circ C}{W} \right) f_{cl}$	
Nude	0	1.0
Typical business suit	0.2	1.32
Shorts and short-sleeve shirt	0.6	1.10
Knee-length skirt and short-sleeve shirt	0.1	1.26
Light trousers and short-sleeve shirt	0.9	1.15

Higher values of  $I_{clo}$  indicate more insulative clothing, such as a parka. Lower values of  $I_{clo}$  allow more heat to pass through and are generally cooler. Fanger (1970) and ASHRAE (1997) give a more extensive range of clothing.

Radiation is incorporated into Fanger's model by using the Stefan-Boltzmann law and relates the outer surface clothing temperature to the mean radiant temperature. It depends on the emissivity of the clothing. A value of 0.97 is suggested for most clothing (Fanger, 1970).

The human body partially radiates to itself and, therefore, the surface area used to compute radiation from the human body is not the actual body surface area but a reduced effective radiation area. The effective radiation area is the DuBois area corrected for the parts of the body radiating back to the body and the clothing. The variable  $f_{cl}$  given in the third column of Table 2.2 is the ratio of the outer surface area of the clothed body to the outer surface area of the nude body and adjusts the surface area for clothing.

The last expression needed to evaluate the thermal comfort equation is the convective heat transfer in watts from the clothed body, which is expressed in the standard form for convection. The convective coefficient depends on the air velocity and activity of the person. These relationships are given in Fanger (1970) and ASHRAE (1997).

## 2.2.2 Predicted Mean Vote

Fanger (1970) utilized the data from the Rohles-Nevins study together with his thermal comfort equation to develop an expression that predicts thermal sensation. This

expression is known as the predicted mean vote (*PMV*). The *PMV* is the mean thermal sensation of a large group of people on a scale of seven points:  $-3$  cold,  $-2$  cool,  $-1$  slightly cool,  $0$  neutral,  $1$  slightly warm,  $2$  warm, and  $3$  hot.

Fanger developed *PMV* tables for various activity levels. Fanger's comfort model also predicts the percentage of persons dissatisfied (*PPD*) with a particular environment. Predicted mean vote and *PPD* are used today to analyze thermal sensations and are used primarily in ISO Standard 7730 (1994).

### 2.3 GAGGE MODEL

Gagge developed a thermal comfort model in an attempt to improve the effective temperature equation formulated by Houghten and Yaglou (1923). Their effective temperature model combined air temperature and relative humidity into a single index. However, the model overestimates the effects of humidity at cold temperatures and underestimates the effects of humidity at warm temperatures (Yaglou, 1947).

Gagge et al. (1971) developed a physiological model based on body heat generation and regulatory sweating, suitable for low and medium activity levels. For the purposes of evaluating thermal comfort, the model considers a human to consist of two thermal compartments: the skin and the core. This model is shown in Fig. 2.3. All metabolic heat ( $M$ ) produced by the person is generated in the core. Shivering, muscle tension, and activity create metabolic heat. Energy is lost from the core by the muscles doing work on the environment and by respiratory heat losses. Heat is transported from the core to the skin by conduction and peripheral blood flow, labeled as Heat Transported from Core to Skin in Figure 2.3. The peripheral blood flow occurs as warm blood is pumped from the core to the skin in

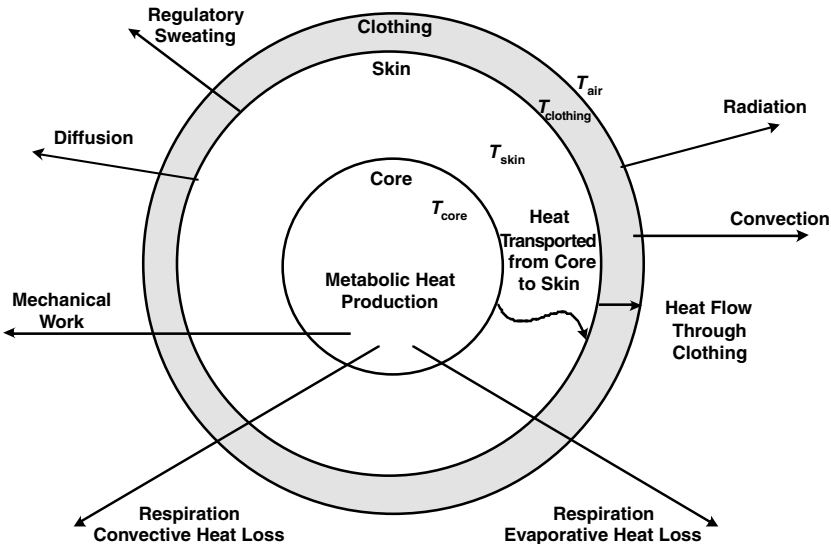


FIGURE 2.3 Gagge two-node model (1971).

an attempt to cool the person and then returns to the core at a cooler temperature. Energy is conducted from the skin to the outer surface of clothing and dissipated from the clothing surface by convection, radiation, regulatory sweating, and diffusion of water vapor.

The sources of heat transfer in the Gagge model are combined into heat balances on the core and skin. These heat balances take the form:

$$\begin{aligned} \text{(Rate of increase in internal energy of the core)} = & \text{(activity)} + \text{(shivering)} - \text{(work)} \\ & - \text{(respiration)} - \text{(conduction)} - \text{(convection by blood)} \quad (2.2) \end{aligned}$$

$$\begin{aligned} \text{(Rate of increase in internal energy of the skin)} = & \text{(heat from core)} - \text{(radiation)} \\ & - \text{(convection)} - \text{(diffusion)} - \text{(evaporation)} - \text{(heat lost from clothing)} \quad (2.3) \end{aligned}$$

The heat from conduction and convection by blood in Eq. (2.2) is equal to the heat from the core in Eq. (2.3). ASHRAE (1997) gives detailed equations for each term in Eqs. (2.2) and (2.3) as mathematical relationships. Each term depends on additional parameters calculated or found on a table. Again, the process for calculating thermal comfort becomes a time-consuming process even for the simplest cases. By numerical integration, these equations provide core and skin temperatures.

Skin wettedness can also be determined in the model. It is defined as the ratio of actual evaporative loss to the maximum possible evaporative loss at the same conditions with completely wet skin. Since it is a ratio, it is dimensionless. Skin wettedness is more closely related to the sense of discomfort than an occupant's thermal sensation (ASHRAE, 1997). Detailed equations and an example are not provided here because the calculations and equations are extremely involved, but Chapter 8 of the ASHRAE *Fundamentals Handbook* (1997) provides equations and charts.

The Gagge model predicts thermal sensation (*TSENS*) by first standardizing the actual environment. The standard environment produces the same physiological effects as the actual environment and is typical of a common indoor environment. The following characteristics are chosen for the standard environment:

1. Sea level
2. Uniform temperature
3. Ambient air movement of 0.1 to 0.18 m/s
4. 50 percent relative humidity
5. Clothing insulation of 0.6 clo

The thermal sensation is based on an 11-point scale. Positive values are the warm side of neutral; negative values are the cool side. *TSENS* is a measure of thermal sensation and calculated from cold and hot set points. The ASHRAE *Fundamentals Handbook* (1997) provides the necessary equations to calculate these limits and *TSENS* for an occupant's activity level.

Gagge's two-node model is based on steady-state experimental measurements on people. However, reaching steady state takes at least an hour when the person is exposed to a constant room condition. There are many instances in which the transient heat transferred from the body must be considered. Therefore, Jones and Ogawa (1992) modified the Gagge two-node model to include a transient clothing model capable of simulating a clothed person in transient situations.

## 2.4 IMPROVEMENTS TO THE GAGGE AND FANGER MODELS

---

Since the Gagge and Fanger models were first created, several improvements have been made to account for the complex nature of thermal comfort. This section briefly discusses three improvements.

### 2.4.1 Spline Analysis of Rohles-Nevins Study

After Fanger (1967) developed a basic comfort equation and Gagge et al. (1971) developed an improved effective temperature ( $ET^*$ ), the conditions converted temperature-humidity conditions from the Rohles-Nevins study into effective temperatures (in  $^{\circ}C$ ) and conducted a spline analysis. The details of this analysis are relatively complex and involve many parameters. Therefore, the discussion is only in brief, general terms.

A probit analysis was used to give the standard deviations from the mean at the given value of  $ET^*$  and are used for predicting cold and hot discomfort. By entering the table of areas under the normal probability curve with values for standard deviation, predicted percent dissatisfied [(PPD), i.e., the percentage of people unhappy with their thermal environment] can be calculated.

The clothing worn by the subjects in the Rohles-Nevins study have an insulation value of  $0.093m^2K/W$  (0.6 clo) and is not generally worn at effective temperatures below  $26.1^{\circ}C$  ( $70.9^{\circ}F$ ). Thus, it is unrealistic to use those equations at temperatures below  $26.1^{\circ}C$  ( $70.9^{\circ}F$ ). Therefore, Rohles et al. (1973) developed a relationship for determining clothing insulation that provides thermal comfort at various effective temperatures.

### 2.4.2 KSU Model

The KSU model is similar to the Gagge model. However, heat conducted and convected from the core to the skin is combined into an overall thermal conductance term determined empirically from experimental data. Rather than converting the actual environment to a standard environment, the KSU model predicts thermal sensation directly from physiological strain. Two equations are developed to predict hot and cold thermal sensation. A vasoconstriction factor is used to predict cold thermal sensations. The KSU model contains empirical equations for cold and warm thermal sensations under various conditions ranging from very hot to very cold at activities from  $58W/m^2$  to  $3400W/m^2$  (1.0 to 6.0 mets) and clothing insulation from  $0.008m^2K/W$  to  $0.1m^2K/W$  (0.05 to 0.7 clo).

### 2.4.3 Multinode Models

Multinode models are useful when people are exposed to nonuniform environments. Asymmetric radiation fields are one cause of these nonuniform environments. Stolwijk's multinode model (Stolwijk and Hardy, 1970) divides each part of the body into four segments: skin, muscle, fat, and the core compartment.

A comparison of the Stolwijk model to experimental measurements on human subjects has been made, and the skin temperatures and evaporative weight loss pre-

dictions of the model are in close agreement to the measurements. However, this model does not predict comfort or incorporate the effects of clothing.

Smith (1991) developed a model describing heat transfer from the body and how the heat is affected in a nonuniform and transient environment. As a foundation for these models, Smith requires an additional detailed model of the human physiological system similar to the Stolwijk multinode model. However, the physiological model developed by Smith is designed to interface specifically with the heat transfer models. The result of Smith's work is a three-dimensional transient computer model of the human thermal system employing finite element analysis.

## **2.5 RECENT THERMAL COMFORT TOOLS**

---

Thanks to many research dollars, several public domain computerized thermal comfort models are available to the HVAC design engineer. This section describes three more publicized thermal comfort models.

### **2.5.1 ASHRAE Research Project-657 and Research Project-907**

ASHRAE Research Project-657 developed a thermal comfort distribution tool that included a robust energy balance (Jones and Chapman, 1994). Building Comfort Analysis Program (BCAP) was further modified and validated in ASHRAE Research Project-907 (Chapman and DeGreef, 1997). Section 8 discusses the specific details of BCAP in depth.

The energy balance formulation completely describes the room interactions and contains a robust radiant energy exchange model. The parameters calculated include a mean radiant temperature distribution and an operative temperature distribution based on a mass-average air temperature. In addition, this program provides conduction, transmission, infiltration losses, and other environmental parameters.

### **2.5.2 BLAST/DOE2**

This thermal comfort model again boasts a sophisticated energy balance including conduction, convection, and radiation. However, the radiation model is based on the MRT correction method. In addition, this model calculates a zone humidity ratio, which is particularly of interest when considering radiant cooling. BLAST and DOE2 are currently being combined into one, more robust, model. Blast/DOE2 was designed to analyze a complete building and does not provide localized information that can be used to size and position in-space convective and radiative heating systems. It cannot be easily used to analyze the effect of setback for fast-acting radiant heating systems.

### **2.5.3 ASHRAE Research Project-781**

Research Project-781 sponsored by ASHRAE developed a thermal comfort prediction tool to be used easily by HVAC design engineers. This tool has a graphic user interface and incorporates three heat balance models, three empirical models, and two adaptive models (Fountain and Huizenga, 1996). The user enters various environmental parameters (e.g., air temperature, air velocity, relative humidity, season,

activity level, and the clothing insulation value of the occupant) and then the program calculates several thermal comfort parameters such as predicted mean vote and thermal sensation.

This model is very user friendly with a relatively sophisticated user interface and quickly calculates the parameters. However, it does not take into account detailed room geometry or robust energy calculations. The operative temperature is not explicitly calculated. The user of this program must realize it does not give a definitive answer on compliance with ASHRAE Standard 55-1992 (Fountain and Huizenga, 1996).



---

# CHAPTER 3

---

## THE MEAN RADIANT TEMPERATURE

---

The previous chapters repeatedly have developed the idea that thermal comfort is not easily modeled. It is intuitively obvious that every occupant desires to be thermally comfortable. However, achieving thermal comfort is not as easy as setting the traditional thermostat for a desired air temperature. Most quantities discussed in the previous chapters are not easily converted to a standard measurement device. Current technology is developing ways to measure the mean radiant temperature discussed in this chapter and the operative temperature discussed in Chapter 4.

This chapter explains the mean radiant temperature, which measures the average temperature of surfaces in the room weighted by a position relationship between them and the occupant. When used in conjunction with the air temperature, the mean radiant temperature gives a more realistic picture of the thermal comfort in a room. Unfortunately, due to the complex nature of radiant heat transfer, the mean radiant temperature is easy to define and understand conceptually but difficult to measure and calculate.

### 3.1 DEFINITION

---

Most thermal distribution systems are designed to maintain a baseline air temperature. Since radiant energy does not directly heat air, the air temperature does not take into account the radiant energy exchange in a room. The mean radiant temperature (MRT) indicates average temperature of the surfaces relative to the occupant. The MRT is defined as “the uniform surface temperature of an imaginary black enclosure in which the radiation from the occupant equals the radiant heat transfer in the actual nonuniform enclosure” (ASHRAE, 1992). This definition is given pictorially in Fig. 3.1. In the left uniform enclosure, all the surface temperatures are at the MRT, and the occupant is exchanging the same amount of heat in all directions. The right enclosure is very nonuniform. The occupant sees patches of cold surfaces to the left and warm patches to the top and bottom. The energy exchange is very nonuniform. However, the net radiant energy exchange of both the left and right occupant is the same. The MRT represents the temperature of the left enclosure surfaces equating both energy exchanges.

Because the MRT depends on the radiant energy exchange in a room, the room's

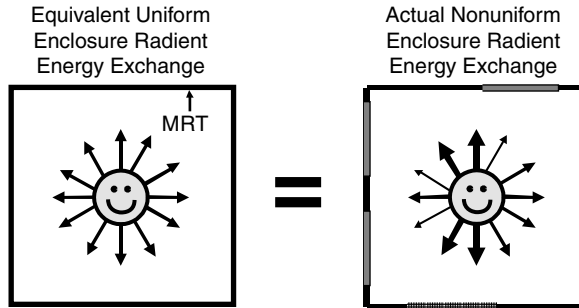


**FIGURE 3.1** Pictorial representation of the mean radiant temperature (MRT).

geometry and wall properties and window placement and type also affect the MRT. In addition to room characteristics, the MRT depends on the person's location and orientation in the room. Not only is the MRT different at different spots in the room but also possibly for occupants who are sitting and standing at the same location in the same room. The many variables affecting the MRT cause its calculation to quickly become complex.

Although the MRT is defined in terms of standard radiant heat transfer quantities, it is not a standard heat transfer quantity itself. The meaningful scope of the MRT is thermal comfort. Standard texts dealing solely with heat transfer will not mention the MRT. However, this does not devalue the MRT. In the realm of thermal comfort, the MRT plays a crucial role.

### 3.2 RELATIONSHIP TO THERMAL COMFORT

The purpose of the MRT in thermal comfort calculations and design is to represent the radiant energy exchange of the occupant at a particular point in a room. Consider the room with a large cold window shown in Fig. 3.2. The room is at a uniform air temperature of 20°C (68°F). At the back of the room (top of the picture) there is a large window to the outside at -18°C (0°F). An occupant at point 1 could be thermally comfortable, but the occupant at point 2 could complain of feeling chilly. The air temperature at both points is the same, so the room thermostat does not give the answer. The difference between the two points is the radiant energy exchange. Point 1 is sheltered from the full extent of the net radiant loss to the cold outdoors through the window. Point 2 is directly in front of the window and is subject to much larger radiant energy losses. Comparatively, this means the MRT at point 1 will be higher than at point 2, as shown later in the calculation examples.

### 3.3 MEASUREMENT TECHNIQUES

Measurement of the MRT requires accurately quantifying the radiant energy exchange at a given point. Tests have been performed and a comparison made between

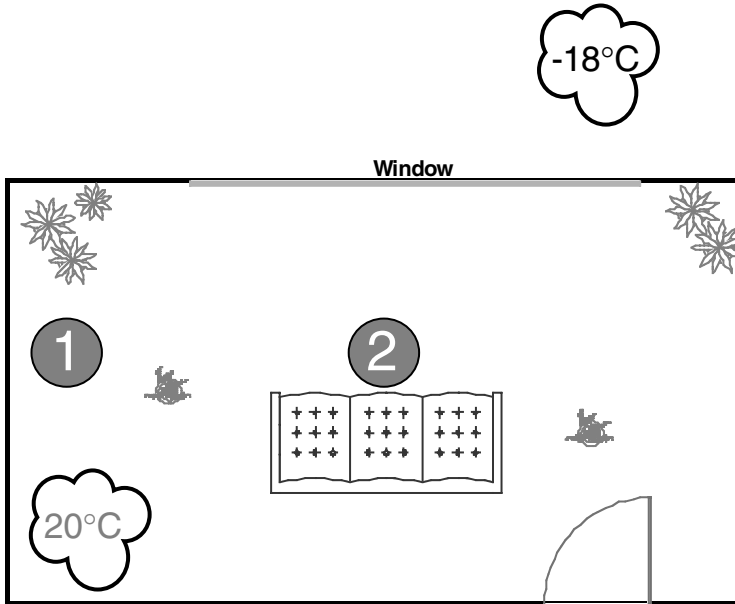


**FIGURE 3.2** Analyzing thermal comfort at two locations in the same room.

the following methods for calculation and measurement of MRT (Olesen et al., 1989): (1) use of a weighted mean value of the plane radiant temperature in six directions, (2) use of a spherical globe sensor, and (3) use of an ellipsoid-shaped “globe” sensor.

The plane radiant temperature used in the first option describes the radiation coming in one direction (ASHRAE, 1997) versus the mean radiant temperature, which encompasses all directions. For enclosures with uniform surface temperatures, differences between the three methods are small.

### 3.4 CALCULATION

There are several ways to calculate the MRT that differ in difficulty of computations and accuracy of the end result. This chapter presents three ways to calculate the MRT. The first two are given in the ASHRAE *Fundamentals Handbook* (1997). The last method was recently developed to perform the MRT calculations directly from the radiant energy exchange calculations with minimal reference to charts and tables. Although this method is slightly more mathematically intense than the former two, the development of personal computers reduces the repetitive calculations to a matter of seconds.

#### 3.4.1 Method 1

The first method of calculation uses the values of the surrounding surface (i.e., wall, window, or sofa) temperature. Each temperature is weighted according to its posi-

tion relative to the person. The equation assumes the surface materials have a high enough emittance ( $\epsilon$ ) to be considered black or ideal. This assumption is reasonably valid for most rooms, but its effect should be considered when analyzing the results. If the surfaces of the enclosure being analyzed do not have a high emittance, the results may not be reliable. This assumption imposes a small yet important limitation on the use of this method.

In addition, this method does not take into account low-E glass. The published emissivity of low-E glass is less than 0.1 in the infrared wavelength range (Carmody et al., 1996). Since the glass is opaque in that range, the rest of the radiant energy is reflected back into the room. The classical ASHRAE standard method does not have the capability to handle this situation. Another case in which the ASHRAE method would fail is solar radiation, which is short-wavelength radiation shining through a window. This method fails to consider any window transmission and only considers the wall surface temperatures as boundary conditions.

Each of the surfaces is considered to be isothermal or having a uniform temperature ( $T_N$ ). If this assumption is not valid for a single large surface, the surface is subdivided until the assumption is valid. The view factors ( $F_{P \rightarrow N}$ ) between the point to be analyzed and all the surfaces are calculated. The sum of all the view factors must equal unity (i.e., one). The MRT is then calculated as (ASHRAE, 1997):

$$\bar{T}_r^4 = T_1^4 F_{P \rightarrow 1} + T_2^4 F_{P \rightarrow 2} + \dots + T_N^4 F_{P \rightarrow N} \quad (3.1)$$

The temperatures for the calculation are in Kelvin and the view factors are unitless. The view factors are tricky to calculate. Standard heat transfer texts (e.g., Incropera and DeWitt, 1990) give standard equations to estimate the view factors. For rectangular surfaces, ASHRAE (1997) and Fanger (1967) provide view factor charts for estimation. Using standard equations or charts is a time-consuming process where human computation errors could easily occur.

If the difference in surface temperatures is small, around 5°F (2.8°C), Eq. (3.1) can be linearized to a simpler form:

$$\bar{T}_r = T_1 F_{P \rightarrow 1} + T_2 F_{P \rightarrow 2} + \dots + T_N F_{P \rightarrow N} \quad (3.2)$$

Although this form is slightly less complicated looking than Eq. (3.1), the view factors still need to be calculated or approximated, which may be a time-consuming task. Caution should be exercised before using the linear form. A large difference in surface temperatures could yield misleading results.

### 3.4.2 Method 2

The second method to calculate the MRT uses a quantity called the plane radiant temperature ( $T_{pr}$ ). The *plane radiant temperature* is defined as “the uniform temperature of an enclosure in which the incident radiant flux on one side of a small plane element is the same as that in the actual environment” (ASHRAE, 1997). The plane radiant temperature represents the radiant energy exchange from one direction, whereas the MRT represents the radiant energy exchange from all directions (ASHRAE, 1997). In a typical room there are six directions to consider: left, right, front, back, up, and down. It logically follows that a weighted average of the six plane temperatures could be used to estimate the MRT. ASHRAE (1997) gives the equations for estimating the MRT from the six plane temperatures. Equation (3.3) is for a standing occupant, and Eq. (3.4) is for a seated occupant.

$$\bar{T}_{r,\text{standing}} = \frac{0.08(T_{pr,\text{up}} + T_{pr,\text{down}}) + 0.23(T_{pr,\text{right}} + T_{pr,\text{left}}) + 0.35(T_{pr,\text{front}} + T_{pr,\text{back}})}{2(0.08 + 0.23 + 0.35)} \quad (3.3)$$

$$\bar{T}_{r,\text{seated}} = \frac{0.18(T_{pr,\text{up}} + T_{pr,\text{down}}) + 0.22(T_{pr,\text{right}} + T_{pr,\text{left}}) + 0.30(T_{pr,\text{front}} + T_{pr,\text{back}})}{2(0.18 + 0.22 + 0.30)} \quad (3.4)$$

Equations (3.3) and (3.4) have the form of weighted averages based on the occupant position. The plane radiant temperature for each surface is calculated by using the same equations as for the MRT given in the previous method [Eqs. (3.1) and (3.2)]. Again this method requires the tedious calculation of the view factors. If the plane temperatures are known (i.e., a given wall is at an approximately uniform temperature), this method is quite simple. The advantage of calculating the plane radiant temperature is the calculation of radiant temperature asymmetry in two opposite directions (ASHRAE, 1997). The radiant asymmetry between two sides is the difference in net radiant gain from each side. For example, the radiant asymmetry between the left and right of an occupant would be the difference between the left and right plane radiant temperatures. This simple calculation does not measure the radiant asymmetry in two nonopposite directions (e.g., between the top and left planes or, more practically, between the head and left arm).

### 3.4.3 Method 3

The third method uses the definition to calculate the MRT in terms of the radiant intensity balance at a particular point in the room. The fundamental radiation property is intensity (Siegel and Howell, 1981). To determine the radiant energy exchange in the room, the intensity field is balanced and calculated, as would a temperature distribution for the heat energy distribution in a room, as discussed in Sec. 2. Therefore, the intensity field throughout the room is already calculated during a robust room energy balance. Another advantage to calculating the MRT from the intensity field is the lack of assumption about wall surface properties. This radiant intensity method solves directly for the intensity field and, therefore, would include low-E glass reflection and solar radiation as boundary conditions in the radiant intensity field calculation. These conditions would not be considered as special cases. Any boundary conditions affecting the radiant intensity field are considered inherently in the radiant intensity balance. Once the intensity field for any given room is accurately calculated, the MRT can be accurately calculated for any point in the room.

The basic formulation begins with writing the definition of the MRT in terms of mathematical quantities, instead of words. The net radiation on a person is described as

$$Q = \int I(\Omega)A_p(\Omega)d\Omega \quad (3.5)$$

This equation is a continuous summation (i.e., an integral) over all the directions represented by the solid angle  $\Omega$  (Siegel and Howell, 1981; Modest, 1993). The intensity and projected area in the direction  $\Omega$  are represented by  $I(\Omega)$  and  $A_p(\Omega)$ , respectively. Using the discrete ordinates method discussed in Sec. 2, the net radiation is calculated by using a discrete approximation to the continuous form [Eq. (3.5) above] by:

$$Q \cong I^i A_p^i w^i \quad (3.6)$$

The variable  $I^j$  is the intensity in coming from a given discrete direction measured in  $W/m^2$  sr and  $A_p^j$  is the projected area in the given direction. The variable  $w^j$  is the quadrature weighting function for that direction as part of the integration technique to approximate the sum. The projected area from a given direction is given in the ASHRAE *HVAC Systems and Equipment Handbook* (1996). The general equation is:

$$A_p^j = f_p^j f_{\text{eff}} A_D \quad (3.7)$$

where  $f_p^j$  is the projected area factor in a given direction. Charts for these factors for sitting and standing people are given in Fanger (1967) and ASHRAE (1996). The effective radiation area of a person to adjust for the body reradiating to itself ( $f_{\text{eff}}$ ) equals 0.73 for a standing person (ASHRAE, 1996). The DuBois area ( $A_D$ ) is estimated from a person's height and mass. For an average person,  $A_D$  equals 1.82 m<sup>2</sup> (19.6 ft<sup>2</sup>) (ASHRAE, 1996).

The radiation emission from a blackbody enclosure is:

$$Q_{\text{black}} = A_{\text{eff}} \sigma T_{\text{MRT}}^4 \quad (3.8)$$

where:

$$A_{\text{eff}} = f_{\text{eff}} A_D \quad (3.9)$$

According to the definition of mean radiant temperature, Eqs. (3.5) and (3.8) are equal. Solving for  $T_{\text{MRT}}$  results in

$$T_{\text{MRT}} = \left[ \frac{\sum_j I^j A_p^j w^j}{f_{\text{eff}} A_D \sigma} \right]^{1/4} \quad (3.10)$$

This equation provides an alternative approach to calculating the  $T_{\text{MRT}}$  using the surrounding surface temperatures given in the previous two methods. This approach, using the localized radiant intensity field, is more flexible than using radiosities or temperatures and view factors from room surfaces, as shown in the following paragraphs. Furthermore, this approach is easily incorporated into radiant energy exchange computer algorithms since the intensity field is calculated throughout the room in most robust methods.

Carefully collected data were used to validate the BCAP methodology (Chapman and DeGreef, 1997). The purpose of the data collection process was to validate the BCAP methodology over a variety of typical room conditions, not to gain a better understanding of thermal comfort. The conditions shown in the explanation are not considered thermally comfortable. Details of the data collection, summarized in the next paragraph, are presented in Chapman and DeGreef (1997).

The test data were collected for a 100 percent radiant, a 100 percent forced-air, and a 50 percent radiant/50 percent forced-air heating system with varying wall emissivity, airflow rate, and room shape. Only one condition was varied at a time. Operative temperature readings were collected by using precision sensors at four different locations in the test room with five heights above the floor at each location. The sensors collected the air temperature and MRT, averaged them, and reported a voltage representing the operative temperature. These measurements were compared against simulation results from the BCAP methodology.

The following graphs show the following: (1) experimental data represented by dots, (2) simulated results calculating the MRT based on using view factors (Fanger,

1970) represented by a solid line, and (3) simulated results calculating the MRT based on the radiant intensity method represented by a dotted line.

Both simulations calculate the air temperature and MRT separately and then approximate the operative temperature as the average of the two. The air temperature and all other calculations are identical for both simulations. The only difference between the simulations is the MRT calculation. The results for the classical MRT calculation method were compared and found accurate by Chapman and Jones (1994). The purpose of these comparisons is illustrating that the radiant intensity method provides results that are more accurate than the classical method.

The first comparison is a 100 percent radiant heating system. Figure 3.3 shows the operative temperature readings in °C and °F on the left and right vertical axes, respectively. The top and bottom horizontal axes show the height above the floor in meters and feet, respectively, at that particular measurement location. The circle data points labeled Experimental show the experimental operative temperature readings. The solid line labeled Classical shows the operative temperature calculations using the view factor method used by ASHRAE (1997). The dotted line labeled Radiant Intensity shows the operative temperature calculations using the radiant intensities. The radiant intensity method is within 4°C (7.2°F) of the classical method and the experimental data.

The second type of heating system was a 100 percent forced-air heating system. Figure 3.4 shows the operative temperature versus height above the floor for a forced-air heating system. There is a small difference of 1.2°C (2°F) between the experimental data represented by dots and the classical calculation method represented by the solid line.

The third heating system type was 50 percent radiant/50 percent forced-air. The operative temperature comparison is shown in Fig. 3.5. As with the previous comparisons, the vertical axis represents the operative temperature, and the horizontal axis represents the height above the floor for the measurement. For this system, the classical MRT calculation shown by the solid line agrees almost exactly with the experimental values represented by dots. The MRT temperatures calculated by the radiant intensity method vary 0.6° to 1.2°C (1° to 2°F). For this particular case, the agreement for both calculation methods is extremely good.

As briefly shown by these example comparisons, calculating the MRT, and hence the operative temperature, based on the radiant intensities does provide slight improvement in MRT calculation. Chapman and DeGreef (1997) give a complete description of the data collection and handling process. Work is completed that thoroughly compares the two methods of calculating the MRT.

The next focus is on understanding the differences between constant air temperature versus constant MRT and the relationship between them. Several examples are given in the remainder of this chapter and the next. For all the examples, the air temperature is uniform throughout the room. This is not true for typical rooms. However, since this a relative comparison of air temperatures and MRT and focuses primarily on difference, this assumption is adequate.

**EXAMPLE 3.1** *Since MRT calculations are lengthy and not conducive to hand calculation, the results of a computer algorithm's calculation of the MRT from the radiant intensity field are given. The room is the same as shown in Fig. 3.2. Compare the MRT for an occupant at points 1 and 2 at 1.0 m (3.2 ft) above the floor. Consider two different heating systems: a primarily forced-air system (e.g., a vent and diffuser providing warm air from a central furnace) and a primarily radiative system (e.g., a low temperature radiant panel). Both heating systems supply energy to the room from the center of the ceiling. Both systems provide the same room average air temperature of 20°C (68°F) to the room.*

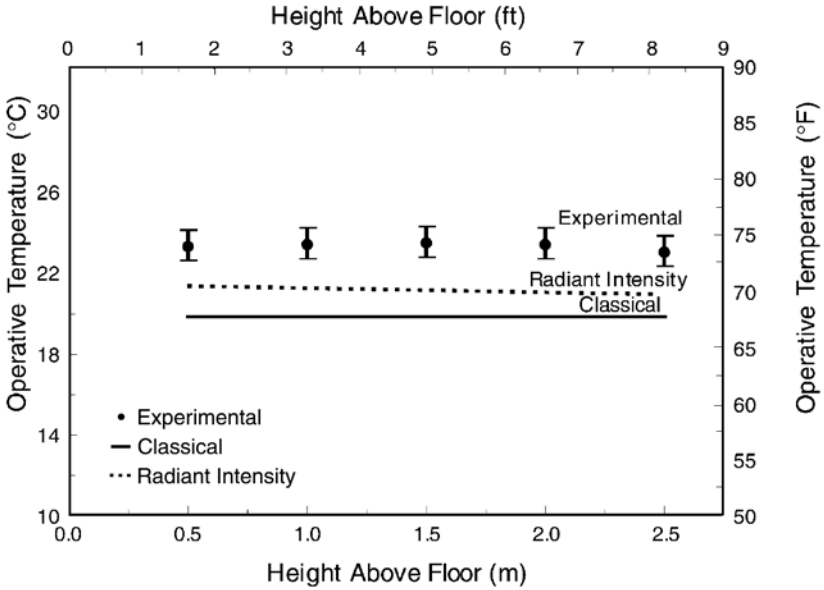


FIGURE 3.3 100 percent radiant heating system operative temperature measurements.

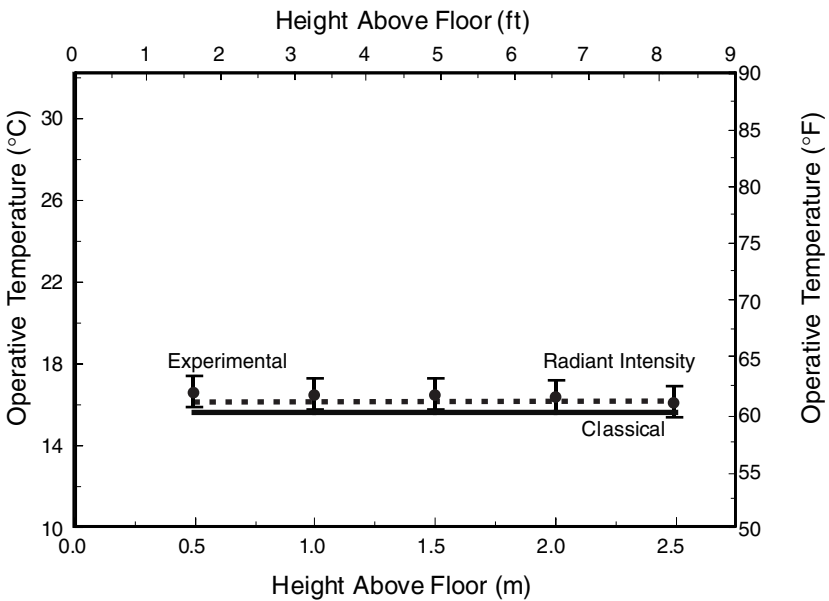
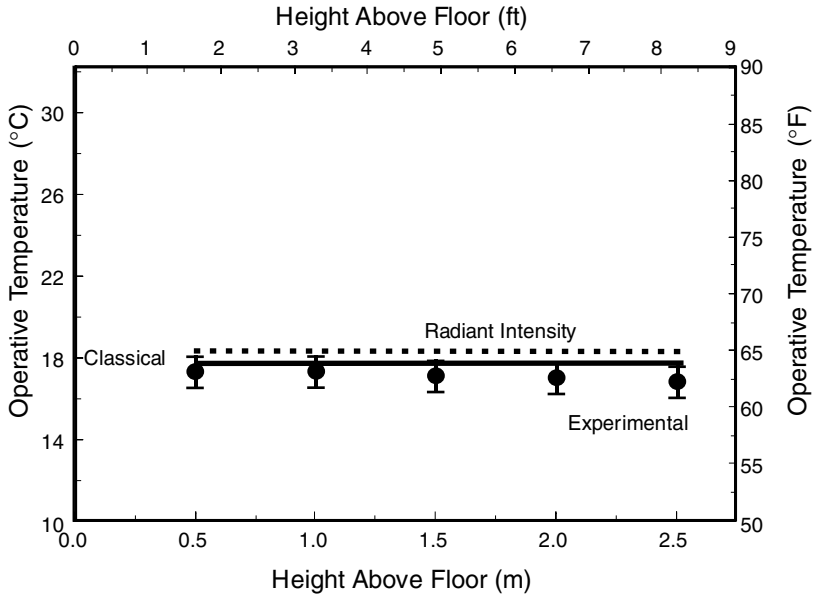


FIGURE 3.4 100 percent forced-air heating system operative temperature measurements.



**FIGURE 3.5** 50 percent radiant/50 percent forced-air heating system operative temperature measurements.

Given:

- Two different heating systems.
- Two different occupant locations.
- Both heating systems provide the same air temperature of 20°C (68°F).

Solution: Table 3.1 shows the results of the computer algorithm calculating the MRT from the radiant intensity field.

**TABLE 3.1** Example Mean Radiant Temperatures for Average Air Temperature of 20°C (68°F)

Heating system	MRT [°C (°F)]	
	Point 1	Point 2
Radiative	21.8 (71.3)	30.4 (86.7)
Forced-air	15.8 (60.4)	15.1 (59.2)

At both points the MRT for the radiative system is higher than the forced-air system. Second, the radiative system MRT at both points is also above the air temperature, whereas the forced-air system MRT at both points is below the air temperature. These statements are illustrated in Fig. 3.6. The left and right bars for each group show the MRT for the radiative and forced-air system, respectively. The horizontal line extending across the graph indicates the constant air temperature of 20°C (68°F).

To better understand the MRT differences for the two heating systems, consider the two identical rooms shown in Fig. 3.7, one heated by a forced-air system shown on top, the other by a radiative system. Both systems operate to achieve equal air temperatures. The much warmer radiant heater surface increases the intensity field at the given point, indicated by the heavier lines. Since the MRT is calculated directly from the radiation intensities, the room with the radiative system with the larger intensities at that point will have a higher MRT. The forced-air heater heats the air first, providing an average room air temperature ignoring for this example the impact of high-temperature air from the duct on local thermal comfort. However, this will not directly affect the MRT, calculated from the intensity field from the wall surfaces, which is smaller than the intensities from a radiant heater surface.

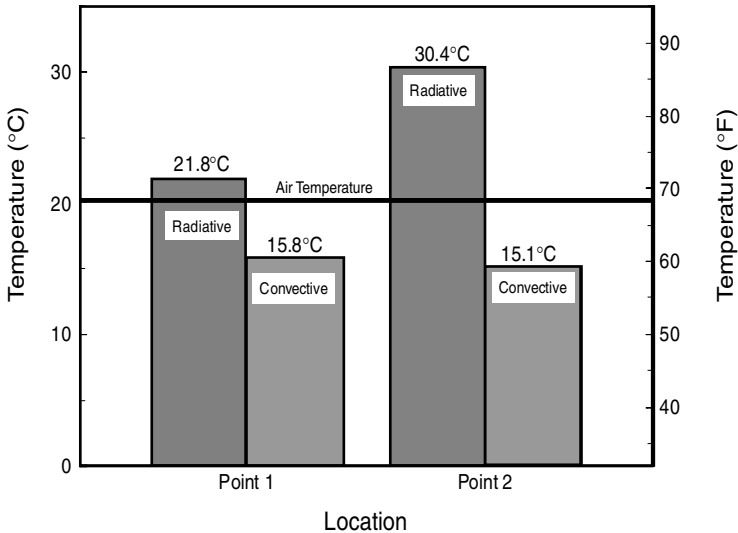


**FIGURE 3.6** Comparison of heating systems MRT for same average room air temperature of 20°C (68°F).

Earlier in the chapter, it was discussed that the large window would cause a lower MRT at point 2. From this comparison, it is clearly seen that point 2 does have a slightly lower MRT than point 1 for the forced-air system. However, for the radiative system, point 2 has a much higher MRT than point 1. The explanation is given by examining the intensity field each heating system provides. Without the window, the forced-air system provides approximately the same net radiant gain to both points 1 and 2 despite the presence of the forced-air heater directly over point 2. Adding the window lowers the net radiant gain at point 2 because the cold window does not radiate to the occupant as much energy as a warm wall. The radiative system located in the center of the room directly above point 2 supplements the net radiant gain and more than compensates for the occupant's radiative losses to the cold window surface.

**EXAMPLE 3.2** Using the same room from Fig. 3.2, compare the MRT for an occupant at points 1 and 2 for two heating systems: a primarily forced-air system (e.g., a vent and

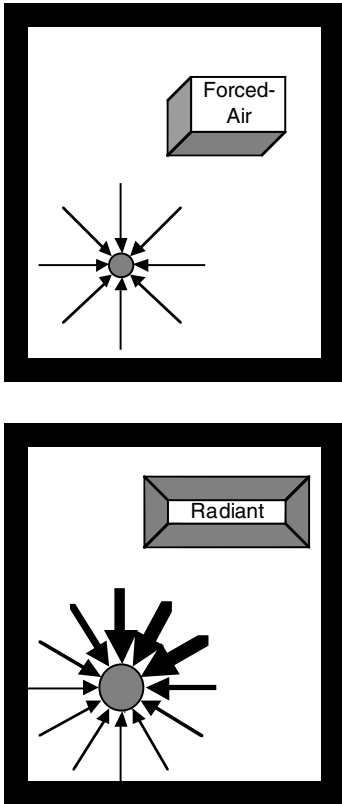


FIGURE 3.7 Radiant intensities differences for two heating systems.

diffuser providing warm air from central furnace) and a primarily radiative system (e.g., a low-temperature radiant panel). Both heating systems supply energy to the room from the center of the ceiling. Both systems supply the same room average MRT of 20°C (68°F) to the room, where room average MRT is the average MRT for all the points in the room.

Given:

- Two different heating systems.
- Two different occupant locations.
- Both heating systems provide the same average MRT of 20°C (68°F).

Solution: Table 3.2 shows the results of the computer algorithm calculating the MRT from the radiant intensity field.

This set of data follows the same trend observed with the constant air temperature data. The radiative system provides an MRT at both points above the air temperature. Point 2 directly under the radiative heater is much warmer than point 1 off to the side of the radiative heater. The forced-air system provides an MRT at both points below the air temperature. Again, the MRT for the forced-air heater at point 2 directly in front of the window is slightly cooler than at point 1 away from the full effects of the window.

Figure 3.8 summarizes this heating system comparison for a room average MRT of 20°C (68°F). The bars on the left and right of each group represent the radiative and forced-air systems, respectively. The last group of bars represents the air temperature provided by each system. Notice at point 1, the MRT provided by the radiative system is actually lower than the forced-air system’s MRT. This seems strange since the radiative system should have a larger intensity field than the forced-air system at all locations in the room. However, this comparison is based on a room average MRT. The radiative system’s MRT is more diverse than the forced-air system’s.

TABLE 3.2 Example Mean Radiant and Air Temperatures for Average Room MRT of 20°C (68°F)

Heating system	MRT [°C(°F)]		Air temperature [°C(°F)]
	Point 1	Point 2	
Radiative	18.6 (65.5)	26.7 (80.1)	16.9 (62.5)
Forced-air	20.3 (68.6)	19.6 (67.4)	25.1 (77.2)

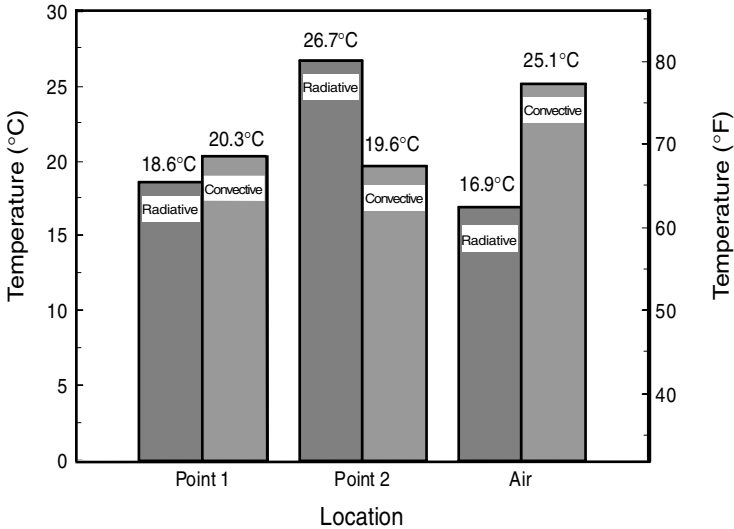


**FIGURE 3.8** Comparison of heating systems MRT for average room MRT of 20°C (68°F).

The forced-air system heats the air, which mixes and then heats the wall relatively uniformly, except, of course, the window. The radiative system heats a small section of the ceiling to a temperature well above the other wall surfaces. This causes the radiative systems MRT throughout the room to be more diverse.

The differences in the low and high MRT for the given room are shown in Fig. 3.9 for the radiative and forced-air systems. The difference between the room maximum and minimum MRT for the radiative system, shown on the left, is significantly greater than the difference for the forced-air system, shown on the right. The room maximum for the radiative system is 43.9°C (111°F), which is generally considered to be thermally uncomfortable. However, this room maximum is right next to the heater surface on the ceiling, which is typically unoccupied space.

As a side note, the surface temperature of the radiant panel is 81.3°C (178°F). The surface temperature is well below the temperature of a halogen lightbulb, and is safe to touch with a bare hand for brief periods. As seen by the MRT at point 2, the MRT at 1.0 m (3.2 ft) above the floor is 26.7°C (80.1°F), which is the typical level of a seated occupant, is warm but not unbearable.

Looking at the MRT gradients across the room shows the other reason the MRT at point 1 is higher for the forced-air system than the radiative system. Figure 3.10 shows the MRT gradients at 1.0 m (3.2 ft) above the floor for the forced-air system. Each contour line represents a line of constant MRT in °C. The horizontal axis is along the width of the room, and the vertical axis is along the room depth. The closeness of the contour lines represents the magnitude of the MRT gradient. For example, the lines are farther apart toward the bottom of the plot than at the top of the plot. This translates to steeper gradients toward the back of the room (top of the plot) and smaller gradients toward the front of the room (bottom of the plot). The difference between each contour line is 1°C (1.8°F). The distance between each contour line is the distance required for the MRT to change 1°C (1.8°F). The coldest regions are indicated by the smallest temperatures toward the top of the chart near the window. The rest of the

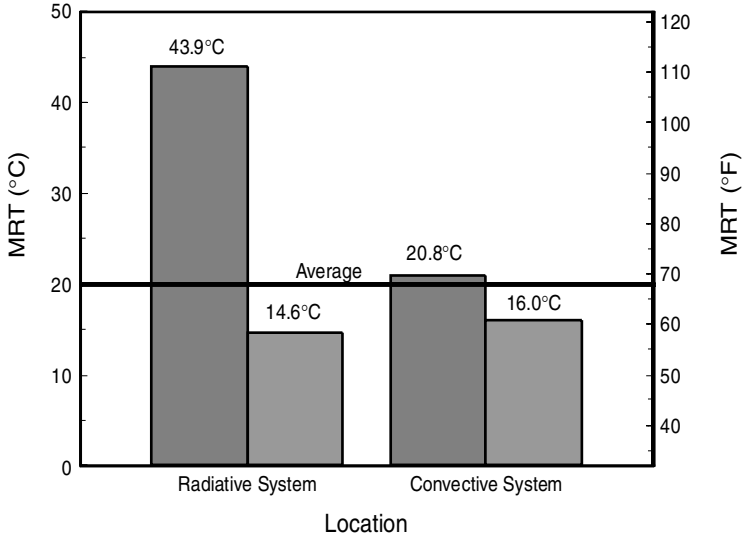


**FIGURE 3.9** Comparison of heating system maximum and minimum MRT for average room MRT of 20°C (68°F).

room is relatively uniform. The MRT varies 4°C (7.2°F) for a low of 17°C (62°F) near the window to a high of 21°C (70°F) far away from the window.

Now compare the gradients for the radiative system with Fig. 3.11, showing the MRT gradients at 1.0 m (3.2 ft) above the floor. Again each contour line represents constant MRT, and the difference between each contour line is 1°C (1.8°F). The coldest region is near the top of the chart where the window is located. The warmest spot is directly under the heater in the middle of the plot. The MRT gradients form

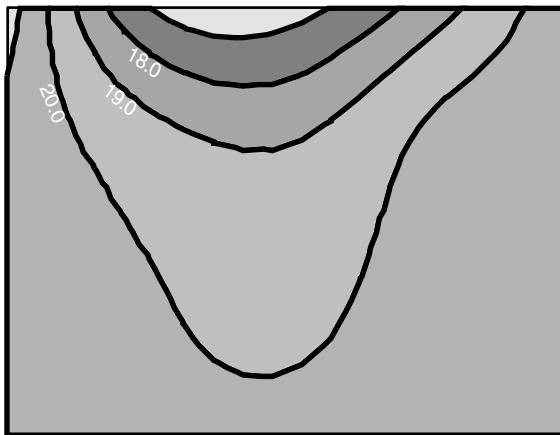


**FIGURE 3.10** Contour plot of MRT gradients for forced-air heating system with average room MRT of 20°C.

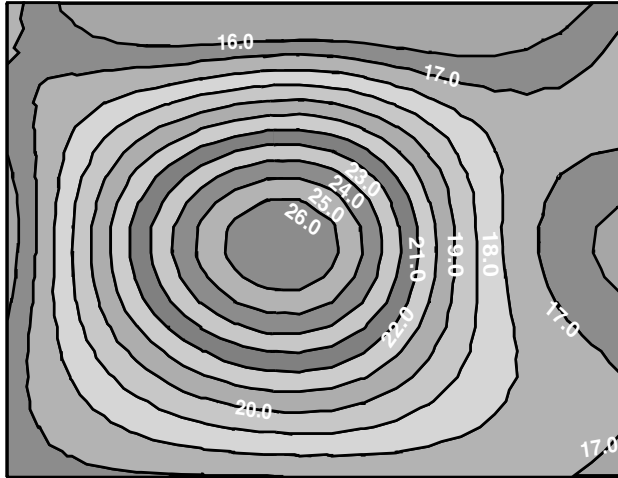


**FIGURE 3.11** Contour plot of MRT gradients for radiative heating system with average MRT of 20°C

concentric circles radiating from the center of the radiative heater. The MRT varies 10°C (19°F) from a low of 16°C (60°F) by the window to a high of 26°C (79°F) underneath the center of the heater.

The contour lines for the radiative heater are much closer together than for the forced-air heater. Physically, this means, in this example of a radiative system, an occupant walking across the room will feel a greater temperature change. The MRT gradients also indicate the intensity field across the room. The intensity field is much more concentrated under the heater for the radiative system than for the forced-air system as simulated in this example.

These differences must be considered when designing a thermally comfortable room. The type of heating system can alter the heat energy distribution. The MRT temperature gradients across the room are related to thermal comfort. Steeper gradients may indicate places where the MRT and operative temperature fall outside of the acceptable region. ASHRAE Standard 55-1992 specifies acceptable MRTs and operative temperatures that should be carefully factored into the room design. In most design conditions, judicious placement of the heating system, especially a radiative system, can reduce temperature gradients (Chapman et al., 1997). These factors are discussed in Sec. 8.

---

# CHAPTER 4

---

## THE OPERATIVE TEMPERATURE

---

The operative temperature combines the air and mean radiant temperatures into one numerical quantity. It is a measure of the body's response to the convection and radiation energy exchange. The discussion of the operative temperature is very similar to the mean radiant temperature (MRT).

### 4.1 DEFINITION

---

*Operative temperature* is defined as “the temperature of a uniform isothermal black enclosure in which the occupant exchanges the same amount of heat by radiation and convection as in the actual nonuniform environment” (ASHRAE, 1995). In a physical sense, it is the temperature the occupant perceives his surroundings to be due to convection and radiation.

The operative temperature is calculated as the weighted average of the air temperature, ( $T_{\text{air}}$ ) and the MRT ( $T_{\text{MRT}}$ ). Equation (4.1) gives the equation provided by ASHRAE (1995):

$$T_{\text{op}} = \frac{h_r T_{\text{MRT}} + h_c T_{\text{air}}}{h_r + h_c} \quad (4.1)$$

where  $h_r$  and  $h_c$  are the linearized radiant and the convective heat transfer coefficients, respectively. Standard heat transfer texts [e.g., Incropera and DeWitt (1990)] contain relationships for calculating general radiant and convection coefficients. However, ASHRAE (1997) contains coefficients specifically for the human body. In an environment with air velocities of 0.4 m/s (1.3 ft/s) and an MRT of 50°C (122°F) or less, the operative temperature is approximately the average of the air temperature and MRT (ASHRAE, 1995). The ASHRAE *Applications Handbook* (1995) provides specific calculations for the weighting factors for other design situations.

### 4.2 RELATIONSHIP TO THERMAL COMFORT

---

The room used in the previous examples clearly displays a nonuniform radiant field and shows the air temperature alone is not a good thermal comfort indicator. The air temperature does not account for the heat loss due to radiant energy exchange with

the walls or window or the radiative heating system. The mean radiant temperature does not account for the warming effects of the surrounding air. For this case, the operative temperature, first suggested by Fanger (1967), is a better indication of the local thermal comfort.

### 4.3 MEASUREMENT TECHNIQUES

---

There are two methods to measure the operative temperature. The first method is a direct measurement using a temperature sensor with a diameter between 5 and 10 mm (2 to 4 in). A black sensor will overestimate the effect of direct sunshine. ASHRAE Standard 55-1992 recommends gray or pink sensors for locations with a high-temperature radiant source [e.g., the sun or a temperature radiant heater of greater than 927°C (1700°F)]. In rooms with no high-temperature radiant source, color has little impact.

The second method does not measure the operative temperature directly. Rather, it calculates the operative temperature from a measured air temperature and MRT. The convective and radiative coefficients provide factors for calculating the weighted average of the air temperature and MRT shown in Eq. (4.1).

### 4.4 CALCULATION

---

The approximation of the operative temperature is straightforward in most design situations once the air temperature and MRT are found. It is done by adding the air and mean radiant temperature and dividing by two. Dividing by two adds the assumption of an equal weighting of the radiative and convective coefficients. The examples presented here will build on the discussion presented in Chapter 3 on the MRT.

**EXAMPLE 4.1** *Using the same room from Fig. 3.2 shown previously in Chap. 3, compare the MRT 1.0 m above the floor for an occupant at points 1 and 2 for two heating systems: a primarily forced-air system (e.g., a vent and diffuser providing warm air from central furnace) and a primarily radiative system (e.g., a low temperature radiant panel). Both heating systems supply energy to the room from the center of the ceiling. Both systems supply the same room average operative temperature of 20°C (68°F) to the room.*

Given:

- Two different heating systems.
- Two different occupant locations.
- Both heating systems provide the same average operative of 20°C (68°F).

*Solution: Table 4.1 shows the results of the computer algorithm calculating the MRT from the radiant intensity field.*

Again, this set of data follows the trends observed in the two examples in Chapter 3 for constant air temperature and constant MRT. The radiative system has a

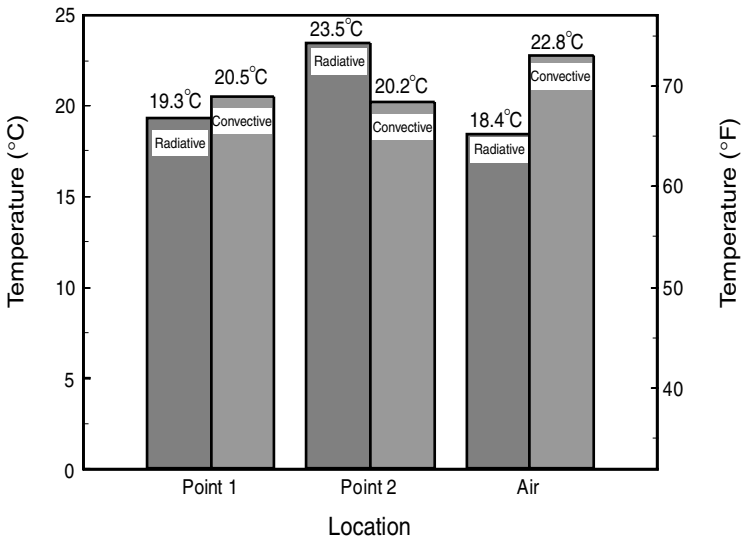
**TABLE 4.1** Example Mean Radiant, Operative, and Air Temperatures for Average Operative Temperature of 20°C (68°F)

Heating system	MRT [°C(°F)]		Operative temp. [°C(°F)]		Air temp. [°C(°F)]
	Point 1	Point 2	Point 1	Point 2	
Radiative	20.2 (68.4)	28.5 (83.3)	19.3 (66.7)	23.5 (74.3)	18.4 (65.2)
Forced-air	18.2 (64.8)	17.6 (63.9)	20.5 (68.9)	20.2 (68.4)	22.8 (73.0)

higher MRT than air temperature at both points. The forced-air system has a higher air temperature than the MRT at both points. As dictated by definition, the operative temperatures are between the air temperatures and the MRTs.

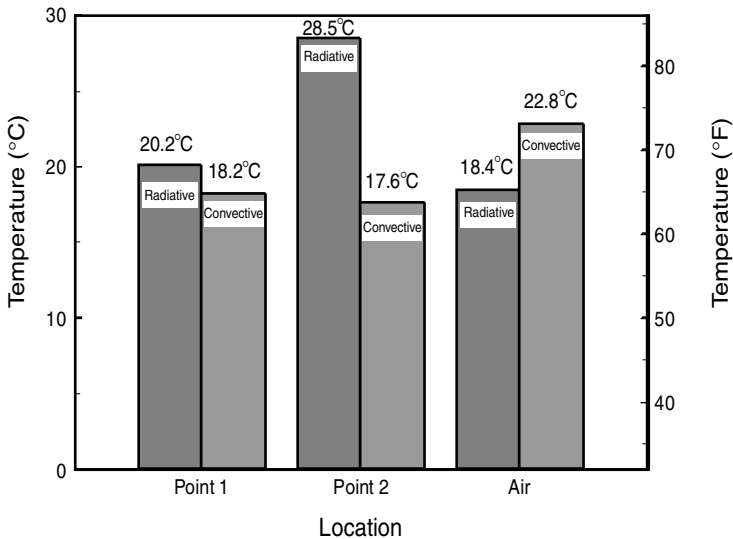
As shown in Table 4.1 with the radiative system, the MRT at point 2 directly under the heater is much higher than at point 1 off to the side. The MRT of 28.5°C (83.3°F) at point 2 could be considered thermally uncomfortable to some occupants. However, when coupled with the air temperature, the operative temperature at point 2 is 23.5°C (74.3°F), which generally is considered to be within a thermally comfortable range.

Figure 4.1 summarizes the comparison of the heating systems' operative temperatures that result with a room average operative temperature of 20°C (68°F). The bars on the left and right of each group represent the radiative and forced-air systems, respectively. The last group represents the air temperature provided by each system. Notice at point 1 the operative temperature provided by the radiative sys-



**FIGURE 4.1** Comparison of heating system operative temperature for average operative temperature of 20°C (68°F).

tem is lower than the operative temperature provided by the forced-air system. Remember the rooms are compared on a room average operative temperature. Also remember the radiative heating system has a more diverse MRT throughout the room than the forced-air heating system. Figure 4.2 summarizes the MRT temperatures to achieve the same room average operative temperature. Again the left and right bars of each group represent the MRT for the radiative and convective heating systems, respectively. The last group repeats the air temperature comparison for each system. At point 1, the MRT for the radiative system is above the forced-air system. However, the air temperature is much lower for the radiative system. When the operative temperatures are computed as the average of the MRT and air temperature, the operative temperature for both heating systems are the same. Despite the difference in MRT and air temperatures in the room, both heating systems give similar operative temperatures. This illustrates the flexibility in methods to achieve equivalent thermal comfort.



**FIGURE 4.2** Comparison of heating system MRT for average room operative temperature of 20°C (68°F).

At point 2, the MRT for the radiative system is much higher and the operative temperature is also slightly higher than for the forced-air system. It should be noted that the temperature differences are very small. Table 4.2 summarizes the differences in the mean radiant, operative, and air temperatures between the radiative and forced-air system for the two points under consideration. A positive number indicates the radiative heating system yielded the higher temperature. Conversely, a negative number indicates the forced-air heating system yielded the higher temperature.

Another interesting characteristic is the variation in the operative temperature across the room. Figure 4.3 shows the operative temperature gradients for the

**TABLE 4.2** Example Differences in Mean Radiant, Operative, and Air Temperatures for Average Operative Temperature of 20°C (68°F)

Location	MRT difference [°C(°F)]	Operative temp. difference [°C(°F)]	Air temp. difference [°C(°F)]
Point 1	2.0 (3.6)	-1.2 (-2.2)	-4.4 (-7.8)
Point 2	10.9 (19.4)	3.3 (5.9)	-4.4 (-7.8)

forced-air heating system at 1 m (3.2 ft) above the floor. Each contour line represents a line of constant operative temperature in °C. The horizontal axis is along the width of the room, and the vertical axis is along the room depth. The closeness of the contour lines represents the magnitude of the operative temperature gradient. For example, the lines are closer together at the top of the plot (back of the room) where the window is located. Closer lines translate into a shorter distance for the operative temperature to vary 1°C (1.8°F), since each line represents a 1°C (1.8°F) change in operative temperature. The operative temperature is relatively uniform across the room, which is highly desirable from a comfort standpoint.

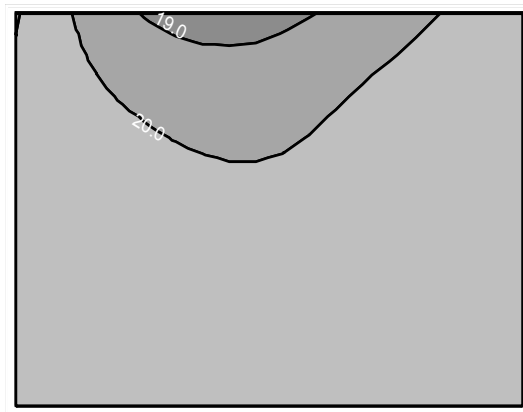
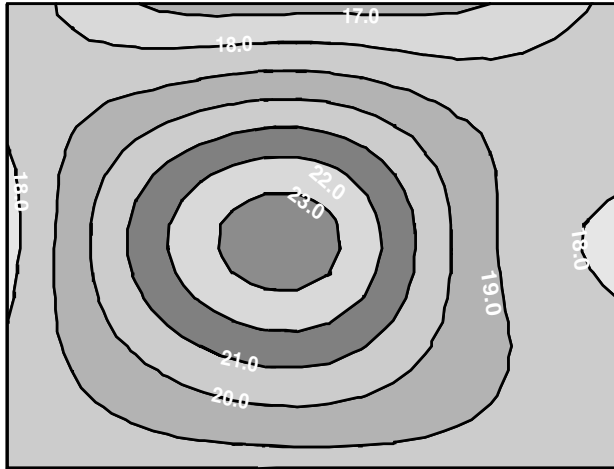
**FIGURE 4.3** Contour plot of MRT gradients for forced-air heating system with average room operative temperature of 20°C (68°F).

Figure 4.4 shows the operative temperature gradients for the radiative heating system at the same 1 m (3.2 ft) above the floor. Again each contour line represents constant operative temperature, and the difference between contours is 1°C (1.8°F). The operative temperature gradients for the radiative system are more severe than for the forced-air heating system. This is due to the radiative heating system's strong intensity field directly under the heater in the center of the room. This elevates the MRT and, consequently, the operative temperature.



**FIGURE 4.4** Contour plot of MRT gradients for radiative heating system with average room operative temperature of 20°C (68°F).

This example illustrates that the room average operative temperature does not completely define the entire picture of the room. The operative temperature gradients should be considered for each design situation. The type of heating system affects the heat distribution in the room. For this example, the heater was placed in the center of the room. Moving the heater would alter the operative temperature at points 1 and 2 and the gradients. Moving the heater to a different location could even alter the average operative temperature of the room.

**S · E · C · T · I · O · N · 4**

**SIZING AND LOAD  
ESTIMATION**



---

# CHAPTER 1

---

## ASHRAE STANDARD METHODS

---

Several standard methods are available to size heating and cooling systems for specific applications. All methods follow a fairly regimented procedure that involves identifying the indoor design conditions, the outdoor design conditions, and the heat losses and gains through the structure. Once these parameters are determined, the next step requires information about the internal heating and cooling loads (e.g., people, computers, and lights), followed finally by the selection of the heating and cooling equipment.

The ASHRAE standard methods for sizing heating and cooling systems first specify the indoor dry-bulb temperature and the design outdoor temperature. The heat transfer rates into and out of the occupied space are calculated from the methods described in Sec. 2 of this Handbook. The infiltration rates are also calculated, along with any heat gains due to lights, people, and other equipment. The final balance equation is developed from the conservation of energy equation as:

$$\dot{Q}_{\text{gain}} - \dot{Q}_{\text{cond}} - \dot{Q}_{\text{loss}} + \dot{m}_{\text{inf}} c_p (T_{\text{amb}} - T_{\text{in}}) + \dot{Q}_{\text{system}} = 0 \quad (1.1)$$

Note that the heat transfer rates may be functions of the indoor temperature, the outdoor temperature, and the insulation values of the walls, floors, ceilings, windows, and doors as shown in Sec. 2. The variable  $\dot{Q}_{\text{system}}$  is the amount of energy that must be added to the room to maintain the indoor dry-bulb temperature at the design condition.

This chapter provides an overview of the standard methods used by practicing engineers to specify and size heating and cooling systems for occupied spaces. Additional information that can be used to calculate the heating and cooling loads can be found in Chaps. 25 through 27 of the ASHRAE *Fundamentals Handbook* (ASHRAE, 1993). One common parameter used throughout standard sizing methods is the dry-bulb temperature. The indoor dry-bulb temperature is frequently used as the measure of occupant thermal comfort. At this point in the Handbook, it is hoped that the reader has determined that the dry-bulb temperature is at best an estimate of occupant thermal comfort. In many cases, as will be shown later, sizing based on the dry-bulb temperature can lead to oversized systems.

---

### 1.1 DESIGN POINT METHODS

---

The design point method is based explicitly on Eq. (1.1). The indoor and outdoor design temperatures are specified, and the equipment is sized accordingly. There are

two accepted design point methods: the modified degree-day method and the variable-base degree-day method. These methods are described in the following sections.

### 1.1.1 The Modified Degree-Day Method

The modified degree-day method (MDD) is based on the assumption that the typical occupied space will be comfortable when the outdoor temperature is 65°F. The premise behind this assumption is that the heat gains from the sun, people, and equipment will be exactly offset by the heat losses through the structure to the ambient. With this assumption in place, the designer now has to determine the heat loss at some outside design temperature that is less than 65°F. The assumption is then that the heat loss is directly proportional to the difference between the average outdoor temperature and 65°F.

This proportionality can be used to determine the heating requirement at any temperature when the heating requirement is known at some temperature. For example, if the heating requirement is 20,000 Btu/h when the temperature is 45°F, then the heating requirement when the temperature is 20°F can be calculated by:

$$\dot{Q}_T = \dot{Q}_{45^\circ\text{F}} \times \left( \frac{T - 65^\circ\text{F}}{45^\circ\text{F} - 65^\circ\text{F}} \right) = \dot{Q}_{45^\circ\text{F}} \times 2.25 = 45,000 \text{ Btu/h} \quad (1.2)$$

The variable  $T$  is the temperature at which the heating load is required. The *ASHRAE Fundamentals Handbook* provides an empirical relationship between the degree days (DD) over a certain period of time, the design heat loss, the temperature difference between the design outdoor conditions and 65°F, and the heating value of the fuel. This relationship also includes two correction factors ( $k$  and  $C_D$ ):

$$E = C_D \frac{24\dot{Q}_{\text{systems},T}DD}{kV(65^\circ\text{F} - T)} \quad (1.3)$$

The result of this equation is the energy required to heat the occupied space over the period of time necessary for the number of degree days. The correction factor  $C_D$  is usually between 0.6 and 0.8. The design heat loss is calculated from Eq. (1.1) at the design outdoor temperature.

The design point temperature should at best be considered an approximate sizing method. It does not include the effects from weather peaks and certainly does not include the sophistication necessary to reliably and consistently deliver occupant thermal comfort.

### 1.1.2 Variable-Base Degree-Day Method

The variable-base degree-day (VBDD) method tries to improve on the MDD method by recognizing that not all structures are “balanced” at 65°F. The VBDD method provides a technique to determine the structure’s balance temperature that is then used in the analysis instead of the 65°F baseline temperature.

By definition, the balance temperature depends on the building structure, equipment inside the occupied space, heat gain from the sun, and so forth. From this definition, the balance temperature is determined by:

$$\dot{Q}_{\text{gains}} = \frac{T_{\text{in}} - T_{\text{bal}}}{R_{\text{th,building}}} \rightarrow T_{\text{bal}} = T_{\text{in}} - \dot{Q}_{\text{gains}}R_{\text{th,building}} \quad (1.4)$$

The variable  $R_{th,building}$  is the overall building thermal resistance to heat transfer from the indoor temperature to the outdoor temperature. Once the balance temperature is calculated, the system heating requirement is then determined from the energy conservation equation:

$$E + \dot{Q}_{gains} - \dot{Q}_{losses} = 0 \quad (1.5)$$

As in the single design point method, the losses are proportional to the difference between the outdoor temperature and the balance temperature. ASHRAE (1993) provides an empirical correlation that is frequently used to size heating systems is:

$$E = \frac{24DD_{T_{bal}}}{\bar{\eta}R_{th,building}} \quad (1.6)$$

where the total degree days over the period is the difference between the average daily temperature and the balance temperature, and the parameter  $\bar{\eta}$  is an average efficiency of the heating equipment.

The variable-base degree-day method improves on the MDD method only by recognizing that structures have unique balance temperatures. However, as with the MDD method, the VBDD method does not consider the ability of the heating system to directly affect the operative temperature of the occupied space. In fact, both of these methods are “equipment” neutral since they do not consider the type of system. Consequently, the only distinction these make between a central heating plant and, say, an in-space woodstove is the parameter  $\bar{\eta}$ , the average efficiency of the heating equipment. Another recognized shortcoming of these methods is that some heating equipment (e.g., an air-to-air heat pump) perform differently at different outdoor temperatures. Consequently, the basic assumption that the size of the heating system is directly proportional to the difference between the design balance temperature and the outdoor temperature fails. In the case of the air-to-air heat pump, backup heating capacity must be installed when the outdoor temperature drops below about 30°F.

## 1.2 MULTIPLE-MEASURE SIZING METHODS

Multiple-measure sizing methods provide more accurate information than the design point methods by recognizing that the proportionality factor is not constant. Instead, the proportionality factor varies with outdoor temperature. Note that the multiple-measure methods do not incorporate the effect of operative temperature or any other thermal comfort parameter except the indoor dry-bulb temperature.

The multiple-measure sizing methods provide a methodology in which the designer can assess the heating and cooling requirements over a wide range of outdoor temperatures. The basic methodology employs the design point methods at various outdoor temperatures over the heating and cooling seasons. The most popular methods are the classical bin method and the modified bin method.

### 1.2.1 Classical Bin Method

The classical bin method divides the heating season into several bins of temperature data. Each bin then is assigned the number of degree days that exist in a particular region. Table 1.1 provides the heating and cooling degree days for several regions of the United States. The temperature range is then divided into 5°F bins. Each bin con-

**TABLE 1.1** Fractional Bin Hours and Climatic Data for the United States\*

Climatic region		I	II	III	IV	V	VI
Cooling hours ( $N_C$ )		6720	5040	3360	2240	1120	560
Heating hours ( $N_H$ )		1826	3148	4453	5643	6956	6258
Bin number	Midpoint $T$ (°F)	Fractional bin hours ( $f$ )					
8	102			0.214			
7	97			0.231			
6	92			0.216			
5	87			0.161			
4	82			0.104			
3	77			0.052			
2	72			0.018			
1	67			0.004			
1	62	0.291	0.215	0.153	0.132	0.106	0.113
2	57	0.239	0.189	0.142	0.111	0.092	0.206
3	52	0.194	0.163	0.138	0.103	0.086	0.215
4	47	0.129	0.143	0.137	0.093	0.076	0.204
5	42	0.081	0.112	0.135	0.100	0.078	0.141
6	37	0.041	0.088	0.118	0.109	0.087	0.076
7	32	0.024	0.056	0.092	0.126	0.102	0.034
8	27	0.005	0.024	0.047	0.087	0.094	0.008
9	22	0.001	0.008	0.021	0.055	0.074	0.003
10	17		0.002	0.009	0.036	0.055	
11	12			0.005	0.026	0.047	
12	7			0.002	0.013	0.038	
13	2			0.001	0.006	0.029	
14	-3				0.002	0.018	
15	-8				0.001	0.010	
16	-13					0.005	
17	-18					0.002	
18	-23					0.001	

\*The bins are 5°F.

tains the fraction of the degree days for each climatic region. The classical bin procedure provides two pieces of information: the total energy consumption and the peak energy consumption.

The parameter term  $f$  is a weighting factor that specifies how long the heating system must operate at a particular ambient temperature. For example, in Arizona this weighting factor would be high at the upper temperatures and small at lower temperatures, whereas in Minnesota the opposite would be true. The classical bin method is demonstrated in the following example.

**EXAMPLE 1.1** A structure is built in climatic region V and has a design heat loss of 30,000 Btu/h at an outdoor temperature of 47°F. Calculate the total energy consumption and the required size of the heating system.

The following unnumbered table illustrates the classical bin calculation. The first column has been copied from Table 1.1 and is the midpoint of each temperature bin.

The second column is the fraction of hours that each temperature bin exists in region V. The third column is the total number of hours spent in each bin. From Table 1.1, the total number of heating hours required in region V is 6956 h. Hence, the value in column 3 is the fraction  $f$  times the total number of hours (6956). The fourth column is the actual heat load for each bin. This calculation assumes for the sake of convenience that the heat load is directly proportional to the temperature difference. The heat load at each bin temperature is then calculated by:

$$\dot{Q}(T_{bin}) = \dot{Q}_{design} \left( \frac{T_{bin} - 65^{\circ}F}{T_{design} - 65^{\circ}F} \right) = 30,000 \text{ Btu/h} \times \left( \frac{T_{bin} - 65^{\circ}F}{47^{\circ}F - 65^{\circ}F} \right)$$

This particular column shows the peak heating capacity necessary to heat this structure. Obviously, as the temperature decreases, the heat load increases to the maximum heat load of 146,667 Btu/h. The problem now is to determine how large the heating system needs to be to achieve the design dry-bulb temperature. If one wanted to be completely safe, a 146,667-Btu/h heating system would be specified after allowance for system efficiencies. However, this capacity would only be required 0.1 percent of the year ( $f = 0.001$ ). However, if one studies the fraction column, it becomes apparent that the outdoor temperature is below 2°F only 3.6 percent of the time (add the fractions in the last five rows of the table). Hence, a 105,000-Btu/h heating system could be specified with little risk.

The last column in the table is the result of multiplying the third and fourth columns to get the total energy consumption for each bin. This column shows that the highest consumption is in the 27°F bin where the size of the heating system needs to be 63,333 Btu/h. This column can be totaled to calculate the energy consumption for the entire heating system. In this example, that total is 343,742,333 Btu. If the system is heated by natural gas with a heating value of 1,000 Btu/ft<sup>3</sup>, and the average system efficiency is 32 percent, then the total fuel consumption is:

$$\begin{aligned} V_{fuel} &= \frac{E_{total}}{\eta_{system}HV} = \frac{343,742,333 \text{ Btu}}{\text{Season}} \times \left( \frac{\text{ft}^3}{1,000 \text{ Btu}} \right) \left( \frac{1}{0.32} \right) \\ &= \frac{1,074,195 \text{ ft}^3}{\text{Season}} \end{aligned}$$

The cost to operate the system for the entire heating system is approximated by (assuming natural gas is \$4 per 1000 ft<sup>3</sup>):

$$\text{Cost} = \frac{1,074,195 \text{ ft}^3}{\text{Season}} \times \frac{\$4.00}{1000 \text{ ft}^3} = \frac{\$4297}{\text{Season}}$$

$T_{bin}$	$f$	$N_b$	$\dot{Q}(T)$	E
62	0.106	737.336	5,000.00	3,686,680
57	0.092	639.952	13,333.33	8,532,693
52	0.086	598.216	21,666.67	12,961,347
47	0.076	528.656	30,000.00	15,859,680
42	0.078	542.568	38,333.33	20,798,440
37	0.087	605.172	46,666.67	28,241,360
32	0.102	709.512	55,000.00	39,023,160
27	0.094	653.864	63,333.33	41,411,387
22	0.074	514.744	71,666.67	36,889,987
17	0.055	382.580	80,000.00	30,606,400
12	0.047	326.932	88,333.33	28,878,993
7	0.038	264.328	96,666.67	25,551,707

$T_{bin}$	f	$N_b$	$\dot{Q}(T)$	E
2	0.029	201.724	105000.00	21181020
-3	0.018	125.208	113333.33	14190240
-8	0.010	69.560	121666.67	8463133
-13	0.005	34.780	130000.00	4521400
-18	0.002	13.912	138333.33	1924493
-23	0.001	6.956	146666.67	1020213

### 1.2.2 Modified Bin Method

The modified bin method incorporates several corrections into the classical bin method. The calculation procedure is essentially the same as in the classical method, except solar gains, equipment heat loads, and adjustments to recognize occupied and unoccupied times are incorporated into the weighting factors. Since these corrections and adjustments simply represent a fine-tuning of the classical method, the details are left to the *ASHRAE Fundamentals Handbook*, which includes a detailed example problem in Chap. 28.

## 1.3 DETAILED SIMULATIONS

Detailed simulations offer a more precise method of calculating the hour-by-hour or day-by-day heat load for a building. They calculate the instantaneous rate of heat flow into the air contained within the occupied space. These simulations must accurately calculate the convective heat transfer rate from surfaces to the room air and the conductive heat transfer rate through walls to adjacent spaces.

Two of the more popular methods are the heat balance method and the weighting factor methods. Each of these methods is described in the following two sections.

### 1.3.1 Heat Balance

The heat balance method is based primarily on the conservation of energy and the conservation of mass equations described in Sec. 2. The method requires one conservation equation for each bounding surface and an additional energy conservation equation for the room air itself.

Consider a room enclosed by three interior walls, one exterior wall, and a floor and ceiling. The air enclosed by the surfaces is treated as one large control volume. The energy conservation equations are written for each surface and for the air as:

$$\sum_{i=1}^n \dot{Q}_{\text{surf}} + \dot{Q}_{\text{gain}} + \dot{m}c_p(T_{\text{inf}} - T_{\text{in}}) + \dot{Q}_{\text{system}} = 0 \quad (1.7)$$

$$\dot{Q}_{\text{conv}} - \dot{Q}_{\text{cond}} = 0 \quad (1.8)$$

The first equation is for the room air, and the second equation is for each of the surfaces bounding the room air. The heat transfer terms within these equations need to be evaluated according to definitions provided in Sec. 2. For example, the convective heat transfer at a surface is evaluated by:

$$\dot{Q}_{\text{conv}} = hA(T_{\text{in}} - T_{\text{surf}}) \quad (1.9)$$

where  $h$  is the convective heat transfer coefficient,  $A$  is the surface area, and  $T_{\text{surf}}$  is the temperature of the particular surface. These equations become more complex when radiative heat transfer is included in the calculations.

To solve these equations, an iterative method must be employed. In addition, the radiation terms must be linearized. In the end, the computations are well beyond the capabilities of a pencil and sheet of paper. Hence, a computer algorithm of some sort is necessary.

Chapter 28 of the ASHRAE *Fundamentals Handbook* (1997) provides several equations that can be used to analyze heating and cooling requirements for a room. However, they are not stressed here since they, as with the bin methods, do not provide a means to calculate the operative and mean radiant temperatures throughout the occupied space. Neither do they provide a satisfactory means of calculating the radiative heat transfer rates within the enclosure.

### 1.3.2 Weighting Factor Method

The weighting factor method, as with the heat balance method, provides a prescription to calculate the instantaneous heat load to the air in an enclosed room. This method differs from the heat balance method by using weighting factors to relate various temperature distributions instead of the conservation equations.

The method uses what is called the Z-transform method of solving differential equations at discrete points. The method uses two sets of weighting factors, one for heat gain by the enclosed air and one for the air temperature itself.

Again, though, this method does not provide the critical information that is necessary for evaluating thermal comfort. The solution from the weighting factor method does not provide enough information to calculate the radiative heat transfer rates throughout the enclosed space. Because of this major limitation, the method is only mentioned here for completeness.

### 1.3.3 Computerized Simulations

Computerized sizing programs probably offer the designer the greatest flexibility. Most computer simulations in use today run fairly quickly on a desktop computer. From the author's experience, most computerized sizing programs employ the bin methods described in the previous section.

The benefit of computerized sizing programs is that they are fairly easy to learn and they allow the user to assess many different configurations in a relatively short period of time. The downside is that most, if not all, computerized solutions lack the sophistication necessary to properly size radiant heating and cooling systems. The reason for this is because they are all based on the room dry-bulb temperature. In some cases (e.g., Blast), the algorithm calculates the mean radiant and operative temperatures, but only in a coarse way.

Computerized solutions are discussed in detail in Sec. 8. They are mentioned here only as an alternative to doing hand calculations.



---

## CHAPTER 2

---

# THE BUILDING COMFORT ANALYSIS PROGRAM METHODOLOGY

---

The Building Comfort Analysis Program resulted from a research project that was sponsored by ASHRAE. Research Project 657, *Simplified Method to Factor Mean Radiant Temperature (MRT) into Building and HVAC System Design*, was completed at Kansas State University in 1994 and represents what the authors believe to be a significant advance in the methodology used to size and specify radiant heating and cooling systems. The basic objective of the research project was to develop a method in which any heating and cooling system would be sized according to the mean radiant and operative temperatures created in the occupied space. The idea was to advance beyond the specification of the room air dry-bulb temperature.

The Building Comfort Analysis Program [BCAP (pronounced be-cap)] is actually a methodology that is a unified collection of computer programs intended to aid in the sizing and design of building heating systems. The BCAP programs were developed to allow system designers to accurately account for radiant heat exchange in the design process. Radiant heat exchange that is addressed in BCAP includes radiant exchange between heaters and coolers and building surfaces, radiant exchange between heaters and building occupants, radiant exchange between building surfaces and building occupants, and radiant exchange between different building surfaces. All of these exchanges are important considerations in determining how a heating and cooling system will perform in a given application. The premise behind BCAP recognizes that the purpose of a heating and cooling system should not be to generate some specific indoor temperature; rather, the purpose should be to provide comfort for the building occupants. Thus, the BCAP methodology uses occupant comfort, in addition to physical parameters, as a measure of performance of a heating system. Because of the detailed treatment of radiant heat exchange, BCAP is particularly suited for use in designing radiant systems. Its use is not limited to these systems, however. The BCAP methodology includes provisions for convective heat inputs. Therefore, since radiant heat exchange is an important factor in designing any heating system, designers of nonradiant systems are likely to find BCAP useful, especially when factors such as hot or cold windows, walls, and floors are addressed.

The BCAP methodology does not design heating and cooling systems. The BCAP methodology is intended to speed the design process and to allow engineers

to do a much better job of designing a system by accurately including the effect of radiant heat exchange in the design calculations.

**2.1 MATHEMATICAL MODELS  
OF RECTANGULAR ENCLOSURES HEATED  
BY RADIANT PANELS**

---

Two promising methods that addressed the concept of the mean radiant and operative temperatures were developed prior to the BCAP methodology. These methods are the Khan and Coutin-Rodicio model and the Howell and Suryanarayana model. Each is described in the following sections.

**2.1.1 Khan and Coutin-Rodicio Model**

A mathematical model of a radiantly heated rectangular enclosure was developed (Khan and Coutin-Rodicio, 1990). The model calculates the transient heat transfer from radiant panels located symmetrically in the center of the ceiling. Conduction through the ceiling, radiation from the ceiling and radiant panels, and natural convection on all room surfaces are included in the calculations. The floor and four walls of the enclosure are considered to participate in the radiant heat transfer. However, the air within the enclosure is assumed to be a nonparticipating medium. View factors between the participating members have been compiled and reported by Hamilton et al. (1952). To simplify the calculations, all participating members in the enclosure are treated as blackbodies.

The model consists of a set of partial and ordinary differential equations. Three sets of equations are developed. First, an energy balance on the ceiling results in:

$$\frac{\partial^2 T_c}{\partial x^2} + \frac{\partial^2 T_c}{\partial y^2} - \frac{h}{k_c b} (T_c - T_a) - \frac{\sigma}{k_c b} \sum_{i=1}^4 F_{ci} (T_c^4 - T_i^4) = \frac{\rho_c C_c}{k_c} \frac{\partial T_c}{\partial \theta} \quad (2.1)$$

The initial and boundary conditions are as follows:

$$T = T_i \quad t = 0$$

$$\frac{\partial T}{\partial x} = 0 \quad x = 0 \quad y = 2l$$

$$\frac{\partial T}{\partial y} = 0 \quad x = l \quad y = 0$$

Second, an energy balance is performed on the floor and four walls, resulting in the following five equations:

$$A_c F_{c1} (E_{b,c} - E_{b,1}) - A_1 \sum_{i=1}^{4,f} F_{1i} (E_{b,1} - E_{b,i}) - h_c A_1 (T_1 - T_a) = 2ldb_w C_w \rho_w \frac{dT_1}{d\theta} \quad (2.3)$$

$$A_c F_{c2} (E_{b,c} - E_{b,2}) - A_2 \sum_{i=1}^{4,f} F_{2i} (E_{b,2} - E_{b,i}) - h_c A_2 (T_2 - T_a) = 2ldb_w C_w \rho_w \frac{dT_2}{d\theta} \quad (2.4)$$

$$A_C F_{C3}(E_{b,C} - E_{b,3}) - A_2 \sum_{i=1}^{4,f} F_{3i}(E_{b,3} - E_{b,i}) - h_C A_3(T_3 - T_a) = 2ldb_w C_w \rho_w \frac{dT_3}{d\theta} \quad (2.5)$$

$$A_C F_{C4}(E_{b,C} - E_{b,4}) - A_4 \sum_{i=1}^{4,f} F_{4i}(E_{b,4} - E_{b,i}) - h_C A_4(T_4 - T_a) = 2ldb_w C_w \rho_w \frac{dT_4}{d\theta} \quad (2.6)$$

$$A_C F_{Ci}(E_{b,C} - E_{b,i}) - A_f \sum_{i=1}^{4,f} F_{fi}(E_{b,i} - E_{b,j}) - h_C A_i(T_i - T_a) = 2ldb_w C_w \rho_w \frac{dT_i}{d\theta} \quad (2.7)$$

The first five terms to the left of the equal sign in each equation represent the radiation exchange between surfaces in the enclosure. Convection heat transfer is accounted for in the sixth term. The remaining term to the right of the equal sign accounts for the transient heat transfer response.

Third, an energy balance is performed on the air within the enclosure and is given by:

$$A_C h(T_C - T_a) + \sum_{i=1}^n A_i h(T_i - T_a) + A_f h(T_f - T_a) = \rho_a s l^2 d c_a \frac{dT_a}{d\theta} \quad (2.8)$$

Figure 2.1 illustrates the results of a computer simulation.

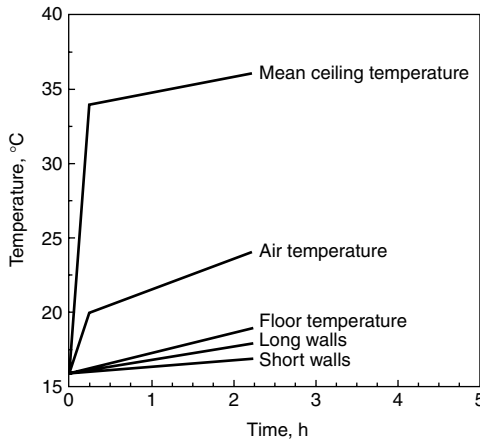


**FIGURE 2.1** Transient response to participating members and air in a rectangular enclosure (Kahn and Coutin-Rodicio, 1990).

The sharp initial rise in the mean ceiling temperature and air results from the rise in temperature of the radiant panels and natural convection between the radiant panels and the air, respectively. Once the radiant panels reach their maximum temperature (approximately 20 min), the mean ceiling temperature rises at a slower rate resulting from the slow rate of heat conduction through the ceiling. The same phenomenon occurs with the air. As the participating members begin exchanging heat convectively with the air (approximately 20 min), the air temperature begins rising at a slower rate (Khan and Coutin-Rodicio, 1990). For the case shown in Fig. 2.1, a

heater surface area to ceiling surface area ratio of 0.36 is used. The radiant heater contains a water inlet temperature of 70°C and a water flow rate of 0.05 kg/s.

This particular mathematical model incorporates conduction and convection into the radiation calculations. Seven equations were solved by using a computer program based on the finite difference method. The ceiling was divided into 200 control volumes, and the temperature for each control volume was calculated explicitly. However, the temperature of the four walls and floor were solved implicitly for each time step.

**2.1.2 Howell and Suryanarayana Model**

Howell and Suryanarayana (1990) also developed a mathematical model for sizing radiant heating systems. Their model is calibrated for three radiant heating systems: ceiling panels, heated floors, and infrared units. Howell and Suryanarayana performed a heat balance on a rectangular room by using the Fanger comfort equations to define comfort for human occupancy (Fanger, 1972). The heat balance was written as:

$$q_{r,i} + q_{cv,i} + q_{cd,i} = 0 \tag{2.9}$$

where the sum of the radiant exchange with the other surfaces ( $q_{r,i}$ ), and convective exchange with the air in the room ( $q_{cv,i}$ ) is equal to the conduction ( $q_{cd,i}$ ) through the surface. The radiative term in Eq. (2.9) is expressed as:

$$q_{r,i} = \epsilon_i \sigma T_i^4 - \sum_{j=1} \epsilon_j \sigma T_j^4 F_{i-j} \tag{2.10}$$

assuming surface emittances to be at or above 0.9. The convective term in Eq. (2.9) is expressed as:

$$q_{cv,i} = h_{c,i}(T_i - T_a) \tag{2.11}$$

Values for  $h_c$  were taken from ASHRAE (1975, 1985), Altmayer et al. (1983), and Min et al. (1956). The remaining conductive term in Eq. (2.9) is expressed as:

$$q_{cd,i} = C_{k,i}(T_i - T_0) \tag{2.12}$$

and accounts for conduction from the inside surface of the wall to the outside air.

**2.1.3 Thermal Comfort Model Conclusions**

The Rohles-Nevins study provides the primary comfort database used throughout the world. Although other studies have been conducted since that time, none of these more recent studies are of a comparable size and scope; rather, they have tended to focus on specific questions rather than developing a comprehensive database. Essentially all comfort modeling uses the Rohles-Nevins database either directly or indirectly. This database did not specifically address questions associated with radiant heating of the human body. No attempt was made to separate radiant interchange between the body and the environment from other thermal interchanges.

Fanger’s work describing the projected areas of the human body as a function of elevation and orientation was conducted in the 1970s. It remains the primary data-

base for describing radiant interchange between the body and the environment. With appropriate descriptions of the surrounding environment, these data can be used to calculate the total radiant exchange for the body. The primary limitation of these data is that they are only for the whole body and cannot be used to describe local effects of nonuniform radiant fields.

The Fanger model and the various forms of the two-node model are often used for comfort research. The Fanger model is much simpler and, consequently, has found more use outside the laboratory. Its PMV and PPD are used in ISO comfort standards. The two-node model has the advantage of being more complete in its representation of evaporative heat loss from the body and is applicable to a wider range of physiological conditions. Both are limited in that they use a one-dimensional description of the body and the thermal interaction with the environment. Neither can describe local effects due to nonuniform environments and/or nonuniform clothing coverage. Multinode models have the potential for describing such nonuniformity, but thus far have found little application outside the laboratory due to their complexity.

Neither the currently available radiant database nor the commonly used comfort models support effective analysis of nonuniform radiant environments. The mean radiant temperature not only is the simplest method of describing the radiant environment, but also has the same limitation of not describing nonuniformities. Empirical studies that measure human subjective responses to asymmetric radiation can be used to set limits on radiant asymmetry. At the present time, these data have not been incorporated into comfort models due to the limitations described above.

The thermal circuit models provide simple techniques to calculate radiant heat transfer in a room. They are limited, however, in application since they can only be applied to rectangular enclosures. Other limitations that impact accuracy range from a well-insulated room to a room with little or no ventilation.

The MRT method, described in Chap. 3 of Sec. 2, is an approximation to the exact solution of radiative heat transfer in an enclosure. As an aside, the reader should not confuse the terminology between the MRT method to calculate the radiant exchange within an enclosure and the mean radiant temperature. They have nothing to do with each other, and it is unfortunate that the names are the same. The approximations are made in such a way that energy is not conserved in the room. Consequently, the balanced MRT scheme was developed. This scheme divided the net heat transfer imbalance among the room surfaces to guarantee that energy was conserved. This method of balancing the energy equation, however, may provide for a maldistribution of energy between the interior surfaces. Finally, the balanced MRT calculations were found to significantly deviate from the exact solution when the room geometry became even slightly complex. This deficiency was somewhat remedied by adding a correction term to the energy equation. Although the correction improved the accuracy for an L-shaped room, there is little reason for the calculations to exhibit improved accuracy for complex geometries that include partitions and so forth. As a final point, the linearized form of the radiation term does not reduce to the original radiation term unless the fictitious plane temperature and the surface temperature are the same. This problem can be resolved by linearization, using a first-order Taylor's series expansion about the surface temperature.

The discrete ordinates method provides one of the more rigorous, yet flexible, methods for efficiently calculating radiant exchange within a geometrically complex enclosure. This method is based on fundamentals of radiation heat transfer and can be made more precise by increasing the fineness of the numerical grid. Sanchez and Smith (1992) have successfully used this method to model a two-dimensional enclou-

sure with arbitrary surfaces and obstacles. Their calculations, however, are only two-dimensional.

The Monte-Carlo method of solving the radiant transfer equation has been successfully used for rectangular enclosures. The accuracy, however, is suspect unless several thousand rays are used. This tends to result in excessive computational effort and large memory requirements when the enclosure becomes geometrically complex.

From the above review, the most flexible and efficient method for calculating radiation heat transfer within a geometrically complex enclosure is the discrete ordinates method. The MRT method is simply not founded on the fundamental principles of radiation heat transfer and has yet to be shown that it can accurately calculate radiant exchange in a complex enclosure.

## 2.2 THE BCAP METHODOLOGY

This section focuses on developing the mathematical energy model for a radiantly heated enclosure by simplifying and developing a general set of equations based on heat transfer and physical fundamentals. When solved, the ensuing set of equations provides the radiant heat flux distribution throughout the room and the total, convective, and radiative heat fluxes on each surface. In addition, the room and surface temperatures can be calculated from the methodology.

Figure 2.2 illustrates the various modes of heat transfer that occur in a radiantly heated room. In this figure, the radiant heater is positioned on the ceiling and radiates to the other interior surfaces of the enclosure. The interior surfaces, in turn, radiate to the other interior surfaces. The room air exchanges energy with the interior enclosures by convective heat transfer. Energy enters and leaves the room through air infiltration. Finally, energy is lost to the ambient by heat conduction through the walls.

The governing equations for energy (heat) transfer for the room air and for each wall surface within the room are written as:

$$\sum_{i=1}^N [h_i A_i (T_{\text{air}} - T_i)] + \dot{m} \int_{T_0}^{T_{\text{air}}} C_p(T) dT + \dot{Q}_{\text{h,c}} = \frac{\partial E_{\text{air}}}{\partial t} \quad (2.13)$$

$$\frac{(T_0 - T_i)}{R_{\text{th}}} + h_i (T_{\text{air}} - T_i) + \left\{ \alpha_i \int_{\Omega'} \ln \cdot \Omega | I(\Omega) d\Omega' - \epsilon_i \sigma T_i^4 \right\} + \alpha_i \dot{Q}_{\text{source}} + \dot{Q}_{\text{panel}} = \frac{\partial E_{\text{air}}}{\partial t} \quad (2.14)$$

Since the work in this project is limited to steady-state calculations, Eqs. (2.13) and (2.14) are simplified to:

$$\sum_{i=1}^N [h_i A_i (T_{\text{air}} - T_i)] + \dot{m} \int_{T_0}^{T_{\text{air}}} C_p(T) dT + \dot{Q}_{\text{h,c}} = 0 \quad (2.15)$$

$$\frac{(T_0 - T_i)}{R_{\text{th}}} + h_i (T_{\text{air}} - T_i) + \left\{ \alpha_i \int_{\Omega'} \ln \cdot \Omega | I(\Omega) d\Omega' - \epsilon_i \sigma T_i^4 \right\} + \alpha_i \dot{Q}_{\text{source}} + \dot{Q}_{\text{panel}} = 0 \quad (2.16)$$

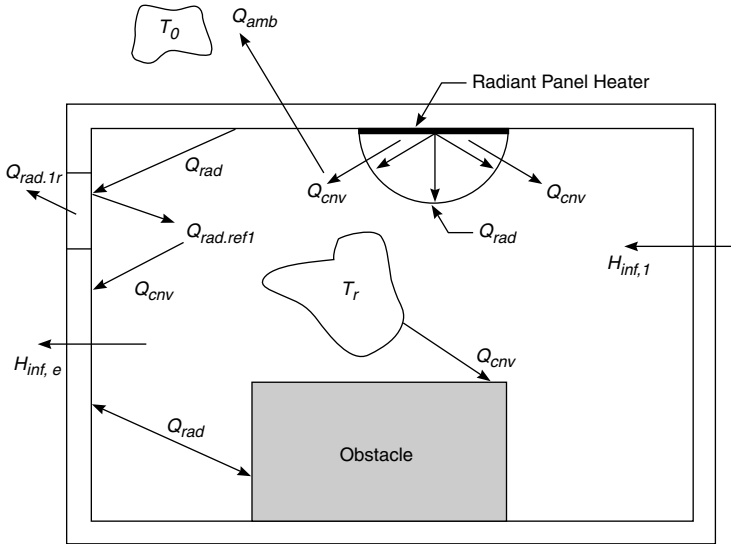


**FIGURE 2.2** Schematic of a radiantly heated room showing the various modes of heat transfer.

Equation (2.15) mathematically describes the energy balance on the room air. The first term represents convective losses to the bounding surfaces, and the second term represents the air infiltration rate, where  $T_0$  is the temperature of the infiltrating air. The last term represents convective heat transfer to the air from the radiant heater. The first term in Eq. (2.16) represents conduction through the wall where  $R_{th}$  is the thermal resistance of the wall and the outer convective boundary layer. The second expression is the convective heat flux between the inside surface and the room air. The third expression represents the incident radiant heat flux absorbed by the wall surface, whereas the parameters  $I$  and  $\Omega$  are the spectral intensity and solid angle. The fourth expression is the radiant emission from the wall. Together, these two terms equal the net radiant heat flux at the bounding surface. The fifth term represents the heat source input, and the sixth term is the heating panel heat flux.

The following sections focus on these two equations by simplifying and developing a general set of equations based on heat transfer and physical fundamentals.

### 2.2.1 Radiation Mathematical Model

The radiative heat transfer model developed in this section is founded on accepted fundamental relationships to ensure the broadest possible generalizations. Although simplifying approximations are necessary to solve the fully three-dimensional radiative transfer equation, they are introduced only in the final stages of the mathematical model development. To this end, the mathematical model developed in this part starts with the fundamental radiative transfer equation and proceeds to the point of calculating surface radiative heat fluxes and intensities necessary to solve equation (2.16).

The radiative heat transfer equation discussed in Chap. 3 of Sec. 2 has been derived in many places (Viskanta and Menguc, 1987; Siegel and Howell, 1981). It

includes a balance of radiant energy emitted and scattered into the direction of propagation ( $\Omega$ ) and the radiant energy attenuation due to absorption and scattering by the medium out of the direction of propagation. When solved, the radiative heat transfer equation provides the radiant intensity as a function of position, direction, and wavelength.

The parameters  $I_\lambda$  and  $I_{b,\lambda}$  are the spectral intensity and the blackbody spectral intensity, and  $\kappa_\lambda$  and  $\sigma_\lambda$  are the spectral absorption and scattering coefficients. Figure 2.3 schematically describes the coordinate parameter  $r$  and the solid angle parameter  $\Omega$ .

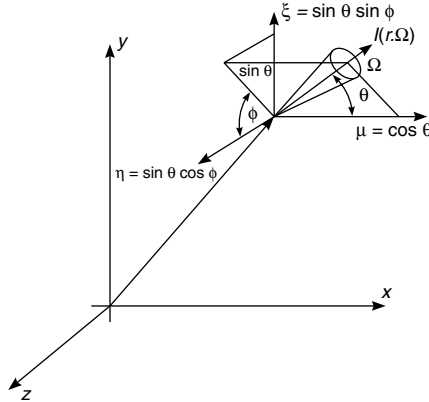


**FIGURE 2.3** Schematic showing the coordinate system and direction cosines for the radiative transfer equation.

Finally, the parameter  $\Phi$  is the phase function, which controls scattering of radiant intensity into the direction  $\Omega$ . For the special case of radiant heating where the air is not radiatively participating,  $\kappa_\lambda$  and  $\sigma_\lambda$  are zero and, for a rectangular coordinate system, the radiative transfer equation reduces to:

$$(\nabla \cdot \Omega)I_\lambda(r,\Omega) = \mu \frac{\partial I_\lambda}{\partial x} + \xi \frac{\partial I_\lambda}{\partial y} + \eta \frac{\partial I_\lambda}{\partial z} = 0 \tag{2.17}$$

The variables  $\mu$ ,  $\xi$ , and  $\eta$  are the direction cosines, as described in Chap. 3 of Sec. 2. Referring to Fig. 2.3, the direction cosines are defined as  $\mu = \cos\theta$ ;  $\xi = \sin\theta \sin\phi$ ; and  $\eta = \sin\theta \cos\phi$ . The boundary conditions for Eq. (2.17) are developed by considering the energy emitted by the boundary and the incident radiant energy reflected by the boundary, as shown in Fig. 2.4. If the boundary is considered to be a diffuse emitter and absorber, and the incident radiation is transmitted through the boundary surface, the boundary conditions are written as:

$$I_{\lambda,\text{bound}} = \epsilon_\lambda I_{b,\lambda} + \frac{\rho_\lambda}{\pi} \int_{n \cdot \Omega'} |n \cdot \Omega| I_\lambda(\Omega') d\Omega' \tag{2.18}$$

$$= \epsilon_\lambda I_{b,\lambda} + \frac{(1 - \epsilon_\lambda - \tau_\lambda)}{\pi} \int_{n \cdot \Omega'} |n \cdot \Omega'| I_\lambda(\Omega') d\Omega'$$

The parameters  $\epsilon_\lambda$ ,  $\tau_\lambda$ , and  $\rho_\lambda$  are the surface spectral emissivity, transmissivity, and reflectivity. The first term on the right side of Eq. (2.18) represents the spectral emission from the surface, whereas the second term represents the reflected radiant intensity due to incident radiation on the surface. By including the transmissivity in the second term, radiation lost through a window or other opening is taken into account.

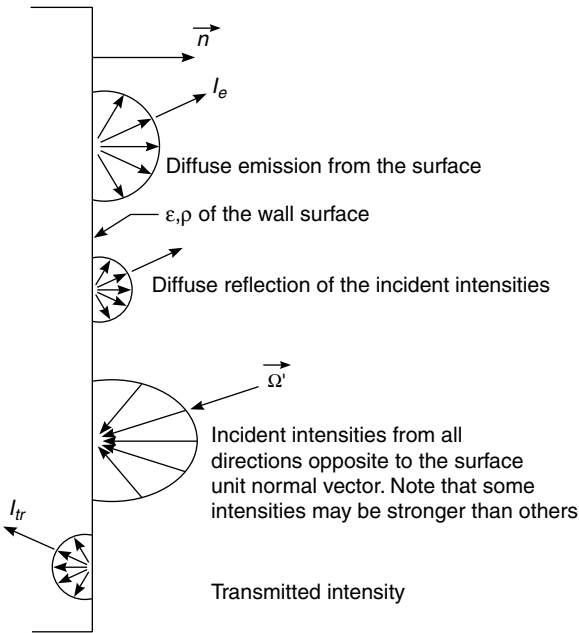


**FIGURE 2.4** Schematic showing the boundary conditions for the radiative transfer equation.

Equations (2.17) through (2.18) represent a coupled set of equations that, when solved, result in the radiation intensity as a function of direction, position, and wavelength. Once  $I_\lambda(r, \Omega)$  is known, it is substituted into Eq. (2.16) to solve for the air and surface temperatures. The spectral dependency has been retained in these equations for generality. However, if the surfaces are radiatively gray, which is usually a valid assumption for room surfaces, the wavelength subscripts can be dropped.

The intensity equations may be solved by using one of several different methods. The method employed in this work is the discrete ordinates method. The discrete

ordinates method has been successfully used in combination with convection and conduction heat transfer, providing a full mathematical model of the energy transfer processes. The basic premise behind this method is to divide the enclosure into control volumes and then to integrate the radiant transfer equation [Eq. (2.17)] over each control volume, resulting in a discretized set of algebraic equations (Fiveland, 1988; Truelove, 1988). Equation (2.17) is discretized by integrating over the three-dimensional control volume with respect to  $dx$ ,  $dy$ , and  $dz$ , in a specific direction  $j$ :

$$\int_z^{z+\Delta z} \int_y^{y+\Delta y} \int_x^{x+\Delta x} \left[ \mu \frac{\partial I'_\lambda}{\partial x} + \xi \frac{\partial I'_\lambda}{\partial y} + \eta \frac{\partial I'_\lambda}{\partial z} = 0 \right] dx dy dz \quad (2.19)$$

The integration is completed by assuming the control volume interface spectral, directional intensity invariant about the other two coordinate directions [i.e., the intensity along the interface at  $x$ ,  $I'_{x,\lambda}$ , is independent of  $y$  and  $z$  (Patankar, 1980)]. Applying this assumption to the other control volume interfaces, Eq. (2.19) is approximated for each discrete direction  $j$  by:

$$0 = \mu^j \Delta z \Delta y (I'_{x+\Delta x,\lambda} - I'_{x,\lambda}) + \xi^j \Delta z \Delta x (I'_{y+\Delta y,\lambda} - I'_{y,\lambda}) + \eta^j \Delta x \Delta y (I'_{z+\Delta z,\lambda} - I'_{z,\lambda}) \quad (2.20)$$

The final form of the discretized spectral radiative transfer equation that can be applied to an enclosed space is:

$$I'_{p,\lambda} = \frac{\mu^j \Delta z \Delta y I'_{x,\lambda} + \xi^j \Delta z \Delta x I'_{y,\lambda} + \eta^j \Delta x \Delta y I'_{z,\lambda}}{\mu^j \Delta z \Delta y + \xi^j \Delta z \Delta x + \eta^j \Delta x \Delta y} \quad (2.21)$$

The discretized form of the radiative transfer equation presented in Eq. (2.19) is valid for a beam propagating in the positive  $x$ ,  $y$ , and  $z$  directions at a specific wavelength. All the direction cosines must be positive. For the case in which the beam is propagating in the positive  $y$  and  $z$  directions, but in the negative  $x$  direction, the term  $I'_{x,\lambda}$  is replaced by  $I'_{x+\Delta x,\lambda}$ . For this case, the direction cosine  $\mu^j$  would be negative and, therefore, the upstream and downstream intensities defined would be reversed. By using this solution scheme, the direction cosines in Eq. (2.19) are always positive and should, therefore, be represented by absolute values. The boundary conditions associated with Eq. (2.19) are derived from Eq. (2.18) and represented by:

$$I'_{x=0,\lambda} = \epsilon_\lambda I_{b,\lambda}(T_{x=0}) + \frac{(1 - \epsilon_\lambda - \tau_\lambda)}{\pi} \sum_i w_i |\mu_i| I'_{x=0,\lambda}, \quad \mu_i < 0 \quad (2.22)$$

$$I'_{x=L,\lambda} = \epsilon_\lambda I_{b,\lambda}(T_{x=L}) + \frac{(1 - \epsilon_\lambda - \tau_\lambda)}{\pi} \sum_i w_i |\mu_i| I'_{x=L,\lambda}, \quad \mu_i > 0 \quad (2.23)$$

$$I'_{y=0,\lambda} = \epsilon_\lambda I_{b,\lambda}(T_{y=0}) + \frac{(1 - \epsilon_\lambda - \tau_\lambda)}{\pi} \sum_i w_i |\xi_i| I'_{y=0,\lambda}, \quad \xi_i < 0 \quad (2.24)$$

$$I'_{y=H,\lambda} = \epsilon_\lambda I_{b,\lambda}(T_{y=H}) + \frac{(1 - \epsilon_\lambda - \tau_\lambda)}{\pi} \sum_i w_i |\mu_i| I'_{y=H,\lambda}, \quad \xi_i > 0 \quad (2.25)$$

$$I'_{z=0,\lambda} = \epsilon_\lambda I_{b,\lambda}(T_{z=0}) + \frac{(1 - \epsilon_\lambda - \tau_\lambda)}{\pi} \sum_i w_i |\eta_i| I'_{z=0,\lambda}, \quad \eta_i < 0 \quad (2.26)$$

$$I'_{z=W,\lambda} = \epsilon_\lambda I_{b,\lambda}(T_{z=W}) + \frac{(1 - \epsilon_\lambda - \tau_\lambda)}{\pi} \sum_i w_i |\eta_i| I'_{z=W,\lambda}, \quad \eta_i > 0 \quad (2.27)$$

The parameter  $w_i$  is the quadrature weighting factor used to approximate the integral over the solid angle. The angular quadrature technique of approximating the integral by carrying out the summation in Eqs. (2.22) through (2.27) has been discussed in detail by Fiveland (1984, 1987, and 1988) and Truelove (1987 and 1988). In general, the angular quadrature weights and directions must satisfy the physical constraints defined by the following equations:

$$\int_{4\pi} d\Omega = \sum_j w_j \quad (2.28)$$

$$\int_{2\pi} \mu d\Omega = \sum_j \mu_j w_j = \pi, \quad \mu_j < 0 \quad (2.29)$$

$$\int_{4\pi} \mu^2 dW = \sum_j \mu_j^2 w_j = \frac{4\pi}{3} \quad (2.30)$$

Similar equations are required for the other two directional cosines  $\xi$  and  $\eta$ . Equation (2.28) represents the integral of the solid angle over all directions (Truelove, 1988), whereas Eqs. (2.29) and (2.30) represent the half-range flux and the diffusion theory, respectively. The weights and directions that satisfy these equations are shown in Table 2.1 for the  $S_4$  model (three directions per octant). This particular model has been evaluated by Truelove (1988) and Fiveland (1988) and found to be quite accurate. Once the weights and directions have been determined, they can be used to approximate any angular integral.

**TABLE 2.1** Directional Cosines and Quadrature Weighting Factors for the Positive  $x$ -,  $y$ -, and  $z$ -Coordinate Octant (Truelove, 1988)

$\mu_j$	$\xi_j$	$\eta_j$	$\omega_j$
0.30	0.30	0.91	$\pi/6$
0.30	0.91	0.30	$\pi/6$
0.91	0.30	0.30	$\pi/6$

The simultaneous solution of Eq. (2.21) through (2.27) produces the spatial, directional, and spectral radiant intensity throughout the enclosure. If the surfaces of the enclosure are gray, all the terms in Eq. (2.21) through (2.27) are treated independent of wavelength by dropping the subscript  $\lambda$ .

Obstacles inside the enclosure (e.g., a truck, airplane, or a piece of furniture) are included in much the same way as was done by Sanchez and Smith (1992). As a beam of radiant intensity travels through the enclosure, it may or may not encounter an obstacle. If the beam does encounter an obstacle, a boundary condition must be imposed by using the surface emissivity of the obstacle. This situation is schematically shown in Fig. 2.5. The schematic shows the computational grid and the obstacle, denoted by the shaded area. Starting from the left wall boundary, the intensity field is diffusely emitted and reflected, even though the wall incident radiation may be directional in nature. The intensity propagates through the air according to Eq. (2.21) until it becomes incident on the surface of the obstacle. Assuming the obsta-

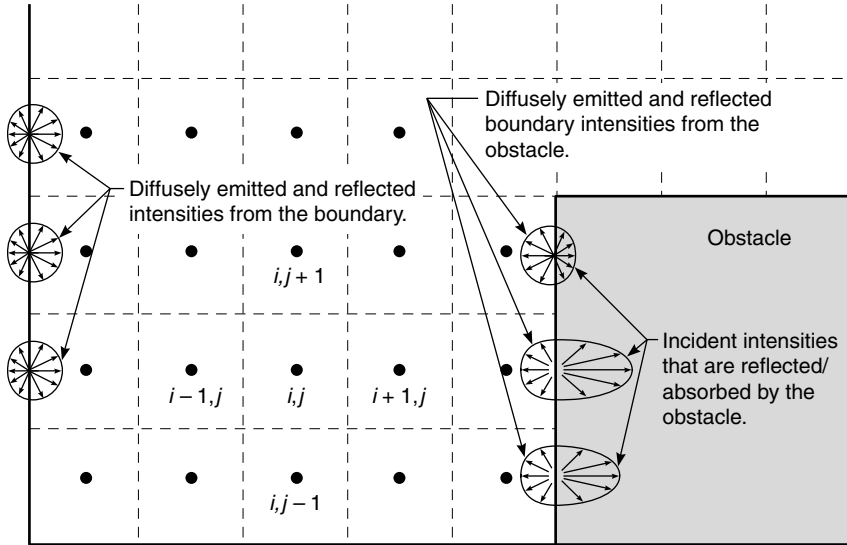


**FIGURE 2.5** Schematic showing how obstacles are incorporated into the discrete ordinates model.

cle is at the same temperature as the room air, the gray boundary condition at the obstacle surface is:

$$I_{\text{bound}} = \epsilon I_b (T_{\text{air}}) + \frac{\rho}{\pi} \int_{n \cdot \Omega' < 0} |n \cdot \Omega'| I(\Omega') d\Omega' \quad (2.31)$$

The boundary intensity is the intensity that diffusely propagates in the opposite direction from the obstacle surface, as shown in the figure. The first term on the left side of Eq. (2.31) represents the intensity emitted from the obstacle, and the second term represents the intensity reflected by the obstacle. Consequently, each control volume must be tested to determine if it is part of an obstacle or a portion of the room air.

For the  $S_4$  discrete ordinates model employed in this work, there are 24 directions that must be considered (three directions per octant). Therefore,  $\mu$ ,  $\xi$ , and  $\eta$  are set for the first of the 24 directions. Next, the boundary intensities are calculated at each solid surface. The computation then proceeds by starting at the first node in the domain and solving Eq. (2.21). To prepare for the calculation at the next sequential node, the downstream control volume interface is tested to determine if it is an obstacle. If it is not, the computation proceeds by calculating the interface intensity. Otherwise, the interior nodes of the obstacle are bypassed. Equation (2.31) is then solved to obtain the emitted and reflected intensity from the opposite obstacle surface. If there are more nodes, the computation continues; otherwise, a new direction is set. Once this procedure has been applied to all directions and nodes, convergence is tested by comparing the intensities from the current iteration to those computed during the previous calculation sweep. If the convergence criteria are not satisfied, the entire iteration is repeated. If the spectral nature of the surfaces is considered, an additional loop is added to cycle through the wavelength spectrum. However, the work presented here assumes gray surfaces.

The intensity field is then used to calculate the radiant heat flux at each surface. The net incident radiant heat flux at a surface is calculated by (Brewster, 1992):

$$q_{\text{rad}} = \int_{\Omega'} |n \cdot \Omega'| I(\Omega') d\Omega' \tag{2.32}$$

For a radiant heat flux in the *x* direction, the foregoing equation is approximated by using a quadrature (Fiveland, 1988):

$$q_{\text{rad}} = \sum_j \mu^j I^j \omega_j \tag{2.33}$$

**2.2.2 Conduction and Convection Mathematical Models**

The conductive heat flux is calculated by using a thermal resistance (*R<sub>th</sub>*). Conduction heat transfer through each surface is calculated by:

$$q_{\text{cond},i} = \frac{Q_{\text{cond},i}}{A_i} = \frac{1}{R_i} (T_{0,i} - T_i) \tag{2.34}$$

The subscript *i* represents the particular surface, *T<sub>i</sub>* represents the inside surface temperature, and *T<sub>0,i</sub>* represents the air temperature on the outer side of the surface. The thermal resistance includes the thermal conductivity and thickness of the wall, and the exterior convective heat transfer coefficient.

The convective heat flux from the room air to the interior surfaces is calculated by using the appropriate heat transfer coefficient from the literature. The convective heat flux to surface *i* is:

$$q_{\text{conv},i} = \frac{Q_{\text{conv},i}}{A_i} = h_i(T_r - T_i) \tag{2.35}$$

The heat transfer coefficient *h<sub>i</sub>* is determined by assuming natural (free) convection in the room. Chapman (1984) recommends the Nusselt number correlations for free convection past a vertical plane surface and around horizontal plates summarized in Table 2.2.

**TABLE 2.2** Empirical Correlations for Air Viscous Fluid Flow (White, 1991)

Property	Correlation	Constant
Thermal expansion β	$\beta = 1/T_m$	$T_m = (T_{\text{surface}} + T_{\text{air}})/2$
Kinematic viscosity ν	$\nu = \frac{\mu}{\rho} = \frac{1}{\rho} \mu_0 \left( \frac{T_m}{T_0} \right)^n$	$\mu_0 = 1.716 \times 10^{-5} \text{ kg/m} \cdot \text{s}$ $T_0 = 273 \text{ K}$ $n = 0.666$ $\rho = 1.2 \text{ kg/m}^3$ $g = 9.8 \text{ m/s}^2$
Thermal conductivity <i>k</i>	$k = k_0 \left( \frac{T_m}{T_0} \right)^n$	$k_0 = 0.0241 \text{ kg/m} \cdot \text{s}$ $n = 0.81$
Prandtl number Pr	$\text{Pr} = 0.875 - (9.2 \times 10^{-4}) \times T_m + (1.2 \times 10^{-6}) \times T_m^2$ $(-10^\circ\text{C} \leq T_m \leq 100^\circ\text{C})$	

The thermophysical properties  $k$ ,  $v$ , and  $\beta$  used in the convection correlations for air are calculated by using empirical relationships provided by White (1991). These empirical relationships are summarized in Table 2.2.

### **2.3 USING THE BCAP METHODOLOGY**

---

The BCAP methodology is an aid to the designer of building heating systems. It is still the individual, not the methodology, who designs the heating systems. The design process using BCAP is iterative by nature. The designer selects a heating system design; the BCAP methodology is used to assess the suitability of the design; modifications are made to the design, if necessary, based on the results of the BCAP analysis; the revised design is evaluated using BCAP; and so forth. The heating system is refined by using this process until the designer is satisfied with the results. Obviously, the better the first system design, the quicker a final design is achieved. Many equipment manufacturers, vendors, and system designers have their own techniques for sizing and laying out heating systems. Individuals experienced with these techniques are encouraged to use them for their initial designs. If these techniques are good, then BCAP is only needed for refining the resulting initial designs.

Some individuals may need guidance in developing an initial design. There are two major factors to consider in designing a heating system: (1) layout and (2) sizing. The layout of the heating systems will depend on the type of equipment used and the heating application. There is no one single correct way to lay out a system in a given application, and good engineering judgment is an essential part of the job. There are far too many possibilities to include suggestions on this topic in the BCAP programs. The user who needs more information on this topic is referred to the ASHRAE Handbooks for advice.

The methods described in Chap. 1, "ASHRAE Standard Methods," of this section provide a reasonable first guess of the size of a heating system. The BCAP methodology can then be used to fine-tune the heating system to provide optimal thermal comfort and energy consumption.

The estimate provided by the ASHRAE standard methods is usually reasonably accurate for uniformly heated buildings. The more localized the heating and the more the unheated surfaces are at nonuniform temperatures, the less reliable the estimate. This relatively simple calculation is the result that would be obtained if no special attention is given to radiant heat transfer within the building and is typical of calculations often used by heating system designers.

### **2.4 BCAP METHODOLOGY EXAMPLE CALCULATION**

---

This section provides an example of using the BCAP methodology and comparing the BCAP results to several different building heating analyses. The final results are shown, as opposed to the detailed step-by-step calculations, due to the complexity of the calculations. However, the CD-ROM included with the Handbook can be used to reproduce these results.

### 2.4.1 Comparing BCAP Calculations to Field-Test Data

The BCAP methodology was validated by using data collected from the Adaptable Fire-Safe Demonstration House located in Bowie, Maryland. The two-story house has about 2200 ft<sup>2</sup> of living space, 8-ft ceilings, and is typical of houses built in the mid-Atlantic region of the United States. A complete first story floor plan of the house is illustrated in Fig. 2.6. During the 1993 to 1994 winter, the house was equipped with and heated by radiant panel heaters. During this time, the room air and the operative air temperatures were measured in various locations around the house.

The best reported data available for validation were collected in the dining room. During a 5-h period of time, the outside air temperature was  $-2.22^{\circ}\text{C}$  ( $28^{\circ}\text{F}$ ). The dining room air and operative temperatures were reported over this 5-h period. The room air floor directly underneath the center of the heater is  $21.3^{\circ}\text{C}$  ( $70.4^{\circ}\text{F}$ ). In addition, the calculated mean radiant temperature at this location is  $24.3^{\circ}\text{C}$  ( $75.7^{\circ}\text{F}$ ). Since the methodology calculates a mass averaged room air temperature, the calculated value was compared to the temperature measured at 109.22 cm (43 in) from the floor. This location, since it is near the vertical center of the room, should be very close to the mass averaged room air temperature. Comparing the measured and calculated mean room air temperatures shows a difference of only  $0.3^{\circ}\text{C}$  ( $0.5^{\circ}\text{F}$ ). The difference between the measured and calculated operative temperatures is  $0.4^{\circ}\text{C}$  ( $0.6^{\circ}\text{F}$ ). Both these differences are well within the expected tolerance of the methodology showing that it accurately predicts room air and operative temperatures.

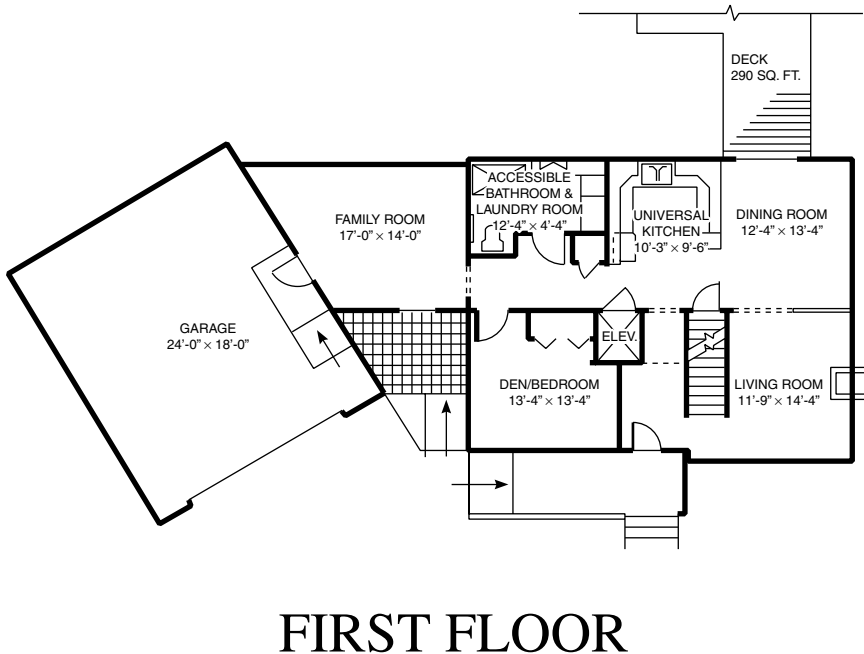


**FIGURE 2.6** Schematic showing the first floor of the house used for validation.

**2.4.2 Example Calculations and Results**

Heating analysis examples of four different buildings were performed to show the utility of the BCAP programs. These structures are listed in Table 2.3(a) along with the insulation values, infiltration rates, inside and outside design air temperatures, and the door and window surface areas. The dimensions listed in Table 2.3(b) are all length × height × width, and the coordinate system for all dimensions is shown in Fig. 2.7. Each structure was analyzed by comparing different radiant heating systems to each other and to a convective heating system. The convective heating analyses must be qualified by noting that the BCAP methodology does not include the effect of

**TABLE 2.3(a)** NAHB Results for the Dining Room (3.759 m × 4.064 m × 2.438 m) with Outside Temperature of -2.22°C (28.0°F)

Walls	R-19, ε = 0.9
Windows	R-2, ε = 0.4, τ = 0.1
Floor	R-11, ε = 0.9
ACH	0.5 (22.7 kg/h)
Indoor measured temp	18.1°C (64.5°F)
Indoor measured $T_{op}$	21.7°C (71.0°F)
Heater	
2 ft × 8 ft Enerjoy People Heater	
50 W/per ft <sup>2</sup>	
Centered 2 ft from back wall,	
6 ft 2 in from side walls	
800 W total output, 90% radiant	
Evaluation location	1.88 m from front kitchen wall, 3.45 m from front wall, 1.09 m from floor
BCAP calculations	$T_{air} = 18.4°C (65.0°F)$ $T_{mrt} = 24.3°C (75.7°F)$ $T_{op} = 21.3°C (70.4°F)$

**TABLE 2.3(b)** Descriptions of the Example Buildings Used to Demonstrate the Utility of the BCAP Programs

Building data	Warehouse	House	Office	Factory
	12 m × 6 m × 6 m (40 ft × 20 ft × 20 ft)	12 m × 3 m × 6 m (40 ft × 8 ft × 20 ft)	12 m × 3 m × 6 m (40 ft × 8 ft × 20 ft)	12 m × 6 m × 6 m (40 ft × 20 ft × 20 ft)
Wall	R-11	R-19	R-11	R-11
Window	R-2	R-3	R-2	R-2
Window surface area	5%	20%	20%	10%
Door	R-2	R-3	R-2	R-2
Door surface area	10%	5%	10%	10%
Ceiling	R-19	R-38	R-19	R-19
Floor	R-1	R-19	R-1.5	R-1
Infiltration	2 ACH	0.4 ACH	1.5 ACH	2 ACH
Outside temp (°C)	0°C	0°C	0°C	0°C
Indoor design temp (°C)	10°C	18°C	20°C	10°C

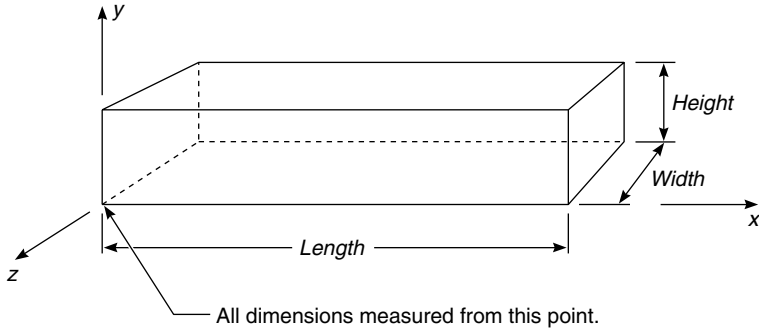


**FIGURE 2.7** Schematic showing the coordinate system and dimensions used to define the buildings.

room air movement on the thermal comfort of the occupants. Consequently, this may, in some unknown way, impact the analyses. The various heaters used in the analyses are listed in Table 2.4 and the evaluation locations for each building are listed in Table 2.5. Unless otherwise stated, all heaters exhibit 70 percent of the output as radiant heat, whereas the remaining 30 percent output is convective.

**2.4.2.1 Warehouse.** The results from the warehouse heating analysis are shown in Table 2.6. The first radiant heating system is a tube-type heater located in the center of the ceiling between the left and right surfaces as shown in Fig. 2.8(a). The tube-type heater is modeled by using four uniform cylindrical radiant flux segments (type 10 in Table 2.4). Each heater was assigned a power output of 2200 W for a total heat input of 8800 W. For this case, all the evaluation locations were 2 m (6.56 ft) above the floor surface. The result for the first location, which is positioned

**TABLE 2.4** Types of Discrete Heaters Used in the Examples and Validation of the BCAP Programs

1	Uniform hemispherical radiant flux, 180°
10	Uniform cylindrical radiant flux segment, 90°
12	Uniform cylindrical radiant flux segment, 30°
—	Fixed-temperature slab heating

**TABLE 2.5** Evaluation Locations in Each Building

Building	Location 1	Location 2	Location 3	Location 4
Warehouse	1 m × 2 m × 1 m	6 m × 2 m × 3 m	11 m × 2 m × 3 m	
House	7 m × 1 m × 5 m	4 m × 1 m × 5.5 m	6 m × 1 m × 3 m	0.5 m × 1 m × 0.5 m
Office	2 m × 1 m × 3 m	6 m × 1 m × 3 m	9 m × 1 m × 5 m	10 m × 1 m × 1 m
Factory	2 m × 1 m × 3 m	6 m × 1 m × 3 m	6 m × 1 m × 1 m	4 m × 1 m × 1 m

The dimensions are given in terms of  $x$ -,  $y$ -, and  $z$ -, as shown in Fig. 2.7.

**TABLE 2.6** Warehouse Heater Evaluation Using a Tube-Type Radiant Heater, a Temperature-Controlled Floor Slab Heater, and a Convective Heater

Heater type	Heater information		Evaluation location			
	Number of heaters	Power/heater* (W)	$T_{op}/T_{mrt}$ (°C)	$T_{op}/T_{mrt}$ (°C)	$T_{op}/T_{mrt}$ (°C)	$T_{op}/T_{mrt}$ (°C)
Tube-type (type 10) located in center of ceiling	4	2200	10.6/11.8	14.6/19.9	11.0/12.6	
Floor heating ( $T_{floor} = 20^{\circ}\text{C}$ )	Slab	5433	11.8/13.7	12.3/14.6	12.0/14.1	
Convection	1	5800	8.1/6.2	8.0/5.9	8.1/6.2	

The air temperature for each heating system was  $10^{\circ}\text{C}$  ( $50^{\circ}\text{F}$ ).

\* The slab heat input into the building is 2810 W by convective heat transfer and 2633 W from radiative heat transfer. These results show that 52 percent of the heat to the room is by convection and 48 percent is by radiation.

well away from the heater, is the coldest temperature. The second location, which is directly beneath the heater, is substantially warmer. The higher operative temperature is due to the increased radiant field from the heater. The calculations show that the operative temperature is  $4.6^{\circ}\text{C}$  higher than the mean air temperature, leading to a thermally warmer climate compared to a system without radiant heating. The third location is directly underneath the right edge of the heater and, therefore, is slightly cooler than the second location. All three locations, however, exhibit an operative temperature greater than the mean air temperature.

The second heating system is a floor slab heater with a temperature of  $20^{\circ}\text{C}$  ( $68^{\circ}\text{F}$ ). Although all locations exhibit approximately the same operative temperature, the first location, which is closer to a wall, is between  $0.2^{\circ}\text{C}$  and  $0.5^{\circ}\text{C}$  lower than the other operative temperatures. This lower temperature is due to the effect of the proximity of the walls. Since the walls lose heat to the ambient, the wall surface temperatures are lower than the floor temperatures. The calculations show that the wall temperatures in the vicinity of the first location are about  $12^{\circ}\text{C}$  ( $53.6^{\circ}\text{F}$ ), leading to the lower mean radiant temperature which, in turn, leads to the lower operative temperature. The total heat that is added to the room by the floor slab heater is 5433 W. The calculations show that 52 percent of the floor heat is convective and 48 percent is radiative.

The third heating system is a convective system. From a modeling standpoint, the heat is added directly to the air, and then the air heats the building surfaces. The power necessary to achieve the design air temperature is 5800 W. However, the results in Table 2.6 show that even though the room air temperature is  $10^{\circ}\text{C}$  ( $50^{\circ}\text{F}$ ), the operative and mean radiant temperatures are substantially lower than for the previous two heating systems. Consequently, even though the convective system requires less energy to maintain the design air temperature, the occupants would feel colder with the convective system than with either of the radiant systems. As a final comparison, the convective heating system required 10,900 W to provide an  $11^{\circ}\text{C}$  ( $51.8^{\circ}\text{F}$ ) operative temperature. The mean room air temperature was, however,  $18.1^{\circ}\text{C}$  ( $64.6^{\circ}\text{C}$ ). Consequently, the convective system required 2100 W more power than the radiant tube-type heating system to provide the same level of thermal comfort.

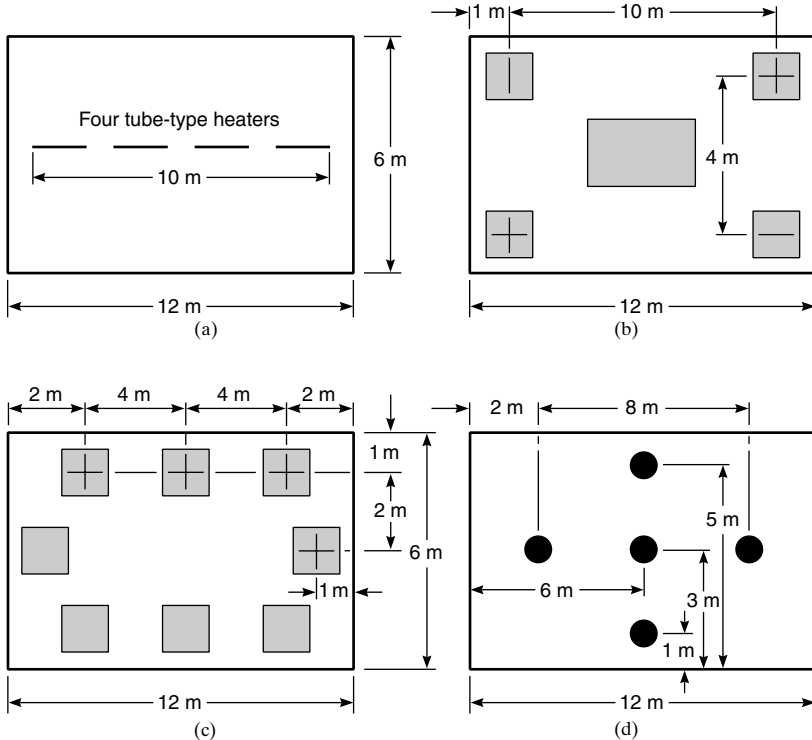


**FIGURE 2.8** Schematics showing the radiant heater systems for the various examples. The schematics are shown from the top. (a) Warehouse. (b) House. (c) Office. (d) Factory.

**2.4.2.2 House.** The heating system analysis for the house is shown in Table 2.7. The first system is a radiant heating panel mounted flush with the ceiling and located in the center of the ceiling. The power output necessary to maintain the 18°C (64.4°F) design air temperature is 3000 W. All the evaluation locations exhibit an operative and mean radiant temperature greater than the mean air temperature. The third location (Table 2.5), which is directly under the radiant heater, exhibits very high operative and mean radiant temperatures. This is due to the proximity of the heater to the evaluation location.

The second heating system is composed of four radiant panels again mounted flush with the ceiling. Each panel is located in a corner of the ceiling with the heater center 1 m (3.28 ft) from each wall, as shown in Fig. 2.8(b). Each panel was powered at 730 W to achieve the design room air temperature. All the evaluation locations exhibit a fairly uniform operative temperature with the fourth location about 1°C (1.8°F) higher than the other three locations. The reason for this is that the fourth evaluation location is positioned under one of the heaters.

The convective heating system required 2500 W to achieve the design room air temperature. As with the previous example, the mean radiant and operative temperatures are lower than the room air temperature, leading to a colder feeling than

**TABLE 2.7** House Heater Evaluation Comparing Two Different Panel-Type Radiant Heating Systems and a Convective Heating System

Heater information			Evaluation location			
Heater type	Number of heaters	Power/heater (W)	$T_{op}/T_{mrt}$ (°C)	$T_{op}/T_{mrt}$ (°C)	$T_{op}/T_{mrt}$ (°C)	$T_{op}/T_{mrt}$ (°C)
Panel heater (type 1) located in the center of the ceiling	1	3000	19.3/20.4	19.1/20.0	27.1/36.1	18.5/18.9
Panel heaters (type 1) located in corners of the ceiling. Heater center is 1 m from each wall	4	730	18.5/18.9	18.6/19.1	18.8/19.6	19.5/20.9
Convective	1	2500	16.4/14.9	16.4/14.9	16.5/15.1	16.5/15.0

The room air temperature was 18°C (64.4°F) for each case.

for the radiant cases. Consequently, to achieve the same level of comfort, the air temperature would have to be increased by increasing the power to the heater. The convective heating system required 2950 W to provide a 19.2°C (66.6°F) operative temperature. The mean room air temperature for this case was 21.0°C (69.8°C). Consequently, the convective system required slightly more power than the second radiant panel system and slightly less power than the first radiant panel system to provide the same level of thermal comfort. The difference between this example and the warehouse example is the insulation. Since the house is well insulated, the inside wall temperatures are approximately the same for both heating systems; however, the calculations did not include air stratification or air movement.

**2.4.2.3 Office Building.** The heating system analysis for the office building is illustrated in Table 2.8. The radiant heating system, shown schematically in Fig. 2.8(c), is a perimeter system composed of eight panel-type radiant heaters powered at 1200 W per heater. The combined heater output is 9600 W. The design air temperature is 20°C (68°F). The operative and mean radiant temperatures for the office

**TABLE 2.8** Office Building Heating Analysis Comparing Eight Panel-Type Radiant Heaters Positioned Around the Perimeter of the Room with a Convective Heater

Heater information			Evaluation location			
Heater type	Number of heaters	Power/heater (W)	$T_{op}/T_{mrt}$ (°C)	$T_{op}/T_{mrt}$ (°C)	$T_{op}/T_{mrt}$ (°C)	$T_{op}/T_{mrt}$ (°C)
Panel-type (type 1) located around room perimeter	8	1200	21.3/22.5	20.8/21.6	21.0/22.0	21.1/22.1
Convection	1	6950	16.2/12.2	16.0/12.0	16.2/12.3	16.2/12.3

The air temperature was 20°C (68°F) for each case.

building are uniform, with the second location (center of the room) exhibiting a 0.2°C to 0.5°C lower operative temperature than the other locations. The reason for this lower operative temperature is that the heaters are on the perimeter of the room, whereas the evaluation location is at the center of the room.

The convective system required 6950 W to maintain the design air temperature. The operative temperatures are approximately 5°C (9°F) lower than for the radiant heating system, whereas the mean radiant temperatures are about 10°C (18°F) lower than those exhibited by the radiant heating system. Some possible reasons why the operative and mean radiant temperatures for the office convective heating system are substantially lower than the corresponding temperatures for the house are the lower ceiling and wall insulation values. These lower values would, in turn, lead to lower wall and ceiling inside surface temperatures that then lead to lower mean radiant temperatures. The convective heating system required 9150 W to provide a 21.0°C (69.8°F) operative temperature. The mean room air temperature for this case was, however, fairly high at 26.0°C (78.80°F).

**2.4.2.4 Factory.** The factory heating analysis is shown in Table 2.9. The goal of this analysis is to show the benefit that can be achieved from localized and selective heating. To show this comparison, five heating systems were evaluated. The first is a spot-type radiant heating system (type 12 from Table 2.5) positioned 6 m (19.7 ft) above the local workstation and spaced as shown in Fig. 2.8(d). The second system is the same as the first, except located 3.5 m (11.5 ft) above the floor. The third is the same as the second, except powered at a lower rating. The final two heating systems are convective heating systems. The first radiant spot heating system required a power output of 2200 W per heater to maintain the design air temperature of 9.5°C (49.1°F). The first two locations are at two of the individual workstations, whereas the other two locations are positioned away from the workstations. The results show that, although the room air temperature is only 9.5°C (49.1°F), the workstations are maintained at an operative temperature of approximately 13°C (55.4°F). The two nonworkstation locations exhibit operative temperatures slightly higher than the mean air temperature since the wall temperatures are greater than the building mean air temperature.

The second case exhibits the situation in which the same heaters are used, except

**TABLE 2.9** Factory Heating Analysis Comparing Six Spot-Type Radiant Heaters Positioned Above Workstations to a Convective Heater

Heater information			Evaluation location			
Heater type	Number of heaters	Power/heater (W)	$T_{op}/T_{mrt}$ (°C)	$T_{op}/T_{mrt}$ (°C)	$T_{op}/T_{mrt}$ (°C)	$T_{op}/T_{mrt}$ (°C)
Spot-type (type 12) on ceiling (6 m above floor)	5	2200	13.2/16.9	12.9/16.2	11.3/13.1	10.0/10.4
Spot-type (type 12) 3.5 m above floor	5	2200	17.5/25.7	17.7/26.2	9.6/9.9	9.3/9.4
	5	1500	12.2/18.1	12.4/18.5	6.6/6.7	6.3/6.4
Convective	1	6000	7.2/4.9	7.1/4.8	7.2/4.9	7.3/5.2

The spot heaters were first positioned at 6 m, and then at 3.5 m. A second case was investigated at 3.5 m with 1500 W spot heaters. The air temperature for all cases except the 1500 W spot heater case was 9.5°C (49.1°F). The air temperature for the 1500 W spot heater case was 6.3°C (43.3°F).

they are lowered from the 6-m (19.7-ft) elevation to an elevation 3.5 m (11.5 ft) above the floor. This action increases the operative temperature at the workstations by 4.3°C to 4.8°C (7.7°F to 8.8°F). Conversely, the operative and mean radiant temperatures at the nonworkstation locations exhibit a corresponding decrease. The reason for this decrease is that the radiant heat is more focused when the spot heaters are closer to the workstation. Consequently, the workstation operative temperatures increase while the nonworkstation operative temperatures decrease as the heaters are moved closer to the floor.

The third case illustrates the energy savings that can be accomplished through selective and focused radiant heating. In this case, the radiant heaters remain in the same location as for the second case, but the power per heater is reduced from 2200 W to 1500 W. This power reduction results in a room air temperature of 6.3°C (43.3°F). The data in the table show, however, that the workstation operative temperature is within 1°C (1.8°F) of the workstation operative temperatures from the first case. The nonworkstation operative temperatures, as expected, approach the room air temperature.

The convective heating system required 6000 W to maintain the design air temperature at 9.5°C (49.1°F). As expected, the operative and mean radiant temperatures are substantially lower than those calculated for the three radiant heating systems. An interesting comparison is between the convective and 1500 W radiant heating systems. Although the radiant system results in a mean air temperature that is 3.2°C (5.8°F) lower than that produced by the convective heating system, the workstation operative temperatures are 5.0°C to 5.3°C (9.0°F to 9.5°F) greater than those produced by the convective heating system. To provide a better comparison, the 1500 W radiant heating system was reexamined with each heater at 1200 W, resulting in a total heat input of 6000 W. The workstation operative temperatures decreased to 9.9°C (49.8°F) and 10.0°C (50.0°F), respectively. The nonworkstation operative temperatures decreased to 5.2°C (41.4°F) and 5.0°C (41.0°F), whereas the room air temperature decreased to 5.0°C (41.0°F). Consequently, the radiant system, with task heating, can produce a more favorable thermal climate than the convective heating system with the same power input.

## 2.5 CONCLUSIONS

---

The BCAP methodology advances the sophistication of sizing and placing heating and cooling systems. The examples provided in this chapter show that a heating and/or cooling system can be optimized to provide thermal comfort to particular regions of an enclosed space (e.g., in the factory setting).

At this point, the reader should have an appreciation for the complexity necessary to design, specify, and place heating and cooling systems. Designing for a specific dry-bulb temperature is much easier than designing for human thermal comfort; however, the rewards of increased fuel economy can be enormous.

**S · E · C · T · I · O · N · 5**

**RADIANT HEATING  
SYSTEMS**



---

# CHAPTER 1

---

## INTRODUCTION TO RADIANT PANELS

---

### 1.1 RADIANT PANEL BASICS

---

A radiant heating panel, normally a flat surface, is defined as a surface from which at least 50 percent of energy transfer is accomplished through radiation. The balance of surface or panel face heat transfer occurs by convection. Radiant heating panels include concealed and visible panels that cover or encompass a large or small fraction of a wall, floor, or ceiling. Panel form ranges from discrete ceiling units to cove, recessed, or surface-mounted wall units, and embedded floor, ceiling, or wall hydronic tubing, or electric cables, wire, and mats.

Research results and physical governing laws prove that the radiative emission from a surface is independent of surface orientation. However, it is well documented that convection heat transfer is a strong function of surface orientation. For example, Nusselt number (Nu) correlation for a heated horizontal plate facing downward versus the same heated horizontal plate facing upward leads to substantially different convective heat transfer coefficients. As long as the surface temperature and other characteristics remain the same, the radiation heat transfer rate is unchanged. However, the varying heat transfer coefficient changes the percentage of the total energy that is represented by the radiant energy emitted from the surface.

For example, a heated plate facing downward with a surface temperature of 370 K exposed to an air temperature of 290 K results in a natural convection Nu of 98, leading to a convective heat flux from the surface of 110 W/m<sup>2</sup>. The same plate exposed to the same conditions—but facing upward—results in a natural convection Nu of 491, almost five times larger, equating to a fivefold increase in the convective heat transfer rate—552 W/m<sup>2</sup>.

For this plate at the given temperature, the radiative emission is 1063 W/m<sup>2</sup>. Consequently, changing the orientation of the heated plate from horizontally facing downward to horizontally facing upward changes the percentage of the radiative emission from about 90 percent to 48 percent for these example conditions.

Large-percentage variation significantly impacts heating system design. The orientation can be adjusted to achieve the desired level of occupant thermal comfort, which may be determined from a combination of convective and radiant heating. The level of occupant thermal comfort obtainable from surface conditions and orientations is explained in Sec. 8 of this Handbook, where the BCAP design methodology is demonstrated.

Thermal radiation is transmitted at the speed of light, travels in straight lines that can be reflected, and elevates the temperature of solid objects by absorption but does not perceptibly heat the air through which it travels. All bodies in the built environment exchange thermal radiation continuously. The rate at which heat transfers depends on the following four factors:

1. Emitting surface and receiver *temperature*
2. Radiating surface *emittance*
3. Receiver *reflectance, absorptance, and transmittance*
4. Emitting surface and receiver *view factor*—viewing angle of the occupant to the radiant source

All types of radiant panels can be successfully designed if the preceding factors are taken into consideration in the analysis. The impacts of the physics involved often determine which type of radiant panel or heater is more appropriate for a given application as well as the operational efficiency of the installation.

## 1.2 RADIANT PANEL CHARACTERISTICS

---

Radiant heating panels are used in residential, commercial, institutional, and industrial buildings. Each type of panel has found application in all types of buildings, although certain applications are more likely candidates for each type of radiant panel. For example, discrete-metal or framed-fiberglass modules are common for T-bar grid ceiling heating, whereas hydronic tubing and electric cables and mats are used for floor heating or warming panels. Gypsum panel ceilings with embedded or surface-affixed resistance wire were commonly used in residential, all-electric homes in the 1960s. Where low-intensity, high-temperature heating is required, gas-tube, electric quartz, or filament heaters are used.

Radiant heat is fuel-neutral. A radiant heater is not defined by the energy input; rather, it is defined by the predominant method of heat output. Most electric radiant heaters are available in 120, 208, and 240 V, and for some types 277 and 480 V is available. International use requires design for additional specific voltages including 100, 200, 220, and 347 if uniform wattage output is desired for standard sizes or models. Hydronic radiant panels may receive heated fluid from almost any source designed to heat water, including geothermal heat pumps, boilers, combination potable water heaters, and alternate energy sources.

Radiant panels provide unique opportunities for the provision of thermal comfort and conservation of energy. Occupants of radiantly heated buildings confirm comfort satisfaction. State-of-the-art design programs graphically verify comfort conditions through a thermal comfort signature. Based upon comparative comfort satisfaction, you would expect that radiant systems would be very common. In fact, radiant heating, although very popular, is far from challenging the dominant market share of traditional forced-air systems. There are many explanations, but it is very hard for both users and the radiant industry to fathom why everyone does not have one form or another of radiant heating.

Occasional failure of metal, rubber, and plastic concealed conduit has had little impact on hydronic radiant heating growth. Electric radiant heating growth was hampered by the rapid escalation of electricity costs following the oil embargo and concealed radiant ceiling failures due to a few publicized materials and installation

failures. However, failures are extremely rare when licensed contractors who specialize in radiant installations install materials with prominent testing organization marks and labels.

Air conditioning is now a standard feature in new homes throughout the United States. This has led some contractors to front-load air-conditioning costs, while lowering the heating cost, thus making it harder for someone selling only heating to compete. But perhaps the biggest hindrance to growth is the lack of comparative system information output availability from the design programs in common use. When convection and radiant systems are compared as though both are convection systems, the radiant advantages are not apparent. Design programs must incorporate the performance characteristics unique to radiant systems in order to provide robust comparative information.

The lesson to be learned is that designers need access to computer simulation programs that factor mean radiant temperature (MRT) into dynamic heat transfer analysis that is related to occupant thermal comfort. It is essential that codes and standards be monitored for inclusion of radiant, as well as other, heating systems. Finally, additional research is needed to more precisely define occupant health and productivity relationships to heating and cooling system thermal comfort performance. ASHRAE Standard 55-92, *Thermal Environmental Conditions for Human Occupancy*, provides a means by which this process could proceed were the Standard to become central to system design.

There are proven materials, components, and equipment listed or marked by leading nonprofit testing organizations for all radiant designs and applications. There is also a large pool of qualified installers, many who are members of the Radiant Panel Association (RPA) and are listed in the RPA Internet directory. The benefits of radiant heating and cooling merit the “learning curve” investment to develop the same specification confidence that is enjoyed with convection systems.

### **1.3 RADIANT PANEL SYSTEM EVALUATION**

---

There are many advantages unique to radiant panel systems. The authors have included those recognized in *ASHRAE Handbook Fundamentals*, research, and manufacturers’ literature. The importance of each feature will vary with the application and geographic location. However, a full understanding of the impact of radiant panel features on design comparison is essential to a robust comprehensive evaluation.

Radiant panel evaluation features include the following:

- Better comfort levels because radiant loads are satisfied directly and air motion is at normal ventilation levels.
- Energy savings due to reduced air infiltration and exfiltration, lower or nonexistent heat transmission losses compared with ducted systems, and lower heat loss due to dry-bulb air temperatures that are no higher than the level required for occupant thermal comfort.
- Low or minimal maintenance is required for radiant panels.
- Reduced air filtration as makeup air is required only for ventilation and not for deliveries of heat as forced-air systems require.
- One hundred percent usable floor space and simplified wall, floor, and structural systems because there is no space-conditioning equipment at the outside walls.

- Cleanliness due to elimination of mechanical equipment in the conditioned floor space satisfies certain legal requirements.
- Window treatment freedom as installation is not restricted by space-conditioning equipment.
- Simultaneous hydronic heating and cooling without central zoning or seasonal changeover when a four-pipe system is used.
- Common central air system can serve both interior and perimeter zones.
- Space partitioning and use flexibility with modular radiant panel systems.
- Reduced air quantities for 100 percent outside air systems mean smaller penalties in terms of refrigeration load.
- Draft-free environment due to a minimum supply of air quantities with radiant heating and cooling.
- Little or no noise compared with induction and fan-coil units.
- Peak load reduction due to mass thermal energy storage in the panel structure, exposed walls, partitions, and furnishings.
- Hybrid system problem solving when coupled with other conditioning systems for heat loss (gain) compensation for cold or hot floors, walls, windows, skylights, fireplaces, or other cold surfaces.

Radiant panel disadvantages include the following:

- Slow response is a characteristic of high-mass systems that can be ameliorated by careful selection and installation of heating elements and controls.
- Nonuniform surface temperatures due to improper element sizing, piping installation spacing, or insufficient heat capacity.
- Options may be restricted for building materials selection, floor coverings, furnishings location, and heater proximity.
- Renovation, redesign, and furnishings options and costs may be impacted.

Radiant heat panels provide natural, direct source-to-object heating that does not require a heat transfer medium. A radiant panel is noiseless, odorless, and generally maintenance-free. Panel design and planar location establish basic heat transfer characteristics that can be managed by thermostats, and fluid controls in the case of hydronic systems.

## **1.4 RADIANT SYSTEM COST ANALYSIS FACTORS**

---

Electricity, oil, gas, propane, wood, and alternative energy sources have all been used successfully as the source of energy for radiant heating. Deciding which energy source to choose requires rigorous analysis. Factors to be determined include not only the usual series of equipment and insulation iterations, but also the use, lifestyle, and building-as-system control implications on operating cost. Initial, life-cycle, and maintenance cost analysis add yet another dimension.

The simple first-order fuel cost per Btu analysis shows how the market currently prices the various energy options, using Btus as the common indicator. Incorporation of actual installation, use, and control factors leads to operating cost informa-

tion that reflects the actual system-specific Btu requirement under conditions of use. The real-world, or miles-per-gallon, information may be expressed in a form that can be used with Btu cost to determine which heating system using which fuel is the most cost-effective in terms of annual operating cost.

A simple comparative indicator of overall Btu lifestyle efficiency is expressed as *Btus per heating degree day per square foot of total heated space*. This index is an excellent indicator of just how efficiently a heating system is able to address occupant thermal comfort requirements in the routine use of occupied space and is expressed in terms of known parameters as:

$$\zeta = \frac{E \text{ (Btu)}}{\text{HDD (day} \cdot \text{ }^\circ\text{F)} \times A_{\text{total}} \text{ (ft}^2\text{)}} \quad (1.1)$$

The performance parameter  $\zeta$  is then given in units of Btu/ft<sup>2</sup> per heating degree-day in a heating system. Typical numbers range from 2.5 to greater than 10. The lowest number represents the lowest comparative conditioned space Btu usage. As an example, consider a home where  $\zeta$  is 4.0 for a 2000-ft<sup>2</sup> house in a region of the country where there are 7000°F-days. Employing this equation shows that the annual energy consumption to heat the home would be approximately 20,515 kWh, which, at a rate of \$0.06/kWh, would cost approximately \$1231 per heating season. The simple multiplication of  $\zeta$  by the cost per Btu of the various fuels provides the actual cost per degree-day per square foot of space as actually used for each system being analyzed. The operating analysis provides perspective for the life-cycle cost analysis and is worth looking at in detail.

Life-cycle analysis incorporates all original installed cost factors associated with each heating system selection in relation to the building in which the system is to be installed. To prevent surprises, review local code, building, or association regulations to determine that all requirements for specific systems and equipment have been included. Minimum energy standards adopted by most jurisdictions are those from ASHRAE Standards 90.1 and 90.2 for commercial and residential buildings, respectively.

Accurate maintenance, repair, and equipment life input is essential. An appropriate *cost of capital*, or *discount*, rate is applied in order to reduce each alternative to what is known as the *net present value* of the expenditure stream for each system. The Federal Energy Management Program (FEMP) website provides extensive discount rate information.

While there are life-cycle costing models in many texts, a universally accepted model for energy analysis may be found on the Internet at the U.S. Department of Energy website. The FEMP Building Life Cycle Cost (BLCC) program is designed for use by both for-profit and nonprofit organizations with adjustment of tax input. While the program is designed for the entire building, a similar approach can be developed for heating- or cooling-system-only analysis. However, a true appreciation of radiant system life-cycle cost performance stands out in a BLCC analysis.

Finally, although out of the scope of engineering analysis, it is important to obtain projections for long-term fuel cost and to incorporate an assessment of the impact of market and technology changes. The array of projections may seem intimidating. However, information developed by the U.S. Government Department of Commerce contains long-term trend analysis, which provides perspective to other information being reviewed. Analysis, which includes occupant comfort-based operating, life-cycle, and present and projected fuel costs, provides meaningful information for comparative radiant and convection heating system evaluation.

### 1.5 RADIANT APPLICATIONS ARE EXTENSIVE

---

Electric and hydronic radiant heating panels are appropriate for all buildings. They are commercially available in the configurations required to provide heating for all building types. The characteristic features of radiant heating panels are common to both hydronic and electric radiant heating systems. Key radiant panel features include lack of dust, noise, odor, maintenance, and impact on relative humidity.

Electric radiant systems exhibit the control flexibility characteristic of electricity, including very fast-acting systems. Temperature setback and thermal storage is also possible over a broad range of comfort requirements. Electric utility rate structures often are an important factor in economic analysis for electric radiant panel systems. The local Public Utility Commission has historically overseen electric rates, which differed by use and customer classification. In some areas, the rates in a given class were flat all year long. In other areas, the rates per kilowatt-hour were fixed, but different during different seasons and varied by time slots over a 24-h period.

With deregulation and the associated industry dynamics, real-time pricing is likely to become more common. In fact, in areas where electricity charges in relation to system-wide demand—*real-time pricing*—are in place, users have the option (indeed, incentive) to schedule electric consumption when rates are most attractive. With real-time pricing the rates may change frequently and fluctuate widely. Real-time pricing eliminates the rate stability and predictability that are characteristic of time-of-day or peak and off-peak time periods during which flat rates are either high or low.

Identification of the daily time periods with low and stable rates is an important factor in determining the thermal storage potential of a radiant system. Building mass retention of radiant heat or cool enables a level of thermal sailing that could be important under a condition of power interruption necessary to gain the full benefit of time-of-day rates or real-time pricing.

Electric radiant heating panels generally consist either of discrete manufactured panels, modules, or fixtures ready for electrical connection on-site, or of terminated-component heating elements consisting of cable, wire, or assembled mats. In some cases, terminations are field constructed. Electric radiant panels and component products are described in some detail in Chap. 2 of this section because these components are integral to the radiant panel. Hydronic mechanical systems, such as boilers, geothermal heat pumps, and combination heaters are not part of the radiant hydronic panel, but are discussed in Chap. 3 of this section in terms of characteristics that could influence radiant panel performance and control.

Hydronic systems involve a broad selection of radiant panel configurations. Traditional high-mass systems are most common. The growing interest in radiant hydronic heating has spurred the development of many new radiant panel approaches. Innovations include small-diameter capillary-style mats, interconnected routed aluminum-covered plywood flooring, routed plywood flooring, and under-floor-suspended or heat conduction plate-routed hydronic tubing. The proponents of each of the many system and design options provide information about important features of their system. The literature identifies features and benefits that manufacturers believe give their system a performance, installation, or cost advantage.

Warm-air radiant heating involves the routing of heat transfer ducting through the concrete floor or slab. Figure 1.1 shows a common approach using air for floor heating and cooling. The heated or cooled air may be in a closed system, or all or part of the air may pass through the space being conditioned to provide supplemental heating or ventilation on its way back to the furnace. Systems like this have been developed for many different types of building using either the floor or the ceiling, or both.

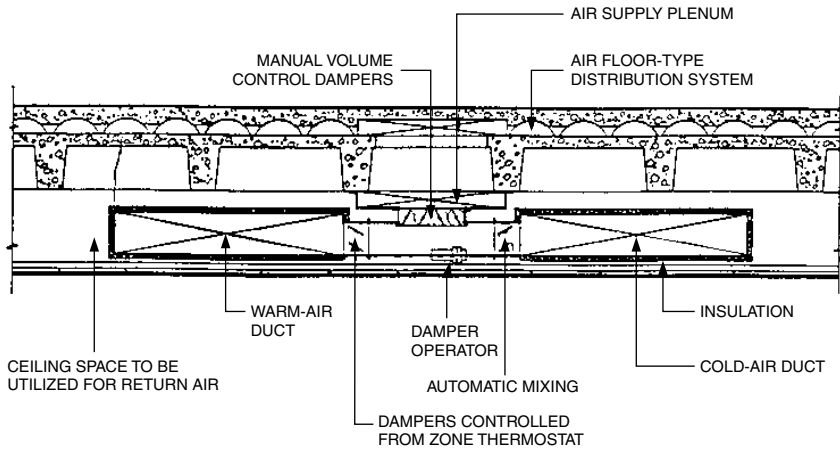


**FIGURE 1.1** Ducted radiant panel. Section showing air-conditioning distribution system.

Panel design methodology is governed by the same opportunities for output maximization as other radiant systems. However, the air dynamics of such a system where the air usually flows into the room and out through a return in a manner similar to a forced-air system are beyond the scope of this Handbook. Application of this approach to duct routing provides floor warming in buildings with concrete floors that might be uncomfortable with ceiling delivery of warm air convection heat.

Radiant heating has long been especially valued for its successful use in very specific situations in conjunction with conventional heating. For the most part, unless part of a carefully engineered project, the installation of radiant heating or cooling has usually occurred as a retrofit to solve a comfort, operational, or energy cost problem. In fact, hybrid or combination radiant heating or cooling offers not only comfort, but also economic operating benefits. The use of radiant systems in combination with other systems is covered in detail in Sec. 7 of this Handbook.

## 1.6 BASICS OF RADIANT DESIGN

Maximizing radiant output is the goal of radiant panel design. Minimizing backloss and edge loss is an important first step toward maximizing frontal heat output. Panel planar location and airflow past the panel determine the split between radiant and convection heat output. Evaluation of radiant panel efficiency is essential to determining panel sizing and estimating system energy use. The analysis of the surface heat balance applies the first law of thermodynamics to the surface of the radiant panel. Figure 1.2 shows the thermal resistance factors, represented by  $R$ , the series of resistors.

Although the ratio of heat delivered is an important design factor, it is essential to factor in the thermal boundaries imposed by occupant thermal comfort to develop a practical radiant system design. The chart in Fig. 1.3 shows the percentage

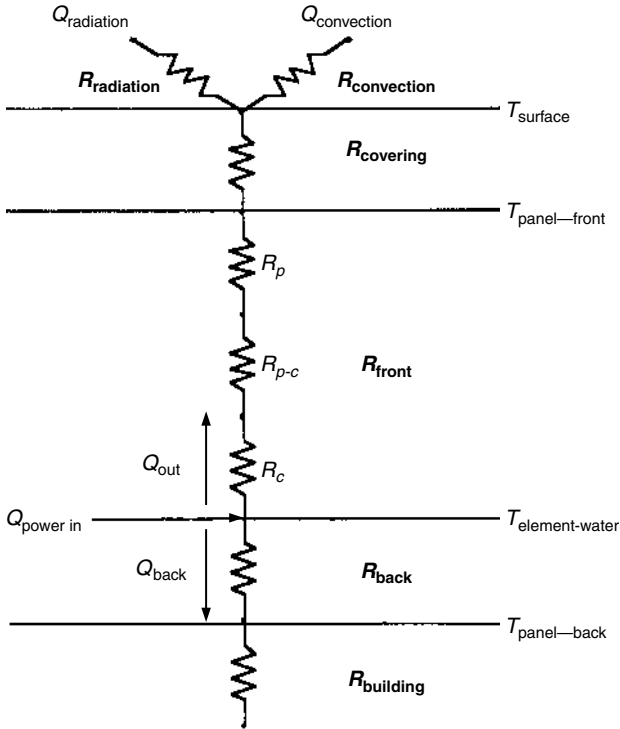


FIGURE 1.2 Thermal resistance network for a radiant panel system.

of dissatisfied people related only to discomfort due to cold or warm feet related to floor temperature. The participants were in a condition of thermal neutrality. The results were not gender-sensitive.

Another significant factor is the impact of air movement, whether natural or mechanical, in reducing the surface temperature of the radiant heat panel, thereby reducing the radiant output. In the built environment, air movement is primarily a function of the heating system design. Coordination of air distribution design is important for radiant panel sizing and design to assure desired performance, and conformance to indoor air change code requirements. Studies of the effect of air velocity over the whole body have found thermal acceptability unaffected in neutral environments by air speeds of 50 feet per minute (fpm) or less. Subjective responses indicate that there is no interaction between air speed and radiant temperature asymmetry. Changes in percent dissatisfied due to draft and radiant asymmetry are independent and additive. There was no significant difference between responses of men and women to draft.

The chart in Fig. 1.4 shows the relationship of occupant thermal comfort to draft in terms of the percentage of people dissatisfied (PPD) as a function of mean air velocity.

Radiant panel planar location is the primary determinant of the split between radiant and convection frontal heat output. In a laboratory study, zero-clearance framed insulated heat panels placed upon the ceiling have 95 percent radiant output.

## Thermal Comfort

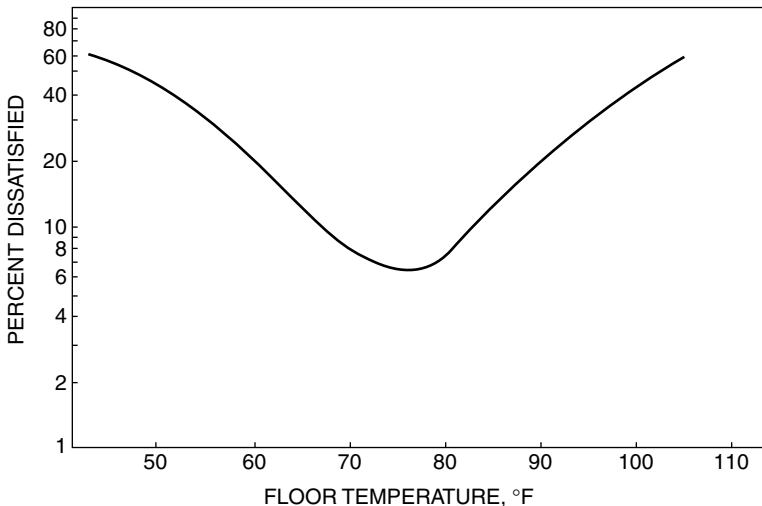


**FIGURE 1.3** Floor temperature comfort graph—percentage of people dissatisfied as a function of floor temperature.

The same panel placed on the wall will have from 60 to 70 percent radiant frontal outputs. Face-up floor placement further increases convection and reduces radiant output to between 50 and 60 percent or less. These differences are important sizing determinants. For example, an ASHRAE-sponsored University of Illinois research project found the wattage requirements for identical radiant output to be 250 W for ceiling location, 325 W for wall location, and 350 W for floor location. Radiant output is a key factor in reducing the energy required to provide conditions of equivalent human thermal comfort with a radiant system in comparison with a convection heating system.

### **1.7 RADIANT DESIGN PROGRAMS INCLUDE THERMAL COMFORT**

Early energy design and simulation programs did not incorporate mean radiant temperature (MRT) and human thermal comfort design factors into their governing algorithms. The result is the design assumption that average unheated surface temperatures (AUSTs) are equal to the air temperature. There are many architectural features, building materials, and operating conditions that result in circumstances in which this assumption is invalid. The programs were not able to model dynamic occupancy-oriented use of radiant systems.

Computer programs that incorporate these factors recognize the performance characteristics that are unique to radiant heating panels in terms of design load, human thermal comfort, and energy consumption. For design purposes, radiant panels were treated as though their heat transfer process was identical to that of con-

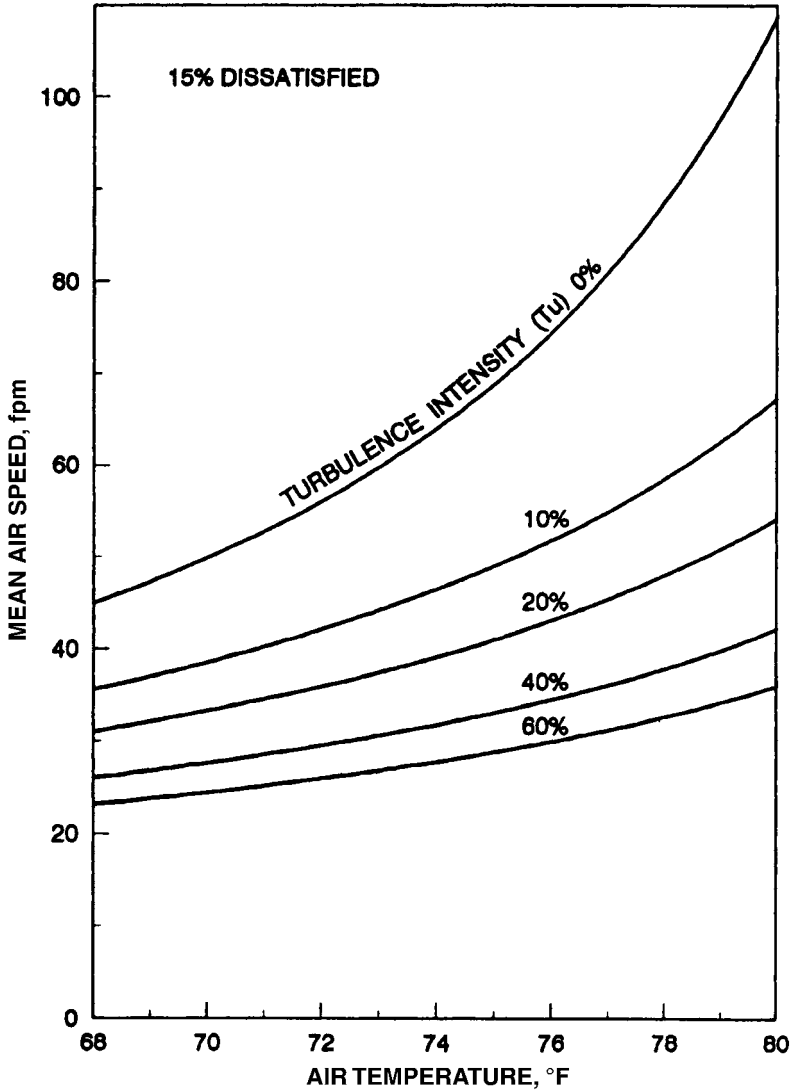


**FIGURE 1.4** Draft thermal comfort graph—draft conditions dissatisfying 15 percent of the population.

vection heating systems. A Btu was considered to be a Btu, regardless of its use, heat transfer mode, or actual quantity requirement for the particular design purpose and heating system. The heating Btu requirement using each system was accepted as being the same.

Efforts to increase the efficiency of heating treating processes and travel into outer space necessitated accurate calculation of all three forms of heat transfer. The expo-

nential increase in computer and programming capability make it practical to address the built environment with the same precision. Dynamic computer programs closely link lifestyle, building use, weather conditions, internal load contribution, indoor air quality requirements, and human thermal comfort in order to provide engineers with better information for heating system selection and design optimization.

## 1.8 FUEL SELECTION ANALYSIS

Fuel cost projection and analysis have become a more difficult input to the complex process of system selection than has historically been the case. Fuel costs have fluctuated widely, and significant long-term influences are emerging. The advance in seismic and extraction technology has identified and unlocked oil and gas reserves. Advances in gas steam turbine heat recovery, secondary combustion, and electric power generation technology have increased efficiency from 30 percent to more than 80 percent, using natural gas. (See Fig. 1.5.)

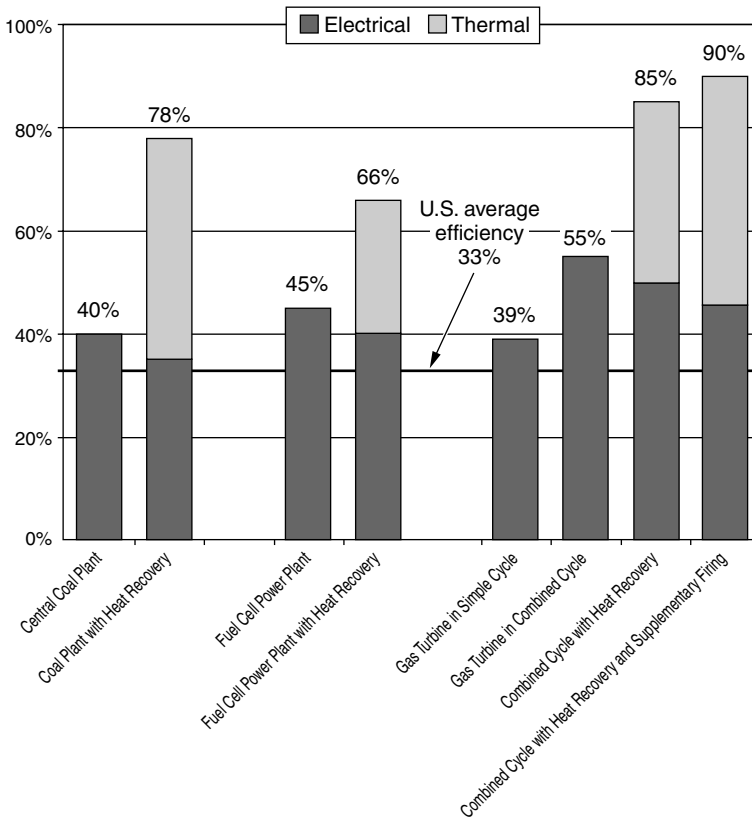


**FIGURE 1.5** Electric power generation efficiencies.

Computer, electronics, and programming technology advances combined with investment in related transmission infrastructure and industry mergers, have vastly increased the ability of electric utilities to route power to serve need. Vast energy trading operations present new energy supply and cost management options for both utilities and consumers. The economic practicality of less expensive, smaller generation facilities designed for intermittent and peak power generation is another important factor to be considered in electricity cost and availability analysis projections.

The dramatic advances in electric power generation efficiency are being incorporated into new and existing generation facilities. The strategies include combined-cycle gas generation, heat recovery, and secondary combustion for both gas and coal plants, where coal is first converted into gas. These techniques can dramatically increase the Btu conversion efficiency from the historic average of approximately 33 percent to a somewhere between 40 and 80 percent, depending upon the circumstances. Aside from the normal shareholder-driven quest for greater economic returns, public policy is driving utilities to reduce pollution while increasing capacity to facilitate economic expansion through the provision of adequate electric power at rates that increase with or below the rate of inflation. The impact of public policy, industry deregulation, and foreign energy pricing are the wild cards in energy pricing and availability projections.

Deregulation of the natural gas and electric utility industries not only opens markets to competition, but also unleashes a torrent of technology investment. Inter-industry corporate mergers create companies that provide a selection of energy choices. All of these developments tend to narrow fuel economic differences and to lessen the significance of fuel heating and cooling energy selection. A leveling of the fuel selection options enables review of the full range of comparative qualitative as well as quantitative system performance features.

Section 5 presents each of the radiant panel options because evaluation of all radiant heating system options is important to assuring selection of the system that best suits the overall objectives and optimizes system performance. The goal of this section is to familiarize the reader with the characteristics and features of each radiant panel system. Once the system selection is made, the reader will proceed to Sec. 8. Discussion will begin with electric radiant heating, because those systems are relatively simple when compared with gas-fired and hydronic systems, which involve combustion and fluid-flow control dynamics, respectively. The objective is mastery of basic radiant design principles. The following chapters empower the reader to develop input appropriate for inclusion of electric, gas, or hydronic radiant panel heating systems in the selection process. The reader will be equipped to perform a complete evaluation of system and equipment alternatives.

---

# CHAPTER 2

---

## ELECTRIC RADIANT HEATING PANELS

---

### 2.1 ELECTRIC RADIANT PANEL OVERVIEW

---

*Electric radiant heating panel* is defined as a flat surface from which at least 50 percent of energy transfer is accomplished through radiation from the electrically powered panel. The source of the energy that produces heat radiation from the panel surface is the product of electric geothermal, or resistance heat, processes. Electric geothermal heat pumps extend the option of electric radiant heating and cooling to hydronic design.

Electric radiant heating panels include concealed and visible panels that cover or encompass a large or small fraction of a wall, floor, or ceiling. Panel form includes discrete surface-mounted, recessed, or suspended ceiling units; recessed or surface-mounted wall units; embedded floor, ceiling, or wall cables, wire, and mats; and hydronic tubing circulating an electrically heated or earth- or evaporative-cooled fluid.

Electric radiant heating panels are used in residential, commercial, institutional, and industrial buildings. Most electric radiant heaters in the United States are available in 120, 208, and 240 V. Some types are available in commercial voltages of 277 and 480 V. To maintain rated wattage output, electric heaters must be operated at nameplate voltage. Foreign voltages, which are often different, would require products designed to operate at the specific voltage specified.

Electric radiant heating panels and/or their components are subjected to a series of specific safety tests, procedures, and inspections by recognized testing agencies, and sometimes are required under national, local, or foreign electrical codes. Components and connection wire may have stamped or printed certification or listing marks. Discrete or modular panels have listing or certification nameplate or labels showing wattage output at rated nameplate voltage.

International use requires voltage design for 100-, 200-, 220-, and 347-V applications. However, voltage fluctuation can be very wide in some countries. Transformer devices are used to stabilize voltage to improve performance consistency and prevent equipment damage. Evaluation of power reliability, consistency, and quality are important to the development of equipment and control design and selection.

Unlike nameplate wattage ratings on office equipment and some appliances, the actual wattage output normally is within a range of between +5 percent and -10 percent of nameplate rating in conformance to the listing or certification. (See Fig. 2.1.) Field wattage verification is made through the application of Ohm's law by using an ohmmeter to obtain the panel electrical circuit resistance rating.

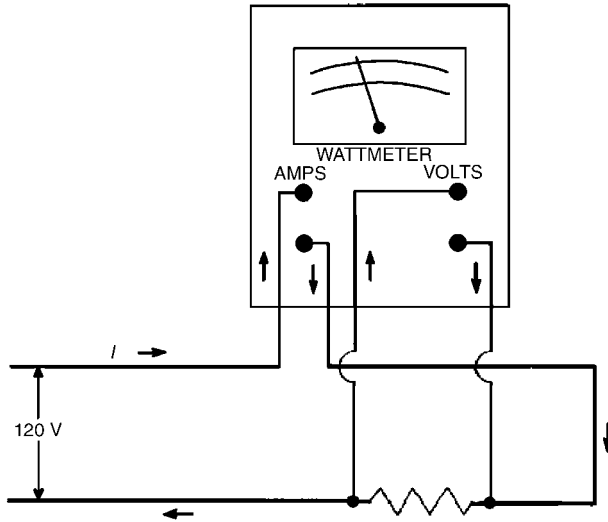


FIGURE 2.1 Basic wattmeter connections.

An understanding of basic electrical principles is essential to converting the radiant system design load to an electric radiant panel installation circuit and control layout. Once the designer has determined the Btu requirements, the conversion to wattage will enable determination of amperage required, which will determine circuit design. There are control options to serve whatever electrical circuit is designed. In general, single 20-A circuits are often served by in-line controls, and larger loads and complexes are often served with low-voltage or energy management system (EMS) controls.

## 2.2 ELECTRICAL PRINCIPLES

The physical laws of electricity and related calculations will assist the designer in relating the equipment alternatives to the available energy resources, circuits required, and performance validation. *Electricity* is the movement of electrons, the negatively charged particles of atoms, through a conductor (e.g., wire) and known as *current*. Materials that impede electron or current flow are known as *insulators*, or *dielectric materials* (e.g., plastic, glass, and wood). A conductor or series of conductors is known as a *circuit*.

A circuit consists of a voltage source that utilizes a conductor to allow the flow of current to the load. The current flow is measured in amperes, or amps. The capacity of a conductor to carry current is called its *ampacity*. The force that causes electrons to move through the conductors is called the *electromotive force*, or EMF, of the circuit. This is also known as the *potential difference*, or the imbalance in a circuit that causes current flow. This is shown in a wiring diagram by labeling one side of the power source as *positive* and the other side as *negative*. Current flows from the negative to the positive and is generally referred to as *amps* and *volts*.

Thinking about electricity as water flowing through a pex tube is a good way to understand the difference between amperage and voltage. Water in the tube is like current in the circuit, measured not in gallons per minute, but in amperage. Both can be measured in volume and do work. However, the water must move due to water pressure from a pump or gravity to do work, normally transfer heat from the boiler to the radiant panel. With electricity you need both volts and amps to run the heater. The pex tubing used in radiant hydronic systems is like the conductor in the electric circuit.

### 2.2.1 Resistance to Current Flow

*Resistance*, caused by friction to the movement of electrons, is measured in ohms. The product of resistance is heat, which is to be minimized in conductors, and controlled in heaters. ASHRAE defines *electric resistance* as:

The property of an electric circuit or of any object used as part of an electric circuit that determines for a given circuit the rate at which electric energy is converted into heat or radiant energy, and that has a value such that the product of the resistance and the square of the current gives the rate of conversion of energy.

It is important to note that the definition differentiates heat and radiant energy. We will find that line resistance and internal component heat can be important factors to review in control selection later in Sec. 6.

The flow resistance heat from excessive current flow is the means used to activate circuit breakers and fuses when a *short*, or the touching of two conductors, occurs. A wire shorting to its conduit or making contact with the enclosure, is a *ground fault*. A *ground fault interrupter* is required for damp interior and exterior areas (e.g., bathrooms, near sinks, and pool areas) for all electrical devices that might be touched (grounded) by a human. Unlike the typical fuse or circuit breaker that is designed to withstand short-term power surges and doesn't open until its rated limit is exceeded, a ground fault interrupter responds in about one-eighth of a second upon detection of very small current flow, thereby preventing dangerous, hazardous electrical shocks.

### 2.2.2 Common Voltages

Electric radiant heat encompasses a broad range of products, each of which utilizes the range of voltages appropriate to the product category. As a result, electric radiant heaters may be found for each of the common voltages. Residential and light commercial products are normally available in both 120- and 240-V models. In some cases dual-voltage models are available. Commercial usage often requires 208- or 277-V models, whereas industrial applications sometimes require 480 V. Voltage is often country-specific. For example, most of Western Europe is 220 V, Japan is 100 or 200 V, and China is 220 V.

Voltage drops due to line resistance is the reduction in voltage that can occur between the power source and the load. For most applications, this is not a factor, but where long feeds are required, the drop must be calculated to determine the impact on the rated output of the equipment shown. The wire material, diameter, and length determine resistance. The product of the resistance and the current is the *voltage drop*. For electric heat, if the drop is more than 1 percent, the equipment sizing should be carefully reviewed because, as we will see, the wattage output drop is much larger.

Voltage drop due to inability of the energy source to provide power at the normal levels results in a much larger corresponding drop in resistance heat output. This will become very apparent as we discuss power, the rate of moving or changing energy. We measure electric power in watts (W).

The following chart provides the unit of measure and abbreviations used for the common descriptors used in discussing basic electrical principles:

<i>Name</i>	<i>Unit of Measure</i>	<i>Abbreviation</i>
Current ( <i>I</i> )	Ampere, amp	A, a
Potential difference ( <i>E</i> )	Voltage, volt	V, v
Electromotive force		EMF
Resistance ( <i>R</i> )	Ohm	$\Omega$
Power ( <i>P</i> )	Wattage, watt	W, w
1000	Kilo-	k
1/1000	Milli-	m

### 2.2.3 Watt's Law and Ohm's Law

Watt's law relates voltage and amperage to power.

$$\text{Power} = \text{voltage} \times \text{amperage}$$

$$\text{Watts} = \text{volts} \times \text{amps}$$

$$W = V \times A$$

Ohm's law, the most fundamental law of electricity, relates voltage, amperage, and resistance, stating that current is equal to voltage divided by resistance:

$$\text{Current} = \text{voltage} \div \text{resistance}$$

or

$$\text{Amperes } (I) = \text{volts} \div \text{ohms}$$

or

$$I = E \div R$$

The resistance of a circuit can be found by substituting and cross-multiplying. Resistance readings may be taken when an electric heat circuit is without power. So-called cold resistance is an important reading used to verify that the heat output will match the rated output at nameplate voltage. Resistance readings should be taken at each step in the installation process, much as a doctor continually monitors blood pressure.

Because Watt's law states that power is equal to current times voltage and Ohm's law states that current is equal to voltage divided by resistance, we can substitute the elements and state Watt's law in terms of current and resistance:

$$W = I^2 \times R \quad (2.1)$$

The power law may be stated in terms of voltage and resistance:

$$W = E^2 \div R \quad (2.2)$$

With algebraic manipulation the equation confirms what the resistance should be at a given voltage and wattage:

$$R = E^2 \div W \quad (2.3)$$

Solving the equation where the voltage is 120 V and the rated wattage is 1000 W, yields a resistance of 14.4  $\Omega$ . Normally, the actual cold resistance reading of the heat circuit will be very close to the calculated number. If the variance is significant, there is a problem, which requires investigation to determine whether the product is defective, the reading was incorrect, or the wrong voltage was assumed. Some electric heat products can operate under dual voltages, which requires that they be wired as required for the specific voltage available. Electric heaters may be composed of multiple elements. The failure of any one circuit will change the wattage output and resistance. Checking resistance with an ohmmeter is one of the most fundamental parts of electric heat installation and performance validation.

Electric circuits may be designed for series or parallel connection of the loads. A line connection is where the loads are connected like links in a chain (Fig. 2.2). If one breaks, the circuit is down, and current flow is halted. To avoid failure of the whole circuit due to failure of one component, loads are normally connected in parallel, or across the line. The failure of one load will not affect the other loads in the circuit. It is always preferable to connect heater loads in parallel so that only the inoperable heater is out of service and may be removed from the circuit (Fig. 2.3).

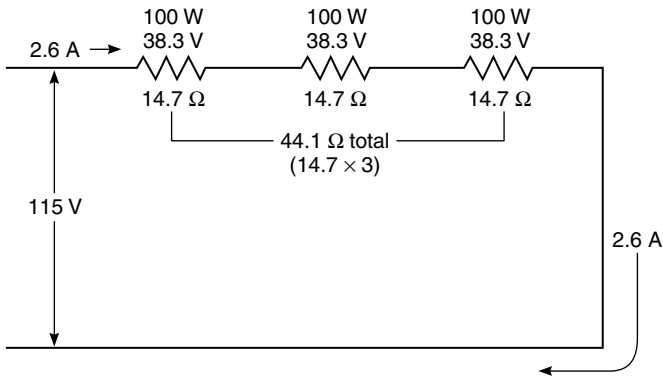


**FIGURE 2.2** Schematic of three heaters in series.

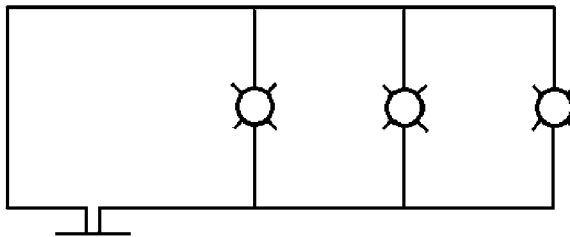


**FIGURE 2.3** Schematic of parallel circuit.

Three types of loads are encountered in radiant heating. Two are common to hydronic heating, whereas resistive loads are common to electric heating. Resistive loads will always have an *in-phase*, or balanced, circuit, and therefore may be operated on either alternating (ac) or direct (dc) current. In-phase power is considered real, or positive, power, and results in a value on the wattmeter that is equal to the volts times the amps. The test reading shows the power available in the circuit.

Inductance and capacitance are found in motor loads and result from EMFs. Fans and pumps are examples of such loads. Inductance and capacitance differ from resistive loads in that they can put the circuit *out of phase*, which means the current and the voltage travel at different rates. The significance of this is that where thermostats or controls are used to control both resistance heat loads as well as inductive fan loads, the designer must verify that the control is designed to handle both types of loads.

The reader is encouraged to coordinate the electrical demands of any heating system with the electrical engineer, to consult the manufacturers' detailed installation instructions, and to assure that all designs are in conformance with the National Electrical Code (NEC) and local building and electrical codes. Electric radiant heating products can be installed in conformance with all electrical codes if they carry the required Underwriters Laboratory (UL), Electronic Testing Laboratory (ETL), or other recognized product safety listing.

### 2.2.4 Electromagnetic Fields

Electromagnetic fields (EMFs) have been the subject of much discussion and considerable research. Most concern has focused upon the impact of long-term residency in proximity to electric power high-voltage transmission lines. Considerable research has been funded by the electric utility industry and conducted through the Electric Power Research Institute in the United States, and by universities and concerned science and health organizations worldwide. To date the research has been unable to establish a causative link between EMF and health effects.

Electric and magnetic fields occur throughout nature and in all living things. Positive electric charges and negative charges occur in all things electrical (Fig. 2.4). A handheld or laboratory gauss meter is used to measure the magnetic field in milligauss (mG), which is one-thousandth of a gauss. Readings have been established for all major electrical appliances, including electric heating equipment. The fourth power characteristic of electromagnetic waves tells us that intensity rapidly diminishes from the designated base distance reading.

Of common electric appliances using a heating element, perhaps the most frequently used is the hair dryer, which is normally arm's length at most from the head. A 1500-W hair dryer employs resistance coils compacted in a circular area approximately  $1\frac{1}{2}$  in in diameter. The milligauss reading, including the fan motor, measured from a comprehensive representation of products, ranged from a low of 1 at 6 in to a high of 700. Along with electric razors, this represented the high end of appliance milligauss readings in daily use within 2 ft of the body (Fig. 2.5).

Radiant panel readings for 1600 W requiring an area of  $48 \times 96$  in that is permanently ceiling mounted has a milligauss reading of 1.6 at 2 ft, and 0.2 or less at 4 ft, which is normal sedentary head height. Portable floor heaters tested had a range at 6 in of 5 to 150 mG, which dropped to a range of negligible to 8 mG at 2 ft. Radiant electric floor heating elements producing 1500 W might encompass anywhere from 100 to 500 ft<sup>2</sup>. In all likelihood, the electric field would be blocked by the panel mass, and the magnetic field may be self-canceling depending upon the element design and control. Although the examples provided are representative, each product and

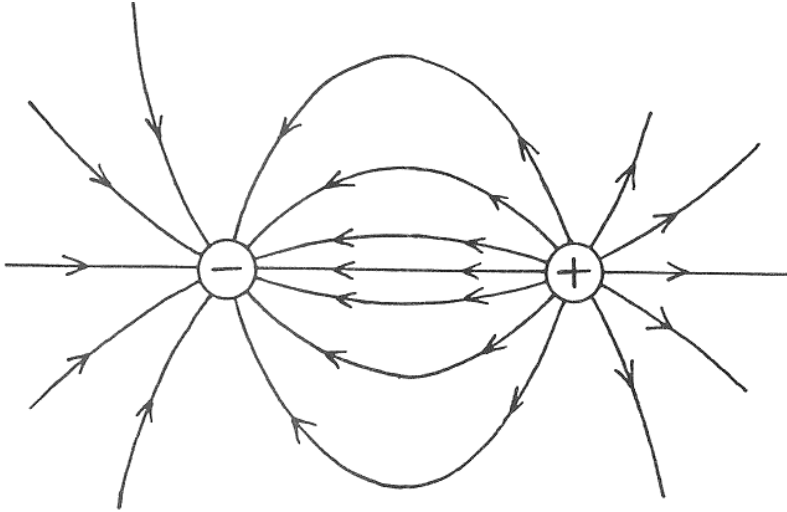


**FIGURE 2.4** Electric field lines begin and end on charges.

installation should be reviewed with the manufacturer in order to determine relevant EMF specification information.

Within the built environment, the general guideline is “prudent avoidance” of long-term exposure to magnetic fields with readings above 4 mG, although no known harmful relationship has been established. Formal health and safety standards do not exist because there is no agreement on whether setting standards would do more harm than good.

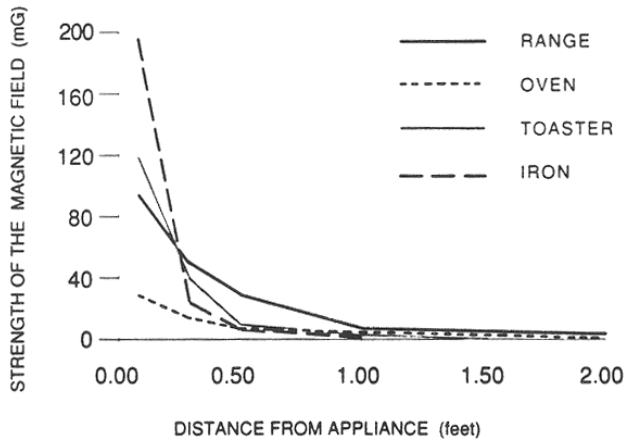


**FIGURE 2.5** Median magnetic field strengths of four typical electric appliances.

Section 2118 of the Energy Policy Act designates lead responsibilities to the National Institute for Environmental Health Sciences and the U.S. Department of Energy to oversee EMF health effects research and engineering research, respectively. The reader looking for current information is advised to contact these organizations, the Electric Power Research Institute, and the relevant state health services department.

### **2.3 RADIANT PANEL FEATURES AND APPLICATION**

---

Each form of electric radiant panel has found application in a wide variety of buildings. Some applications are more common for each form of electric radiant panel. For example, discrete-metal or framed-fiberglass modules are common for T-bar grid ceiling heating, whereas heating cables, mats, and tubing are used as floor heaters and floor warmers. Gypsum panels with embedded or surface-affixed resistance wire were introduced in residential, all-electric homes in the 1940s. Where concentrated heat output is needed, high-temperature heating elements are required. Glass, quartz, ceramic, carbon-rod, and filament heaters are used.

Electric radiant heating panels utilize a power source readily available in all buildings. They are commercially available in the configurations required to provide heating for all building types and a broad range of special heating needs. Features characteristic of all radiant heating systems are present in electrically powered radiant heating systems. The distinguishing feature of all radiant systems is the dominance of radiant energy in providing human thermal comfort. The capacity, sizing, and energy consumption implications are system design- and equipment selection-dependent. Yet, comfort is attainable under conditions of lower ambient air temperature than normally required with convection heating systems.

Key features of radiant electric heating systems include lack of dust, noise, odor, maintenance, and impact on relative humidity. The elimination of convection heat air distribution of airborne particles, pollen, and bacteria is a compelling characteristic of radiant heat transfer to the chemically sensitive and allergic members of the population.

The design characteristics, components, and nonmechanical nature of electric radiant heat panels eliminate the possibility of noise and odor, while virtually eliminating maintenance. Relative humidity is virtually unaffected by radiant heat panels due to the benign impact on building infiltration and exfiltration.

Electric resistance radiant systems exhibit the control flexibility characteristic of electricity, including virtual occupancy control of very fast-acting systems. Line-voltage mechanical or electronic air or operative sensing thermostats frequently control the dry electric radiant systems. Low-voltage centrally or locally programmed controls are also used. Programmable thermostats of each type are also appropriate for radiant panel control. Various designs are employed to monitor floor temperature, including bulb and capillary thermostats. The control of hydronic and electric radiant systems is more complex than simple convection systems. The reader is referred to Sec. 6 for comprehensive information.

An important characteristic of discrete electric panels distinguishing them from central heating system hydronic panels is their complete performance and control independence from the other heated areas. The entire designed capacity of the electric radiant panel may be controlled by a single thermostat or linked with other panels. Central hydronic systems may be designed and controlled discretely, but there is usually an efficiency penalty that diminishes the energy benefits of zoning.

The same efficiency penalties from fractional output due to zoning apply to forced-air systems. However, the penalties are usually greater than simulation programs project. At least two factors are often overlooked in the program and assumptions. The first is interior duct leaks, which result in diversion of heat away from the zoned space, but are not incorporated as duct loss or wasted heat. The second is the impact on system balance during zonal operation. The cost of equipment to balance on demand makes its inclusion in convection systems rare. In addition, doors are often closed as a means of zoning, which may actually increase energy usage. Finally, even if zoning were economic and technically practicable, the impact on building pressure balance and air infiltration could create building condensation problems.

In-space electric radiant panels have distinguishing zonal advantages over zoned baseboard or wall convection heaters as well as over central systems. The normal process of heating air to transfer heat creates an air temperature gradient that significantly increases the airflow from the heated zone, unless the space is enclosed. In-space radiant panels raise the mean radiant temperature (MRT), while the dry-bulb air temperature gradually increases, without creating large air gradients that result in significant airflow. Radiant panel heat within the heated area is transferred out by means of conventional heat loss and natural convection from the radiantly heated surfaces. Although it is impractical with convection systems, zoning is practical for open floor plans with electric panel systems.

Electric radiant thermal mass heat storage options encompass a broad range of comfort and energy use options. The objective may be to accommodate electric utility rate structures or simply to manage building mass temperatures in the overall comfort design. Electric cables and mats, including hydronic thermal storage tubing, are buried under or placed in the thermal mass, in order to charge the earth or mass with heat during periods when electricity rates are lower. Hydronic systems may use a variety of mechanical, evaporative, or conductive methods to cool a fluid for radiant cooling, thereby eliminating or reducing the mechanical cooling load.

There are opportunities for mass heat storage with alternative energy systems in combination with radiant electric systems. For example, passive solar heating strategies often require maintenance of mass temperatures during certain seasons or time periods in order to even out the natural solar cycle. Successful application of radiant thermal storage requires a comprehensive, overall system design including an occupancy-responsive temperature and/or comfort control program. See Sec. 7 in this Handbook for comprehensive information on combination system design and task heating.

Although most energy design and simulation programs have not incorporated MRT or human thermal comfort factors, nor have they been dynamic programs, those programs that do incorporate thermal comfort parameters have not refined the calculation to a high level. When computer programs incorporate these factors, they will capture performance characteristics that are unique to electric radiant heating panels. These characteristics include reduced electrical load, human thermal comfort at lowered ambient air temperatures, and reduced energy consumption.

Neither common nor individual radiant system characteristics are recognized when all-electric, resistance heating systems are treated the same and are identical in the model. The advent of computer programs that more closely link occupant lifestyle and building use, weather conditions, internal load contribution, indoor air quality requirements, and human thermal comfort provides engineers with better information for system selection, which would be much more likely to be radiant.

Characteristics of radiant panels are shown in Table 2.1. Of note, studies at the University of Illinois and Kansas State University have demonstrated that electric ceiling panel radiant output may exceed 0.9 to 0.95 under common conditions in the built environment (see Chap. 5 in this section of the Handbook for ASHRAE RP

**TABLE 2.1** Characteristics of a Typical Electric Panel Heater

Resistor material	Graphite or nichrome wire
Relative heat intensity	Low, 50–125 W/ft <sup>2</sup>
Resistor temperature	180–350°F
Envelope temperature (in use)	160–300°F
Radiation-generating ratio*	0.7–0.8
Response time (heat-up)	240–600 s
Luminosity (visible light)	None
Thermal shock resistance	Excellent
Vibration resistance	Excellent
Impact resistance	Excellent
Resistance to drafts or wind <sup>†</sup>	Poor
Mounting position	Any
Envelope material	Steel alloy or aluminum
Color blindness	Very good
Flexibility	Good—wide range of power density, length, and voltage practical
Life expectancy	Over 10,000 h

\* Ratio of radiant output to power input (elements only).

<sup>†</sup> May be shielded from wind effects by louvers, deep-drawn fixtures, or both.

876, and also RP 657). There is a discussion relative to the design and thermal comfort impacts of draft in both Secs. 3 and 8 of this Handbook.

Evaluation of all radiant heating options is important to ensure selection of the system that best suits the overall design and performance objectives. This chapter empowers the reader to assemble the appropriate panel information for analysis of electric radiant heat in comparison with any heating system. The reader is equipped to perform comprehensive system evaluation and equipment selection.

## **2.4 FRAMED FAST-ACTING RADIANT CEILING PANELS**

Factory-made radiant heaters include visible wall or cove units that are not generally preinsulated. Visible radiant ceiling panels are usually constructed with internal insulation. Framed preinsulated electric radiant heating modules are constructed with the surface-heating element affixed directly to an insulation substrate without an interceding air space, metal encapsulation, or protective surface grill. An insulated surface element is characterized by higher radiant output than integral concealed heating elements, but lower watt density than metal-encapsulated or grill-protected elements. Framing secures the fiberglass perimeter and provides the structure for mounting (Fig. 2.6).

### **2.4.1 Impact of Preinsulation**

The use of insulation as a substrate for a visible radiant panel increases the maximum permissible watt density compared with concealed or uninsulated zero-clearance systems. Concealed systems are limited in watt density by the characteristics of the

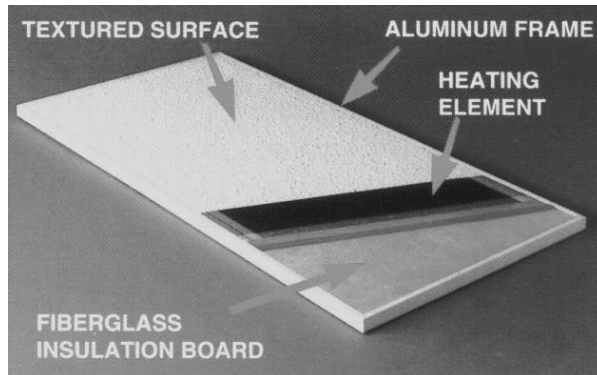


**FIGURE 2.6** Framed panel with insulation-backed heating element.  
(Photo courtesy of SSHC, Inc.)

materials with which they are, or may potentially be, in contact. For a visible ceiling panel, thermal bridging (i.e., the transfer of heat across beams, joists, and other contiguous surfaces) is eliminated. The insulation substrate reduces transmission of heat through the backside of the heater, thereby permitting zero-clearance mounting to commonly encountered building surfaces. These are distinguishing features of preinsulated visible radiant ceiling panels.

Insulated surface element panels also feature a very fast warm-up cycle, generally reaching full output temperature in approximately 5 minutes. The resulting surface temperature is a function of heat capacity, surrounding air temperature, and proximity and magnitude of heat loss. The normal operating surface temperature range is between 150°F and 210°F, yet is safe to touch due to the lightly textured surface. The significance of fast warm-up is quick comfort restoration through MRT elevation without increasing output sizing.

The feature of occupancy setback recovery without increased sizing results in significant comparative capacity reduction for radiant panel systems. The ASHRAE Handbook recommended a sizing increase of 40 percent for conventional forced-air systems for both day and night setback. However, actual convective equipment size is often defaulted by the available equipment capacity selection. In addition, contractors often oversize equipment with the idea that more is better, and that oversizing is likely to reduce callbacks. Finally, owner bias is toward having a safety factor for additions, space conversions, and as insurance against being cold. Radiant panel location and sizing is precise and important in order to assure that comfort requirements are met under dynamic operating conditions. See Sec. 8 of this Handbook for sizing information.

The significance of and the potential for backloss vary with the application. The absence of additional backside insulation normally impacts energy cost and comfort performance, necessitating incorporation of appropriate design factor compensation. In many T-bar grid ceiling applications, additional insulation is absent, yet heat loss to the space above may be sizable and of little benefit. At the other extreme, installation direct to a superinsulated *R*-70 ceiling reduces backloss to the point where it is almost nonexistent. Determination of the amount and impact of backside heat loss is an important design factor for sizing and/or equipment specification.

Maximizing radiant output is the goal of radiant panel design. Minimizing backloss is an important first step toward maximizing frontal radiant output. Another sig-

nificant factor is the impact of air movement, whether natural or mechanical, in reducing the surface temperature of the radiant heat panel, thereby reducing the radiant output. In the built environment, air movement is usually primarily a function of the heating system design. This is especially significant design input for radiant panel sizing and performance analysis (Fig. 2.7).



**FIGURE 2.7** Surface-mounted panels used for primary heating.

Radiant panel planar placement is the primary determinant of the split between radiant and convection frontal heat output. Preinsulated heat panels placed upon the ceiling have 95 percent radiant output. The same panel placed on the wall will have from 60 to 70 percent radiant frontal outputs. Face-up floor placement further increases convection, while reducing radiant output to between 50 and 60 percent. These differences are important sizing determinants. Radiant output is a key factor

in reducing the energy that is required to provide conditions of equivalent human thermal comfort with a radiant system.

### 2.4.2 Comfort Recovery

Quick attainment of full operating temperature is a performance and energy characteristic unique to a preinsulated module. Radiant panel surface temperature is dependent upon the surrounding thermal conditions. For example, exact ceiling placement of a heater with a fixed-wattage output is determined in relation to the heat loss of the cold window so that the desired radiant surface temperature may be attained. With proper preinsulated panel sizing and layout, there will be 95 percent radiant output in ceiling installations. Heat loss through convection and conduction under normal built environment conditions is minimized. Under these conditions, preinsulated heater maximum output is attained in about 5 minutes.

The significance of quick comfort recovery is important in considering control protocols. Comfort recovery for a radiant panel is defined by restoration of the radiant field, or MRT. This is very quick for a low-mass, preinsulated panel, and slows proportionately as panel mass increases. For convection systems, the time constant to restore comfort is determined by the length of time that is required to raise the dry-bulb air temperature to a level that is sufficient to offset the below-comfort-level average unheated surface temperature (AUST). This process is also dependent upon the impact of temperature gradients on the escape of heated air from the controlled space being heated. The energy impacts of radiant heating system and equipment selection performance are ultimately defined by the ability of the control to enhance panel performance and minimize required energy.

Thermal comfort studies by the John Pierce Foundation Laboratories (Berglund et al.) confirm that occupants will accept exposure to cool conditions on entry, at 59°F, if thermal comfort can be restored within 15 minutes. The study concluded, "Fast-acting radiant systems are now another tool to be investigated and applied by environmental designers for comfort and energy economy." Fast-acting radiant panels are one of the few design options with a proven capability to quickly restore occupant comfort following a period of temperature setback. Energy reduction is especially significant because sizing may be unaffected by the design of setback protocol, unlike convection systems, which are normally significantly oversized to accommodate day and night setback options.

### 2.4.3 Task Heating, Zoning, and Temperature Setback

Determination of setback sizing implications and requirements are critical to HVAC conventional system design analysis. Equipment oversizing of 20 to 60 percent is commonly recommended for convection systems operated with night setback, or both day and night setback, respectively. Fast-acting, preinsulated radiant heat panel systems do not require additional capacity or equipment for effective occupant-oriented setback. Recovery is not system, convection, or mass restrained. Recovery is defined by radiant field restoration as defined for thermal comfort. Dynamic setback capability is a standard feature of fast-acting radiant heat panel installations. As their sizing accommodates normal setback, these strategies can always be pursued, regardless of original installation and operational practice design.

Zoning or individual room or area control is a comfort and energy conservation feature of fast-acting radiant panels. Direct source-to-object radiant heat transfer

enables restoration of comfort in open rooms and open areas. Migration of warmed air, through natural convection or mechanical distribution, complicates convection system zoning. Issues include enclosure of space to be zoned, air distribution pressure balance, heat generation output reduction, duct zoning capability, and control requirements. Achievement of savings through zoning with convection systems requires careful system design and increased initial cost. Standard design practice for fast-acting, preinsulated radiant panels incorporates individual room or area control. The base cost is unaffected (Fig. 2.8).

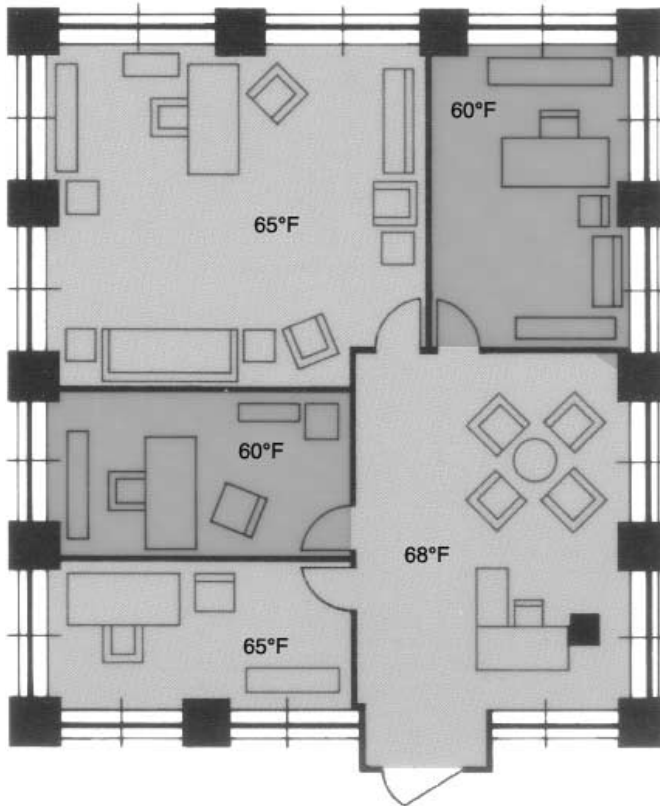


**FIGURE 2.8** Temperature setback zone plan.

The radiant fast-acting feature makes radiant heat panels suitable for task heating, a form of hybrid system with energy benefits comparable with those achieved with task lighting. Installation directly over occupied areas provides localized comfort in the presence of lower air temperatures in surrounding areas. The magnitude of difference between surrounding air and the required local heated area operative temperature depends on the task being performed. The idea of heating people, not space, though impractical for convection systems, is a practical and standard feature of many radiant heaters, especially fast-acting panels (Fig. 2.9).



**FIGURE 2.9** Example of task heating during weekend setback.

#### 2.4.4 Heating Applications and Sizing

Hybrid, or combination radiant and convection, systems are the subject of Sec. 7 of this Handbook. Commercial variable air volume (VAV) systems utilize perimeter radiant heat panels in place of in-duct convection electric resistance heating coils. Perimeter radiant panels are used in combination with heat pumps without central resistance backup coil heaters in order to reduce the potential usage peak in areas with demand-based electric rates. The same potential for installed capacity reduction is possible with all heat pump installations that have resistance backup (Fig. 2.10).

Sizing capacity is significantly lower for framed fast-acting radiant heat panels than for conventional convective systems and other radiative systems. Delivery of almost all heat output in the form

of comfort-producing radiant energy within the occupied space is one characteristic among many that are explained in Secs. 4 and 8 of this Handbook.



**FIGURE 2.10** Lay-in for T-bar grid ceilings using panel size required (4 × 4 ft).

For purposes of preliminary planning, radiant ceiling panels can be likened to lighting due to their diffuse radiant output. The flat panel configuration of heat delivery usually requires from 10 to 15 percent of ceiling coverage for common watt densities in residential building rooms or commercial building perimeter rooms. Although the panels are generally positioned in relation to heat loss requirements in each room, an exterior wall perimeter offset of 1.5 ft is normally recommended. Where the design falls in the 10 to 15 percent range of ceiling coverage depends upon insulation, ceiling height, glazing, doors, and other sources of heat loss, as well as geographic location. For size estimating purposes, the range for the footprint of the common commercial office is from 4 to 7 W/ft<sup>2</sup>. The use of 4 W is appropriate for supplemental heating; 7 W is appropriate for perimeter corner rooms and bathrooms; the average remaining office types fall somewhere in between. Refer to Sec. 8 of this Handbook for design information and system sizing.

Framed fast-acting radiant panels are used as primary and supplemental heating in all types of buildings. Their use in multifloor buildings eliminates the increase in stack effect that can be caused by a convection heating system. In buildings where the stack effect causes discomfort, comfort can be restored through the use of radiant heating, which may be the only cost-effective solution. Concrete floors that are in contact with the earth will tend to take on the temperature of the substrate that in most heating climates approximates 50°F. Radiant ceiling panels are an easy retrofit solution to warm the surface of cold floors.

Use in housing for the elderly and nursing homes allows the provision of required comfort through increased MRTs and equal or lower air temperatures (Fig. 2.11). Ceiling location permits architect, owner, or occupant determination of floor space requirement, utilization, and unobstructed floor maintenance. Elimination of air distribution for heat delivery reduces filtration and blower costs, permitting optimum air distribution design in conformance with code. Ease and simplicity of control, lack of mechanical maintenance, and long heater life may reduce or eliminate building engineering support, often required with mechanical heating, ventilating, and air-



**FIGURE 2.11** Radiant panel primary heating for nursing home dining room.

conditioning (HVAC) systems. These are a few of the many reasons why inclusion of radiant heating in the overall analysis process arms the designer with an important addition to the pool of HVAC selection options.

## **2.5 METAL-ENCASED RADIANT HEAT PANELS**

---

Metal-encased electric radiant heat panels have been in use for more than 50 years. The most common application used is in suspended ceiling grids as either primary or perimeter heating (Fig. 2.12). The revealed-edge and flat lay-in T-bar grid or fine-line grid units are normally lightly textured or silk-screened to match the ceiling tiles. For many years, choice was confined to two wattage densities. System sizing and design was usually based upon manufacturer recommendations. Users experienced over-sizing when following traditional design methodologies.



**FIGURE 2.12** Standard lay-in T-bar grid ceiling panel heating.

### 2.5.1 Features and Sizing

The most common sizes are  $2 \times 2$  ft in 250- and 375-W models, and  $2 \times 4$  ft in 500- and 750-W models, and custom wattage in between these ranges. Voltage choice includes the most common 120 and 240 V, which can be manufactured as a dual-voltage model, and commercial 208- and 277-V models. Although sizes as large as  $2 \times 8$  ft are made, metal encapsulation makes these panels heavy to ship, handle, and install. Each 2- by 2-ft increment is approximately 15 lb in weight so that a 2- by 8-ft panel weighs 60 lb or more. It is important to confirm that the weight of the panels specified conforms to the ceiling support and structural weight rating.

The choice of wattage and watt density is related not only to the heat loss, but also to the comfort parameters of the design application. Even though it might be appropriate to use a high-watt density panel, a 750- or 1000-W, 2- by 4-ft panel over an open-floor-plan factory workstation at an 8-ft height, it might be uncomfortable for someone sitting at a desk in an office with an 8-ft ceiling. The key factor is that the radiant asymmetry, or the temperature difference that the occupant feels, be within the guidelines for human thermal comfort in each case.

In general, lower watt densities are more commonly used in well-insulated building environments with average 8-ft ceilings and controlled air distribution. The industry offers a range of watt densities that provide design flexibility. The deciding factor is not cost per watt, which was common field design methodology when energy was cheap. The incentive to oversize is fed by the relationship between capacity and price per unit of capacity with products like baseboard convection heaters that are the cheapest heaters on the market. In well-insulated buildings that are designed to provide occupant thermal comfort, radiant panel sizing is precisely defined. The result usually is that proper watt density and lower installed capacity provide better occupant thermal comfort and operating economy.

In fact, both oversizing and the use of higher watt density than conforms to comfort parameters can result in uneconomic operation and an unsuccessful installation. In early installations, it was not uncommon to find a high-watt-density panel specified because it was placed directly adjacent to an air diffuser. The result was, in effect, air washing of the panel face, significantly lowering the surface temperature due to the increased convection heat transfer while the diffuser was active, and uncomfortable asymmetric radiation due to the much higher panel surface temperature when the diffuser was inactive. Similarly, oversizing at the perimeter results in short cycling as the heat loss is satisfied too quickly, thereby negating performance of the design objective of reducing downdraft due to cold window surfaces. Short cycling will occur with the use of high-density panels in most buildings using code-conformant glazing, as opposed to the plate glass that was common in buildings built before energy prices escalated. Lower-watt-density panels will have a longer "on" cycle, thereby eliminating discomfort problems caused by window downdraft.

### 2.5.2 Characteristics

Resistance elements used to provide heat for metal-encapsulated panels include fiberglass graphite-impregnated cloth, metallic ribbon, wire, insulated wire, plastic-encapsulated graphite, and wire sheet or element capsules. Element temperature, form, and conditions of failure require metal encapsulation. Element failure may produce normal electrical failure odor or smoke, surface paint discoloration, and possibly a small, black mark or hole in the panel face. Encapsulated metal panels are known to have an excellent safety record.

Maintenance of metal panels is minimal. When ceiling panel placement is coordinated with ventilation air distribution, little dust collection or dirt soiling occurs. Panels placed near diffusers to offset draft chill may collect some dust soil, as will other adjacent surfaces. However, if repainting is done, the paint must be water-based and able to tolerate the highest temperature as well as the longest time duration likely to be encountered in panel operation. Always consult the manufacturer for current information. Panel life expectancy is dependent on the resistance element, which normally will have a long life. Field experience reports, manufacturers' brochures, and warranty are the best sources of information for use in life-cycle costing.

Warranties for metal panels are similar to most electrical heaters. One-year warranties are common. Over the years, extended warranties have been sold, and some warranties have been prorated based upon percentage adjustment for years of service applied to the manufacturer's list price prevailing at the time of product failure. Similar to most electrical product, failure is rare. The largest percentage of failure due to defects in manufacture occurs within the first full year of use.

### 2.5.3 Application, Selection, and Installation

The most common suspended ceiling T-bar grid application (shown in Fig. 2.13) is commercial office perimeter heating, combination perimeter heating with variable air volume systems, primary heating, and problem solving. Mounting and frame kit designs extend use to other ceiling constructions like gypsum sheetrock and concrete for the full range of building types and uses. Revealed-edge models and silk screening enable a reasonable panel match to most ceiling tiles. However, the flat panel surface is a limiting factor in matching to three-dimensional tiles (Fig. 2.14).

Installation is facilitated by a standard 3-ft± conduit panel lead for connection to a plenum-mounted electrical box, the typical procedure for commercial buildings

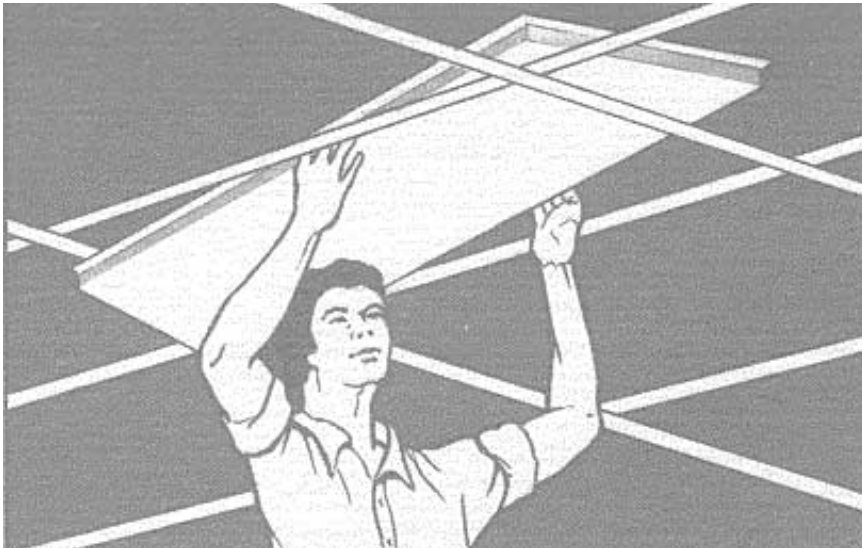


**FIGURE 2.13** Installation is easy.

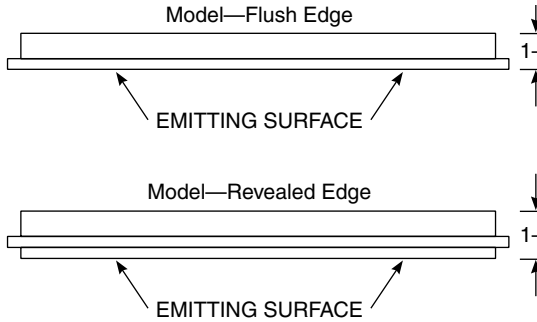


**FIGURE 2.14** Flush and revealed-edge lay-in models.

(Fig. 2.15). Wiring is unique to each voltage. Installers should consult manufacturers' wiring instructions (Fig. 2.16). Installation must conform to electrical and building codes in terms of clearance from other surfaces, fixtures, and materials as well as electric circuit design and amperage load. Space use and other factors may also impact product selection, installation, and design requirements.

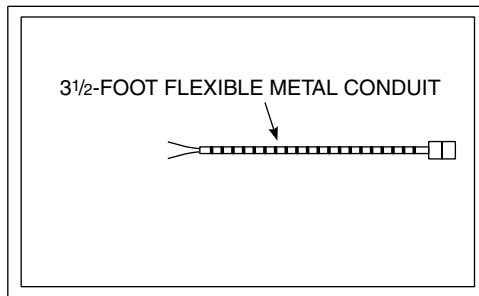


**FIGURE 2.15** Flexible wiring conduit on panel back.

Encapsulated metal panel designs serve high-humidity locations and some classes of hazardous locations. The wattage output range is approximately 65 to 125 W/ft<sup>2</sup> of ceiling panel area. The range of watt density and design application provides opportunities for consideration of encapsulated metal heat panels for a variety of ceiling and wall locations 6 ft or more above the floor (Fig. 2.17). Encapsulated electric metal radiant ceiling panels may address both spot and general heating needs.

## **2.6 WALL FLAT PANEL COVE, RECESSED, SURFACE, AND BASEBOARD HEATERS**

Wall flat panel heaters include a broad array of products encompassing a wide selection of wattage capacities. Heater surface temperatures determine wall location and

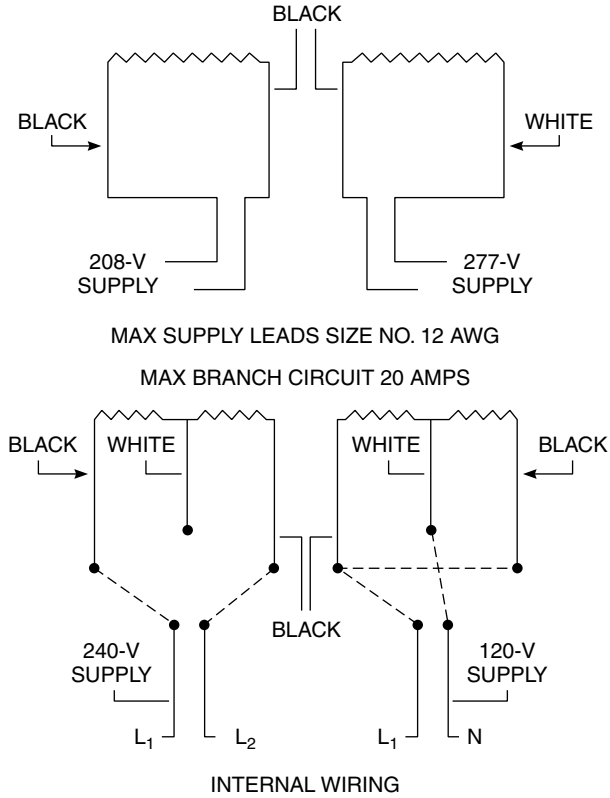


**FIGURE 2.16** Wiring diagram for each voltage.

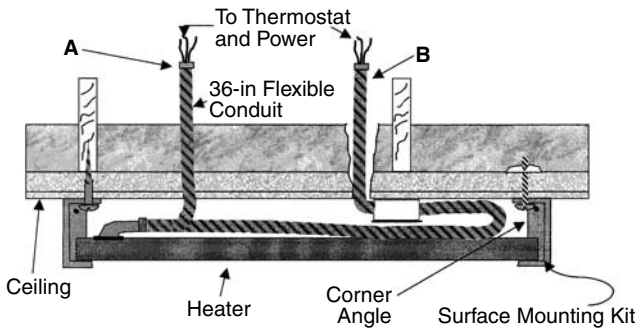


**FIGURE 2.17** Surface mounting with wiring to plenum box (A) or ceiling box (B).

installation specifications. Wall flat panel heaters are available in voltages that are appropriate for designed watt capacity and use application. Flat panel grill-faced glass and ceramic heaters and cove heaters have provided safe, comfortable heat since the 1940s (Fig. 2.18).



**FIGURE 2.18** Flat ceramic or glass panel recessed wall heater. (Photo courtesy of Radiant Electric Heat.)

Electric wall heater nameplate ratings list the wattage output of heat and radiant energy. The actual wattage output may vary by between +5 percent and -10 percent. Establishing the split between radiant and convection heat transfer may be an even more significant design factor. Evaluation of actual panel design is an important first step in determining the radiant and convection heat transfer split of the equipment being considered. The reduction in surface temperature occurs through transfer of heat to the air film adjacent to the panel. A temperature gradient results in natural convection across the element and through the open panel housing. Radiant wall installation specification, sizing, energy, and comfort analysis must consider the radiant and convection heat transfer split in the actual built environment. Because the thermal comfort process is absent in many heating calculations, all types of radiant heating panels are frequently employed as problem solvers in order to provide the missing MRT requirement.

### 2.6.1 Low-Temperature Baseboard Heaters

Lower-temperature panels are designed for wall surface mounting, including flat low-temperature baseboard panels (Fig. 2.19). Low-temperature panels are bounded by temperature limits that permit casual touching. The flat-panel surface area must be

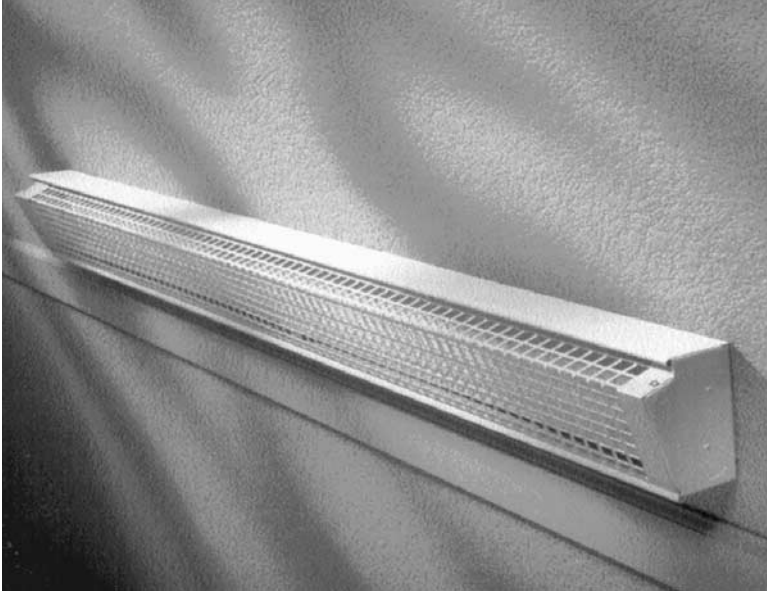


**FIGURE 2.19** Baseboard low-temperature radiant panel heater.

large due to the lower watt capacity of touchable wall or baseboard heaters. The larger surface area required by the low watt capacity of wall heaters distinguishes them from housing- or grill-protected common convection baseboard and reflector wall heaters.

Low-temperature flat-wall baseboard panels are available in many different dimensional configurations in order to meet the wattage required for the specified application. Safety surface temperature limits constrict wattage output to a range of approximately 15 to 75 W/ft<sup>2</sup> of panel radiating surface. The wattage output in relation to appropriate installation space defines whether the system capacity is adequate to provide primary or supplemental heat. The wattage capacity required is commonly 15 to 25 percent less than for traditional baseboard convectors.

Some enclosed baseboard wall heat panels are insulated, but most are uninsulated. When used for primary heating, low-temperature baseboard radiant panels may require all available perimeter baseboard space in order to provide the wattage required for the heat loss. Both discrete and electrically interlocking designs are used for enclosed radiant panel baseboard installation. Control is commonly achieved by installation of wall thermostats. As with any baseboard heating system, heating radiant efficiency is compromised by obstructions. The surrounding area should be open to the space being heated.

### 2.6.2 Low-Temperature Wall Panels

Whether wall panels are used for primary or supplemental heating depends on the heat loss requirements, design constraints, and circumstances encountered. Growth in the use of radiant low-temperature wall panel heaters is attributed to the design

appeal of colorful decorative shapes and sizes. Developed originally to replace old-fashioned hydronic radiators, the wall-mounted radiant panels are also available as electric panels (Fig. 2.20). When powered by electricity, the characteristic lower wattage and ease of installation is enhanced by the ease of electric system control.



**FIGURE 2.20** Low-temperature electric or hydronic wall surface mounted radiant panels.

### 2.6.3 Glass and Ceramic Higher-Temperature Heaters

The higher radiant output of flat-panel wall heaters provides an attractive option to traditional, much smaller, recessed, high-wattage fan-coil or filament wall heaters. Recessed installation of any heater within an outside wall can compromise insulation. An increase in the temperature differential from the inside to the outside of the insulated wall at the point of installation could result in additional heat loss to the outside, which should be factored into the design analysis. Surface installation of shallow-depth ceramic panels has a smaller impact on adjacent wall heat loss (Fig. 2.21). Comparative installed wattage may be reduced in direct proportion to decreased backloss and radiant versus convection output that is characteristic of wall surface-mounted flat-panel heaters in comparison to wall fan-coil units.

Higher radiating surface temperatures are achieved with ceramic or glass graphite-coated elements that are used for out-of-reach cove and grill-protected recessed wall heaters. With wattage output of approximately 300 W or more per square foot, the heating element surface temperatures are much too hot to touch and require protective grills or location 6 ft or more above the floor. Installation requires clearance from all surfaces. Back enclosures embody a reflective surface to enhance radiant output and reduce back heat loss.

High-watt-density glass and ceramic elements are made in numerous sizes. The actual heater casing is only a few inches larger than the element, but the relatively

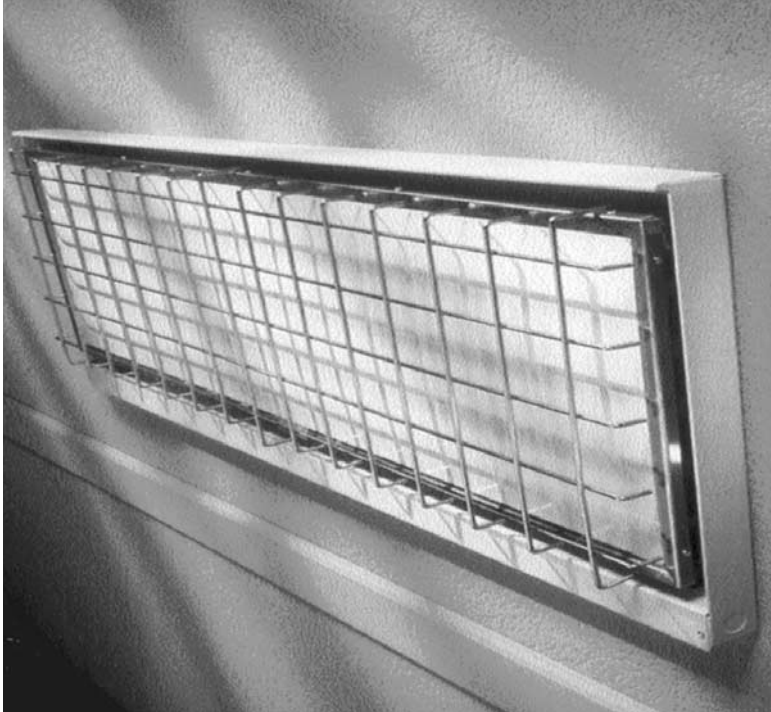


**FIGURE 2.21** Ceramic radiant wall heater.

high material density results in a weight density approximating the 4 lb/ft<sup>2</sup> of metal-encased radiant panels. The various product housings are designed so that the element is relatively easy to replace.

Element replacement is an attractive feature that extends fixture life and avoids the costs that are involved in refinishing a wall in the event of fixture removal. Electrical element life is very long. The ceramic heat element substrate offers structural stability. Failure is rare for ceramic elements. Most failures are due to glass failure, not electrical element failure.

Glass elements, when used, should be manufactured to the same standards as automotive safety glass. The heat-tempering process is intended to ensure that shatter fragments or shards are within defined safety specifications, should breakage occur. The 50-year installation history of glass and ceramic heaters provides useful product life and field performance information.

Higher-watt-density ceramic heaters require less wall space in relation to most other radiant wall heaters due to the significantly higher wattage output. As with most heating systems, occupant comfort may be impacted by occupant location in relation to the heat output source. For someone who longs for the feeling of warmth associated with sitting near a fireplace, concentrated warmth may be a particularly attractive feature unique to high-temperature recessed radiant wall heaters. From a design standpoint, high panel surface temperature requires that radiant asymmetry relationships be reviewed in relation to design objectives.

Ceramic element cove heaters provide a means of installing high wattage capacity in a relatively small space. Installation is usually on an exterior wall about a foot below the ceiling, just above a window. The unobstructed panel element heat transfer is evenly split between radiant and convection. Interior wall placement is an option to be considered for buildings that meet current construction and insulation standards, as defined in ASHRAE Standards 90.1 and 90.2 for commercial and residential buildings, respectively. Location on an interior wall minimizes panel backloss to the outside. Interior wall location facing heavily glazed exterior walls is a popular residential porch application. Ceramic or glass element cove heaters are relatively heavy, requiring connection to structural building members (Fig. 2.22).

Sizing of ceramic wall and cove heaters is commonly 20 percent less than convection baseboard. High element temperature makes these heaters especially effective task heaters. Users report satisfaction with both comfort and operating cost, which suggest that they are taking advantage of the excellent task-heating performance.

Ceramic and glass heater elements reach full operating temperature quickly. Determination of the radiant and convective heat transfer split, relative location to the occupant, setback temperature, and relative sizing in relation to heat loss are important factors in determining the time period that is required for comfort restoration. There are many applications where higher-temperature heaters may be used for problem solving and task heating, as well as primary heating. Popular applications include nursing homes, retirement homes, hotel and motel applications, public and elderly housing, and primary and vacation residences.

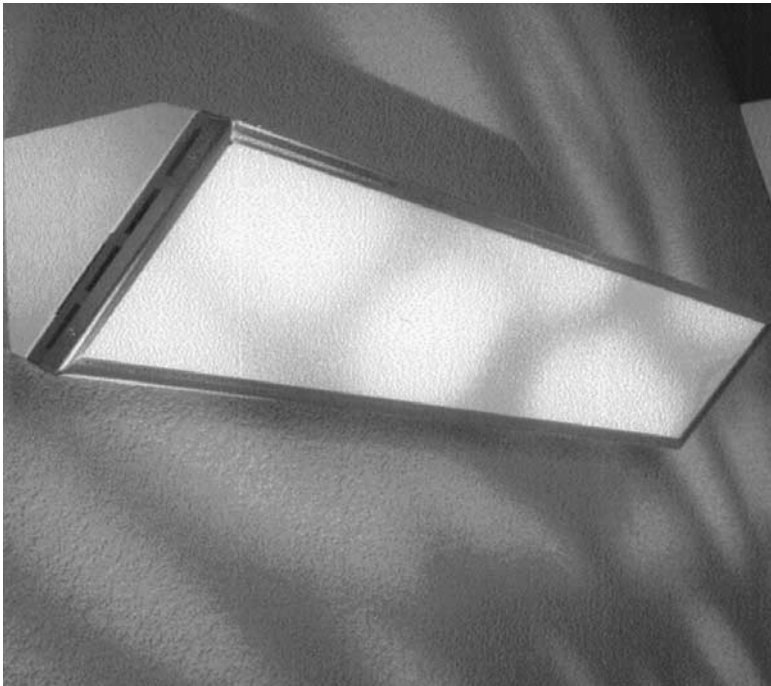


**FIGURE 2.22** Cove ceramic radiant panel.

## **2.7 CONCEALED CEILING CABLES, WIRE, AND FLEXIBLE RADIANT HEAT PANELS**

---

Architectural design championed the monolithic ceiling, leading to the development of several approaches for concealing electric and hydronic radiant heating in the ceiling. These systems included the use of resistance wire, gypsum panels, and flexible radiant panel elements. The engineering compromises in efficiency, control, technical reliability, and service accessibility have culminated in the virtual disappearance of electric concealed ceiling heating.

Concealed radiant ceiling systems merit coverage in this Handbook because the systems are still in use in many areas in the United States and abroad. It is also important to understand that the circumstances, which existed during the period of their greatest popularity, were very different than those that exist currently. For a heating system selection and design to stand up over time, global factors that impact design engineering must be considered. In addition, there are a lot of lessons to be learned from the experience history of concealed radiant ceiling heating, which can be a viable design alternative when all performance factors are addressed.

One of the early techniques for providing ceiling heating involved stapling or adhering insulated resistance wire directly to the ceiling surface before finish plastering was applied. The wire was generally placed in parallel pattern about  $\frac{1}{2}$  to 1 in apart running from one side of a room to the other, covering about 80 percent of the ceiling surface. System life expectancy was 15 to 25 years, or longer. Failures were caused by breaks in the circuit caused by wire failure, moisture, or building stress breaks. When these systems were popular, repair service was available through electric utilities and electricians.

When circuit interruption occurred, current detection wands were used to locate the break; special wire bridge connectors were installed; and the ceiling was patched and repainted. Concealed resistance wire repair has become a lost art. However, as these systems age, wire failures increase and repair ceases to be cost-effective.

Occasionally, an outline, or ghost line, related to the concealed wire would appear on the ceiling surface. This may occur through a process known as *historesis*, where particles in suspension are attracted to surfaces in relation to the nature of the electrical magnetic field, such as may exist on the ceiling surface below the concealed resistance heat wires or hydronic metal conduit.

As the cost of plastering increased, cheaper ways of installing a radiant ceiling system were sought. As sheetrock became economical, embedding resistance wire with backside termination connectors resulted in prefabricated gypsum radiant panels. The entire assembly became both the ceiling and radiant heating system. Users of concealed radiant systems generally found them to be very comfortable. Complaints, when they did occur, related to localized discomfort and slow response time.

Problems relating to localized discomfort sometimes occurred because the general construction and insulation practices at the time were very different from those defined by current building codes. Specifically, glazing was single-pane alone or combined with single-pane storm windows. There was no insulation under the floor above a basement or crawl space, so the floor would likely be cold under a table with any heating system, as would a space by a window or a masonry fireplace.

Two concerns are inherent in concealed systems. Response time is related to the Btu limitations of the gypsum or plaster ceiling materials, which generally results in warm-up recovery times from setback that are too long to make setback practical except for long vacancy periods. As a result, these systems are normally turned on at the desired temperature in the fall and turned off in the spring, which should be factored in to design and operation analysis.

The second area of concern is that watt density or Btu output is normally uniform across the ceiling surface being heated. The Btu limitations of concealed systems may not adequately address areas of high heat loss, such as in front of sliding glass doors, or in rooms where the ceiling area is inadequate to meet the heat loss, such as bathrooms. Concealed system design often incorporates supplemental or hybrid design to ensure uniform occupant thermal comfort and energy-efficient system operation.

Original owners were usually happy with operating costs: electricity was very inexpensive during the days of the “Gold Medallion Home,” and all-electric homes were given an additional rate discount. When energy prices escalated and rates were revised, the level of insulation and construction standards of the time made operating cost comparisons with tighter, better insulated buildings less attractive, and electric heat was universally singled out as being expensive. In reality, for concealed radiant systems, the main cause of high operating cost was inattention to the importance of minimizing radiant panel backloss and edge loss. A second cause was the failure to recognize that the floor is the primary recipient of ceiling radiant energy and, therefore, must be insulated from an unheated space below.

Electric radiant ceiling heating products also include resistance wire-embedded gypsum panels of varying widths and lengths that are laid between the ceiling joists directly upon the top of the gypsum ceiling board. This type of panel is normally connected by routing a connecting wire from the thermostat through an encapsulated feed located at the end of each panel on the circuit.

As with all radiant panels, installation design must incorporate insulation to maximize frontal panel output. Use of loose cellulose or any potentially combustible insulation is not recommended. Loose insulation, like cellulose, can migrate between the panel and the ceiling, where the highest temperatures occur. Product life is similar to ceiling cable heat, but failure occurs on a panel-by-panel basis rather than an entire room, as may be the case when a single ceiling cable comprises the entire heating element.

Repair is virtually impossible for between-floor installation. Replacement of panels that could be up to 10 ft long is very difficult, even with attic access. Due to the weight of the gypsum panels, the use of at least  $\frac{3}{8}$ -in sheetrock is essential to avoid the potential appearance of a wavy ceiling surface. Normally, panel support strapping is installed to position the panels prior to sheetrock installation. However, the panels normally rest directly on the sheetrock to ensure maximum heat conduction to the sheetrock when the installation is completed.

Sheet resistive elements stapled to the ceiling joist are designed to provide heat in the area between the joists, which is conducted directly to the gypsum ceiling that is fastened directly to the same ceiling joists. Common elements include graphite-impregnated fiberglass material and graphite-encapsulated plastic film. Both elements encountered occasional electrical problems. The failures were usually traced to buss bar electrical failure due to manufacturing defect or to wire crimp connection failure during installation.

A third element constructed with etched resistance foil embodied a heat-limiting feature that prevented dangerous overheating by breaking the resistance circuit. However, its use in very tight homes, with as much as *R*-70 insulation placed upon the element, resulted in sufficient temperature buildup to cause premature element failure, thereby leaving the building owner with an inaccessible and virtually unsalvageable or unrepairable heating system.

Flexible elements were popular with installers, who found installation to be easy, quick, and profitable. Builders and owners embraced the technology and marveled at its simplicity and nonmechanical effectiveness. Architects were attracted to the invisibility of the heating system and the resulting monolithic ceiling.

When concealed electric radiant heating systems fail, the most cost-effective option is usually the installation of surface-mounted panels. Room or area thermostats and ceiling wiring are already in place, and electrical circuitry is adequate as installed capacity is normally reduced by 30 to 50 percent. Operating cost should be reduced by 15 to 20 percent, and can be further reduced by the use of temperature setback that is possible with fast-acting surface- or wall-mounted panels.

### 2.7.1 Safety Issues

The safety concerns raised by concealed-element failure resulted in a comprehensive review by the Canadian Standards Association and Underwriters Laboratory. Product testing, installation, and application listing standards were subsequently revised. The most significant factor for design was a reduction in element wattage per square foot of flexible or rigid ceiling panels, which means that more ceiling space and more elements are now required to compensate for the resulting drop in element temperature.

It was found that when gypsum board is subjected to long periods of continuous heat, the moisture content drops to a point at which gypsum becomes a heat insulator rather than performing the heat conduction function as designed. Testing also found that some of the elements were electrically unstable and evidenced declining resistivity and increasing heat output over time. The information developed has led to a reduction in maximum element wattage output. The result is a reduction in element temperature and therefore a reduction in the maximum temperature to which the gypsum ceiling board may be exposed.

The product classification and application listing changes reduced maximum element wattage output and gypsum ceiling panel temperature. This correspondingly increases the area of a ceiling, other things being equal, that would need to be covered by the element to provide the wattage required to meet the heat loss. The interested reader is encouraged to obtain current information from the CSA, UL, ETL, and product manufacturers prior to designing a concealed electric radiant ceiling panel heating system.

### 2.7.2 Electrical Testing and Retrofit Option

The actual performance of concealed ceiling systems can easily be verified against the original installed wattage capacity or in relation to the calculated heat loss. The systems are generally controlled by a line-voltage thermostat, which usually makes access to the connecting wiring quite easy. When the connecting power feed is accessed, an ohmmeter may be used to obtain a resistance reading in order to calculate the current wattage output the system elements are capable of providing to the space to be heated. If the wattage has become inadequate to address the heat loss, further analysis must be conducted to determine if there is a loose panel connection or actual panel failure. If the resistance reading indicates a very high wattage in relation to heat loss, the element may be overheating. Heater output rating should be checked against actual output to determine if the system should be disabled immediately.

In the event that a new heating system is required, the presence of ceiling heat wiring, local thermostat outlet box, and adequate electrical capacity make the retrofit of modular ceiling panels very easy. The importance of performing design analysis should not be overlooked. The tendency to connect “about” the same wattage as before should be resisted. A thorough design analysis takes into account the capabilities of the replacement system.

For framed fast-acting panels, the significant reduction in wattage capacity required assures that the existing circuit power is adequate. Modular configuration provides an opportunity to address areas of high heat loss, which is usually not possible with a concealed system. The panel will cover an opening for whatever ceiling access may be required to route the wiring required for panel installation. The entire existing system should be disabled; only one system should operate; and no surface, which could heat, should be covered in any way.

## **2.8 CABLE, MAT, AND INSULATED-WIRE BURIED, SLAB, OR FLOOR PANELS**

---

Radiant floor panels are made using a wide variety of electric resistance wire heating elements. Some performance characteristics, such as thermal inertia, are similar to concealed radiant ceiling heating that has high thermal mass. However, floor surface temperature is bounded by the thermal conditions of comfort dictated for direct, indirect, and continual occupant contact, rather than solely by encapsulation material temperature limits. Within surface temperature parameters, various design alternatives can impact radiant heating recovery time or mass thermal performance (Fig. 2.23). As with all radiant floor heating systems, the design must accommodate objects that block heat transfer that might subsequently be placed on the floor, either as floor covering, furnishing, or area division.

Radiant floor heating is used for floor warming, primary heating, and electric and solar thermal storage. Thermal storage is designed to take advantage of off-peak electric utility rates or to even out a natural thermal energy charging design strategy. The noncombustible material mass is normally sand, screed, or concrete. The demands for each application can be quite different. The element proximity pattern and location within the mass are determined by the application that the system is serving. Heat-producing element selection is defined by the conditions of design within the mass serving as the radiant panel. Actual installation specifications inherent in the design are also a determinant of whether to use a manufactured mat or field-routed element. Element selection and routing patterns are also determinants of the electric and magnetic field, neither of which normally influences the overall heat transfer or radiant panel design.

### **2.8.1 Application and Characteristics**

The design methodology and materials used for floor warming are similar to those used in radiant panel design except that the sole objective is heat transfer for the purpose of maintaining the floor surface temperature at a predetermined skin contact comfort minimum rather than radiantly heating occupants or space. The use of various ceramic and masonry flooring materials has spawned an interest in ensuring that these floors are comfortable for bare feet whether the central system is heating or cooling.

The main panel design constraint, other than temperature performance, is use of the noncombustible base or screed for element encapsulation without structural design alteration or an increase in architecturally constrained thickness. Inasmuch as foot comfort is the prime objective, the use of low-temperature constant-wattage terminated cable sets or thin-wire mats, which easily fit in designated bathroom floor sections where heat is desired, will facilitate installation as designed (Fig. 2.24).

**APPLICATION METHODS**

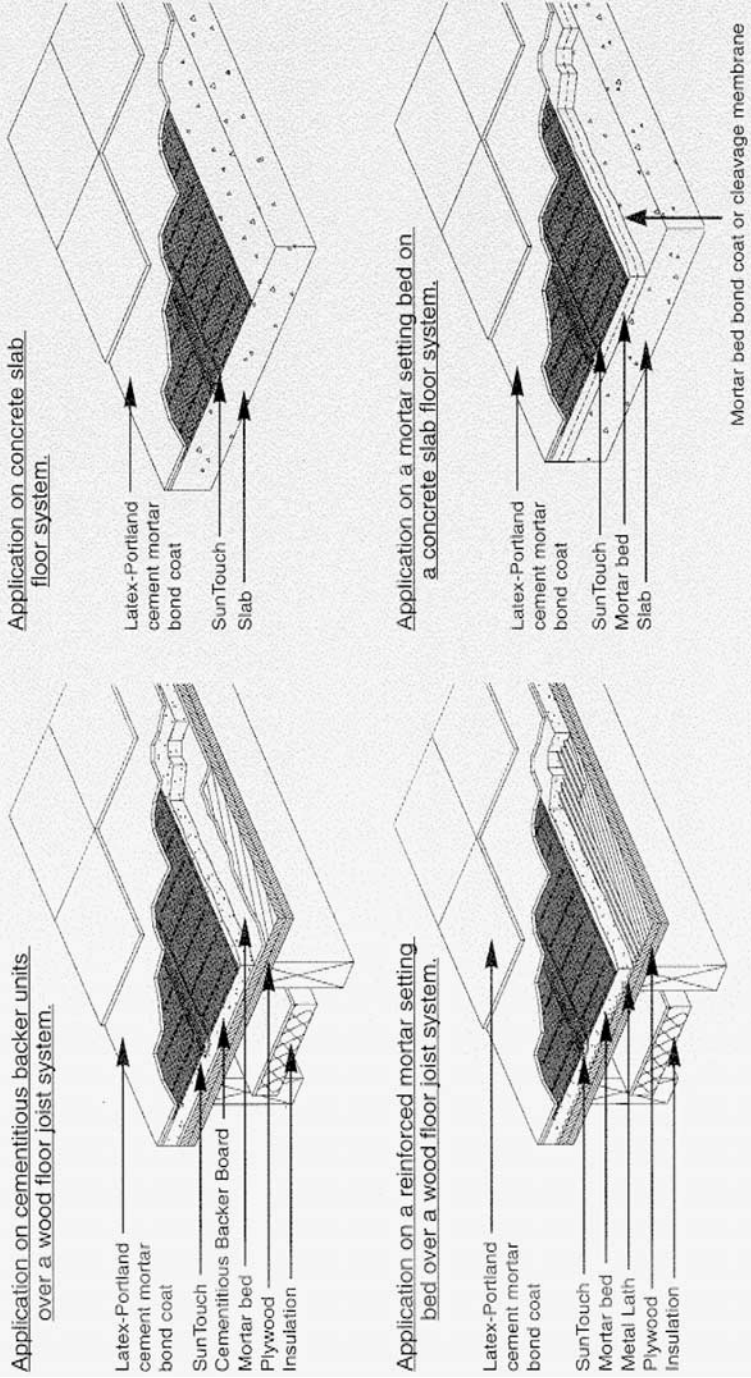


**FIGURE 2.23** Floor cable and mat installation applications.

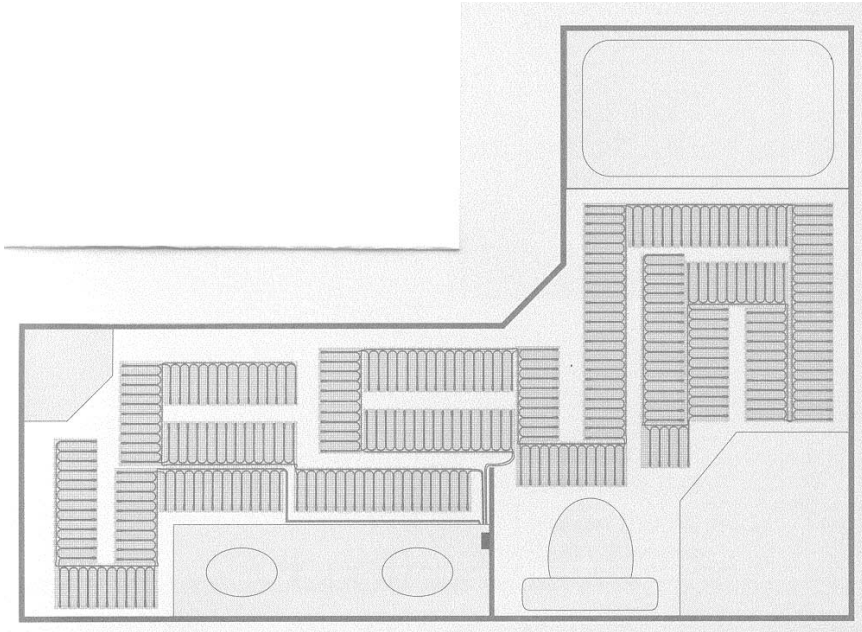


**FIGURE 2.24** Mat application for bathroom heating or floor warming.

Heat transfer cable is used for many applications, some of which are not radiant panels. The cable is manufactured in a broad range of element specifications, sheathings, and coverings. The insulating jacket temperature tolerance range, combustibility, pattern-bending radius, conformation memory, and mass tolerance temperatures are among the important input design factors to be considered.

Use of heat transfer cable extends to very large areas such as may be encountered for snow melting or large-area slab-on-grade industrial heating panels. Heat transfer cable is also used for novel applications. Maintenance of athletic field ground temperatures suitable for the growth of grass throughout the winter eliminates artificial turf, which turned out to be unpopular with players and fans alike. Some other common nonradiant applications include aircraft hangar door freeze prevention, frost heave control, and roof deicing.

Mineral-insulated (MI) cable should be included in cable selection analysis due to long life and ability to withstand the installation field abuse that may be encountered in large-scale radiant floor and heat transfer applications. Mineral-insulated cable installations do not always require ground fault interruption and could offer greater flexibility for termination box location. The MI cable is also flame-resistant and appropriate for use where high temperatures may be encountered.

Self-regulating cable is used for heat transfer applications where heat output regulation by the cable may be accomplished within the specified application design limits. Self-regulating cable is not commonly used for radiant heating panels. The energy consumption characteristics of self-regulating cable in relation to the application should be carefully analyzed. Low-level output generally continues in the absence of external on-off control at varying levels that may or may not be productive or cost-effective.

## 2.8.2 Design Considerations

The heat transfer product chosen and the application design determine the code requirements for installation, including ground fault interruption, termination box specification and location, cold lead routing and enclosure, over-limit cable temperature control, and the entire range of relevant electrical factors (Fig. 2.25). The National Electrical Code and state and local codes should be consulted for design and installation of all electrical products, including heat transfer cable used for mass temperature control and radiant panels, to ensure conformance to national and local safety codes and other jurisdictional regulations.

The selection of cable for use in floor and earth heating requires design of a secured routing system (Fig. 2.26). The element is anchored in the design position and protected as much as possible during the compaction, mass fill, pour, or other field activities that are required to complete the radiant panel design. There are many more or less serpentine design layouts that can be adapted to meet the heat loss and construction demands of a particular room or area. Care must be taken to ensure that both ends of the resistance element circuit are protected and properly secured in position in order to route the cold leads in the conduit, make the required electrical connections, and install the junction box in an accessible location. Where ground and ground fault interruption is required, those connections must also be in place and tested, along with the resistance circuit, both before, during, and after mass construction.

Repair or replacement of a defective or damaged element becomes increasingly difficult as mass construction proceeds toward completion. Problems are not common, as the conduit materials are durable, but testing is essential as the system either works or it doesn't. Continual testing of continuity, resistance, and insulation will reveal problems and is the best insurance against costly callback for installation failure.

The wide range of wire resistance specifications provides a broad selection of design wattage outputs. Determination of cable wattage output enables design of the cable pattern, total capacity, and required volt-amp rating of the electrical circuit. The wattage output must also be designed in relation to the constraints of the radiant panel performance or the heat transfer application. Generally, small areas and floor warming are low-total-wattage applications for which 120-V power may be adequate. The most common design voltage specification is 220 to 240 V. Industrial and snow-melting applications where large wattage is required use 240 V, or 277- or 480-V power when available.

Once the performance parameters and wattage are determined, a formula is used to determine element spacing for the element length required for the wattage specification (Fig. 2.27). The conduit spacing is determined by taking the area of the space to be heated multiplied by 12 and divided by the length of conduit required. An example is

Heated floor area in square feet = 200

Cable length for required wattage = 280

$$200 \times 12 = 2400 \div 280 = 8.6 \text{ in of spacing for the cable pattern}$$

Cable spacing, proximity to the surface, and encapsulation heat transfer characteristics are primary determinants of surface temperature uniformity and system heating response. It is important to review all of the elements of heat transfer to determine that the watt density, heat conduit spacing, and location within the mass provide heat that is consistent with the radiant panel performance objectives.

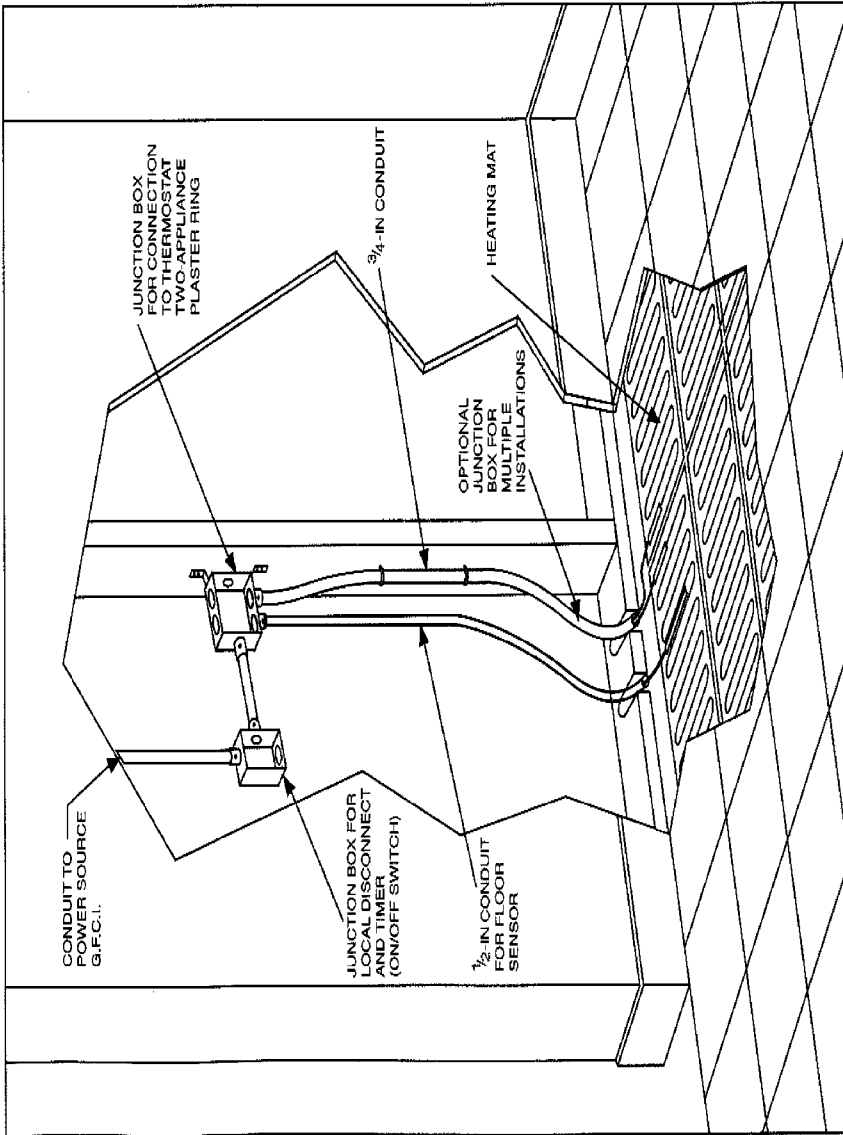
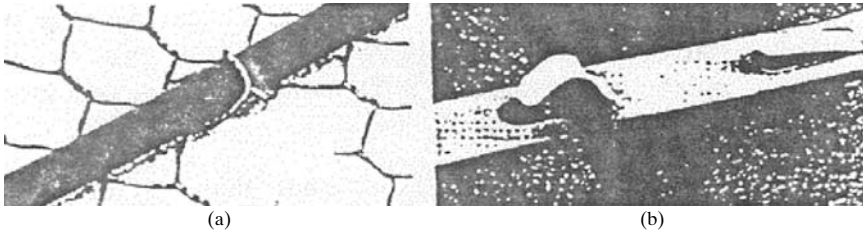
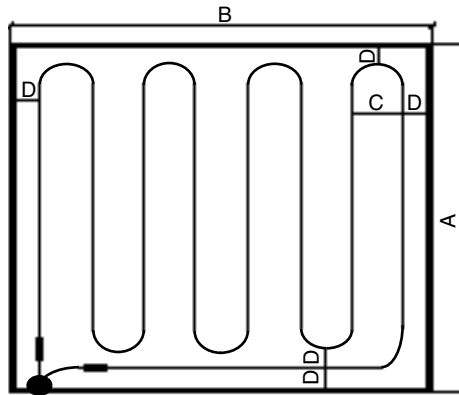


FIGURE 2.25 Typical floor heating or warming installation diagram.



**FIGURE 2.26** Secure heat cable to wire mesh or cleats. (a) Heating cable fixed to wire netting. (b) Heating cable fixed to special strips.



**FIGURE 2.27** Floor cable layout showing important design points. (A, B) Space dimensions; (C) conduit spacing; (D) perimeter and conduit separation spacing.

### 2.8.3 Thermal Storage and Mass Design

Earth thermal storage systems have been encouraged by winter-peaking electric utilities interested in building level, long-term electric heating load (Fig. 2.28). The concept is simple: create a large thermal mass that can be charged with heat by electric resistance elements during periods when excess electricity can be sold to customers at a significant discount. The process may be price-efficient, although off-peak thermal storage generally results in the use of more energy (kWh) than more direct heating systems. Careful comprehensive design analysis is important to ensure that system performance objectives are attained under all conditions encountered. Controls are installed to measure and control mass temperature performance as well as cable temperature over-limit controls to prevent premature element failure or burnout. The reader is referred to Secs. 6 and 7 of this Handbook for more information.

Electrical floor systems offer flexibility of design to overcome some of the thermal inertia characteristics of high-mass systems. Thermal transfer characteristics of the mass material and heat conduit are important design input. The variation in wire

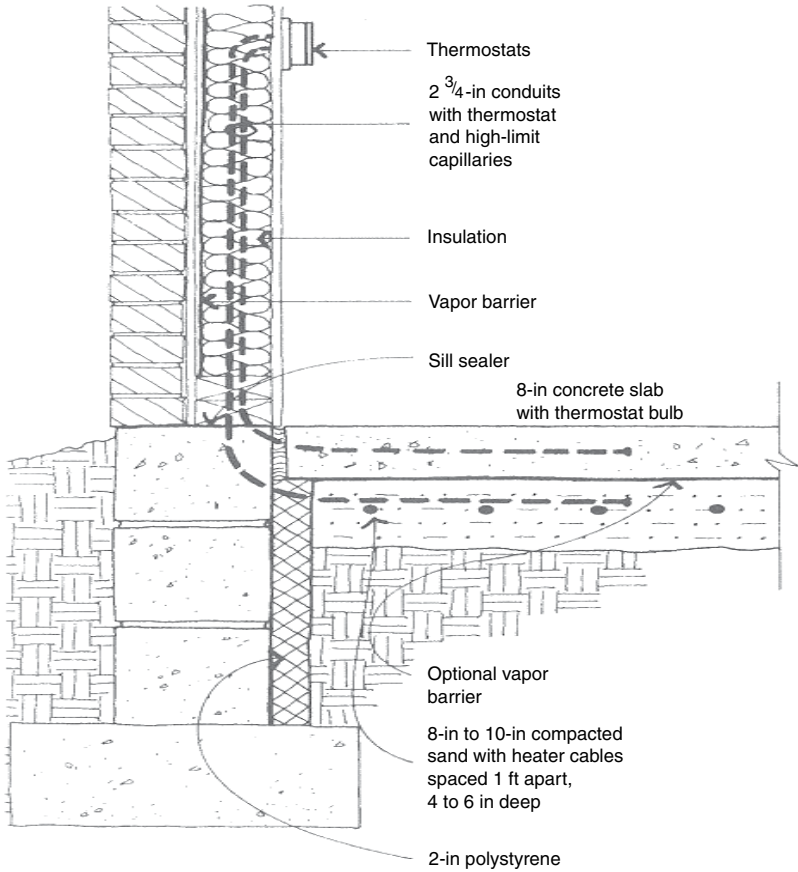


**FIGURE 2.28** Earth thermal storage design elements—typical installation.

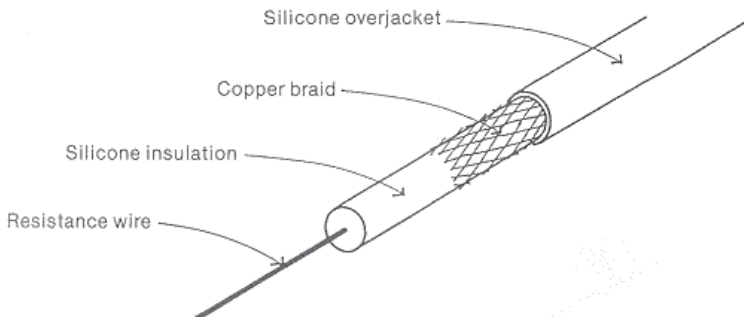


**FIGURE 2.29** Single conductor 150°C rated cable with 12-W lineal foot limit. (Photo courtesy of Delta-Therm.)

diameter, flexibility, and resistivity permit the use of almost any noncombustible mass thickness of  $\frac{1}{2}$  in or more (Fig. 2.29). Variation in wire pass design proximity allows the design of heat output in relation to localized area heat loss in floor systems. For more information on conductive heat transfer and the relationship of wire location and temperature within the mass-to-mass surface temperature, the reader is referred to Sec. 2, Chap. 2 of this Handbook.

The ability to vary wire proximity and resistivity, or wattage output rating, are important design factors in relation to mass thickness and surface temperature performance. Typical wattage ratings per lineal foot range from 3 to 30 W or more. Use and application determine the choice that is appropriate. Factors include the encapsulation mass, and applications that range from floor warming in temperate climates to snow melting. Manufacturer specifications should be consulted to determine recommended product specification, pattern design, and installation options and requirements for each application (Fig. 2.30). It is very important for repair or analysis of system performance that complete installation layout, wattage, circuit resistivity readings, and control mapping be prepared and provided in the commissioning process.

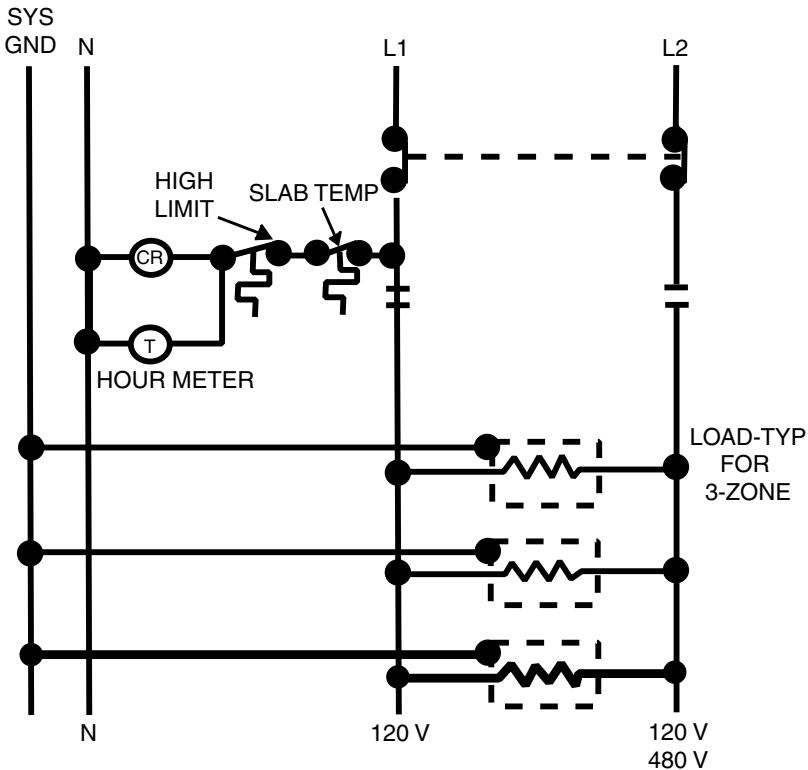


**FIGURE 2.30** Typical earth thermal storage installation—wiring for a typical 240-V installation.



---

# CHAPTER 3

---

## HIGH-TEMPERATURE HEATERS

---

Over the years, high-temperature radiant heaters have been used in many industrial applications and, to a lesser extent, in commercial and space heating. These heaters take on various shapes ranging from flat surfaces to tubes to cylindrical surfaces. A hydrocarbon fuel or electricity via resistive elements can heat these heaters. The definition of a high-temperature heater is one whose surface is greater than 300°F, but they may range up to as high as 1800°F. Due to the high temperature of these heaters, safety dictates location and distance from combustible surfaces.

As energy efficiency and employee comfort are becoming more important issues, engineers have sought a better design and application of these heaters. The following sections introduce types of high-temperature radiant heaters and discuss heat transfer implications of these heaters. The discussions also include some design parameters to size and locate heaters for their optimum operations.

### **3.1 TYPES OF HIGH-TEMPERATURE RADIANT HEATERS: DIRECT AND INDIRECT**

---

For residential thermal comfort utilization, a *direct radiant heater* refers to a radiant heater that typically consists of a porous ceramic or metal screen as a flat combustion surface. One type of direct radiant heater is illustrated in Fig. 3.1. In ASHRAE's *Handbook of HVAC System and Equipment*, these types of heaters are classified as *surface combustion heaters*. Often, the manufacturer's literature refers to these types of heaters as *high-intensity radiant heaters* because of their high temperature at the burning surface. The gas and air are premixed, and the combustion takes place on the burner face. According to the ASHRAE Handbook as well as some heater manufacturers, the temperature of the burning surface ranges from 300°F to 1800°F under regular operating conditions. A direct radiant heater does not normally include an integrated ventilation system. Therefore, areas heated with direct high-temperature radiant heaters need to have sufficient ventilation to ensure that combustion contaminants are removed and air quality is maintained at acceptable levels.

*Indirect radiant heaters* commonly have a tubular combustion cell. A typical tube is made of either heat-resistant steel or ceramic. Tube shapes differ depending on the design. They can be composed of straight-through, U-type, W-type, and blinded-end. A straight-through radiant tube (see Fig. 3.2) is the simplest; however, it suffers from relatively large longitudinal thermal expansion that reduces its service life. The U- and W-types, also shown in Figs. 3.3 and 3.4, have both combustion reactant and product flowing through the same side of the heater. This configuration successfully increases the service life of the heater. Nevertheless, they have a disadvantage as far

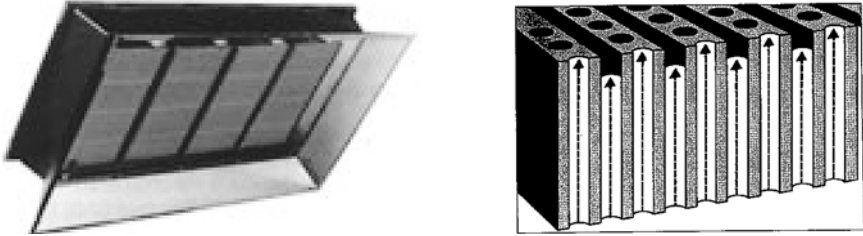


**FIGURE 3.1** Gas-fired direct radiant heater and its surface structure. (Source: Solaronics, Inc.)



**FIGURE 3.2** Straight-through radiant tube heater. (Source: Solaronics, Inc.)

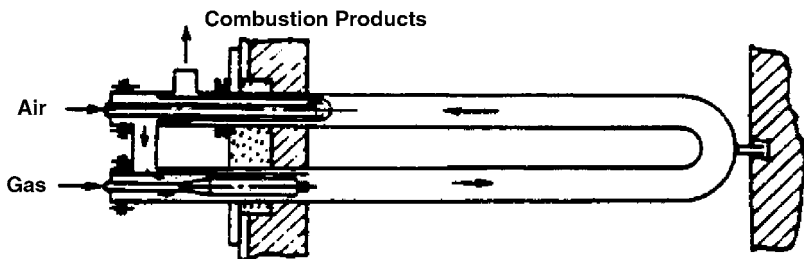


**FIGURE 3.3** U-type radiant heater. (Source: Chapman et al., 1988.)

as maintenance and thermal efficiency are concerned. The blinded-end radiant tube appears to be the optimum with its simple design, uniform temperature distribution, and high thermal efficiency (Chapman et al., 1988). Figure 3.5 illustrates the schematic of the blinded-end radiant tube heater.

### 3.2 HEAT TRANSFER FROM INDIRECT ELECTRIC AND GAS RADIANT HEATERS

Either a hydrocarbon fuel (normally natural gas) or electricity can power indirect radiant heaters. For the purposes of calculating delivered thermal comfort, either

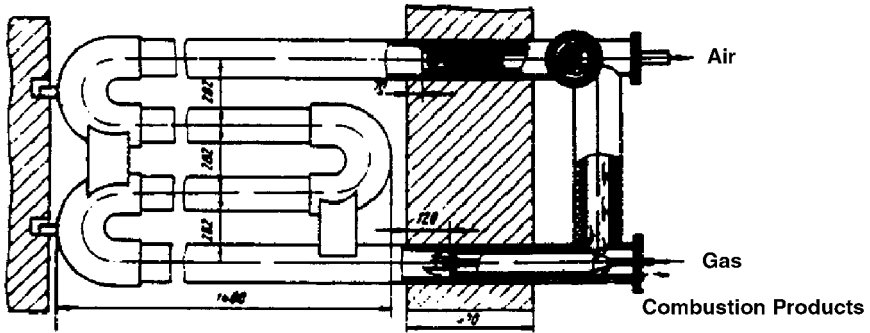


FIGURE 3.4 W-type radiant heater. (Source: Chapman et al., 1988.)

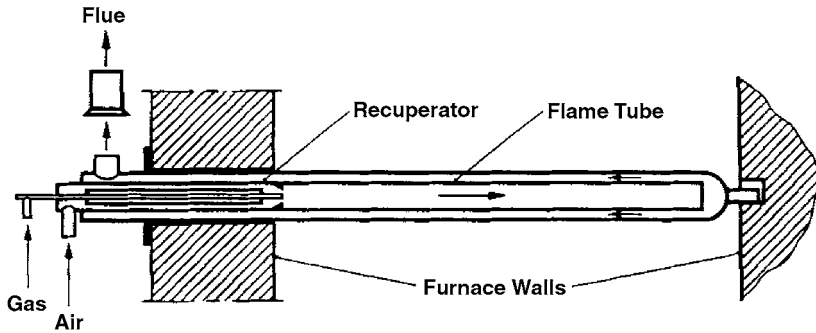
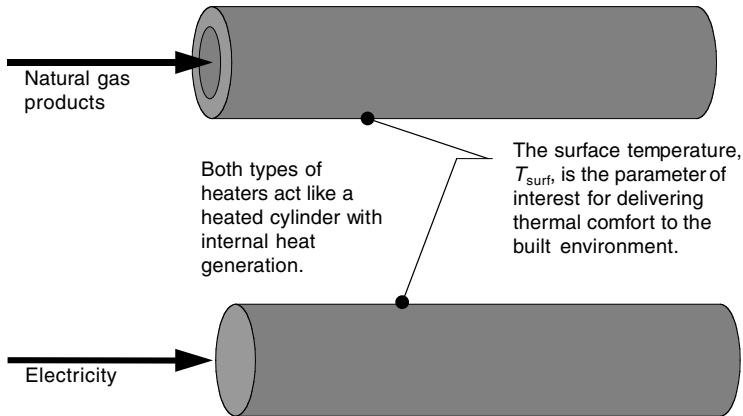


FIGURE 3.5 Blinded-end radiant heater. (Source: Chapman et al., 1988.)

type of heater ultimately has the same final heat transfer and temperature characteristics—the heaters are fuel-neutral relative to thermal comfort. Figure 3.6 illustrates the basic difference between the natural gas-powered and the electric-powered heaters. Both types of heaters can be treated as a cylinder with internal heat generation (refer to the conduction section in Sec. 2, Chap. 2 of this Handbook). The electric heater can be treated exactly like a cylinder with internal heat generation, but the gas-fired radiant tube cannot. The difference is due to the flowing characteristics of the reactants and products through the tube, and the burning rate inside the tube. Because of the complexity introduced by the gas-fired parameters, much of the discussion in this section focuses on gas-fired radiant tubes. Again, the electric-powered tubes can be analyzed exactly like the example in Sec. 2, Chap. 2 of this Handbook.

A gas-fired radiant tube heater generates heat as a result of combustion of hydrocarbon gas (commonly natural gas or propane) at the combustion burner that is inside the tubular structure. The gas and air are partially mixed at the burner so that combustion takes place inside the radiant tube. The combustion products flow from the burner into the radiant tube. Then the energy released during the combustion process is partially transferred to the tube (Harder et al., 1987). The heated tube transports the heat energy via surface radiant and convective heat transfer to the built environment and to the occupants in the room.



**FIGURE 3.6** Fuel-independent radiant tube heaters.

The flow rate of the fuel mixture mainly determines the rate of heat generation available. The parameters that are related to the optimum design of radiant tubes include tube wall temperature uniformity, radiant tube thermal efficiency, and tube service life (Harder et al., 1987). The primary interest is how the quantity of total available heat generated would reach the occupants as far as thermal comfort of the occupants is concerned.

Natural and forced-convection heat transfer occurs due to the temperature difference between the tube surface and air in the room. A rise in temperature of the air by convective heat transfer would certainly contribute to thermal comfort of the occupants. The radiant intensity resulting from surface emission from the tube is, however, the principal mechanism to deliver thermal energy to the occupant. The tube surface emits radiative energy toward all of the other surfaces in all directions in the room. Typically, the tube heater includes a reflector, which is located above the tube that is intended to capture and focus heat that would otherwise transfer to the ceiling or other nonoccupied space. As a result, this intensity field is composed of direct radiant intensity from the tube itself and the reflected radiant intensity from the reflector.

### 3.2.1 Heat Transfer Model

Although the principle of energy transfer from a radiant tube heater to the surroundings is the same for all different designs, mathematical modeling of the heater varies depending on the geometric design and operating characteristics and assumptions. To provide basic concepts of the modeling scheme, this section illustrates one-dimensional modeling for the straight-through radiant tube heater.

The three basic principles of modeling a radiant heater and most thermal systems are conservation of (1) mass, (2) momentum, and (3) energy. Provided that there is a steady-state condition for an axially symmetric flow in the tube, these equations are (Chapman et al., 1988)

$$\frac{d(\rho W)}{dz} = 0 \quad (3.1)$$

$$\rho W \frac{dW}{dz} + \frac{dp}{dz} + \frac{2\tau}{r_i} = 0 \quad (3.2)$$

$$\dot{m}c_p \frac{dT_g}{dz} = h_i P_i (T_w - T_g) + \Delta h_{\text{fuel}} \frac{d\dot{m}_{\text{fuel}}}{dz} - P_i q''_{\text{rad}} \quad (3.3)$$

The subscript  $i$  stands for inside the tube;  $\Delta h_{\text{fuel}}$  represents the heat of formation of the fuel;  $P$  is the perimeter; and  $h$  represents the convective heat transfer coefficient. The shear stress,  $\tau$ , due to friction in the momentum equation, could be expressed as (Chapman et al., 1988)

$$\tau = \frac{\rho W^2}{8} f \quad (3.4)$$

The parameter  $f$  is the friction factor of the tube (refer to Sec. 2, Chap. 6 in this Handbook for more information on the friction factor). The fuel-air mixture is assumed to behave as an ideal gas, and the coexistence of air, fuel, and combustion product is also assumed at any axial location in the tube. To incorporate different compositions of each constituent at an arbitrary location, the notion of a fuel burn-up ratio is employed. This concept was introduced by Lisenko et al. (1986). The functional expression for the fuel burn-up ratio is the following:

$$k = 1 - \exp\left(\frac{-4z}{D_i} \text{Re}_D^{-0.3}\right) \quad (3.5)$$

The parameter  $D_i$  is the inner diameter of the tube. This correlation was developed through an extensive study by Lisenko et al. (1986) on combustion phenomena in the straight-through-type radiant heater. Using this parameter, the mass flow rates of each constituent could be expressed as (Chapman et al., 1988)

$$\dot{m}_{\text{fuel}} = \dot{m}_{\text{fuel initial}} (1 - k) \quad (3.6)$$

$$\dot{m}_{\text{air}} = \dot{m}_{\text{air initial}} (1 - \Phi k) \quad (3.7)$$

$$\dot{m}_{\text{product}} = \dot{m}_{\text{fuel initial}} + \dot{m}_{\text{air initial}} - (\dot{m}_{\text{fuel}} + \dot{m}_{\text{air}}) \quad (3.8)$$

The parameter  $\Phi$  is the equivalence ratio. The convective heat transfer coefficient in Eq. (3.3) and the friction factor in Eq. (3.4) should be evaluated depending on the flow condition that is either laminar or turbulent as explained in Sec. 2, Chap. 6 of this Handbook.

With the assumption of absorbing-emitting medium, the radiative heat transfer between the flowing gases inside the tube and the inner surface of the tube appearing in Eq. (3.3) can be expressed as (Chapman et al., 1988)

$$q''_{\text{rad}} = \frac{\varepsilon_{w_i} \sigma (\varepsilon_g T_g^4 - \alpha_g T_w^4)}{1 - (1 - \varepsilon_{w_i})(1 - \alpha_g)} \quad (3.9)$$

Neglecting axial conduction, the energy balance on the tube wall gives the following (Chapman et al., 1988):

$$h_i (T_g - T_w) + q_{\text{rad}_i} = \frac{r_o}{r_i} [h_o (T_w - T_{\text{surr}}) + q''_{\text{rad}_o}] \quad (3.10)$$

The convective heat transfer coefficient,  $h_o$ , was obtained assuming free convection at the outer tube surface.

At this point, it is finally possible to calculate the radiant tube surface temperature for a given flow rate through the tube. One has to simultaneously solve Eqs. (3.1) through (3.3), along with Eqs. (3.9) and (3.10). The gas emissivity and absorptivity in Eq. (3.9) can be obtained with the aid of the temperature and the pressure-path length product that has been studied by Hottel (1985). Calculating the tube surface temperature almost always requires the use of a computer to solve the complex equations. Solving these equations would be mandatory in order to design a new radiant tube heater. The tube manufacturer should be able to provide the external temperature that can then be used in thermal comfort calculations if one is interested in sizing a particular type of radiant tube. For the interested reader, Chapman et al. (1988) obtained the local tube wall temperature by solving Eq. (3.10) with the underrelaxed Newton-Raphson iteration during each predictor-corrector step.

### 3.3 HEAT TRANSFER FROM DIRECT RADIANT HEATERS

The surface combustion heater (see Fig. 3.7), which is a direct radiant heater, consists of a plenum chamber, porous plate, and reflector around the surface plate. Premixed air and hydrocarbon gas enter the plenum behind the surface plate, and combustion occurs within or at the surface of the porous plate. The flow rate and the ratio of air to fuel of the mixture noticeably affect the burning characteristics of the heater (Severens et al., 1995). The combustion incandesces the porous surface plate that then emits radiant energy to the surroundings. Both direct and reflected radiant intensity reach the occupants as the primary heat transfer mode. However, convective heat transfer takes place due to the temperature difference between the surface plate and the air surrounding the heater.

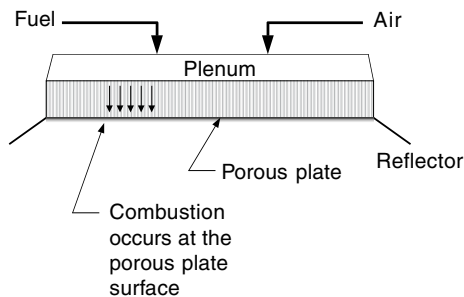


**FIGURE 3.7** Schematic showing the major components of a direct-fired surface radiant heater.

#### 3.3.1 Mathematical Modeling

Heat transfer modeling of direct-type heaters highly depends on the flame behavior of the burner surface. The primary mode of operation is to have the flame front near the burner surface. The burning gases then transfer heat to the porous structure. The porous structure then radiates to the surroundings. The porous structure of the

burner surface is almost always inhomogeneous causing temperature nonuniformity at the burner surface (Severens et al., 1995). When the fuel-to-air ratio is held at a constant value, the flow velocity of the gas mixture at the burner surface controls the flame behavior of the burner. Three different situations of flame behavior could be observed with varying gas mixture flow velocity: (1) within the porous structure, (2) at the porous structure surface, and (3) blown off the porous structure.

Severens et al. (1995) studied the operation of a porous surface burner for a wide range of flow velocity at the surface. When the flow velocity is near the low end, the location of the combusting flame is within the porous burner plate. With increasing flow velocity, the flame location moves toward the burner surface. Usually, when the flame is stabilized at or just beneath the burner surface, it is considered ideal operation because conduction from the flame to the burner surface is optimal and the burner surface temperature is at its peak. This occurs at a flow velocity much lower than the adiabatic flow velocity (Severens et al., 1995). As the flow velocity approaches to the adiabatic flow velocity, the flame departs and can actually blow off from the surface. The burner surface temperature continuously decreases with this transition. Because of nonuniformities within the porous structure, this transition of flame behavior does not occur simultaneously for the entire surface. It is possible for one surface region to exhibit a stabilized flame front while the flame is blown off another portion of the surface (Severens et al., 1995). When all the flames over the entire surface leave the surface of the burner plate at a high-flow velocity, conduction from the flame to the burner is nearly zero. At this condition, radiant transfer is limited to that which volumetrically emits from the gases. Because the gases are not heating the burner surface, the surface no longer radiates, thereby limiting the performance of the heater.

Severens et al. (1995) observed an important relationship between the pressure drop through the porous burner plate and the flame behavior. Both the viscosity and density of the gas mixture are a function of temperature. Temperature dependence of the gas mixture density and viscosity could be accounted for with the notion of ideal gas law and an empirical study by Bird et al. (1960):

$$\rho(x) = \rho_0 \frac{T_{g,0}}{T_g(x)} \quad (3.11)$$

$$\mu(x) = \mu_0 \left( \frac{T_g(x)}{T_{g,0}} \right)^m \quad (3.12)$$

The subscript 0 indicates the mixture state entering the porous plate, and temperature varies at any position  $x$  from the entrance of the pores. The exponent  $m$  was found to be between 0.6 and 0.7 (Bird et al., 1960). Based on conservation of mass, the mixture velocity flowing through the plate changes as follows:

$$u(x) = u_0 \frac{\rho_0}{\rho(x)} \quad (3.13)$$

Then the rate of pressure drop of the gas mixture at any location of  $x$  can be expressed as (Severens et al., 1995):

$$\frac{dp}{dx} = c_1 \mu_0 u_0 \left( \frac{T_g(x)}{T_{g,0}} \right)^{m+1} + c_2 \rho_0 u_0^2 \frac{T_g(x)}{T_{g,0}} \quad (3.14)$$

The coefficients  $c_1$  and  $c_2$  are determined by geometric configuration of the porous structure. The integration of Eq. (3.14) requires finding the mixture temperature

variance within the porous structure. Assuming combustion occurs outside of the porous structure, the energy balance within the plate yields the following (Severens et al., 1995):

$$\phi \left[ \rho_0 \left( \frac{u_0}{\phi} \right) c_p \frac{\partial T_g}{\partial x} - \frac{\partial}{\partial x} \left( k_g \frac{\partial T_g}{\partial x} \right) \right] = hS(T_s - T_g) \quad (3.15)$$

$$-(1 - \phi) \frac{\partial}{\partial x} \left( k_s \frac{\partial T_s}{\partial x} \right) = -hS(T_s - T_g) \quad (3.16)$$

The variables  $T_s$ ,  $k_s$ ,  $k_g$ ,  $c_p$ ,  $h$ , and  $S$  are the solid temperature, solid thermal conductivity, gas thermal conductivity, gas specific heat, the heat transfer coefficient within the porous structure, and the specific surface area that is wetted per unit volume. The thermal conductivity of the gas may include the effect of radiation within the plate. The gradient of porosity,  $\phi$ , is neglected in the preceding equations. Provided that  $c_p$ ,  $k_g$ ,  $k_s$ , and  $h$  are independent of temperature, and radiation takes place only at the surface of the plate, a fourth-order differential equation can be obtained (Severens et al., 1995):

$$\begin{aligned} \rho_0 c_p u_0 \frac{\partial T_{g,s}}{\partial x} - [\phi k_g + (1 - \phi) k_s] \frac{\partial^2 T_{g,s}}{\partial x^2} \\ - \rho_0 c_p u_0 \frac{\phi(1 - \phi)}{hS} k_s \frac{\partial^3 T_{g,s}}{\partial x^3} + k_g k_s \frac{\phi(1 - \phi)}{hS} \frac{\partial^4 T_{g,s}}{\partial x^4} = 0 \end{aligned} \quad (3.17)$$

In Eq. (3.17),  $T_{g,s}$  denotes  $T_g$  or  $T_s$ . Applying the corresponding boundary conditions and neglecting insignificant terms that are based on the experiment data, the solution to Eq. (3.16) can be well approximated with a block profile that gives (Severens et al., 1995):

$$T_g(x) = \begin{cases} T_{g,0} & \text{if } 0 < x < L - \delta \\ T_{g,\text{surf}} & \text{if } L - \delta < x < L \end{cases} \quad (3.18)$$

The variable  $L$  is the thickness of the plate, and  $\delta$  is given by (Severens et al., 1995):

$$\delta = \frac{\phi k_g + k_s(1 - \phi)}{\rho_0 u_0 c_p} \quad (3.19)$$

Upon investigating the boundary conditions necessary for the solution of Eq. (3.18), it was found to be reasonable to assume  $T_{s,\text{surf}} \cong T_{g,\text{surf}}$  (Severens et al., 1995). With the assumption of one-dimensional flame behavior and energy consumption by radiation occurring only at the surface of the burner plate, the energy balance at the burner surface yields (Severens et al., 1995):

$$\rho_0 u_0 c_p (T_b - T'_b) = \epsilon \sigma (T_{s,\text{surf}}^4 - T_{\text{sur}}^4) \quad (3.20)$$

where  $T_b$ ,  $T'_b$ , and  $T_{\text{sur}}$  are the adiabatic, nonadiabatic, and surrounding temperatures, respectively. The variable  $\epsilon$  represents the emissivity of the burner surface, and  $\sigma$  is the Stefan-Boltzmann constant. In Eq. (3.20), the constant specific heat and the emissivity for the temperature range between  $T_b$  and  $T'_b$  are assumed. A burner-stabilized flame occurs when the mixture gas velocity is at a nonadiabatic velocity of  $v'_L$ . Many researchers have studied the relationship between the nonadiabatic flame temperature and velocity. Among them, Kaskan (1967) empirically found the following relationship:

$$u = ke^{-E_a/2RT'_b} \quad (3.21)$$

The value of the coefficient,  $k$ , with an effective energy activation,  $E_a$ , was obtained through experiments by Kasan (1967). The variable  $R$  appearing in Eq. (3.21) is the universal gas constant. Equation (3.21) is valid only when the reaction takes place outside the porous plate (Severens et al., 1995). Then the relationship between the adiabatic temperature and velocity was found as follows (Severens et al., 1995):

$$\frac{v'_L}{v_L} = \exp\left(-\frac{E_a}{2RT'_b} + \frac{E_a}{2RT_b}\right) \quad (3.22)$$

Combining Eqs. (3.20) and (3.22) with experimentally determined values of  $T'_b$  and  $v_L$  gives the surface temperature as a function of the gas mixture velocity (Severens et al., 1995):

$$T_{\text{surf}}^4 = \begin{cases} T_{g,0}^4 + \frac{\rho_0 u_0 c_p T_b}{\varepsilon \sigma} \left[ 1 - \frac{E_a}{2RT_b \ln\left(\frac{u_0}{v_L}\right)} \right] & \text{if } u_0 < v_L \\ T_{g,0}^4 & \text{if } u_0 > v_L \end{cases} \quad (3.23)$$

The calculated plot is of the burner surface temperature with varying average gas mixture velocity that enters the burner plate from the back. In their study, methane was used for fuel. When the velocity exceeds the adiabatic burning velocity, all of the flame is blown off from the surface, and the heat from the flame does not transfer to the burner surface any longer despite an increase in the flame temperature itself (Severens et al., 1995).

### 3.4 APPLICATIONS

The most attractive advantage of a radiant heater is its capability to supply heat to the occupants without having to use the surrounding air as the medium of energy transfer. This is the major reason why radiant heaters have been used for large open spaces such as an aircraft hangar or storage. Radiant heating is considered more energy-efficient than the warm-air heating, especially for spaces that have a high air change rate per hour. For example, ASHRAE Standard 90.1 requires the use of radiant heaters when unenclosed spaces such as loading docks need to be heated. Either gas or electric units may be used (see Fig. 3.8).

To maintain thermal comfort and energy performance, combustion design parameters must be maintained. Thermal cutoffs limit combustion extremes, but thermal performance can vary within the cutoff ranges. These thermal cutoffs and adjustments must be maintained within the design specifications specified by the manufacturer.

#### 3.4.1 Radiant Heating Design

The ASHRAE *Handbook of Fundamentals* outlines system modeling and energy estimating strategies for heating system designs that have been widely accepted by engineers. Following this ASHRAE standard method, various manufacturers have developed heating design guidebooks. These guidebooks usually summarize a heat-

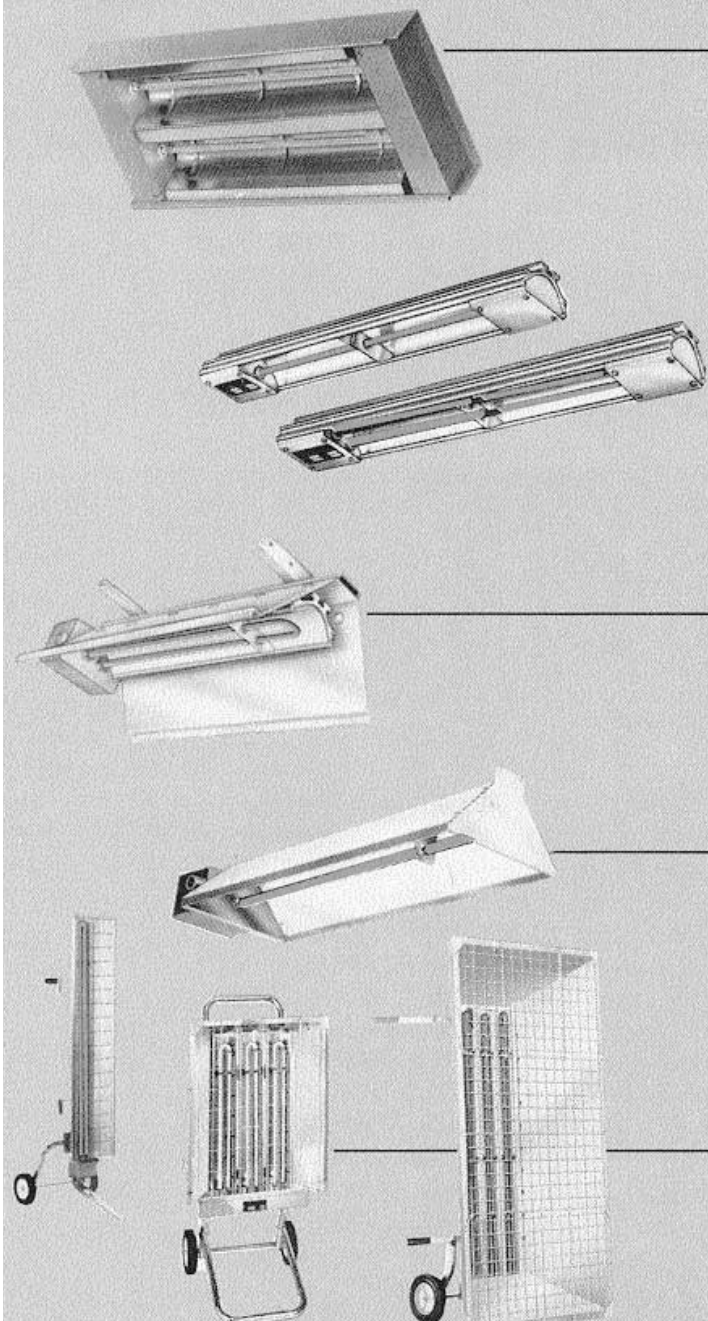


**FIGURE 3.8** Electric high-temperature, various-wattage heaters. (Photo courtesy of Aitken.)

ing system design procedure that can be used for radiant heaters. The reader should realize, however, that these methods are not based on delivering thermal comfort but, instead, are based on an energy balance for the room. As discussed in Sec. 4, Chap. 3 of this Handbook, a better method is to base designs on thermal comfort delivery. However, the method described here is to illustrate the common approaches in use today. These approaches will be contrasted in the last section of this Handbook by comparing the localized comfort delivery-based strategies with the energy-based strategies.

Based on the first law of thermodynamics, determination of the amount of heat required to accomplish a desired heating for any space relies on estimation of heat loss of the space. Estimation of heat loss involves obtaining the total transmission loss through the walls, roof, and floor of the space to be heated and amount of air passing through the space per unit time. To develop these factors, a complete survey of the space to be heated is necessary. The survey basically includes the desired inside temperature, outside design temperature, building construction, and anything that affects the rate of air change per hour.

The  $R$  value for each wall, roof, and floor of the conditioned space needs to be determined. The  $R$  value, described in Sec. 4, Chap. 2 of this Handbook, is resistance to heat transfer through a solid surface. The higher the  $R$  value, the lower the heat transfer rate through the surface. The lists of  $R$  values are available in the ASHRAE Handbook for common materials. For new insulation products, consult the manufacturer.

Desired inside temperature varies depending on usage of the building and customer's preference. It is common for manufacturers of high-temperature radiant heating systems to suggest the inside temperature. This temperature is typically between 8°F and 10°F lower than the dry-bulb air temperature for a conventional warm-air heating system to achieve the same level of thermal comfort. [Note: This approximates in a rough way the effect of the mean radiant temperature (MRT). Indirectly, this approach attempts to size radiant heaters based on thermal comfort delivery.] This approach is an approximation of the level of thermal comfort measurement that should be based on the operative temperature (OT) rather than the dry-bulb air temperature in the case of radiant heating.

The outside design temperatures are presented in the ASHRAE *Handbook of Fundamentals* for various cities. With the design temperature, the total transmission loss for the building can be calculated by the following expression:

$$q_{\text{trans loss}} = \sum_{i=1}^N \left[ \frac{A_i(T_{\text{inside}} - T_{\text{outside}})}{R_i} \right] \quad (3.24)$$

where  $N$  is the number of enclosure elements of the room (normally, six), and  $R_i$  and  $A_i$  are the  $R$  value and area of the corresponding element, respectively.

The infiltration and ventilation rates also affect the sizing and placement of radiant heaters. The heat loss through the exchange of room air is based on the estimation of air change rate and infiltration rate, which is a function of the outside wind velocity, atmospheric pressure, building design, and various other key factors. The number of doors and their frequency of use and any powered exhaust are main factors that determine the rate in addition to recommended minimum rate to maintain the room comfort at a design OT. The heat loss through air change is the product of the air change rate plus infiltration rate, air specific heat, and design temperature difference between inside and outside:

$$q_{\text{air loss}} = \dot{V}_s \rho_s c_p (T_{\text{inside}} - T_{\text{outside}}) \quad (3.25)$$

In Eq. (3.25),  $c_p$  is the specific heat of air at standard temperature and atmospheric pressure, and the density  $\rho_s$  is the standard density of air. The sum of the transmission loss and air loss is the total heat loss for the building. Heat gains are those from lights, equipment, occupants, and solar radiation transmitted through the windows. Finally, the required heat input to accomplish the design inside temperature would be expressed as

$$q_{\text{input}} = \frac{1}{\eta} (q_{\text{trans loss}} + q_{\text{air loss}} - q_{\text{heat gain}}) \quad (3.26)$$

where  $\eta$  is the efficiency of the radiant heaters. Therefore, the appropriate heater size would be the product of the heat input and the efficiency. Again, the reader should realize that this method of sizing a heater does not take advantage of thermal comfort delivery as measured by OT.

### 3.4.2 Optimal Use of Radiant Heaters

The concept of spot or area heating would be of importance to optimally utilize radiant heaters for some practical applications such as warehouses and aircraft hangars. It is especially suitable for a case in which heating is desired in only a certain area of the whole space. The definition of spot heating is to maintain no net heat loss of an individual surface by providing the heat that is equal to the surface heat loss of the individual. The spot and area heating differ only by the size of area for which the radiant intensity field is desired. The optimum location of the heater would depend on the geometry of the reflector and the availability of the space to evaluate the size of radiation intensity field (see Fig. 3.9).

High-temperature heater locations relative to glass must be carefully analyzed because window glass is not completely opaque to the short-wavelength heater. High-temperature heaters located close to outside windows will radiate a significant amount of heat directly to the outside. Design analysis must factor in the impact of high-temperature heater location on equipment sizing.

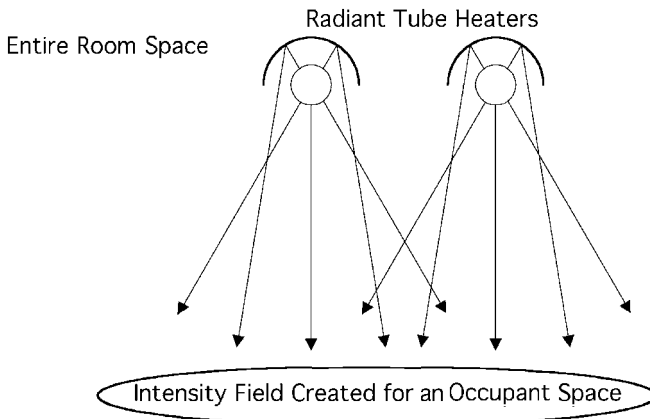


**FIGURE 3.9** Area heater's creation of an intensity field.

### 3.5 VENTILATION CONSIDERATION

The porous structure that is utilized for the burning surface induces continuous conduction from the flame to the surface plate. At a relatively low flow velocity, this phenomenon appreciably lowers the flame temperature compared with the other conventional combustion process and results in a significant reduction in polluting products such as nitrogen oxides (Severens et al., 1995). Regardless of this significant decrease in polluting emissions, use of direct radiant heaters still requires a higher rate of ventilation than that of indirect radiant heaters. This is due to the fact that the combusting surface is directly exposed to the surroundings. Required ventilation of room air lowers the room temperature that then influences estimating either body surface heat loss of the occupants or simply net heat loss of the building, in relation to the temperature of the ventilating air.

### 3.6 RELATIVE HUMIDITY AND THE ABSORPTION COEFFICIENT

Air as a transparent gas is normally considered a radiatively nonparticipating gas except when its temperature is extremely high. However, water vapor certainly absorbs and/or emits radiative energy. This indicates an effect of the moisture content of the ambient air on the radiative heat exchange of a system containing ambient air. A quantity that is often used to express the amount of water vapor content in the ambient air is the *relative humidity*. Therefore, to incorporate the effect of moisture content in the air into the radiative heat exchange analysis, a correlation between the relative humidity and the *absorption coefficient* of the water vapor may be desirable. The absorption coefficient is a parameter that appears in the radiative transfer equation (Sec. 2, Chap. 3 of this Handbook) and determines the attenuation of the radiative energy by the medium, which in this case is humid air. It is known that water vapor is an important participant of radiative heat exchange at high temperature as for radiation of combustion product. The following sections present the fundamental ideas to establish the relationship between relative humidity and the absorption coefficient for humid air.

#### 3.6.1 Absorption in Gas Layers

As shown in Fig. 3.10, for a beam of radiation that penetrates a gas layer in a coordinate system, the spectral intensity along this beam can be written as (Özişik, 1977)

$$\frac{dI_{\lambda}(S)}{dS} + \kappa_{\lambda}I_{\lambda}(S) = 0 \quad (3.27)$$

In Eq. (3.27),  $dI_{\lambda}$  is the spectral absorption coefficient of the gas layer. The solution to this differential equation with an appropriate boundary condition gives

$$I_{\lambda}(S) = I_{\lambda 0}e^{-\kappa_{\lambda}S} \quad (3.28)$$

where  $I_{\lambda 0}$  is the spectral intensity evaluated at  $S = 0$ . When the thickness of the medium that the beam penetrates is a length  $L$ , the spectral intensity at the location  $L$  is evaluated as

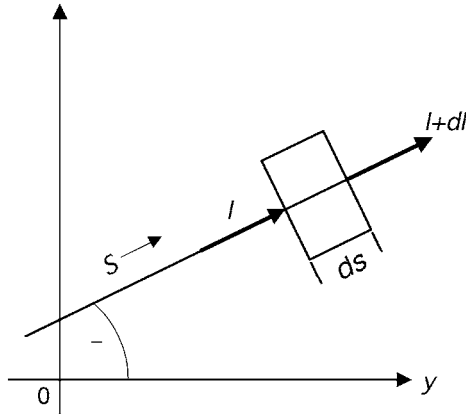


**FIGURE 3.10** Intensity beam in a space. (Source: Özişik, 1977.)

$$I_{\lambda}(L) = I_{\lambda 0} e^{-\kappa_{\lambda} L} \quad (3.29)$$

The decrease in the intensity between  $S = 0$  and  $S = L$  is the spectral radiation attenuated by the gas layer of its thickness  $L$ . This can be written as (Özişik, 1977)

$$I_{\lambda}(0) - I_{\lambda}(L) = I_{\lambda 0}(1 - e^{-\kappa_{\lambda} L}) \quad (3.30)$$

Equation (3.30) leads to obtain the spectral absorptivity,  $\alpha_{\lambda}$ , of the gas layer that forms the following relation (Özişik, 1977):

$$\alpha_{\lambda} \equiv 1 - e^{-\kappa_{\lambda} L} \quad (3.31)$$

Equation (3.31) shows a direct relationship between the absorptivity and the absorption coefficient of the gas layer for a known beam length of radiation. This beam length can be determined by the notion of mean beam length for any desired geometry. To solve Eq. (3.31) for the absorption coefficient, the absorptivity of the gas must be found.

### 3.6.2 Absorption Coefficient, Absorptivity, and Emissivity of Water Vapor

Accurately evaluating either gas absorption or emission is a very complicated matter that involves quantum physics. The spectral nature of gaseous matter attributes to this complexity. To avoid delving into the quantum physics of gaseous matter, a simpler and more convenient method to evaluate gas absorptivity is desirable for a practical engineering calculation.

Hottel developed a simplified method to estimate the total emissivity and absorptivity of water vapor within a nonradiating gas. The word *total* in this case means that the emissivity and absorptivity were averaged over all wavelengths, and the total quantity is often preferred to the spectral quantity for a typical engineering calculation. The gas was assumed to have a hemispherical volume at a uniform temperature. The emissivity of the water vapor was correlated with its temperature, partial pressure, the total pressure of the entire gas, and the radius of the hemisphere.

The experimental results of water vapor emissivity, conducted by Hottel et al., are available as a chart with any arbitrary given parameter values. Because these empirical results were based on the total gas pressure of 1 atmosphere (atm), the emissivity obtained from the chart must be multiplied by a correction factor for gas mass having its total pressure other than 1 atm. Hottel et al. also developed a chart of the correction factors. The notion of mean beam length must be incorporated for any arbitrary shape of gas mass inasmuch as the charted values are valid for a hemispherical gas volume.

The emissivity for water vapor that can be obtained from Hottel's charts is a total value for a given pressure and temperature. They were experimentally measured values that included some extrapolations. Leckner and others also investigated the water vapor emission. For homogeneous gases, it was found that values for extrapolated regions from Hottel's charts did not agree well with the calculated values based on statistically available spectral data (Leckner, 1972). Leckner also formed a chart for water vapor emissivity with the same parameters as the ones used in Hottel's chart. The results of Leckner agreed with the ones derived by some other investigators, such as Ludwig et al., who also studied water vapor emissivity after Hottel (Modest, 1993). For the purpose of computer programming, Leckner also developed a functional expression of the emissivity that was consistent with his results. This expression has less than  $\pm 5$  percent maximum error with the chart for temperatures greater than  $100^\circ\text{C}$ . These studies focus more on the higher temperature range of gases because of their particular interest in radiative transfer of combustion products. However, some data for the range of room temperature could be developed from these studies.

The functional relationship for the emissivity and absorptivity of water vapor for their charts are the following (Modest, 1993).

$$\varepsilon = \varepsilon(p_g L_m, p, T_g) \quad (3.32)$$

$$\alpha = \alpha(p_g L_m, p, T_g, T_s) \approx \left(\frac{T_g}{T_s}\right)^{0.5} \varepsilon\left(p_g L_m \frac{T_s}{T_g}, p, T_s\right) \quad (3.33)$$

The temperatures  $T_g$  and  $T_s$ , shown in Eq. (3.33), are the temperatures of the water vapor and an external blackbody heat source surface, respectively (Modest, 1993).

### 3.6.3 Partial Vapor Pressure and Relative Humidity

The partial pressure of water vapor is a parameter that must be known to obtain the emissivity and absorptivity for a given state of the gas mixture containing dry air and water vapor. The relative humidity relates directly to the partial pressure of the water vapor within humid air. The relative humidity measures the ratio of the mol fraction of water vapor to the mol fraction of the maximum moisture possible, which is saturated condition, within the given moist air. The relative humidity, normally denoted by  $\phi$ , is defined as (Moran and Shapiro, 1992)

$$\phi = \left(\frac{y_v}{y_{v,\text{sat}}}\right)_{T,p} \quad (3.34)$$

In Eq. (3.34),  $y_v$  is the mol fraction of water vapor in a given moist air, and  $y_{v,\text{sat}}$  is the mol fraction of the saturated vapor at the same mixture temperature,  $T$ , and pressure,  $p$ . Because the partial pressure of the water vapor is directly proportional to its mol fraction, Eq. (3.34) can also be written as (Moran and Shapiro, 1992)

$$\phi = \left( \frac{p_v}{p_g} \right)_{T,p} \quad (3.35)$$

where  $p_v$  is the partial pressure of the water vapor actually present in the sample air, and  $p_g$  is the pressure of the saturated vapor at the temperature and pressure of the sample. Then, solving Eq. (3.35) for the vapor partial pressure readily results in the following expression:

$$p_v = \phi p_g(T) \quad (3.36)$$

The saturated vapor pressure could be determined for given pressure and temperature of the moist air. Therefore, the partial pressure of water vapor for the same humid air is obtainable with a given relative humidity.

### 3.6.4 Effect of Humid Air on the Radiative Intensity Field

The foregoing sections illustrate an approach to evaluate the absorption coefficient for moist air that would be present for a radiant heating, thermal comfort calculation. Once the absorption coefficient of the humid air is found, the radiative transfer equation can be solved, including the effect of medium absorption. When sizing a radiative heater for thermal comfort delivery, one should take air humidity into consideration unless it can be proven insignificant. Because combustion products contain significant moisture levels, the analysis of high-temperature direct heaters should always include the effect of humid air.

To examine the effect of radiative energy absorption by moist air, simple radiant heating models were simulated using the discrete-ordinate module solver described in Sec. 2, Chap. 3 of this Handbook. Three different dimensions of rectangular parallelepiped geometry were used to implement these simulations. The schematic that describes the geometry for the simulations is shown in Fig. 3.11.

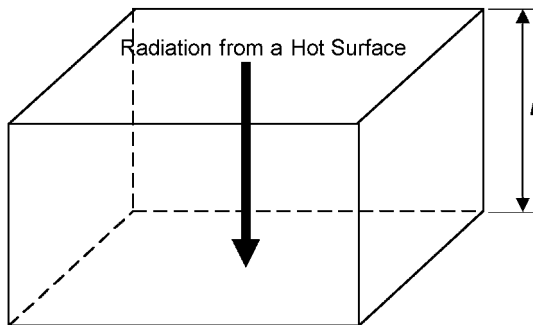


FIGURE 3.11 Schematic of simulation geometry.

The top and bottom surfaces have the same dimensions of  $100 \times 100$  m, and they were maintained the same throughout all simulations. All the surfaces were assumed to be blackbody. The temperature of the top surface and the other surfaces were also kept unchanged at 500 K and 290 K, respectively. The distance,  $L$ , was varied with

three different values of 1, 5, and 10 m. For each distance of  $L$ , a fraction of the radiation from the top surface would reach the center of the bottom surface was observed for three different medium temperatures of 280 K, 290 K, and 300 K with varying relative humidity.

During these simulations, the spectrally averaged absorption coefficient was repetitively evaluated for each situation of different distance  $L$ , medium temperature, and relative humidity. The total medium pressure of 1 atm was assumed for every situation. First, the saturated vapor pressure for each given temperature was directly utilized from a table of saturated vapor under a constant total pressure of 1 atm. The product of this saturated vapor pressure and a relative humidity gave the partial pressure of the vapor that was present in the medium air. Under the optically thin medium assumption that is almost always valid for a gaseous medium, Eq. (3.28) was used to evaluate the averaged mean beam length for a given geometry. Leckner's functional expression of the vapor emissivity in Eq. (3.33) was used to evaluate the absorptivity. This expression is a set of two second-order polynomials. The original polynomial expressions of Leckner (1972) to obtain the vapor emissivity of Eq. (3.32) follow:

$$\ln \varepsilon = a_0 + \sum_{i=1}^2 a_i \lambda^i \quad (3.37)$$

$$a_i = c_{0i} + \sum_{j=1}^2 c_{ji} \tau^j \quad (3.38)$$

The variable  $\lambda$  in Eq. (3.37) and  $\tau$  in Eq. (3.38) are defined as

$$\lambda = \log p_g L_m \quad (3.39)$$

$$\tau = T_g / 1000 \quad (3.40)$$

Nonetheless,  $p_g L_m$  in Eq. (3.39) and  $T_g$  in Eq. (3.40) were replaced by  $p_g L_m (T_s / T_g)$  and  $T_s$ , respectively, to obtain the vapor absorptivity. The values of coefficients  $c_{ji}$  for Eq. (3.37) are listed in Table 3.1.

**TABLE 3.1** Coefficient Values for Eq. (3.37)

$i$	$c_{0i}$	$c_{1i}$	$c_{2i}$
0	-2.2118	-1.1987	0.035596
1	0.85667	0.93048	-0.14391
2	-0.10838	-0.17156	0.045915

Source: Leckner, 1972.

Once the absorptivity was determined, Eq. (3.31) without spectral dependence was solved for the spectrally averaged absorption coefficient with the parameter  $L$  being the averaged mean beam length. Figure 3.12 shows a graph containing nine different plots that resulted from the simulations. The quantity on the vertical axis,  $\psi$ , is the nondimensional heat flux that is the ratio of irradiation flux at the center of the bottom surface to the net radiation flux from the top surface that would

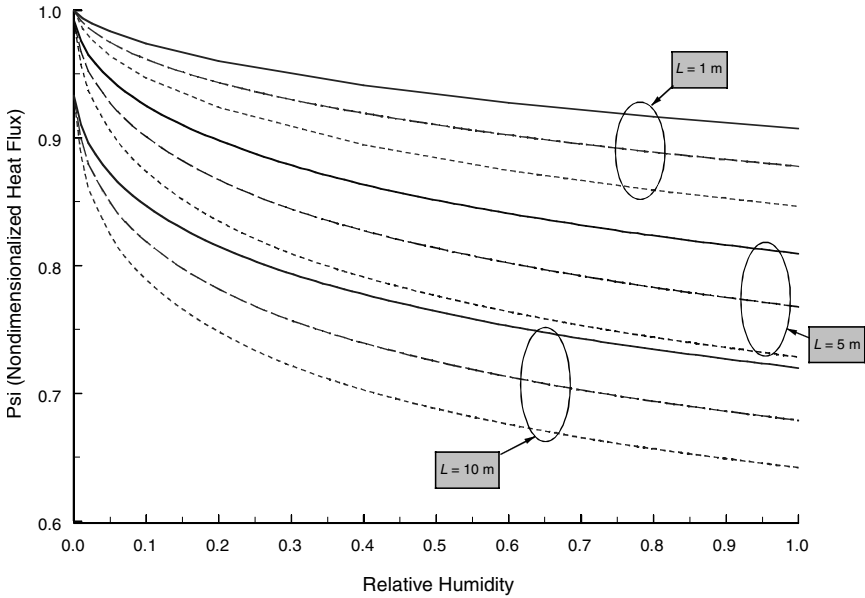


**FIGURE 3.12** Impact of relative humidity on radiation heat transfer.

occur for the temperature difference between the two surfaces. It is mathematically defined as

$$\Psi = \frac{q''_{\text{irradiation}}}{\sigma(T_{\text{top}}^4 - T_{\text{bottom}}^4)} \quad (3.41)$$

This parameter illustrates how much radiation leaving the ceiling arrives at the floor.

Solid lines, coarsely dashed lines, and finely dashed lines represent the medium temperatures of 280 K, 290 K, and 300 K, respectively. The larger quantity of the distance  $L$  means the thicker medium of the moist air at each given relative humidity. As medium gets thicker, less radiation reaches the center of the bottom surface. Because of the increase in saturated vapor pressure, higher medium temperature results in more absorption by the medium.

At the distance  $L$  equal to 10 m, about 93 percent of the radiant energy leaving the ceiling reaches the bottom surface center for zero relative humidity. While radiant beams from the top travel to reach the bottom, they become spread out and some of them intercept the other walls. This is why all the radiant heat flux from the top does not reach the bottom center even for the zero relative humidity case. However, for  $L$  equal to 1 m with zero relative humidity, almost all of the emitted radiation from the top surface is absorbed by the bottom center surface. As the relative humidity increases, less radiative flux arrives at the bottom center for all different situations of the medium temperature and the distance  $L$ . This is due to the increased absorption coefficient and, hence, increased absorption by the humid air medium.

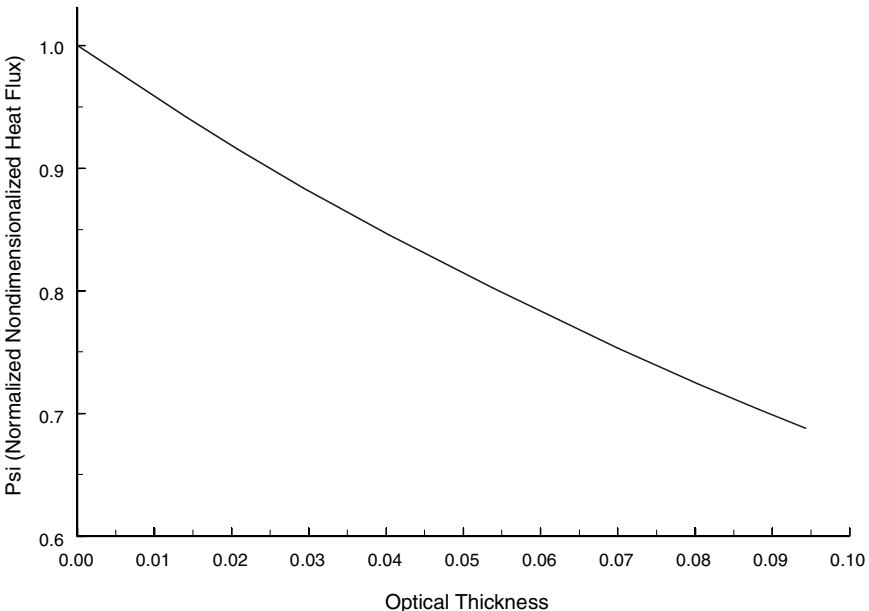
For instance, at the medium temperature of 290 K with the relative humidity of 70 percent that could be a practical value during the winter, only about 80 percent of the radiation flux reaches the bottom center for the distance  $L$  of 5 m. In other words, the medium air absorbs nearly 20 percent of the radiation flux emitted from the top surface.

Figure 3.13 shows how the nondimensional heat flux changes with respect to the optical thickness for the medium temperature of 300 K and the distance  $L$  of 10 m. The optical thickness is a nondimensional representation of the medium size and level of radiative participation. Mathematically, the optical thickness is the product of the absorption coefficient and the medium characteristic length. The medium characteristic length is the ratio of the volume,  $V$ , and the surface area,  $A_s$ , of the medium that is defined as

$$L_c = \frac{V}{A_s} \quad (3.42)$$

The optical thickness is a nondimensional quantity, and it physically represents the absorbing density of the medium. The largest optical thickness that occurs during the simulations was 0.095.

When the absorption coefficient for each situation of the simulations was evaluated, Leckner's functional expression of vapor emissivity was employed. Leckner's expression has a maximum error of less than  $\pm 5$  percent to evaluate the emissivity for the vapor temperatures higher than 100°C as mentioned earlier. The simulations utilized three different medium temperatures of 280 K, 290 K, and 300 K that are 7°C, 17°C, and 27°C, respectively. This implies that the results of the simulations



**FIGURE 3.13** Optical thickness versus radiative heat transfer.

may contain errors that would be greater than  $\pm 5$  percent. Even taking this possible error into account during the simulations, a noticeable effect of the absorption of radiative energy by the moist air could not be denied.

In general, high-temperature radiant equipment sizing and operating characteristics will be impacted significantly by the presence of high relative humidity. Whether these conditions are transient or normal for the application will determine the level of impact to be considered in system design.

---

# CHAPTER 4

---

# RADIANT HYDRONIC HEATING SYSTEMS

---

## **4.1 INTRODUCTION TO RADIANT HYDRONIC SYSTEMS**

---

Radiant hydronic heating systems accomplish heat delivery by means of panels that transfer 50 percent or more of total panel energy radiantly, a characteristic by which the ASHRAE Handbooks define all radiant systems. The distinguishing feature of radiant hydronic heating systems is the use of a liquid or fluid to transfer heat from the originating source to the radiant panel at the location of heat delivery. The focus of this chapter is the development of information about hydronic heating panel design, performance, and control characteristics.

Radiant hydronic systems employ a broad range of radiant panel configurations located on or in the floor, wall, or ceiling. The performance characteristics are impacted by the planar selection. Occupant proximity to the heat source, the split between radiant and convective heat transfer, and potential for heat-obstructing or surface-covering materials—all are important considerations in plane selection for radiant heat delivery. Each location can accommodate a broad selection of hydronic equipment and design options.

Common radiant hydronic panels encompass a variety of floor design options to accommodate the complex range of new and existing building architectural requirements. Even though radiant hydronic floor systems normally embed the heat transfer conduit directly into the floor as the panel, the heat transfer conduit may also be placed on the underside of the floor. Each radiant floor panel design should be analyzed carefully to determine its unique performance requirements, as planned, as it could be installed, and as it might later be used.

Radiant hydronic wall panels include embedded and surface-mounted systems. Old-fashioned radiators are, in fact, not considered radiant panels, as heat transfer is often more than 70 percent convective. However, large-panel-face, narrow-profile, wall-mounted radiant hydronic panels transfer a larger portion of heat radiantly than the cast-iron radiators that heated the buildings of yesteryear, and are included in the review of radiant hydronic systems.

Embedded radiant hydronic ceiling systems were more common in the United States in the 1940s, when ceilings were composed of lathe and plaster, in which copper or iron piping was embedded. For such applications, narrow-profile polymeric conduit and mats have replaced metal for embedded radiant hydronic ceiling systems. A less expensive design routes flexible conduit through the ceiling joists above

the topside of the ceiling surface or under the subfloor for floor heating. Insulation is placed above or below the conduit to maximize panel face heat output.

Metal panels are more common for hydronic ceiling heating in commercial and institutional applications. Metal panels transfer heat radiantly that is delivered by copper conduit routed through heat transfer brackets integral to the panel. Manufactured radiant hydronic ceiling panels are made of various metal alloys and designs. Metal radiant hydronic panels may be installed flush with the ceiling or surface-mounted on the ceiling. The performance characteristics of each of the radiant ceiling panel equipment and design selections are unique. Each alternative should be carefully designed to ensure that desired comfort and energy performance is achieved.

## 4.2 COMPONENT FEATURES

Much of the credit for the resurgence of radiant hydronic heating is attributed to the development of various semirigid and flexible polymeric tubing materials. Cross-linked polyethylene tubing, known simply as *PEX* (Fig. 4.1), has largely replaced metal conduit in designing low-temperature, concealed radiant hydronic panels. Although there are proprietary chemical and production formulations for different

brands of *PEX*, the common performance characteristic is very long life.

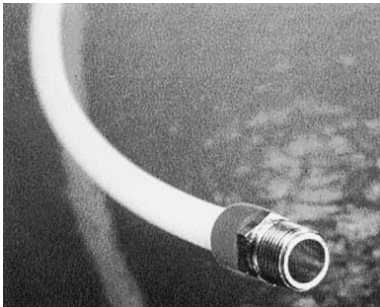


**FIGURE 4.1** PEX tubing with connection fitting. (Photo courtesy of Rettau.)

Performance standards for a pressure-rated in-floor heating application are contained in ANSI/NSF Standard 14. Products meeting these standards, which are tested by NSF, carry the End Use Mark NSF-rfh. Field failures that have occurred may be due to formulation failure, faulty fittings, or failure to adequately test the systems at each step. Each product specification should conform to testing standards that at least mirror field performance exposure. All specifications should be carefully reviewed in relation to the demands of the planned installation.

Warranties require careful examination to determine the nature of coverage and use process required to ensure that the warranty applies in the event of product failure. There is an abundance of material, components, and equipment to choose from that perform dependably and have a very long life when installed in conformance with good design practice.

Advantages of *PEX*, compared with metal, are that the conduit is nontoxic and free of lead, copper, and other metal ions that can complicate the choice of heat transfer fluid and fittings. *PEX* generally survives mild freezing without the failures encountered with other conduit options. *PEX* tubing is also used for potable water distribution, including hot water. Cross-linking provides strength under pressure as well as chemical, high-temperature, and water pressure stability, and the flexibility required for installation design formation.

Of equal importance for the increase in performance reliability of radiant hydronic heating is the development of long-lived, noncorrosive metal fitting alloys.

The alloys are used to make connection fittings and control valves engineered for use with the cross-linked polyethylene tubing for radiant heating installations. Some fittings may require special tools. The combination of conduit, connection, housing, and valve material improvements has virtually eliminated leaks and contamination due to material failure or chemical reaction. The chance for faulty installation due to component manufacture materials is virtually eliminated through proper design material specification. Careful inspection at each step in the installation process, coupled with system cleanout and flushing, heat transfer fluid filtration, and performance pressure testing at each stage of start-up, in spite of the significant time investment, remains the best insurance against costly leaks and performance surprises.

Steel and aluminum alloys are employed for both wall and ceiling panels, as well as for flooring and underfloor heat transfer plates. Brass of various alloys is used for connectors, manifolds, and valves. Conduit layout, component selection, and panel material composition each impact radiant panel performance. The details of each variable are important design determinants that must be included in the comprehensive system design. (See Table 4.1.)

**TABLE 4.1** Thermal Conductivity of Typical Tube Material

Material	Thermal conductivity, $k_t$ [Btu/(h · ft · °F)]
Carbon steel (AISI 1020)	30
Copper (drawn)	225
Red brass (85 Cu-15 Zn)	92
Stainless steel (AISI 202)	10
Low-density polyethylene (LDPE)	0.18
High-density polyethylene (HDPE)	0.24
Cross-linked polyethylene (VPE or PEX)	0.22
Textile-reinforced rubber heat transfer hose (HTRH)	0.17
Polypropylene block copolymer (PP-C)	0.13
Polypropylene random copolymer (PP-RC)	0.14
Polybutylene (PB)	0.13

### 4.3 DESIGN CHARACTERISTICS

The insulation and routing of heat transfer plumbing lines or circuit tails is important for the overall performance and energy efficiency of the system. ASHRAE SPC-152P, *Method of Test for Determining the Steady-State and Seasonal Efficiencies of Residential Thermal Distribution Systems*, details a methodology for determining the heat loss from the point of heat origin to the point of heat delivery for residential and heating and cooling systems. Transmission loss reduces the actual point-of-use heat or cool output of the radiant panel, baseboard, or forced-air register or diffuser. Normally found to be in the range of 15 to 40 percent or more in residential forced-air convection systems, duct sealing and new construction design duct loss targets are 15 percent or less. Energy transmission loss is not likely to exceed 5 percent for a radiant system. (See Fig. 4.2.)

Design strategies for minimization of transmission and panel heat loss are well known. When the specification for reducing heat loss is detailed, implementation is

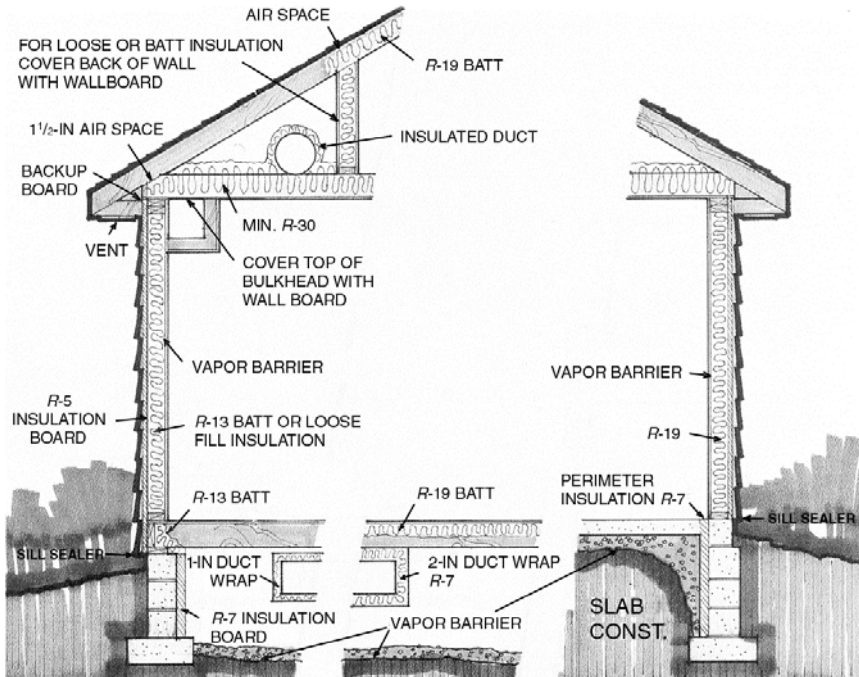


**FIGURE 4.2** Building, ductwork, and radiant slab insulation designs.

successful and installed performance matches design. Fluid leaks are usually unrelated to heat loss, except in the case of freeze-ups. Though sometimes damaging, fluid leaks are quickly detected. Forced-air system leaks may go undetected until the system is actually tested as a result of high bills, or discovered during service inspection that includes duct pressurization or system balancing. In either case, repair is more difficult when either the air duct or the radiant conduit is not readily accessible.

In addition to transmission loss, other potential heat loss from the radiant panel is also detailed in ASHRAE SPC-152P. Such loss may occur at the perimeter and backside of the radiant hydronic panel system. (See Fig. 4.3.) Insulation, planar location, and nature of surrounding space usage are among the conditions defining the magnitude of heat transfer potential from surfaces other than the designed primary radiant output surface.

Radiant hydronic floor heating panel performance is affected by the addition of any material that changes the rate of designed panel heat transfer. For example, carpeting, furniture, walls, or cabinets may be added, which would impact the designed rate of heat transfer from the panel to the occupied space. (See Table 4.2.) Other factors to be considered relate more to the potential likelihood of penetration, which is also a concern for radiant ceilings when lighting, ventilation, smoke detection, security, or other equipment is installed. For any concealed system the installation documentation is essential to reduce the risk of system damage from penetration.

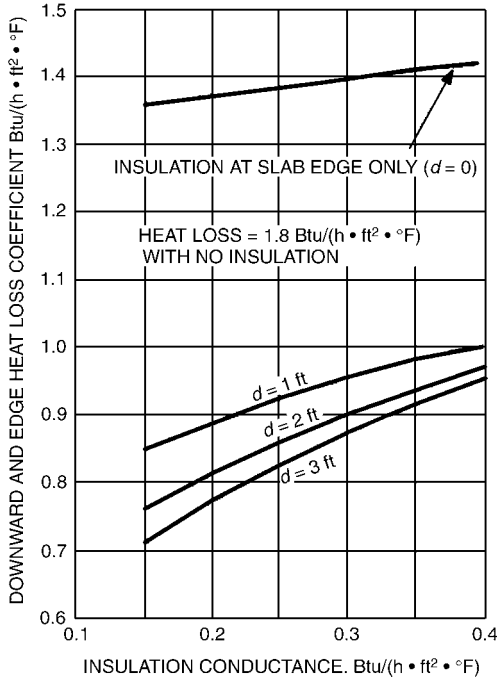
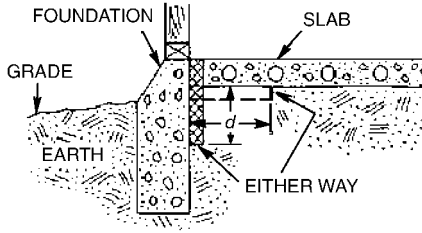


**FIGURE 4.3** Slab-on-grade heat loss coefficients—downward and edgewise heat loss coefficient for concrete floor slabs on grade.

#### 4.4 INSTALLATION DOCUMENTATION

Documentation, including photographs, is especially important for ensuring consistent operation of radiant hydronic systems over the long expected operating life. The complexity of supply and conduit routing and radiant panel design make service diagnosis without the aid of a complete scale plan difficult, time-consuming, and more costly. A complete explanation of the original design conditions on which overall system design was based is just as important as the layout, actual equipment, panel sizing, and electrical schematic. (See Fig. 4.4.)

**TABLE 4.2** Thermal Resistance of Floor Coverings

Description	Thermal resistance, $r_c$ [(ft <sup>2</sup> · h · °F)/Btu]
Bare concrete, no covering	0
Asphalt tile	0.05
Rubber tile	0.05
Light carpet	0.60
Light carpet with rubber pad	1.00
Light carpet with light pad	1.40
Light carpet with heavy pad	1.70
Heavy carpet	0.80
Heavy carpet with rubber pad	1.20
Heavy carpet with light pad	1.60
Heavy carpet with heavy pad	1.90
¾-in hardwood	0.54
¾-in wood floor (oak)	0.57
½-in oak parquet and pad	0.68
Linoleum	0.12
Marble floor and mudset	0.18
Rubber pad	0.62
¾-in prime urethane underlayment	1.61
48-oz waffled sponge rubber	0.78
½-in bonded urethane	2.09

\* Carpet pad should be no more than ¼ in thick.

† Total resistance of the carpet is more a function of thickness than of fiber type.

‡ A general rule for approximating the  $R$  value is 2.6 times the total carpet thickness in inches.

§ Before carpet is installed, it should be established that the backing is resistant to long periods of continuous heat up to 120°F.

Examples of documentation categories recommended by the Radiant Panel Association (RPA) include the following:

1. Piping schematic of entire system
2. Electrical control schematic
3. Scaled floor plans showing placement of heat emitters and pipe
4. Description of system operation
5. Component data sheets manual
6. Photographs and/or videotape of as-built installation
7. Service record

The documentation should include detail of all final control settings after the installation is up and running in line with design performance. Finally, the information should include complete parts-listing information required for maintenance, purchase, repair, and replacement, as well as warranty terms of compliance, schedule of maintenance, and duration from date of commencement. The supply source and manufacturer detail forms should include name, address, and telephone number, as well as provision for a complete record of service performed and parts replaced.

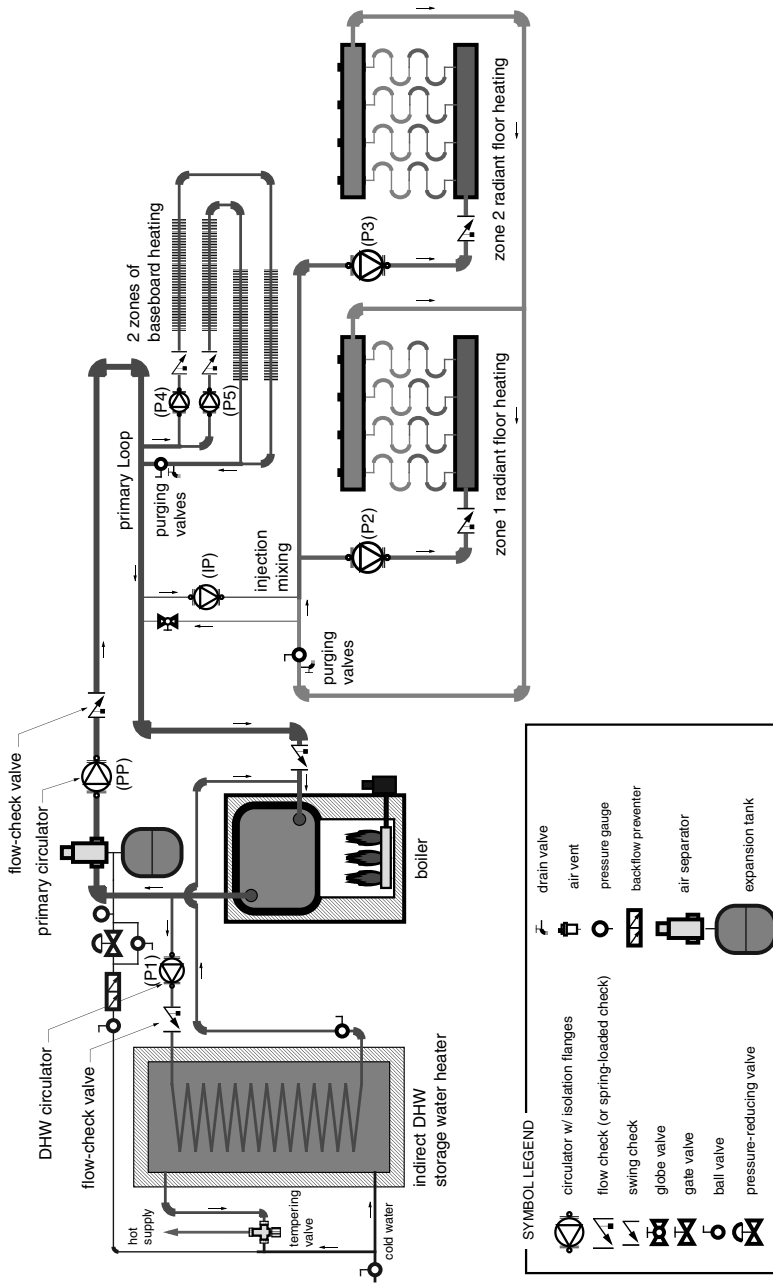


FIGURE 4.4 Radiant Panel Association documentation example for radiant hydronic system.

## 4.5 PANEL CHARACTERISTICS

---

Radiant hydronic panel systems (Fig. 4.5) are normally considered to be high-mass systems. In fact, the array of design and equipment options provides a broad range of high- and low-panel mass designs. Embedded floor heating mass specification and performance options include varying conduit depth and proximity, mass thickness, or material composition in relation to design and performance requirements. (See Fig. 4.6.) Modular ceiling panels, whether steel or aluminum, are a relatively low-mass hydronic option compared with the embedded ceiling and floor systems. Mass is an important interactive determinant for system design to match radiant panel performance and control parameters.

The surface temperature of the radiant hydronic panel is a function of fluid temperature, flow rates, conduit layout pattern, mass transfer characteristics, and heat delivery balance. Uniform heat delivery is accomplished by control and circuit design that minimizes fluid temperature drop across the panel. (See Fig. 4.7.) Panel temperature design strategies include continuous fluid-flow analysis. Adjusting conduit proximity, fluid input, and return locations are additional design options for heat output optimization within the panel circuit. The interrelationship of radiant panel conduit heat delivery, panel heat transfer characteristics, and control design is important in evaluating and determining the parameters necessary to provide for energy management and comfort control of radiant hydronic panel systems.

Radiant hydronic heating systems, like forced-warm-air heating systems, have control points in the transmission system that provide opportunity for adjustment. Flow, balance and mixing valves, booster pumps, flow meters, temperature and pressure monitors, and zone controls represent a few of the intermediary points that may be balanced and adjusted mechanically or electronically in relation to the point-of-use temperature control and energy management requirements. Refer to manufacturers' published conduit specifications for heat transfer rates, pressure capabilities, and pressure drop.

The range of panel temperature and heat output capability varies with panel design and is bounded by occupant comfort requirements. In general, low panel temperatures are associated with a high-mass, high percentage of plane panel coverage. For example, the floor panel surface, with which occupants come in contact, is designed within a surface temperature range of 65°F to a maximum of 85°F. Radiant hydronic wall panels that cover a small part of the total wall surface are designed within safe, casual touch temperature limits. Radiant hydronic ceiling panel coverage is inversely related to panel surface temperature, which normally ranges from 85°F to 185°F. Common ceiling materials such as gypsum dictate ceiling temperatures for embedded-conduit concealed ceiling systems. The phase change limits of the heat transfer fluid is a determinant of the maximum supply temperature for modular panels. As heat loss and ceiling height increase, the relative portion of ceiling panel coverage increases in relation to the maximum surface temperature, heat output capability, and thermal comfort specifications.

## 4.6 THERMAL COMFORT

---

Although material and safety limits define relevant radiant panel temperature boundaries, comfort requirements are the defining design determinant within the physical temperature limits. Selection of occupant thermal comfort parameters

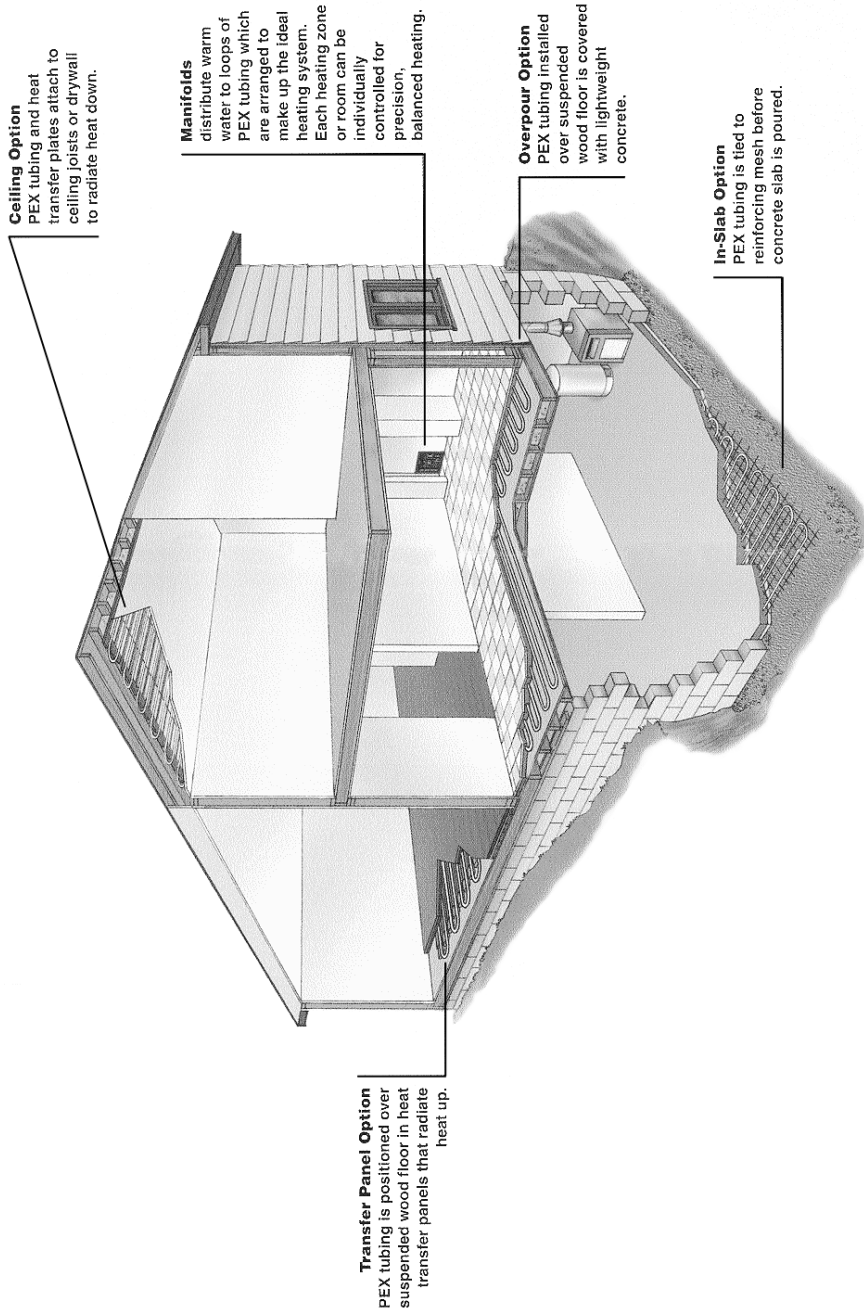


**FIGURE 4.5** Basic components of a radiant hydronic heating system.

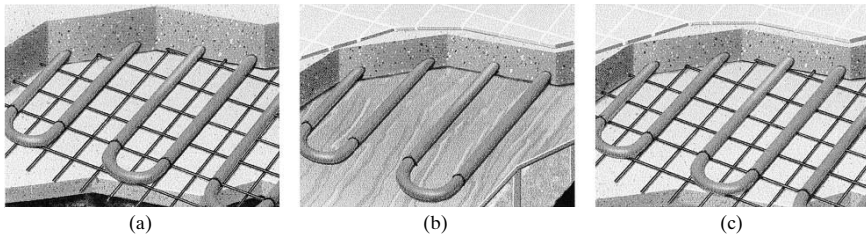


**FIGURE 4.6** Installation and mass design options. (a) Concrete on grade with insulation. (b) Topping pour on suspended floor. (c) Topping pour on concrete floor.

defines the range of mean radiant temperatures (MRTs) within which the radiant panel design must operate. Radiant temperature asymmetry is a design determinant. Radiant temperature asymmetry is defined as the plane radiant temperature difference between the surface temperature of the two defined parallel planes.

The methodology for determining the planar human thermal comfort limits is detailed in ASHRAE Standard 55-92, *Thermal Environmental Conditions for Human Occupancy*. Additional information on the relationship between the MRT, thermal comfort, and radiant heat transfer is available in the final report for ASHRAE Research Project 657 by Jones and Chapman (1994). Section 3 of this Handbook covers the entire subject of thermal comfort in detail, reviewing the thermal comfort models, MRT, and operative temperature (OT).

Thermal comfort delivery from a radiant hydronic system may be provided using controls that sense fluid, panel surface, dry-bulb air, mean radiant, operative, or some combination of these temperatures. Control algorithms may be employed, or the occupant, in relation to whichever temperature reading it is capable of developing, may simply adjust the control. Control may be automatic, electronic, or occupant-activated automatically or manually.

The system may be zoned by means of local valves—an array of circuit, injection, flow, or mixing valves—zone controls functioning directly through the central system or operating on a discrete zone basis with finite, independent heat generation capability. Zone control may be designed for the purpose of providing individual room or area comfort control, for energy conservation, or for other reasons.

Control of radiant hydronic systems, though sometimes complex, is almost always successful in providing occupant comfort because a key factor of human thermal com-

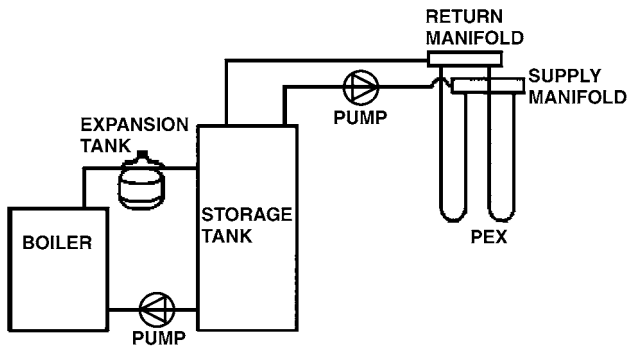


**FIGURE 4.7** Radiant hydronic system component schematic.

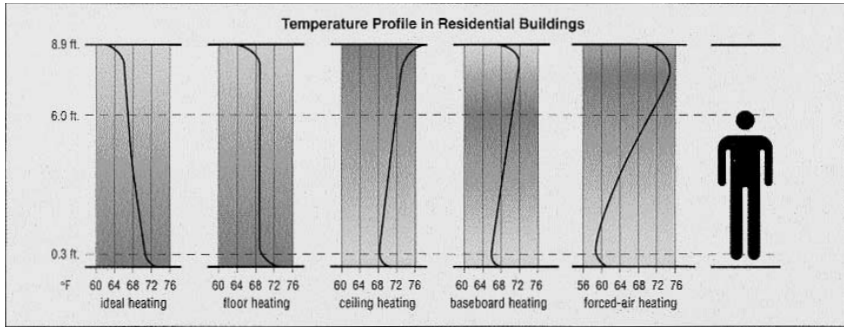


**FIGURE 4.8** Comparative heating system floor-to-ceiling dry-bulb air temperatures.

fort, MRT, is satisfied. Forced-hot-air convection systems, normally controlled solely to dry-bulb air temperature, correct MRT deficiencies by elevating dry-bulb air temperatures to produce the OT required for human thermal comfort. The temperature profile for residential buildings graphically shows the comparative floor-to-ceiling dry-bulb air temperatures. (See Fig. 4.8. Also, see Sec. 8 for additional information.)

#### 4.7 HYDRONIC ENERGY SOURCES

Radiant hydronic systems require electricity for pumping, control, and operating functions, but may use electricity, gas, propane, fuel oil, or alternate energy for warming the heat transfer fluid. Radiant hydronic heating panels are fuel neutral and are not impacted by the source of heat energy. However, the fuel choice selection does define and limit heating equipment selection, which may impact performance capability. A review of equipment and system performance capability provides important input in relation to the impact of energy selection.

Most boilers are fossil fuel fired, and geothermal heat pumps are electric. Combination potable and/or hot-water heaters may use either fossil fuel or electricity as the energy source. The use of alternate energy may require a hybrid system and impact system design and performance significantly compared with the more common energy source and equipment approaches. Systems using solar or wood-heated fluid as a base thermal input are successfully installed in solar-sparse Maine climates as well as in moderate, more solar-dependable climates.

Selection of the heat generation source may be a determining factor in heat transfer fluid selection. Though water has been used through the ages, modern chemistry has developed fluids to meet radiant system component demands. Careful attention to fluid selection can eliminate serious problems. In the past, corrosion, contamination, filtration, freezing, evaporation, and other problems have created a need for continuous surveillance and service. Most of these conditions are virtually eliminated, except for routine service, with careful attention to the material chemical performance interrelationships with the heat transfer fluid.

Detailed discussion of heat generation equipment is beyond the scope of this Handbook. However, it should be noted that radiant hydronic systems have used the entire range of heat generation equipment. The increasing popularity of hydronic radiant heating systems is driving technology. Boilers are designed to encompass a

broader range of output and return fluid temperatures. Many are packaged with appropriate manifolds, valves, and controls to facilitate performance and simplify installation. Geothermal heat pumps incorporate control and output capabilities appropriate for radiant hydronic heating systems. Combination potable and hot-water heaters support a variety of radiant hydronic panels and design requirements. Passive solar collection, storage, distribution, and control strategies are reliable and present an additional option for radiant system design.

The 1992 Energy Policy Act set national policy for defining heat generation equipment performance standards for use in new and existing buildings. ASHRAE Standards 90.1, *Energy Standard for Buildings Except Low-Rise Residential Buildings*, and 90.2, *Energy Design of Low-Rise Residential Buildings*, are documents that provide the prescriptive information on which local building and energy performance codes for boilers, geothermal heat pumps, water heaters, and other equipment and design applications are based.

## 4.8 HYDRONIC APPLICATIONS

---

Radiant hydronic heating systems are appropriate for the full range of building designs and uses. As with most emerging technologies, the most common uses are those in which other forms of heating have not fully satisfied their users. These include slab-on-grade residential and commercial applications; use where cold floors are associated with specified materials like ceramic tile, bare wood, and other types of uncarpeted flooring; large areas of window expanse; stratification-impacted split-level constructions; drive and walkway snow melting; and so forth.

Documentation of conduit placement is the best way to reduce risk of system damage should entry into the panel be necessary. However, the need for extensive documentation for the radiant operating system is symptomatic of the complexity of system design. Radiant system design and installation has had the aura of an art. Packaging of components is emerging, including boilers, heat pumps, manifolds, electronic valve assemblies, connector packages, and so on. The simplification that comes from prefabricated component modules takes the mystery out of radiant panel support components and installation, lowers overall system cost, and could propel radiant hydronic heating into the mainstream as more contractors become comfortable with its installation and confident in its operation.

The reader is encouraged to read on with the mind open to nonmechanical radiant heat transfer through the use of hydronic radiant panels. The applications that are appropriate for radiant hydronic heating are endless. Increased use is limited only by the development of the design tools, knowledge, and skill level required for specification of radiant hydronic systems as easily as other heating systems.

## 4.9 OVERHEAD HYDRONIC PANELS

---

Overhead hydronic radiant ceiling panels may be concealed or visible. Choosing whether to design for a visible or invisible system is perhaps the most challenging hurdle to the selection of a radiant ceiling system. System visibility and appearance are subjective. System selection and performance design are normally objective. Yet, whether a system is visible or invisible significantly impacts design and can impact comfort and energy performance.

### 4.9.1 Concealed Radiant Hydronic Ceiling Systems

Concealed radiant ceiling panels are normally field-constructed. Concealed design of radiant hydronic ceiling panels defines the ceiling as the panel and radiant delivery surface. As with all radiant panels, the objective is maximization of radiant frontal output and minimization of side and back heat loss. Regardless of building construction, panel surface output is maximized when the panel contact with cold building surfaces is buffered by an enclosed air space and separated by insulation. A defined and closed air space eliminates thermal bridging and conductive heat loss. (See Fig. 4.9.) Insulation reduces heat transfer outside of the space to which the panel is designed to radiate heat, and should be designed based upon cost-effective site analysis.

Concealed panel composition and construction alternatives impact panel performance, control, and energy consumption. For embedded ceiling panel systems, determination of conduit material and design configuration is an important factor determining mass minimum thickness and material composition alternatives. Mass thickness and material composition define thermal mass and heat transfer design alternatives. Weight and architectural constraints may establish boundary conditions for concealed radiant system design. For example, a concrete floor may be impractical except as a slab or basement floor.

In the case of panels that are designed using flexible hydronic conduit routed through ceiling joists, the same panel design principles apply. Energy efficiency and performance will depend upon comprehensive definition of the radiant concealed panel in relation to the performance design. The emergence of this application is driven by the economics of competition with ducted warm-air heating systems. An important factor for performance success is panel design simplicity and plan detail that ensures consistent field construction and installation. As with any concealed system, detailed comprehensive documentation of installation, con-

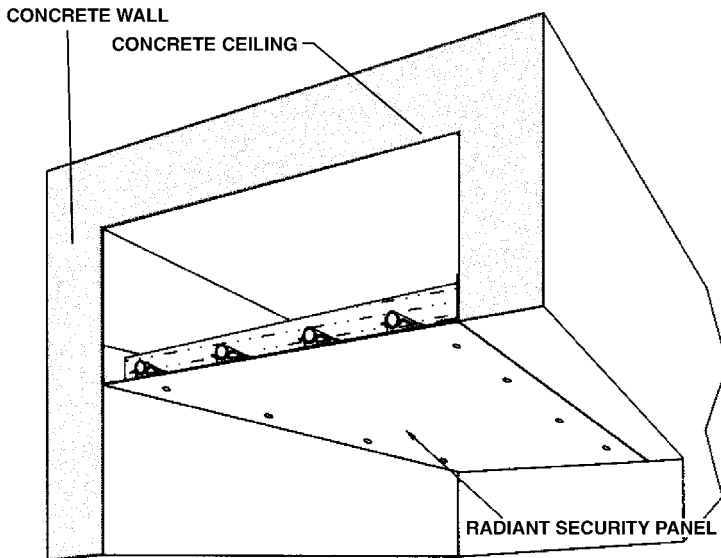


**FIGURE 4.9** Concealed or flush radiant hydronic panel system.

nections, operating control settings, and the like is essential to system service and management.

Encapsulated or concealed radiant ceiling systems, whether PEX tubing or narrow-diameter capillary tubing or mats, are inherently higher-mass systems. (See Fig. 4.10.) The key performance design factor of mass systems is determination of temperature change–time increments under dynamic external and internal design conditions. Thermal stability, mass temperature lags, and mass charges and discharges are characteristics that are essential design inputs. Solar impact, occupancy patterns, and energy source for fluid heating are but a few of the interacting factors that must be integrated into overall system design and control.

Surface characteristics of the panel face are not a design constraint on concealed or other radiant systems. The emissivity of the normally encountered building materials used for building ceilings is on the order of 90 percent whether painted or textured. The surface temperatures are also within the range tolerated by standard surfacing materials, paints, and finishes. The placement over the ceiling of wood or other materials that provide thermal resistance will impact performance and will require careful analysis. The details of ASHRAE Research Project 876, *Impact of Surface Characteristics on Radiant Heat Transfer*, are covered in more detail in Chap. 5 at the end of Sec. 5 of this Handbook.

Concealed radiant ceiling heating is commonly specified and designed for conditions where it is practical to turn the heating on to a set point that is maintained over the entire winter period until turned off for the summer. Interim adjustment is not recommended because short-term adjustment may not be economic or practicable due to the thermal inertia of a concealed ceiling system. Selection of the optimum operating protocol is essential to the energy efficiency and comfort performance of all heating systems, including concealed radiant ceiling systems.

Economic heating system operation involves a strategy designed to complement and maintain building mass at temperature levels compatible with occupant comfort



**FIGURE 4.10** Capillary radiant ceiling panel system.

or other building use specifications, thereby minimizing the initial start-up heat energy investment. For concealed radiant ceiling systems, it is important to account for the thermal properties of the ceiling material in designing ramp-up and ramp-down strategies to avoid cracks, expansion, and contraction stress, or other problems. In some cases, the material limitations prevent rapid warm-up. In new installations, the mass materials must always be dry and fully cured naturally before any heat is applied. Even though there may be adequate conduit heat capacity, the thermal transfer properties of the panel design or material may prohibit exploitation for rapid warm-up or cool-down. On the plus side, high-mass systems provide an even longer period of building thermal stability than low-mass radiant systems, which is an important benefit of any radiant system during power, energy source, or equipment outages.

#### 4.9.2 Visible Radiant Hydronic Ceiling Heating Panels

Visible radiant hydronic ceiling heating panels are steel or aluminum panels that may be mounted on the surface, flush with the surface, or suspended in, on, or from the ceiling. The panel may be factory-assembled and ready for field installation and connection or supplied in the form of components for further fabrication and assembly on-site. If related building design or insulation changes are not specified, factory panel or component construction is the sole determinant of panel back and side heat loss potential and actual frontal output—essential factors for design and performance specification.

The growth in specification of visible radiant hydronic panels has been hindered primarily by higher first cost than more common gas or heat pump forced-air systems. Growth in visible radiant hydronic panel systems is attributed to appreciation of the normal benefits of radiant heating and the flexibility of energy choice. A discussion of operating cost and lower comfort temperatures follows in Sec. 3, Chap. 3; Sec. 5, Chap. 5; and Sec. 8, all in this Handbook. Features of radiant ceiling systems are the absence of mechanical equipment within the occupied space and the freedom to use all wall and floor space for whatever purpose is required.

Office productivity is an increasingly important consideration in heating system selection. Proponents of ceiling radiant heating point to the noiseless, odorless, draft-free comfort at lower temperatures from a heat source that is away from the occupants' personal space. Flexibility of modular panel relocation to accommodate office layout alterations ensures that comfort need not be compromised by redesign of space use. Localized heat delivery, characteristic of radiant heat transfer, contrasts with convection heat delivery that is impacted by air temperature gradients, buoyancy, and resulting air currents.

When radiant heating is used, air distribution for the purpose of heat delivery is eliminated. Instead, air distribution is dictated solely by ventilation requirements. ASHRAE Standard 62, *Ventilation for Acceptable Indoor Air Quality*, defines the requirements. The determination of comparative system air to be moved and filtered or infiltrating is important input for determining overall system sizing, comfort, and energy performance. The reader is referred to Sec. 7, Chap. 3 of this Handbook.

#### 4.9.3 Installation and Characteristics

Surface and flush mounting of hydronic ceiling panels is accomplished through use of mounting frames and accessories, which provides for required surface clearance and allowance for installation and connection servicing. (See Fig. 4.11.) The panels



**FIGURE 4.11** Visible radiant hydronic ceiling panel system.

may be either linear or modular with flat, grooved, or channeled surfaces. Linear panels are generally either extruded aluminum or steel heating strips in 1- to 2-ft widths and lengths to approximately 16 ft. The individual panels can be fastened together by brackets or be formed as tongue-and-groove units to form panels of the length and width required. Modular panels utilize similar framing that facilitates recess mounting in gypsum or T-bar grid ceiling systems.

The face of the metal panel is the radiating surface to which the heat is conducted from the copper tubing that is routed through heat transfer channels. The tubing is mechanically held in direct contact with the back of the panel plank or trays to facilitate heat conduction. (See Fig. 4.12.) Some manufacturers specify use of a nonhardening heat paste between the tubing and the aluminum faceplate to increase thermal efficiency. Insulation may be placed over the heat panel to reduce backloss and increase frontal heat output. The generally open plenum space, dictated by visible hydronic panel specification, installation, and service requirements, provides a fertile environment for convection air currents. The amount and nature of convection heat transfer and other panel heat loss are important inputs

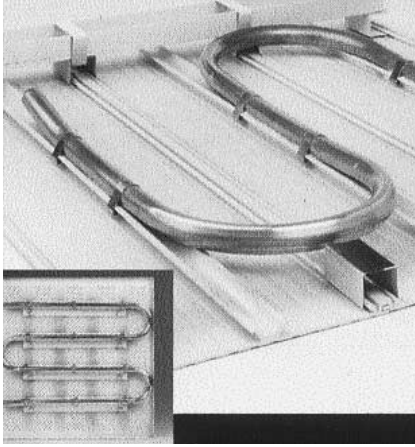


**FIGURE 4.12** Hydronic modular ceiling panel construction. (Photo courtesy of Mestek.)

for insulation specification, panel design, overall system design, and energy projections.

Radiant hydronic ceiling panels originally were made from heavy steel, but are more commonly made with various lighter-weight, noncorrosive, highly conductive aluminum alloys, except in security or industrial applications. Heat delivery response time is a function of the energy source, transmission performance factors, and the thermal conductivity and mass of the heat delivery panel. Thermal mass is less than concealed hydronic systems with correspondingly faster response time, and greater opportunities for energy management. These features also give visible linear and modular hydronic panels the control flexibility required for radiant cooling.

As linear and modular radiant hydronic panels are normally made to order, a variety of surface features are standard options. (See Fig. 4.13.) Finishes are almost always factory-applied. The selection, finish, color, and silk screening may be made without concern for panel performance impact, except in the case of acoustic perforations if they are determined to contribute to convection heat loss. T-bar grid modular panels are made in tegular models also, which reveal  $\frac{1}{4}$  to  $\frac{1}{2}$  in of panel below the ceiling grid.

As with any hydronic system, pressure testing, system flushing, and cleaning are important initial installation procedures. The inspection and cleaning of filters prior to dry-pressure testing for leaks are final steps in the process of venting air as the system is gradually brought up to temperature. Observance of expansion bushings, fittings, and connections is important to detect noise, leaks, or stress as the system reaches full operating temperature.

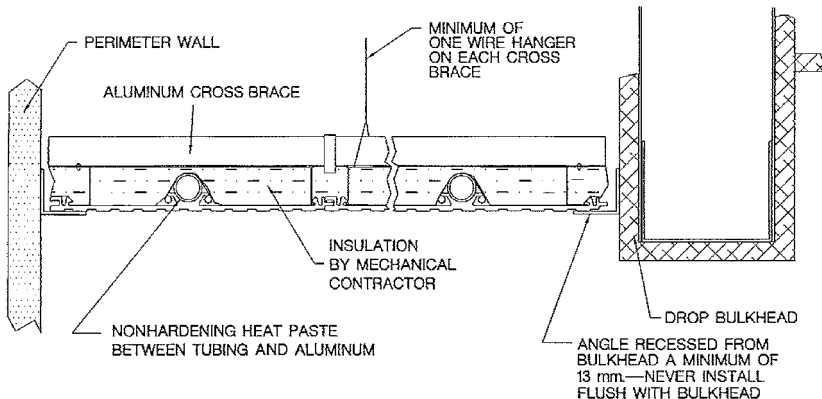


**FIGURE 4.13** Radiant hydronic ceiling panel installation. (Courtesy of TWA Panel Systems.)

Visible hydronic panels may be retrofit in buildings that have baseboard hydronic heating. Supply and return connection and control capabilities are important retrofit design factors to ensure satisfactory performance. Hydronic ceiling panels enjoy widespread commercial application in offices, hospitals, schools, nursing homes, and assisted-care living centers. Though used most commonly for heating, radiant hydronic panels are appropriate for hydronic cooling, as discussed in more detail in Sec. 7, Chap. 4 of this Handbook. The development of hybrid hydronic systems may remove the higher first-cost barrier, now associated with hydronic ceiling heating as a heating-only system.

#### 4.10 RADIANT HYDRONIC FLOOR PANELS

---

The most common form of radiant hydronic heating involves use of the entire floor mass as the radiant floor heat transfer panel. The encapsulation of steel or copper pipe in concrete has been superseded by the use of cross-linked polyethylene (PEX) tubing. PEX is available in several formulations that exhibit varying characteristics of rigidity, flexibility, temperature tolerance, pressure strength, chemical stability and resistance, and heat transfer efficiency. Conduit diameters commonly used for radiant floor heating are  $\frac{3}{4}$ ,  $\frac{1}{2}$ , and  $\frac{3}{8}$  in for residential and up to 1 in or more in large-scale commercial applications. Conduit characteristics must accommodate heat distribution pattern design, heat delivery capacity, panel construction requirements, and be accounted for in mass volume calculations. (See Fig. 4.14.)



**FIGURE 4.14** Large, high-mass radiant hydronic floor installation. (Photo courtesy of Watts Heatway.)

#### 4.10.1 Concrete Slab Heating

For buildings that already incorporate a concrete slab construction design feature, installation of radiant conduit may be a relatively inexpensive heating solution. Slab conversion to a radiant panel requires design review to determine what additional insulation, mass thickness, or other features may require modification to ensure that radiant performance parameters are met. For buildings that do not incorporate a convenient encapsulation medium, there may be alternative design options that are also cost-competitive.

Radiant slabs are high-mass systems. The panels' surface temperature change is a function of the heat transfer characteristics of the composition, tubing, and system heat delivery capability. For many reasons mass temperature change is gradual and a significant design characteristic. Temperature setback strategies, if used at all, must be tempered in relation to the performance characteristics of the application. Radiant slab thermal control in relation to seasonal heating requirements is accomplished through the use of outdoor reset controls and anticipation. Thermal stability is a key feature around which design control is based. For additional information, refer to Sec. 6 of this Handbook.

In a sense, the entire foundation for concrete slab radiant floor heating becomes part of the radiant panel system and requires comprehensive design specification in order to ensure optimum performance. This requires finite definition of the radiant panel in order to minimize side and back heat loss. Depending on design, the underlayment may function as insulation, mass thermal storage, or heat conduit. Attention to insulating the perimeter of the slab is especially important for smaller slabs due to the larger proportional relationship to overall slab heat loss and the influence on thermal comfort within the small designed space.

For slabs that are brought up to temperature in the fall and allowed to discharge at the end of the heating season, the energy expended to initially charge the mass may be small in relation to total heating season energy usage. Side loss reduction insulation, appropriate for the climate and frost depth, ensures that perimeter heat loss is cost-effectively minimized. The ongoing loss through the backside may also be relatively small if surrounding materials and soil are kept dry, are porous, and not compacted, so that heat conduction is minimized. In most climates the ground temperature, approximately 5 to 10 ft inside of the perimeter and 2 to 3 ft below the heated slab, will remain at the stable year-round temperature indigenous to the region, usually just above or below 50°F.

#### 4.10.2 Design Alternatives

Several strategies may be employed to overcome thermal inertia and mass dominance of radiant slab temperature change. From the perspective of panel design, mass thickness may be reduced, thermal breaks inserted, or material changed. The thermal heating profile is impacted by changes in conduit diameter, proximity, location, pattern, and supply thermal output. The objective is the achievement of the required thermal profile using the lowest heat transfer fluid temperature. Each alternative that is considered introduces new overall design considerations. (See Fig. 4.15.)

Conduit patterns used for radiant floor heating encompass many different designs that are responsive to site-specific heat loss and building use. The perimeter deadband and other areas where conduit may not be routed are an initial input for

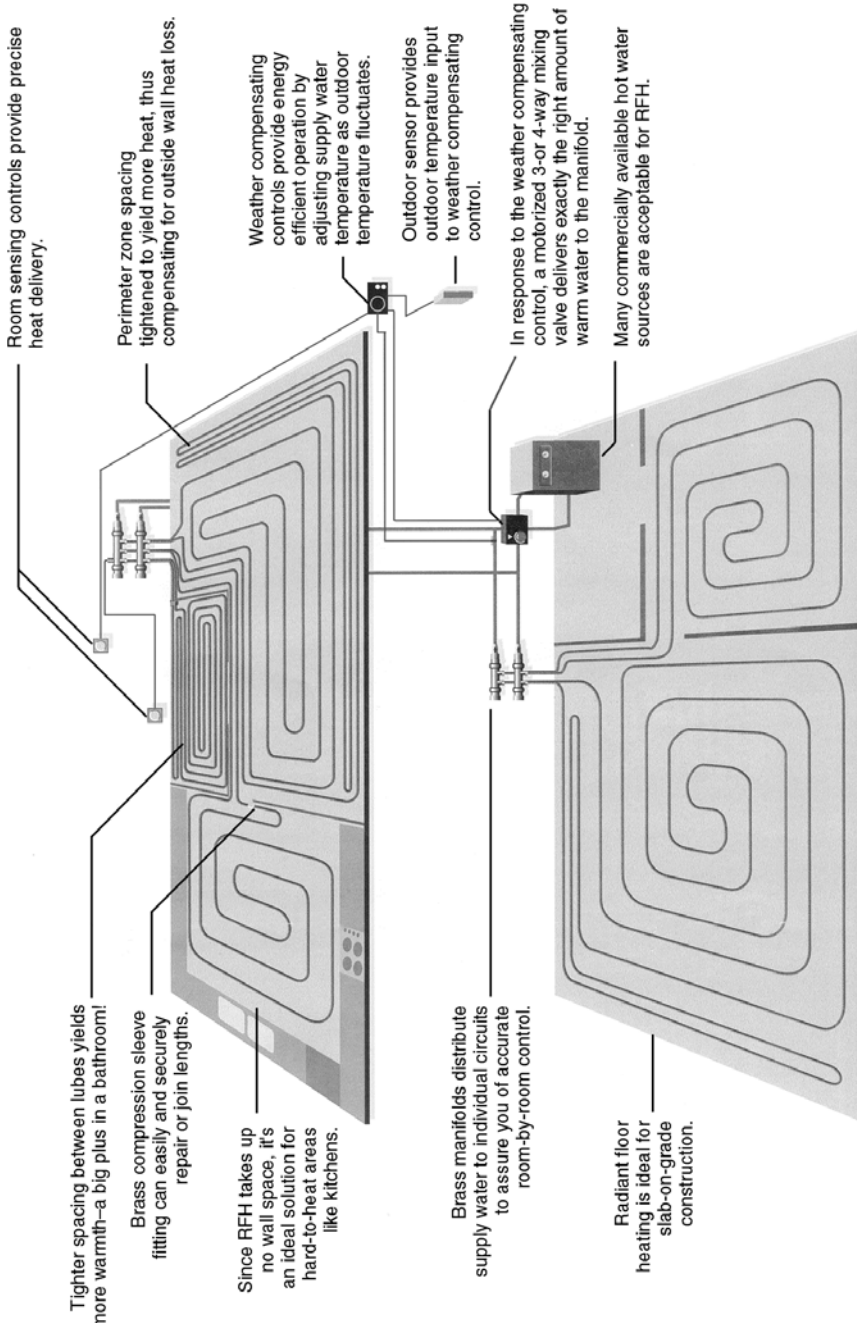


**FIGURE 4.15** Radiant hydronic floor system design.

determination of pattern design options. The common serpentine pattern routes conduit in a parallel pattern, permitting spacing variation, which enables increased heat output for perimeter and high-loss areas. Close spacing may facilitate floor temperatures approaching 95°F in a narrow-perimeter band, and wider uniform spacing is used elsewhere to provide surface temperatures within the thermal comfort parameters. Depending on conduit flexibility and memory, radial retention brackets or braces may be required.

Counterflow spiral pattern design is an option that uses alternating flow design to facilitate even heat distribution. (See Fig. 4.16.) Conduit tube-bending radius constraints have less influence on conduit proximity with counterflow spiral routing than with serpentine patterns. (See Fig. 4.17.) Combinations of serpentine and spiral flow patterns are used to meet a wide range of application demands. Multiple-circuit conduit design is employed to meet performance requirements, for zoning, or required due to the size of the area to be heated. Similarity of supply heat requirements, heat loss, area control isolation, or other reasons may dictate the grouping of circuits.

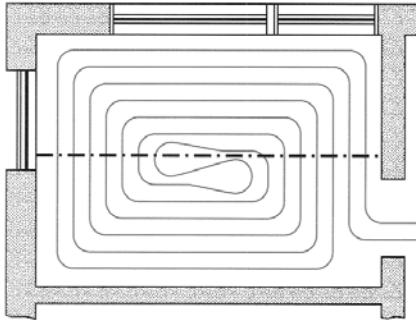


**FIGURE 4.16** Counterflow spiral conduit pattern.

Conduit length is constrained by the characteristics of the conduit, which include among other factors the design conditions for temperature and heat capacity and loss, conduit pressure drop, and individual material stock lengths.

Conduit connection tail length and proximity to supply manifolds are additional design input. (See Table 4.3.) Whichever design is ultimately chosen, the rate of panel radiating surface temperature change determines flexibility for comfort control, space temperature control, and energy management. (See Table 4.4.)

Similar strategies are employed for multifloor concrete buildings or buildings where a screed or nonstructural pour is used as a subset for ceramic tile or other

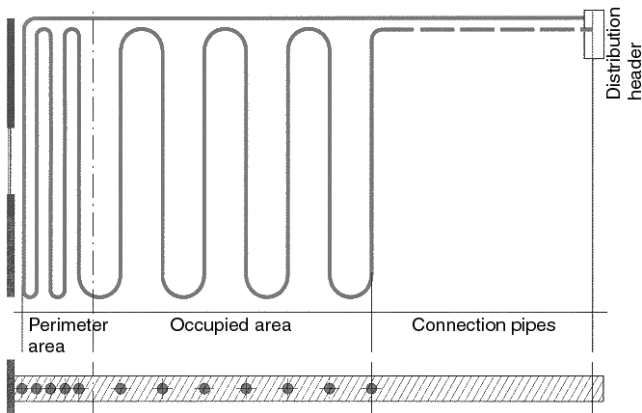


**FIGURE 4.17** Serpentine conduit pattern in hydronic floor panel.

**TABLE 4.3** Radiant Panel Manifold Circuit Length Guidelines

Maximum tube length
Residential manifolds
3/8-in tube—200 ft
1/2-in tube—300 ft
Commercial manifolds
1/2-in tube—300 ft
High-capacity manifolds
1/2-in tube—500 ft
3/4-in tube—1000 ft

**TABLE 4.4** Tube Size and Hydronic Floor Output (Btu/ft<sup>2</sup>) Range

Tube size	Floor output in Btu/ft <sup>2</sup>		
	10–20	20–30	30–40
3/8 in	9 in	6 in	4 in
1/2 in	12 in	9 in	6 in
3/4 in	15 in	12 in	9 in

flooring materials with which radiant heating is coupled. Regardless of the application, the heat transfer characteristics of the materials separating the conduit from the panel face and the heat loss to be satisfied determine the heat delivery design. In each case, a manageable but essential set of design decisions is required in order to ensure compatibility, desired performance, and code compliance.

Another consideration in pattern and layout design is provision for slab dimensional stress and variation. The use of expansion joints, floating floors, and forging material formulations are all common preventive measures. Routing parallel to expansion joints minimizes pattern design influence, and may limit exposure to feeder conduit only. Wherever exposed to stress, the conduit must be protected as needed. Layout design must always be altered in order to minimize and accommodate stress exposure.

With thin-pour bathroom applications, a common objective is floor warming. For bathroom floor-warming applications, tubing may be smaller in diameter, somewhat closer together, or formed-mat narrow-diameter connected tubing. The tubing specifications are designed to facilitate quick response. In some applications, users choose a set point for continuous temperature continuity throughout the year. If

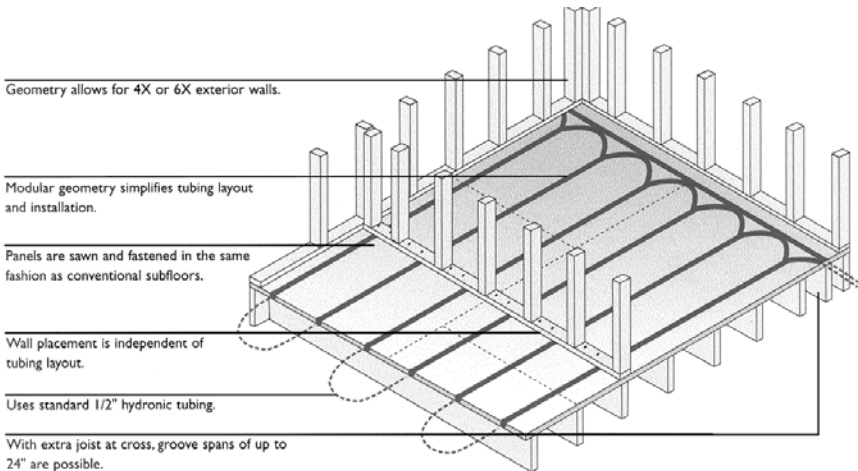


**FIGURE 4.18** Continuous heat transfer radiant panel and floor structure system.

floor warming is the sole objective, an additional source of heat will be required in moderate and northern climates.

Hydronic floor system popularity has spurred the development of alternative installation design options that enable installation of hydronic floor heating with almost any construction approach. PEX tubing is installed with heat transfer plates under subflooring and in heat transfer channels in subflooring. Metal-clad floorwide interconnected channeled primary flooring, allowing residential installation of radiant floor heating prior to partition wall construction, is an example of innovative design alternatives. (See Fig. 4.18.) The prechanneled tubing layout in the modular subfloor assembly is ready for field PEX insertion and connection to the fluid control and heat source components.

A key factor in radiant floor design capacity is provision for the additional resistance to heat transfer of potential floor coverings. (See Fig. 4.19.) The surface characteristics of the floor covering do not impact radiant heat transfer, but the  $R$  value of the intervening flooring or carpet does. In fact, even the change from a worn, dirt-impregnated carpet to a plush new carpet may provide a noticeable change in heat output if the change is made on the coldest day of the winter. Dirt-impregnated,

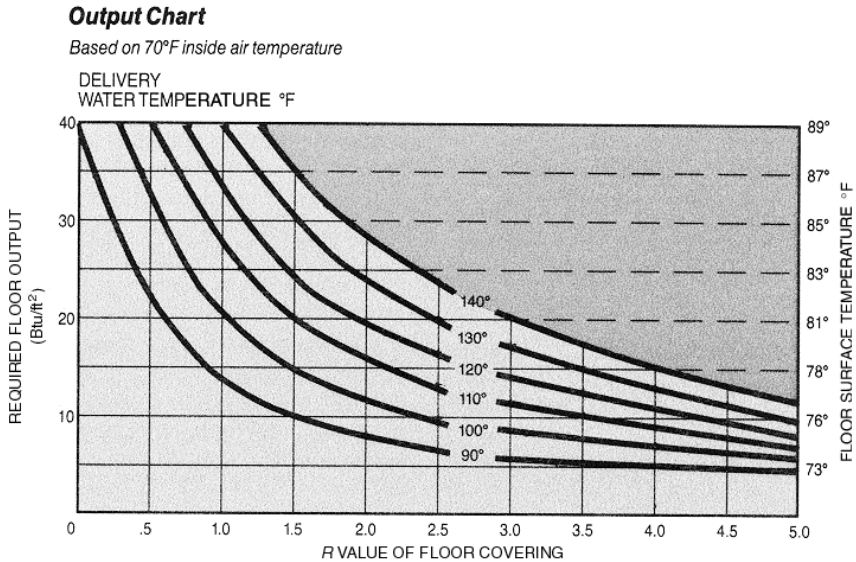


**FIGURE 4.19** Radiant hydronic floor panel heat output chart.

1. Find the required floor output on the left side of the chart and extend a line to the right to read the floor surface temperature.
2. Locate your selected floor covering  $R$  value on the bottom of the chart ( $R$  value from  $R$ -value table). Extend a line up to cross your first line.
3. Read the delivery water temperature at the intersection of the two lines.
4. If the lines intersect beyond the 140°F line, do one or more of the following:
  - a. Select a floor covering with a lower  $R$  value.
  - b. Reduce the heat loss of the area to lower the required floor output.
  - c. Figure supplemental fin tube baseboard heating.
    - Extend a line up from your floor covering  $R$  value until it intersects the 140° line.
    - From that point, extend the line to the left to find the actual output of the floor.
    - Subtract the actual output from your required output to find the amount of supplemental heat needed.

**TABLE 4.5** Guidelines for Use *Only* for Preliminary Estimating Purposes\*

Application	Residential	Commercial	Industrial	Snowmelt
Room temperature	65–72°F	60–72°F	55–70°F	25°F
Water temperature	95–140°F	90–140°F	85–120°F	90–130°F
Surface temperature	75–85°F	75–85°F	70–85°F	35–40°F
Heat output	15–30 Btu/ (h · ft <sup>2</sup> )	15–30 Btu/ (h · ft <sup>2</sup> )	10–25 Btu/ (h · ft <sup>2</sup> )	80–150 Btu/ (h · ft <sup>2</sup> )
Temperature drop	15–20°F	15–20°F	15–20°F	20–35°F
Flow/loop	≈0.3 gpm	≈0.7 gpm	≈2.5 gpm	≈2.5 gpm
Pressure drop	2–6 ft H <sub>2</sub> O	3–10 ft H <sub>2</sub> O	15–40 ft H <sub>2</sub> O	20–50 ft H <sub>2</sub> O
Loop length	200 ft	300 ft	1000 ft	300 ft
Tube size	¾ in	½ in	¾ in	¾ in
Tube centers	4–9 in	6–12 in	9–15 in	8–12 in

\* *Note:* These design factors are dependent upon each other. Do not use these values as a base for a system design. All numbers are averages only. A heat loss analysis is required for an actual system design.

compacted pile carpet has good conductivity and minimal insulation value in comparison with the same carpet when it is new and exhibits maximum *R* value.

Radiant hydronic floors last a long time. The longevity of PEX is unknown, but after 25 years or more of use, rated PEX tubing failure due to tubing deterioration is unknown to the authors. What is important relative to system material longevity is selection of fittings that are compatible with the fluids to be used. By choosing the correct metal alloy fitting, problems caused by corrosive deterioration and ultimate failure are eliminated. When compatible rated materials are properly installed, the main risks of system failure are due to lack of proper maintenance.

To have general information for guideline estimating, the accompanying chart is provided. Once a radiant system has been chosen, careful design using manufacturers' information is required. The guidelines also provide a useful benchmark reference. (See Table 4.5.)

#### 4.11 RADIANT HYDRONIC WALL PANELS

Radiant hydronic wall panels encompass concealed conduit systems and surface-mounted panels. The same design features addressed with ceiling and floor panels in order to ensure the highest frontal heat output apply to radiant wall panel design. The wall is a viable surface for radiant use that is sometimes overlooked in review of radiant design alternatives.

Embedded radiant wall panel systems are commonly designed to accommodate low-temperature radiant systems. Remember that the panel surface area required for heat transfer is inversely related to the radiating surface temperature. When floor area is inadequate to meet the heat loss at the design surface temperature chosen, the walls may be designed as additional radiant heating panels. Given the series of openings for windows and doors, as well as electric outlets, switches, and other wall penetration demands, careful attention to design layout, control, and documentation is important to ensure conformance to codes and performance design parameters.

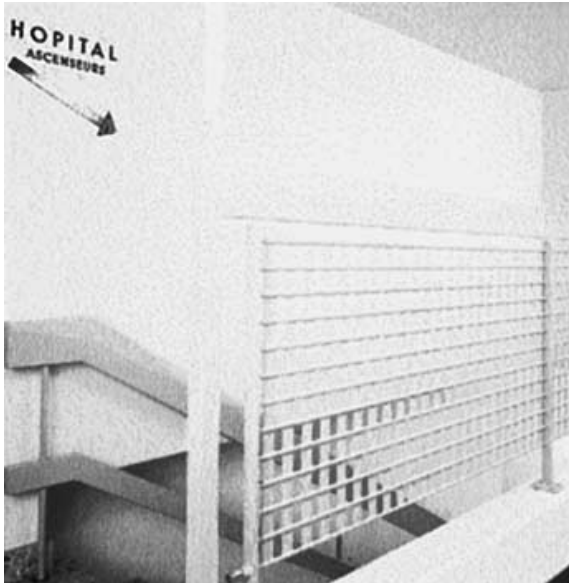


**FIGURE 4.20** Hydronic panels used for heat, safety, and design accent.

Narrow-profile decorative flat-panel radiant wall heaters are often used for spot warming in conjunction with concealed radiant hydronic systems. The variety of sizes and shapes provides attractive design flexibility to easily address special needs independent of or in conjunction with other hydronic heating systems. (See Fig. 4.20.) The same radiant panel performance design features common to other radiant panel systems applies to factory-manufactured radiant wall heat panels.

The location of a surface-mounted radiant panel on the wall impacts the radiant and convection division of panel heat transfer. For a flush-mounted radiant wall panel operating at approximately 100°F, the radiant percentage heat transfer ranged between 60 and 70 percent, and convective balance ranged between 30 and 40 percent. For radiant wall panels with open space between the radiant panel and the wall, air movement similar to panel face convection will occur, further reducing the radiant percentage output. Determination of the radiant-convective split is important input for design sizing and panel layout. (See Fig. 4.21.)

Wall panel surface temperatures range from the building maintenance temperature level to safe-for-casual-touch levels determined for safety considerations for installations from floor level up to 6 ft above the floor. Wall panels installed 6 ft or more above floor levels are considered the same as ceiling panels in regard to surface temperature safety limitations. Normal occupied building wall temperatures for concealed systems will range from 65°F to a maximum of 85°F, with temperatures of 68°F to 72°F being more common. For surface-mounted radiant panels that are less than 6 ft above the floor, common design temperature ranges are from 85°F to 125°F, unless surrounded by a grill or protective cover.

Surface-mounted radiant hydronic wall panels are replacing the convection baseboard radiation of yesteryear. Common applications include both supplemental and primary heating in all climates. Availability of an attractive array of enamel color fin-

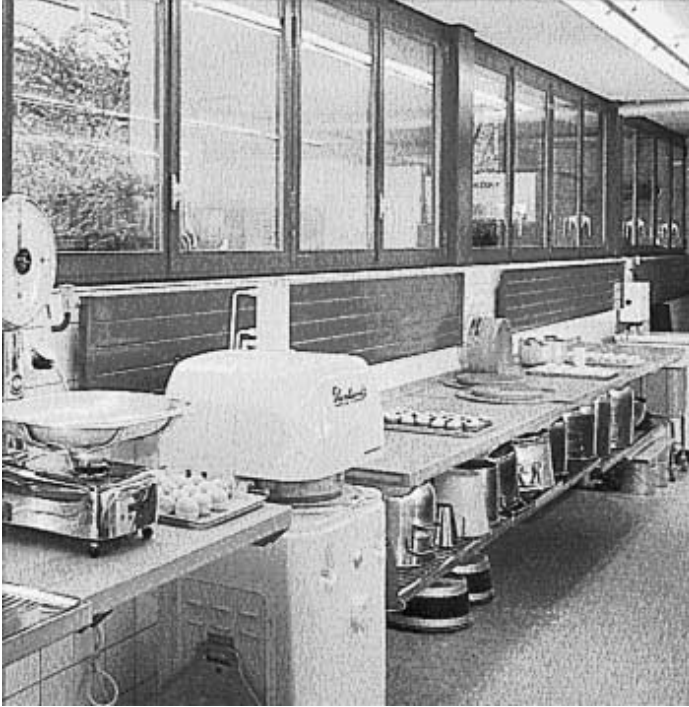


**FIGURE 4.21** Colorful hydronic wall panel designed for localized heating.

ishes increases their appeal to interior designers and architects who often are responsible for fixture selection. Nonetheless, proper engineering analysis is essential to meeting performance specifications.

#### **4.12 ALTERNATE-ENERGY RADIANT HYDRONIC HEATING SYSTEMS**

---

The principles, which apply to other radiant hydronic panel heating systems, apply to hydronic system design for alternate-energy applications. The key difference is the focus on design impacts dictated by the decision that alternate energy is the driving design influence. A characteristic of alternate energy is the need to take advantage of intermittent and sometimes unpredictable availability and to provide for required storage of thermal capacity in order to minimize the use of more costly or less desirable backup or complimentary energy sources when alternate energy is inadequate or unavailable. (See Fig. 4.22.)

Alternate-energy fluid temperature varies with heat source, collector, fluid warmth enhancement, and retention equipment and design. Thermal storage strategies seek to match thermal input capacity with thermal heating requirements. Thermal storage in building mass has been maximized through increased mass design

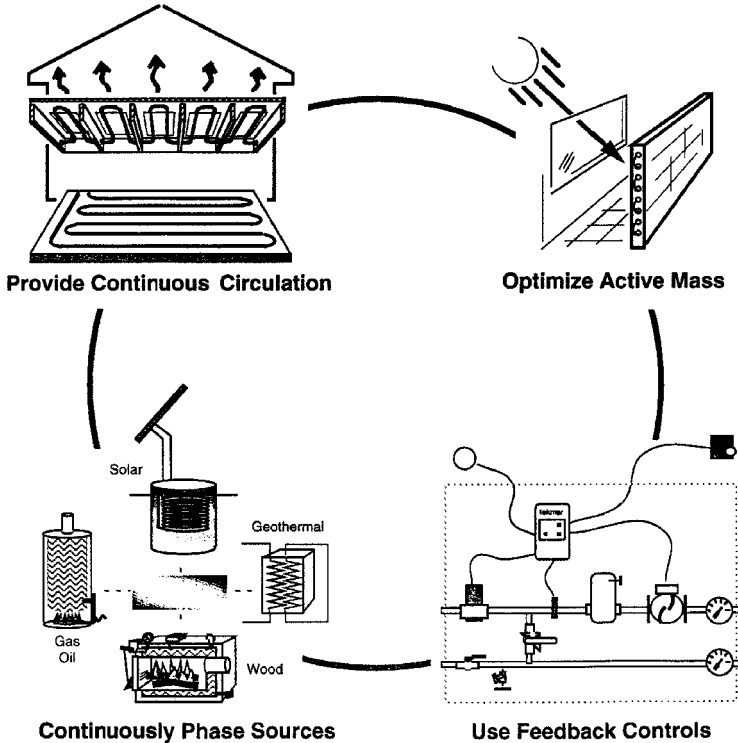


**FIGURE 4.22** Design considerations for radiant hydronic solar or alternate-energy system.

and utilization of all available mass, including everything from countertops to wall, floor, and ceiling surfaces. Fast-acting radiant ceiling and wall electric panels are appropriate guarantors of occupant thermal comfort during periods of alternate-energy supply deficit. As with other hydronic systems, material selection, fluid filtration and pH balance, and regular maintenance throughout the year are essential factors for consistent long-term operability.



---

# CHAPTER 5

---

## CASE STUDIES\*

---

Case study information is frequently requested, but seldom fully understood in terms of relating the conditions under which it was conducted to the actual results reported. In fact, the real need is for studies with populations that are of sufficient size to provide a statistically representative sample of actual field performance of heating or cooling systems “as used” in buildings “as built.” Unfortunately, the costs, politics of energy source, equipment involved, and proponents of the study make it almost impossible for the major consensus research-funding agencies and organizations to set up and conduct large-scale comparative heating or cooling system performance studies. One possible large-scale study approach would be a government-funded study of identical existing government buildings. Oversight would be provided by an ASHRAE committee composed of the relevant technical committee chairs and convened for the purpose of conducting a comparative operating analysis, the results of which would be incorporated in the ASHRAE Handbook and related standards.

Yet, there is considerable solid research that addresses specific research aspects of radiant heating and radiant system performance, capacity design, and human thermal comfort. The performance and design of radiant heating systems is not a secret or a mystery, but it is not incorporated into mainstream engineering system selection and design or familiar to most building contractors. The objective of this Handbook is to provide the information required to include radiant heating systems in all heating system selection analyses.

By reading this entire Handbook, the reader develops a comprehensive knowledge of the comparative differences between radiant and alternative convection heating and cooling systems. There are also broadly based studies that provide additional foundation for understanding. The advantage of recognizing mean radiant temperature (MRT) and the role of human thermal comfort has been recognized by many visionaries, including Richard Hayter who later served as the president of ASHRAE. He noted in *Education for Energy Conservation*, “Research regarding human comfort has led to the creation of numerous opportunities for energy conservation in the built environment.” But as this book is published more than 10 years later, the relationship is still not well understood. Therein lies the usefulness of the information, which forms the skeleton of this Handbook.

A study that conforms to the scientific standard of analysis seeks to isolate all but the variables being studied. A number of so-called micro studies have produced very useful information, some of which are included in this Handbook. However, in overall system performance, or macro, studies, human thermal comfort, which is subject-

---

\* Tables and figures mentioned in this chapter and followed by an asterisk are in the original ASHRAE publication; these items have not been reproduced.

tive, must be involved. The introduction of lifestyle influences requires a very large population and comprehensive data collection protocol to develop information that is applicable to the general population about the way they use their heating and cooling systems. Because this is difficult, costly, and may be outdated by technological and construction practice changes, there are not many useful macro case studies where sufficient information is available to determine comparative system field performance. Finally, when benchmarking to research, it is always important to carefully examine the research test conditions in order to determine that the information that was developed is robust. Sufficient technical information is now available to define comparative system performance within the defined operating protocol of the system design and performance.

## 5.1 RESEARCH

---

Much radiant heating and cooling technical research has been funded through the ASHRAE Research Program made possible by the contributions of the membership. Projects originate in the technical committees that are responsible for the area of research involved. Committee members annually prepare a research plan, which includes their prioritized research projects. A statement of work is developed, voted on by the committee, and forwarded to the Research Activities Committee and oversight committees for approval to be presented in the semiannual request for proposal listing. The project-monitoring subcommittee reviews the bids, makes a recommendation on which the entire technical committee votes for referral to the Technical Activities Committee and oversight committees for approvals of contract award. Once contracts are signed, the work may begin.

The technical committee (2.1) responsible for physiology and human comfort and predecessor committees initiated the original work on thermal comfort. Following over 40 years of research, including legendary field studies involving human participants, the committee work culminated in the development of the first edition of ASHRAE Standard 55 in 1984, *Thermal Environmental Conditions for Human Occupancy*. The significance of mean radiant temperature (MRT) in the provision of human thermal comfort led to the creation of an additional Technical Committee for Radiant Heating and Cooling (TC-6.5).

This section will look in depth at four representative research projects that entail comprehensive review of the subject covered, encompassing the entire range of radiant heating and cooling. The first, one of the most significant radiant heating and cooling research projects developed by TC-6.5, is *A Study to Determine Methods for Designing Radiant Heating and Cooling Systems*, conducted by Ronald Howell, final report ASHRAE RP-394, May 1987. The project is noteworthy for its comprehensive assimilation of information when mainframe computer capability was less than today's personal computer! The study concluded that heat load requirements and therefore the radiant equipment sizing could be reduced considerably from those shown in this study, which were based upon ASHRAE design procedure. Exerpts from this and other reports are included in the Handbook, along with other ASHRAE research with permission.

The Howell study is an annotated bibliography that is included as an addendum to this Handbook. The bibliography has been updated to include additional annotated references published since the original work. The study ties together information covering the entire spectrum of radiant heating and cooling equipment, sizing, and design, and it provided a springboard for the advances in knowledge made possible by subsequent research.

The information developed in the Howell report confirmed the need for the second landmark research project: ASHRAE RP-657, *Simplified Method to Factor Mean Radiant Temperature (MRT) into Building and HVAC System Design*, in September 1994. This research and the resulting methodology, developed by Byron W. Jones and Kirby S. Chapman of Kansas State University, are covered in detail in Sec. 8 of this Handbook. Each ASHRAE study is representative of the wealth and quality of useful ASHRAE research that has been conducted over many years and is available to members and the public alike for a nominal cost. Arguably, RP-657 is the most significant technical contribution of the last decade because it provides the design methodology to implement Standard 55, *Thermal Environmental Conditions for Human Occupancy*, for any space in the built environment.

The second comprehensive study is ASHRAE RP-876, *The Impact of Surface Characteristics on Radiant Panel Output*, in March 1997. The report is useful in the breadth of explanation and analysis related to determining radiant panel performance under various location and surface conditions. Basic information was presented in a form that is easy to understand and useful to all participants in the radiant heating design and installation process. The research reaffirmed that surface characteristics are not a significant factor in radiant panel output, but that insulation values of panel surface coverings and panel planar location as it relates to the radiative-convective split are factors that must be incorporated into the design process.

The third report is *An Evaluation of Thermal Comfort and Energy Consumption for the ENERJOY® Radiant Panel Heating System*, by the NAHB Research Center, May 1993. The landmark study uses occupant thermal comfort as the indicator on which electric energy consumption information is based over the course of the heating season. The study, in an occupied 2300-ft<sup>2</sup> research park house produced comparative sizing, comfort, performance under design conditions, energy usage, and operating cost data for both an air-to-air heat pump and electric baseboard heating system. This study was also used to validate the BCAP model developed in RP-657 because the data collection was comprehensive and robust.

Comprehensive comparative heating system energy consumption data for most of the common heating systems are presented in the fourth research demonstration project reported in ASHRAE Transactions SF-98-9-4, *Case Study: Seven-System Analysis of Thermal Comfort and Energy Use for a Fast-Acting Radiant Heating System*. The retrofit case study was conducted in a large retirement community over several years and uses electric and gas utility billing information adjusted for base load consumption to derive the estimated heating energy usage. In addition to useful comparative energy data, the study addresses the wide range of issues that need to be factored into analysis of installation and operating cost estimates for retrofit applications that are unique to each heating system under consideration.

The research projects and case studies included in this chapter were selected because they provide the reader with comprehensive information to distinguish radiant from convection system design and performance. For additional information on any radiant area of interest, please refer to the annotated bibliography at the end of this book.

### **5.1.1 Extracts from *A Study to Determine Methods for Designing Radiant Heating and Cooling Systems (RP-394)***

Selected passages from RP-394 are presented here with permission from ASHRAE. They have been edited in the context of this Handbook to serve the reader. For more detailed information, including the results of each of the analyses conducted, the reader is referred to the final report.

The goal of this study was to obtain design data and relevant manufacturers data concerning the design procedures for radiant heating and cooling systems. A comprehensive literature search was conducted which resulted in an annotated bibliography with over 250 entries. This bibliography was subdivided into the following sections: load analysis and modeling, convection coefficients, comfort conditions, radiant thermal comfort, floor panels, panel heating and cooling, infrared heating, design procedures, energy consumption, transient effects, controls, and spot heating and cooling.

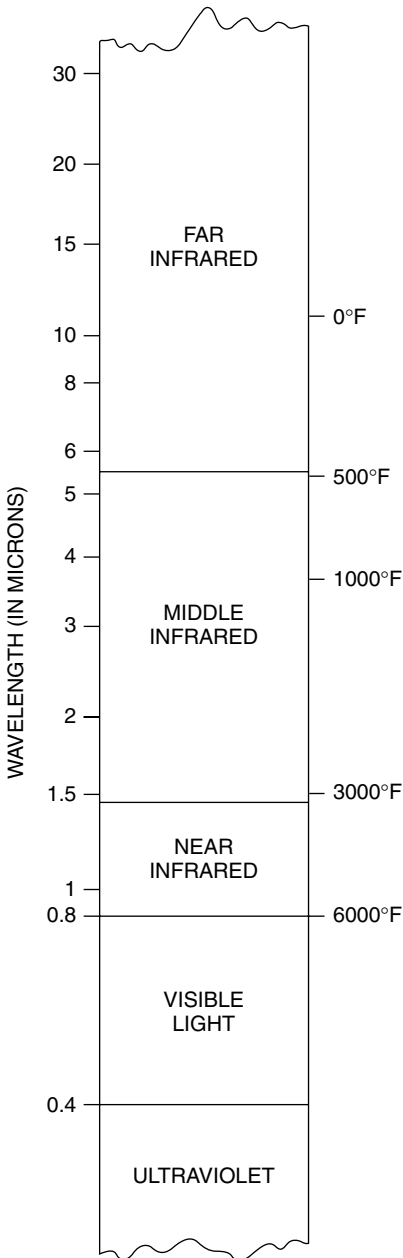


FIGURE 5.1 Wavelength.

The manufacturers survey resulted in identifying three commonly used categories of radiant heating/cooling surface temperature ranges. The low surface temperature range is 80°F to 200°F for heating and 50°F to 70°F for cooling. The medium surface temperature range is from 700°F to 1100°F and the high surface temperature range is from 1200°F to 2000°F. These surface temperature ranges identify the four commonly used systems for radiant heating and cooling: ceiling panel heating and cooling and floor heated panels operate in the low temperature range, U-tube infrared units operate in the medium temperature range, and modular gas-fired or electric infrared units operate in the high temperature range (Fig. 5.1).

Analysis of the above information indicated that the only reliable or appropriate design consideration would involve looking at the surface-to-air design process and not the means, which is used to obtain the heated surface temperature. There are many variations or schemes used to obtain appropriate surface temperatures and it was not the object of this study to evaluate all of these schemes. Each manufacturer or designer has a unique method for obtaining a specific surface temperature. Descriptions and applications are provided for eleven of the most common configurations. These are: hydronic floor panels, electric floor panels, air floors, hydronic wall panels, electric wall panels, hydronic ceiling panels, electric ceiling panels, gas fired radiant ceramic tube surface infrared units, gas fired radiant ceramic tube surface

infrared units, gas fired radiant tube infrared units, electric infrared units, and miscellaneous electric systems.

A computerized technique was developed to relate heater surface temperature to the space heating requirements while maintaining the Fanger comfort constraints. For each variation, the required area of heater surface was calculated and the actual design heat loss for the radiant heating system was calculated and compared to the ASHRAE standard design procedure. Calculations were made for the four types or radiant systems (ceiling panel heating and cooling, heated floor panels, U-tube infrared, and modular infrared) for typical ranges of many of the variables. The variables considered were:  $U$  factors, quantity of glass, heater surface temperature, surface emissivities, convection coefficients, outside air design temperature, room size, ceiling height, infiltration rate, number of heating surfaces, heater placement, and use of reflectors or deflectors on infrared units.

The major variable which was found to have a significant effect on the difference between the actual design heat loss and the ASHRAE standard heat loss was the infiltration rate. The percent difference in these two design-heating loads varied from  $-4\%$  at 0.5 ACH to  $-16\%$  at 4 ACH. The actual design heat loss is less than the ASHRAE standard design heat loss.

It was also recognized that room air temperature stratification can affect the heat loss calculations and thus the required heating unit size. However, there is inconclusive evidence concerning the amount of room air temperature stratification and when room air temperature stratification will occur.

There was also evidence from this study that the ASHRAE design heat loss procedure will over predict the radiant unit size by up to 16% when the occupants are engaged in medium activity wearing a medium level of clothing. However, the effects due to radiant temperature asymmetry and its interaction with comfort conditions at various activity and clothing levels are not completely known. It should be recognized that higher activity levels and clothing levels appear to allow smaller radiant heater sizes than those predicted by the common ASHRAE heating design procedure (Table 5.1). This being due to a higher mean radian temperature experienced by the occupants and an accompanying lower room air temperature necessary to satisfy comfort criteria. The resulting lower room air temperature leads to a reduced heat load requirement for the structure than what is predicted by the common ASHRAE heating design procedure. Given all of the conditions implicit in the parameters required for the design load calculation, the heat load requirements and therefore the radiant equipment size can be reduced considerably from those shown in this study.

Additional work was found to be needed in several areas that are described in the report. This work involves prediction of surface convection coefficients, room air temperature stratification, surface emissivities, comfort criteria during radiant temperature asymmetry, radiant system dynamics, and design procedures for heated floor systems.

Design methods considering techniques for calculating loads, sizing equipment and positioning equipment are presented for each of the common types of radiant heating systems. The design procedure for radiant cooling which is presented in the *1984 ASHRAE Systems Handbook* (ASHRAE, 1984), was found to be adequate and is recommended for use.

The Objectives and Scope stated

The goal of this project was to obtain a body of accurate and relevant data on method of designing radiant heating and cooling systems. The data includes methods of calculating loads, sizing equipment, and positioning equipment.

**TABLE 5.1** Comparison of Room Air Temperature and MRT for Comfort Conditions at Different Activity and Clothing Levels with 30% Relative Humidity and 0.2 m/s Relative Velocity

Sedentary activity, light clothing		Sedentary activity, medium clothing		Medium activity, light clothing		Medium activity, medium clothing	
MRT, °F	$t_{a}$ , °F	MRT, °F	$t_{a}$ , °F	MRT, °F	$t_{a}$ , °F	MRT, °F	$t_{a}$ , °F
68	87.8	60.8	82.4	60.8	75	50	67.6
71.6	85.1	62.6	81.5	62.6	74.5	51.8	66.2
75.2	83.3	64.4	80.6	64.4	72.3	53.6	65.5
78.8	81.5	66.2	79.9	66.2	71.4	55.4	63.9
•	•						
80.6	80.6	68	79	68	70.2	57.7	63.0
				•	•		
82.4	79.7	69.8	78.1	69.8	69.8	59.0	62.6
						•	•
86.0	75.6	71.6	77	71.6	67.8	61.2	61.2
89.6	72.9	73.4	75.2	73.4	66.0	62.6	59.9
		•	•				
93.2	71.6	76.5	76.5	75.2	64.4	64.4	57.6
96.8	68.4	77	74.7	77	63.5	68.0	56.3
		80.6	72	78.8	62.8	71.6	53.1
		84.2	69.3			75.2	50.7
		86	68.4				

The study has focused on identifying all significant types of radiant heating and cooling systems by means of a literature search and analysis of appropriate available data and technical material. From this material, a procedure for designing radiant heating and cooling systems has been developed. This procedure includes methods of calculating loads, sizing equipment, and positioning equipment.

A major effort of the project has been the preparation of an annotated bibliography of published sources of information for radiant heating/cooling systems. As a result of the preparation of this annotated bibliography, additional research needed in order to improve the recommended methods for calculating loads, sizing equipment, positioning equipment, and system dynamics has been provided.

Convective and radiant heating and cooling systems have been used for many years in providing comfort systems in rooms occupied by people and/or materials. These two types of systems produce different comfort environments due to their nature of heat delivery or removal, and thus there is no fundamental reason to expect them to be sized by the same technique or to require the same energy to produce identical levels of comfort. Proponents of radiant heating systems assert that these types of systems offer the potential for reduced heating unit sizes and reduced energy consumption. They claim that the room may be operated at a lower air temperature than if it is heated by a convective system because the radiant heat from the heater falls directly on the occupants, producing comfort conditions. However, there is also the opposite factor, that radiant heating systems produce higher floor, wall, and glass temperatures due to the radiant heaters heating these surfaces and not the air, and thus producing greater heat losses to the surroundings. *The calculations in Sec. 8 of this Handbook illustrate that this statement is not necessarily true for all cases and, in fact, is only true for limited applications. In addition, the research publication*

The Impact of Heating Systems on Wall Surface Temperatures, *ASHRAE Transactions 106 (I)*, demonstrates that the wall temperatures are, in most cases, less for radiant heating systems than for forced-air heating systems. In essence, the high emissivity of common wall surfaces and the opacity and reflectivity of glass for long-wave radiant energy result in lower wall surface temperatures and less heat loss under conditions of equivalent occupant thermal comfort. The key factor to remember is that design of the built environment should be based on operative, not dry-bulb, air temperature. Under these conditions, wall heat loss with radiant systems is generally less than with forced-air systems.

The thermal environment within a room and its rate of heat loss are determined by the configuration and structural materials used in the walls, floor, and ceiling; the amount of infiltration air forced through the room; and the nature of the heat suppliers. A convective type of system produces an environment where the air temperature is greater than the MRT in the space. A radiant heating system on the other hand, produces an environment in which the MRT (or average room surface temperature) is higher than the air temperature. For this reason, the infiltration air losses will be greater in convective than in radiant heating systems. Convective types of systems using fans for delivering heated air that cause slight air pressure differences will tend to increase the air infiltration loss. Radiant heating systems also have the advantage of increasing the MRT to which occupants are exposed and thereby allowing comfort at lower air temperatures.

There are two fundamentally different characteristics to be considered: (1) the concept of sizing of radiant heating systems, and (2) estimating the energy required by radiant systems for providing comfort conditions over a heating season. For sizing, design calculations are made to indicate what is the expected *maximum rate of total heat delivery*, which is to be expected from the heater. Along with the total size of the heating system is the positioning of the individual heating units so that they provide uniform comfort conditions throughout the space. In Chap. 25 of the *ASHRAE Handbook of Fundamentals* (Ref. 1) a procedure is presented for determining the design-heating load for a structure. The fundamental objective of this project has been to determine if this ASHRAE Design Heating Load Procedure is applicable to radiant heating systems.

The estimation of the energy used by a radiant heating system over a heating season is a separate and more complicated problem. System dynamics and thermal storage characteristics of the structure are important factors in answering this question. It is questionable whether some of the simpler procedures presented in Chap 28 of the *ASHRAE Handbook of Fundamentals (HBF)* (1) (ASHRAE, 1985), such as degree-day method, full load hours, or BIN method are applicable to radiant heating systems. This project does not address the energy requirement calculation. Section 8 demonstrates calculations and results for several types of radiant heating applications.

There are three general categories of radiant heating and cooling systems, and the temperature range in which they operate can identify these. One category is that of panel heating and cooling systems where the surface temperature can be called *low* and is in the range of 80°F to 200°F for heating and 50°F to 70°F for cooling. In these systems, the surface temperature is controlled in order to vary the quantity of heat being delivered or absorbed. The controlled temperature surfaces may be in the floor, walls, or ceiling, and the temperature is maintained by circulating water, air, or electric current.

The second type of radiant system comprises the medium-temperature-range units, which operate from about 700°F to 1100°F and consist of radiant tubes through which the products of combustion from a gas burner are circulated and then exhausted to the outside. These units come in integral lengths, which can be placed in specific patterns

or in U-tube-shaped units of different lengths. They have the advantage of exhausting the exhaust products to the outdoors rather than inside the structure.

The third type of radiant unit are the modular high-temperature infrared units, operating in the range of 1200°F to 2000°F surface temperature. These consist of gas- or electric-operated units placed at various locations throughout the space and are generally used for spot-heating applications, or in many cases, for full-area comfort heating. The gas-fired units have the disadvantage of discharging the products of combustion inside the conditioned space.

One of the advantages, and in some cases a disadvantage, is the maintenance of comfort conditions when using radiant heating. The advantage occurs when the units are properly sized and located, providing a higher MRT for the occupants, which then permits a lower air temperature for equal comfort conditions. The disadvantage can occur if the radiant heat is concentrated to such a condition that the asymmetric temperature felt by the occupant is such that discomfort occurs in the space. Any design procedure that is specified must account for maintaining comfort and not creating severe asymmetric temperature conditions. Typically, by satisfying the Fanger comfort equation (Fanger, 1967) and limiting the asymmetric temperature to 9°F, no discomfort should be experienced by the occupants.

Another advantage claimed for radiant heating systems is that the negligible air temperature gradient experienced by spaces using radiant sources rather than convective sources for heating. This occurs because radiant systems heat surfaces, which in turn heat people and objects and by their nature create very little air motion resulting in a more uniform room air temperature distribution. Convective heating systems will generally have air temperature gradients due to the higher temperature of the air brought into the space for heating purposes with a resultant higher air temperature at the ceiling than at the floor.

In Fig. 5.2, a schematic is given of room air temperature gradients for heated ceiling panels and heated floors. These schematics were prepared from data from 1953 results taken at the ASHRAE Laboratory in Cleveland, Ohio. These two examples show that there is virtually no air temperature stratification for radiant heated systems (ceiling or floor) with ceilings up to about 12 ft in height.

In Fig. 5.3, some room air temperature profiles are given for some gas-fired infrared radiant heating systems and oil-fired forced-air rooftop units. These results were extracted from "Engineering Principles Support an Adjustment Factor When Sizing Gas-Fired Low-Intensity Infrared Equipment," by N. A. Buckley and T. P. Seel (1986). The situation considered in Fig. 5.3 is for a garage-type building, with eight overhead doors, that is 80 ft wide by 200 ft long with a 22-ft ceiling. The air temperature was measured at the centerline of the building 18 ft from the doors. Results are shown when the outside air temperature is 41°F and 15°F. At 15°F outside air temperature, there is very little room air temperature stratification for either the radiant system or the convection system. It should also be noted in Fig. 5.3 that the forced-air rooftop unit was not maintaining comfort condition in the garage because the air temperature was at 56°F. Both systems show only a 3°F to 4°F room air temperature variation up to 22 ft. When the outside air temperature is 41°F, the radiant heating system exhibits only a 4°F (66°F floor to 62°F ceiling) temperature change in the room air in the 22-ft height. However, at this same outside air temperature, the oil-fired rooftop unit exhibits a 9°F (64°F near the floor to 73°F at the ceiling) temperature variation in the room air temperature. It appears from these results that when the outside temperature was 15°F the convection unit operated all the time, maintaining a constant room air temperature. When the outside temperature was 41°F, the convection heating unit cycled on and off, allowing air temperature stratification to occur.

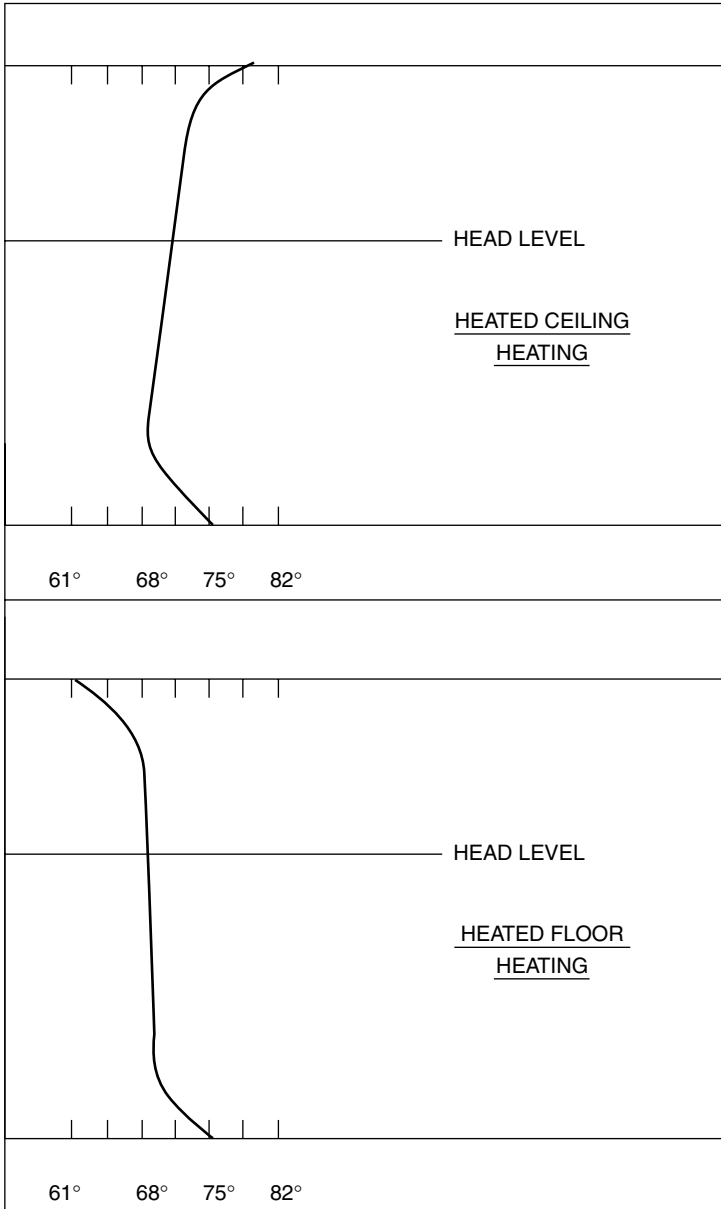


**FIGURE 5.2** Schematic of air temperature gradients for radiant ceiling heating and radiant floor heating. (Source: *ASHVE Laboratory Data, July 1953.*)

RADIANT HEATING SYSTEMS

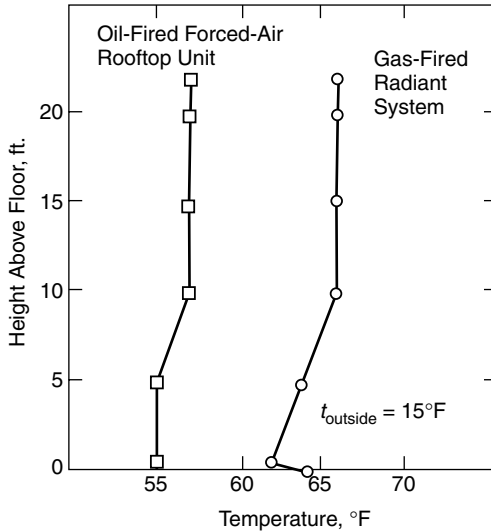
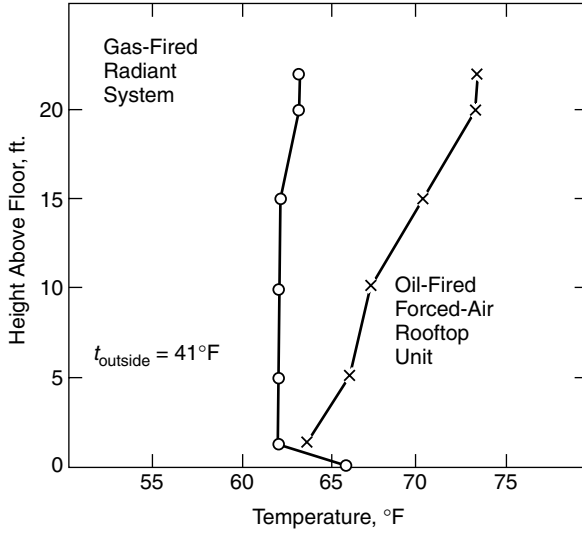


**FIGURE 5.3** Temperature stratification in a highway garage building—80 × 200 ft with 22-ft ceiling. (a) Outside temperature = 41° F. (b) Outside temperature = 15° F (Source: N. A. Buckley and T. P. Seel, 1987.)

In Fig. 5.4, some additional room air temperature stratification data are presented from the same source as that of Fig. 5.3. These data are for a different building, a warehouse that was well insulated with 6 in or more of insulation on the walls and roof. This building had two walk-in doors and two overhead doors. The estimated infiltration rate was about one-half air change per hour. The warehouse was 30 ft wide by 100 ft long with 21-ft-high ceilings. It can be seen in Fig. 5.4 that for this situation with a gas-fired radiant heating system, room air temperature stratification did occur. In this case, the room air varied by 8°F (61°F near the floor to 69°F near the ceiling).

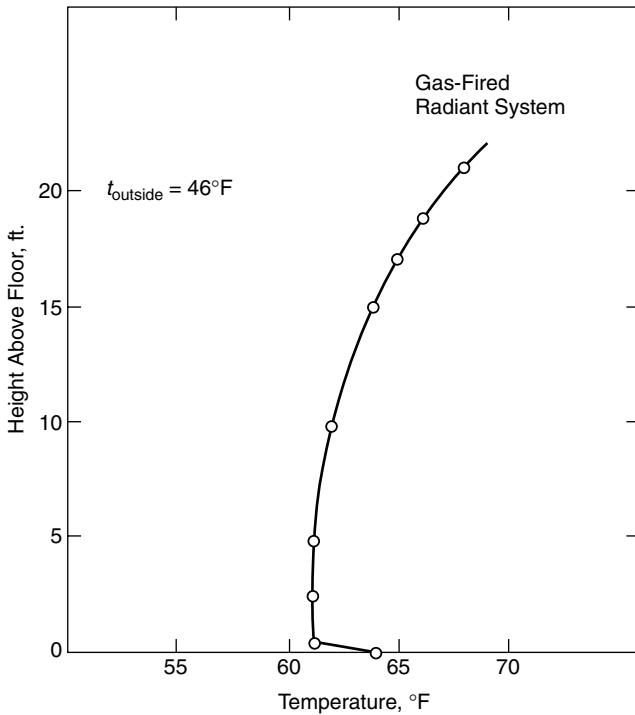


**FIGURE 5.4** Temperature stratification with infrared heating system in a well-insulated warehouse. (Source: N. A. Buckley and T. P. Seel, 1987.)

Figure 5.5 shows some room air temperature measurements for a heated floor case and a cooled ceiling panel case. These are results from 1953 data taken at the ASHVE Laboratory in Cleveland, Ohio. Articles containing this type of data are listed under “G-Panel Heating and Cooling” in the annotated bibliography.

From the results given here and other results in the literature, room air temperature gradients of 0.5°F to 1.5°F per foot could be experienced in both forced-air convection heating systems and in some situations for radiant heating systems. The room air temperature gradient depends on room size, quantity of ceiling and wall insulation, and the air distribution system design and operation. *For radiant heated*

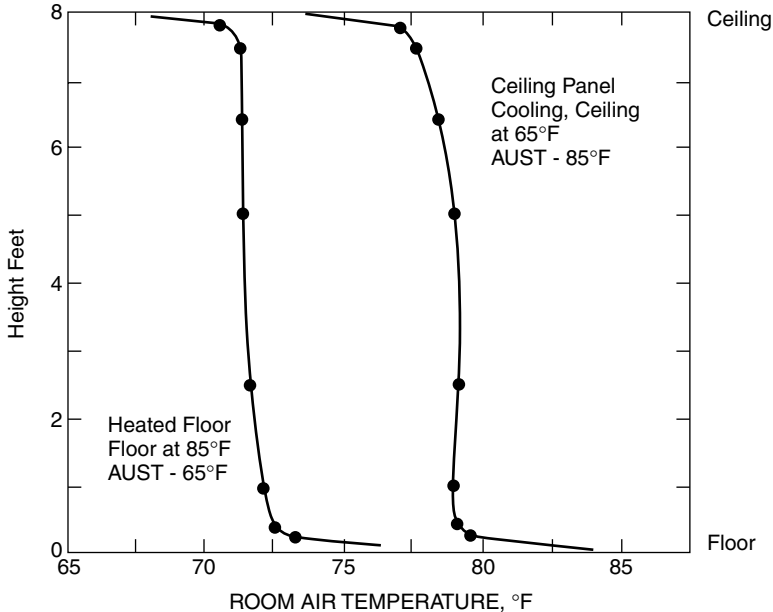


**FIGURE 5.5** Measured air temperatures for radiant heating and cooling situations. (Source: ASHVE Laboratory Data, July 1953.)

and cooled rooms, it is most common to observe a negligible room-at-air-temperature gradient. It should be kept in mind, however, that application of the available room air temperature gradient requires careful consideration of all of the parameters under which the data were measured and collected. All data cannot arbitrarily be applied to any situation. From analysis of the available data on room air temperature stratification, it is recommended that additional research be done in order to assess the effects of the variables just discussed.

With a temperature gradient in the room, the infiltration heat loss is greater than when a gradient does not exist. Because of this, it is expected that convection types of heating systems will have larger design infiltration losses than radiant systems. During the heating mode, infiltration air will enter at the bottom of the space and exfiltration will occur at the top of the space. This exfiltrated air will be at a higher temperature in the convection-type systems, thereby creating a larger heat loss than experienced in radiant types of systems. This is another expected benefit of radiant heating types of systems.

Also, when a temperature gradient in the room air exists, there will be a higher temperature at the ceiling-roof and upper walls for the heating mode. This will require a larger heating unit in order to account for the larger temperature difference between the roof and upper wall area and the outside air. For radiant heating systems where it is common to have a negligible room air temperature gradient, another expected benefit could be a smaller required unit size due to this decrease in ceiling-roof and upper-wall heat losses.

Radiant heating systems are used in many types of applications such as offices, hospitals, homes, warehouses, and manufacturing or industrial situations. For hospitals and offices ceiling panel radiant systems are typically used. For homes, offices,

and warehouses, very often radiant floor panels are used. The medium- and high-temperature infrared systems are generally found in warehouses, manufacturing, and industrial situations. These general types of applications are not meant to be restrictive, because each application should be addressed individually by weighing the advantages and disadvantages of each type of system. Additional details on applicability are given in the applications matrix (Table 5.2).

This project investigated a *system design procedure* for radiant heating and cooling. The evaluation of the energy requirements for radiant heating systems was not considered. The system design procedure involves the estimation of the design heating or cooling load; the selection of the type of radiant system to be used (ceiling panels, floor panels, U-tube modular units, or infrared modular units), which is partially based on the allowable heater surface temperatures for the application considered; and the positioning of the heaters in the space. In addition, a literature survey has been conducted and is included in the annotated bibliography.

The report contains the ASHRAE standard procedure from the Handbook, which is reprinted here so the reader can be clear on the benchmark with which the report examples were compared (Table 5.3).

### 5.1.2 Calculation of Design Heating Load

This investigation is directed at providing a design procedure for radiant heating and cooling systems. The major concern is whether the ASHRAE standard heating load design procedure can be used for radiant systems. The procedure developed for this project is based on the best available information for radiant and convective exchange, but has not been validated with experimental data. This procedure will be presented first, followed by a procedure developed specifically for this project, and a discussion on the differences between these techniques and some other techniques found in the literature.

***Design Inside Air Temperature.*** It is common practice to select the inside design dry-bulb temperature at 75°F in most localities in the United States. Generally, this is done without accounting for the comfort constraints previously described. This temperature is used in both the transmission loss and infiltration loss calculations, and a choice of this value will affect the design loads for the space in proportion to the temperature difference between the inside and outside at design conditions. As indicated in Sec. 3.0 of the ASHRAE RP-394, "Definitions and Terminology," the value used for the inside design temperature in this analysis has been set at 75°F.

***Room Air Temperature Gradients.*** For rooms, which are 8 to 10 ft high, a small temperature gradient in room air may exist as discussed, but is usually not incorporated into the design heat loss calculation. For higher ceiling-roof or spaces, this gradient can affect the design heat loss due to higher transmission and infiltration losses. For the ASHRAE standard design heat loss calculations (HLD) made later, it is assumed that there is no air temperature gradient. However, this ceiling temperature gradient is incorporated into another design heat loss ceiling gradient (HLCG) to illustrate what effect it has on the results. Typical values of this air temperature gradient are 0.5°F to 2.0°F per foot.

***Wall, Ceiling, Floor Convection Coefficients.*** The  $U$  factors indicated in the transmission loss component include convection on the inside walls, floors, and ceiling that contain a contribution from radiation as well as convection. These values

**TABLE 5.2** Applications Matrix

Type of radiant system	Surface temperature, °F	Integral with construction or add-on possibility	Response time	Total or spot heating	Cooling capacity	Exhaust venting system required	Condensation to be considered
Hydronic floor	05	Integral	Slow	Total	No	No	No
Electric floor	85	Integral	Slow	Total	No	No	No
Air floor	85	Integral	Medium	Total	No	No	No
Hydronic wall	100	Integral	Medium	Total	Yes	No	If cooling
Electric wall	100	Integral	Medium	Total	No	No	No
Hydronic ceiling	85–200	Add-on	Good	Total	Yes	No	If cooling
Electric ceiling	120–200	Add-on	Good	Total or spot	No	No	No
Ceramic infrared	1500–1700	Add-on	Good	Total or spot	No	Yes	If not vented
Tube infrared	720–1300	Add-on	Good	Total or spot	No	Yes	If not vented
Electric infrared	1100–4000	Add-on	Good	Total or spot	No	No	No

*Source:* ASHRAE RP-394.

have been standardized over the years and are commonly used in all design heating and cooling load calculations. When radiant systems are considered, it is important to realize that these standard coefficients may no longer apply due to higher surface temperatures. For the standard ASHRAE design heat loss procedure (HLD), the convection coefficients in Ref. 1 were used and these are given in Table 4.\* Also shown as Table 5\* are common emissivity values for building materials.

The  $U$  factors for the transmission losses also contain outside convection coefficients for the walls and floors and ceilings if appropriate.

### 5.1.3 Development of Design Heat Loss Procedure for Radiant Systems

It is necessary with radiant types of systems to be able to estimate the design heat loss value so that units can be sized and located. It is also important for this study to be able to compare this design load with the ASHRAE standard procedure (HLD) described earlier and to investigate the effect of changing specific parameters in the design process for radiant units. These include effect of higher room surface temperatures, consequences of higher MRTs, and lower air temperatures, and changes in the infiltration heat loss term.

Residential	Applications						
	Industrial	Warehouse	Garage	Commercial office	Sports	School facility	Hospital
X	X	X	X			X	
X		X	X			X	
X							
X				X			
X				X			
X				X	X	X	X
X	X		X	X	X	X	X
	X	X	X		X		
	X	X	X		X		
	X	X	X		X		

In Fig. 5.6, a schematic of the room configuration used for the calculation of the radiant design heat loss values is shown. There are six surfaces specified: four walls, a floor, and a ceiling. For the floor, an emissivity ( $\epsilon$ ), convection coefficient ( $h_c$ ) and a  $U$  factor ( $U$ ) are specified. The ceiling is composed of several portions: heating or cooling panels and ceiling.

For all of the equally sized panels an emissivity ( $\epsilon$ ) and convection coefficient ( $h_c$ ) must be specified. There is no  $U$  factor specified for the heating-cooling panels because this would vary considerably from unit to unit and it can be taken into account in the design process. The remainder of ceiling (see Fig. 5.6) has an emissivity ( $\epsilon$ ), convection coefficient ( $h_c$ ), and a  $U$  factor ( $U$ ) specified.

The four walls can be individually described by giving an emissivity ( $\epsilon$ ), convection coefficient ( $h_c$ ), and a  $U$  factor ( $U$ ) for each wall. This allows the walls to be outside or inside walls by using the actual  $U$  or a small  $U$  [0.001 Btu/(hr · ft<sup>2</sup> · °F)] value. Also, specifying appropriate values of the wall  $U$  factor can vary the contribution of glass in the outside walls.

By specifying the size of the room (length and width), the room height, the number of ceiling panels, and their coordinate locations, the geometry of room is defined. From this information the angle factors between all of the room surfaces can then be calculated.

**TABLE 5.3** General Procedure

---

To calculate a design heating load, prepare the following information about building design and weather data at design conditions.

1. Select outdoor design weather conditions: temperature, wind direction, and wind speed. Winter climatic data can be found in Chap. 24.
  2. Select the indoor air temperature to be maintained in each space during coldest weather.
  3. Estimate temperatures in adjacent unheated spaces.
  4. Select or compute heat transfer coefficients for outside walls and glass; for inside walls, nonbasement floors and ceilings, if these are next to unheated spaces; and the roof if it is next to heated spaces.
  5. Determine net area of outside wall, glass, and roof next to heated spaces, as well as any cold walls, floors, or ceilings next to unheated spaces. These determinations can be made from building plans or from the actual building, using inside dimensions.
  6. Compute heat transmission losses for each kind of wall, glass, floor, ceiling, and roof in the building by multiplying the heat transfer coefficient in each case by the area of the surface and the temperature difference between indoor and outdoor air or adjacent unheated space.
  7. Compute heat losses from basement or grade-level slab floors using the methods in this chapter.
  8. Select unit values and compute the energy associated with infiltration of cold air around outside doors, windows, and other openings. These unit values depend on the kind or width of crack, wind speed, and the temperature difference between indoor and outdoor air. An alternative method is to use air changes. (See Chap. 22.)
  9. When positive ventilation using outdoor air is provided by an air-heating or air-conditioning unit, the energy required to warm the outdoor air to the space temperature must be provided by the unit. The principle for calculation of this load component is identical to that for infiltration. If mechanical exhaust from the space is provided in an amount equal to the outdoor air drawn in by the unit, the unit must also provide for natural infiltration losses. If no mechanical exhaust is used and the outdoor air supply equals or exceeds the amount of natural infiltration that can occur without ventilation, some reduction in infiltration may occur.
  10. The sum of the transmission losses or heat transmitted through the confining walls, floor, ceiling, glass, and other surfaces, plus the energy associated with cold air entering by infiltration or required to replace mechanical exhaust, represents the total heating load.
  11. In buildings with a sizable and reasonably steady internal heat release from sources other than the heating system, compute, and deduct this heat release under design conditions from the total heat losses computed above.
  12. Consider using pickup loads that may be required in intermittently heated buildings or in buildings using night thermostat setback. Pickup loads frequently require an increase in heating equipment capacity to bring the temperature of structure, air, and material contents to the specified temperature.
- 

As indicated in Fig. 5.6, there is a contribution to the total design heat loss by the infiltration term. For this analysis an air change per hour (ACH) was specified as input information and then with the room volume known an air volume could be calculated.

It is important to understand that all of the surfaces are coupled thermally through their radiant exchange and their convective exchange with the room air. In addition, the outside walls will transfer heat to the surroundings as will the floor and

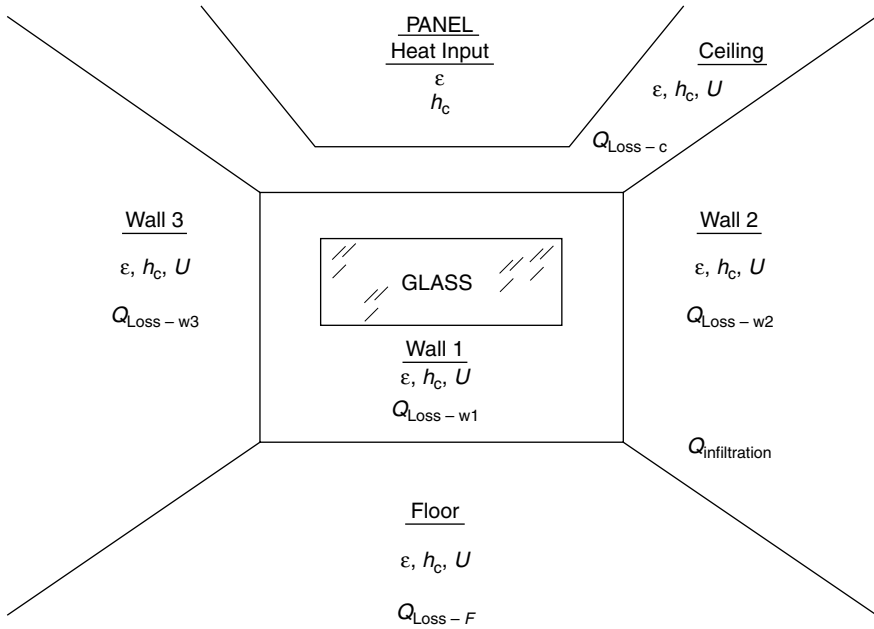


**FIGURE 5.6** Schematic of room configuration used for the calculation of radiant design heat loss values.

the ceiling. The heating panels will be supplying heat by radiation and convection to the other surfaces and the room air. At the same time, the infiltration air will be affecting the overall heat balance of the room air.

The following sections contain a description of the system of equations solved using a computer program and how these equations were formulated. To achieve this aim, it was found that the following system of equations needed to be solved:

1. Heat balance on the room surfaces (six surfaces)
2. Heat balance on the complete room
3. The comfort equations (two equations)
4. The definition of MRT

These resulted in 10 equations that need to be solved, where 9 of the equations are coupled and 8 of the 9 are nonlinear. This required solving a system of nine nonlinear equations simultaneously. The solution was done using an algorithm based on Newton's method. Once this system of equations was solved and all of the temperatures known, the design heat losses and other parameters were evaluated.

**Heat Balance on Room Surfaces (Ref. 4).** Each room surface area  $A_j$  is in radiant exchange with all the other surfaces and is in convective exchange with the air in the room. The sum of these two heat flows,  $q_r$  and  $q_{cv}$  will, under steady-state conditions, be equal to the conductive heat flow through the surface as shown by:

$$q_r + q_{cv} + q_{cd} = 0 \quad (5.1)$$

where:  $q_r$  = net radiation heat transfer from  $A_i$   
 $q_{cv}$  = convection between air and surface  $A_i$   
 $q_{cd}$  = conduction through surface  $A_i$

**Radiant Exchange Rate.** For emittance of surfaces at or above 0.9, surface reflections can be ignored from surfaces, and the radiant exchange can be expressed as:

$$q_{r,i} = \varepsilon_i \sigma T_i^4 - \sum_{j=1} \varepsilon_j \sigma T_j^4 F_{A_i \rightarrow A_j} \quad (5.2)$$

**Convective Heat Transfer.** This term is evaluated from the following equation:

$$q_{cvi} = h_{c,i}(T_i - T_a) \quad (5.3)$$

where  $T_i$  is the temperature of surface  $A_i$ . The heat transfer coefficient  $h_{c,i}$  that was selected was different for the nonradiant heating and radiant heating cases. The reason for this is that in the nonradiant heating systems, higher air velocities and lower surface temperatures are expected. For the *nonradiant heating calculation*, the following coefficients were used:

$$\text{Ceiling/floor, upward heat flow} \quad h_c = 0.712 \text{ Btu}/(\text{h} \cdot \text{ft}^2 \cdot ^\circ\text{F})$$

$$\text{Ceiling/floor, downward heat flow} \quad h_c = 0.162 \text{ Btu}/(\text{h} \cdot \text{ft}^2 \cdot ^\circ\text{F})$$

$$\text{Walls} \quad h_c = 2.03 \left( \frac{\Delta T}{H} \right)^{0.22} \left[ \frac{\text{W}}{\text{m}^2 \cdot ^\circ\text{C}} \right]$$

where  $\Delta T$  is the average temperature difference between the surface and the air in degrees Celsius ( $^\circ\text{C}$ ), and  $H$  is the height of the room in meters (m).

For the radiant heating systems, the following coefficients were used:

*Heated Ceiling.* Heated ceiling panels:

$$h_c = 0.041 \left( \frac{\Delta T}{D_e} \right)^{0.25} \left[ \frac{\text{Btu}}{\text{h} \cdot \text{ft}^2 \cdot ^\circ\text{F}} \right]$$

where  $D_e$  is the equivalent diameter (four times the area divided by the perimeter).

Unheated ceiling portion:

$$h_c = 0.162 \text{ Btu}/(\text{h} \cdot \text{ft}^2 \cdot ^\circ\text{F})$$

Walls:

$$h_c = 0.29 \left( \frac{\Delta T^{0.32}}{H^{0.05}} \right)$$

Floor:

$$h_c = 0.712 \text{ Btu}/(\text{h} \cdot \text{ft}^2 \cdot ^\circ\text{F})$$

*Heated Floor.* Heated floor portion:

$$h_c = 0.39 \frac{\Delta T^{0.31}}{D_e^{0.08}}$$

Unheated floor/ceiling area:

$$h_c = 0.712 \text{ Btu}/(\text{h} \cdot \text{ft}^2 \cdot ^\circ\text{F}) \quad \text{upward heat flow}$$

$$h_c = 0.162 \text{ Btu}/(\text{h} \cdot \text{ft}^2 \cdot ^\circ\text{F}) \quad \text{downward heat flow}$$

Walls:

$$h_c = \frac{0.29\Delta T^{0.32}}{H^{0.05}}$$

**Conductive Heat Transfer.** Under steady-state conditions, the heat conduction per unit area  $A_i$  is given by:

$$q_{\text{cd},i} = C_i(T_i - T_o)$$

$$C_i \equiv \text{overall wall conductance from inside surface to outside air} \quad (5.4)$$

$$= \frac{1}{\frac{x_1}{K_1} + \cdots + \frac{1}{a_1} + \cdots + \frac{1}{h_o}}$$

where  $x$  is the wall section thickness,  $K$  is the material thermal conductivity,  $a$  is the air space conductance in the wall, and  $h_o$  is the convection and radiation coefficient of heat transfer from the outside surface of the wall.

For calculation in the program,  $C_i$  was calculated by:

$$\frac{1}{C_i} = \frac{1}{U_i} - \frac{1}{h_i} \quad (5.5)$$

where  $U_i$  is the overall heat transfer coefficient from the inside air to the outside air using standard or typical ASHRAE values, and  $h_i$  is the heat transfer coefficient from the inside air to the surface. This was the typical design value for this coefficient as given in Table 5.2. These are standard or typical values used by designers and include convection and radiation heat transfer.

Equation (5.5) was used in order to eliminate the standard dual convection coefficient, which includes both radiation and convection terms. It was necessary to use only the true convection coefficient because the procedure in the calculation method accounted for the radiation.

**Heat Balance on the Complete Room.** It is necessary from the first law of thermodynamics to maintain a heat balance on the air within the room (see Fig. 5.6). This is given by the following equation:

$$(\text{Total heat gain}) - (\text{total heat loss}) = 0 \quad (5.6)$$

where the total heat gain is the sum of the heat input, heat added by people, and heat added by lights. The total heat loss is that via transmission through walls and other parts of the structure, and by infiltration.

**Comfort Equations.** The objective of the heating or cooling system is to provide thermal comfort for people in the room illustrated in Fig. 5.6. To do this, a set of com-

fort criteria needed to be selected. For this study, the Fanger Comfort Criteria (Fanger, 1967) were chosen and were discussed earlier in Sec. 4.1.1 of this Handbook. Fanger considers the simultaneous influence of six operating variables for comfort. These are:

1. Activity level
2. Thermal resistance of clothing
3. Air temperature
4. MRT
5. Humidity level
6. Relative air velocity

The comfort equations can be expressed as:

$$t_{cl} = f\left(\frac{M}{A_{Du}}, \eta, p_a, T_a\right) \quad (5.7)$$

$$T_{MRT} = f(F_{pi} \text{ for } i = 1, 6 \quad t_i \text{ for } i = 1 \text{ to } 6) \quad (5.8)$$

$$0 = f\left(T_a, t_{cl}, T_{MRT}, p_a, \frac{M}{A_{Du}}, \eta\right) \quad (5.9)$$

For details of the development of these equations, one should see Fanger (Fanger, 1967).

### 5.1.4 Comparison of Calculated Design Radiant Loads with the Standard ASHRAE Design Load Calculation

Many cases have been run for both forced-air and radiant systems in order to determine the effect of various parameters and variables on the design heat loss. A base configuration was selected and this was used to make initial calculations and then changes in the parameters were made in order to test their effect on the value of the design heat loss. The configuration was the following:

Outside design temperature: 3°F.

Room dimensions:

Length: 30 ft.

Width: 30 ft.

Height: 9 ft.

*U* factors, Btu/(h · ft<sup>2</sup> · °F):

Wall 1: half wall with *U*-0.1, and half glass with *U*-0.58. Glass distributed uniformly over the wall.

Walls 2, 3, and 4: *U*-0.1.

Floor: *U*-0.07.

Ceiling: *U*-0.07.

Emissivities:

Panels: 0.9.

Walls: 0.9.

Floor: 0.9.

Ceiling: 0.9.

Convection coefficients,  $\text{Btu}/(\text{h} \cdot \text{ft}^2 \cdot ^\circ\text{F})$ : See previous convective heat transfer, starting with Eq. (5.3).

Comfort variables:

Metabolic rate:  $75 \text{ kcal}/(\text{h} \cdot \text{m}^2)$ .

Clothing resistance:  $0.75 \text{ clo}$  (fcl: 1.1).

Relative air velocity:  $0.15 \text{ m/s}$ .

Relative humidity: 30 percent.

Infiltration rate:  $0.5 \text{ ACH}$ .

Convection heating: The air temperature gradient was set at  $0.75 \text{ CFM/ft}$  with a reference height of  $5 \text{ ft}$  from the floor.

Convection heating: The supply airflow rate was set at  $0.75 \text{ CFM/ft}^2$  of floor area.

Radiant heating: There was no supply air, and the room air temperature gradient was set at  $0^\circ\text{F/ft}$ .

For these design calculations, the number of people was set at zero, and no lighting load was considered. For cooling cases, this would not be the case.

### 5.1.5 Test Case Calculations

To be able to evaluate the performance of the computational scheme, the forced-air heating case was taken as a test case. This allowed the design heat loss values to be calculated and compared with the standard ASHRAE procedure. In these calculations, the convection coefficient on the walls, floors, and ceiling were not changed during the operation of the system. The values given in Sec. 5.1.4 of the ASHRAE RP-394 were used and remained constant (except for the walls where they were a function of the  $\Delta t$ ).

The standard forced-air heating cases are given in Table 5.4 for various heights of the room. As the room height increases, the ASHRAE design heat loss (HLD) increases and, correspondingly, so does the supply air temperature. This is due to increased infiltration as well as the increase in wall and glass areas as the wall height is raised, causing larger heat losses. This shows up also in a reduced value of average unheated surface temperature (AUST) with increasing height. As the room height increases, the infiltration air leaving the room at the ceiling level is at a higher temperature due to an air temperature gradient. The ASHRAE HLD overestimates the calculated heat loss HLC or HLCG by about 7 percent for an 8-ft-high room and by about 3 percent for a 25-ft-high room even with a temperature gradient. It is also important to notice that the room air temperature for comfort is about  $77^\circ\text{F}$  for the 8-ft-high room and almost  $80^\circ\text{F}$  for the 25-ft-high room. This is due to the MRT dropping because of more glass surface in the higher room and, therefore, a higher air temperature being required to satisfy the comfort equations. These higher air temperatures are consistent with the results presented in Table 5.5 for comfort conditions.

Tables 7 through 9\* show similar results as Table 6,\* except that the air temperature gradient was changed to  $0.5$ ,  $1.0$ , and  $1.5^\circ\text{F}$  per foot, respectively. Similar results are exhibited except that the ASHRAE HLD underestimates the heat loss by about 2 percent for the 25-ft-high room with a temperature gradient of  $1.5^\circ\text{F/ft}$ .

Tables 10\* and 11\* give the results for the forced-air heating system standard case with different infiltration rates and for a 15-ft- and 25-ft-high room, respectively. The results in Table 12\* are for the same conditions as in Table 11\* except that the  $U$  factors were increased to what might be expected in industrial situations. Comparison of these results show that the ASHRAE HLD calculation can under-

TABLE 5.4 Forced-Air Heating—Standard Case Calculations

Room height, ft	8.0	9.0	10.0	12.0	15.0	20.0	25.0
ASHRAE design heat loss, Btu/h	24796.8	26762.4	28728.0	32659.2	38556.0	48384.0	58212.0
Actual design heat loss, Btu/h	25642.2	27792.8	29895.6	34124.6	40482.8	51256.8	62055.1
Percentage difference 1	3.4	3.9	4.1	4.5	5.0	5.9	6.6
Conduction design heat loss 1, Btu/h	22796.8	24645.9	26443.6	30039.1	35399.4	44389.9	53297.4
Percentage difference 2	-8.1	-7.9	-8.0	-8.0	-8.2	-8.3	-8.4
Conduction design heat loss 2, Btu/h	22942.6	24864.6	26747.4	30549.4	36310.7	46212.4	56334.9
Percentage difference 3	-7.5	-7.1	-6.9	-6.5	-5.8	-4.5	-3.2
Actual heat input, Btu/h	22942.6	24864.6	26747.4	30549.4	36310.7	46212.4	56334.9
Percentage difference 4	-7.5	-7.1	-6.9	-6.5	-5.8	-4.5	-3.2
Floor temperature, °F	61.5	61.4	61.2	60.9	60.3	59.7	59.1
Room air temperature, °F	77.5	77.8	77.9	78.2	78.6	79.3	79.8
Mean radiant temperature, °F	62.6	62.2	61.9	61.5	61.0	60.0	59.3
Operative temperature, °F	69.2	69.1	69.1	69.0	68.8	68.6	68.4
Effective radiant field, Btu/(h · ft <sup>2</sup> )	-10.7	-11.3	-11.5	-12.1	-12.7	-13.9	-14.7
AUST °F	62.4	62.3	62.1	61.7	61.1	60.4	59.8
Supply air temperature, °F	101.1	103.4	105.4	109.7	116.0	126.8	137.7

**TABLE 5.5** Comparison of Room Air Temperature and MRT for Comfort Conditions at Different Activity and Clothing Levels with 30 Percent Relative Humidity and 0.2 m/s Relative Velocity

Sedentary activity, light clothing		Sedentary activity, medium clothing		Medium activity, light clothing		Medium activity, medium clothing	
MRT, °F	$t_a$ , °F	MRT, °F	$t_a$ , °F	MRT, °F	$t_a$ , °F	MRT, °F	$t_a$ , °F
68	87.8	60.8	82.4	60.8	75	50	67.6
71.6	85.1	62.6	81.5	62.6	74.5	51.8	66.2
75.2	83.3	64.4	80.6	64.4	72.3	53.6	65.5
78.8	81.5	66.2	79.9	66.2	71.4	55.4	63.9
•	•						
80.6	80.6	68	79	68	70.2	57.7	63.0
				•	•		
82.4	79.7	69.8	78.1	69.8	69.8	59.0	62.6
						•	•
86.0	75.6	71.6	77	71.6	67.8	61.2	61.2
89.6	72.9	73.4	75.2	73.4	66.0	62.6	59.9
		•	•				
93.2	71.6	76.5	76.5	75.2	64.4	64.4	57.6
96.8	68.4	77	74.7	77	63.5	68.0	56.3
		80.6	72	78.8	62.8	71.6	53.1
		84.2	69.3			75.2	50.7
		86	68.4				

estimate the size of the heating load for high (greater than 2) infiltration air changes. This underestimation can be up to 16 percent at 4 ACH. It should be noted in Tables 10\* through 12\* that the supply air temperatures are not appropriate. The airflow rate was set at 0.75 CFM/ft<sup>2</sup>, and for higher heat losses, as found here, this would have to be raised to approximately 3 CFM/ft<sup>2</sup> to yield reasonable supply air temperatures. This calculation does not affect the design load calculations.

The convective calculations appear to be reasonable and correct and do not show any unusual results. They indicate that the program is calculating values that are expected and show that the ASHRAE standard design procedure tends to slightly overestimate design losses even with an air temperature gradient present except for high (above 2) ACH of infiltration.

The same base case was taken as in the forced-air system except a single radiant heating panel was used to supply heat to the room and there was no heated supply air. In this procedure, the panel temperature was assumed as input information and a trial-and-error procedure was used to determine the required area for the heat loss from the space. In this calculation, the emissivity of the panel heater was set at 0.9 and its convection coefficient was as previously specified.

In Table 5.6, the results for panel surface temperatures from 120 to 180°F are shown for the base case room. As expected, the area required for heating with panels reduced as the panel temperature increased. For 120°F, approximately 49 percent of the ceiling area was covered with radiant panels, whereas for a 180°F panel temperature approximately 20 percent of the ceiling was covered with radiant panels. The areas calculated here were compared with the required area from two manufacturers' procedure, which indicated 453 ft<sup>2</sup>, and the other manufacturer's procedure indicated 415 ft<sup>2</sup>. The calculation here indicated 439 ft<sup>2</sup>. At 180°F the two numbers were 216 and 185 ft<sup>2</sup> and the calculated area was 176 ft<sup>2</sup>. This information

TABLE 5.6 Base Case for Radiant Panel Heating: Single Panel Heating—Ceiling Height = 9 ft

Panel temperature, °F	120.0	130.0	140.0	150.0	160.0	170.0	180.0
Panel area required, sq ft	438.8	359.7	302.2	258.7	224.7	197.9	175.6
ASHRAE design heat loss, Btu/h	26762.4	26762.4	26762.4	26762.4	26762.4	26762.4	26762.4
Actual design heat loss, Btu/h	23664.8	23667.7	23671.1	23674.1	23676.3	23678.0	23679.1
Percentage difference 1	-11.6	-11.6	-11.6	-11.5	-11.5	-11.5	-11.5
Conduction design heat loss 1, Btu/h	25662.7	25654.4	25650.1	25647.6	25646.1	25645.2	25644.4
Percentage difference 2	-4.1	-4.1	-4.2	-4.2	-4.2	-4.2	-4.2
Conduction design heat loss 2, Btu/h	25662.7	25654.4	25650.1	25647.6	25646.1	25645.2	25644.4
Percentage difference 3	-4.1	-4.1	-4.2	-4.2	-4.2	-4.2	-4.2
Actual heat input, Btu/h	23655.1	24005.8	24263.4	24459.6	24613.7	24735.2	24836.8
Percentage difference 4	-11.6	-10.3	-9.3	-8.6	-8.0	-7.6	-7.2
Percentage radiation	95.3	95.3	95.3	95.3	95.4	95.4	95.4
Percent ceiling covered by panels	48.8	40.0	33.6	28.7	25.0	22.0	19.5
Heat output per unit panel area, Btu/(h · sq ft)	53.9	66.7	80.3	94.6	109.6	125.0	141.5
Floor temperature, °F	74.4	74.7	74.8	74.8	74.9	74.9	74.9
Room air temperature, °F	66.7	66.7	66.7	66.7	66.7	66.7	66.7
Mean radiant temperature, °F	77.0	77.0	77.0	77.0	77.0	77.0	77.0
Operative temperature, °F	72.4	72.4	72.4	72.4	72.4	72.4	72.4
Effective radiant field, Btu/(h · sq ft)	7.6	7.5	7.5	7.5	7.5	7.5	7.5
AUST deg F	68.7	68.6	68.5	68.5	68.4	68.4	68.4
Parameter 1, Btu/(h · sq ft · °F)	1.0091	1.0523	1.0937	1.1338	1.1730	1.2111	1.2497
Parameter 3, dimensionless	0.0168	0.0142	0.0124	0.0109	0.0098	0.0089	0.0081

appears to verify the calculation procedure because reasonable agreement is found with rated heating panels.

The HLC here is about 4 percent below the ASHRAE standard HLD calculation. This is attributed to the higher wall, floor, and ceiling temperatures experienced in the radiant system than in the forced-air systems. For the radiant case, the AUST remained at about 68°F to 69°F, and in the forced-air system it ranged between 60°F to 62°F, causing additional heat loss through the surfaces. The room air temperature for comfort conditions in the radiant cases (about 67°F) is 10°F less than in the forced-air case, which reduces infiltration loss. However, this reduction in infiltration loss does not overcome the increased loss due to higher surface temperatures. Comparison with the forced-air case shows about 3 percent more loss in the radiant situation. This result is not significant in light of the many assumptions made in both cases.

It should be noted in Table 5.6 that higher floor temperatures are present in the radiant case than in the forced-air case. This is significant because it illustrates that the radiant systems heat surfaces, which in turn heat the occupants and the air, whereas forced-air systems heat the air, which then heats the occupants and the surfaces. Also, keep in mind that comfort conditions were satisfied at the center location for a seated person and that due to radiant temperature asymmetry, discomfort could be experienced at the higher panel temperatures. Normally, the higher panel temperature would be used in rooms with higher ceilings.

The values for floor temperature, room air temperature, MRT, operative temperature (OT), effective radiant field, and AUST remain relatively constant as the panel temperature increases. Parameter 1 and parameter 3 were calculated just to observe their behavior in the radiant types of systems. Parameter 1 is a “pseudo” overall heat transfer coefficient, and parameter 3 is a dimensionless factor related to the radiant exchange process. There does not appear to be any significant trends to either of these parameters.

Figure 5.7 shows the expected nonlinearity of the required panel area as a function of panel temperature for the radiant base case given in Table 5.6.

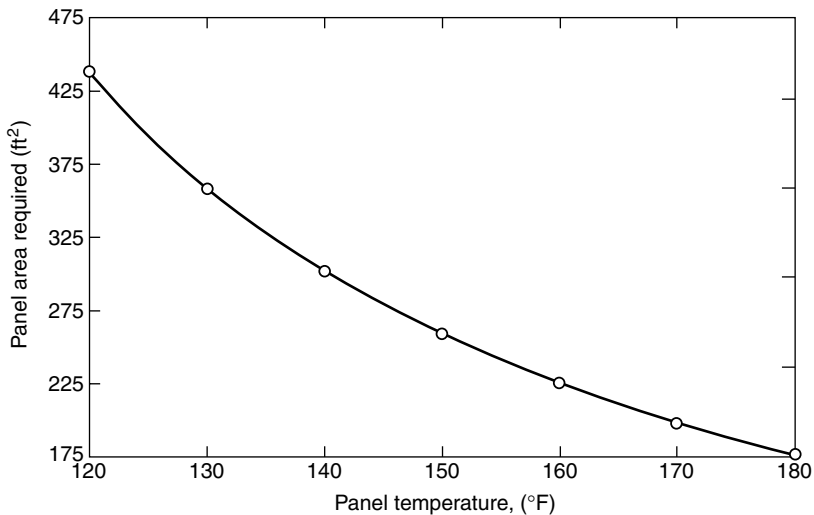


**FIGURE 5.7** Required heating panel area as a function of panel temperature.

**TABLE 5.7** Effects of Panel Emissivity with Panel Temperature = 140°F

Panel emissivity	0.88	0.90	0.92	0.94
Panel area required, sq ft	316.8	301.9	288.3	275.8
ASHRAE design heat loss, Btu/h	26762.4	26762.4	26762.4	26762.4
Actual design heat loss, Btu/h	23628.0	23684.5	23735.9	23782.9
Percentage difference 1	-11.7	-11.5	-11.3	-11.1
Conduction design heat loss 1, Btu/h	25654.1	25728.6	25796.5	25858.4
Percentage difference 2	-4.1	-3.9	-3.6	-3.4
Conduction design heat loss 2, Btu/h	25654.1	25728.6	25796.5	25858.4
Percentage difference 3	-4.1	-3.9	-3.6	-3.4
Actual heat input, Btu/h	24203.7	24342.1	24468.7	24585.0
Percentage difference 4	-9.6	-9.0	-8.6	-8.1
Percentage radiation	95.1	95.3	95.6	95.8
Percent ceiling covered by panels	35.2	33.5	32.0	30.6
Heat output per unit panel area, Btu/(h · sq ft)	76.4	80.6	84.9	89.1
Floor temperature, °F	74.3	74.5	74.7	74.9
Room air temperature, °F	66.6	66.7	66.9	67.0
Mean radiant temperature, °F	77.1	77.0	76.8	76.6
Operative temperature, °F	72.5	72.4	72.4	72.4
Effective radiant field, Btu/(h · sq ft)	7.7	7.5	7.2	7.0
AUST, °F	68.3	68.5	68.7	68.8
Parameter 1, Btu/(h · sq ft · °F)	1.0392	1.0990	1.1590	1.2194
Parameter 3, dimensionless	0.0117	0.0124	0.0131	0.0138

Table 5.7 shows a comparison for the different assumptions concerning the radiant panel emissivity. The emissivity was varied between 0.88 and 0.94 for a panel temperature of 140°F. This resulted in significant changes in required radiant panel area (a 13 percent drop in area as emissivity changed from 0.88 to 0.94). This variation in emissivity also affected the heat output per unit area and parameters 1 and 3. Some of the other quantities showed only slight changes as the emissivity was varied. Manufacturers indicate that a panel emissivity of 0.9 is typical over the life of the radiant panel.

In Table 5.8, the emissivities of the walls, floor and ceiling were varied between 0.8 and 0.95 for a situation when the panel temperature was at 140°F. This caused the required panel area to increase by only 3 percent. The only other variable to change significantly with this change in surface emissivity was the floor temperature, which went from 72°F to 76°F as emissivity went from 0.8 to 0.95. For the remainder of the calculations, a value of 0.9 for the surface emissivities has been used, and the calculations do not appear to be sensitive to changes in the surface emissivity.

Tables 5.9 through 5.11 show the effects obtained when the convection coefficient for the radiant panel is changed by a factor of 2, 5, and 10, respectively. This calculation was carried out because there is a great deal of uncertainty concerning the value of the convection coefficient from surfaces when there is a large  $\Delta T$  such as exists in the radiant panel case. Min et al. (1956) have made this point in their work and indicated that it is a difficult parameter to evaluate because of geometrical considerations.

By increasing the panel convection coefficient by 100% (Table 5.9), the area required for heating the space is reduced by 4.5 percent for a 150°F panel temperature. By increasing the convection coefficient by 500 percent (Table 5.10), the area is reduced by 15.8 percent; therefore, it is not a significant variation if the convection

**TABLE 5.8** Effects of Wall, Floor, and Ceiling Emissivity with Panel Temperature = 140°F

	0.80	0.85	0.90	0.95
Wall emissivity	0.80	0.85	0.90	0.95
Panel area required, sq ft	295.8	299.3	302.2	304.8
ASHRAE design heat loss, Btu/h	26762.4	26762.4	26762.4	26762.4
Actual design heat loss, Btu/h	23700.0	23671.8	23671.1	23678.1
Percentage difference 1	-11.4	-11.5	-11.6	-11.5
Conduction design heat loss 1, Btu/h	26303.1	25984.5	25650.1	25317.7
Percentage difference 2	-1.7	-2.9	-4.2	-5.4
Conduction design heat loss 2, Btu/h	26303.1	25984.5	25650.1	25317.7
Percentage difference 3	-1.7	-2.9	-4.2	-5.4
Actual heat input, Btu/h	25015.2	24645.2	24263.4	23882.0
Percentage difference 4	-6.5	-7.9	-9.3	-10.8
Percentage radiation	95.6	95.4	95.3	95.2
Percent ceiling covered by panels	32.9	33.3	33.6	33.9
Heat output per unit panel area, Btu/(h · sq ft)	84.6	82.3	80.3	78.4
Floor temperature, °F	71.9	73.4	74.8	76.0
Room air temperature, °F	66.8	66.7	66.7	66.7
Mean radiant temperature, °F	76.9	77.0	77.0	77.0
Operative temperature, °F	72.4	72.4	72.4	72.4
Effective radiant field, Btu/(h · sq ft)	7.4	7.5	7.5	7.5
AUST, °F	69.2	68.9	68.5	68.1
Parameter 1, Btu/(h · sq ft · °F)	1.1531	1.1218	1.0937	1.0677
Parameter 3, dimensionless	0.0131	0.0127	0.0124	0.0120

coefficient is known within a factor of two. It is interesting to note that the percent difference in design heat losses remains about the same (-4 percent) for all of these cases. Some of the other parameters change slightly with significant changes in panel convection coefficient. The percent radiation delivered by the panels does change as the convection coefficient is increased and this variation is illustrated in Fig. 5.8.

Different values of infiltration rates (0.5 to 4.0 ACH) were assumed for the base case configuration, and these results are given in Tables 19\* through 21\* for 130°F, 150°F, and 170°F panel surface temperatures, respectively.

As seen in these tables, the ASHRAE standard HLD overpredicts the HLC by up to 16 percent for an infiltration rate of 4 ACH. If this were compared with a forced-air system with an air temperature gradient, approximately 1 percent more loss would be added to this number (see Sec. 5.4) so that there might be a difference of approximately 17 percent. The percent difference in the design loads as a function of infiltration is shown in Fig. 5.9.

As the infiltration rate increases, the floor temperature, MRT, OT, effective radiant flux, and AUST increase significantly. These changes need to be considered in the design process for radiant panel systems.

Different combinations and quantities of glass have been considered in the radiant base case, which was previously described. The results from these calculations are given in Table 5.12 for a panel temperature of 140°F. The radiant base case is shown as case 2 in Table 5.12 and a room with no glass is given as case 1. Case 3 is one wall that is all glass; case 4 is one wall with all glass and half of another wall with glass; and case 5 is the room with two walls with all glass. As anticipated, as the quantity of glass increases, the panel area increases. Also, as can be seen in Table 5.12, the difference between HLD and HLC becomes smaller as the quantity of glass in the

TABLE 5.9 Effects of Changing Panel Convection Coefficient by a Factor of Two

Panel temperature, °F	120.0	130.0	140.0	150.0	160.0	170.0	180.0
Panel area required, sq ft	418.7	343.1	288.2	246.8	214.4	188.9	167.7
ASHRAE design heat loss, Btu/h	26762.4	26762.4	26762.4	26762.4	26762.4	26762.4	26762.4
Actual design heat loss, Btu/h	23827.2	23833.8	23839.8	23841.5	23841.7	23841.0	23839.6
Percentage difference 1	-11.0	-10.9	-10.9	-10.9	-10.9	-10.9	-10.9
Conduction design heat loss 1, Btu/h	25637.2	25626.9	25620.5	25618.8	25618.5	25618.9	25619.5
Percentage difference 2	-4.2	-4.2	-4.3	-4.3	-4.3	-4.3	-4.3
Conduction design heat loss 2, Btu/h	25617.2	25626.9	25620.5	25618.8	25618.5	25618.9	25619.5
Percentage difference 3	-4.2	-4.2	-4.3	-4.3	-4.3	-4.3	-4.3
Actual heat input, Btu/h	23719.9	24053.3	24297.1	24484.9	24632.8	24749.8	24847.8
Percentage difference 4	-11.4	-10.1	-9.2	-8.5	-8.0	-7.5	-7.2
Percentage radiation	91.2	91.1	91.1	91.2	91.2	91.2	91.3
Percent ceiling covered by panels	46.5	38.1	32.0	27.4	23.8	21.0	18.6
Heat output per unit panel area, Btu/(h · sq ft)	56.7	70.1	84.3	99.2	114.9	131.0	148.2
Floor temperature, °F	74.1	74.3	74.4	74.4	74.5	74.5	74.5
Room air temperature, °F	67.1	67.1	67.1	67.1	67.1	67.1	67.1
Mean radiant temperature, °F	76.5	76.4	76.4	76.4	76.4	76.4	76.4
Operative temperature, °F	72.3	72.3	72.3	72.3	72.3	72.3	72.3
Effective radiant field, Btu/(h · sq ft)	6.8	6.8	6.8	6.8	6.8	6.8	6.8
AUST, °F	68.5	68.4	68.3	68.2	68.2	68.2	68.2
Parameter 1, Btu/(h · sq ft · °F)	1.0691	1.1133	1.1554	1.1961	1.2360	1.2747	1.3140
Parameter 3, dimensionless	0.0177	0.0150	0.0130	0.0115	0.0103	0.0093	0.0085

**TABLE 5.10** Effects of Changing Panel Convection Coefficients by a Factor of Five

Panel temperature, °F	120.0	130.0	10.0	150.0	160.0	170.0	180.0
Panel area required, sq ft	369.9	302.9	254.4	217.8	189.8	166.9	148.2
ASHRAE design heat loss, Btu/h	26762.4	26762.4	26762.4	26762.4	26762.4	26762.4	26762.4
Actual design heat loss, Btu/h	24233.1	24236.0	24237.1	24236.6	24235.0	24232.3	24228.7
Percentage difference 1	-9.5	-9.4	-9.4	-9.4	-9.4	-9.5	-9.5
Conduction design heat loss 1, Btu/h	25563.7	25561.6	25561.6	25562.5	25563.5	25564.7	25565.9
Percentage difference 2	-4.5	-4.5	-4.5	-4.5	-4.5	-4.5	-4.5
Conduction design heat loss 2, Btu/h	25563.7	25561.6	25561.6	25562.5	25563.5	25564.7	25565.9
Percentage difference 3	-4.5	-4.5	-4.5	-4.5	-4.5	-4.5	-4.5
Actual heat input, Btu/h	23866.9	24170.0	24391.8	24560.1	24689.6	24795.9	24882.9
Percentage difference 4	-10.8	-9.7	-8.9	-8.2	-7.7	-7.3	-7.0
Percentage radiation	81.1	80.9	80.9	80.9	80.9	81.0	81.0
Percent ceiling covered by panels	41.1	33.7	28.3	24.2	21.1	18.5	16.5
Heat output per unit panel area, Btu/(h · sq ft)	64.5	79.8	95.9	112.7	130.1	148.6	167.9
Floor temperature, °F	73.3	73.4	73.5	73.5	73.6	73.6	73.6
Room air temperature, °F	68.2	68.2	68.2	68.2	68.2	68.2	68.2
Mean radiant temperature, °F	75.1	75.1	75.1	75.1	75.1	75.1	75.1
Operative temperature, °F	72.0	72.0	72.0	72.0	72.0	72.0	72.0
Effective radiant field, Btu/(h · sq ft)	5.0	5.0	5.0	5.0	5.0	5.0	5.0
AUST, °F	67.8	67.8	67.7	67.7	67.7	67.7	67.7
Parameter 1, Btu/(h · sq ft · °F)	1.2433	1.2893	1.3337	1.3768	1.4185	1.4606	1.5024
Parameter 3, dimensionless	0.0204	0.0172	0.0149	0.0132	0.0118	0.0107	0.0097

TABLE 5.11 Effects of Changing Panel Convection Coefficients by a Factor of Ten

Panel temperature, °F	120.0	130.0	140.0	150.0	160.0	170.0	180.0
Panel area required, sq ft	313.6	256.0	214.7	184.1	159.9	140.6	124.9
ASHRAE design heat loss, Btu/h	26762.4	26762.4	26762.4	26762.4	26762.4	26762.4	26762.4
Actual design heat loss, Btu/h	24671.3	24678.6	24682.8	24684.4	24683.9	24681.6	24677.9
Percentage difference 1	-7.8	-7.8	-7.8	-7.8	-7.8	-7.8	-7.8
Conduction design heat loss 1, Btu/h	25513.7	25514.2	25515.2	25516.3	25517.4	25518.5	25519.6
Percentage difference 2	-4.7	-4.7	-4.7	-4.7	-4.7	-4.6	-4.6
Conduction design heat loss 2, Btu/h	25513.7	25514.2	25515.2	25516.3	25517.4	25518.5	25519.6
Percentage difference 3	-4.7	-4.7	-4.7	-4.7	-4.7	-4.6	-4.6
Actual heat input, Btu/h	24071.3	24335.3	24525.9	24667.2	24779.7	24869.6	24943.0
Percentage difference 4	-10.1	-9.1	-8.4	-7.8	-7.4	-7.1	-6.8
Percentage radiation	69.1	68.8	68.6	68.5	68.4	68.5	68.6
Percent ceiling covered by panels	34.8	28.4	23.9	20.5	17.8	15.6	13.9
Heat output per unit panel area, Btu/(h · sq ft)	76.8	95.0	114.2	134.0	154.9	176.8	199.6
Floor temperature, °F	72.4	72.4	72.5	72.5	72.5	72.5	72.5
Room air temperature, °F	69.4	69.4	69.4	69.4	69.4	69.4	69.4
Mean radiant temperature, °F	73.5	73.5	73.5	73.5	73.5	73.5	73.5
Operative temperature, °F	71.7	71.7	71.7	71.7	71.7	71.7	71.7
Effective radiant field, Btu/(h · sq ft)	3.0	3.0	3.0	3.0	3.0	3.0	3.0
AUST, °F	67.3	67.2	67.2	67.2	67.2	67.2	67.2
Parameter 1, Btu/(h · sq ft · °F)	1.5134	1.5657	1.6161	1.6642	1.7122	1.7596	1.8065
Parameter 3, dimensionless	0.0246	0.0208	0.0180	0.0159	0.0142	0.0128	0.0117

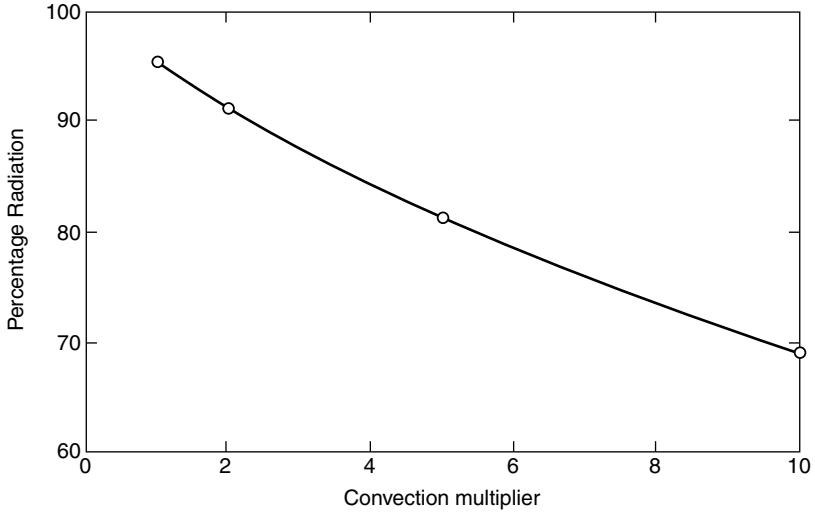


**FIGURE 5.8** Effects on percent radiation delivered by the panel as the convection multiplier is changed.

room increases with only a  $-2$  percent difference showing up in case 5. Because the panel area increases in order to make up increased heat losses as the quantity of glass increases, the floor temperature also rises. This in turn causes the room air temperature for comfort to be reduced from  $67^{\circ}\text{F}$  to  $64^{\circ}\text{F}$ . In Fig. 5.10, the required panel area is plotted for each case shown in Table 5.12. Likewise, in Fig. 5.11, the floor tem-

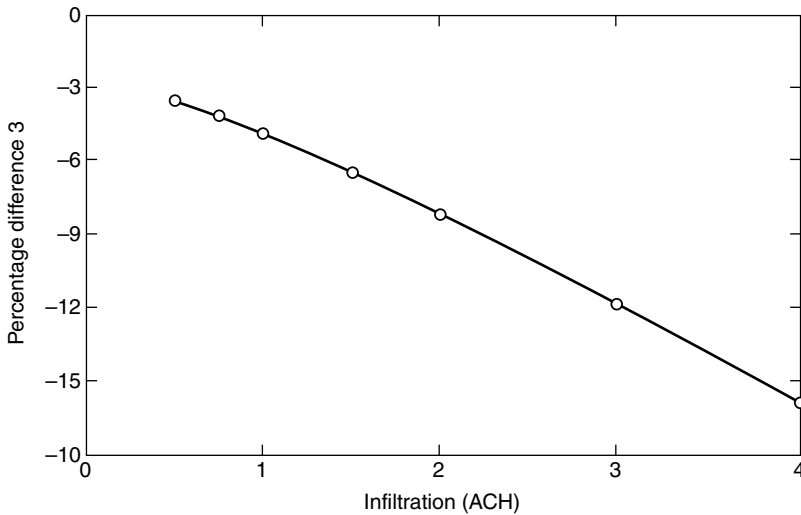


**FIGURE 5.9** Effect of air infiltration in panel heating on percent difference in design load calculations.

**TABLE 5.12** Effects of Changes in Glass Distribution—Panel Temperature = 140°F

Class distribution case number	1	2	3	4	5
Panel area required, sq ft	249.0	302.2	359.3	410.9	466.5
ASHRAE design heat loss, Btu/h	22096.8	26762.4	31428.0	36093.6	40759.2
Actual design heat loss, Btu/h	19744.9	23671.1	27407.1	31189.3	34757.8
Percentage difference 1	-10.6	-11.6	-12.8	-13.6	-14.7
Conduction design heat loss 1, Btu/h	21110.2	25650.1	30469.1	34945.1	39796.1
Percentage difference 2	-4.5	-4.2	-3.1	-3.2	-2.4
Conduction design heat loss 2, Btu/h	21110.2	25650.1	30469.1	34945.1	39796.1
Percentage difference 3	-4.5	-4.2	-3.1	-3.2	-2.4
Actual heat input, Btu/h	19954.8	24263.4	28839.3	33107.3	37737.7
Percentage difference 4	-9.7	-9.3	-8.2	-8.3	-7.4
Percentage radiation	95.4	95.3	95.2	95.2	95.2
Percent ceiling covered by panels	27.7	33.6	39.9	45.7	51.8
Heat output per unit panel area, Btu/(h · sq ft)	80.1	80.3	80.3	80.6	80.9
Floor temperature, °F	73.8	74.8	75.8	76.6	77.4
Room air temperature, °F	67.3	66.7	65.8	65.2	64.4
Mean radiant temperature, °F	76.2	77.0	78.1	78.8	79.9
Operative temperature, °F	72.3	72.4	72.7	72.8	73.0
Effective radiant field, Btu/(h · sq ft)	6.4	7.5	9.0	10.0	11.3
AUST, °F	69.4	68.5	67.8	66.8	66.0
Parameter 1, Btu/(h · sq ft · °F)	1.1013	1.0937	1.0803	1.0761	1.0687
Parameter 3, dimensionless	0.0126	0.0124	0.0121	0.0119	0.0117
Case number 1: no glass in any wall					
Case number 2: one wall, half glass					
Case number 3: one wall, all glass					
Case number 4: one wall, all glass-second wall, half glass					
Case number 5: two walls, all glass					

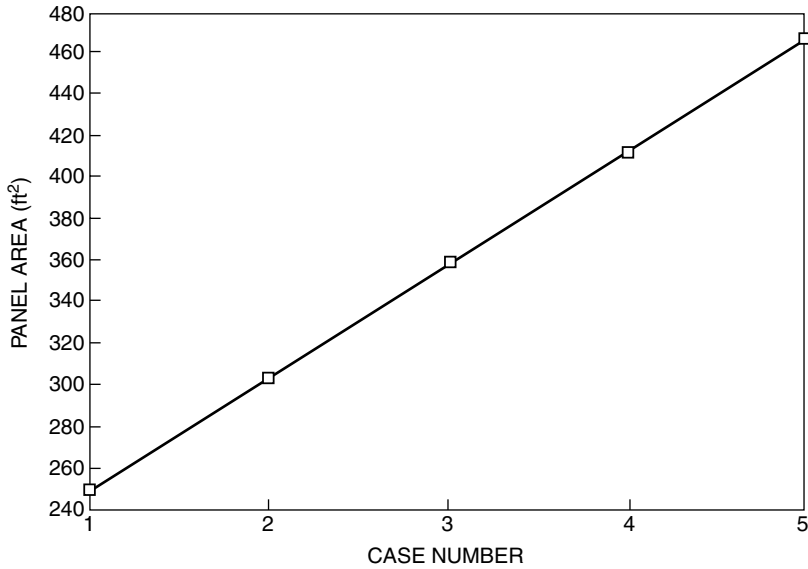


**FIGURE 5.10** Panel area required as a function of the quantity of glass.

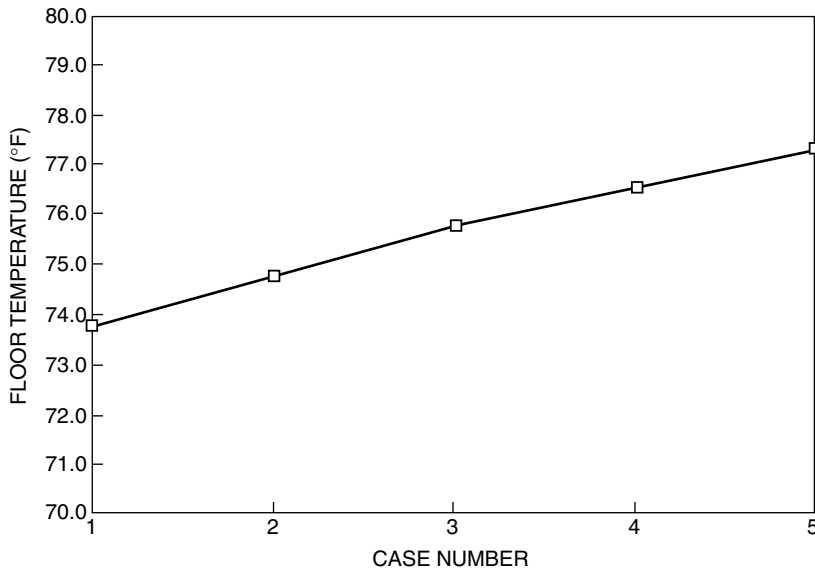


**FIGURE 5.11** Floor temperature as a function of the quantity of glass.

perature is plotted. It is interesting to note that an 87 percent increase in panel area in the room results in only a 3.6°F increase in floor temperature.

The  $U$  factors in the radiant base case were changed and various calculations were made to determine this effect on the design heat loss. The wall  $U$  factors were changed from 0.1 to 0.2 Btu/(h · ft<sup>2</sup> · °F) and the floor and ceiling values from 0.07 to 0.1 Btu/(h · ft<sup>2</sup> · °F). The  $U$  factor for the glass was changed from 0.58 to 1.0 Btu/(h · ft<sup>2</sup> · °F). All of these were changed at one time so that an initial and new case was compared at three panel temperatures of 130°F, 150°F, and 170°F. These results are given in Table 5.13. The variation is very much as expected in that with increased  $U$  factors there is an increased floor temperature and MRT and a decreased air temperature and AUST. In each case, the difference between HLD and HLC has been reduced by about one-half so that the ASHRAE standard design procedure more closely predicts the required heat input.

In Table 5.14 are the results for five different-size rooms: (1) 20 × 20 ft, (2) 30 × 30 ft, (3) 40 × 40 ft, (4) 40 × 20 ft, and (5) 30 × 15 ft. All five rooms measured 9 ft high. The important thing to notice about these results is that as the room size increases, the ASHRAE standard design load procedure tends to increasingly overpredict the required heater size. This tendency is not great (3.7 percent for 20 × 20 ft and 5.6 percent for 40 × 40 ft), but it is an important trend.

Also illustrated here is the fact that a square room or building will tend to be oversized if the ASHRAE standard design load is used. In Table 5.15, results for four, square buildings are tabulated. Again, as the building becomes larger, the ASHRAE standard design procedure (HDL) tends to oversize (6 percent for a 10,000-ft<sup>2</sup> building) the radiant heating systems.

The radiant base case room was modified to have a ceiling height between 8 and 25 ft. The results from these calculations are presented in Table 5.16. There are two important trends to observe from these results. First, as the height is increased, more panel area is required to counteract the increased room heat loss, and because of changing room geometry, more of the walls intercept the radiant energy, thus increasing the AUST. This in turn causes the second trend to occur in that the difference between HLD and HLC decreases because of more heat conduction through the walls. This decrease in the difference between HLD and HLC as room height is increased is illustrated by the plot shown in Figure 5.12.

To see what effect outside design temperature had on the design load calculation, five other outside design temperatures were used, and these results are given in Table 5.17. There is a slight tendency for the percent difference between HLD and HLC to increase with milder climates (−3.6 percent at −5°F to −5.3 percent at 15°F). This does not appear to be a significant trend and is apparently due to reduced infiltration and conduction losses at the higher outside temperatures.

Several cases were run with a perimeter (narrow panel running parallel to the outside wall) radiant panel system, and these results are given in Table 5.18. These cases are for a 15- × 15- × 8-ft room with three inside walls and one outside wall with half glass. The  $U$  factor for the floor and ceiling were the same as the radiant base case. The radiant panel was 36 in wide and ran parallel to the outside wall with the window. There is no apparent difference between HLD and HLC as far as the design loads are concerned. This is apparently due to the proximity of the radiant heating surface to the cold surface or wall resulting in higher convective losses. This is only about 4 percent different than the results shown in Table 5.6 for the single-panel radiant base case. This is not a significant trend considering all of the unknown variables that can enter into consideration in the actual case. The other variables in Tables 5.6 and 5.18 are quite similar so that this special type of application of panels does not alter the conclusions from the single-panel calculations.

TABLE 5.13 Effects of Increased *U* Factors on Radiant Heating Panel Performance

<i>U</i> -factor case	New		Old		New		Old	
	Old	New	Old	New	Old	New	Old	New
Panel temperature, °F	590.0	590.0	610.0	610.0	630.0	630.0	630.0	630.0
Panel area required, sq ft	359.7	546.3	258.7	397.3	197.9	305.3	197.9	305.3
ASHRAE design heat loss, Btu/h	26762.4	41536.8	26762.4	41536.8	26762.4	41536.8	26762.4	41536.8
Actual design heat loss, Btu/h	23667.7	35605.8	23674.1	35622.0	23678.0	35611.4	23678.0	35611.4
Percentage difference 1	-11.6	-14.3	-11.5	-14.2	-11.5	-14.3	-11.5	-14.3
Conduction design heat loss 1, Btu/h	25654.4	40542.8	25647.6	40403.9	25645.2	40374.7	25645.2	40374.7
Percentage difference 2	-4.1	-2.4	-4.2	-2.7	-4.2	-2.8	-4.2	-2.8
Conduction design heat loss 2, Btu/h	25654.4	40542.8	25647.6	40403.9	25645.2	40374.7	25645.2	40374.7
Percentage difference 3	-4.1	-2.4	-4.2	-2.7	-4.2	-2.8	-4.2	-2.8
Actual heat input, Btu/h	24005.8	37107.6	24459.6	37890.3	24735.2	38435.0	24735.2	38435.0
Percentage difference 4	-10.3	-10.7	-8.6	-8.8	-7.6	-7.5	-7.6	-7.5
Percentage radiation	95.3	95.2	95.3	95.2	95.4	95.3	95.4	95.3
Percent ceiling covered by panels	40.0	60.7	28.7	44.1	22.0	33.9	22.0	33.9
Heat output per unit panel area, Btu/(h · sq ft)	66.7	67.9	94.6	95.4	125.0	125.9	94.6	95.4
Floor temperature, °F	74.7	75.6	74.8	76.4	74.9	76.7	74.9	76.7
Room air temperature, °F	66.7	64.7	66.7	64.7	66.7	64.7	66.7	64.7
Mean radiant temperature, °F	77.0	79.5	77.0	79.4	77.0	79.5	77.0	79.5
Operative temperature, °F	72.4	72.9	72.4	72.9	72.4	72.9	72.4	72.9
Effective radiant field, Btu/(h · sq ft)	7.5	10.8	7.5	10.7	7.5	10.8	7.5	10.8
AUST, °F	68.6	66.3	68.5	65.9	68.4	65.7	68.4	65.7
Parameter 1, Btu/(h · sq ft · °F)	1.0523	1.0390	1.1338	1.1176	1.2111	1.1947	1.1338	1.1176
Parameter 3, dimensionless	0.0142	0.0136	0.0109	0.0105	0.0089	0.0086	0.0109	0.0105
Surface	Wall 1	Wall 2	Wall 3	Wall 4	Floor	Ceiling		
Initial <i>U</i>	0.34	0.1	0.1	0.1	0.07	0.07		
New <i>U</i>	0.60	0.2	0.2	0.2	0.10	0.10		

**TABLE 5.14** Effects of Changes in Room Length and Width with a 140°F Panel Temperature

	20 · 20	30 · 30	40 · 40	40 · 20	30 · 15
Room length · width, ft · ft					
Panel area required, sq ft	162.6	302.2	468.9	300.9	197.2
ASHRAE design heat loss, Btu/h	14659.2	26762.4	42048.0	26726.4	17658.0
Actual design heat loss, Btu/h	12901.9	23671.1	36820.0	23579.7	15571.1
Percentage difference 1	-12.0	-11.6	-12.4	-11.8	-11.8
Conduction design heat loss 1, Btu/h	14121.6	25650.1	39711.4	25826.0	17178.8
Percentage difference 2	-3.7	-4.2	-5.6	-3.4	-2.7
Conduction design heat loss 2, Btu/h	14121.6	25650.1	39711.4	25826.0	17178.8
Percentage difference 3	-3.7	-4.2	-5.6	-3.4	-2.7
Actual heat input, Btu/h	13384.0	24263.4	37571.6	24454.1	16284.6
Percentage difference 4	-8.7	-9.3	-10.6	-8.5	-7.8
Percentage radiation	94.9	95.3	95.6	95.2	94.9
Percent ceiling covered by panels	40.7	33.6	29.3	37.6	43.8
Heat output per unit panel area, Btu/(h · sq ft)	82.3	80.3	80.1	81.3	82.6
Floor temperature, °F	73.7	74.8	74.0	74.6	74.3
Room air temperature, °F	66.4	66.7	66.0	66.5	66.5
Mean radiant temperature, °F	77.4	77.0	77.8	77.2	77.2
Operative temperature, °F	72.5	72.4	72.6	72.5	72.5
Effective radiant field, Btu/(h · sq ft)	8.1	7.5	8.6	7.8	7.9
AUST, °F	67.9	68.5	68.0	68.0	67.8
Parameter 1, Btu/(h · sq ft · °F)	1.1191	1.0937	1.0822	1.1047	1.1217
Parameter 3, dimensionless	0.0126	0.0124	0.0122	0.0124	0.0126

**TABLE 5.15** Effects of Changing Room Size with a 140°F Panel Temperature

	20 · 20	30 · 30	40 · 40	100 · 100
Room length · width, ft · ft	162.6	302.2	468.9	2285.8
Panel area required, sq ft	14659.2	26762.4	42048.0	200952.0
ASHRAE design heat loss, Btu/h	12901.9	23671.1	36820.0	176195.8
Actual design heat loss, Btu/h	-12.0	-11.6	-12.4	-12.2
Percentage difference 1	14121.6	25650.1	39711.4	188495.6
Conduction design heat loss 1, Btu/h	-3.7	-4.2	-5.6	-6.0
Percentage difference 2	14121.6	25650.1	39711.4	188495.6
Conduction design heat loss 2, Btu/h	-3.7	-4.2	-5.6	-6.0
Percentage difference 3	13384.0	24263.4	37571.6	177908.1
Actual heat input, Btu/h	-8.7	-9.3	-10.6	-11.3
Percentage difference 4	94.9	95.3	95.6	96.4
Percentage radiation	40.7	33.6	29.3	22.9
Percent ceiling covered by panels	82.3	80.3	80.1	77.8
Heat output per unit panel area, Btu/(h · sq ft)	73.7	74.8	74.0	73.7
Floor temperature, °F	66.4	66.7	66.0	66.2
Room air temperature, °F	77.4	77.0	77.8	77.6
Mean radiant temperature, °F	72.5	72.4	72.6	72.5
Operative temperature, °F	8.1	7.5	8.6	8.3
Effective radiant field, Btu/(h · sq ft)	67.9	68.5	68.0	69.0
AUST, °F	1.1191	1.0937	1.0822	1.0566
Parameter 1, Btu/(h · sq ft · °F)	0.0126	0.0124	0.0122	0.0120
Parameter 3, dimensionless				

TABLE 5.16 Effects of Changing Room Height with a 140°F Panel Temperature

Room height, ft	8.0	9.0	10.0	12.0	15.0	20.0	25.0
Panel area required, sq ft	274.2	301.9	323.6	367.8	432.0	556.1	677.8
ASHRAE design heat loss, Btu/h	24796.8	26762.4	28728.0	32659.2	38556.0	48384.0	58212.0
Actual design heat loss, Btu/h	21765.7	23684.5	25332.6	28675.0	33584.5	42498.0	51235.5
Percentage difference 1	-12.2	-11.5	-11.8	-12.2	-12.9	-12.2	-12.0
Conduction design heat loss 1, Btu/h	23528.2	25728.6	27642.7	31529.6	37271.5	47707.2	57951.5
Percentage difference 2	-5.1	-3.9	-3.8	-3.5	-3.3	-1.4	-0.4
Conduction design heat loss 2, Btu/h	23528.2	25728.6	27642.7	31529.6	37271.5	47707.2	57951.5
Percentage difference 3	-5.1	-3.9	-3.8	-3.5	-3.3	-1.4	-0.4
Actual heat input, Btu/h	22280.8	24342.1	26159.7	29847.7	35307.3	45149.8	54824.8
Percentage difference 4	-10.1	-9.0	-8.9	-8.6	-8.4	-6.7	-5.8
Percentage radiation	95.3	95.3	95.3	95.3	95.3	95.3	95.3
Percent ceiling covered by panels	30.5	33.5	36.0	40.9	48.0	61.8	75.3
Heat output per unit panel area, Btu/(h · sq ft)	81.2	80.6	80.8	81.1	81.7	81.2	80.9
Floor temperature, °F	73.5	74.5	74.6	74.7	74.4	74.8	74.6
Room air temperature, °F	66.2	66.7	66.5	66.2	65.7	66.2	66.4
Mean radiant temperature, °F	77.6	77.0	77.2	77.6	78.2	77.6	77.4
Operative temperature, °F	72.6	72.4	72.5	72.6	72.7	72.5	72.5
Effective radiant field, Btu/(h · sq ft)	8.3	7.5	7.9	8.3	9.1	8.3	8.1
AUST, °F	67.7	68.5	68.6	68.7	68.8	70.1	70.8
Parameter 1, Btu/(h · sq ft · °F)	1.0995	1.0990	1.0983	1.0983	1.0989	1.0994	1.0971
Parameter 3, dimensionless	0.0123	0.0124	0.0124	0.0124	0.0124	0.0126	0.0127

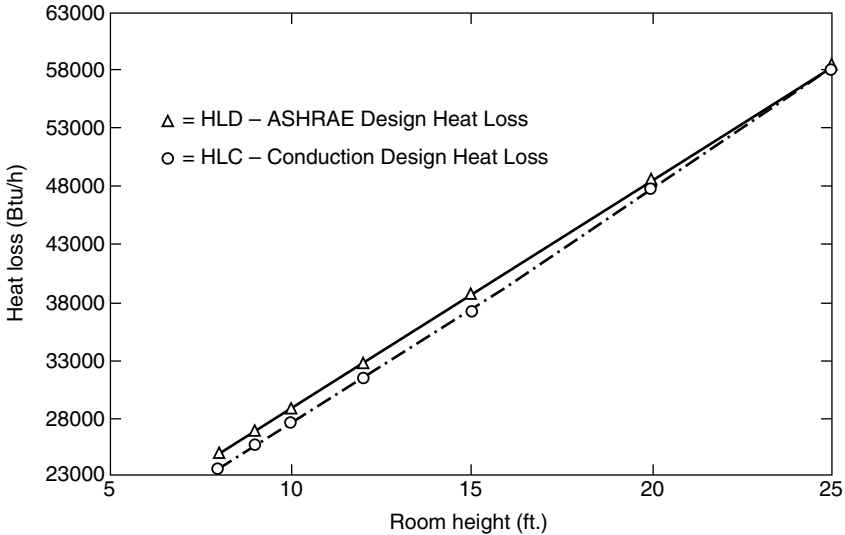


**FIGURE 5.12** Effect of room height change on design heat loss for radiant panels.

Several of the situations from forced-air and radiant ceiling panel systems were compared, and these are shown in Figs. 25\* and 26.\* Figure 25\* shows radiant ceiling panels at 120°F (rad—120) and at 180°F (rad—180) compared with forced-air heating systems with an air temperature gradient of 0.75°F/ft (con—0.75) and a gradient of 1.5°F/ft (con—1.50). From this figure, it appears that the increased infiltration heat loss, including an air temperature gradient in the forced-air cases, is not enough to overcome the effect of an increased AUST in the radiant case (“Bar-Conduction 2” in Fig. 25\*). Keep in mind that these results are for a 9-ft-high room and one-half ACH.

In Fig. 26,\* two different room heights are compared for forced-air and radiant heating systems. The con—8 case is for an 8-ft-high ceiling forced-air system, and rad—8 is for an 8-ft-high ceiling radiant system. The con—25 and rad—25 are for the same variables except that the ceiling is 25 ft high. These results show the same trends as previously discussed, except that panel heating system design loads become equivalent to the forced-air design loads and the ASHRAE standard design heating loads as long as room air temperature gradients are considered. This is due to more of the radiant energy falling on the walls as the height of the building is increased.

The radiant heated floor-type of system has also been simulated. The base case that was used for this was the same as that previously described, except that it has a room height of 8 ft, and the outside design temperature was selected to be 10°F. The room height of 8 ft was chosen for this case because the radiant floor-type system is commonly applied to residential structures. The 10°F outside temperature was selected because the floor temperature is limited to 85°F for comfort requirements and with a 3°F outside temperature not many floor temperature variations were available. For this case, the floor temperature was varied between 81°F and 85°F, and the required floor area for heating was calculated assuming a uniform and constant floor temperature. These results are presented in Table 5.19.

**TABLE 5.17** Effects Due to Outside Design Temperature Changes with a 130°F Panel Temperature

Outside design temperature, °F	0.0	3.0	5.0	10.0	15.0
Panel area required, sq ft	399.0	359.7	349.7	324.8	299.5
ASHRAE design heat loss, Btu/h	29736.0	26762.4	26019.0	24160.5	22302.0
Actual design heat loss, Btu/h	26437.8	23667.7	22975.2	21243.8	19512.3
Percentage difference 1	-11.1	-11.6	-11.7	-12.1	-12.5
Conduction design heat loss 1, Btu/h	28675.7	25654.4	24899.4	23012.1	21125.4
Percentage difference 2	-3.6	-4.1	-4.3	-4.8	-5.3
Conduction design heat loss 2, Btu/h	28675.7	25654.4	24899.4	23012.1	21125.4
Percentage difference 3	-3.6	-4.1	-4.3	-4.8	-5.3
Actual heat input, Btu/h	26634.3	24005.8	23343.1	21675.5	19992.8
Percentage difference 4	-10.4	-10.3	-10.3	-10.3	-10.4
Percentage radiation	95.3	95.3	95.3	95.3	95.4
Percent ceiling covered by panels	44.3	40.0	38.9	36.1	33.3
Heat output per unit panel area, Btu/(h · sq ft)	66.8	66.7	66.7	66.7	66.7
Floor temperature, °F	75.0	74.7	74.6	74.4	74.1
Room air temperature, °F	66.1	66.7	66.8	67.2	67.5
Mean radiant temperature, °F	77.7	77.0	76.8	76.4	76.0
Operative temperature, °F	72.6	72.4	72.4	72.3	72.2
Effective radiant field, Btu/(h · sq ft)	8.5	7.9	7.3	6.8	6.2
AUST, °F	68.4	68.6	68.7	68.8	69.0
Parameter 1, Btu/(h · sq ft · °F)	1.0437	1.0523	1.0546	1.0604	1.0663
Parameter 3, dimensionless	0.0141	0.0142	0.0143	0.0144	0.0145

**TABLE 5.18** Results for a Perimeter Radiant Panel Heating System\*—15' × 15' × 8' Room with Three Inside Walls and One Outside Wall with Half Glass—36" Wide Panel—Floor and Ceiling at Radiant Base Case Conditions

Perimeter heater temperature, °F	175.0	180.0	185.0
Panel area required, sq ft	45.0	42.5	40.2
ASHRAE design heat loss, Btu/h	6397.9	6397.9	6397.9
Actual design heat loss, Btu/h	5770.2	5769.3	5768.5
Percentage difference 1	-9.8	-9.8	-9.8
Conduction design heat loss 1, Btu/h	6381.1	6390.0	6397.3
Percentage difference 2	-0.3	-0.1	0.0
Conduction design heat loss 2, Btu/h	6381.1	6390.0	6397.3
Percentage difference 3	-0.3	-0.1	0.0
Actual heat input, Btu/h	6171.7	6192.3	6210.1
Percentage difference 4	-3.5	-3.2	-2.9
Percentage radiation	94.8	94.8	94.8
Percent ceiling covered by panels	20.0	18.9	17.9
Heat output per unit panel area, Btu/(h · sq ft)	137.2	145.7	154.4
Floor temperature, °F	71.2	71.3	71.4
Room air temperature, °F	67.9	67.9	67.9
Mean radiant temperature, °F	75.4	75.4	75.4
Operative temperature, °F	72.1	72.1	72.1
Effective radiant field, Btu/(h · sq ft)	5.4	5.5	5.5
AUST, °F	69.5	69.5	69.5
Parameter 1, Btu/(h · sq ft · °F)	1.2808	1.2993	1.3176
Parameter 3, dimensionless	0.0089	0.0085	0.0081

Room measures 15 × 15 × 8 ft with three inside walls and one outside wall with half glass (36-in-wide panel). The floor and ceiling are at radiant base conditions.

From the data in Table 5.19, it can be seen that the percent difference between HLD and HLC is constant at about -7 percent. The actual heat input is lower than HLD because most of the floor is covered with radiant heating surface and no loss from the floor to the surroundings is considered for the heated area. *In the design process, this heat loss would be taken into account.* The room air temperature remains constant at about 70°F, and the MRT was approximately 73°F.

Next, the outside design temperature was varied between 5°F and 20°F to indicate its effect on the design heat loss, and these results for an 84°F floor temperature are given in Table 5.20. The trend from these calculations is that as the climate becomes milder, HLD and HLC begin to diverge. However, this is only 1.5 percent for an outside temperature change from 5°F to 20°F.

In Table 5.21, the  $U$  factor for the floor was changed between 0.07 and 0.15 Btu/(h · ft<sup>2</sup> · °F), and the floor temperature was maintained at 84°F. It is seen that there is a slight increase (-6.9 to -7.9) in the deviation from the ASHRAE standard design procedure. The other variables in the calculation (except actual heat input and floor area) are affected very little by this change.

In Table 5.22, the infiltration rate was varied from 0.5 to 1.25 air changes per hour for the base configuration room with an 84°F floor temperature. The percent change in design load only increased an insignificant amount (½ %). At 1.25 ACH the floor is 100 % active with heating surface. There are reductions in room temperature and an increase in MRT and resulting increase in the AUST. This results also in the percent from the heated floor portion going from 61.7 % to 55.5 %.

TABLE 5.19 Results for Heated Floors—Base Case

Heated floor temperature, °F	81.0	82.0	83.0	84.0	85.0
Panel area required, sq ft	875.7	815.8	762.8	724.4	681.0
ASHRAE design heat loss, Btu/h	22386.0	22386.0	22386.0	22386.0	22386.0
Actual design heat loss, Btu/h	20536.8	20564.8	20591.8	20612.8	20638.0
Percentage difference 1	-8.3	-8.1	-8.0	-7.9	-7.8
Conduction design heat loss 1, Btu/h	20846.5	20842.5	20835.3	20830.5	20825.4
Percentage difference 2	-6.9	-6.9	-6.9	-6.9	-7.0
Conduction design heat loss 2, Btu/h	20846.5	20842.5	20835.3	20830.5	20825.4
Percentage difference 3	-6.9	-6.9	-6.9	-6.9	-7.0
Actual heat input, Btu/h	17326.8	17561.1	17767.9	17917.9	18087.3
Percentage difference 4	-22.6	-21.6	-20.6	-20.0	-19.2
Percentage radiation	63.3	62.7	62.1	61.7	61.2
Percent floor covered by panels	97.3	90.6	84.8	80.5	75.7
Heat output per unit panel area, Btu/(h · sq ft)	19.8	21.5	23.3	24.7	26.6
Ceiling temperature, °F	69.9	69.9	70.0	70.0	70.0
Room air temperature, °F	69.6	69.7	69.8	69.9	69.9
Mean radiant temperature, °F	73.2	73.1	73.0	72.9	72.8
Operative temperature, °F	71.6	71.6	71.6	71.6	71.5
Effective radiant field, Btu/(h · sq ft)	2.6	2.5	2.3	2.2	2.1
AUST, °F	67.0	66.8	66.7	66.6	66.5
Parameter 1, Btu/(h · sq ft · °F)	1.7252	1.7378	1.7504	1.7606	1.7734
Parameter 3, dimensionless	0.1170	0.1086	0.1016	0.0967	0.0913

**TABLE 5.20** Effects of Outside Air Temperature Change for a Heated Floor at 84°F

Outside design temperature, °F	5.0	10.0	15.0	20.0
Panel area required, sq ft	755.8	724.4	681.6	636.5
ASHRAE design heat loss, Btu/h	24108.0	22386.0	20664.0	18942.0
Actual design heat loss, Btu/h	22286.9	20612.8	18943.4	17273.4
Percentage difference 1	-7.6	-7.9	-8.3	-8.8
Conduction design heat loss 1, Btu/h	22545.9	20830.5	19115.1	17400.9
Percentage difference 2	-6.5	-6.9	-7.5	-8.1
Conduction design heat loss 2, Btu/h	22545.9	20830.5	19115.1	17400.9
Percentage difference 3	-6.5	-6.9	-7.5	-8.1
Actual heat input, Btu/h	19258.4	17917.9	16598.5	15260.1
Percentage difference 4	-20.1	-20.0	-19.7	-19.4
Percentage radiation	61.7	61.7	61.7	61.6
Percent floor covered by panels	84.0	80.5	75.7	70.7
Heat output per unit panel area, Btu/(h · sq ft)	25.5	24.7	24.4	24.0
Ceiling temperature, °F	69.9	70.0	70.1	70.2
Room air temperature, °F	69.7	69.9	70.0	70.2
Mean radiant temperature, °F	73.1	72.9	72.7	72.5
Operative temperature, °F	71.6	71.6	71.5	71.5
Effective radiant field, Btu/(h · sq ft)	2.5	2.2	2.0	1.7
AUST, °F	66.3	66.6	66.9	67.2
Parameter 1, Btu/(h · sq ft · °F)	1.7713	1.7606	1.7523	1.7441
Parameter 3, dimensionless	0.0947	0.0967	0.0977	0.0989

**TABLE 5.21** Effects of Floor  $U$  Factors on a Heated Floor at 84°F

Floor $U$ factor, Btu/(h · sq ft · °F)	0.07	0.10	0.15
Panel area required, sq ft	724.4	734.2	747.5
ASHRAE design heat loss, Btu/h	22386.0	24141.0	27066.0
Actual design heat loss, Btu/h	20612.8	22239.9	24952.9
Percentage difference 1	-7.9	-7.9	-7.8
Conduction design heat loss 1, Btu/h	20830.5	22372.0	24928.2
Percentage difference 2	-6.9	-7.3	-7.9
Conduction design heat loss 2, Btu/h	20830.5	22372.0	24928.2
Percentage difference 3	-6.9	-7.3	-7.9
Actual heat input, Btu/h	17917.9	18160.7	18515.5
Percentage difference 4	-20.0	-24.8	-31.6
Percentage radiation	61.7	61.8	61.9
Percent floor covered by panels	80.5	81.6	83.1
Heat output per unit panel area, Btu/(h · sq ft)	24.7	24.7	24.8
Ceiling temperature, °F	70.0	70.0	69.9
Room air temperature, °F	69.9	69.9	69.9
Mean radiant temperature, °F	72.9	72.9	72.8
Operative temperature, °F	71.6	71.6	71.5
Effective radiant field, Btu/(h · sq ft)	2.2	2.2	2.1
AUST, °F	66.6	66.4	66.2
Parameter 1, Btu/(h · sq ft · °F)	1.7606	1.7640	1.7692
Parameter 3, dimensionless	0.0967	0.0961	0.0952

**TABLE 5.22** Effects Due to Infiltration for a Heated Floor at 84°F for a 30 × 30 × 8-ft Room

Infiltration rate, ACH	0.50	0.75	1.00	1.25
Panel area required, sq ft	724.4	777.6	837.5	896.0
ASHRAE design heat loss, Btu/h	22386.0	24492.0	26598.0	28704.0
Actual design heat loss, Btu/h	20612.8	22302.4	23955.1	25570.9
Percentage difference 1	-7.9	-8.9	-9.9	-10.9
Conduction design heat loss 1, Btu/h	20830.5	22800.8	24734.4	26574.8
Percentage difference 2	-6.9	-6.9	-7.0	-7.4
Conduction design heat loss 2, Btu/h	20830.5	22800.8	24734.4	26574.8
Percentage difference 3	-6.9	-6.9	-7.0	-7.4
Actual heat input, Btu/h	17917.9	19661.0	21337.7	22984.8
Percentage difference 4	-20.0	-19.7	-19.8	-19.9
Percentage radiation	61.7	59.5	57.5	55.5
Percent floor covered by panels	80.5	86.4	93.1	99.6
Heat output per unit panel area, Btu/(h · sq ft)	24.7	25.3	25.5	25.7
Ceiling temperature, °F	70.0	70.6	71.1	71.6
Room air temperature, °F	69.9	69.2	68.5	67.9
Mean radiant temperature, °F	72.9	73.8	74.6	75.4
Operative temperature, °F	71.6	71.7	71.9	72.1
Effective radiant field, Btu/(h · sq ft)	2.2	3.4	4.4	5.5
AUST, °F	66.6	67.1	67.7	68.3
Parameter 1, Btu/(h · sq ft · °F)	1.7606	1.6959	1.6378	1.5842
Parameter 3, dimensionless	0.0967	0.0947	0.0944	0.0946

In Tables 5.23 and 5.24, cases for three inside walls and two inside walls are presented. In these two situations, the room is 15 × 15 × 8 ft, and in each case one outside wall contains half glass. The other variables are as given in the base case. There is little effect in either situation on the difference between HLD and HLC.

Analysis has also been carried out for infrared modular (square or rectangular) and U-tube heating types of units. For the infrared base cases (both modular and U-tube types), the base case described in Sec. 5.3 for ceiling panels and floors was somewhat modified. The configuration for the *infrared base case*, which was compared for both modular and U-tube units, was the following:

Outside design temperature: 3°F.

Room dimensions:

Length: 30 ft.

Width: 30 ft.

Height: 9 ft.

$U$  Factors, Btu/(h · ft<sup>2</sup> · °F):

Wall 1: half wall with  $U = 0.25$ , and half glass with  $U = 1.0$ .

Walls 2, 3, and 4:  $U = 0.25$ .

Floor:  $U = 0.25$ .

Ceiling:  $U = 0.25$ .

Emissivities:

Panels: 0.9.

Walls: 0.9.

Floor: 0.9.

Ceiling: 0.9.

Convection coefficients,  $\text{Btu}/(\text{h} \cdot \text{ft}^2 \cdot ^\circ\text{F})$ : See previous convective heat transfer, starting with Eq. (5.3).

Comfort variables:

Metabolic rate:  $75 \text{ cal}/(\text{h} \cdot \text{m}^2)$ .

Clothing resistance: 0.75.

Relative air velocity: 0.15 m/s.

Relative humidity: 30 percent.

Infiltration rate: 0.5 ACH.

Room air temperature gradient:  $0^\circ\text{F}/\text{ft}$ .

It should be noted that the following items were changed from the base case for the ceiling and floor panel calculations.

Walls:  $U = 0.25 \text{ Btu}/(\text{h} \cdot \text{ft}^2 \cdot ^\circ\text{F})$ .

Floors:  $U = 0.25 \text{ Btu}/(\text{h} \cdot \text{ft}^2 \cdot ^\circ\text{F})$ .

Ceiling:  $U = 0.25 \text{ Btu}/(\text{h} \cdot \text{ft}^2 \cdot ^\circ\text{F})$ .

Glass:  $U = 1.0 \text{ Btu}/(\text{h} \cdot \text{ft}^2 \cdot ^\circ\text{F})$ .

This change in wall and floor construction was made because modular and U-tube types of radiant units are most commonly applied to industrial buildings where the  $U$  factors are normally higher than what was given in the base case applied to ceiling and floor panel heating systems. The room height was kept at 9 ft in order to be consistent with the previous calculations. It is recognized that infrared U tubes and modular units are not normally installed at this height but at a height usually greater than 12 ft. The installed height was changed in some of the following calculations in order to determine its effect on the design heat loss value.

**TABLE 5.23** Heated Floor Cases—Three Inside Walls and One Outside Wall with Half Glass for a  $15 \times 15 \times 8$ -ft Room

Floor temperature, $^\circ\text{F}$	83.0	84.0	85.0
Panel area required, sq ft	197.7	184.9	173.5
ASHRAE design heat loss, $\text{Btu}/\text{h}$	5775.9	5775.9	5775.9
Actual design heat loss, $\text{Btu}/\text{h}$	5318.6	5324.3	5329.7
Percentage difference 1	-7.9	-7.8	-7.7
Conduction design heat loss 1, $\text{Btu}/\text{h}$	5433.4	5434.2	5434.8
Percentage difference 2	-5.9	-5.9	-5.9
Conduction design heat loss 2, $\text{Btu}/\text{h}$	5433.4	5434.2	5434.8
Percentage difference 3	-5.9	-5.9	-5.9
Actual heat input, $\text{Btu}/\text{h}$	4617.2	4672.0	4720.1
Percentage difference 4	-20.1	-19.1	-18.3
Percentage radiation	60.3	59.9	59.5
Percent floor covered by panels	87.9	82.2	77.1
Heat output per unit panel area, $\text{Btu}/(\text{h} \cdot \text{sq ft})$	23.4	25.3	27.2
Ceiling temperature, $^\circ\text{F}$	69.2	69.2	69.2
Room air temperature, $^\circ\text{F}$	69.9	69.9	70.0
Mean radiant temperature, $^\circ\text{F}$	72.9	72.8	72.8
Operative temperature, $^\circ\text{F}$	71.6	71.5	71.5
Effective radiant field, $\text{Btu}/(\text{h} \cdot \text{sq ft})$	2.2	2.1	2.0
AUST, $^\circ\text{F}$	68.0	68.0	67.9
Parameter 1, $\text{Btu}/(\text{h} \cdot \text{sq ft} \cdot ^\circ\text{F})$	1.7634	1.7819	1.7988
Parameter 3, dimensionless	0.1112	0.1045	0.0986

In addition, the metabolic rate was left at  $75 \text{ cal}/(\text{h} \cdot \text{m}^2)$  (or 1.5 MET), the clothing resistance at 0.75 clo (halfway between light and medium clothing), and the relative air velocity was at 0.15 m/s (which is at the lower range for this variable). For industrial applications these values might be somewhat low for the three variables. The effect due to some changes in these variables is addressed later in Table 45B.\*

A second point to be made is that the room air temperature gradient was kept at  $0^\circ\text{F}/\text{ft}$  for all of these calculations. The reason for this was discussed in Sec. 2.0 of RP-394 and specifically illustrated in Figs. 5.2 through 5.5. The small amount of reliable data shows almost no air temperature stratification for ceiling heights of up to about 12 ft and then conflicting values for gradients at room heights above 12 ft. Because there were no available consistent data for air temperature stratification in infrared heated structures, it was felt that this variable should be kept at  $0^\circ\text{F}/\text{ft}$ , which is the most commonly reported value. It should be kept in mind, however, that if air temperature gradients do exist, this would affect the design heat loss value of the structure. It is difficult to assess how much the air temperature gradient will affect the heat loss since the placement of convection units, amount of insulation in the structure, and the mixing of warm and cool air will affect the actual temperature difference between inside and outside air. This is an area that needs additional study before any realistic numerical differences can be estimated for heat loss due to air stratification.

A *single case for a convection heating system* for an industrial type building was calculated and discussed in Sec. 5.4 of RP-394. For this convection case calculation, the room parameters were the same as the new base case specified previously *except* that the room was 25 ft high, which would be more common in an industrial situation, and the infiltration rate was varied between 1 and 4 ACH. For this convection heating case, the supply airflow rate was set at  $0.75 \text{ CFM}/\text{ft}^2$  of floor area, and the room air temperature gradient was  $0.75^\circ\text{F}/\text{ft}$ , with a reference height of 5 ft from the floor. The results from these calculations were presented in Table 12.\* Examination of these results show that the ASHRAE design heat loss calculation procedure can underestimate the size of the heating load by 11 percent at an air infiltration rate of 4 ACH. For infiltration rates of up to 2 ACH, the ASHRAE design procedure estimates the heating load quite closely or overestimates. It was pointed out in Table 5.4 that the ASHRAE design heat loss procedure could overestimate the design heat loss by 3 to 8 percent for various room heights with 0.5 ACH for infiltration. It is not unexpected that the ASHRAE procedure would be conservative by up to 10 percent in order to account for unexpected conditions in a structure. It should be pointed out here that the present calculations show an increased heat loss due to stratification of up to 20 percent (11 percent underestimate at 4 ACH in Table 12\* and up to 8 percent overestimate in Table 5.4). However, the numerical values are strongly dependent on building geometry, wall and ceiling  $U$  factors, infiltration rates, and room air temperature gradients. *These results emphasize that additional research is needed in order to properly predict room air temperature stratification and the resulting increase in design heat loss values. It is apparent that with higher air temperatures at the ceiling, there will be increased heat losses from the structure.* In radiant heating systems design, if there is lesser stratification in the room air temperature, recognition should be given to this in the design heat loss calculation.

Again, it should be noted that in Table 12\* the supply air temperatures are not appropriate values. The airflow rate was set at  $0.75 \text{ CFM}/\text{ft}^2$ , and for higher heat losses, such as found here, this value would have to be approximately  $3 \text{ CFM}/\text{ft}^2$  to yield reasonable supply air temperatures. *This calculation does not affect the design load calculations.*

Two situations were calculated for the modular and U-tube infrared cases. *The first situation was when there were no reflectors or deflectors on the units (which is not*

the normal operating condition), and the second is when there were reflectors or deflectors on the units and these reflectors are perfect and that the placement of the units is such that none of the direct radiation from the infrared units falls on the walls of the structure. This second situation would be the ideal design and placement case for infrared modular and U-tube infrared heaters. In these calculations, the model that was used had a well-insulated back surface so that the heat output from the infrared units was from the surface facing the room. This results in minimum convection heat transfer from the infrared heaters. Figures 4\* and 5\* illustrate the first situation, and Fig. 5.13 illustrates the ideal situation with no direct radiation falling on the walls. This appeared to be the most reasonable approach to this type of heater because each manufacturer has a series of different reflector designs and suggestions or directions for placement of the units. By looking at these two extremes—no reflectors or deflectors and perfect reflectors or deflectors—the range of performance of generic units can be identified.

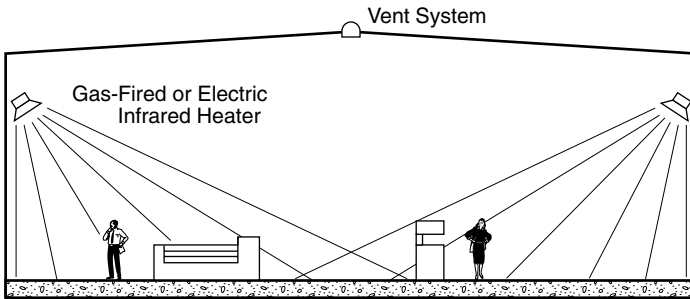


**FIGURE 5.13** Placement of infrared modular units with deflectors and reflectors to prevent direct wall radiation.

Table 5.25 summarizes results for three infrared surface temperatures when there are *no reflectors or deflectors*. The areas of the heaters that are shown in Table 5.25 are the total of four infrared heaters located at the ceiling (without reflectors) and compared with several manufacturers and found to be in good agreement with their published ratings. The percent difference between HLD and HLC was constant at approximately +3 percent. This increase in design heating load is apparently due to a lower AUST because of increased  $U$  factors and also more of the radiant energy being intercepted by the walls.

In Table 5.26, results are presented for four 1700°F infrared units located at the ceiling (*without reflectors or deflectors*) for the base case as the ceiling height is extended to 25 ft. This indicates that as the heaters are raised in the room, more of the radiant energy is absorbed by the larger wall area resulting in greater conduction losses. This results in a greater design heat loss (up to 10 percent at 25 ft). It should be kept in mind, however, that high-temperature radiant units are normally mounted at the 12- to 15-ft level in an industrial building and use reflectors to direct the radiant energy away from the walls and toward the floor or occupants. This lowering of the units and use of directive reflectors would nullify this 3 to 10 percent difference in design heat loss as illustrated in the following calculations.

In Table 5.27, the room was 15 ft high, the modular infrared units were at 1700°F, and they did not have reflectors or deflectors. In this case (Table 5.27), the infiltra-

**TABLE 5.24** Heated Floor Cases—Two Inside Walls and Two Outside Walls, One with Half Glass for a 15 × 15 × 8-ft Room

Floor temperature, °F	83.0	84.0	85.0
Panel area required, sq ft	217.2	203.7	191.7
ASHRAE design heat loss, Btu/h	6548.1	6548.1	6548.1
Actual design heat loss, Btu/h	6031.3	6038.3	6045.0
Percentage difference 1	-7.9	-7.8	-7.7
Conduction design heat loss 1, Btu/h	6091.4	6090.2	6089.3
Percentage difference 2	-7.0	-7.0	-7.0
Conduction design heat loss 2, Btu/h	6091.4	6090.2	6089.3
Percentage difference 3	-7.0	-7.0	-7.0
Actual heat input, Btu/h	5216.5	5269.9	5317.6
Percentage difference 4	-20.3	-19.5	-18.8
Percentage radiation	61.5	60.9	60.4
Percent floor covered by panels	96.5	90.5	85.2
Heat output per unit panel area, Btu/(h · sq ft)	24.0	25.9	27.7
Ceiling temperature, °F	69.0	69.0	69.1
Room air temperature, °F	69.9	69.9	70.0
Mean radiant temperature, °F	72.9	72.8	72.7
Operative temperature, °F	71.6	71.5	71.5
Effective radiant field, Btu/(h · sq ft)	2.2	2.1	2.0
AUST, °F	67.2	67.1	67.1
Parameter 1, Btu/(h · sq ft · °F)	1.8152	1.8269	1.8385
Parameter 3, dimensionless	0.1088	0.1022	0.0964

**TABLE 5.25** Infrared Modular Units—Base Case with No Reflectors or Deflectors and Variable Surface Temperature

Infrared heater temperature, °F	1600.0	1700.0	1800.0
Panel area required, sq ft	2.4	2.0	1.6
ASHRAE design heat loss, Btu/h	64378.8	64378.8	64378.8
Actual design heat loss, Btu/h	51343.2	51328.3	51315.4
Percentage difference 1	-20.2	-20.3	-20.3
Conduction design heat loss 1, Btu/h	66224.4	66228.8	66232.6
Percentage difference 2	2.9	2.9	2.9
Conduction design heat loss 2, Btu/h	66224.4	66228.8	66232.6
Percentage difference 3	2.9	2.9	2.9
Actual heat input, Btu/h	66188.0	66198.6	66207.4
Percentage difference 4	2.8	2.8	2.8
Percentage radiation	99.4	99.5	99.5
Percent ceiling covered by panels	0.3	0.2	0.2
Heat output per unit panel area, Btu/(h · sq ft)	27832.4	33635.6	40312.8
Floor temperature, °F	73.7	73.7	73.7
Room air temperature, °F	60.4	60.4	60.4
Mean radiant temperature, °F	84.7	84.7	84.8
Operative temperature, °F	74.0	74.0	74.0
Effective radiant field, Btu/(h · sq ft)	17.8	17.8	17.9
AUST, °F	62.6	62.6	62.6
Parameter 1, Btu/(h · sq ft · °F)	18.0769	20.5157	23.1746
Parameter 3, dimensionless	0.0006	0.0006	0.0005

TABLE 5.26 Infrared Modular Units with No Reflectors or Deflectors and Surface Temperature at 1700°F.—Effect of Room Height

Room height, ft	9.0	10.0	12.0	15.0	20.0	25.0
Panel area required, sq ft	2.0	2.1	2.3	2.6	3.3	4.0
ASHRAE design heat loss, Btu/h	64378.8	67932.0	75038.4	85698.0	103464.0	121230.0
Actual design heat loss, Btu/h	51328.3	53973.1	59514.3	67341.4	83916.3	99536.9
Percentage difference 1	-20.3	-20.5	-20.7	-21.4	-18.9	-17.9
Conduction design heat loss 1, Btu/h	66228.8	69934.7	77682.6	88684.3	111769.5	133661.2
Percentage difference 2	2.9	2.9	3.5	3.5	8.0	10.3
Conduction design heat loss 2, Btu/h	66228.8	69934.7	77682.6	88684.3	111769.5	133661.2
Percentage difference 3	2.9	2.9	3.5	3.5	8.0	10.3
Actual heat input, Btu/h	66198.6	69903.0	77647.5	88644.7	111718.1	133599.0
Percentage difference 4	2.8	2.9	3.5	3.4	8.0	10.2
Percentage radiation	99.5	99.5	99.5	99.5	99.5	99.5
Percent ceiling covered by panels	0.2	0.2	0.3	0.3	0.4	0.4
Heat output per unit panel area, Btu/(h · sq ft)	33635.6	33646.9	33646.8	33648.2	33646.8	33646.2
Floor temperature, °F	73.7	73.5	73.4	72.4	73.7	73.3
Room air temperature, °F	60.4	60.2	60.1	59.6	61.4	62.1
Mean radiant temperature, °F	84.7	85.0	85.1	85.7	83.5	82.7
Operative temperature, °F	74.0	74.0	74.1	74.2	73.8	73.6
Effective radiant field, Btu/(h · sq ft)	17.8	18.2	18.3	19.2	16.2	15.1
AUST, °F	62.6	62.6	62.8	62.7	65.1	66.3
Parameter 1, Btu/(h · sq ft · °F)	20.5157	20.5179	20.5167	20.5109	20.5327	20.5414
Parameter 3, dimensionless	0.0006	0.0006	0.0006	0.0006	0.0006	0.0006

tion rate was changed between 1 and 4 ACH. As can be seen in Tables 5.26 and 5.27, the percent difference in HLD and HLC goes from =3.5 percent at 0.5 ACH to -9.4 percent at 4 ACH. This illustrates how much the infiltration rate affects the design load calculation. This is due to the exchange of lower-temperature air for radiant systems when compared with forced-air systems. With this increase in the infiltration rate, the floor temperature has increased to 80.9°F, the room air temperature for comfort has decreased to 49°F, and the MRT has increased to 100°F. In this situation, the 4 ACH would most likely be beyond any normal situation (except for something such as spot heating) and does not represent a realistic situation. However, the importance of the change in the design heat loss load compared with the standard ASHRAE design load as infiltration is changed is strongly supported.

In Table 5.28, the convection coefficient at the modular infrared units was changed by up to a factor of 5 for a 15-ft-high room with 3 ACH and a modular infrared heater surface at 1700°F *without reflectors or deflectors*. The first case with a convection coefficient multiplier of 1 is identical to the 3 ACH case given as the third column in Table 5.27. Using a convection coefficient five times larger has had only a slight effect on the results. A negligible effect was found for the design heat loss calculations. If reflectors are used, there might be more of an effect due to more area available for convection heat transfer; however, it is expected to be negligible also.

In Tables 5.29 through 5.31, cases were run where the modular infrared units had *perfect reflectors or deflectors and were positioned such that none of their direct radiation fell on the walls*. This situation is illustrated in Fig. 5.13 for an individual application.

**TABLE 5.27** Infrared Modular Units with No Reflectors or Deflectors and Surface Temperature at 1700°F and 15-ft Height—Effect of Infiltration Rate

Air changes per hour, ACH	1.0	2.0	3.0	4.0
Panel area required, sq ft	2.9	3.2	3.6	4.0
ASHRAE design heat loss, Btu/h	94446.0	111942.0	129438.0	146934.0
Actual design heat loss, Btu/h	71677.8	79646.7	86809.3	93065.8
Percentage difference 1	-24.1	-28.9	-32.9	-36.7
Conduction design heat loss 1, Btu/h	95968.8	109202.3	121735.1	133075.9
Percentage difference 2	1.6	-2.4	-6.0	-9.4
Conduction design heat loss 2, Btu/h	95968.8	109202.3	121735.1	133075.9
Percentage difference 3	1.6	-2.4	-6.0	-9.4
Actual heat input, Btu/h	95926.2	109154.3	121680.9	133015.7
Percentage difference 4	1.6	-2.5	-6.0	-9.5
Percentage radiation	99.5	99.5	99.5	99.5
Percent ceiling covered by panels	0.3	0.4	0.4	0.4
Heat output per unit panel area, Btu/(h · sq ft)	33647.4	33646.5	33644.7	33644.1
Floor temperature, °F	73.7	76.0	78.5	80.9
Room air temperature, °F	57.6	54.2	51.3	48.6
Mean radiant temperature, °F	88.0	92.1	96.2	100.0
Operative temperature, °F	74.6	75.4	76.4	77.4
Effective radiant field, Btu/(h · sq ft)	22.3	27.8	33.2	38.0
AUST, °F	63.3	64.3	65.8	67.3
Parameter 1, Btu/(h · sq ft · °F)	20.4863	20.4432	20.4057	20.3721
Parameter 3, dimensionless	0.0006	0.0005	0.0005	0.0005

**TABLE 5.28** Infrared Modular Units with No Reflectors or Deflectors and Surface Temperature at 1700°F, 15 ft High, 3 ACH—Effect of Convection Coefficient Multiplier

Convection multiplier	1.0	2.0	5.0
Panel area required, sq ft	3.6	3.6	3.5
ASHRAE design heat loss, Btu/h	129438.0	129438.0	129438.0
Actual design heat loss, Btu/h	86809.3	87104.7	87964.9
Percentage difference 1	-32.9	-32.7	-32.0
Conduction design heat loss 1, Btu/h	121735.1	121714.3	121664.4
Percentage difference 2	-6.0	-6.0	-6.0
Conduction design heat loss 2, Btu/h	121735.1	121714.3	121664.4
Percentage difference 3	-6.0	-6.0	-6.0
Actual heat input, Btu/h	121680.9	121660.5	121611.7
Percentage difference 4	-6.0	-6.0	-6.0
Percentage radiation	99.5	98.9	97.3
Percent ceiling covered by panels	0.4	0.4	0.4
Heat output per unit panel area, Btu/(h · sq ft)	33644.7	33830.2	34381.6
Floor temperature, °F	78.5	78.4	78.0
Room air temperature, °F	51.3	51.5	51.9
Mean radiant temperature, °F	96.2	96.0	95.3
Operative temperature, °F	76.4	76.4	76.2
Effective radiant field, Btu/(h · sq ft)	33.2	32.9	32.0
AUST, °F	65.8	65.7	65.5
Parameter 1, Btu/(h · sq ft · °F)	20.4057	20.5200	20.8606
Parameter 3, dimensionless	0.0005	0.0006	0.0006

**TABLE 5.29** Infrared Modular Units with Perfect Reflectors in a 9-ft-High Base Case Room—Effect of Surface Temperature

Infrared heater temperature, °F	1600.0	1700.0	1800.0
Panel area required, sq ft	2.3	1.9	1.6
ASHRAE design heat loss, Btu/h	64378.8	64378.8	64378.8
Actual design heat loss, Btu/h	51189.5	51177.4	51166.8
Percentage difference 1	-20.5	-20.5	-20.5
Conduction design heat loss 1, Btu/h	63752.4	63755.6	63758.2
Percentage difference 2	-1.0	-1.0	-1.0
Conduction design heat loss 2, Btu/h	63752.4	63755.6	63758.2
Percentage difference 3	-1.0	-1.0	-1.0
Actual heat input, Btu/h	63716.9	63726.2	63733.7
Percentage difference 4	-1.0	-1.0	-1.0
Percentage radiation	99.4	99.5	99.5
Percent ceiling covered by panels	0.3	0.2	0.2
Heat output per unit panel area, Btu/(h · sq ft)	27819.0	33621.7	40298.0
Floor temperature, °F	83.3	83.3	83.3
Room air temperature, °F	60.2	60.2	60.2
Mean radiant temperature, °F	84.9	84.9	85.0
Operative temperature, °F	74.0	74.0	74.0
Effective radiant field, Btu/(h · sq ft)	18.1	18.1	18.1
AUST, °F	61.4	61.4	61.4
Parameter 1, Btu/(h · sq ft · °F)	18.0661	20.5051	23.1641
Parameter 3, dimensionless	0.0006	0.0006	0.0005

**TABLE 5.30** Infrared Modular Units with Perfect Reflectors with 0.5 ACH and 1700°F Heaters—Effect of Room Height

Room height, ft	8.0	9.0	10.0	12.0	15.0	20.0	25.0
Panel area required, sq ft	1.7	1.9	2.0	2.2	2.4	3.0	3.4
ASHRAE design heat loss, Btu/h	60825.6	64378.8	67932.0	75038.4	85698.0	103464.0	121230.0
Actual design heat loss, Btu/h	47042.2	51177.4	53685.4	58866.2	65878.9	80311.5	92743.0
Percentage difference 1	-22.7	-20.5	-21.0	-21.6	-23.1	-22.4	-23.5
Conduction design heat loss 1, Btu/h	58558.7	63755.6	66870.4	73314.1	82005.6	100056.2	115527.7
Percentage difference 2	-3.7	-1.0	-1.6	-2.3	-4.3	-3.3	-4.7
Conduction design heat loss 2, Btu/h	58558.7	63755.6	66870.4	73314.1	82005.6	100056.2	115527.7
Percentage difference 3	-3.7	-1.0	-1.6	-2.3	-4.3	-3.3	-4.7
Actual heat input, Btu/h	58532.4	63726.2	66839.8	73280.7	81969.2	100011.7	115477.5
Percentage difference 4	-3.8	-1.0	-1.6	-2.3	-4.4	-3.3	-4.7
Percentage radiation	99.5	99.5	99.5	99.5	99.5	99.5	99.5
Percent ceiling covered by panels	0.2	0.2	0.2	0.2	0.3	0.3	0.4
Heat output per unit panel area, Btu/(h · sq ft)	33626.8	33621.7	33621.2	33628.2	33624.5	33614.7	33606.8
Floor temperature, °F	79.4	83.3	84.7	87.8	91.5	101.2	108.5
Room air temperature, °F	58.7	60.2	59.5	59.5	58.3	58.9	58.1
Mean radiant temperature, °F	86.8	84.9	85.3	85.8	87.2	86.5	87.5
Operative temperature, °F	74.4	74.0	74.1	74.2	74.4	74.3	74.5
Effective radiant field, Btu/(h · sq ft)	20.6	18.1	18.7	19.3	21.2	20.3	21.6
AUST, °F	59.7	61.4	61.1	60.8	59.8	60.5	59.8
Parameter 1, Btu/(h · sq ft · °F)	20.4886	20.5051	20.5005	20.4975	20.4811	20.4818	20.4668
Parameter 3, dimensionless	0.0006	0.0006	0.0006	0.0006	0.0006	0.0006	0.0006

**TABLE 5.31** Infrared Modular Units with Perfect Reflectors in 15-ft-High Room with Heaters at 1700°F—Effect of Infiltration

Infiltration rate, ACH	1.0	2.0	3.0	4.0
Panel area required, sq ft	2.6	3.0	3.3	3.6
ASHRAE design heat loss, Btu/h	94446.0	111942.0	129438.0	146934.0
Actual design heat loss, Btu/h	69909.4	77235.9	82915.1	88056.9
Percentage difference 1	-26.0	-31.0	-35.9	-40.1
Conduction design heat loss 1, Btu/h	88556.3	100781.1	112335.0	122314.8
Percentage difference 2	-6.2	-10.0	-13.2	-16.8
Conduction design heat loss 2, Btu/h	88556.3	100781.1	112335.0	122314.8
Percentage difference 3	-6.2	-10.0	-13.2	-16.8
Actual heat input, Btu/h	88517.1	100736.7	112283.9	122257.9
Percentage difference 4	-6.3	-10.0	-13.3	-16.8
Percentage radiation	99.5	99.5	99.5	99.5
Percent ceiling covered by panels	0.3	0.3	0.4	0.4
Heat output per unit panel area, Btu/(h · sq ft)	33622.2	33617.8	33612.4	33607.2
Floor temperature, °F	94.1	99.2	104.4	108.8
Room air temperature, °F	56.3	52.7	49.1	46.1
Mean radiant temperature, °F	89.6	94.3	99.3	103.4
Operative temperature, °F	74.9	75.9	77.2	78.3
Effective radiant field, Btu/(h · sq ft)	24.5	30.6	37.1	42.5
AUST, °F	60.2	61.2	63.1	64.6
Parameter 1, Btu/(h · sq ft · °F)	20.4541	20.4064	20.3592	20.3196
Parameter 3, dimensionless	0.0005	0.0005	0.0005	0.0005

The situation in Table 5.29 is identical to the situation reported in Table 5.25—*infrared base case*—except that Table 5.29 uses perfect reflectors and unit placement. It is now seen that the percent difference between HLD and HLC has gone from +3 to -1 percent, indicating that proper placement of the infrared heaters and use of reflector can account for 4 percent change in design load at these conditions. Also note in Tables 5.25 and 5.29 that the floor temperature has risen by 10°F, the room air temperature for comfort and MRT have not changed, and the AUST has dropped by about 1°F. *In actual situations, the floor temperature would not get this high due to furniture, people, equipment, and material distributed across the floor.*

The situation in Table 5.30 is identical to the situation reported in Table 5.26, except that Table 5.30 issues *perfect reflectors and placement of the heating units*. In these two tables, the effect of room height is considered. It is seen that the percent difference between HLD and HLC has changed from +10 percent with no reflectors to -5 percent with *ideal reflectors and placement indicating that proper placement of the infrared heaters can account for 15 percent reduction in the design heat loss value*. Also note in Tables 5.26 and 5.30 that the floor temperature can reach too high a value in the ideal situation (108°F), but in the actual situation this will not be realized because equipment, furniture, and people will absorb this radiant energy and intercept it before it reaches the floor. Also, observe that in Table 5.30, the air temperature for comfort is lower by up to 4°F, the MRT is increased by up to 5°F, and the AUST is reduced by up to 7°F as compared with the situation in Table 5.26 where no reflectors are used.

The configuration and conditions in Table 5.31 are identical to those considered in Table 5.27, except that Table 5.31 considers *ideal reflectors and unit heater placement*. In these two tables, the effect due to air infiltration is considered. It is seen that the percent differences between HLD and HLC has changed from up to -9.4 percent with no reflectors to up to -16.8 percent with ideal reflectors. This indicates that *with proper reflector design and unit placement of infrared heaters that up to 7 percent of the design heating load can be saved when considering the height of the room*. Again, the floor temperature has increased, theoretically, by up to 25°F by use of reflectors and proper unit placement. The room air temperature for comfort has been reduced by 2°F, the MRT increased by 3°F, and the AUST reduced by 2°F with the use of reflectors and correct unit placement.

The U-tube or straight-tube types of configurations for vented gas-fired infrared units were also analyzed. These units have different orifice sizes for the same size and length of tube; therefore, the units will operate at different average surface temperatures. The same base case parameters were used as described in Sec. 5.8 of RP-394 for the infrared modular units except for this case two U tubes were used in the space instead of the four modular units. Again, two situations were considered: (1) no reflectors and then (2) with ideal reflectors and placement. The results from these calculations are shown in Tables 5.32 through 5.40. Tables 5.32 and 5.33 give results for the U-tube heaters that *do not have reflectors or deflectors*. In Table 5.32, the average surface temperature was varied between 700°F and 900°F. To verify the calculations made here, the required heater area calculated for the average surface temperature of 700°F and 750°F was compared with data presented in the manufacturer's catalog. For the same heat output required here and given in the manufacturer's catalog, the area of the heater listed by the manufacturer and that calculated here agreed reasonably well. The same conclusions can be drawn from these results as from the infrared modular results. In fact, there is very little change in the results, and the trends are similar.

The convection multiplier was not changed from 1 because there is no reason to think that the results would be different from what was shown in Table 5.28. It is expected that more convection heat transfer will result from the tube-type heaters but the total heat transfer will be as calculated in Tables 5.32 through 5.40.

The results given in Table 5.33 are for 750°F average surface temperature; however, the ceiling was extended in steps up to 20 ft. It is interesting to note here that the line source of radiation causes the opposite trend in the difference between HLD and HLC than was observed for the modular infrared units. The behavior of the U-tube units appears to be similar to that of the ceiling panel heating-types of units.

Tables 5.34 through 5.40 present the results for the U-tube infrared units, which *have ideal reflectors and unit placement*. Table 5.34 is the same configuration and conditions as used in Table 5.32, except that ideal reflectors and unit placement is used in Table 5.34. This change results in a decrease in the percent difference between HLD and HLC of up to 5 percent for this set of conditions. Also showing up in this calculation is an increase of about 10°F in the floor temperature when all of the infrared radiant energy from the heater is reflected directly to the floors with none impinging on the walls. In Table 5.35, the average surface temperature was extended down to 400°F. There are no unusual variations here other than an increase in the area of the heater in order to provide enough heat to the room.

In Table 5.36, the same configuration as used in Table 5.35 was considered except that changes in some of the comfort variables were considered so that these results could be compared with the results given in Table 5.1. In Table 5.36, the metabolic rate (activity level) was increased from 75 cal/(h · m<sup>2</sup>) (1.5 MET) to 100 cal/(h · m<sup>2</sup>)

**TABLE 5.32** U-Tube Infrared Units—Base Case with No Reflectors or Deflectors—Change in Tube Surface Temperature

U-tube IR heater temperature, °F	900.0	850.0	800.0	750.0	700.0
Panel area required, sq ft	12.7	14.8	17.3	20.4	24.3
ASHRAE design heat loss, Btu/h	64378.8	64378.8	64378.8	64378.8	64378.8
Actual design heat loss, Btu/h	51692.1	51721.6	51754.5	51791.1	51831.9
Percentage difference 1	-19.7	-19.7	-19.6	-19.6	-19.5
Conduction design heat loss 1, Btu/h	66658.9	66649.9	66640.3	66630.0	66619.3
Percentage difference 2	3.5	3.5	3.5	3.5	3.5
Conduction design heat loss 2, Btu/h	66658.9	66649.9	66640.3	66630.0	66619.3
Percentage difference 3	3.5	3.5	3.5	3.5	3.5
Actual heat input, Btu/h	66464.7	66423.9	66375.5	66317.6	66247.8
Percentage difference 4	3.2	3.2	3.1	3.0	2.9
Percentage radiation	98.5	98.4	98.2	98.1	97.9
Percent ceiling covered by panels	1.4	1.6	1.9	2.3	2.7
Heat output per unit panel area, Btu/(h · sq ft)	5234.8	4494.6	3834.3	3247.3	2728.5
Floor temperature, °F	73.3	73.3	73.2	73.2	73.1
Room air temperature, °F	60.8	60.8	60.9	60.9	61.0
Mean radiant temperature, °F	84.2	84.2	84.2	84.1	84.1
Operative temperature, °F	73.9	73.9	73.9	73.9	73.9
Effective radiant field, Btu/(h · sq ft)	17.2	17.1	17.1	17.0	16.9
AUST, °F	62.1	62.1	62.1	62.1	62.1
Parameter 1, Btu/(h · sq ft · °F)	6.2386	5.6962	5.1883	4.7132	4.2702
Parameter 3, dimensionless	0.0011	0.0012	0.0012	0.0013	0.0014

**TABLE 5.33** U-Tube Infrared Units—750°F Surface Temperature and No Reflectors or Deflectors—Effect of Change in Room Height

Room height, ft	9.0	10.0	12.0	15.0	20.0
Panel area required, sq ft	20.4	21.4	23.4	26.3	30.9
ASHRAE design heat loss, Btu/h	64378.8	67932.0	75038.4	85598.0	103464.0
Actual design heat loss, Btu/h	51791.1	54135.7	58689.3	65300.3	75864.0
Percentage difference 1	-19.6	-20.3	-21.8	-23.8	-26.7
Conduction design heat loss 1, Btu/h	66630.0	69924.7	76463.0	86012.3	101112.3
Percentage difference 2	3.5	2.9	1.9	0.4	-2.3
Conduction design heat loss 2, Btu/h	66630.0	69924.7	76463.0	86012.3	101112.3
Percentage difference 3	3.5	2.9	1.9	0.4	-2.3
Actual heat input, Btu/h	66317.6	69600.3	76115.4	85632.0	100683.5
Percentage difference 4	3.0	2.5	1.4	-0.1	-2.7
Percentage radiation	98.1	98.1	98.1	98.1	98.1
Percent ceiling covered by panels	2.3	2.4	2.6	2.9	3.4
Heat output per unit panel area, Btu/(h · sq ft)	3247.3	3248.2	3249.7	3251.5	3254.3
Floor temperature, °F	73.2	72.6	71.5	69.7	66.5
Room air temperature, °F	60.9	60.4	59.3	57.9	55.8
Mean radiant temperature, °F	84.1	84.8	86.0	87.7	90.2
Operative temperature, °F	73.9	74.0	74.2	74.6	75.0
Effective radiant field, Btu/(h · sq ft)	17.0	17.9	19.6	21.9	25.2
AUST, °F	62.1	61.7	61.1	60.1	58.6
Parameter 1, Btu/(h · sq ft · °F)	4.7132	4.7107	4.7056	4.6984	4.6884
Parameter 3, dimensionless	0.0013	0.0013	0.0013	0.0013	0.0013

TABLE 5.34 U-Tube Infrared Units—Base Case with Ideal Reflectors and Placement—Change in Tube Surface Temperature

U-tube heater temperature, °F	700.0	750.0	800.0	850.0	900.0
Panel area required, sq ft	23.3	19.6	16.6	14.2	12.2
ASHRAE design heat loss, Btu/h	64378.8	64378.8	64377.9	64378.8	64378.8
Actual design heat loss, Btu/h	51414.1	51396.1	51377.9	51360.1	51343.0
Percentage difference 1	-20.1	-20.2	-20.2	-20.2	-20.2
Conduction design heat loss 1, Btu/h	63618.7	63639.0	63655.9	63670.0	63682.0
Percentage difference 2	-1.2	-1.1	-1.1	-1.1	-1.1
Conduction design heat loss 2, Btu/h	63618.7	63639.0	63655.9	63670.0	63682.0
Percentage difference 3	-1.2	-1.1	-1.1	-1.1	-1.1
Actual heat input, Btu/h	63256.8	63334.9	63398.2	63450.2	63493.2
Percentage difference 4	-1.7	-1.6	-1.5	-1.4	-1.4
Percentage radiation	97.9	98.1	98.2	98.4	98.5
Percent ceiling covered by panels	2.6	2.2	1.8	1.6	1.4
Heat output per unit panel area, Btu/(h · sq ft)	2714.1	3233.3	3820.1	4480.8	5220.7
Floor temperature, °F	83.3	83.3	83.3	83.3	83.3
Room air temperature, °F	60.5	60.5	60.5	60.4	60.4
Mean radiant temperature, °F	84.6	84.6	84.7	84.7	84.7
Operative temperature, °F	74.0	74.0	74.0	74.0	74.0
Effective radiant field, Btu/(h · sq ft)	17.7	17.7	17.7	17.8	17.8
AUST, °F	61.4	61.4	61.4	61.4	61.4
Parameter 1, Btu/(h · sq ft · °F)	4.2447	4.6898	5.1662	5.6757	6.2189
Parameter 3, dimensionless	0.0014	0.0013	0.0012	0.0012	0.0011

**TABLE 5.35** U-Tube Infrared Units—Base Case with Ideal Reflectors and Placement—Change in Tube Surface Temperature down to 400°F

U-tube IR heater temperature, °F	400.0	500.0	600.0	700.0
Panel area required, sq ft	84.5	51.7	33.9	23.3
ASHRAE design heat loss, Btu/h	64378.8	64378.8	64378.8	64378.8
Actual design heat loss, Btu/h	51353.2	51452.4	51445.4	51414.1
Percentage difference 1	-20.2	-20.1	-20.1	-20.1
Conduction design heat loss 1, Btu/h	63359.4	63479.7	63563.8	63618.7
Percentage difference 2	-1.6	-1.4	-1.3	-1.2
Conduction design heat loss 2, Btu/h	63359.4	63479.7	63563.8	63618.7
Percentage difference 3	-1.6	-1.4	-1.3	-1.2
Actual heat input, Btu/h	62043.1	62675.6	63036.8	63256.9
Percentage difference 4	-3.6	-2.6	-2.1	-1.7
Percentage radiation	96.5	97.1	97.5	97.9
Percent ceiling covered by panels	9.4	5.7	3.8	2.6
Heat output per unit panel area, Btu/(h · sq ft)	734.1	1211.1	1857.9	2714.2
Floor temperature, °F	84.6	83.8	83.5	83.3
Room air temperature, °F	60.4	60.5	60.5	60.5
Mean radiant temperature, °F	84.7	84.6	84.6	84.6
Operative temperature, °F	74.0	74.0	74.0	74.0
Effective radiant field, Btu/(h · sq ft)	17.8	17.6	17.6	17.7
AUST, °F	61.4	61.4	61.4	61.4
Parameter 1, Btu/(h · sq ft · °F)	2.1611	2.7554	3.4444	4.2448
Parameter 3, dimensionless	0.0027	0.0021	0.0017	0.0014

**TABLE 5.36** U-Tube Infrared Units with Same Condition as Table 5.35 Except: Metabolic Rate = 100 cal/h m<sup>2</sup> (2MET), ICL = 1 clo, Relative Air Velocity = 0.2 m/s

Panel temperature, °F	400.0	500.0	600.0	700.0
Panel area required, sq ft	71.7	44.1	29.0	19.9
ASHRAE design heat loss, Btu/h	64378.8	64378.8	64378.8	64378.8
Actual design heat loss, Btu/h	44390.8	44419.6	44396.5	44362.7
Percentage difference 1	-31.0	-31.0	-31.0	-31.1
Conduction design heat loss 1, Btu/h	54397.1	54506.1	54580.8	54631.2
Percentage difference 2	-15.5	-15.3	-15.2	-15.1
Conduction design heat loss 2, Btu/h	54397.1	54506.1	54580.8	54631.2
Percentage difference 3	-15.5	-15.3	-15.2	-15.1
Actual heat input, Btu/h	53441.2	53918.4	54194.8	54365.8
Percentage difference 4	-17.0	-16.2	-15.8	-15.6
Percentage radiation	96.5	97.1	97.5	97.9
Percent ceiling covered by panels	8.0	4.9	3.2	2.2
Heat output per unit panel area, Btu/(h · sq ft)	745.5	1221.4	1869.0	2725.3
Floor temperature, °F	73.4	72.9	72.7	72.6
Room air temperature, °F	52.6	52.7	52.7	52.6
Mean radiant temperature, °F	74.0	74.0	74.0	74.1
Operative temperature, °F	63.5	63.5	63.5	63.5
Effective radiant field, Btu/(h · sq ft)	14.9	14.8	14.9	14.9
AUST, °F	53.2	53.2	53.2	53.2
Parameter 1, Btu/(h · sq ft · °F)	2.1457	2.7310	3.4152	4.2103
Parameter 3, dimensionless	0.0026	0.0020	0.0017	0.0014

**TABLE 5.37** U-Tube Infrared Units at 750°F Surface Temperature and with Ideal Reflectors and Placement—Effect of Change in Room Height

Room height, ft	9.0	10.0	12.0	15.0	20.0
Panel area required, sq ft	19.6	20.6	22.6	25.2	30.9
ASHRAE design heat loss, Btu/h	64378.8	67932.0	75038.4	85698.0	103464.0
Actual design heat loss, Btu/h	51396.1	53903.5	59074.6	66060.5	80365.5
Percentage difference 1	-20.2	-20.7	-21.3	-22.9	-22.3
Conduction design heat loss 1, Btu/h	63639.0	66742.1	73156.1	81802.6	99714.2
Percentage difference 2	-1.1	-1.8	-2.5	-4.5	-3.6
Conduction design heat loss 2, Btu/h	63639.0	66742.1	73156.1	81802.6	99714.2
Percentage difference 3	-1.1	-1.8	-2.5	-4.5	-3.6
Actual heat input, Btu/h	63334.9	66424.8	72810.8	81425.3	99252.0
Percentage difference 4	-1.6	-2.2	-3.0	-5.0	-4.1
Percentage radiation	98.1	98.1	98.1	98.1	98.1
Percent ceiling covered by panels	2.2	2.3	2.5	2.8	3.4
Heat output per unit panel area, Btu/(h · sq ft)	3233.3	3231.7	3228.7	3225.0	3214.3
Floor temperature, °F	83.3	84.7	87.9	91.7	101.7
Room air temperature, °F	60.5	60.1	59.7	58.5	58.9
Mean radiant temperature, °F	84.6	85.1	85.6	87.0	86.5
Operative temperature, °F	74.0	74.0	74.1	74.4	74.3
Effective radiant field, Btu/(h · sq ft)	17.7	18.3	19.0	20.9	20.2
AUST, °F	61.4	61.1	60.8	59.7	60.4
Parameter 1, Btu/(h · sq ft · °F)	4.6898	4.6852	4.6777	4.6643	4.6517
Parameter 3, dimensionless	0.0013	0.0013	0.0013	0.0013	0.0013

**TABLE 5.38** U-Tube Infrared Units at 500°F Surface Temperature and with Ideal Reflectors and Placement—Effect of Change in Room Height

Room height, ft	9.0	10.0	12.0	15.0	20.0
Panel area required, sq ft	51.7	54.3	59.7	66.9	82.2
ASHRAE design heat loss, Btu/h	64378.8	67932.0	75038.4	85698.0	103464.0
Actual design heat loss, Btu/h	51452.4	53930.0	59025.1	65864.5	79776.8
Percentage difference 1	-20.1	-20.6	-21.3	-23.1	-22.9
Conduction design heat loss 1, Btu/h	63479.7	66558.5	72916.3	81461.2	99150.0
Percentage difference 2	-1.4	-2.0	-2.8	-4.9	-4.2
Conduction design heat loss 2, Btu/h	63479.7	66558.5	72916.3	81461.2	99150.0
Percentage difference 3	-1.4	-2.0	-2.8	-4.9	-4.2
Actual heat input, Btu/h	62675.6	65719.0	72001.8	80460.6	97920.1
Percentage difference 4	-2.6	-3.3	-4.0	-6.1	-5.4
Percentage radiation	97.1	97.1	97.1	97.0	97.0
Percent ceiling covered by panels	5.7	6.0	6.6	7.4	9.1
Heat output per unit panel area, Btu/(h · sq ft)	1211.1	1209.5	1206.3	1202.2	1190.7
Floor temperature, °F	83.8	85.3	88.7	92.8	103.4
Room air temperature, °F	60.5	60.2	59.6	58.3	58.5
Mean radiant temperature, °F	84.6	85.0	85.7	87.2	87.0
Operative temperature, °F	74.0	74.0	74.2	74.4	74.4
Effective radiant field, Btu/(h · sq ft)	17.6	18.2	19.1	21.2	20.9
AUST, °F	61.4	61.1	60.8	59.7	60.3
Parameter 1, Btu/(h · sq ft · °F)	2.7554	2.7495	2.7387	2.7213	2.6965
Parameter 3, dimensionless	0.0021	0.0021	0.0021	0.0020	0.0020

**TABLE 5.39** U-Tube Infrared Units at 750°F with Ideal Reflectors and Placement in a 15-ft-High Room—Effect of Changes in Air Infiltration

Infiltration rate, ACH	1.0	2.0	3.0	4.0
Panel area required, sq ft	27.3	31.1	34.7	37.8
ASHRAE design heat loss, Btu/h	94446.0	111942.0	129438.0	146934.0
Actual design heat loss, Btu/h	70097.6	77439.9	83180.1	88205.4
Percentage difference 1	-25.8	-30.8	-35.7	-40.0
Conduction design heat loss 1, Btu/h	88345.6	100498.5	111983.4	121984.8
Percentage difference 2	-6.5	-10.2	-13.5	-17.0
Conduction design heat loss 2, Btu/h	88345.6	100498.5	111983.4	121984.8
Percentage difference 3	-6.5	-10.2	-13.5	-17.0
Actual heat input, Btu/h	87940.0	100038.2	111454.4	121393.1
Percentage difference 4	-6.9	-10.6	-13.9	-17.4
Percentage radiation	98.1	98.0	98.0	98.0
Percent ceiling covered by panels	3.0	3.5	3.9	4.2
Heat output per unit panel area, Btu/(h · sq ft)	3222.2	3217.3	3211.9	3207.3
Floor temperature, °F	94.4	99.6	104.8	109.4
Room air temperature, °F	56.4	52.8	49.3	46.2
Mean radiant temperature, °F	89.4	94.1	99.1	103.3
Operative temperature, °F	74.9	75.9	77.2	78.3
Effective radiant field, Btu/(h · sq ft)	24.2	30.4	36.8	42.4
AUST, °F	60.1	61.1	62.9	64.5
Parameter 1, Btu/(h · sq ft · °F)	4.6466	4.6152	4.5842	4.5577
Parameter 3, dimensionless	0.0013	0.0013	0.0013	0.0013

(2 MET), the clothing level was increased from 0.75 to 1.0 clo (medium clothing), and the relative air velocity was increased from 0.15 to 0.2 m/s. For the four tube temperatures (400°F, 500°F, 600°F, and 700°F) given in Table 5.36, values of some of the appropriate variables are as follows:

Floor temperature  $\approx 73^\circ\text{F}$

Room air temperature  $\approx 52^\circ\text{F}$  to  $53^\circ\text{F}$

OT  $\approx 63.5^\circ\text{F}$

MRT  $\approx 74^\circ\text{F}$

Percentage difference 3  $\approx -15$  percent

From Table 5.1 (last column, last rows) for medium *activity* and *medium* clothing the *room air temperature* and *MRT for comfort* are as follows:

$t_a$	MRT
53.1°F	71.6°F
50.7°F	75.2°F

It is seen that the results from Table 5.36 are in agreement with the comfort conditions in Table 5.1—room air temperature is approximately  $52^\circ\text{F}$ , and MRT is approximately  $74^\circ\text{F}$ . *Comfort is obtained at lower air temperatures for medium activity and*

**TABLE 5.40** U-Tube Infrared Units at 500°F with Ideal Reflectors and Placement in a 15-ft-High Room—Effect of Changes in Air Infiltration

Infiltration rate, ACH	1.0	2.0	3.0	4.0
Panel area required, sq ft	72.4	82.7	92.4	101.1
ASHRAE design heat loss, Btu/h	94446.0	111942.0	129438.0	146934.0
Actual design heat loss, Btu/h	69837.7	76983.3	82640.9	87271.4
Percentage difference 1	-26.1	-31.2	-36.2	-40.6
Conduction design heat loss 1, Btu/h	87933.6	100013.3	111253.0	121155.0
Percentage difference 2	-6.9	-10.7	-14.0	-17.5
Conduction design heat loss 2, Btu/h	87933.6	100013.3	111253.0	121155.0
Percentage difference 3	-6.9	-10.7	-14.0	-17.5
Actual heat input, Btu/h	86857.5	98784.8	109839.9	119565.8
Percentage difference 4	-8.0	-11.8	-15.1	-18.6
Percentage radiation	97.0	97.0	96.9	96.9
Percent ceiling covered by panels	8.0	9.2	10.3	11.2
Heat output per unit panel area, Btu/(h · sq ft)	1199.4	1193.8	1188.2	1183.0
Floor temperature, °F	95.6	101.1	106.5	111.3
Room air temperature, °F	56.2	52.5	49.0	45.8
Mean radiant temperature, °F	89.6	94.5	99.5	104.0
Operative temperature, °F	74.9	76.0	77.3	78.4
Effective radiant field, Btu/(h · sq ft)	24.5	30.9	37.4	43.2
AUST, °F	60.1	61.1	62.8	64.6
Parameter 1, Btu/(h · sq ft · °F)	2.7022	2.6674	2.6340	2.6040
Parameter 3, dimensionless	0.0020	0.0020	0.0020	0.0020

*medium clothing levels.* Also demonstrated in this calculation is the fact that at this level of activity and clothing, the ASHRAE design heat loss procedure *overpredicts the required heating by 15 percent.* For lesser activities and clothing (see Table 5.35) the overprediction was only 1 to 2 percent. This overprediction is a strong effect of the occupant's activity level, relative air velocity, and the quantity of clothing being worn.

In Table 5.37, the same configuration and conditions as in Table 5.33 are considered, except that in Table 5.37, *ideal reflectors and unit placement can reduce the installed heating capacity up to 5 percent.* The trend in the floor temperature has been changed in Table 5.37 because more area of heating surface has been installed and the walls intercept none of this heat directly. This causes the floor temperature to approach 100°F for the 20-ft-high room. In the actual situation, a floor temperature of 100°F will not be realized because people, materials, and equipment will intercept and redistribute some of the radiant energy from the heaters.

Another case Table 5.38, identical to Table 5.37, was run except that the heaters were kept at an average surface temperature of 500°F rather than 700°F. There are no significant changes here in the percent difference in the design heat loads.

There is a significant increase in the area of the heaters required because the surface temperature has been reduced by 250°F.

In Table 5.39, the results for U-tube infrared units at 750°F with ideal reflectors and placement in a 15-ft-high room are given for infiltration rates changing from 1 to 4 ACH. This shows that the percent difference between HLD and HLC can be up to 17 percent by use of ideal reflectors. However, at the same time, the floor temperature

becomes very high (up to 109°F in the theoretical undisturbed case), and the air temperature for comfort has been reduced to 46°F. These are rather extreme situations and most likely would not be encountered in a total-heat situation for infrared heaters.

In Table 5.40, the results for a U-tube infrared at 500°F rather than at 750°F (as done in Table 5.39) are given. This shows that the percent difference between HLD and HLC can be up to *19 percent at 4 ACH by use of ideal reflectors and placement*. Again, high floor temperatures are calculated for the theoretical situation. These high floor temperatures would not be realized in the actual situation because equipment, people, and materials would intercept some of the radiant energy from the heaters.

The results in the changes in percent difference between HLD and HLCG given in Tables 5.4 through 5.40 have been summarized in Table 48.\* The HLD is the ASHRAE standard heat loss calculation procedure, and HLC is the design heat loss for a space considering the actual conduction through the walls and the infiltration load based on the air change method. Table 48\* describes the basic cases from the previous tables, gives the variable being changed, its rate of change, and the percent difference in the two design heat loss calculations. Each of the types of heating systems are identified, such as: Forced-Air Heating—C1—C7, Panel Heating—P1—P16, Heated Floor—F1—F6, Infrared Modular Units—I1—I7, and Infrared U-Tubes—U1—U5.

This summary in Table 48\* shows that the ASHRAE design heat loss calculation can *oversize a system up to about 17 percent but the most common value is 4 to 7 percent oversizing for all of the variables and conditions considered here*. For some situations (C6 and C7), the ASHRAE standard procedure can undersize the system by up to 15 percent.

It was also shown in Table 5.36 that the metabolic rate, clothing level, and room air relative velocity can result in the ASHRAE design heat loss calculation procedure oversizing a system by up to 16 percent. However, the effects due to radiant temperature asymmetry and its interaction with comfort conditions at various metabolic rates, clothing levels, and air velocities are not completely specified. *There is evidence from these calculations that the ASHRAE design heat loss procedure will overpredict the radiant unit size by up to 16 percent for medium clothing levels.*

A listing of the computer program that was used to perform all of these calculations is given in Appendix C of ASHRAE RP-394. A list of the input variables is also given there.

### 5.1.6 Design Procedures

In the previous section, "Calculation of Design Heating Loads," it was shown in Table 48\* that the use of the ASHRAE design heating load procedure (HLD) (ASHRAE, 1985) would result typically in a *slightly* oversized heating system. Examination of Table 48\* shows for panel heating systems (P1—P16) that for variations in panel temperature, room size, and room height that this oversizing is about 3 to 6 percent for 0.5 ACH. However, for larger infiltration rates, this oversizing can be up to 15 percent for 4.0 ACH. In a similar way for the heated floor situation, the oversizing is about 7 percent at 0.5 ACH. Likewise, for modular and U-tube infrared (high- and medium-temperature, respectively) units with good reflectors and proper location such that no direct infrared radiation impinges on the walls, this oversizing is up to 5 percent at 0.5 ACH. If the infiltration rate is at 4 ACH, the oversizing can be up to 17 percent.

The conclusion of this investigation is that the air infiltration rate is the only variable in the design heat loss calculation that affects in a meaningful way the results for the sizing of radiant heating units. In Fig. 5.14, the percent reduction of standard

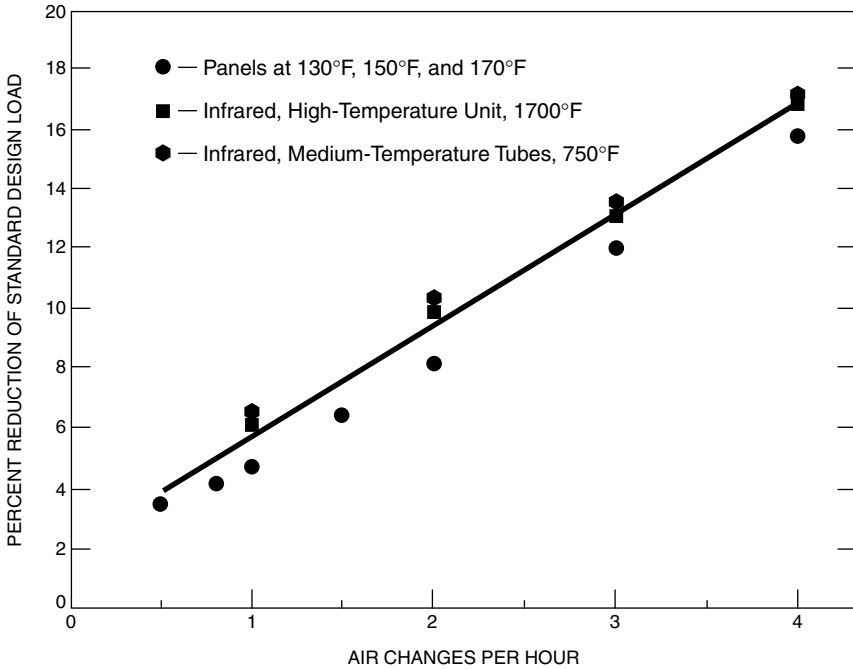


**FIGURE 5.14** Percent reduction of standard design load as a function of air infiltration rate.

design load is plotted against the air infiltration rate for panel heating, heated floor, and infrared modular and U-tube units. A single line has been drawn through the data to represent all four types of radiant heating systems, such that at 0.5 ACH, the reduction in heating unit size is 4 percent; at 1.0 ACH, it is 5.5 percent; at 1.5 ACH, it is 7.5 percent; at 2.0 ACH, it is 9.5 percent; at 3.0 ACH, it is 13 percent; and at 4.0 ACH, it is 16 percent. The variation shown in Fig. 28 is recommended as the only reduction factor to use for sizing radiant heating systems.

From these results, it is recommended for radiant heating systems that the ASHRAE design heat loss calculation procedure presented in Chap. 25 of the *Handbook of Fundamentals* (ASHRAE, 1985) be used with a reduction in the final value made according to the estimated infiltration rate as presented in Fig. 5.14. There is not any overwhelming evidence to reduce the design heat loss values for any of the other parameters in the radiant heating situation. The following procedures are suggested for designing radiant heating and cooling systems.

In Chap. 8 of the *1984 AHSRAE Systems Handbook* (ASHRAE, 1984) there is a section entitled "Panel Heat Systems Design," and this includes data and examples for metal ceiling panels, warm-water panels with embedded pipe (plaster ceiling and concrete ceiling), and electric ceiling panels. Appendix D of ASHRAE RP-394 contains a reproduction of Chap. 8 from the *1984 AHSRAE Systems Handbook*.

The current design steps and procedures given in Chap. 8 of the *1984 ASHRAE Systems Handbook* have been reviewed and compared with the original work in the literature, which is presented in the annotated bibliography of this Handbook. There were no serious problems or difficulties with the assumptions made in compiling the

curves and tables used in the procedures. In addition, various manufacturers have used these procedures for many years and have not reported any deficiencies in the design procedures.

The following are the recommended design steps for panel heating systems. The only change from what appears in Chap. 8 of the *1984 ASHRAE Systems Handbook* is that the design heat loss is reduced as a function of infiltration rate as given in Fig. 5.14. Some additional recommendations are also added.

### ***Panel Heating System Design Steps***

1. Calculate the hourly rate of heat loss for each room using procedures given in Chap. 25 of the *1985 ASHRAE Handbook of Fundamentals* (ASHRAE, 1985). Reduce this heat loss by the amount given in Fig. 5.14 for the specific estimated air infiltration rates.
2. Determine the available area for panels in each room.
3. Calculate the required unit panel output.
4. Determine the required panel surface temperature.
5. Select the means of heating the panel and the size and location of the heating elements.
6. Select insulation for the reverse side and edge of panel.
7. Determine panel heat loss and required input to the panel.
8. Determine any other temperatures that are required.
9. Design the systems for heating the panels according to conventional practice.

In the design steps, the effect of each assumption or choice on comfort should be considered carefully. *Always consider the manufacturers' recommendations for pre-engineered heating panel systems.* The following general rules should be followed:

1. Place panels near cold areas where the heat losses occur.
2. Do not use high-temperature ceiling panels in very low ceilings.
3. Keep floor temperatures at or below 85°F (29°C).

The computer procedure that was developed has been applied to several cases of radiant panel cooling. The calculation procedure was not able to calculate the actual outside wall or glass temperature for summer conditions because it did not consider solar effects on the wall or glass. The procedure was developed basically for heating design load calculations where solar effects would not be considered at the design time. The analysis for the procedure for sizing radiant panel cooling systems involved examination of the original ASHRAE research work and the procedure for panel cooling given in Chap. 8 of the *1984 ASHRAE Systems Handbook*. This appears to be sufficient for the cooling situation, because in that case the portion of sensible heat removed by radiation is significantly less because surface temperature differences are less in the cooling mode than in the heating mode. In addition, the infiltration load for summer design is expected to be significantly less because the inside-outside air temperature difference (stack effect) is much smaller, and the summer design wind velocity (typically 7.5 mph) is typically half of the winter design wind velocity (15 mph). Also, the radiant cooling system is not able to absorb the latent load so that the ventilation air brought to the cooling space absorbs this latent load and, at the same time, absorbs some of the sensible load. For these reasons, the correction to the design load given in Fig. 5.14 *does not apply for the design cooling load*. It is recommended that

the ASHRAE design cooling load procedures (for commercial buildings and residential buildings) presented in Chap. 26 of the *1985 ASHRAE Handbook of Fundamentals* (ASHRAE, 1985) be used directly. There are no engineering and/or comfort reasons to expect a reduction in the design cooling load calculations. In addition, there has not been any research located since the ASHRAE work in the 1950s that would invalidate the current design procedures.

The procedures given in Chap. 8 of the *1984 ASHRAE Systems Handbook* (ASHRAE, 1984) were checked and verified with the references and original work done by ASHRAE. Also, several manufacturers have been using this procedure for many years and have not reported any deficiencies in the procedure. The procedure is as follows.

### ***Panel Cooling System Design***

1. Determine the room design dry-bulb temperature, relative humidity, and dew-point.
2. Calculate room sensible and latent heat gains using the ASHRAE procedure given in Chap. 26 in the *1985 ASHRAE Handbook of Fundamentals* (ASHRAE, 1985).
3. Select mean water temperature for cooling.
4. Establish minimum-supply air quality.
5. Calculate the latent cooling available from the air.
6. Calculate the sensible cooling available from the air.
7. Determine panel cooling load.
8. Determine required panel area.

Now, design for the heating situation.

9. Calculate room heat loss using the procedures given in Chap. 25 of the *1985 ASHRAE Handbook of Fundamentals* (ASHRAE, 1985). Reduce this heat loss by the amount given in Fig. 5.14 for the specific estimated air infiltration rate.
10. Select mean water temperature for heating.
11. Determine panel area for heating.
12. Determine water flow rate and pressure drop.
13. Design the panel arrangement.
14. Always consider the manufacturers' recommendations for placement, sizing, and insulation of preengineered panel heating and cooling systems.

In the evaluation of this design procedure, it is seen that the location of the air diffusers relative to the panel sections does not enter into the design procedure. It would be expected that if the air is diffused in close proximity to the ceiling panels, the cooling and heating performance would be altered slightly. For typical design situations, this should not alter the design procedure. It should also be pointed out that the lighting load for the cooling case should be carefully evaluated because it would be a major contributor to the cooling load. The design procedure does not account for different types of lighting fixtures, and these loads should be incorporated into the design heat gain calculation. Also, it should be emphasized that the latent heat gain must be absorbed by an independent source. The source specified in the design procedure is the ventilation air, which is dehumidified separately. It would also be possi-

ble to operate various types of dehumidifiers within the space to absorb this latent load or to use chemical dehumidification.

**Heated Floor Systems.** A design procedure for heated floors (concrete floor panels for slab-on-grade, concrete floor panels for intermediate slabs, and electric floor slab heating) is presented in Chap. 8 of the *1984 ASHRAE Systems Handbook* (ASHRAE, 1984), which is included in Appendix D of ASHRAE RP-394.

There were some papers obtained in the literature search, which discussed the physical parameters (slab thickness, tube spacing, and lower insulation) in the design process and their effect on the upward heat delivered by the system. The actual design process for radiant systems was not part of this project. Here, we are only interested in the design heat loss calculation and the placement of the *heat surfaces*.

Grammling (1985) in a 1985 ASHRAE paper pointed out that in the German standard DIN 4725, methods were developed for testing the thermal performance of hydronic floor heating systems. In addition, numerous measurements have been made for these types of heating systems. Most of the systems have been tested with the so-called plate apparatus. The results of the tests show that measured values of performance differ significantly from figures published in the literature or company catalogs. *It is clear from these results that exact performance measurements under controlled thermal conditions are necessary for designing and laying out unique floor heating systems.*

Hogan (1979) in a M.S. thesis reviewed and evaluated the ASHRAE design recommendations given in Chap. 8 of the *1984 ASHRAE System Handbook* (ASHRAE, 1984). This was done using a steady-state and a transient numerical model of the heated floor slab. The ASHRAE panel heating model does not represent the panel heat loss mechanisms correctly, but the design recommendations are adequate and slightly conservative for designing both bare and covered radiant floor heating panels with no infiltration and an AUST equal to the room air temperature. These design recommendations are conservative because both the downward and edgewise heat loss and panel thermal resistance are overestimated. These conclusions were also presented in an ASHRAE paper by Hogan and Blackwell (1986).

Shamsundar, Lienhard, and Tezduyar (1985), in an unpublished private report, presented some similar conclusions. They have shown that the ASHRAE procedure is erroneous (using numerical simulation) and that it can be modified to make it more correct. Some of the error that they note is on the conservative side, and some of it is underestimating the requirements so that the errors appear to cancel each other for most conditions. This is most likely why it has not been detected in existing designs. However, because this is an unpublished report, it is not a valid source of information for changing the current design. They indicate that the ASHRAE procedure can also be used for systems with plastic pipe by using simple multipliers for various pipe diameters.

**High- and Medium-Temperature Infrared Systems.** The design guidelines provided by manufacturers of infrared heating systems (14 were made available) have been reviewed. They cover gas and electric as well as various intensity levels (porous refractory, radiant tube, quartz tube, and metal sheath electric). The design guidelines for all of these units are very similar, with minor variations between manufacturers. These begin with a heating survey taking note of building materials, design temperatures, usage schedules, combustible or potentially toxic vapors in the building, and restrictions for moisture level requirements. A standard ASHRAE heat loss calculation is suggested along with a reduction recommendation ranging from 0 to 25 percent, with the usual value being about 15 percent. Various reasons are given

for this reduction in design heat load: unvented gas-fired units are more efficient; there is less heat loss due to a reduction in air temperature stratification in the building; and a lower air temperature is required for comfort when radiant energy is used for heating.

The size of the heaters are then selected from the manufacturers' published data. These units are usually mounted along the perimeter where the high heat losses occur. They have specific types of reflectors and are mounted at various angles so as to prevent radiating the wall. Specific details are given concerning mounting height, lateral spacing of heaters, and distance from combustible materials.

At some point in the design of the unvented gas units, consideration of minimum dilution air to control the CO<sub>2</sub> and condensation possibilities must be taken into account. Providing the necessary makeup air and exhaust for these systems is an extremely important consideration.

A design procedure follows for gas and electric infrared heaters. It must be stated, however, that the designer or engineer *must follow the manufacturers' design and layout suggestions in order to be protected by their guarantee*. The following basic steps are suggested as a design procedure.

1. Determine if the building and/or operations are suitable for infrared heaters. Do not install units where combustible vapors are presented.
2. Calculate building transmission losses using ASHRAE design procedures in Chap. 25 of the *1985 ASHRAE Handbook of Fundamentals* (ASHRAE, 1985).
3. Compute the air infiltration and any forced-ventilation loads using procedures given in Chap. 22 of the *1985 ASHRAE Handbook of Fundamentals*.
4. Calculate total heat loss by adding together the transmission losses and infiltration and ventilation losses. Reduce this number based on the information given in Fig. 5.14 and the estimated infiltration air changed per hour.
5. Select heater size or sizes and type of control. This should take into account the mounting height, reflector style, clearance to combustible materials, and general layout of the building. Take into account the manufacturers' recommendations and requirements. Select the type of control suitable for the heaters and the specific application.
6. Determine the number of heaters by dividing the total load from item 4 by the heater size selected in item 5.
7. Determine heater placement using the manufacturers' suggestions regarding mounting height, distance from combustibles, reflector design (they should be designed and placed so that no direct infrared radiation falls on the walls and that the floor is covered with direct infrared radiant energy in proportion to the building heat loss), and building dimensions. Perimeter-mounted heaters are usually angled toward the interior of the building (at about 30°), and heaters in the interior of the building are usually mounted horizontally with appropriate reflectors. They should avoid interior obstructions such as crane sprinkler systems, storage racks, forklift travel, and light fixtures.
8. Determine the method of mounting heaters using manufacturers' recommendations. Use manufacturers' recommendations concerning mounting devices, brackets, flexible gas lines, and flexible electrical conduit. Avoid having heaters too close to structural members. Always conform to local codes.
9. Select and locate thermostats to control zone loads and provide uniform heating. They should be mounted according to the manufacturers' recommendations. Generally, they should be about 5 ft from the floor, out of direct view of the heaters, and not in direct contact with cold outside walls.

10. Determine minimum air needed to dilute CO<sub>2</sub> in unvented units to a safe level. In unvented gas-fired systems, check for condensation possibilities. Check design values of inside surfaces and roof with the dewpoint temperature of the inside air.
11. Comply with all of the manufacturers' installation and operation instructions.

**Other Design Procedures.** A few other suggestions were found in the literature for modification of the design heat load for a radiant heating system when the design heat load is calculated for a forced-air system. McIntyre (1980, 1984) used a theoretical computer program and a simplified method in the *CIBS Guide* to compare the difference in design heating load for radiant and warm-air systems. In addition, he also looked at estimated energy requirements for the various types of systems. He came to the following conclusions:

1. The simplified *CIBS Guide* method and the computer model show very good agreement.
2. Theoretical studies showed little difference (5 percent) in the power required to maintain comfortable conditions in residential size and types of rooms with either radiant or warm-air heating.
3. Radiant heating was more economical (5 to 20 percent) than forced-air heating systems in large spaces with high infiltration rates.

In another paper by Harrison (1975), the differences between design heating loads for convective and radiant systems are discussed. These contain multiplying factors to be applied to transmission losses and air change losses. These are all based on theoretical calculations and show the same trend of a decrease in the design heat loss as infiltration increases and an increase in the design heat loss as more radiant energy falls on the walls, floors, or ceiling. For about the greatest change illustrated, a combined modifier of 0.82 was given. This is comparable with the value of a 17 percent reduction given in Fig. 5.14.

In another unpublished discussion of this problem, the author calculates a percent reduction in the design heat loss of about 12 percent at 1 ACH. This is somewhat higher than what others have calculated, however, this model is considerably different than what others propose.

**System Dynamics.** System dynamics for heating and cooling enter into the calculations only when actual operation is considered and not when design heating loads are being calculated. The dynamics of the systems are important during transient load situations in order to estimate comfort conditions and energy requirements. This is discussed in several references in the annotated bibliography. The heated concrete floor and embedded heaters in plaster ceilings were found to present the slowest response times and require more sophisticated control systems to account for temperature lag. The hydronic metal and nonembedded electric ceiling panels and high-temperature (infrared) systems do not appear to present any dynamic problems if properly designed and controlled.

## **5.2 RESEARCH CONDUCTED IN RESPONSE TO IDENTIFIED RESEARCH NEEDS**

---

The Howell report identified areas further than the ASHRAE Technical Committees have addressed by several research projects. ASHRAE Research Project 927, *Simpli-*

*fied Methodology to Factor Room Air Movement and the Impact on Thermal Comfort into Design of Radiative, Convective, and Hybrid Heating and Cooling Systems*, provides a methodology leading to development of convection coefficients and stratification. Extensive information on surface emissivities is presented in *Impacts of Surface Characteristics on Radiant Panel Output*, which is the next research report included in this chapter. Radiant temperature asymmetry is one of the many thermal comfort outputs of the BCAP program from *Simplified Method to Factor Mean Radiant Temperature (MRT) into Building and HVAC System Design*. Radiant system dynamics are a feature of the Actual Building Occupant Verification Efficiency (ABOVE®) program on the demo CD provided in the inside back cover pocket. High-temperature radiant heater design methodology needs are addressed in ASHRAE Research Project 1037, *Development of a Simplified Methodology to Incorporate Radiant Heaters Over 300°F into Thermal Comfort Calculations*. Finally, ASHRAE Research Project 1036, *Development of Simplified Methodology to Factor Heat Transfer of Common Radiant Conduit into the Design of Radiant and Heating Cooling Systems*, will provide design information about panel operating performance related to radiant panel element design and construction. Though there are many areas that are fertile for research, the major needs identified in the comprehensive Howell report have been addressed.

### 5.2.1 Impact of Surface Characteristics on Radiant Panel Output

The impact of surface characteristics on radiant heat panels had been a topic of mystery in the field, although well understood in the lab. This report validates and explains in detail the factors that are important, as well as those that are not significant to radiant panel radiant and convective heat transfer. The sections presented are taken directly from the final report with the permission of ASHRAE.

**Executive Summary.** RP-876 was designed to determine “the impact of surface characteristics on radiant panel output.” In some respects the results were predictable. The characteristically high emissivities of smooth building materials for the most part obviated the need to measure emittance of textured building materials. In most cases the maximum theoretical change in emittance was known a priori to be no more than 5 percent. The question of surface diffuseness was bounded in the same way. Textured surfaces are predictably more diffuse than smooth surfaces, and all common building materials, whether textured or not, show the characteristic behavior of diffuse emitters. Although there were some interesting textured surface results, such as the effect of finishing techniques on the diffuseness of concrete and the relationship between effective surface temperature and apparent carpet diffuseness, in general the impact of surface texture on radiation properties, though measurable, was not significant in the engineering sense of the word.

Likewise, convective correlation was more or less impervious to surface texture. That is, surface texture did not measurably affect the rate of convective heat transfer from a radiant panel. Under the same environmental conditions and for the same surface temperature, a carpeted panel convected heat at the same rate as a painted panel—the convective heat transfer coefficient (or Nusselt number) was nearly the same for both.

The immediate conclusion of the research is that radiant panel surface texture does not significantly affect either surface radiative output or surface convective output. At a given temperature in the same environment, the textured surface will radiate and convect heat to the space at the same rate as the untextured surface. However, surface coverings can significantly affect both panel capacity and efficiency and, therefore,

must be considered in the design of the radiant system. A radiantly heated floor with carpet requires additional back insulation to operate at the same efficiency as an uncarpeted radiant floor. Additionally, a carpeted floor must operate at a higher element or water temperature in order to attain the same total panel output as its uncarpeted counterpart. To avoid a reduction in panel capacity, either the heating element (or water) must be able to reach the higher temperature, or the power density (tube or wire density) of the panel must be increased. Although surface coverings do not affect surface radiative or convective output, they do affect system operation and therefore must be accounted for in a comprehensive design strategy.

The second conclusion of the research, then, is that evaluation of radiant panel efficiency and application of experimental results (such as convection correlations) must occur in the context of the surface heat balance—the first law of thermodynamics applied to the surface of the radiant panel. The surface heat balance is often described using the analogy of a resistance network. A typical network for a hydronic panel is shown in Fig. 5.15. The total power input into the system is the sum of  $Q_{out}$  and  $Q_{back}$ , the rate of conduction heat transfer out the front and back of the radiant panel, respectively.  $Q_{out}$  is transferred from the heating element to the panel surface through conduction and then to the conditioned space through radiation and

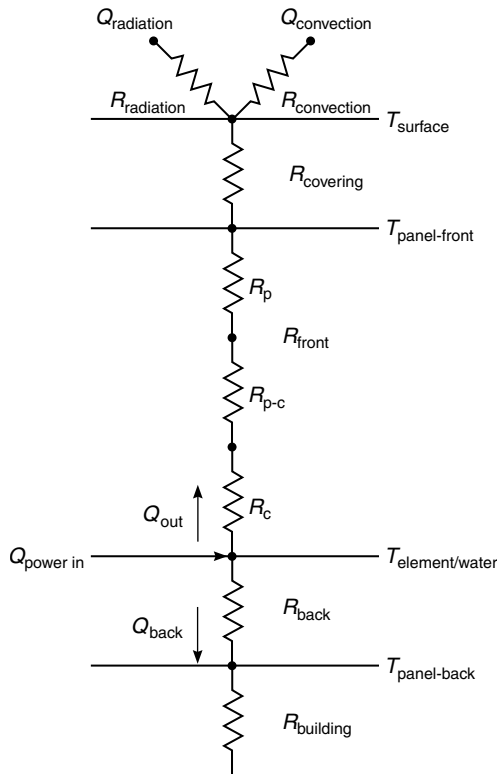


**FIGURE 5.15** Thermal resistance network for a radiant panel system.

convection.  $Q_{\text{back}}$  is transferred from the heating element to the back of the heating panel as a backloss. The *insulation value*, or *thermal resistance*, to the heat flow in both directions (out the front and back of the panel) is represented by the series of resistors,  $R$ , where:

$R_{\text{radiation}}$	Thermal resistance to radiation heat transfer, often expressed as a linearized radiation heat transfer coefficient.
$R_{\text{convection}}$	Thermal resistance to convection heat transfer, often expressed as a <i>film</i> , or convective heat transfer coefficient.
$R_{\text{covering}}$	Thermal resistance of the panel covering (carpet, vinyl, etc.)
$R_{\text{front}}$	Total thermal resistance between the heating or cooling element and the front of the panel, including: $R_p$ = thermal resistance of the panel $R_{p-c}$ = thermal resistance between tube (electric cable) and panel per unit spacing $R_c$ = thermal resistance of tube wall per unit tube spacing in a hydronic system
$R_{\text{back}}$	Total thermal resistance between the heating or cooling element and the back of the panel.
$R_{\text{building}}$	Total thermal resistance of the building element (floor, ceiling, etc.) behind the panel.

The second conclusion leads immediately to a final conclusion concerning radiant system design methods in general and SPC-138P (*Method of Test for Rating Hydronic Radiant Ceiling*) in particular. The research showed that for a rated power input (or water flow rate for hydronic panels) the two critical panel design parameters are  $R_{\text{front}}$  and  $R_{\text{back}}$ , as shown in Fig. 5.15. These two parameters should be explicitly required in radiant panel rating standards and clearly incorporated in radiant system design procedures. A method of test that requires explicit calculation of these two thermal resistances not only allows for a fair comparison of different panel designs, but also provides the necessary information to correctly size radiant systems under virtually any set of environmental conditions.

Tables 5.41 through 5.44 represent a summary of the experimental observations made over the course of three ASHRAE research projects (RP-529, RP-664, RP-876) in the experimental room at the University of Illinois. The tables assume that a radiant heating system is operating at a constant power input at steady-state conditions in a space with all other surfaces having a uniform and equal surface temperature. The first column of the tables shows changes to the radiant system itself or to the environment. The remaining columns show the expected effect on the various heat fluxes shown in Fig. 5.15 and estimate the effect on overall system comfort. The direction of the arrows indicates whether the change in col. 1 is expected to reduce or increase the rate of heat transfer. The number of arrows gives an indication of the relative significance of this effect. The notes referenced in the last column explain the cause-and-effect relationship between the change in the system or environment and the change in the system comfort.

It must be stressed that the results shown in Tables 5.41 through 5.44 represent the change in only one parameter under the specified condition. Quantitative results must assess all interactions and competing processes to determine the overall effect on system performance. Tables 5.41 through 5.44 provide a quick overview of the effect of most design parameters on radiant system performance. Once alerted to the potential impact of design changes on radiant system operation, the system com-

**TABLE 5.41** Impact of Design Changes on Radiantly Heated Floor System

Change radiant panel or environment	$Q_{back}$	$Q_{out}$	% $Q_{out}$ to convection	% $Q_{out}$ to radiation	Change in thermal comfort	Notes*
Add carpet	↑↑↑	↓↓↓	—	—	↓↓↓	1
Add ceramic tile	↑↑	↓↓	—	—	↓↓	1
Add rough (brick) tile	↑↑	↓↓	—	—	↓↓	1
Add vinyl	↑	↓	—	—	↓	1
Insulate back of panel	↓↓↓	↑↑↑	—	—	↑↑↑	1
Insulate other side of floor	↓↓↓	↑↑↑	—	—	↑↑↑	1
Improve element surface contact	↓↓	↑↑	—	—	↑↑	2
Reduce element base floor contact	↓↓	↑↑	—	—	↑↑	2
Change vinyls	—	—	—	—	—	3
Change tiles	—	—	—	—	—	3
Change carpets	—	—	—	—	—	3
Paint the floor	—	—	—	—	—	3
Add a cold draft to carpeted room	↓	↑	↑↑↑	↓↓↓	↓↓↓	5
Add a cold draft to vinyl room	↓	↑	↑↑↑	↓↓↓	↓↓↓	5
Add a cold draft to tiled room	↓	↑	↑↑↑	↓↓↓	↓↓↓	5
Add a cold window	↓	↑	↑↑	↓↓	↓↓	6
Lower the wall temperature	↓	↑	↑	↓	↓↓	6
Lower the air temperature	↓	↑	↑↑	↓↓	↓↓	7

\* Notes are found in Table 5.44.

fort can be recalculated on the basis of the new conditions. It should also be stressed that incorporating the change as a parameter in the design procedure can compensate for virtually all of the detrimental effects on total panel output or thermal comfort. Tables 5.41 through 5.44 show the effect of modifying an existing system or neglecting a design parameter, but do not imply that the changes could not be compensated for by proper consideration during the design process.

Tables 5.45 and 5.46 illustrate that a number of factors determine the performance of a radiant system. It is difficult (and dangerous!) to isolate one particular factor and attempt to determine its impact on overall panel performance without considering the entire panel heat balance. However, based on the research results, it is possible to propose some guidelines for radiant panel and system design.

The research project examined a number of factors related to surface characteristics and their impact on radiant panel output. Some of the key findings are:

1. The various materials tested (vinyl, carpet, plastic, paint) had uniformly high surface emittance of 0.9 and greater. The significance of this is that these surfaces are all equivalent radiators.

**TABLE 5.42** Impact of Design Changes on Radiantly Heated Ceiling System

Change radiant panel or environment	$Q_{\text{back}}$	$Q_{\text{out}}$	% $Q_{\text{out}}$ to convection	% $Q_{\text{out}}$ to radiation	Change in thermal comfort	Notes*
Add texture finish	↑	↓	—	—	↓	4
Texture finish instead of smooth	—	—	—	—	—	4
Add wallpaper	—	—	—	—	—	3
Insulate back of panel	↓↓↓	↑↑↑	—	—	↑↑↑	1
Insulate other side of ceiling	↓↓↓	↑↑↑	—	—	↑↑↑	1
Improve element-surface contact	↓↓	↑↑	—	—	↑↑	2
Reduce element-base contact	↓↓	↑↑	—	—	↑↑	2
Paint the ceiling	—	—	—	—	—	3
Add a cold draft to room	↓	↑	↓	↑	↓	5
Add a cold window	↓	↑	↓	↑	↓	6
Lower the wall temperature	↓	↑	↓	↑	↓	6
Lower the air temperature	↓	↑	↑	↓	↓	7

\* Notes are found in Table 5.44.

2. These same materials can be considered to be diffuse emitters. The surfaces will radiate almost equally well in all directions from the surface normal.
3. When backlosses were eliminated, the total panel output, for radiant panels using different surfaces given the same power input and operating conditions, was equal. For high thermal resistance surfaces such as carpet there was, however, up to a 35°C temperature difference from the back to the surface.
4. The natural convection output for a ceiling panel is approximately 10 percent of the total panel output. This research found that for a floor or wall panel, the natural convection output was approximately 30 percent of total panel output. It should be noted that other research has shown that for a floor or wall panel, the natural convection output for a floor or wall panel can be as high as 50 percent.
5. Surface characteristics have a negligible effect on natural- and low-speed forced convection. For air speeds of 1 m/s and less, the convective output for a radiant panel does not depend on the surface characteristics.

Finally, the research results corroborated existing guidelines for panel design and provide some direction for future research.

1. The surface covering of the radiant panel should have a high emittance. This is typically not a problem, because most nonmetals have a high emittance. When an aluminum surface is used, it should always be painted. A painted aluminum surface will have the radiative properties of the paint.

**TABLE 5.43** Impact of Design Changes on Radiantly Heated Wall System

Change radiant panel or environment	$Q_{\text{back}}$	$Q_{\text{out}}$	% $Q_{\text{out}}$ to convection	% $Q_{\text{out}}$ to radiation	Change in thermal comfort	Notes*
Add texture finish	↑	↓	—	—	↓	4
Texture finish instead of smooth	—	—	—	—	—	4
Add wallpaper	—	—	—	—	—	3
Insulate back of panel	↓↓↓	↑↑↑	—	—	↑↑↑	1
Insulate other side of wall	↓↓↓	↑↑↑	—	—	↑↑↑	1
Improve element surface contact	↓↓	↑↑	—	—	↑↑	2
Reduce element base contact	↓↓	↑↑	—	—	↑↑	2
Paint the wall	—	—	—	—	—	3
Add a cold draft to room	↓	↑	↑↑	↓↓	↓↓	5
Add a cold window	↓	↑	↑	↓	↓	6
Lower the wall temperature	↓	↑	↑	↓	↓	6
Lower the air temperature	↓	↑	↑	↓	↓	7

\* Notes are found in Table 5.44.

2. To increase the surface radiative output of the panel, minimize the convection from the panel by designing for reduced air movement in the vicinity of the panel.
3. The overall thermal resistance of the panel should be minimized. Coverings should be chosen that have a small conductive resistance.
4. Insulating the back of the radiant system should minimize panel backlosses.
5. When increased surface resistance (carpet) is offset by a commensurate increase in backloss resistance (insulation), higher element temperatures will result.

The most promising research area appears to be in the development and application of natural- and forced-convection correlation, which should be verified for enclosures with various types of radiant heating and cooling systems. Finally, guidelines that facilitate selection of appropriate convection correlation should be developed for various radiant systems, room surface temperature, and room airflow configurations.

**Background.** In recent years, low-temperature radiant systems have been the focus of numerous research projects. New materials, new heating elements, and innovative system designs have spurred a renaissance of this old technology. Low-temperature radiant systems are built into or attached to a building element such as a ceiling, wall, or floor. Electrical resistance heating elements or hot or cold water circulated through pipes or tubes produces a net heating or cooling effect on the room.

Low-temperature radiant designs fall broadly into two categories, depending on the power density of the system. The floor system shown in Fig. 5.16 is an example of

**TABLE 5.44** Notes to Tables 5.41 Through 5.43

Number	Notes
1	For a constant power input, the thermal resistances shown in Fig. 1.1 simply determine which way the heat will flow—out the front or back of the panel. Adding a layer of material either to the front or back of the panel adds a thermal resistance to the system. Adding a layer to the front of the panel (e.g., carpet) increases the resistance to heat flow toward the front: $Q_{out}$ is reduced and $Q_{back}$ is increased. The result is a lower surface temperature and reduced panel output. Conversely adding a layer of material to the back increases the resistance to heat flow out the back of the panel: $Q_{out}$ is increased and $Q_{back}$ is decreased. The result is a higher surface temperature and increased occupant comfort.
2	Changing the contact between layers changes the resistance in the system. Good contact lowers the resistance; poor contact increases the resistance. Changing the resistance in this way has the same effect as described in note 1.
3	Painting a surface or adding wallpaper results in an insignificant change to the surface resistance. All standard paints and wallpapers are equivalent radiators and convectors, so changing a radiant surface in this way will not affect panel output. Likewise, tiles and carpets can be considered equivalent radiators and convectors for engineering calculations. If changing materials does not change the surface resistance, there will be no effect on system performance. It should be noted that exchanging old carpet for new almost always results in a significant increase in surface resistance.
4	Adding a textured finish to a panel will slightly increase the surface resistance and result in a slight decrease in panel output. For thin textured layers, the change in output will not be noticeable. Replacing a smooth layer with a textured layer will result in no change in panel output.
5	A cold draft primarily affects floor and wall system performance by changing the radiative convective split at the surface without changing the total panel output. An increase in surface convection will lower the surface temperature and result in a decrease in radiation (and, in this case, system performance). Because cold drafts typically move along the floor, the effect on floor panels is expected to be significantly higher than on wall panels. Cold drafts affect ceiling system performance through a slightly different mechanism. The draft reduces the floor temperature, resulting in increased radiation to the floor. As a result, however, the radiant panel moves to a new equilibrium point at a lower surface temperature.
6	Cold windows and walls have two effects on radiant system performance. First, they affect the buoyantly driven flow in the space. This may change the rate of convection heat transfer from the panel. Second, they provide a “sink” for radiant energy from the heated panel (as described in note 5 for ceilings). This results in a new equilibrium point (at a lower temperature) for the radiant panel.
7	Lowering the room air temperature increases the rate of convective heat transfer from both the heated panel and unheated surfaces. This adversely affects the radiative convective split as described in note 5.

a radiant system with a relatively low power density. Typically, systems of this type have power outputs on the order of 15 to 20 W/ft<sup>2</sup>. Fast-acting radiant panels with graphite electrical resistance heating elements are an example of a relatively high-power-density panel. The power output of these units is usually on the order of 50 W/ft<sup>2</sup>. Fast-acting radiant panels usually cover a small percentage of the surface (approximately 10 percent of the surface for a typical room) (Watson, 1995), whereas systems with lower power densities typically cover the entire floor or ceiling of a room.

**TABLE 5.45** Radiant Panel Design

Objective	Approach	Recommended procedure
1. Increase panel capacity.	Reduce panel thermal resistance between heating-cooling element and radiating surface.	<ul style="list-style-type: none"> <li>• Eliminate contact resistance between panel components by welding or using thermally conductive adhesive.</li> <li>• Consider alternative high-conductivity materials such as aluminum-filled epoxies and plasters.</li> </ul>
2. Reduce panel backlosses.	Increase panel thermal resistance between heating-cooling element and the "outside" environment.	<ul style="list-style-type: none"> <li>• Add insulation to back of panel. (Recalculate element temperature for new panel construction.)</li> </ul>
3. Increase panel efficiency.	Combine recommendations for nos. 1 and 2.	<ul style="list-style-type: none"> <li>• If published emittance &gt; 0.8, panel is already operating at near-optimal conditions. (Most nonmetal building materials are near 0.9.)</li> </ul>
4. Increase panel radiative output.	Check published emittance of surface material in IR region (>1 $\mu\text{m}$ ).	<ul style="list-style-type: none"> <li>• Paint or otherwise coat low-emittance materials (such as bare aluminum).</li> </ul>

**TABLE 5.46** Radiant System Troubleshooting

Problem	Probable cause	Recommended procedure
<b>1.</b> Radiant surface temperature too low or high.	Front and/or back thermal resistance of panel is higher or lower than design values, or “outside” environment temperature is lower or higher than design value.	<ul style="list-style-type: none"> <li>• Ensure proper installation of “back” insulation.</li> <li>• Compare actual “outside” temperature with design value.</li> <li>• Include all surface coverings in estimation of panel thermal resistance.</li> <li>• Select “forced-convection” correlations for ventilated and drafty rooms (including rooms with ceiling fans).</li> <li>• Select “natural convection” correlations for rooms that are not mechanically ventilated.</li> <li>• Check actual room air temperature against design conditions.</li> <li>• If the room has one “cold (or hot) wall” and the radiant panel is not centrally located in the room, or the aspect ratio of the room is not close to 1, calculate the rate of radiation heat transfer using a more detailed radiant exchange model.</li> <li>• For centrally located panels in rooms with aspect ratios near 1, simply recalculate the AUST.</li> <li>• Adjust operating temperature of radiant panel. Calculate panel temperature required to ensure thermal comfort at given location. Use detailed radiation exchange program.</li> <li>• Adjust location of radiant panel to improve the occupant’s view of the panel.</li> <li>• Install “radiation shields” between occupant and hot or cold surfaces. These include shades, curtains, and wall hangings. For maximum effect, use “low-emittance” material.</li> </ul>
	Rate of convection heat transfer is higher or lower than design conditions due to “off-design” heat transfer coefficient or room air temperature.	
	Rate of radiation heat transfer is higher or lower than design conditions due to “off-design” AUST or surface properties.	
<b>2.</b> Radiant surface temperature at design value, but occupants are not comfortable.	Occupants are located near cold or hot surfaces with poor “view” of radiant panel.	
<b>3.</b> Radiant surface temperature at design value, but system consuming more energy than predicted.	Same as no. 1, with the exception that this system has adequate capacity. The system in no. 1 is capacity limited.	

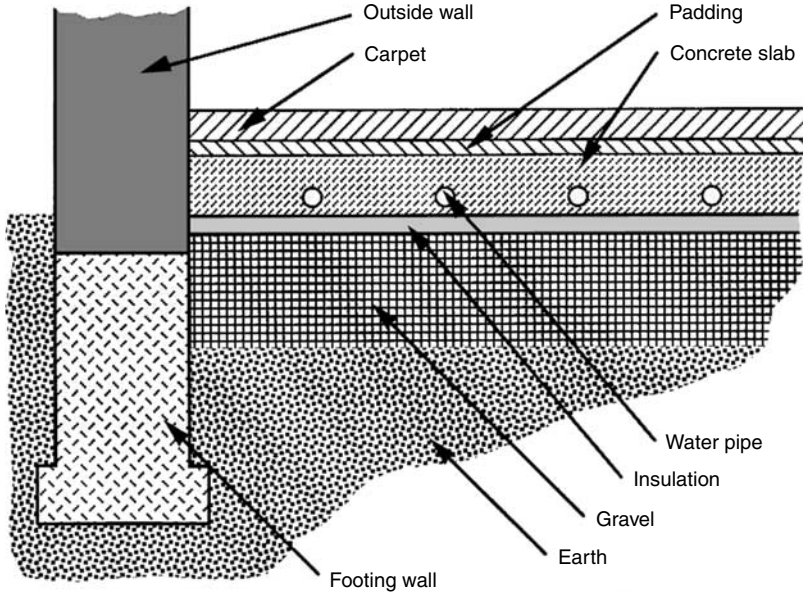


**FIGURE 5.16** Example of a radiant floor system. (Source: Strand, 1995.)

Because low-temperature radiant systems are in close contact with the building occupants, there are limits to their operating temperatures. Whereas high-temperature systems can have relatively small heating elements that exceed  $2500^{\circ}\text{C}$ , low-temperature systems have surface temperatures well below  $100^{\circ}\text{C}$ , with low-temperature floors operating below  $30^{\circ}\text{C}$ . The focus of this project is on these low-temperature radiant systems (Fig. 5.17).

**Surface Characteristics.** Many problems in heat transfer have an associated length scale. For radiative heat transfer, the important length scale in terms of properties is the wavelength of thermal radiation. Any surface over 0 K will radiate over the continuum of all wavelengths. However, the wavelength region important for low-temperature radiative heat transfer in buildings is typically from  $0.1\ \mu\text{m}$  to  $1\ \text{mm}$ .

Like wavelengths, surface characteristics also have an associated length scale. Striking a piece of metal with a hammer changes its surface characteristic by putting a dent in the metal. The length scale that is associated with this surface characteristic is on the order of the diameter of the hammerhead. Heat-treating the same piece of metal changes its surface characteristics by diffusing carbon into dislocations in its crystalline structure. The length scale associated with this surface characteristic is on the order of the lattice spacing of the metal's microstructure.

With this in mind, two definitions that clarify *surface characteristics* as they apply to thermal radiation are given. *Microsurface characteristics* refer to the surface characteristics that are on the order of the wavelength of thermal radiation. *Macrosurface characteristics* refer to the surface characteristics that are much greater in scale than the relevant wavelength of thermal radiation.

The project work statement uses the term *impact of surface characteristics* to include the effect of both micro- and macrosurface characteristics on radiative

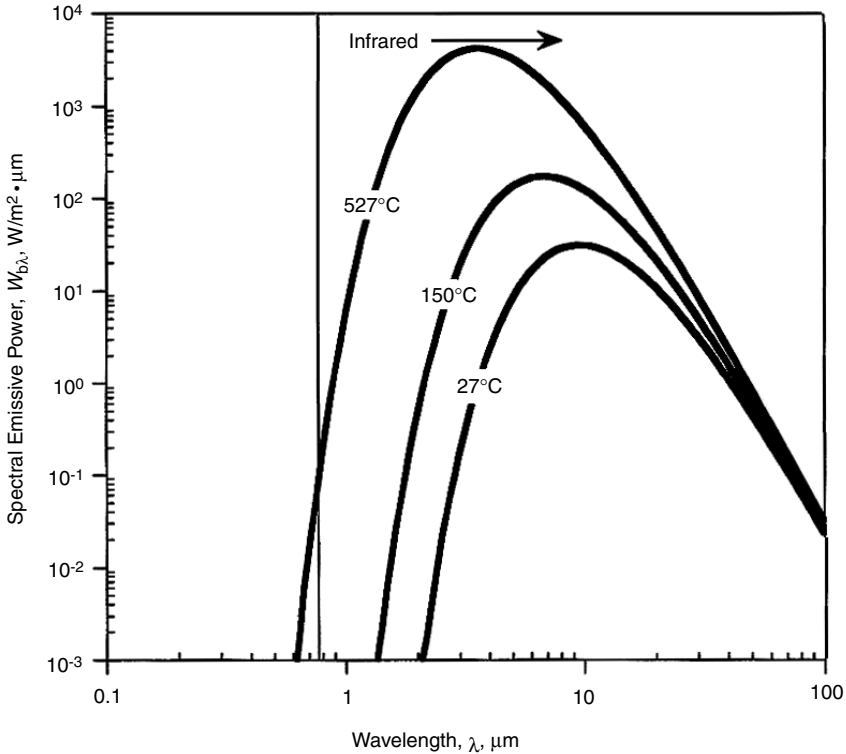


**FIGURE 5.17** Spectral blackbody emissive power.

properties. In this report, we will distinguish between the length scales associated with surface characteristics by referring to microsurface and macrosurface characteristics. Microsurface characteristics include, but are not limited to, material properties. For example, the microsurface characteristics of aluminum include both the chemical composition and crystalline structure of the metal as well as the surface polish of the surface. Macrosurface characteristics include the texture and roughness of the surface. The roughness of a surface for a metal can be a microcharacteristic in terms of the preceding definitions. The radiative properties of a surface include its emissivity, absorptivity, reflectivity, and transmissivity. It should be noted that the radiative properties of metals and nonmetals (conductors and nonconductors) are often significantly different, and the impact of both micro- and macroscale surface characteristics can also be significantly different for a metal and nonmetal.

Figure 5.18 shows the parameters that affect radiative properties. Both micro- and macrosurface characteristics can be important. In addition, temperature can also have a strong influence on the radiative properties of a surface.

**Objective.** Despite the renewed interest in low-temperature radiant systems no experimental work in the area of panel output has been undertaken since the early 1950s. Both building materials and radiant system technology have changed signifi-

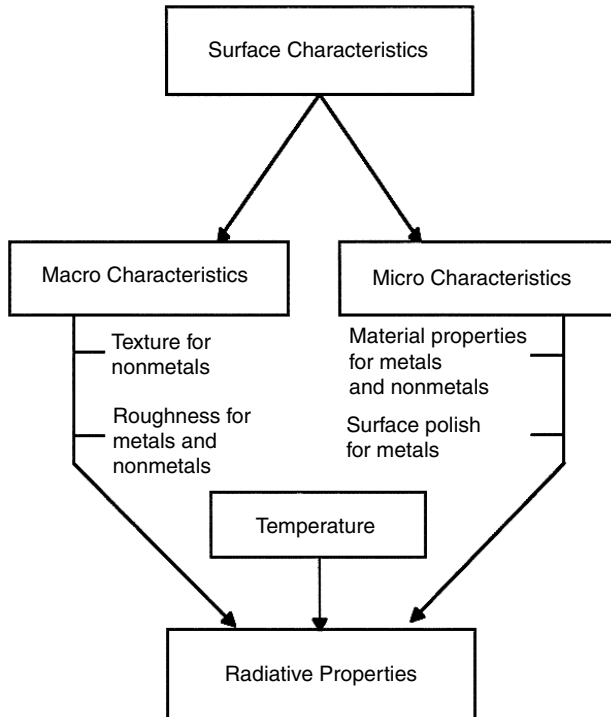


**FIGURE 5.18** Parameters important for radiative heat transfer.

cantly since then. This project was designed to update the literature by examining the impact of modern floor and wall coverings on panel output.

The project's main objective was to obtain relevant and accurate data pertaining to the effects of surface characteristics on heat transfer from radiant panels, which will assist system designers in predicting the actual panel output required for thermal comfort as well as energy performance.

To meet this objective, the effect of macro- and microsurface characteristics on radiative properties and panel output were examined.

The effect of microsurface characteristics was examined by testing different materials. The effect of macrosurface characteristics was examined by testing different surface textures. Hemispherical and directional emittance measurements were made in order to compare how the emittance varied with surface type and to verify existing assumptions and corroborate existing surface property data. In looking at panel output, panel surfaces were tested in three geometries and under varying operating conditions. In this manner, the radiative-conductive split could be studied along with the room panel interactions.

**Literature Review.** Although few recent studies specifically address radiant panel output (i.e., the radiative output of a radiant system), in the last decade there have been a number of attempts to investigate the performance of radiant systems. Various modeling and experimental investigations have attempted to relate the physical

nature of radiant systems to their output and thereby either justify their reemergence or prove their shortcomings. Most of the recent experimental work can be classified as case studies. As such they are of little value to designers of radiant systems. The most recent controlled experiments designed to determine the significance of various parameters on radiant panel output were performed in the 1950s in the American Society of Heating and Ventilating Engineers (ASHVE) Environment Laboratory.

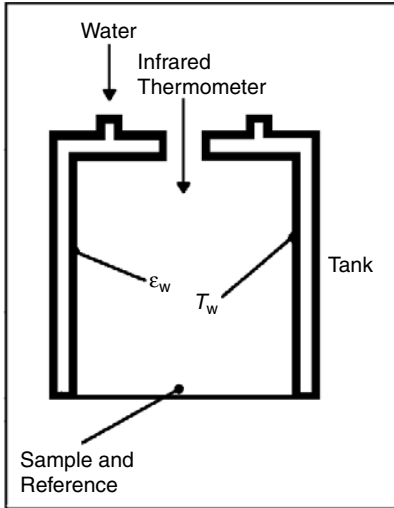


**FIGURE 5.19** Equipment for measuring hemispherical emittance.

*Measurement of Hemispherical Emittance.* The thermal emittance of a surface determines how well that surface will perform as a radiator. Therefore, it is an important property that needs to be determined. In the literature there are some practical methods for measuring emittance. The discussion of these methods will involve only the primary measurements and setup and not the theoretical basis for the techniques.

Jian Liu and Cai-gen Zhang (1994) devised a technique that involves using an infrared (IR) thermometer and a cylindrical, double-walled, bottomless cavity. The space between the walls is filled with water controlled at temperature,  $T_w$ . The inner wall of the cavity is painted with a paint of known emittance,  $\epsilon_w$ . Another plate with a known emittance,  $\epsilon_r$ , is used as the reference. The cylinder is placed over the sample, which has an unknown emittance,  $\epsilon_s$ . (See Fig. 5.19.)

When the IR thermometer is focused on the sample and the wall of the cylinder, respectively, it will give signal voltages  $V(T_{cs})$  and  $V(T_{cw})$ , corresponding to the respective brightness temperatures of the surfaces. The brightness temperature is the temperature a blackbody could have and still emit at the same intensity as the nonblackbody source being measured.

$$V(T_{cs}) = \epsilon_s V(T_s) + (1 - \epsilon_s) \epsilon_w V(T_w) \quad (5.10)$$

$$V(T_{cw}) = \epsilon_w V(T_w) + (1 - \epsilon_w) \epsilon_s V(T_s) \quad (5.11)$$

The procedure is repeated to obtain signal voltages from the reference target and the wall.

$$V(T_{cr}) = \epsilon_r V(T_s) + (1 - \epsilon_r) \epsilon_w V(T_w) \quad (5.12)$$

$$V'(T_{cw}) = \epsilon_w V(T_w) + (1 - \epsilon_w) \epsilon_r V(T_s) \quad (5.13)$$

When  $V(T_{cr})$  is subtracted from  $V'(T_{cw})$ , the result is:

$$V'(T_{cw}) - V(T_{cr}) = \epsilon_r [\epsilon_w V(T_w) - \epsilon_w V(T_s)] \quad (5.14)$$

A similar result is obtained by subtracting  $V(T_{es})$  from  $V(T_{ew})$ . Equating the quantity in brackets allows for the solution of the unknown emittance in terms of the reference emittance and the measured voltages. The unknown emissivity is then:

$$\epsilon_s = \frac{\epsilon_r [V(T_{ew}) - V(T_{es})]}{[V'(T_{ew}) - V(T_{er})]} \quad (5.15)$$

V. C. Sharma (1989) devised an additional method from measuring hemispherical emittance. The experimental setup included an emissometer (differential thermopile), a reference surface with known hemispherical emissivity, and a digital voltmeter. The detector portion of the emissometer was heated to an environment temperature so that the samples did not have to be heated. The hemispherical emittance of the sample could then be calculated as a function of the power input to the detector surface and the emittance of the reference surface:

$$\epsilon_h = \frac{V(\text{sample})}{V(\text{standard})} \times 0.93 \quad (5.16)$$

where 0.93 is the hemispherical emittance of a matte-black aluminum reference surface. Sharma noted that the hemispherical emittance of the building materials he measured (clay, concrete, cement, paper, wood, and paint) were high and varied from 0.8 to  $0.92 \pm 0.02$ .

*Measurement of Angular and Spectral Emittance.* Aydin Umur, G. V. Parmelee, and L. F. Schutrum (1955) conducted an experimental investigation of directional (angular) emittance. The researchers constructed an apparatus to measure surface radiation at various angles of emission in a controlled environment. The apparatus consisted of a double-walled tank with a sighting port through the double wall into the test chamber. Water was circulated through the tank wall, and the test chamber was painted with a coating of known emittance. As a result, both the surface temperature and the emittance of the test chamber were known and constant. The test surface was attached to a heated base instrument and was calibrated with thermocouples. The base could be rotated so that a radiometer could view the sample (through the sighting port) at different angles.

The experimental results agreed with the theoretical angular emittance for non-metal surfaces predicted by Schmidt and Eckert. For nonmetals the emittance remains nearly constant for angles (measured from the normal) of emission between  $0^\circ$  and  $60^\circ$ , then drops off very quickly to 0 near angles of  $90^\circ$ . As a result, the hemispherical emittance for nonmetal surfaces is approximately 95 percent of the normal emittance. Nonmetal surfaces can be considered to be diffuse emitters.

A slightly more recent work by A. A. Voznesenskii and A. R. Fert (1967) investigated the spectral emittance of various types of concretes and plasters used in buildings. The presence of silicates ( $\text{SiO}_2$ ) in the aggregate mixes resulted in widely varying spectral distributions of emittance. Their research showed emissivities ranging from as low as 0.5 to as high as 0.9 for various types of concretes and plasters. Although the emittance of these materials was not temperature dependent, it was dependent on the way the surface was finished. Apparently various finishing techniques result in different concentrations of silicates near the surface. It should be noted that the practical implications of these findings are minimized by the fact that bare-plaster panels are virtually nonexistent in buildings, and uncoated concrete surfaces are rare.

*Development of Natural Convection Correlation for Radiant Applications*

RADIANT PANEL HEATED ROOM EXPERIMENTS: In 1951, T. C. Min et al (1956) performed experiments to quantify the effects of natural convection and radiation in a panel-heated room. The natural convection correlations they developed are still used in the *ASHRAE HVAC Systems and Equipment Handbook* as an integral part of the currently recommended procedure for radiant panel design.

The six surfaces in the ASHVE experimental room used by Min and his fellow researchers were composed of painted aluminum panels having a hemispherical emittance of 0.88. The surface temperature was controlled by liquid circulation with one of the surfaces being controlled to a higher temperature than the others. The experiments covered room sizes of  $24.5 \times 12 \times 8$  ft,  $24.5 \times 12 \times 12$  ft, and  $12 \times 12 \times 8$  ft. The total output of the panel surface was measured using plate-type heat flow meters. The radiation output measured with a radiometer was subtracted from the total panel output to obtain the convection heat flow.

Min used the general equation for radiation interchange developed by Hottel (1954). Although Hottel's formulation has been nearly lost in recent years, it is a clever and intuitive formulation of the radiant exchange between gray diffuse surfaces and, as such, deserves a second look. Hottel's formulation is based on the fact that if a surface is a perfectly diffuse emitter and reflector, and if its emittance is independent of temperature (a gray surface), then a so-called interchange factor between two surfaces,  $\bar{F}_{1,2}$ , can be defined as:

$$\bar{F}_{1,2} = \frac{1}{\frac{1}{F_{12}} + \left(\frac{1}{\epsilon_1} - 1\right) + \frac{A_1}{A_2} \left(\frac{1}{\epsilon_2} - 1\right)} \quad (5.17)$$

where  $F_{12}$  is the view factor between the two surfaces. The general equation for radiation interchange as given by Hottel then becomes:

$$q_r = \bar{F}_{1,2} \sigma (T_1^4 - T_2^4) \quad (5.18)$$

Note, when the area of the radiant panel,  $A_1$ , is much smaller than the rest of the area of the enclosure, the interchange factor simplifies to the emittance of the radiant panel surface.

The painted aluminum surfaces in the ASHVE environment chamber had a normal emittance of 0.92 and a hemispherical emittance of 0.88. For the conditions in the room, the interchange factor calculated, as earlier, was 0.85. Through radiation measurements, the interchange factor between the floor panel and its environment was determined to be 0.876. For a ceiling panel, the interchange factor was found to be 0.90. After these factors were determined, they were used to calculate the radiation exchange between the warm panel and its environment.

The experiments were run with still air conditions and used the entire floor or ceiling as a single heated panel. All of the other surfaces were at a uniform temperature. The heated floor tests were run at temperatures from  $24^\circ\text{C}$  to  $43^\circ\text{C}$  ( $75^\circ\text{F}$  to  $100^\circ\text{F}$ ), and the heated ceiling tests were run at temperatures from  $32^\circ\text{C}$  to  $66^\circ\text{C}$  ( $90^\circ\text{F}$  to  $150^\circ\text{F}$ ). The other surfaces were run at temperatures between  $45^\circ\text{F}$  and  $70^\circ\text{F}$  ( $7.2^\circ\text{C}$  and  $21.1^\circ\text{C}$ ). The correlation (in S.I. units) from the research are as follows:

1. In a floor-heated space
  - a. Convection from floor:

$$q_{pc} = 2.42(T_p - T_a)^{1.31} / D_e^{0.08} \quad (5.19)$$

*b.* Convection to walls:

$$q_{pc} = 1.87(T_p - T_a)^{1.32} / H^{0.05} \quad (5.20)$$

*c.* Convection to ceiling: same as convection from floor.

2. In a ceiling-heated space

*a.* Convection from ceiling:

$$q_{pc} = 0.20(T_p - T_a)^{1.25} / D_e^{0.25} \quad (5.21)$$

*b.* Convection to walls: same as for floor heated space.

*c.* Convection to floor: same as convection from ceiling.

In these correlations,  $q_{pc}$  is the convective heat flux ( $\text{W}/\text{m}^2$ ) from the panel, and  $T_p$  is the radiant panel temperature.  $D_e$  is the equivalent diameter of the panel, and  $H$  is the height of a wall panel.

The researchers noted that the natural convection correlation compared well with other experimental work except for natural convection from a heated ceiling. The convection coefficient from a small free-edge plate, they noted, may be 6 to 10 times as great as that for a heated ceiling. Although this appears to be an important consideration, the magnitude of natural convection heat transfer for a ceiling-mounted radiant heating panel is in all cases very small, usually under 10 percent of the total panel output.

The convection correlation used for radiant heating can also be used for radiant cooling with a slight twist. Correlation applicable for floor heating is applicable for ceiling cooling. Similarly, a convection correlation for ceiling heating is now applicable for radiant floor cooling.

EFFECTS OF ROOM SIZE AND FURNISHINGS ON PANEL OUTPUT: In 1952, Schutrum and Vouris (1954) studied the effects of room size and nonuniform panel surface temperatures on panel output. This research, performed in ASHVE's Environment Laboratory, has been largely obviated by the advent of computer-based engineering analysis. Calculating the radiant exchange between a modest number of heat transfer surfaces for a simple geometry was a difficult problem for the practicing engineer at the time this research was completed. Today these calculations are more or less routine.

Although the data presented in the paper did not admit to the development of correlation, several interesting qualitative observations were made. First, the researchers noted that for heated ceiling systems, the aspect ratio of the room appeared to be insignificant. For the three ceiling heights tested (4, 8, and 12 ft), there was no measurable effect on either the panel output or the room air temperature, regardless of the average unheated surface temperature (AUST) and the air infiltration rate. This finding, which was corroborated by the research results reported in this paper, indicates that radiant ceiling panels do not significantly disturb the flow field of the room.

For heated floor systems, room size did significantly affect both the power output and the room air temperature. The lack of data coupled with virtually no information about the flow field (such as where and how the infiltration air was introduced into the room), once again precluded the possibility of developing general correlation.

The effect of surface temperature nonuniformity was also observed. Ceiling-heated panel power output increased slightly when alternate ceiling panels were heated. Because the air temperature also increased slightly, the researchers concluded that nonuniform ceiling temperatures do induce some airflow in the room.

A companion paper by Schutrum and Humphreys (1954) reported additional panel performance data for rooms with nonuniform surface temperature environments. The results confirmed the previous conclusion that nonuniform surface temperatures had a small effect on both ceiling and floor systems. Panel output was adequately predicted using the AUST of the room. Additional carpeted room tests were also performed. The results of these tests demonstrated that the heat transfer from a carpet surface is essentially the same as the heat transfer from an ordinary bare panel surface at the same surface temperature. They of course also noted the addition of carpet greatly increases the thermal resistance of the panel system.

Finally, the paper reported on the effect of household furnishings in the room. Furnishings acted both as radiative fins (increasing the air temperature in the room) and as radiation shields (decreasing the radiative exchange between the heated panels and the rest of the room). The net effect on panel output was small—on the order of 5 percent for a normally furnished room.

One noticeable flaw in the experiments was the failure to calculate comfort parameters. Air temperatures, surface temperatures, and panel power were all reported but without the context of thermal comfort. Very little useful design information could be extracted from the data. In addition, no effort was made to calculate the uncertainty associated with the data, and correlations were implied by drawing curves through widely scattered data points.

**COMPARISON OF NATURAL CONVECTION CORRELATIONS:** To properly predict total panel output, it is necessary to predict the contribution of both radiation and natural convection to the total surface heat transfer rate. For some configurations and operating conditions, the natural convection contribution is nearly as large as the radiation contribution.

E. Dascalaki et al. (1994) performed a substantial review of published natural convection correlation for surfaces in unconfined flows and in enclosures. Their work shows that for unconfined flows there is, in general, good agreement between the correlation. The same cannot be said for enclosures. Tables 5.47 and 5.48 present the maximum and minimum correlation for unconfined flows and enclosures.

The correlations in Tables 5.47 and 5.48 are based on the Grashof number ( $Gr$ ), which is defined as:

$$Gr_L = \frac{g\beta(T_s - T_a)L^3}{\nu^2} \quad (5.22)$$

**TABLE 5.47** Maximum and Minimum Correlations for Unconfined Flows

Vertical surface	
Laminar	Turbulent
Max: $Nu = 0.564 Gr^{1/4}$	Max: $Nu = 0.124 Gr^{1/3}$
Min: $Nu = 0.474 Gr^{1/4}$	Min: $Nu = 0.079 Gr^{1/3}$
% difference = 19	% difference = 57
Horizontal surface (hot side up)	
Max: $Nu = [(0.52 Gr^{1/4})^6 + (0.126 Gr^{1/3})^6]^{1/6}$	Max: $Nu = [(0.52 Gr^{1/4})^6 + (0.126 Gr^{1/3})^6]^{1/6}$
Min: $Nu = 0.487 Gr^{1/4}$	Min: $Nu = 0.117 Gr^{1/3}$
% difference (at $Gr = 1E8$ ) = 34	% difference (at $Gr = 1E10$ ) = 22

**TABLE 5.48** Maximum and Minimum Correlations for Enclosures

Vertical surface
Max: $Nu = 0.197 Gr^{0.32}$
Min: $Nu = 1.53 Gr^{0.14}$
% difference (at $Gr = 1E10$ ) = 88%
Horizontal surface
Max: $Nu = 0.297 Gr^{0.31}$
Min: $Nu = 1.24 Gr^{0.24}$
% difference (at $Gr = 1E10$ ) = 17%

where  $g$  = local acceleration due to gravity  
 $\beta$  = volumetric thermal expansion coefficient  
 $T_s$  = surface temperature  
 $T_a$  = reference air temperature  
 $L$  = characteristic length  
 $\nu$  = kinematic viscosity

Although the extreme differences between the correlations are rather large, most of the correlations agree quite well with each other. One thing that makes comparisons difficult is the uncertainty in what was used as the correlating length scale. As Goldstein et al. (1972) pointed out, for many published correlations, the details of the experimental setup are not known. Dascalaki's paper does not provide any additional help.

The researchers noted that the correlation for unconfined flows and for enclosures were often significantly different. For horizontal surfaces, the enclosure correlation predicts a larger Nusselt number than predicted by the unconfined geometry correlation. The opposite is true for vertical surfaces (except for the Min correlation). The authors concluded that more investigation needs to be performed with full-scale rooms and typical operating conditions.

Several problems are then encountered when using a correlation to predict natural convection.

- What is the appropriate length scale?
- What is the appropriate reference temperature?
- What surface temperature distribution drives the flow field?
- Is the correlation valid when the room is conditioned with a radiant system?

The differences in the enclosure equations show that not all of these problems have been adequately addressed.

EXPERIMENTAL INVESTIGATION OF RADIANT HEATING AND COOLING SYSTEMS: One of the most widely held assumptions is that radiant systems can provide an equally comfortable thermal environment at a lower (or higher) air temperature than forced-air systems. The reason for this is that thermal comfort is a function of a number of parameters including both the air temperature and the interior surface temperatures of the building. The interior surface temperatures are often approximated by a single value called the *mean radiant temperature* ( $T_{mrt}$ ). This effectively reduces the enclosure radiation exchange to a two-surface problem. For this calcu-

lation,  $T_{\text{mrt}}$  is approximated as the area-emittance weighted surface temperature, as shown in Eq. (5.23):

$$T_{\text{mrt}} = \frac{\sum_{k=1}^n A_k \epsilon_k T_k}{\sum_{k=1}^n A_k \epsilon_k} \quad (5.23)$$

where  $n$  is the number of surfaces in the room,  $A_k$  is the surface area,  $\epsilon_k$  is the surface emittance, and  $T_k$  is the surface temperature. In a radiant heating system, because the MRT is higher than in a forced-air system, the air temperature can be lower to achieve the same comfort level. It is hypothesized that a lower air temperature should result in a lower heat loss through the surfaces of the building. A similar effect is obtained in a radiant cooling system by lowering the MRT and raising the air temperature.

On the other hand, several researchers have pointed out that due to the nature of radiant systems, the energy savings realized by favorably adjusting the air temperature may be negated by the energy used to radiantly heat or cool the building surfaces. Because heat transfer through the building elements is more closely connected to the surface temperatures than the air temperature, some claim that there should be an increased heat loss from the structure due to the higher temperature difference between the inside and outside of the building walls, floors, and ceilings.

One would think that scientific study of low-temperature radiant heating systems would clearly support one of the expected trends. This is not the case. There is quite a large range of reports in the literature as to the effectiveness of the different systems that are available. Most, but certainly not all, of the studies have concluded that low-temperature radiant heating systems are more efficient than forced-air systems due to either lower life-cycle cost or lower energy consumption. Yet, the actual benefit reported varies anywhere from none to extremely significant. Several studies have even pointed out that the steady-state design procedures reported by ASHRAE (1984) need to be enhanced (Ling, 1990; Howell, 1990).

Experimental studies on low-temperature radiant systems have not clarified the issue of overall building energy efficiency. Berglund and Gagge (1985) performed a series of experiments using a typical office structure that was fitted with four different heating systems: (1) radiant ceiling, (2) forced-air, (3) baseboard, and (4) radiant floor. The structure was surrounded by a controlled airspace, and the system control was based on operative temperature,  $T_{\text{op}}$ , which is defined by ASHRAE (1989) as:

$$T_{\text{op}} = \frac{(h_r T_{\text{mrt}} + h_c T_{\text{air}})}{(h_r + h_c)} \quad (5.24)$$

where  $h_r$  is the linearized radiative heat transfer coefficient,  $T_{\text{mrt}}$  is the mean radiant temperature,  $h_c$  is the convective heat transfer coefficient, and  $T_{\text{air}}$  is the mean air temperature. In addition, human subjects inhabited the space during the experiments to give the researchers insight into the thermal perceptions of the participants.

The researchers reported that the ceiling system was the most energy-efficient. The forced-air system caused the most local discomfort, followed by the radiant ceiling system. The floor system was the preferred alternative by the occupants, but it consumed the most energy. Although the results of this study are equipment-specific and cannot be generalized to other ceiling or floor systems, the study does highlight the importance of thermal resistance as a radiant panel design parameter.

Another experimental investigation was performed by Dale and Ackerman (1993) over a period of three years. In this study, two nearly identical, two-story residential buildings were built. One was considered the reference house and was heated using a forced-air system. The other house had both a forced-air and radiant floor system installed. The second house was in general better insulated and had more window area. Energy consumption measurements from the second building were normalized with respect to the first in order to discount the effect of weather on the study.

The researchers found that, after normalization, there was very little difference in energy consumption between the two systems. In fact, they felt that the radiant floor system was less efficient due to increased losses through the exterior surfaces. However, this study did not control on OT but rather solely on air temperature. Mean radiant temperatures were higher in the radiant system, and this could have been used to reduce the air temperature and thus the heat losses.

Yost, Barbour, and Watson (1995) were involved in an experimental study comparing energy consumption and thermal comfort in a test house for an air-to-air heat pump system and a surface-mounted ceiling radiant heating system. Heating systems were operated alternately in two-week blocks when possible and for one-week blocks otherwise. During periods of radiant heating, room thermostats were set back to 60°F when unoccupied and 68°F when occupied. Individual zones could therefore be turned on or left off as desired. The heat pump system used a setback of 60°F and a set point of 68°F.

A regression analysis of energy consumption versus outdoor temperature showed a lower slope for the radiant system. Typical record year data from a nearby air force base allowed translation of the regression lines into expected average energy consumption for the systems. Based on the analysis, energy consumption savings of 33 percent were estimated for a typical record year in the Washington, D.C. area for the radiant system in comparison with the air-to-air heat pump system. The predicted savings over an electric baseboard system for the radiant system was 52 percent. Though it must be noted, the baseboard system was not tested in the same experiment and had an air temperature approximately 2°F higher than the other two systems. The authors note the comparative energy performance is specific to the house and its occupancy by a working couple.

While no one experiment can address all of the issues that are related to comfort and energy consumption, the studies as a whole do seem to indicate that radiant systems can provide an equal level of comfort at equal or lower levels of energy consumption. More experimental studies are warranted in comparing different heating systems for different locations and operating conditions. Additionally, experimental work using hybrid systems is also necessary to adequately present the case for radiant heating and cooling systems.

**RADIANT SYSTEM SIMULATION AND MODELING:** The attempts at modeling low-temperature radiant heating systems through computer algorithms has also produced differing opinions on their relative efficiency. Weida (1986) performed a life-cycle cost analysis for a generic hospital structure located at several geographic sites and reported that the radiant system was justifiable on an economic basis. Researchers at the Center for Building Studies at Concordia University (Zmeureanu et al., 1988) reported that their computer model predicted that a ceiling radiant system would use 21 percent less energy and have a 38 percent lower peak load. Saunders and Andrews (1987) studied the effect of unheated surface emittance on radiant system performance. They found that surface emittance did not significantly effect radiant system performance until the emittance of the unheated walls was lowered below 0.8.

Most of the modeling procedures can be broken into two categories: numerical or control theory based. The numerical models typically use some form of a finite control volume to solve transient heat conduction through the building elements. The control theory techniques are derived from efforts to analyze the effect of different radiant heating control schemes. Both are described in detail by Strand (1995). Two recently developed programs that can be used in radiant system design are of particular interest.

**IBLAST Model.** A persistent problem in radiant system design is the inability to correlate the total output of a radiant panel to the performance of an installed radiant system. Under partial ASHRAE funding, a first step in the development of a comprehensive radiant system model was completed (Strand, 1995) using a research version of the BLAST program called Integrated Building Loads Analysis and System Thermodynamics (IBLAST). Recognizing the dual nature of a radiant system as both a building element and a space-conditioning system, this new radiant system model fits well into the heat balance based solution of IBLAST, which solves the zone energy balance and the system response simultaneous. The IBLAST model uses an extension of conduction transfer functions (CTFs) to characterize the transient conduction from the location of a heat source or sink (either electrical resistance wire or mat heating or hydronic circulation loop) embedded in the building element. In conjunction with the IBLAST zone heat balance, the model accounts for convection to the room air as well as radiation to other room surfaces and people occupying the space. The results of the model are also linked to three popular thermal comfort models, allowing architects and engineers the ability to investigate thermal comfort as well as energy consumption. With the completion of the Strand models, IBLAST permits the analysis of both low-temperature radiant heating and cooling and provides the user with the option of selecting either flux or temperature-based control algorithms. IBLAST also employs a zone moisture balance (Liesen, 1994), which is utilized to predict the occurrence of condensation on room surfaces for radiant cooling systems.

**BCAP Program.** The Building Comfort Analysis Programs (BCAP) were also developed under ASHRAE funding (Project RP-657). BCAP allows the mean radiant temperature ( $T_{\text{mrt}}$ ) to be incorporated into building and HVAC system design. BCAP consists of a number of programs that each have a specific function in producing the final results. The programs move from initial building configuration, heater types (both radiant and convective), and desired design conditions to several programs giving a detailed comfort analysis. BCAP allows a variety of building geometry to be modeled. The output from the programs is enormous—everything from air temperatures to the comfort of different body locations. The advantage of BCAP is that it provides detailed comfort results and allows for relatively quick design iterations.

**Heat Balance Method of Calculating Radiant Panel Heat Transfer.** The heat balance method provides the physical framework for understanding the thermodynamic processes that occur simultaneously in a radiantly heated or cooled room. Simply stated, the heat balance method requires that the first law of thermodynamics be satisfied for an arbitrary control volume around a surface or space of interest.

The experimental method developed for this investigation is based on a control volume that encloses the radiant panel as shown in Fig. 5.20. It should be noted that although Fig. 5.20 refers to the heating panel, the principles are equally valid for cooling. Only the direction of heat flow changes.

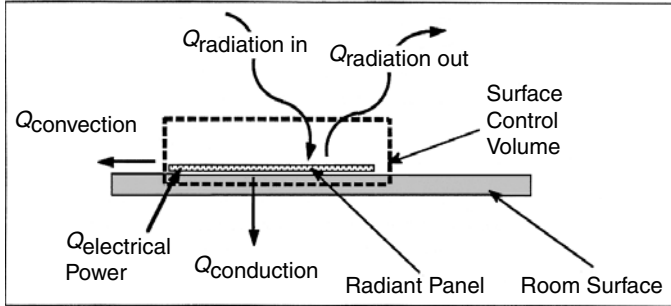


**FIGURE 5.20** Control volume enclosing radiant panel.

Under steady-state conditions, the rate at which electrical energy is dissipated in the control volume by Joule heating must exactly equal the rate at which heat energy is removed from the control volume by the combined processes of conduction, convection, and radiation. A slightly more detailed view of the surface heat transfer processes is shown in Fig. 5.21. This diagram shows that the total heat flux into the panel will include both heat transfer out the front of the panel by radiation and convection and heat transfer out the back of the panel through conduction.

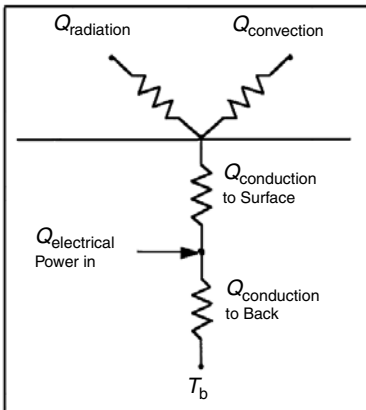


**FIGURE 5.21** Resistance network for panel.

to the natural convection from the panel. It can therefore be difficult to realize improvements in panel output because of the interaction among the various heat transfer processes.

*Radiant panel efficiency* is the ratio of the rate of total heat transfer from the radiant panel to the total input. It is also desired that most of the total input to the panel be transferred by radiation. To increase panel efficiency, first backlosses need to be made as small as possible through proper insulation of the back of the panel. Second, convection from the panel surface should be minimized by eliminating drafts and any sources of forced convection. However, even if forced convection is eliminated, there will always be natural convection from the panel surface. Materials used as the panel surface should have a high emittance. The use of high-conductance materials will also increase panel efficiency by reducing backlosses.

**Experimental Configurations and Procedure**

*Introduction to Experiments.* To satisfy the objective of examining the impact of both microsurface and macrosurface characteristics on radiant panel output, a three-stage experimental procedure was devised.

First, the validity of microsurface assumptions was examined. In accordance with the definition given in Sec. 1 of RP-876, this set of experiments looked only at infrared wavelength scale phenomena. With nonmetals in view, this was accomplished by estimating the total hemispherical emittance of the various building materials of interest.

Second, the validity of macrosurface assumptions was examined. This was accomplished by checking the diffuseness of various surface textures.

Third, the impact of both macrosurface and microsurface characteristics on panel output was examined in a series of experiments designed to separate the impact of surface characteristics on the total panel output into radiation and convection components. These experiments were performed in “still air,” under natural convection conditions, and under forced-convection conditions. It should be noted that in all panel output experiments, the objective was to measure the change in output due to a change in panel surface characteristics. Thus, absolute values and (by extension) correlation were of secondary importance. Although several of the correlations appeared to be quite good, convection correlations—especially natural convection correlations—require a large set of parametric experiments over a wide range of boundary conditions before they can be generalized. Convection experiments on this scale were beyond the scope of this project.

*Description of Radiant Panel Surfaces.* A number of commonly used materials were tested as radiant panel surfaces. Though not every material possible was tested, the materials that were tested cover a broad range of typical surfaces encountered in buildings. Following is a description of the materials that were tested:

1. *Plastic.* A thin, clear high-temperature plastic surface that was attached to the heating element of the radiant panel (abbreviated as *plastic*).
2. *Vinyl.* A typical vinyl floor covering 0.18 cm (0.07 in) thick (abbreviated as *vinyl*).
3. *White.* Thin layer of paint on top of the heating element of the radiant panel (abbreviated as *white*).
4. *Textured.* A textured layer of paint on top of the heating element of the radiant panel (abbreviated as *textured*).
5. *Medium textured.* A slightly smoother textured surface (abbreviated as *med.-tex*).
6. *Carpet.* A nylon fiber carpet with a pile height of about 1.02 cm (0.4 in). The carpet was plush with a medium weave density.

The aforementioned names are used in the figures in Sec. 6 of RP-876.

The following three items were only used in the diffuse testing experiments:

1. *Carpet 2.* A nylon fiber carpet with a pile height of 1.65 cm (0.65 in.) The carpet was a plush with a medium weave density.
2. *Carpet 3.* An olefin fiber carpet with a textured surface (non-uniform height). The carpet had a dense weave.
3. *Concrete.* Two concrete surfaces were tested for surface emittance. One surface was troweled smooth, the other was lightly textured. Concrete was not used in any of the panel output experiments.

**Experimental Results and Discussion.** Experimental results are presented in the following sections and shown in Appendix E of ASHRAE RP-876. In Sec. 6.1 of the

research project, surface properties and basic assumptions are checked. In Sec. 6.2, the combined impact of macro- and microsurface characteristics on radiant panel output is examined. The results of natural and forced-convection experiments are included in Secs. 6.4 and 6.5. The significance of experimental results for panel design and future research are emphasized throughout.

*Surface Properties—Basic Assumptions.* Radiant panel design depends on two basic assumptions that are related to micro- and macrosurface characteristics. The first assumption is that the total emittance of all common, nonmetal building materials (e.g., paints, carpets, and vinyl) is  $0.9 \pm 0.05$ . The second assumption is that for enclosure radiant exchange calculations, a surface can be treated as a diffuse emitter. This assumption recognizes that nonmetal surfaces are in fact not completely diffuse but asserts that the directional dependence of the radiant flux does not significantly affect the calculation of either the total panel output or the radiant exchange in a room.

The emittance assumption and the diffuse assumption are basic to the diffuse, gray, uniform-radiosity formulation of the enclosure, radiant exchange problem. This section concludes with a comparison of measured radiant flux and the theoretical radiant flux calculated on the basis of these two assumptions.

HEMISPHERICAL EMITTANCE EXPERIMENTS: The emittance measurements reported in this section were primarily motivated by the fact that the emittance of some modern building materials such as carpet and vinyl cannot be found in the literature. Because all previously measured nonmetal building materials have emittance approximately equal to 0.9, it is commonly assumed that modern materials have similar properties. These measurements check that assumption.

There is, of course, a limit to which the radiative properties can be changed. The emittance by definition cannot be greater than 1. In addition, roughening a surface will always tend to increase its effective emittance. As the surface roughness increases, the emittance and absorptivity increase because of multiple reflection between surface peaks and valleys. This can be demonstrated theoretically by considering a textured surface as a collection of tiny cavities, with the “bumps” in the surface forming the cavity walls. To the extent that the cavity walls “see” each other, the cavity will appear to be thermally black ( $\epsilon = 1$ ) to a distant surface.

The fact that roughening a surface always increases its emittance greatly simplifies the task of determining the emittance of modern surfaces. For example, if a smooth, painted surface has a measured emittance of 0.9, a textured surface coated with the same paint must have an emittance between 0.9 and 1.0. In this case, estimating the textured-surface emittance at 0.95 will result in a maximum error of  $\pm 5$  percent.

It is important to note that because radiation is a surface phenomenon, it is the surface properties of a material and not its bulk volumetric properties that are significant. Take, for example, aluminum. Smooth, polished aluminum at 300 K can have an emittance of 0.04, but anodized aluminum at 300 K can have an emittance of 0.9. When aluminum is painted, the radiative surface properties are the surface properties of the paint. See the ASHRAE experimental work performed by Aydin Umur (1955). Because uncoated metal surfaces are seldom used in building applications, they are not considered in this study.

The building materials for which emissivities are not reported in the literature can be summarized as petroleum-based polymers and fibers. These include plastics, vinyl, most carpet fibers, and many drapery fibers. The experimental measurements shown in Table 5.49 are reported for carpets, vinyl floor coverings, and a high-temperature plastic. To demonstrate the expected effect of texture on a high-emittance surface, smooth and textured painted surfaces are also compared. The measurements reported in Table 5.49 were obtained using the net radiometer-based procedure reported in Sec. 5 of RP-876. Figure 5.22 plots the results as a function of temperature.

**TABLE 5.49** Results of Hemispherical Emittance Measurements for Various Surfaces

Surface	Surface temperature [°C]	Hemispherical emittance
Vinyl floor covering	35	0.93
Vinyl floor covering	45	0.98
Vinyl floor covering	55	1.04
Textured paint	35	0.97
Textured paint	45	0.97
Textured paint	55	0.98
Plush carpet	35	0.93
Plush carpet	45	0.98
Plush carpet	30	0.98
White smooth paint	35	0.96
White smooth paint	45	0.98
White smooth paint	55	0.99
White smooth paint	30	0.94
High-temperature plastic	35	0.90
High-temperature plastic	45	0.92
High-temperature plastic	55	0.95

The uniformity of the results (even with errors and uncertainties considered) shows that the surfaces are very similar in terms of their radiative properties. Even though the materials have different macroscale properties, their radiative properties are similar.

An examination of the results leads to the following conclusions:

1. Emissivities of petroleum-based building materials fall between 0.9 and 1.0. Therefore, an estimated emittance of 0.95 for these materials is reasonable and will not result in significant error in radiant panel calculations.
2. Texture has the expected effect of slightly increasing emittance.

The apparent scatter in the data is actually a temperature bias most likely introduced by convection conditions that do not match the correction built into the net radiometer.

The radiometer corrects for the natural convection from the surface to the radiometer in order to determine the radiative flux. It appears that this correction does not match actual flow conditions when the radiometer is located in close proximity to a surface. Figure 5.22, which plots the data shown in Table 5.49, tends to support this hypothesis. The smoothest surfaces, which would tend to have the thickest boundary layers, show the greatest temperature dependence. The textured surfaces show much less temperature dependence. The result of this relatively insignificant systematic measurement error is that the uncertainty associated with the direct radiation measurement is approximately the same as the uncertainty associated with the theoretical radiant exchange calculation.

The emittance measurements have relevance for radiant cooling purposes also. A desirable property for radiant cooling is a high surface absorptance. Because the surfaces commonly used in radiative heating and cooling applications can be considered gray surfaces, the emittance and absorptance are equal. Therefore, a surface having a high emittance will also have a high absorptance; therefore, it is a good sur-

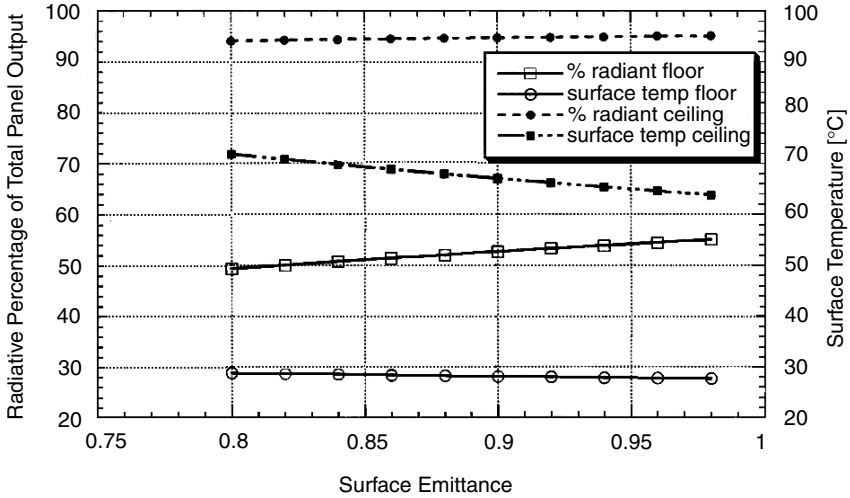


**FIGURE 5.22** Emittance of various surfaces as a function of temperature.

face to use for radiative cooling. Although surface temperatures for radiative cooling are significantly less than for heating, there is not a significant change in surface properties when used for heating or cooling.

ASHRAE Research Project 876 also examined other materials. As noted in the literature review, concrete surfaces appear to exhibit a slight surface property dependence on finishing technique. Even if concrete were not usually coated with a sealer or paint of some kind, this effect would be largely of academic interest. It is included here both for completeness and to form the basis of an interesting example.

Emittance was measured for two concrete surfaces, which were prepared from the same batch of concrete. One sample was troweled smooth, and the other was lightly textured to simulate a no-slip safety surface.

The data for the concrete surface tests are shown in Table 5.50 with comparable results reported by Sharma.

**TABLE 5.50** Results of Emittance Measurements for Concrete

	RP-876	Results reported by Sharma (1990)
$\epsilon_{\text{smooth}}$	$0.89 \pm 0.06$	$0.87 \pm 0.02$
$\epsilon_{\text{rough}}$	$0.96 \pm 0.07$	

The results from the concrete tests are reasonable. The smooth-surface results agree well with published data. Roughening the surface (changing the macrosurface characteristics) can increase the emittance to a slightly higher value. Yet, because the smooth surface has a relatively high emittance, the percentage increase in emittance (and in surface radiative output) is not large.

At this point, an example illustrating the impact of emittance on panel output may be appropriate. Consider a radiantly heated concrete floor. Assume that the

wall, ceiling, and air temperatures are all equal. Additionally, assume that the natural convection from the floor can be predicted using the ASHRAE Handbook equations (Chap. 6, "HVAC Systems") and that the radiation from the floor panel can be predicted with a two-surface exchange model. Now, what will the effect of surface emittance be on the energy radiated from the floor? Assume that the total output of the floor is  $130 \text{ W/m}^2$  [ $41.2 \text{ Btu/(h} \cdot \text{ft}^2)$ ] and the surrounding temperatures are at  $15^\circ\text{C}$ . Under these conditions, Table 5.51 shows that a change in emittance from 0.8 to 0.98 changes the percentage of heat transfer from the surface by radiation from 49 to 55 percent. The reason the change is not large is because convective heat transfer accounts for nearly one-half of the total output of the floor. When the natural convection from a surface is less, then the surface emittance will have a greater effect on the radiant output of the heated surface.

The same example can be repeated for a ceiling system. For this case, assume that the total output is  $350 \text{ W/m}^2$  [ $111 \text{ Btu/(h} \cdot \text{ft}^2)$ ] along with the previous mentioned assumptions. As seen in Table 5.51, the percentage of heat transfer from the surface by radiation remains relatively constant at nearly 95 percent. Changing the emissivity from 0.8 to 0.98 results in a change in surface temperature from  $71^\circ\text{C}$  to  $63^\circ\text{C}$ . If surface temperature is one of the design constraints, a higher emissivity surface will have a higher output for the same temperature.

Although the preceding example may be somewhat simplistic, it does demonstrate that surface emittance has a greater effect for a ceiling system than for a floor system. However, this research project has shown that most surfaces have an emissivity of 0.9 and greater.

**ERROR ANALYSIS FOR EMITTANCE MEASUREMENTS:** The uncertainty in the emittance measurements mainly comes from nonuniform surface temperatures. For some of the tests, there was a temperature difference of up to  $2^\circ\text{C}$ . The emittance is calculated using the expression:

$$\epsilon_s = \frac{q_{\text{net}}}{\sigma(T_s^4 - T_\infty^4)} \quad (5.25)$$

The uncertainty in the measurements is then expressed as:

$$e_\epsilon = \left[ \left( \frac{\partial \epsilon_s}{\partial T_s} e_{T_s} \right)^2 + \left( \frac{\partial \epsilon_s}{\partial T_\infty} e_{T_\infty} \right)^2 + \left( \frac{\partial \epsilon_s}{\partial q_{\text{rad}}} e_{q_{\text{rad}}} \right)^2 \right]^{1/2} \quad (5.26)$$

Expressions for each of the partial derivatives are:

$$\frac{\partial \epsilon_s}{\partial T_s} = \frac{-4q_{\text{rad}}T_s^4}{\sigma(T_s^4 - T_\infty^4)^2} \quad \frac{\partial \epsilon_s}{\partial T_\infty} = \frac{4q_{\text{rad}}T_\infty^4}{\sigma(T_s^4 - T_\infty^4)^2} \quad \frac{\partial \epsilon_s}{\partial q_{\text{rad}}} = \frac{1}{\sigma(T_s^4 - T_\infty^4)} \quad (5.27)$$

The uncertainty in the surface temperature was estimated to be  $1^\circ\text{C}$ . The uncertainty in the AUST was estimated at  $0.5^\circ\text{C}$ . And the uncertainty in the radiometer reading was estimated to be  $2 \text{ W/m}^2$ . These values give an uncertainty for the emittance measurements approximately equal to  $\pm 0.06$  on average.

**DIRECTIONAL PROPERTY EXPERIMENTS:** A diffuse surface radiates uniformly in all directions. All surfaces including nonconductors depart from the diffuse assumption. Figure 5.23 gives a representative description of the directional emittance for a metal and nonmetal.

As shown in Fig. 5.23, at viewing angles near the normal, both metals and nonmetals exhibit diffuse behavior. For metals, the emittance remains nearly constant up to about  $40^\circ$  from the normal, after which the emittance increases until it drops

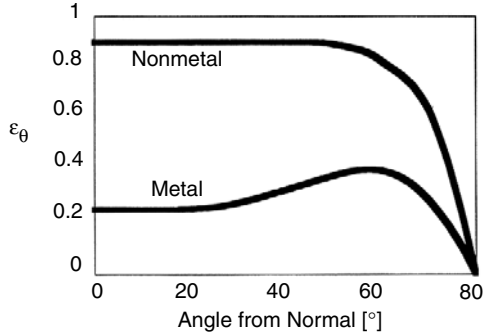


**FIGURE 5.23** Emittance as a function of angle from normal for a nonmetal and metal.

off sharply to zero. For nonmetals, the typical trend is nearly constant emittance to about  $60^\circ$  from the normal. After that, emittance sharply decreases to zero. For metals, the hemispherical emittance is usually slightly larger than the normal emittance, whereas for nonmetals the opposite is true.

At first glance it appears that calculating radiant exchange using the assumption of diffuse behavior will result in large errors. There are two reasons why this is not true. First, for nonmetals the hemispherical emittance is approximately 0.95 times the normal emittance. That is, the error incurred by approximating the hemispherical emittance as the normal emittance is approximately 5 percent. It should be noted that for all simplified computational methods (two-surface method, MRT method), it is the hemispherical emittance that is used in the calculation.

The second reason why the diffuse assumption is reasonable, despite the large differences at angles greater than  $60^\circ$ , is that the emittance is multiplied by the view factor in the radiant exchange calculation. The view factor also exhibits a cosine dependence on  $\theta$ ; as  $\theta$  approaches  $90^\circ$ , the view factor approaches zero. Thus, in the region where departure from diffuse behavior is greatest, the view factor is the smallest.

The experimental procedure described in Sec. 5.4 of ASHRAE RP-876 provides for a check on the diffuse assumption. The thermometer is, however, limited in spectral range (8 to  $14\ \mu\text{m}$ ), and the experimental apparatus and procedure are rather crude compared with what is required for precise measurements of diffuseness.

An initial check showed that the procedure was sufficient to differentiate between metals and nonmetals. Figure 5.24 shows the angular emittance normalized with respect to the normal emittance for the high-temperature plastic, carpet, vinyl, and textured surface. The experimental uncertainty is shown for one of the carpet tests. Figure 5.25 shows an aluminum panel for comparison. The data for the aluminum surface show some interesting behavior. The surface condition of the aluminum is not known, but the data do tend to agree to some extent with published results, as is shown in Fig. 5.25. It is not known why the emittance ratio decreases for small angles from the normal. It must be remembered, though, that the infrared thermometer only detects radiation in the range of 8 to  $14\ \mu\text{m}$ . The data could be quite different in another spectral range.

The experimental method was not only adequate to differentiate between metals and nonmetals, but it was also able to differentiate to some extent between nonmetals of varying diffuseness. A textured, painted panel was compared with a previ-

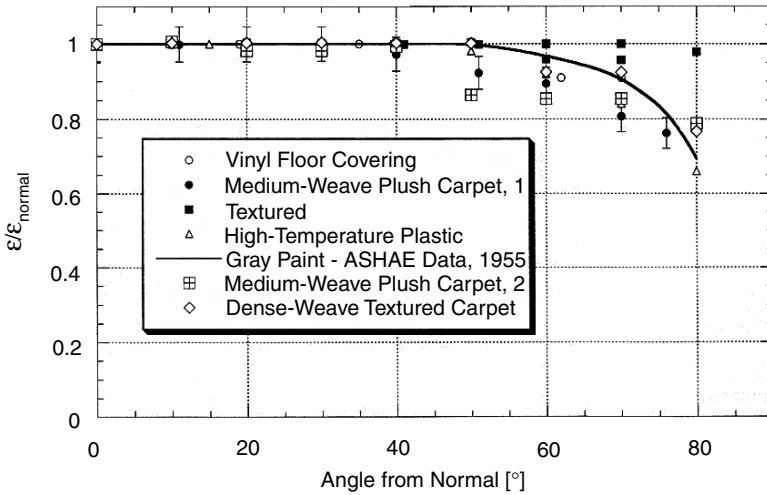


**FIGURE 5.24** Ratio of angular to normal emittance for various surfaces as a function of angle from normal.

ously measured smooth, painted panel. Because the elemental surfaces of the textured panel are not coplanar, this panel is expected to be more diffuse than a similarly painted smooth surface. The experimental data demonstrate this effect. In fact, the emittance ratios differ by more than 20 percent at 80° from normal.

Caution must be exercised in interpreting the difference. A 20 percent error in the angular emittance measured at 75° represents less than a 3 percent error in the

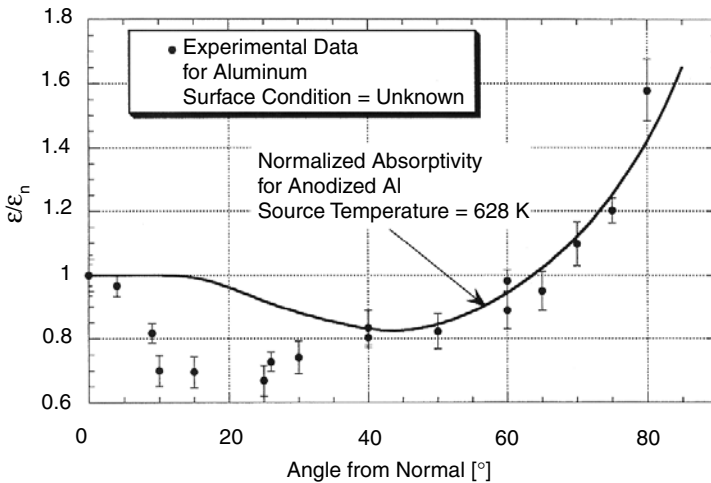


**FIGURE 5.25** Ratio of angular emittance to normal emittance for an aluminum surface. (Source: Redrawn from Siegel and Howell.)

total power output of the panel. As stated previously, at large angles from the normal, large changes in angular emittance have little impact on total panel output due to the magnitude of the view factors.

The data from these experiments also agree well with the ASHRAE data (Umur et al., 1955). The results from the ASHRAE experiments demonstrated that the hemispherical emittance for surfaces such as asphalt, black paint, and gray paint was approximately equal to 0.95 times the normal emittance.

The results from the experiments were numerically integrated to obtain hemispherical emittance ratios presented in Table 5.51.

**TABLE 5.51** Ratio of Hemispherical to Normal Emittance for Various Surfaces Along with Average Uncertainty for the Measurements

Sample	$\epsilon/\epsilon_n$ hemispherical	Average uncertainty
High-temperature plastic	0.92	$\pm 0.044$
Vinyl floor covering	0.94	$\pm 0.054$
Medium-weave plush carpet, 1	0.90	$\pm 0.044$
Gray paint	0.96	—
Medium-weave plush carpet, 2	0.90	$\pm 0.078$
Dense-weave textured carpet	0.94	$\pm 0.090$
Painted textured	0.96	$\pm 0.052$

As noted in Table 5.51, the data do indicate that the surfaces can be considered diffuse. Except for several of the carpets, all of the other ratios are near 0.95, which is a typical value for a nonmetal. Although the most important conclusion that can be drawn from the data is that for all practical engineering calculations the surfaces are diffuse, there are several interesting features that should be mentioned. As has already been noted, texturing a surface does make it more diffuse. Although this may seem like a panel design aspect that warrants additional investigation, the potential return is small. The other point, also primarily of academic interest, is the fact that the diffuse behavior of carpets varies noticeably from one type to another. It should be noted at this point that the results of all the tests were highly repeatable within the uncertainty intervals shown. The results tend to highlight the complexity of a carpeted surface. Carpet differs significantly from a textured, painted surface in that the topography is not well defined. The difficulty in defining the *surface temperature* is also highlighted. The precipitous drop in angular emittance at  $50^\circ$  (see Fig. 5.23) may very well reflect a change in the apparent surface temperature. At angles near  $0^\circ$  the IR thermometer “sees” the warm “roots” of the carpet fibers. At  $50^\circ$  the “roots” are “shaded” by the fibers, and the IR thermometer sees only the relatively cool tops of the fibers. This theory is borne out by the fact that the sharpest drop was measured for the densest weave of plush carpet at  $50^\circ$ , whereas no drop was measured for the textured carpet at the same angle.

It must be noted that these ratios do not necessarily indicate what surface has a higher hemispherical emittance. Rather they are a measure of diffuseness. The diffuse assumption is an important approximation for radiant heat transfer. It allows for the definition of a view factor (shape factor or exchange factor), thus greatly simplifying radiant exchange calculations. The experiments show that although surface

topography noticeably affects panel diffuseness, the diffuse assumption is valid for surfaces used in most buildings.

**ERROR ANALYSIS:** The ratio of the angular emittance to the normal emittance is calculated as:

$$\epsilon_r = \frac{T_s^4 - T_\infty^4}{T_{s,n}^4 - T_\infty^4} \quad (5.28)$$

where  $T_{s,n}$  = The normal surface temperature measurement made by the infrared thermometer

$T_s$  = The temperature measured by the infrared thermometer

$T_\infty$  = The temperature of the surroundings

An expression for the uncertainty in this measurement is:

$$e_{\epsilon_r} = \left[ \left( \frac{\partial \epsilon_r}{\partial T_s} e T_s \right)^2 + \left( \frac{\partial \epsilon_r}{\partial T_{s,n}} e T_{s,n} \right)^2 + \left( \frac{\partial \epsilon_r}{\partial T_\infty} e T_\infty \right)^2 \right]^{0.5} \quad (5.29)$$

Expressions for each of the partial derivatives are:

$$\frac{\partial \epsilon_r}{\partial T_s} = \frac{4T_s^3}{T_{s,n}^4 - T_\infty^4} \quad \frac{\partial \epsilon_r}{\partial T_{s,n}} = \frac{-4T_{s,n}^3(T_s^4 - T_\infty^4)}{(T_{s,n}^4 - T_\infty^4)^2} \quad \frac{\partial \epsilon_r}{\partial T_\infty} = \frac{-4T_\infty^3(T_{s,n}^4 - T_s^4)}{(T_{s,n}^4 - T_\infty^4)^2} \quad (5.30)$$

The thermometer has a listed accuracy of  $\pm 1$  percent of reading (at  $25^\circ\text{C}$ ). Therefore, taking an uncertainty of  $\pm 0.5^\circ\text{C}$  for both the angular surface temperature and the normal surface temperature is reasonable. This same value was used in the uncertainty of the surroundings.

Figure 5.25 displayed the uncertainty for only one of the surfaces, in order to avoid confusion in the figure. Table 5.51 lists the average uncertainty for the angular measurements for each of the surfaces as calculated using the above equations.

**COMBINED EFFECT OF EMITTANCE AND DIFFUSENESS ASSUMPTIONS:** Both the emittance measurements and the checks on surface diffuseness indicate that commonly made assumptions in radiation calculations are valid for modern building materials including carpet and vinyl. Figure 5.26 compares the calculated flux based on an emittance of 0.95 with the flux measured by the radiometer. The data, from a number of the floor experiments, indicate that an emittance of 0.95 (with the diffuse assumption) compares well with the measured radiant exchange.

As was demonstrated in the previous section, there is good reason to believe that the net radiometer overpredicts the radiation heat transfer at high temperatures due to a change in its convective boundary condition. This being the case, the theoretical radiant exchange (Sec. 5.6 in ASHRAE RP-876) provides a more consistent estimate of panel output and will be used in all radiation exchange calculations in the following sections.

#### *Panel Output Experiments*

**PANEL ENERGY BALANCE:** The heat transfer through and from the panel surface can be modeled using a simple thermal resistance network, as shown in Fig. 5.27. The simple resistance network includes the resistance between the heating element and panel surface, the convective and radiative resistance from the panel surface to the room, and the conductive resistance from the heating element to the back of the panel.

The total flux into the panel will include both heat transfer out the front of the panel by radiation and convection and the heat transfer conducted through the back

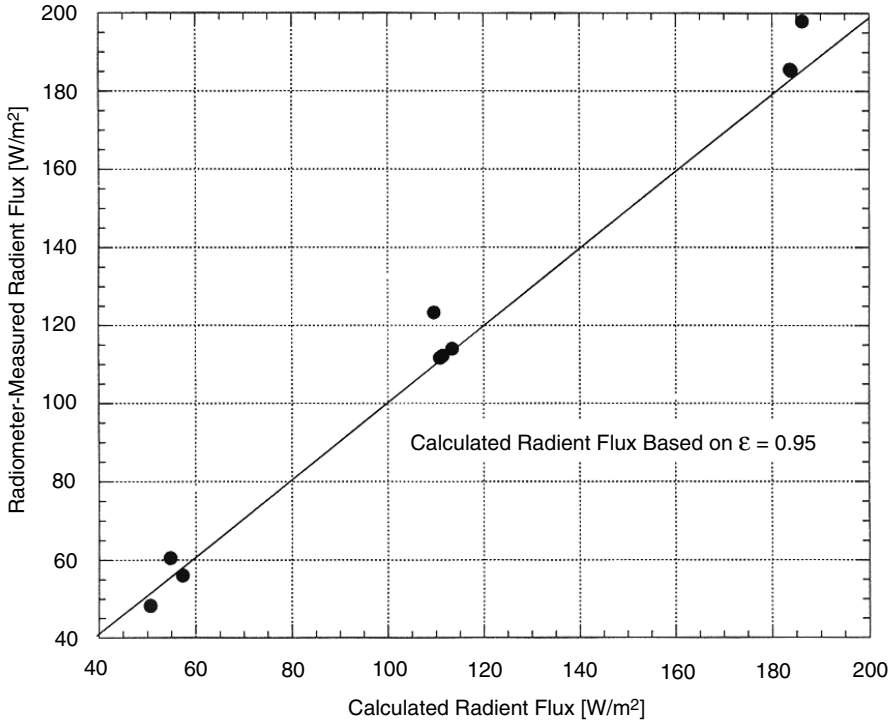


**FIGURE 5.26** Radiant flux measured by radiometer compared with calculated radiant flux. Data from floor experiments are discussed later in the report.

of the panel. For a control volume around the entire panel, the following energy balance can be written:

$$q_{total} = q_{back} + q_{pr} + q_{pc} \tag{5.31}$$

where:  $q_{pc}$  = radiant panel convective heat flux  
 $q_{pr}$  = radiant panel radiative heat flux

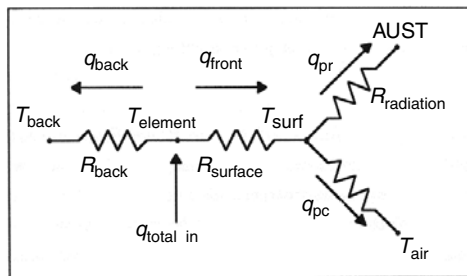


**FIGURE 5.27** Resistance network for panel.

The heat transfer from the front of the panel is

$$\frac{T_e - T_s}{R_s} = q_{pr} + q_{pc} \quad (5.32)$$

where  $R_s$  is the characteristic panel resistance.

When the emissivities of an enclosure are nearly equal and the exposed surfaces are passive, then the temperature of the fictitious surface becomes the AUST exposed to the panels.

The characteristic panel resistance for a hydronic system, where the element temperature is the water temperature, includes the thermal resistance of the tube wall, resistance between tube and panel, the thermal resistance of the panel, and the thermal resistance of the panel covers. For electric resistance heating, the panel resistance is just the resistance of the panel surface.

The total radiant panel output is defined as the sum of  $q_{pc}$  and  $q_{pr}$ ; it includes both the radiative and the convective flux from the front of the panel. Therefore, when the impact of surface characteristics on panel output is discussed, the effect of both convection and radiation are in view. It should be noted, however, that increasing panel output does not necessarily increase comfort. Panel output could be increased for example through forced convection, yet this would not improve comfort. Additionally, a cold window could increase the total output from the panel, yet again comfort for the same power input would be decreased.

**IMPACT OF SURFACE CHARACTERISTICS ON PANEL RADIANT OUTPUT:** Carpet, vinyl, plastic, and painted (textured and nontextured) surfaces were used in these experiments. The carpet was a nylon fiber carpet with a pile height of about 1.02 cm (0.4 in). The vinyl floor covering was 0.18 cm (0.07 in) thick. The surface resistance of the carpet and the vinyl surface was calculated from the various tests. Backlosses were nearly eliminated by controlling the back of the panel temperature to the element temperature. Therefore, all the power input to the panel was assumed to be transferred by radiation and convection from the surface of the panel. It should be noted that calculating and offsetting backlosses by adequate insulation is an important part of radiant panel design. For the purposes of these experiments, it was important to completely eliminate backloss in order to establish the fraction of panel output that was radiative and convective.

By measuring the temperature difference across the surface, a resistance value for the surface could be calculated. The results, shown in Table 5.52, agree well with published data and with the values from Table 3 of *HVAC Systems and Equipment* (1996).

For all of the tests, in order to achieve uniform surface temperatures, the surface temperatures of all room surfaces seen by the radiant panel were approximately 25°C (77°F). Although this temperature is higher than would be encountered in real systems, it is not different enough to change the radiative properties of the materials. The

**TABLE 5.52** Calculated Resistance for Carpet and Vinyl

Material	Resistance [W/(m <sup>2</sup> · °C)]	Resistance [Btu/(h · ft <sup>2</sup> · °F)]
Carpet	0.18	1.0
Vinyl	0.028	0.16

results from the experiments are not dependent on the temperatures used in the tests. Temperatures inside the room tended to rise above this control setting, but the surface temperatures were always monitored and recorded. The surface area of the radiant panel was about 2 percent of the total surface area in the room. The emittance of all the surfaces besides the radiant panel was assumed to be 0.9. The emittance of the radiant panel surfaces was taken to be 0.95. This is a very reasonable value, as was discussed in an earlier section.

The surface temperature of the radiant panel will depend on the following six factors:

1. Power input
2. Surface emittance
3. Air temperature
4. Natural convection
5. Temperature of other surfaces in the enclosure
6. Backlosses

For all experiments, power input to the panel and the temperature of the other room surfaces were controlled. As already mentioned, backlosses were eliminated and the radiant panel temperature was measured. Convective heat transfer was calculated from the heat balance.

Figures 5.28 and 5.29 display the surface temperature as a function of panel power for three different radiant panel locations—ceiling, floor, and wall. It is seen from the three figures that the surface temperature at a given power level is nearly the same regardless of the type of surface finish on the panel. For a constant power input and constant room surface temperature, a change in the experimental variable, surface temperature, could only be caused by either a change in the rate of convective heat transfer or a change in the rate of radiative heat transfer. Based on the emittance and diffusivity experiments in the last section, the radiative flux was not

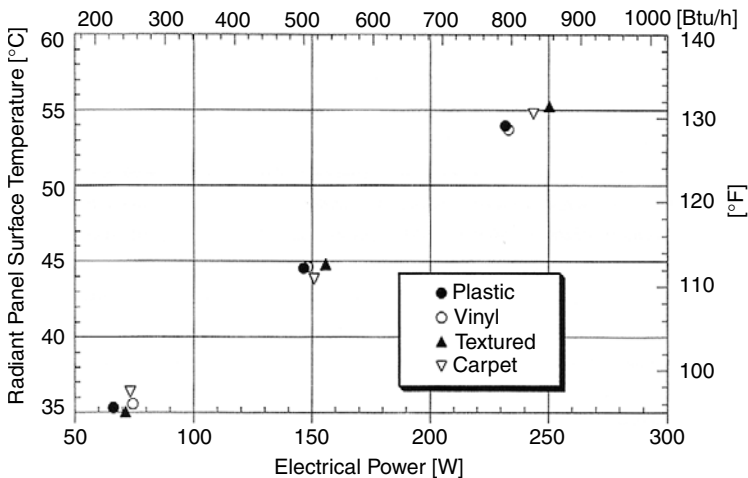


**FIGURE 5.28** Panel surface temperature versus power input into the panels for ceiling panels.

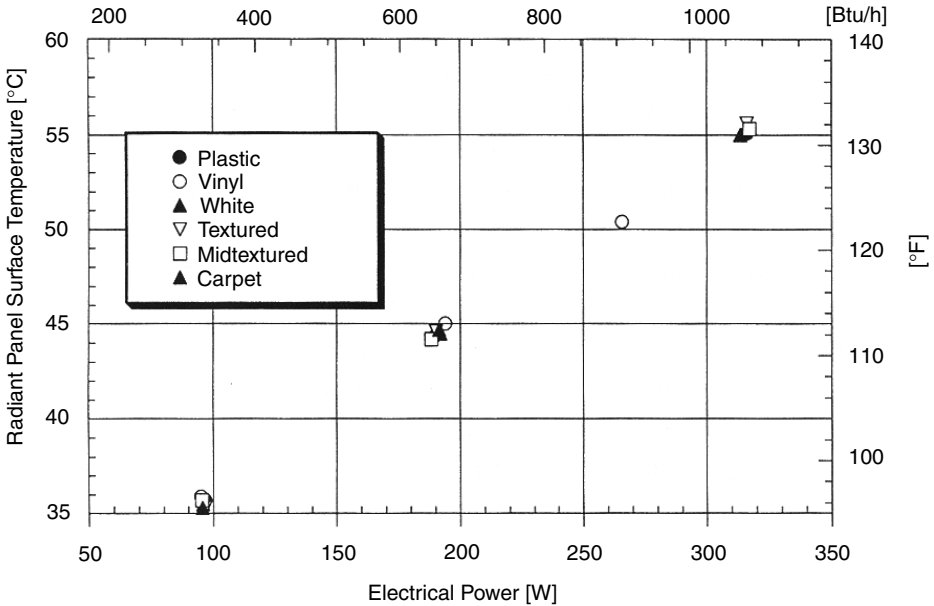
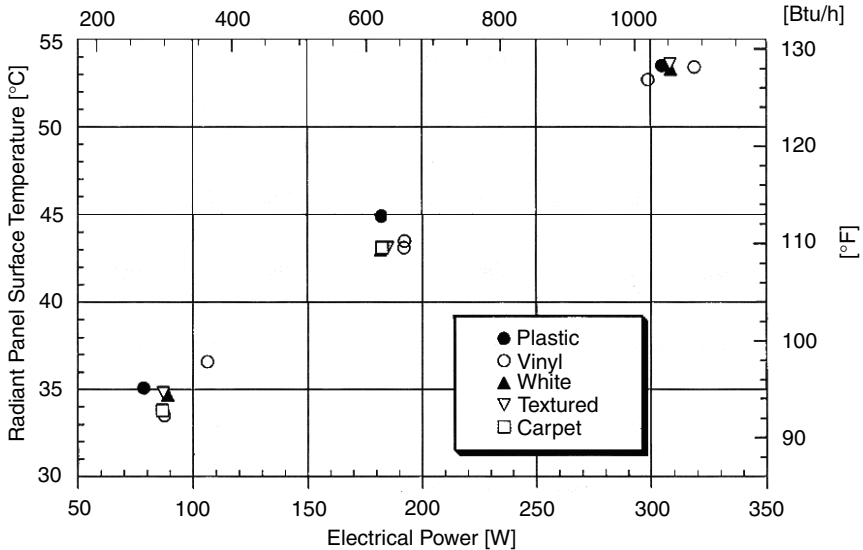


FIGURE 5.29 Panel surface temperature as a function of power input to panel for sidewall tests.

expected to change for different surfaces. Because there was no change in surface temperature for different textures, the plots show that the different surface types were equivalent radiators. They also show that under the natural convection condition in the lab, surface texture had an insignificant effect on the rate of convective heat transfer. The floor tests in Fig. 5.30 show a slight spread in the data, but the wall and floor locations show good agreement between the data.

Several points can be made about the figures. First, texture has no effect on the rate of heat transfer from the surface. The smooth, painted white surface and the textured surface (Figs. 5.28 and 5.29) have the same surface temperature for a given power input. Because the emittance of the white surface is already high, the effect of giving the surface a rough texture is not significant. Second, there is good agreement between all the surfaces supporting the fact that they all have similar radiative properties. The fact that some surfaces were slightly more diffuse does not have any impact, either. Third, it must be noted that the carpet and vinyl surfaces agree with the other surfaces (which have no surface resistance), because backlosses for all surfaces were made negligible. If this were not the case, surface temperature would be a strong function of the surface resistances, (see Fig. 5.31). Finally, the location of the panel does affect the panel output. Nearly 325 W were needed to maintain a surface temperature of 55°C for the wall location as compared with roughly 250 W for the ceiling location. Location has no effect on radiation, because the room has nearly uniform surface temperatures, but location does significantly affect the rate of convective heat transfer. The 30 percent increase in power that was required to maintain the panel surface temperature is due entirely to the increased surface convection at the new orientation. For this reason, it is extremely important to select appropriate convection correlation for each location as discussed in Section 6.6 of ASHRAE RP-876. It is also interesting to note from the three figures, that under the given



**FIGURE 5.30** Panel surface temperature as a function of power input to panel for floor tests.

operating conditions, the surface temperature has a near-linear dependence upon panel power. Though radiation is nonlinear, it exhibits a near-linear response when the range of operating conditions is small.

**SUMMARY OF PANEL OUTPUT EXPERIMENTS:** Although the location of the panel does affect its output, the three sets of experiments illustrate that surface texture does not affect the output of the panel when the surface has a high emittance.

The location of the panel, whether on the floor, ceiling, or wall, will affect the output of the panel by changing the split between the fraction of total power output that is radiated to the room and the fraction of total power that is convected to the room. For the ceiling, the convection-conduction from the panel surface to the air is much less than the natural convection from the floor or wall locations. Table 5.53 compares the percentage of panel output that is radiated for the various tests. For the ceiling, over 90 percent of the panel output is transferred from the panel as radiation. This is a distinct advantage that ceiling radiant systems have over floor systems. For the

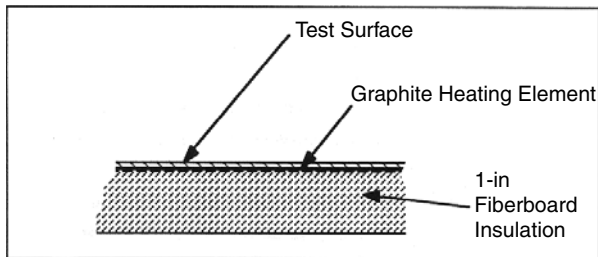


**FIGURE 5.31** Typical cross section of fast-acting radiant heat panel.

**TABLE 5.53** Percentage of Panel Output Due to Radiation for Various Tests

Location— test and surface	Ceiling— % output radiant	Sidewall— % output radiant	Floor— % output radiant
Plastic 35	91.5	75.3	78.7
Plastic 45	92.5	72.5	72.3
Plastic 55	91.1	71.3	70.5
Vinyl 35	93.0	75.5	74.6
Vinyl 45	91.7	72.3	66.1
Vinyl 55	89.7	70.3	67.4
Textured 35	93.1	72.2	72.5
Textured 45	89.4	72.1	68.1
Textured 55	89.3	70.9	68.5
Carpet 35	93.9	71.1	67.3
Carpet 45	87.0	71.7	69.9
Carpet 55	89.4	—	—
White 35	—	74.1	73.9
White 45	—	71.9	70.4
White 55	—	71.2	68.4
Midtexture 35	—	75.6	—
Midtexture 45	—	72.0	—
Midtexture 55	—	71.2	—
Average	91.0	72.4	70.6

floor and sidewall, this percentage is somewhat less. The percent radiant tends to decrease for higher surface temperatures.

The convective-radiative split is a function of the surface emittance and the natural convection from the surface (see Fig. 5.31). If operating conditions are such that the natural convective flow is turbulent, then the percent output that is radiant will be significantly less. For turbulent natural convection from a floor panel, the percent output that is radiant is closer to 50 percent (as compared with around 70 percent for laminar natural convection) and is not highly sensitive to emissivities in the range of 0.8 to 1, as illustrated by the example in Sec. 6.1 of ASHRAE RP-876.

For a radiant system, it is desired that most of the output from the panel be transferred by radiation. By definition, a radiant panel transfers 50 percent or more of its total output by radiation to other surfaces seen by the panel. With the presence of natural convection, it takes more energy to maintain a particular surface temperature. Although convective heat transfer to a zone is not wasted energy, convective heat transfer from the panel will heat the air before heating any of the occupants. Part of the determination of comfort in a conditioned space is the MRT. Natural convection from a panel surface will have a tendency of lowering the MRT.

Because of these reasons, ceiling radiant heating systems are seen to possess some location advantages because natural convection from a ceiling system is typically much less than for a floor or wall heating system. This is of course not to say that floor systems do not possess advantages over ceiling systems. The important conclusion is that the natural convection for a radiant system must be considered because its percentage of the total radiant output can be quite large.

*Research Results and the Simplified Radiant System Design Method.* The radiation heat transfer is the same for a ceiling, floor, or wall panel operating at the same surface temperature, but the convective heat transfer will differ depending

on the particular orientation. The ASHRAE Handbook presents the work of several researchers in developing the equations for natural convection. The panel design method presented in the *HVAC Systems and Equipment Handbooks* (ASHRAE, 1992, 1996) account for natural convection as well as panel resistance and room operating conditions.

The convection correlation presented in the ASHRAE Handbook uses the equivalent diameter,  $D_e$ , which is defined as:

$$D_e = 4 \frac{\text{surface area}}{\text{perimeter}} \tag{5.33}$$

The ASHRAE Handbook natural convection equations are:

S.I. units (W/m <sup>2</sup> )	English units [Btu/(h · ft <sup>2</sup> )]
$q_{pc} = 0.20(T_p - T_a)^{1.25} / D_e^{0.25}$ (ceiling) (5.34)	$q_{pc} = 0.04(T_p - T_a)^{1.25} / D_e^{0.25}$ (ceiling)
$q_{pc} = 2.42(T_p - T_a)^{1.31} / D_e^{0.08}$ (floor) (5.35)	$q_{pc} = 0.39(T_p - T_a)^{1.31} / D_e^{0.08}$ (floor)
$q_{pc} = 1.87(T_p - T_a)^{1.32} / H^{0.05}$ (wall) (5.36)	$q_{pc} = 0.29(T_p - T_a)^{1.32} / H^{0.05}$ (wall)

where:  $q_{pc}$  = heat transfer by natural convection [W/m<sup>2</sup> or Btu/(h · ft<sup>2</sup>)]  
 $T_p, T_a$  = temperature of panel surface and air, respectively (°C or °F)  
 $D_e$  = Equivalent diameter = 1.04 m (3.41 ft) for the test panels  
 $H$  = height of wall panel (m or ft)

The design procedure basically solves the surface heat balance:

$$\frac{T_e - T_p}{R_{\text{surface}}} = q_{pr} + q_{pc} \tag{5.37}$$

Using data from the ceiling panel experiments, new coefficients were calculated to yield the following set of equations:

S.I. units (W/m <sup>2</sup> )	English units [Btu/h · ft <sup>2</sup> ]
$q_{pc} = 0.198(T_p - T_a)^{1.25}$ (5.38)	$q_{pc} = 0.031(T_p - T_a)^{1.25}$
$q_{pr} = 0.95\sigma[(T_p + 273)^4 - (T_\infty + 273)^4]$ (5.39)	$q_{pr} = 0.95\sigma[(460 + T_p)^4 - (460 + T_\infty)^4]$
where $\sigma = 5.67e - 8 \text{ W/(m}^2 \cdot \text{K}^4)$	where $\sigma = 0.174e - 8 \text{ Btu/(h} \cdot \text{ft}^2 \cdot \text{°R}^4)$

where  $T_e$  = element or water temperature (°C or °F)  
 $T_a$  = reference air temperature (AUST was used)  
 $T_\infty$  = Temperature of “fictitious” surface (AUST was used)

The main drawback of the design procedure is that it obscures the importance of the overall heat balance in the panel design problem. The design graphs show panel output as a function of element temperature for various panel resistances. The procedure assumes a constant, known backloss, which, given the diversity of radiant application, is in general not a good assumption. A heat balance-based design procedure, by accounting for all heat flow paths from the radiant panel, ensures that all environmental parameters are properly accounted for.

During the ceiling experiments, the temperature of the surface and the heating element were both measured. The power input to the panel was also measured. Because backlosses were made to be negligible, it is assumed that all the power input into the panel is transferred by natural convection and radiation. Figure 5.32 shows

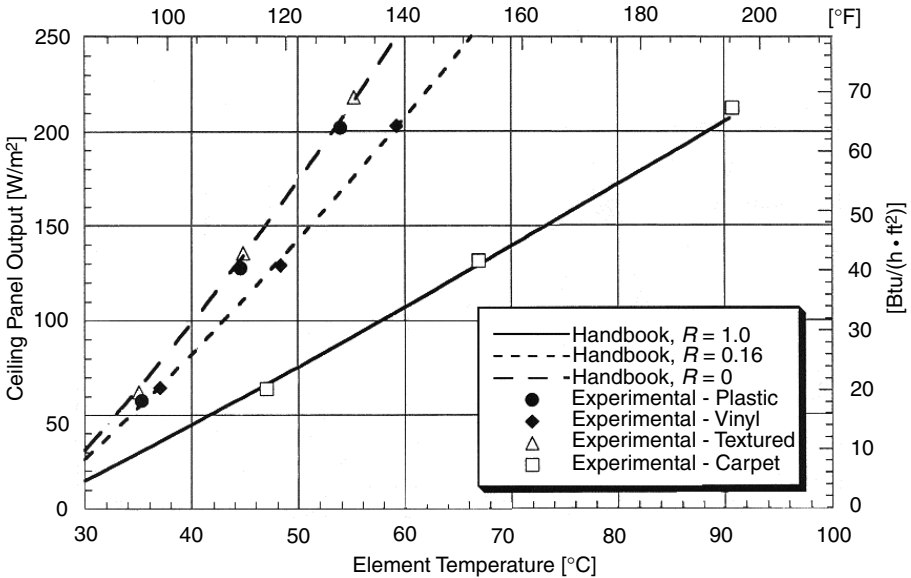


FIGURE 5.32 Ceiling panel design graph and experimental results.

the experimental results along with the curves generated from the ASHRAE Handbook equations. For both the plastic surface panel and the textured surface panel, the resistance of the surface was taken to be zero.

The ASHRAE Handbook curves shown in Fig. 5.32 were generated using the equations listed earlier. During the course of testing a particular surface using different surface temperatures, the AUST would tend to rise. To present the data using a single curve, the average AUST (average of three tests) for a particular surface was used.

The experimental data agree quite well with the ASHRAE Handbook predictions. Because the room geometry is not complex, a two-surface exchange model using the AUST works well in predicting the radiation exchange. Additionally, the AUST for these conditions can be used in predicting the natural convection. This is not a proof that the AUST can always be used as a convection reference temperature. For the ceiling, the convection is only on the order of 10 percent of the total heat transfer from the panel surface. The experimental data for this project therefore agree well with the equations in the ASHRAE Handbook for a ceiling panel. The results also compare well with Fig. 10 in the 1996 *HVAC Systems and Equipment Handbook* (ASHRAE, 1996).

What is also immediately obvious is that surfaces having a higher surface resistance have a higher element temperature. Note that at the highest output, the carpet element temperature is around 90°C. The surface temperature for this test was around 55°C. These results are within the range of carpet thermal resistance data shown in Tables 5.56 and 5.57.

To predict the total power transferred from the panel it is necessary to know the operating conditions of the room, the surface resistance, surface emittance, and an appropriate correlation for the natural convection. The carpet and the vinyl surface have a different surface texture, yet their output can be predicted with knowledge of the preceding information.

The experimental results of the floor and wall tests were similar. Because these tests were run in a sealed room, the wall temperatures tended to rise above the set point temperature of 25°C (77°F). To compare the experimental results with the Handbook equations, the average AUST for a particular surface was used as an approximation for the surface and air temperatures. The element temperature is the independent parameter.

The natural convective heat transfer from the panels during a test was determined by subtracting the radiant heat transfer from the total panel power. This is a reasonable method because backlosses were made negligible. The natural convective correlations resulting from the floor and sidewall experiments follow:

S.I. units (W/m <sup>2</sup> )	English units [Btu/(h · ft <sup>2</sup> )]
$q_{pc} = 1.37(T_p - T_a)^{1.25}$ (floor) (5.40)	$q_{pc} = 0.212(T_p - T_a)^{1.25}$ (floor correlation)
$q_{pc} = 1.23(T_p - T_a)^{1.23}$ (wall) (5.41)	$q_{pc} = 0.190(T_p - T_a)^{1.23}$ (wall correlation)

The experimental correlations are significantly different from those presented in chap. 6 of the Handbook. The difference primarily stems from the fact that the handbook correlation is based on turbulent flow conditions. The experimental results indicated that laminar conditions existed in the laboratory. Figures 5.33 and 5.34 show that the experimental data fit the laminar correlation quite well. Although these correlations are not generally applicable, they do indicate the need for additional research to establish guidelines for the application of natural convection correlation to radiant heating systems. Section 6.4 compares the natural convection correlation in detail, but it is appropriate here to note the difficulty of applying a single convection correlation to all room configurations. In addition to flow regimes, geometry and room surface temperatures also significantly affect the rate of convective heat transfer.

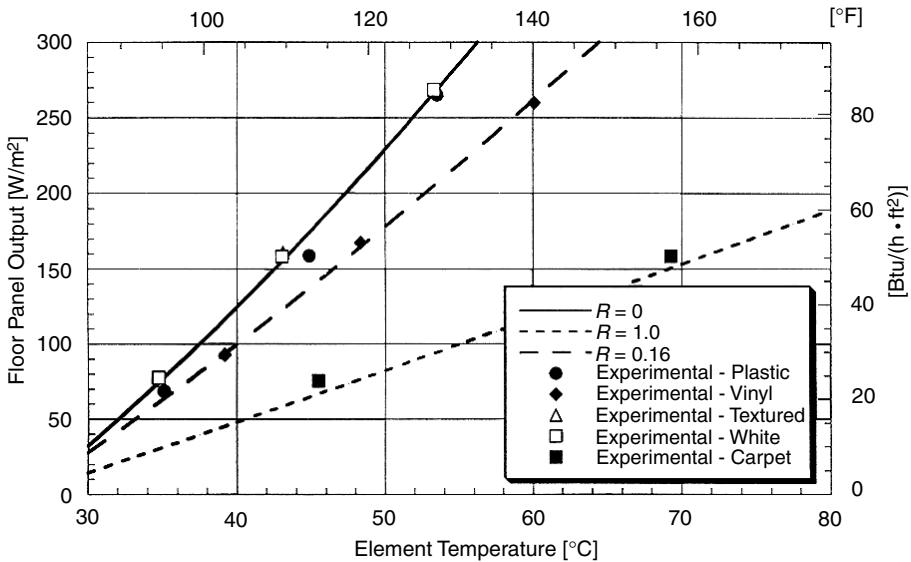


FIGURE 5.33 Floor panel design graph and experimental results.

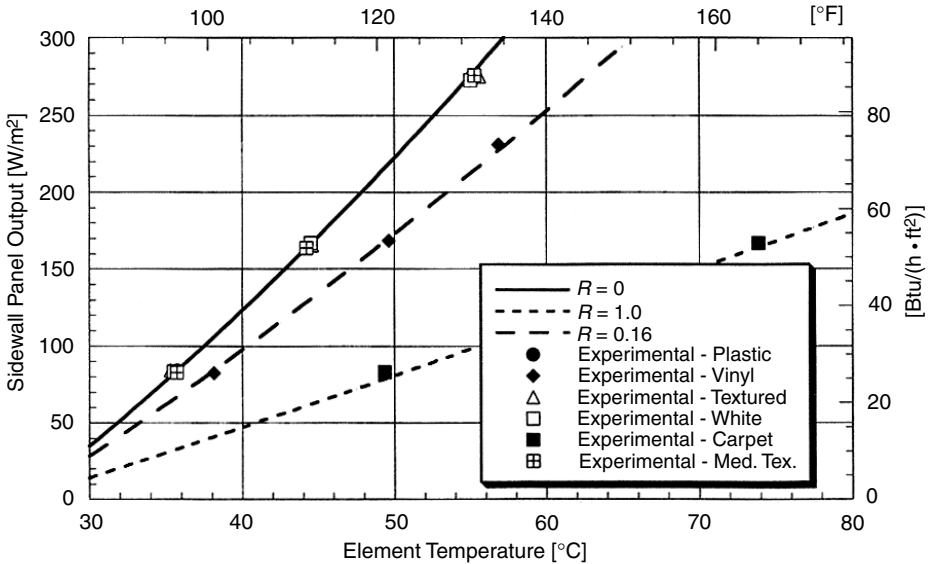


FIGURE 5.34 Sidewall design graph and experimental results.

As shown in Figure 5.35, the radiant flux accounts for approximately 70 percent of the total panel output for the experimental conditions in the laboratory. Under the same conditions, the Handbook correlations predict a radiant flux that is only slightly greater than 50 percent of the total panel output—a difference of 20 percent. This significant difference is directly attributable to the differences in convective correlations.

Figures 5.33 and 5.34 corroborate the ceiling test results, showing that all surface types tested were equivalent radiators. The plastic surface panel, white painted panel, and the textured surface panel had essentially the same output for a given surface temperature. Though the surfaces have a different texture, the radiative properties of the surfaces are nearly the same, and therefore the output from the two surfaces is the same. The differences in the macroscale properties of the surfaces do not affect the panel output, because the surfaces have similar radiative properties. On a surface-by-surface basis, they are found to agree well. This agreement is especially good for the wall tests, where the difference between points is seen to be very small (see Fig. 5.36). The convective flux from the surfaces seems to therefore be independent of the macroscopic properties of the surface Fig. 5.37. Surface texture, which intuitively might be selected as an important parameter in selecting a correlation, is shown to have negligible effect.

#### Natural Convection Discussion

BRIEF REVIEW OF EXISTING CORRELATION: As other researchers have noted, convection is the least understood fundamental heat transfer process. There are several difficulties in addressing natural convection inside of buildings.

1. Although there has been a great deal of work in developing natural convection correlation, the conditions under which the correlation was developed often do not match typical conditions inside a building. In addition, most of the natural

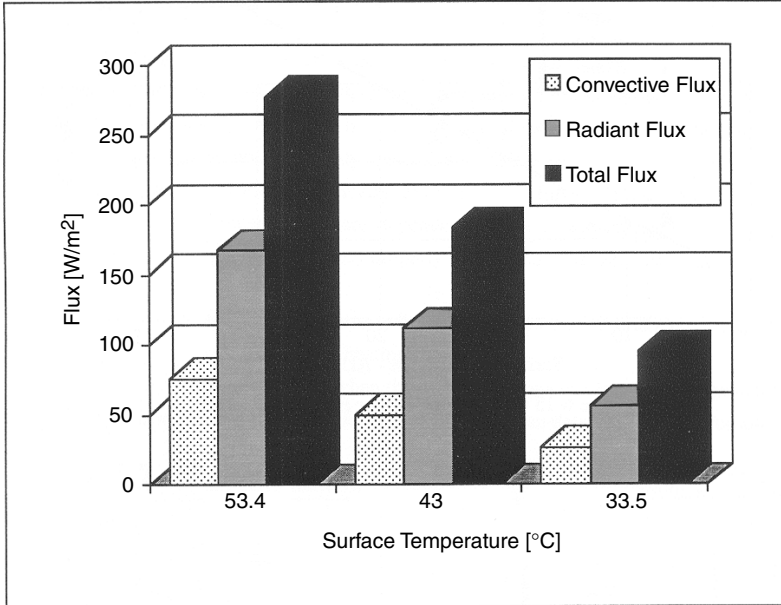


**FIGURE 5.35** Distribution of total flux for three different surface temperatures data are representative of a typical floor test.

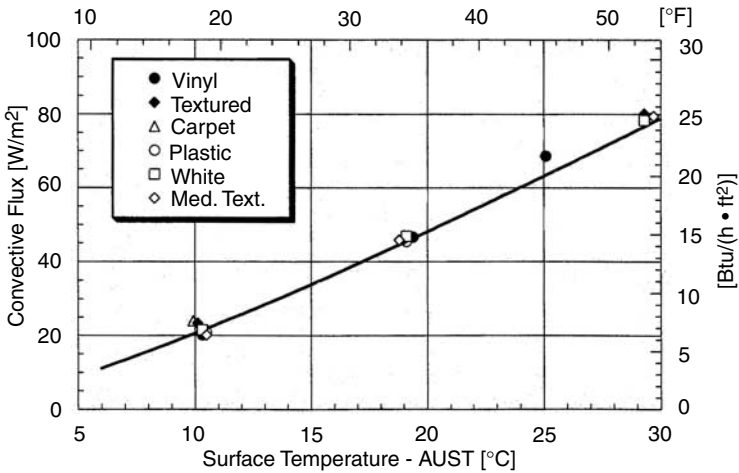


**FIGURE 5.36** Convective flux for wall panel.

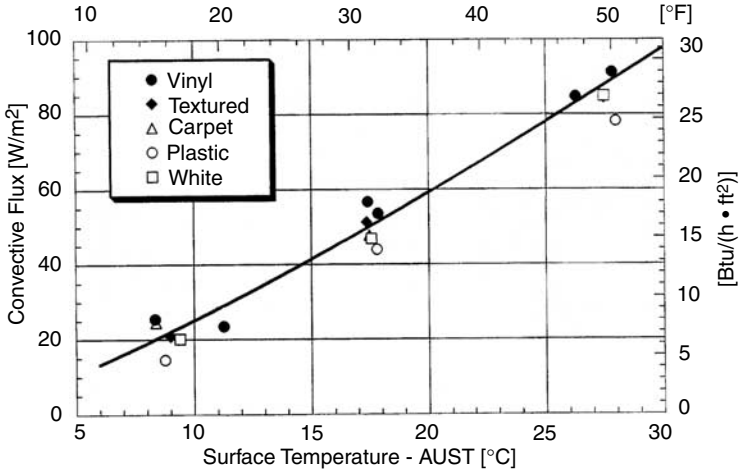


FIGURE 5.37 Convective flux for floor panel.

convection correlation are for free surfaces and are not necessarily applicable to surfaces inside an enclosure.

2. Even correlation specifically developed for full-scale enclosures are often not generally applicable, because they are dependent on the conditions under which they were developed. That is, they have not been properly nondimensionalized (see Figures 5.38 and 5.39).
3. The work done by Min seems to be the only research that looks specifically at natural convection in enclosures with radiant heating systems.

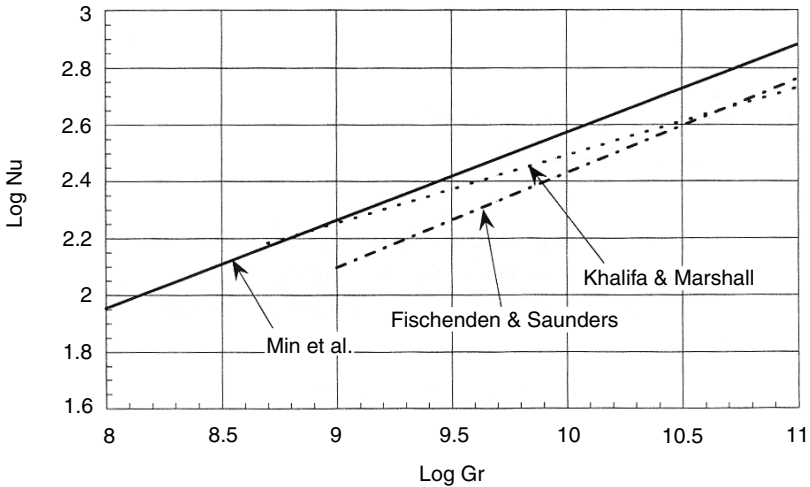


FIGURE 5.38 Natural convection correlations for horizontal surfaces facing upward.

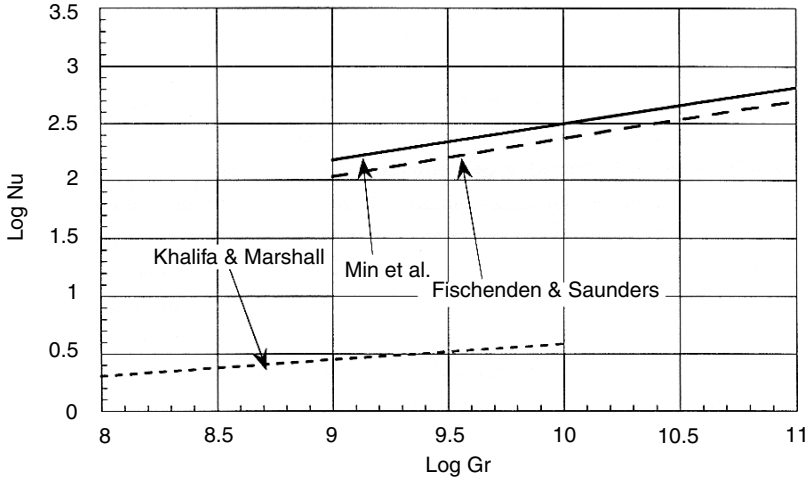


FIGURE 5.39 Natural convection correlations for vertical surfaces.

4. It is not fully understood when the flow conditions inside an enclosure will transition from laminar to turbulent. For an enclosure, the geometry can delay the onset to turbulence.

Buoyancy forces drive the flow in natural convection. Correlation is usually of the form

$$\overline{Nu}_L = \frac{\overline{h}L}{k} = CRa_L^n \quad (5.42)$$

where the Rayleigh number ( $Ra$ ) is related to the Grashof number ( $Gr$ )

$$Ra_L = Gr_L Pr = \frac{g\beta(T_s - T_a)L^3}{\nu\alpha} \quad (5.43)$$

For natural convection, the important parameter is the Rayleigh or Grashof number. It is used to predict whether the buoyantly driven flow is laminar or turbulent. Table 5.54 shows several natural convection correlations for unconfined natural convection flow from horizontal and vertical surfaces.

TABLE 5.54 Natural Convection Correlations for Unconfined Natural Convection Flow from Horizontal and Vertical Surfaces

	Laminar	Correlation	Turbulent	Correlation
Floor	$10^4 \leq Ra_L \leq 10^7$	$\overline{Nu}_L = 0.54 Ra_L^{1/4}$	$10^7 \leq Ra_L \leq 10^{11}$	$\overline{Nu}_L = 0.15 Ra_L^{1/3}$
Wall	$0 \leq Ra_L \leq 10^9$	$\overline{Nu}_L = 0.59 Ra_L^{1/4}$	$Ra_L \geq 10^9$	$\overline{Nu}_L = 0.10 Ra_L^{1/3}$

Source: Incropera, 1990.

As Dascalaki noted (1994), most of the correlations for unconfined flow have good agreement. ASHRAE has several correlations in the various handbooks. The *Handbook of Fundamentals*, in Chap. 3, presents a number of correlations. Chapter 6 of *HVAC Systems and Equipment* presents several correlations applicable for radiant panels. These correlations were the result of Min's work (1956).

Experimental results (by Min, Dascalaki, etc.) clearly illustrate the difference between convection heat transfer from enclosures and unconfined surfaces. Though Dascalaki presents a number of correlations, not many were developed in full-scale rooms. The following figures compare just three of the correlations for vertical and horizontal surfaces. The Fisheden correlation is for an unconfined surface, and the Min and Khalifa correlations are for enclosures.

On a log-log plot, the Min correlations seem to agree with the often-quoted Fisheden and Saunders correlation as shown in Fig. 5.38. Yet the Min correlation for horizontal surfaces at a  $Gr \approx 1E-10$  is almost 50 percent greater than the Fisheden correlation. For vertical surfaces, the Min correlation is 30 percent greater at a  $Gr \approx 1E-10$ . The correlation by Khalifa and Marshall developed for a vertical surface in an enclosure is also shown in Fig. 5.39. It is an order of magnitude less than both of the other correlations. This disparity of results makes it difficult to know what correlation is applicable for a given situation.

**EXAMINATION OF EXPERIMENTAL RESULTS:** A cursory examination of the enclosure natural convection literature reveals a large number of papers presenting unique correlations for every imaginable geometric and surface temperature configuration. The sheer number of correlations highlights the magnitude of the problem; it is virtually impossible to specify a generally applicable correlation for convection heat transfer in enclosures. Natural convection in a room with a heated floor, one cold wall, three warm walls, and a warm ceiling cannot be accurately described by correlations developed for heated-wall or heated-ceiling configurations. Cold spots (e.g., windows) on otherwise warm walls further disturb the flow field, leading to additional sets of unique correlations. Furthermore, for each unique configuration, there are two possible correlations: one for the laminar flow regime and one for the turbulent flow regime.

The experimental data presented in this section were for a single radiant panel, which covered approximately one-ninth of the total wall or floor surface area. The panel was mounted in the center of the wall or floor, respectively, and radiated to an enclosure at a uniform temperature. Thus, the buoyant plume from the radiant panel provided the sole driving force to the recirculating flow in the enclosure. Min's correlations, which are presented in Chap. 6 of the Handbook (and in Sec. 6-3 of RP-876), are based on a substantially different configuration.

Min used the entire floor as a radiant surface, whereas for the RP-876 experiments, the radiant panel is only  $1.15 \text{ m}^2$  and covers one-ninth of the floor. Though in the Min experiments the size of the floor panel was varied, the entire floor area was always used as a radiant panel. The temperature difference between the panel surface and air temperature was also greater for Min's tests. The Rayleigh number range used in the Min experiments was from about  $3.16 \times 10^{10}$  to  $20 \times 10^{10}$ , indicating a turbulent flow regime. (Note the exponent on the Min equations for the floor and wall shown in Sec. 6-3 of RP-876.) The RP-876 experimental data were within the laminar regime.

In developing correlations for vertical surfaces, the Min experiments never used the wall as the radiant surface. The vertical surface correlation is based on natural convection to the wall from a heated floor or ceiling. Wall heights of 8 and 12 ft were used. The characteristic length then is significantly larger than the characteristic length in the present experiments. The characteristic length in this research project

was the width of the panel, which is much smaller than the correlating length in the Min experiments. A greater characteristic length leads to higher Rayleigh numbers, which are indicative of turbulent flow.

Given the significant differences in both configuration and flow regime, it is not surprising that the RP-876 natural convection results cannot be directly compared with the Min correlations shown in the Handbook. They are rather compared with unconfined flow laminar correlations.

Figures 5.40 and 5.41 display the Nusselt number plotted as a function of the Rayleigh number for the floor and wall panels. Table 5.55 lists the information used in developing the correlation. The data not only show excellent agreement with the two-laminar correlation, but also are quite consistent, even at extremely low Rayleigh numbers (very small convective fluxes). Although the purpose of this research was not to develop convection correlation (a much larger parametric set of experiments is needed to establish with reasonable certainty a new set of natural convection correlations), the exercise does provide useful information for future convection research:

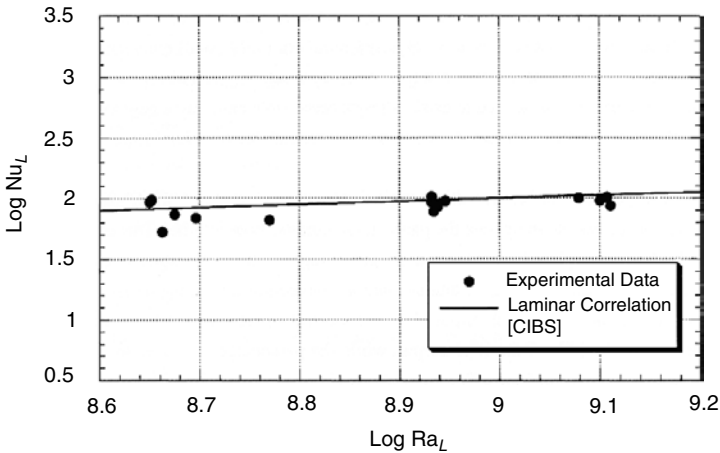


**FIGURE 5.40** Nusselt number versus Rayleigh number for floor tests.

1. For low-temperature radiant panels where the radiant panel covers a small percentage of the room surface, it is possible to operate the panel in the laminar flow regime. The advantage of operating in the laminar regime is that the radiant percentage of the total output is greater than when operating in a turbulent regime. Laminar natural convection output for a ceiling panel is approximately 10 percent of the total panel output. Laminar natural convection output for a wall or floor system is approximately 30 percent of the total output, whereas the percentage increases to nearly 50 percent for turbulent natural convection from a floor or wall panel.
2. Selection of appropriate-length scales is critical to the development of valid and useful correlation. Bejan (1984) provides an excellent discussion in this regard. For engineering calculations, an appropriate-length scale is one that is generally accessible to practitioners.

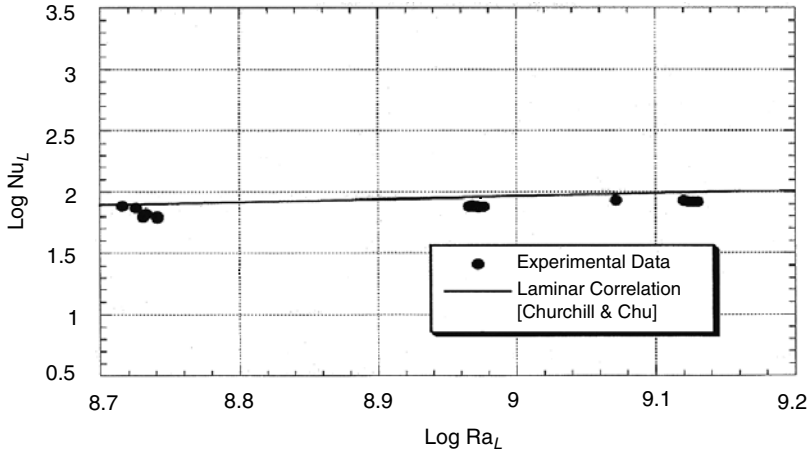


**FIGURE 5.41** Nusselt number versus Rayleigh number for wall tests.

3. In designing natural convection experiments for radiant applications, thoughtful consideration must be given to surface temperature and geometric configurations. Mixed convection configurations should also be considered.

*Forced-Convection Results.* Although most radiant systems operate primarily under natural convection conditions, higher air speeds may occur in drafty rooms or in zones conditioned by hybrid systems. Under these conditions, forced-convection heat transfer correlation (rather than natural convection correlations) should be used to predict the radiation-convection split of the panel output. With few exceptions, forced-convection correlations are based on the Reynolds number, a dimensionless parameter that presumes some knowledge of air speeds in the vicinity of the radiant panel.

The forced convection experiments performed under RP-876 were designed to answer two questions: (1) Does surface texture significantly affect the rate of forced-convection heat transfer at low air speeds up to 1.0 m/s (200 fpm)? (2) How significant is the error that might result from using natural convection correlation to design radiant systems that end up operating under forced-convection conditions?

Figure 5.42 shows the typical magnitude of the convective and radiative fluxes for the 25°C and 30°C surface temperature tests.

**TABLE 5.55** Information for Experimental Correlations

	Horizontal surface*	Vertical surface
Reference temperature	AUST	AUST
Correlating length	Panel width = 0.84 m	Panel width = 0.84 m
Ra <sub>L</sub> range	5 × 10 <sup>8</sup> –1.3 × 10 <sup>9</sup>	5 × 10 <sup>8</sup> –1.3 × 10 <sup>9</sup>
Comparison correlation	$\bar{Nu}_L = 0.56Ra_L^{1/4}$	$\bar{Nu}_L = 0.68 + 0.47 Gr^{1/4}$

\**Source:* CIBS.

†*Source:* Churchill and Chu.

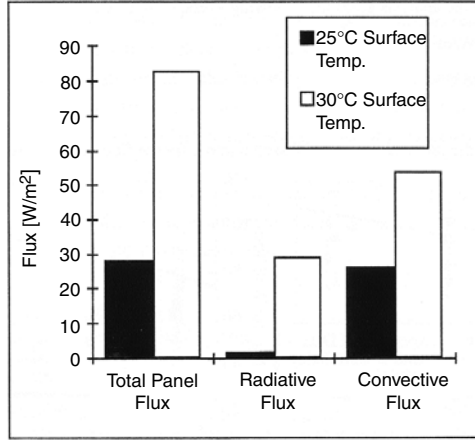


**FIGURE 5.42** Typical magnitudes of fluxes for forced-convection experiments.

**EFFECT OF SURFACE TEXTURE:** The results of the forced-convection experiments are shown in Fig. 5.43. The figure plots the heat transfer coefficient as a function of Reynolds number. For comparison, an “enhanced turbulent” correlation is also shown in the figure. This enhanced correlation is 40 percent greater than a standard turbulent solution. Several researchers found that free-stream turbulence could increase the heat transfer rate by 20 to 40 percent (Blair, 1983; Young, 1991). The data convincingly demonstrate that surface texture has no effect on the forced-convection heat transfer at air speeds up to 1 m/s. Thus forced-convection correlations can be used with confidence on surfaces of varying texture for surface air speeds ranging from near zero (natural convection) to air speeds as high as 1.0 m/s.

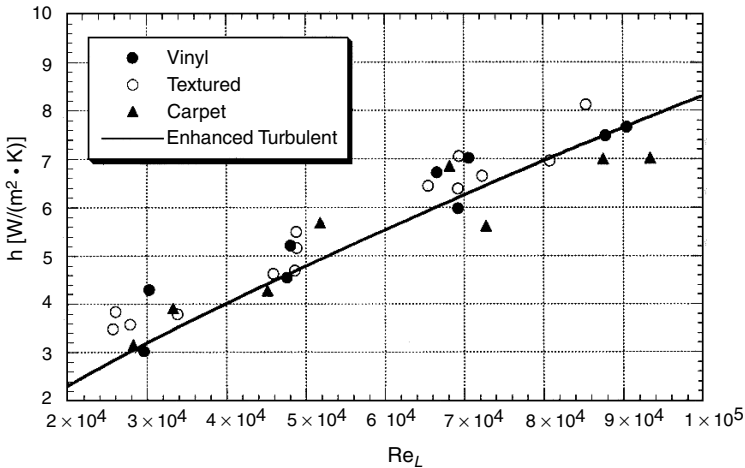


**FIGURE 5.43** Convective heat transfer coefficient versus length Reynolds number with turbulent solutions also displayed.

**PANEL OUTPUT:** Typically, natural convection correlations are used in radiant panel system design regardless of the actual operating conditions of the panel. To bracket the expected error associated with the misapplication of the natural convection correlations, experimental results for natural and forced-convection conditions were compared. Figure 5.44 compares the forced-convection data with the natural convection floor data. The figure shows the panel surface temperature obtained for a given power input for the forced-convection data and for several natural convection data. From Fig. 5.43 it is seen that the convective heat transfer coefficient for an air velocity of 1 m/s is approximately  $7.5 \text{ W}/(\text{m}^2 \cdot ^\circ\text{C})$ . For natural convection, the convective heat transfer coefficient was approximately  $2.5 \text{ W}/(\text{m}^2 \cdot ^\circ\text{C})$ . (The coefficient would be higher if the natural convection from the panel was turbulent as described by the ASHRAE Handbook equations.) An example similar to the one previously given will further explain the importance of the forced-convection results.

As in the previous example, consider a radiantly heated concrete floor. Assume that the wall, ceiling, and air temperatures are all equal. Additionally, assume that the natural convection from the floor can be predicted using the ASHRAE Handbook equations (Chap. 6 of the *HVAC Systems and Equipment Handbook*), and that the radiative exchange can be modeled using a two-surface model ( $\epsilon_{\text{surface}} = 0.95$ ). Now, what will the effect of natural convection be (in comparison with forced convection) on the performance of the system. As in the previous example, the air temperature and the temperature of the unheated surfaces were equal to  $15^\circ\text{C}$ . For forced convection, assume that a worst-case scenario yields a convection heat transfer coefficient of  $7.5 \text{ W}/(\text{m}^2 \cdot ^\circ\text{C})$ . Based on the experimental results, this would correspond to an air velocity of approximately 1.0 m/s.

Figure 5.45 shows the impact that forced convection has in lowering the radiative percentage of the total output. For the natural convection case, as the total panel output increases, the radiative percentage decreases. The reason for this is as follows. As the total panel flux increases, the surface temperature correspondingly increases. For this temperature range (approximately  $30^\circ\text{C}$ ), the natural convection heat transfer

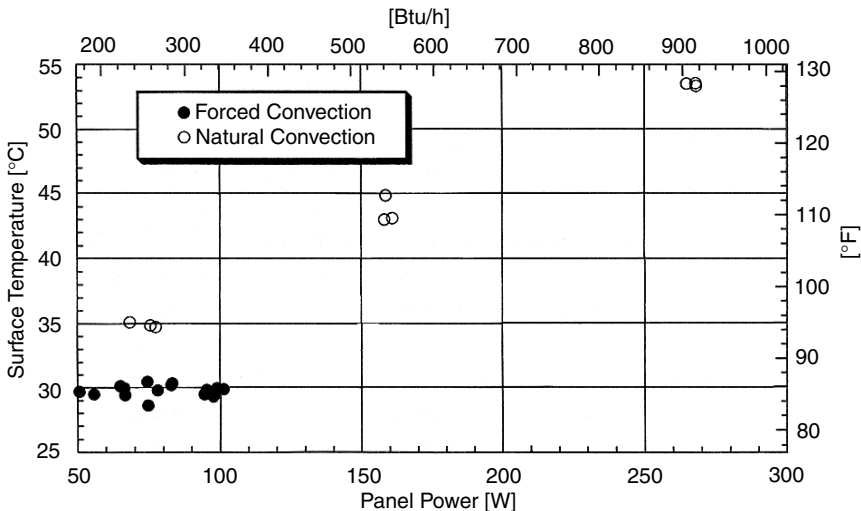


**FIGURE 5.44** Comparison of natural and forced-convection results.

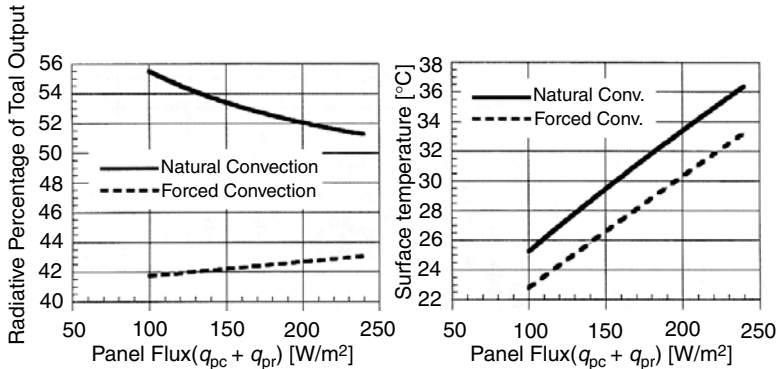


**FIGURE 5.45** Surface temperature as a function of panel output under forced- and natural convection conditions.

increases at a larger rate than the radiation heat transfer in this range. With forced convection, the opposite is true. The reason is that forced convection increases linearly with an increase in surface temperature, whereas the radiation increases at a rate proportional to the surface temperature to the third power.

An examination of Fig. 5.45 reveals that at a panel flux of 100 W/m<sup>2</sup>, there is a difference of nearly 14 percent in the percentage of radiant output. This difference decreases to approximately 8 percent at higher total panel fluxes. Therefore, selecting a natural convection correlation for air speeds of 1.0 m/s and greater can lead to a significant error in the calculated radiant panel output.

**ERROR ANALYSIS:** A simple error analysis will also prove helpful in understanding the data. The uncertainty in the average heat transfer coefficient can be calculated using the following uncertainty equation.

$$e_h \left[ \left( \frac{\partial h}{\partial q_{\text{conv}}} e_{q_{\text{conv}}} \right)^2 + \left( \frac{\partial h}{\partial \Delta T} e_{\Delta T} \right)^2 \right] \quad (5.44)$$

where:

$$\frac{\partial h}{\partial q_{\text{conv}}} = \frac{1}{\Delta T} \quad \text{and} \quad \frac{\partial h}{\partial \Delta T} = \frac{-q_{\text{conv}}}{\Delta T^2} \quad (5.45)$$

Reasonable uncertainty values for the uncertainties in the temperature difference and the convective flux are:

$$e_{\Delta T} = 1^\circ\text{C} \quad \text{and} \quad e_{q_{\text{conv}}} = 3 \text{ W/m}^2$$

Figure 6-26 in RP-876 displays the convective coefficients and their uncertainties as a function of Reynolds number.

Figure 6-26 in RP-876 shows the uncertainty that is associated with the measurements. Larger uncertainties result from relatively small temperature difference between the surface and air temperature. Additionally, the convective fluxes for some of the tests were quite small (on the order of 15 W/m<sup>2</sup>). Smaller uncertainties are associated with the higher surface temperature tests. These tests had a temperature difference nearly twice as large as the 25°C temperature tests. It can also be seen that the spread in the data is within the uncertainty range.

*Summary of Convection Results.* There is still much work to be done in the development of convection correlations for radiant applications. Although correlations exist for many configurations, the applicability of these correlations to the unique set of boundary conditions found in many radiant applications has not been checked. Several things are immediately apparent from the preceding discussion:

1. Convection heat transfer coefficients must be selected for each surface based on its orientation and room airflow conditions. A single coefficient indiscriminately applied to room surfaces without regarding its location and the flow conditions in the room can result in significant error in the calculation of the radiant-convective split for the total panel output.
2. There can be a significant difference between laminar and turbulent correlation for the same type of flow. Any estimate of the flow conditions in the room should include an estimate of the Reynolds number (dimensionless velocity), which will determine the applicability of laminar or turbulent correlation.
3. The available convection correlation represents reasonable approximations and should be used with caution in sizing calculations. Additional research is required in this area to broaden the applicability of convection correlation to include the full range of standard radiant panel applications.

Until the research has been completed, designers of radiant systems should proceed with caution using the best available information to estimate the rate of convection heat transfer from radiant surfaces.

*Ventilated and Drafty Rooms.* For radiant applications in mechanically ventilated and drafty rooms, flat-plate forced-convection correlations offer the best approximation of surface heat transfer. The main drawback of this correlation is that they require the designer to estimate both the air velocity and the air temperature in the vicinity of the surface. The air temperature can often be estimated with relative certainty; air speeds on the other hand are difficult to estimate with any degree of certainty. If air speeds are available, a straightforward procedure can be implemented to calculate the convective heat transfer as follows:

1. Calculate the Reynolds number for the surface where:  
for air where:  
 $\nu$  is the kinematic viscosity in  $\text{ft}^2/\text{s}$   
 $U$  = air velocity in  $\text{ft}/\text{s}$   
 $L$  = the characteristic length in  $\text{ft}$
2. Calculate the Nusselt number for the surface where:  
for  $\text{Re} < 500,000$   
for  $\text{Re} > 500,000$   
for air (is the thermal diffusivity)
3. Convert the Nusselt number to a convective heat transfer coefficient for air.
4. Use the heat transfer coefficient to calculate the rate of convection heat transfer.

*Natural Convection.* A similar procedure can be used for natural convection using the equations presented in Table 5.54. For these correlations, a Rayleigh number [Eq. (5.43)] is calculated instead of a Reynolds number. Alternatively, the ASHRAE Handbook correlations shown in Eqs. (5.34) through (5.36) can be used to provide a reasonable estimate of natural convection heat transfer for most room configurations. It should be noted that these correlations might be applied only to radiantly heated surfaces.

The critical parameter in calculating natural convection heat transfer is the location of the radiant panel in the room. For example, using Eq. (5.34), the rate of convective heat transfer from a 5- × 5-ft radiant ceiling panel operating at 100°F in a 65°F room is 2.3 Btu/(h · ft<sup>2</sup>). For the sake of comparison, assume the same configuration located on the floor. For this configuration, the rate of convection heat transfer [using Eq. (5.35)] is 36.1 Btu/(h · ft<sup>2</sup>)—nearly 16 times the rate of convection heat transfer from the ceiling. This illustrates the importance of designing radiant panels and surfaces with location appropriate convection correlation. It should be noted that the Min correlations (1956) in general predict higher convection rates than some other natural convection correlation. Additional research is required to obtain an optimal set of correlations for radiant heating and cooling applications. Regardless of which correlation is used, the difference between ceiling and floor convection rates is large. It is a serious mistake to neglect location when selecting a natural convection correlation.

*Relative Significance of Surface Emittance and Thermal Resistance.* The impact of emittance on surface radiative output has been discussed in detail in the preceding chapters. It was shown that the potential impact of variable convection coefficients on the rate of radiation heat transfer is much greater than the potential impact of variable emittance for nonmetal building materials. This chapter illustrates that the potential impact of variable thermal resistance is also much greater than the potential impact of variable emittance.

Figure 9 in Chap. 6 of the *HVAC Systems and Equipment Handbook*, (1992 edition) shows the combined heat transfer for ceiling and floor panels, respectively. (This figure is not in the 1996 edition.) The figure shows the effect of the surface resistance. The figure is based on only one particular interchange factor,  $F_e$ . The interchange factor, defined earlier in the report, is a function of the surface emittance. Figures 5.46 and 5.47 show the effect of the surface emittance for the conditions of a room air temperature of 21.1°C (70°F). Applying the analysis and equations from Chap. 6 in the *HVAC Systems and Applications Handbook* derives the two figures. Two families of curves are shown for a surface having an  $R$  value of 1.0 and 0.1 ( $R = \text{Btu}/(^\circ\text{F} \cdot \text{h} \cdot \text{ft}^2)$ ).

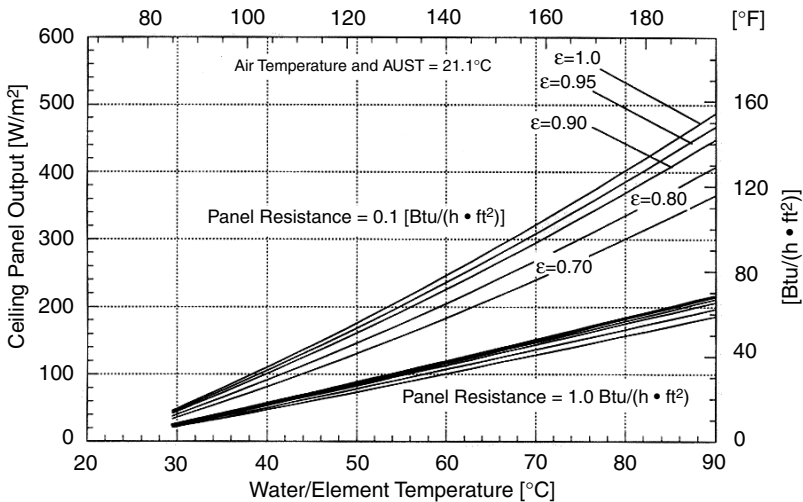
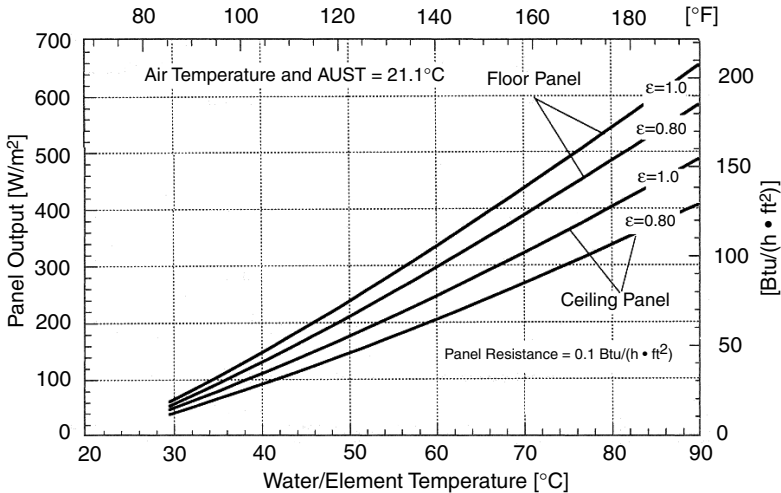


FIGURE 5.46 Ceiling panel design graph showing effect of emittance and resistance.



**FIGURE 5.47** Ceiling and floor design graph showing effect of emittance and resistance.

Figure 5.46 shows that the potential impact of surface resistance on panel output is far greater than the potential impact of surface emittance. The surface emittance has the greatest impact when the surface resistance is small. The percentage difference in panel output between an emittance of 0.90 and 0.7 is about 28 percent for a surface resistance of 0.1. For a surface resistance of 1.0, the percentage difference for the same emissivities is approximately 14 percent. A change in surface resistance from 1.0 to 0.1—a change that can be realized just by changing carpets, as shown in Table 5.56, nearly doubles the panel output! Compared with surface resistance, the surface emittance is therefore a secondary factor in determining ceiling panel output.

Figure 5.47 looks at the results at the effect of emittance for both a floor and ceiling panel and a surface resistance of 0.1. It can be seen that for a floor panel, the effect of emittance is smaller because the effect of natural convection is more significant in terms of panel output.

It should be stressed that both Figs. 5.46 and 5.47 assume a set of environmental conditions and backlosses. With no backlosses, the effect of surface resistance is a significant problem. Both figures show that to obtain the same output with a lower emissivity, the water-heating element temperature needs to be increased. As this temperature increases, backlosses also increase. Table 5.57 shows surface resistances for a number of common materials.

One surface covering that can have a wide range of  $R$  values is carpet. Tables 5.56 and 5.58 show typical  $R$  values for carpet and carpet padding. Though carpets can have a wide range of  $R$  values, their radiative properties are very similar—all have emissivities between 0.90 and 1.0. Therefore, when using carpet as the surface for a radiant panel, the  $R$  value is the most important factor in terms of system performance.

Table 5.59 lists the emittance for a number of common materials. A look at Table 5.59 indicates that most of the materials have an emittance close to 0.9. This is true for most nonmetals. The reason for this is that the spectral emittance of these materials is high in the infrared region where most of the energy is located when the substances are between room temperature and several thousand degrees. This is illustrated in Figure 5.48. For metals, the opposite is usually true. Metals typically

**TABLE 5.56** Typical Carpet R Values

Sample	Fiber type	Yarn type	Style	Pile height (in)	Pile weight (oz/yd <sup>2</sup> )	Gauge	Stitches per inch	Tufts/in <sup>2</sup>	R value
1	Nylon	CF	LL	0.125	10	1/10	8	80	0.68
2	Nylon	CF	LL	0.109	20	1/8	6	48	0.65
3	Nylon	CF	LL	0.192	28	1/8	8.4	67.2	0.67
4	Nylon	CF	LL	0.125	24	1/10	8.6	86	0.55
5	Nylon	S	Plush	0.25	24	1/8	11	88	1.12
6	Nylon	CF	HLL	—	24	5/32	8.6	55	1.33
7	Nylon	CF	Shag	1.07	24	3/16	5.2	27.7	1.51
8	Acrylic	S	LL	0.21	42	1/10	8	80	0.78
9	Acrylic	S	LL(FB)	0.21	42	1/10	8	80	1.03
10	Polyester	S	Plush	0.28	42	5/32	8.5	54.4	0.95
11	Polyester	S	HLL	—	42	5/32	8.5	54.4	1.66
12	Nylon	S	Saxony	0.552	40	3/16	5.5	29.3	1.96
13	Nylon	CF	Shag	1.25	43	3/16	4.2	22.4	2.46
14	Wool	S	Plush	0.487	43	5/32	7	44.8	2.19
15	Nylon	S	Plush	0.812	58	1/8	10	80	1.83
16	Acrylic	S	Plush	0.688	53	5/32	9	57.6	1.9
17	Acrylic	S	Plush	0.53	44	3/16	8.25	44	1.71
18	Olefin	CF	LL	—	20	—	—	—	0.7

**Source:** Carpet and Rug Institute.

**TABLE 5.57** Typical Resistance Values of Common Surfaces

Material	<i>R</i> Value, English units, (1 in)
Cork tiles	1.72
Clay tiles	0.17
Linoleum	0.72
Marble	0.06
Thermoplastic tiles	0.29
Mahogany	0.93
Concrete	0.10
Terrazzo	0.09

**TABLE 5.58** Typical Carpet Cushion *R* Values

Cushion	Thickness (in)	Weight (oz/yd <sup>2</sup> )	Density (lbs/ft <sup>3</sup> )	<i>R</i> value
Prime urethane	0.4	10.3	2.2	1.61
Slab rubber	0.23	622	—	0.62
Waffled sponge rubber	0.43	49.2	—	0.78
Hair and jute coated	0.44	52.6	—	1.71
Bonded urethane	0.5	—	4	2.09

*Source:* Carpet and Rug Institute.

have a low spectral emittance in the infrared. Therefore, at low temperatures, most metals will have a low total emittance.

One particular note in Table 5.59 is that when a normally low-emittance material such as aluminum is painted or coated, the emittance of the paint determines the emittance of the panel. So even though some radiant systems may use aluminum panels, as long as the aluminum is painted, the surface will have a fairly high emittance. (Umur, 1955). An additional note regarding Table 5.59 is that the difference

**TABLE 5.59** Total Emittance Data

Material	Hemispherical/normal	Emittance
Wood	Normal	0.80–0.90
Glass, polished	Normal	0.94
Brick wall	Normal	0.94
Oil paints	Normal	0.89–0.97
Plaster	Normal	0.93
Concrete	Hemispherical	0.87
Marble	Hemispherical	0.88
Lacquer on Al	Hemispherical	0.88
Porcelain tile	Hemispherical	0.85

*Source:* Gubareff et al., 1960; Sharma, 1989.

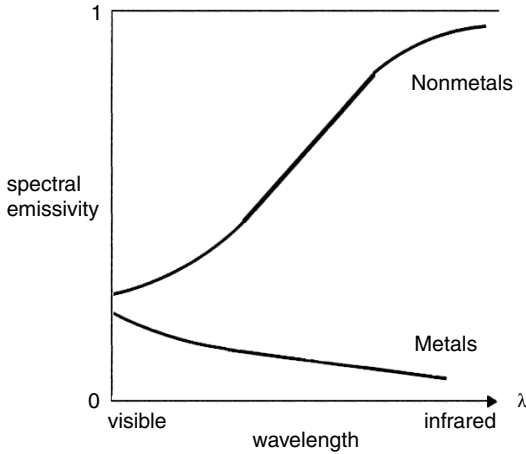


**FIGURE 5.48** Spectral emittance for metals and nonmetals.  
(Source: Brewster, 1992.)

between the normal and hemispherical emittance is usually not large enough to warrant any distinction. Table 5.59 is compiled from two different sources, one source reporting normal values and the other hemispherical. This is the only reason it is noted in the table.

In conclusion, it is seen that effect of emittance (i.e., how will the surfaces disperse heat into the room) is not as significant as it might be thought for several reasons. The first is that most surfaces have an emittance of  $0.9 \pm 0.05$ . Second, the effect of surface resistance decreases the impact of emittance. Finally, natural convection (the location of the radiant panel), also lessens the impact of the surface emittance. This last point is especially true when the radiant panel is located on the floor or wall.

The research on radiant panel surface characteristics not only provides useful information about panel surfaces, but also presents the entire range of performance factors related to surface, orientation, location, heat loss, and air movement. The study served to buttress field experience and remove some of the mystery and confusion about radiant panel construction. Designers can feel very comfortable that they know the design factors required to offer the radiant panel design flexibility customers demand.

### **5.3 AN EVALUATION OF THERMAL COMFORT AND ENERGY CONSUMPTION FOR THE ENERJOY® RADIANT PANEL HEATING SYSTEM**

The first three studies focused on development and evaluation of radiant system design and performance factors unique to radiant heating panel systems. The following case study utilizes a rigorous instrument and occupant monitoring protocol to develop real-world performance data in the occupied seven-year-old Adaptable Fire Safe Research Park house. The entire report is available from the NAHB Research Center. The material presented here is from *ASHRAE Transactions* 1995,

V. 101, Pt. 1, "An Evaluation of Thermal Comfort and Energy Consumption for a Surface-Mounted Ceiling Radiant Panel Heating System."

Many common radiant panel design factors are studied in the occupied environment that was monitored in the unique ENERJOY® Case Study. The objective of the study, conducted by the National Association of Home Builders Research Center under the auspices of the Advanced Housing Technology Program of the U.S. Department of Energy, was to improve product energy efficiency, quality, and cost-effectiveness in the U.S. home building industry. The study develops information that shows how the performance factors of the residential radiant heating system were at significant and favorable variance from two common convection systems.

### 5.3.1 Introduction

Because most homes in the United States are conditioned by forced-air systems, there is a tendency to define heat transfer in buildings with an almost exclusive emphasis on convection. Principles of radiant heat transfer are not well understood by the general public, and the dynamic interplay in buildings among the three forms of heat transfer will, for a long time, generate discussions among heat transfer experts. This case study provided the opportunity to further the understanding of heat transfer in residential structures.

Fast-acting radiant heating panels have been commercially available for more than 10 years. The panels consist of a base of high-density fiberglass insulation board, a patented solid-state heating element with a textured-surface coating, and an aluminum frame. The panels are lightweight, have a 1-in profile, and are available for either 120- or 240-V installations in dimensions ranging from 1 × 2 ft to 4 × 8 ft. The panels have been installed in residential commercial buildings, both new construction and retrofit. (The panel dimensions allow them to be used in suspended ceiling grids without modification.) Their ability to function on either direct or alternating current makes them well suited to all locations, including remote ones. The radiant system operates silently, cleanly, and with little to no required maintenance.

Evaluation of radiant performance was based on energy consumption and thermal comfort data obtained and analyzed from an occupied research home. In this home, the radiant panels were compared with a forced-air, air-to-air heat pump system.

### 5.3.2 Background

Most conventional heating systems in U.S. housing rely primarily on convection and provide thermal comfort by directly heating the interior air space and subsequently heating the contents of the space. Radiant heating systems target surfaces within the space, including occupants, for heating and only indirectly heat the air. Proponents of radiant heating systems claim that the systems have the potential for energy savings without sacrificing thermal comfort by lowering the air temperature and heating people rather than entire buildings. In theory, significant energy savings are possible, but some research and resulting discussions in the literature questioned the soundness of the energy savings claims and raised questions regarding thermal comfort.

There are several different types of radiant heating systems; distinction among them is important because their differences, when ignored, can result in misleading conclusions about their appropriate use and performance. Radiant floor and ceiling systems can be located within the floor-ceiling materials or directly behind the floor-ceiling surface material. All of these electric resistance or hydronic systems are considered high-mass systems whose thermal inertia requires steady-state

operation. Only surface-mounted ceiling panels are considered low-mass systems whose response time makes transient operation possible with substantially reduced installed capacity. Although there are several different types of radiant heating systems that claim greater comfort and/or energy savings, the surface-mounted ceiling radiant panels have a unique combination of qualities.

1. *Quick recovery time.* Panels reach an operating radiant surface temperature of 150°F to 170°F in less than 5 min.
2. *Zoning.* Room zoning with thermostats designed to sense both air and radiant temperatures for more effective operation.
3. *Ease of installation.* The electric resistance panels are wired in the same manner as residential lighting, are lightweight, and have an extremely narrow 1-in profile.
4. *Versatility.* The panels are suitable for primary or supplemental heating in new construction and retrofit.
5. *Panel design.* The solid-state radiant panels used in this case study deliver more than 90 percent of heat output as radiant. Dense insulation reduces conductive losses through the backside. The low-panel profile and surface composition reduce convection. The result is a truly radiant heat exchange system.

### 5.3.3 Comparative Field Test

This case study was designed to address the lack of data on the relative energy efficiency and delivery of thermal comfort by surface-mounted radiant heating systems and more conventional forced-air convection heating systems in residential structures. The specific assertions made by the manufacturer regarding surface-mounted ceiling radiant panels to be evaluated were as follows:

- Ten to twenty percent less air infiltration than conventional convection systems.
- Significantly reduce the installed Btu capacity of the radiant system in comparison with a conventional forced-air convection system at a given design load.
- Significantly lower electricity consumption than zoned, electric baseboard heating.
- Significantly lower energy costs than conventional convection systems, under transient conditions.
- Maintained thermal comfort with quick recovery from a 6°F to 8°F temperature setback.

### 5.3.4 Test House

Prior research has demonstrated the acceptability and even the desirability of testing two heating systems in a single home. The method involves an alternating schedule over the course of half of the heating season, the half-season including a shoulder and conditions at or approaching design conditions for the location. (The winter design temperature is the outdoor air temperature that is exceeded 97.5 percent of the time.) This method has the distinct advantage of eliminating variables that are present when tests are conducted in more than one home. In this study, the two heating systems were operated alternately for 1- to 2-week periods.

The adaptable fire-safe demonstration house (hereafter referred to as the AFSD house), a research home located in Bowie, Maryland, was selected for this case study because of the existence of a database on energy consumption from a previous

research project and its occupancy by the family of a research center employee prepared for the demands of the field study. The AFSD house, built in 1990, is a two-story house approximately 2200 ft<sup>2</sup> in size. The AFSD house is fairly typical of contemporary, single-family detached homes in the mid-Atlantic region of the United States: 2 × 4 wall construction, fiberglass insulation, 8-ft ceilings, and gypsum board interior walls and ceilings. Unique features of the AFSD house were its modular construction, 3-ft passageways and hallways, and a three-story elevator. The only feature to have potential for significant impact on the field study was the elevator, which was disabled and the shaft sealed. The effects of solar and sky conditions were mitigated by heavy drapes kept closed on all south-facing windows and the dining room slider for the entire study period.

The forced-air heating system of the AFSD house was zoned using two heat pumps, with the ducting runs for the two floors being independent because of the structure's modular construction. The air handler and ducting for second-floor heating was located in the unconditioned attic space. All second-floor ducting was wrapped and taped with duct insulation. Ducting for the first floor was located in the semiconditioned space of the basement. Ducting in the basement was not insulated. The exception to this was the family room. Because this room is located over a crawlspace foundation, the ducting for this space was wrapped and taped with duct insulation. Both zones of the forced-air system were equipped with state-of-the-art programmable thermostats for separate weekday and weekend setback strategies. The thermostats are described as *predictive* because of their ability to incorporate previous daily energy requirements into the ramping up of interior temperatures when recovering from setback.

### 5.3.5 Radiant Heating System

The number, size, and location of radiant ceiling panels installed in the AFSD house were specified by the manufacturer. Research has indicated that standard heating design procedures established by the American Society for Heating, Refrigerating and Air Conditioning Engineers (ASHRAE) may require modification for certain types of radiant heating (Howell and Suranarayana, 1990). Although calculation of the heating load of a structure is independent of the type of heating system to be used in a structure, fast-acting radiant systems provide the opportunity for greater reduction in the installed Btu capacity if the heating load (on a room-by-room basis) can be accurately estimated. The research center provided the manufacturer with information from previous research on the heating of the AFSD house for calculations. The radiant heating system installation consisted of 20 panels, 160 ft<sup>2</sup> in 13 zones, with a resulting power density of approximately 4 W/ft<sup>2</sup> of floor area. The panels can be wired as either 240 or 120 V; all panels in the AFSD house were wired as 240 V.

All 13 zones of the radiant system were equipped with hydraulic line-voltage thermostats. The manufacturer specified these thermostats because of their narrow operating differential (+1°F) and the ability to sense both radiant and air temperature effects. The thermostats were located according to the manufacturer's directions; their location was determined by considerations of user convenience and viewing angle with respect to the radiant panels.

### 5.3.6 Monitoring and Data Acquisition System

The monitoring equipment recorded data on the following parameters for approximately three months of the heating season:

- Thermal comfort
  - Dry-bulb temperature
  - Operative temperature (OT)
  - Vertical air temperature difference
- Energy
  - Metered electric consumption
  - Outdoor temperature

The data acquisition system used for the field study consisted of a measured performance rating controller and a data acquisition system.

Thermal comfort stations were located in three of the most frequently used rooms in the house: (1) the family room, (2) the dining room and kitchen, and (3) the master bedroom. (Minute temperature data from three thermal comfort stations and two outdoor temperature sensors were recorded on a 20-channel data acquisition system.) Although the stations should be located to reflect occupancy patterns, the actual rather than simulated occupancy of this test house forced the stations closer to the perimeter of the rooms. The stations consisted of three double-shielded air temperature sensors located 4, 43, and 93 in from the floor and a 6-in hollow copper globe located 43 in from the floor with a temperature sensor sealed at its center. The sensor heights were determined in accordance with ASHRAE Standard 55-1992 (ASHRAE, 1992).

The 6-in hollow copper globes were originally intended to estimate the mean radiant temperature (MRT) as prescribed in Chap. 13 of the ASHRAE Handbook (ASHRAE, 1993). As is the case in the evaluation of most convection systems, when the air temperature and globe temperatures are very similar, the globe is a good approximation of the MRT. If the 43-in air temperature is significantly different from the globe temperature, as was the case during operation of the radiant system, the globe temperature, not the MRT, is a much better estimation of the OT (Berglund et al., 1982). Using the globe temperature as an estimation of the OT simplified evaluation of thermal comfort.

The sensitivity of the OT globes to their location in a room during radiant heating system operation became apparent during the research project. The globes were subsequently relocated to the indicated positions (directly underneath the largest panel in the three monitored rooms) approximately halfway through the testing period. Relative humidity was spot-checked with a handheld humidity sensor over the course of the data acquisition period.

Two calibrated, pulse-initiating watt-hour meters separately monitored incidental and home heating electric consumption. Electric service to both heating systems was wired so that the meter dedicated to the heating system monitored electric current. Counts by both meters were summed hourly and recorded on a separate data acquisition system. The status of radiant panels in the three monitored rooms was recorded on a minute-by-minute basis.

### 5.3.7 Methods of Evaluation

The relative performance of the radiant and conventional heating systems was evaluated according to the following methodology:

1. *Air infiltration.* Two blower door tests were performed on the AFSD house. In the first test, the registers and cold-air returns of the ducted heating system were left open, as they would during normal operation of the forced-air heating system. For the second test, all registers and the two cold air returns were sealed to effec-

tively eliminate the ducting from the house. This simulated the configuration of the AFSD house if the ductless, nonmechanically radiant heating system was the primary, permanent system. In this way, the induced air infiltration losses associated with ducted and nonducted heating systems could be quantitatively compared.

- 2. Installed Btu capacity.** The installed Btu capacities of the heat pump, electric baseboard, and radiant panels are known and can be compared. A critical element of this comparison is the ability of the heating system to deliver thermal comfort during design conditions. Outdoor temperatures down to and below design conditions were encountered during the data acquisition period so that the sufficiency of installed capacity for the two systems could be assessed.
- 3. Energy savings under transient conditions.** The asserted energy savings with the radiant heating system are the result of the combined effect of reduced parasitic losses, room-by-room zoning, quick recovery from setback, and reduced air temperature. The total effect of these phenomena should be significantly reduced building heat loss without sacrifice of occupant thermal comfort.

During periods of radiant heating, thermostats were set back to 60°F when rooms were unoccupied and set to 68°F when occupied. This represented optimal operation of the radiant system under living conditions. During periods of heat pump, forced-air heating, the two programmable thermostats had a setback of 60°F and a set point of 68°F. The weekday and weekend schedules of the AFSD house occupants were used to program day and night setbacks of the heat pump thermostats. The state-of-the-art programmable thermostats are designed to allow flexible timed recovery from setback based on the previous day's power requirements. This represented optimal operation of the heat pumps under living conditions. The comparison of daily electric energy consumption as it relates to outdoor temperature, permitted a comparison of the two alternately operated heating systems.

Previous research at the AFSD house involved installation of baseboard electric heat throughout the house. Room-by-room day and night setback schedules were employed during this study. Energy consumption as it relates to outdoor temperature was quantified for the baseboard heating system. This allowed comparison of the energy consumption of the radiant and baseboard heating systems for the same residential structure.

- 4. Delivery of thermal comfort under transient conditions.** An inextricable element of any comparison of heating system efficiencies is the delivery of thermal comfort to the occupants. Reduction in either the installed Btu capacity or seasonal energy consumption of any heating system is only relevant if thermal comfort can be maintained. Thermal comfort is defined in ANSI/ASHRAE Standard 55-1992 (ASHRAE, 1992) as "the condition of mind that expresses satisfaction with the thermal environment; it requires subjective evaluation." The environmental factors affecting thermal comfort have been determined: ambient air and MRT, relative humidity, and air speed. (Operative temperature is the primary environmental determinant of thermal comfort; relative humidity and air speed, unless extreme, are secondary effects.) In this field study, data on air and operative temperatures were recorded in three rooms on a minute by minute basis, the relative humidity was spot checked, and the air speed was not monitored.

The two heating systems were operated before data collection to allow determination by the occupants of comfortable setback and set point temperature settings. Each heating system was operated in this manner for at least 1 week. The radiant and heat pump temperature strategies established, as results of the trial operations of the two systems were a setback of 60°F and a set point of 68°F.

Thermal comfort was evaluated by reviewing occupant thermal discomfort surveys. Whenever an occupant of the research home experienced thermal discomfort in one of the three monitored rooms, the individual completed a short survey. The environmental conditions corresponding to the time of discomfort as recorded by the monitoring system were later linked to each survey for evaluation. Patterns or generalizations regarding the operation and thermal comfort delivery of the two heating systems could in this manner be established.

### 5.3.8 Field Test Results

**Air Infiltration.** Air infiltration is one of the primary contributors to heat loss in buildings. Air infiltration accounts for somewhere between 25 and 45 percent of the total heat loss in a typical home (Goldschmidt, 1986). As conditioned air moves out of the building envelope, the energy to heat or cool that air is lost. Research has shown that homes with forced-air heating systems can have air infiltration rates up to 36 percent greater than homes with nonducted heating systems (Palmiter et al., 1991). Determination of the difference in air infiltration at the AFSD house with and without ducts aided the researchers in determining the importance of sealing off all ducts during operation of the radiant system.

The blower door test is a common method of estimating air infiltration. It is particularly useful in assessing relative building tightness (Nantka, 1990). The air infiltration tests on the AFSD house were performed on November 29, 1993, in accordance with guidelines set forth in ASTM Standard E779-1987, *Method for Determining Air Leakage by Fan Pressurization* (ASTM, 1987). The results are presented in Table 5.60. The first test was performed with all floor and ceiling registers and cold-air returns covered with foil-faced, bubble-wrap insulation and air-sealed with duct tape. In the second test, all registers and returns were open, as they would be during normal operation of the forced-air heating system.

It is customary to estimate the natural air infiltration rate by dividing the calculated air changes per hour (ACH) at 50 pascal (Pa) by either 16 or 20 (Persily, 1986). This places the natural air infiltration rate between 0.7 and 0.88 during radiant system operation. Though efforts to establish an average U.S. residential ACH show wide variation, an ACH in the range of 0.7 to 0.88 qualifies the AFSD house as an "average" U.S. home (Goldschmidt, 1986). Regardless of the estimating procedure, the reduction in air infiltration with the forced-air distribution system effectively eliminated from the building envelope was approximately 12.5 percent. Clearly, significant air leakage was attributable to the forced-air system's ducting. These results fall within the range of air leakage attributed to ducting by other researchers.

The results of the blower door tests are even more significant in light of research performed by Gammage and Modera (Saunders et al., 1993). Studies performed by Gammage and other work reviewed by Modera estimate that duct air leakage dur-

**TABLE 5.60** Blower Door Test Results

	Ducts sealed— radiant system	Ducts open— heat pump system
Airflow at 50 pascals [air changes per hour (ACH)]	13.97	15.84
Estimated natural infiltration in ACH	0.88	0.99
Percent reduction in ACH	12.5	Base

ing blower operation could result in a doubling of the ACH of the structure. The air leakage attributable to duct losses is a function of the quality of the system installation and the location of the ducts inside or outside the heated space. These are issues of forced-air system installation that are currently being addressed by the industry. The effect of increased air leakage during blower operation of the ducted heat pump system shows up in this case study as an integral part of the energy consumption comparison. The radiant system does not suffer from delivery losses.

**Installed System Capacity.** The installed capacity of any heating system is a function of the estimated building heat loss, the winter design conditions, and the setback strategies, if any, to be implemented in the building. Table 5.61 presents a summary of the installed system capacities for the radiant, electric baseboard, and heat pump systems.

The first column contains information on building heat loss for the AFSD house as calculated using a computer program whose output is certified by the Associated Conditioning Contractors of America (ACCA) to meet all requirements of a widely accepted standard design procedure for heating and cooling systems. Although the calculation utilizes substantial actual information on the building's construction and design, some important assumptions must be made. For example, the air change rate is an input to the calculation that has a significant impact on the building heat loss calculation. Air infiltration can account for one-third of the total heat loss in typical houses. Despite limitations, the building heat loss calculation provides a basis for comparing the installed capacities of the three different heating systems. Note that the units for heat loss and installed system capacity are either Btu or watts. It is customary for heating and cooling contractors to work in Btu and for electric utilities to work in watts or kilowatts; both are provided here for convenience.

The second column presents the installed capacity of the electric baseboard heating system from a previous research project. Note that the installed capacity is approximately 50 percent greater than the calculated design load of the building. System oversizing of up to 60 percent is standard practice when both day and night setback strategies are anticipated (ASHRAE, 1993). Setback strategies and room by room thermostatic control were used in previous research involving the electric

**TABLE 5.61** Comparison of Heating System Installed Capacities—AFSD House

Parameter	Calculated building heat loss (right—J)	Heating system			
		Electric baseboard	Heat pump	Radiant panel (ENERJOY)	Radiant panel (Kansas State)
Indoor/outdoor $\Delta t$ at design conditions, °F	57° (70°–13°)	57° (70°–13°)	57° (70°–13°)	55° (65°–10°)	63° (72°–9°)
Assumed ACH	0.7	0.7	—	0.4	0.7
Day and night setback strategies?	No	Yes	Yes	Yes	Yes
Installed capacity—Btu/h (watts)	45,442 (13,314)	69,967 (20,500)	57,100 (16,700)	27,645 (8,100)	29,864 (8,750)
Percent system oversizing (at design conditions)	NA	+54	+26	–40	–34

baseboard system, making comparison of energy consumption between the electric baseboard and radiant panel systems meaningful.

The third column contains information on the heat pumps installed at the AFSD house. The air-to-air heat pumps were a 1-ton unit for the second floor and a 2-ton unit supplying the first floor. Conventional heat pumps are often not operated on setback strategies. The predictive nature of the state-of-the-art programmable thermostats, however, allowed efficient operation of the heat pumps with setback strategies. The combined installed capacity of just the two heat pumps is actually approximately 41,000 Btu. At design conditions, however, the installed capacity is most accurately estimated by adding the output of the backup strip heat (15 kW) to the output of the heat pump at that particular temperature. This calculation is appropriate because the capacity of the heat pump depends on the outdoor temperature and, at design conditions, the forced-air system is delivering heat primarily from the electric strip heat. Adding the output of the heat pumps at design temperature results in a total installed capacity that is 26 percent greater than the calculated capacity. This extra capacity is the capacity required to meet the demands of day and night setbacks with the heat pump system.

The fourth column shows the installed capacity of the radiant heating system in the AFSD house. The installed capacity of the radiant system is 40 percent less than the installed capacity recommended by the analysis. (Although the indoor-outdoor temperature differential used for the calculations is 2°F less than the differential used to calculate the radiant installed capacity, this difference is only around 4 percent.) Recall that the rapid response time and lower air temperatures possible with the radiant system permit significant reduction in installed capacity, even with day and night setback strategies. The installed capacity of the radiant system is 2.5 times less than that of the electric baseboard system and two times less than that of the heat pump system. This is an important characteristic of the radiant system, as it pertains to the demand on an electric utility during design conditions. (The winter of 1993–1994 was severe, and power outages at the test house did occur as the result of insufficient electric utility capacity.)

***Energy Consumption Comparison.*** For approximately half of the 1993–1994 heating season, electric consumption at the occupied AFSD house was monitored. The heating systems were wired so that their electric consumption was dedicated to one meter, and the second meter monitored all incidental household electric consumption. The radiant and heat pump systems were operated alternately in 2-week blocks when possible and for 1-week blocks otherwise. This was done to minimize the impact of intermittent operation on the heat pump predictive thermostats during heat pump operation and to maximize the routine of room-by-room thermostat use during radiant panel operation. All window coverings on the south and west sides of the house were kept closed for the test period to minimize the effects of solar gain on energy consumption and to prevent direct solar radiation from having any impact on the OT globes. The precision of the pulse tabulations was checked against manual readings on at least three occasions; on all occasions, the pulse counts were within 2 percent of manual readings.

Incidental household electric use contributes indirectly to home heating, and large variances in its consumption could have a significant impact on heating system energy requirements. With two occupants, both fully employed outside the home, little variation was anticipated. Review of incidental electric consumption revealed significantly greater consumption on weekend days than weekdays but no other patterns or large variances. Because heating system operation changes were performed at approximately midnight on Saturdays, weekend variances in incidental electric

consumption should have had very little impact on the heating energy analysis of the two heating systems.

**Regression Analysis of Energy Consumption.** Total daily heating electric consumption was plotted against corresponding daily average outdoor temperature (electric consumption was compiled on an hourly basis, and outdoor temperature was compiled on a minute-by-minute basis). The data were linearly regressed, with the results presented in Table 5.62.

**TABLE 5.62** Regression Analysis on Energy Consumption and Outdoor Temperature for Three Heating Systems

Parameter	Heating system		
	Heat pump	Radiant panel	Baseboard
Constant	250.9472	188.1726	256.2494
Standard error of y estimate	20.82946	9.845121	13.9711
$R^2$	0.897179	0.913999	0.85182
No. of observations	32	31	44
Degrees of freedom	30	29	42
$x$ -coefficient	-4.37728	-3.36296	-3.72808
Standard error of coefficient	0.270549	0.191558	0.239928

The standard errors of both the  $y$ -intercept and the slope coefficient for all three regressions are statistically significant. The  $R^2$  values, which can be interpreted as the percent of variation in the values of  $x$  explained by variation in  $y$ , are quite high, varying between 85 and 91 percent. Inspection of the distribution of data points about the regression lines revealed no evidence of patterns in the residuals that might pose problems during the interpretation of the regression statistics. Linear forms appeared to be the most appropriate functional forms for all three regressions. A streak of very cold weather during the test period resulted in outlying data points for both the heat pump and the radiant panels. None of the outliers was found to be influential. The regression results suggest that the estimated linear relationships between energy consumption and daily average outdoor temperature for the three heating systems are reasonable and can be used with acceptable levels of confidence.

The three regression lines are shown in Figure 5.49. The negative slopes portray decreasing energy consumption with increasing outdoor temperature, as would be expected. The positions of the three regression lines indicate that the radiant panel heating system used less energy regardless of the outdoor temperature.

The balance point of a structure is the outdoor temperature at which the structure requires no heating energy. The  $x$ -intercepts of the three regression lines are of interest, as they estimate the balance point of the AFSD house. All else being equal for the same structure, the outdoor temperature at which no dedicated heating energy is required should be the same; thus, the  $x$ -intercepts of all three regression lines should be approximately the same. The  $x$ -intercepts for the radiant, heat pump, and baseboard systems were 56°F, 57°F, and 68.7°F, respectively. The proximity of the heat pump and radiant panel  $x$ -intercepts is credible because the indoor temperature set point and setbacks, incidental energy gains, and operation of the house were similar during operation of each system. The one major difference was the sealing of

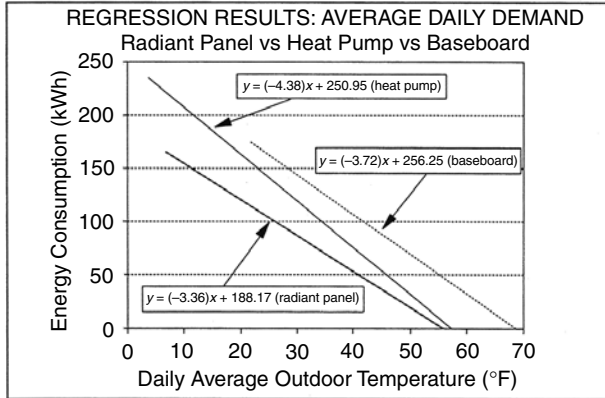


FIGURE 5.49 Regression results.

the forced-air delivery registers and cold-air returns when the radiant system was being operated. This may explain the slightly higher balance point of the heat pump regression line.

The balance point for the baseboard system is significantly different from either the radiant panel or the heat pump regression line. Several factors could account for the difference.

1. The AFSD house was unoccupied during the electric baseboard study. Incidental gains and losses from occupants' activities (cooking, domestic hot-water use, exhaust fan use, entering and exiting, etc.) are not reflected in the baseboard data. Additionally, the interior conditions of the house during the baseboard study (curtain and blind positions, furniture contents, etc.) are not known and could affect the thermal performance of the house.
2. The thermostat set point temperature for the electric baseboard study was 4°F higher than in this study. The actual indoor temperature was approximately 2°F higher (averaging 70.5°F).
3. The room-by-room setback schedules for the baseboard study were designed to simulate occupancy. How well they actually reflected the routines of the AFSD house occupants in this study cannot be determined.

It was not possible to factor these differences out of the present comparison. Accounting for the higher set points would serve to decrease the difference in comparison with the other two regression lines. For the current comparison, it can only be noted that differences exist, and the comparison of the baseboard energy consumption to that of the other systems is limited by these differences.

It is interesting to note that the slopes of the radiant and baseboard system regression lines are similar, suggesting similar relationships between energy consumption and outdoor temperature. It is not possible to determine the reason for the slope similarity, but the room-by-room thermostat control and lack of delivery losses for both systems may be at least part of the explanation.

**Translation of Regression Relationships into Expected Energy Savings.** The estimated relationships between energy consumption and outdoor temperature can be

used to calculate the expected annual heating energy required for the Washington, D.C. area. Typical record year (TRY) data from the nearby Andrews Air Force Base allow translation of the regression lines into the expected average energy consumption for the heating system. The TRY calculation is a method of weighting the individual relationships by outdoor temperatures typically encountered during a heating season. Table 5.63 gives the results of the TRY calculations.

**TABLE 5.63** Typical Record Year Heating Energy Estimations for the Three Heating Systems

Typical record year information: Heating	Heating system		
	Heat pump	Radiant panel	Electric baseboard
Estimated annual electric consumption (kWh)	10,764.1	7,229.4	15,107.5 <sup>24</sup>
Estimated annual heating electric costs (at \$0.055/kWh)	\$592.03	\$397.62	\$830.91
Estimated annual percent savings with radiant	33%	Base	52%

The radiant panel heating system demonstrates a projected 33 percent savings compared to the heat pump for the TRY. A note should be made here that the different slopes of the two regression lines translate into varying savings with varying heating season climates. The fact that the radiant regression line is below the heat pump regression line over the entire range of outdoor temperatures suggests that the panels would outperform the heat pump, regardless of the record year or region in which the house is located. Greater savings would be expected in colder climates, less in warmer climates. The 52 percent energy savings estimated with the radiant heating system in comparison with the baseboard system must be presented with some caution. Different test conditions existed for the radiant panel and baseboard studies, and the impact of these differences has an impact on the relative energy savings.

***Qualifying the Energy Savings Demonstrated by the Radiant System.*** The seasonal heating cost estimates pertain to the AFSD house occupied by a working couple. Significant impact on the operation and, consequently, the energy consumption of either or both heating systems could result from additional occupants. Because the setting forward of thermostats is occupant dependent with the radiant system, more occupants would presumably significantly increase energy use. In other words, the energy consumption of an occupant-dependent heating system may be more sensitive than the floor-zoned conventional system to increases in the number of occupants. On the other hand, the impact of one occupant at home during daytime hours could have a greater impact on the conventional forced-air system than on the radiant system. With the conventional forced-air system, an entire zone(s) would be removed from daytime setback, whereas with the radiant system, an occupant at home during the daytime may only require the setting forward of certain rooms. Though occupation of a 2200-ft<sup>2</sup> house by one working couple does not represent the median living situation in the United States, these circumstances are by no means unusual and the savings demonstrated here are relevant. Actual savings in homes with varying numbers of occupants and schedules will result in different savings.

Furthermore, the relevancy of the projected savings with the radiant system is dependent on the delivery of acceptable levels of thermal comfort. The overall evaluation of the heating systems comparison hinges on analysis of thermal comfort delivery with the two heating systems.

***Delivery of Thermal Comfort Comparison.*** Assessment of thermal comfort delivery assessment of thermal comfort involved a review of the thermal comfort surveys completed by the occupants. The occupants of the AFSD house were asked to complete a short survey whenever they experienced thermal discomfort. By including the exact time of survey completion, the responses could be linked to environmental conditions recorded for the occupied room.

It should be noted that the occupants of the AFSD house were new to the region and had little experience with radiant panels, heat pumps, or forced-air systems in general. Both occupants were accustomed to hydronic baseboard and wood stove heat.

The following generalizations were made based on a review of the surveys and the environmental conditions as recorded by the monitoring system.

1. The setpoint temperature of 68°F for both heating systems was probably at the lower margin of thermal comfort for the female occupant of the research home. During the trial operation period of both heating systems, the male occupant determined the setback and set point thermostat settings. The female occupant completed 20 of the 25 surveys for some level of cold discomfort. Studies have shown that there appears to be no relationship between thermal comfort requirements and gender; however, substantial variation among individual requirements does exist.

ASHRAE Standard 55-1992, a thermal comfort standard, includes a graph showing the relationship between OT and clothing insulation for typical metabolic activity, relative humidity, and air speed. The graph gives the operative temperature range that would satisfy 80 percent of all individuals for a given level of clothing insulation. Given the 1.1 clo value of the AFSD house occupants, the optimum OT was 69.5°F and the lower and upper limits satisfying 80 percent of all individuals were 66.5°F and 72.5°F, respectively (ASHRAE, 1992). (*Note:* These temperatures are for individuals during light, sedentary activity, a relative humidity of 50 percent, and an air speed of less than 0.15 m/s.) Although the set point temperature of 68°F is quite reasonable for a clo value of 1.1, individual variation certainly allows for the responses of both occupants to the temperature setting.

2. For both occupants, an equal number of comfort surveys indicating insufficient thermal delivery were completed for each heating system. If the set point temperature of 68°F was a bit low for the female occupant, at least the reaction to this set point was roughly equivalent for both heating systems.

3. Half of the comfort surveys indicating insufficient thermal delivery were completed for the family room alone. This fact is a combination of the total amount of waking hours spent in this room and the fact that the heat loss from this room may have been greater than that calculated for either heating system. For the forced-air system, the distance of the room from the first-floor thermostat and the room's relative isolation from the remainder of the first floor were most likely important factors. For the radiant system, insufficient panel density and/or panel location may have combined responsibility. Related to this, the temperatures in the family room at the ceiling and floor were, regardless of the operating heating system, well below measured floor and ceiling temperatures for the master bedroom and dining room. The fact that five of the six surfaces in this room were exterior would make any errors in the estimation of the conductive and/or air infiltration load in this room critical in the delivery of thermally acceptable conditions.

4. Occupants found more opportunity to locate for comfort with the radiant system. Although occupant location was not information included on the comfort survey, the occupants noted that they found themselves positioning according to panel location. Locating more directly beneath a panel could accommodate the generally higher thermal requirements of the female occupant, and locating less directly beneath the panel accommodated the lower thermal requirements of the male occupant. AFSD house visitors also demonstrated this pattern on several occasions. One visitor remarked that it was similar to how people might gather around a wood stove, except that the location of the panel on the ceiling meant that nobody's view of the heat source was obstructed. This dependence of thermal comfort delivery on location can be interpreted as either an advantage or a disadvantage of the radiant system, depending on whether occupants can or must locate for comfort in a room during recovery from setback.

Research by Berglund et al. (1982) demonstrated that occupants could find it thermally acceptable for a room to be cool on entry as long as the OT is rapidly raised; here *rapidly* is defined as approximately 15 min. This corresponds to the experience of the AFSD house occupants in this case study as long as the occupant's activity permits location in close proximity to a radiant panel. Roomwide thermal acceptability may require as long as 45 min. During recovery periods, the OT varied depending on occupant location with respect to the radiant panel.

5. On five occasions, comfort surveys indicating insufficient thermal delivery corresponded to periods of radiant panel cycling, Figure 5.50. On all five occasions, inspection of the recorded radiant panel status for the occupied room indicated that a survey was completed only at the tail end of an off cycle. On the one hand, this phenomenon suggests that the radiant thermostat is sensing thermal comfort requirements in the proximity of the panel quite efficiently. On the other hand, this phenomenon suggests that if thermally acceptable conditions are dependent on panel status, cycling as the panels near or achieve set-forward conditions may be problematic for individuals requiring direct radiation for thermal comfort. All five of these surveys were completed by the female occupant of the AFSD house, the occupant whose comfort requirements have already been noted as being more sensitive to the set-forward temperature.

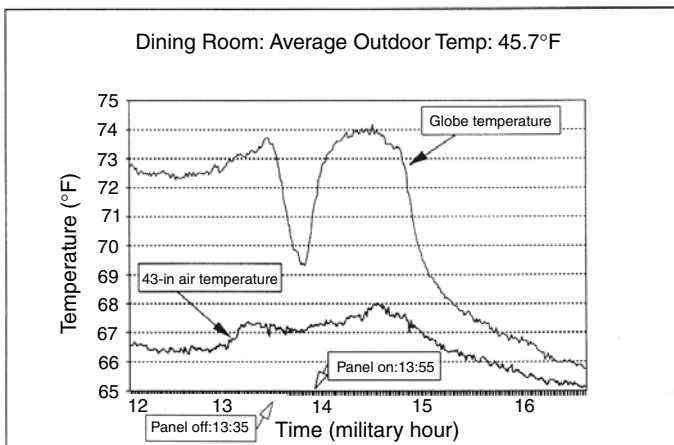
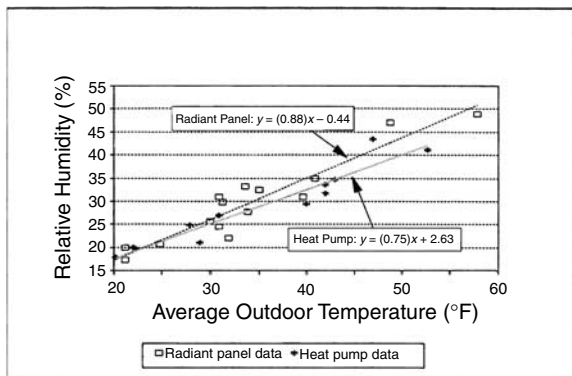


FIGURE 5.50 Panel cycling and thermal comfort.

6. Four of the five comfort surveys indicating excessive thermal delivery were for the forced-air system, all four of these for the master bedroom. The only monitored room that had doors to isolate it from the rest of the house was the master bedroom. The occupants generally slept with this door closed. With the master bedroom entrance door closed, the heat pump thermostat in the upstairs hallway was not receiving feedback from the single largest area on the second floor. Subsequently, overshoot in the master bedroom was quite common. In the early morning hours as the heat pump was ramping up to meet the morning set-forward temperature, 43-in air temperatures could go as high as 78°F. With occupants dressed and blanketed for overnight setback of 60°F, 78°F was quite uncomfortable. The problems of interior door position as it relates to delivery ducts, returns, and zone thermostats are not unusual for conventional forced-air systems.

7. Overshoot occurrences were often coupled with occupant complaints of dry throats and headaches that they attributed to the dryness of the air. It was anticipated that the occupants' sinus problems would be associated with lower relative humidities with the forced-air system than the radiant system, particularly at lower outdoor air temperatures. The infiltration of cold, relatively dry air would be greater with the higher infiltration rate associated with the ducted forced-air system than with the conducted radiant. This would be particularly true during very cold periods when longer periods of blower operation would increase the air infiltration rate associated with the ducted system. In fact, the graph in Fig. 5.51 shows little difference in relative humidities for the two systems and unexpectedly less difference at colder outside temperatures. More continuous and consistent relative humidity measurement may be required to resolve this apparent anomaly. Regardless of the numerical results on relative humidity, sinus complaints were clearly common with forced-air system operation at cold temperatures and nonexistent during radiant system operation. It is possible that sinus and respiratory irritation was related to some other phenomena, such as airborne dust or room pressurization, which are also correlated to forced-air operation.

The degree of vertical air temperature difference associated with any heating system is important in terms of thermal comfort conductive heat loss. The ASHRAE thermal comfort standard sets a maximum difference between floor and head high air temperatures. Stratification can create a stack effect associated with increased heat



**FIGURE 5.51** Heating system comparison: relative air moisture content.

loss. Under recovery or steady state, the vertical air temperature difference associated with radiant heating system operation in the AFSD house was found not to exceed 4°F (Fig. 5.52). This degree of vertical air temperature difference is within the limits set by the ASHRAE thermal comfort standard and less than the degree of vertical air temperature difference identified during some periods of forced-air system operation.

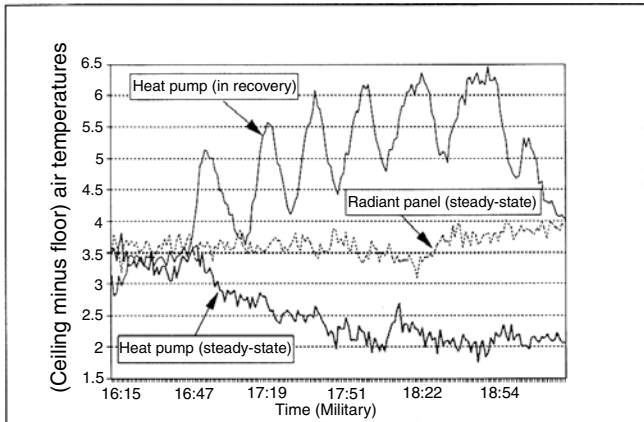


**FIGURE 5.52** Radiant and heat pump system comparison, air temperature stratification.

8. The clo value of both occupants' standard dress may have had an impact on thermal comfort assessment of both heating systems. The occupants made an effort to standardize the total clo value of day- and nighttime dress. Day attire for both occupants was approximated at 1.1. This clo value is, however, significantly higher than the clo value used in most thermal comfort studies, with perhaps the most important difference being the percent exposed skin surface. The total clo value and relatively low percent exposed skin surface may have made occupants less sensitive to air temperature reduction with the radiant system and localized drafts near forced-air delivery registers. The occupants commented that on isolated occasions when substantial skin surface was exposed, walking from room to room during radiant system operation felt quite cool. Similar instances were described for the forced-air system operation, particularly in the bathrooms, where the location of delivery registers near the showers made lower total clo values sometimes unavoidable. Although the occupants' dress may have reduced their sensitivity to certain aspects of operation of both heating systems, the fact that dress was standardized for both systems reduced the impact of this phenomenon.

At the end of the testing period, the two occupants of the AFSD house were asked which heating system they preferred and why. Their preferences were solicited before any information on the comparative energy consumption of the two systems was available. Both occupants stated their preference for the radiant heating system for the following reasons.

1. *Room-by-room control and flexibility.* Both occupants liked being able to control the temperature in the room rather than have a hallway thermostat dictate

the conditions. An activity such as exercising by one occupant in one room did not require changing the environmental conditions of an entire floor. The radiant system accommodated occupants' varying thermal requirements better than did the conventional forced air system.

2. *Silent and still operation.* Both occupants preferred the lack of air movement and fan operation noise.
3. *Sinus comfort.* Particularly during sleeping hours, the occupants preferred the conditions of radiant panel operation to those of forced air operation.

The primary inconvenience cited in the operation of the radiant system was the need to anticipate the setting forward of room thermostats to achieve general room comfort as opposed to more local thermal comfort conditions. Although the occupants felt that acceptable thermal conditions could be achieved in approximately 10 to 15 min if activity was restricted to panel proximity, total room comfort required approximately 30 to 45 min. For example, the master bedroom thermostat was set forward by the earlier riser in the morning so that thermally acceptable whole-room conditions would exist for the other occupant upon rising.

The occupants also felt that it was more difficult to remember to set back the thermostat when exiting than it was to set it forward when entering a room. There was no prompt to set back the thermostat as there is for lighting when exiting a room.

The input from actual occupants was invaluable in assessing the operation and delivery of thermal comfort by the two heating systems. Their input goes beyond the capabilities of measured environmental factors. Their experiences are by nature, however, individual and subjective. Their specific thermal requirements and preferences are important but must be viewed as limited. The recorded environmental parameters from the three thermal comfort stations can be used to broaden the discussion of thermal comfort delivery.

Sufficiency of installed capacity assessment of thermal comfort delivery is, in part, determined by the ability of each heating system to meet heating needs down to design conditions. The installed capacity of a heating system must be sufficient to meet the whole-house requirements for maintenance of acceptable thermal conditions down to an outdoor temperature extreme typical of the region. The design temperature for the area where the AFSD house is located is 13°F.

The 1993–1994 heating season for the mid-Atlantic region of the United States was unseasonably cold, particularly in mid-January and early February. Outdoor temperatures approaching and exceeding design conditions were common during parts of January and February. Data for two full days of outdoors-daily average temperatures below 10°F were available for comparing the performance of the radiant and forced-air heating systems. Of the three monitored rooms, the family room was selected for discussion because the heat loss from this room placed the greatest load on both heating systems.

Figure 5.53 shows the OT recorded in the family room during radiant system operation for the entire 24-h period on January 15, 1994. Outdoor temperatures were at or below design conditions for the entire period. The temperature started at 12°F and worked its way down to 0°F as the day progressed. This means that the AFSD house was experiencing outdoor conditions primarily below design conditions for the entire period.

The pattern of family room OT suggested that the installed capacity was sufficient to at least maintain the setback temperature of 60°F, even at temperatures approaching 0°F. The indoor-outdoor temperature differential at 0°F was 60°F—5°F greater than the differential used for the manufacturer's installed capacity calculations.

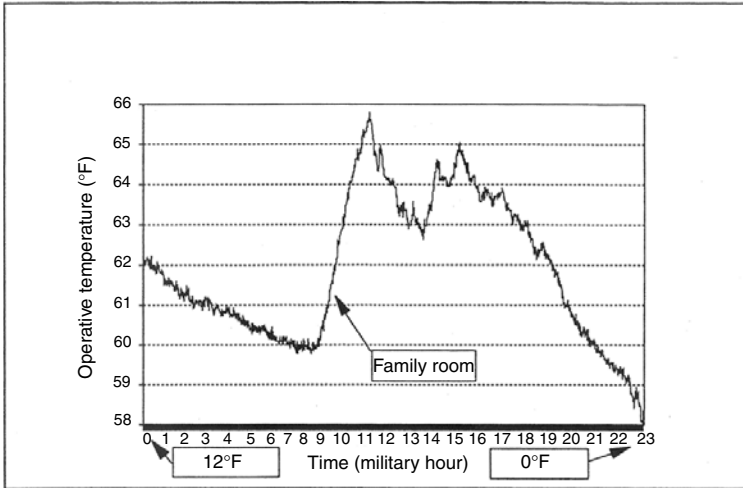


**FIGURE 5.53** Radiant system below design conditions. Average outdoor temperature, 6.7°F.

It is more difficult to determine if the installed capacity was sufficient for recovery from setback. The setpoint of the family room thermostat is known only for the early-morning and late-night hours for this 24-hour period. These periods corresponded to nighttime setbacks of 60°F. On most days, inspection of the status channel for a monitored room in conjunction with the pattern of the OT provided the information necessary to determine when monitored rooms were occupied. For this day, however, inspection of the status channel revealed that the panels in the family room were energized without interruption for the entire 24-h period. Little can be determined regarding family room occupancy and daytime thermostat setting from the database. Although the OT peaks of 65°F suggest some intermittent occupancy, the fact that this was a weekend day meant that nothing could be determined regarding occupancy.

Inspection of data for this 24-h period for the other two monitored rooms indicated frequent panel cycling, even late in the evening when outdoor temperatures were well below design conditions. This suggested that the installed panel capacity in these rooms was more than sufficient to meet design conditions under steady-state conditions. Review of cold days above design conditions (average daily outdoor temperatures in the 20s) revealed no difficulties in the ability of any of the monitored rooms to recover from setback. Although the information available does not prove the sufficiency of installed capacity, there are strong indications to suggest that the installed capacity was adequate for design conditions and day and night setbacks.

Figure 5.54 shows the graph of OT patterns for the family room during forced-air system operation for a day with an average outdoor temperature below design conditions and very similar to the average outdoor temperature shown in Fig. 5.51. Because the forced-air system followed a schedule and it was known that this 24-h period represented a weekend day, the thermostat settings were known. The night setback was 60°F and the day setting was 68°F. The night setback of 60°F was not maintained in the family room. This period did, however, correspond to outdoor temperatures well below the design condition of 13°F. The temperature pattern of

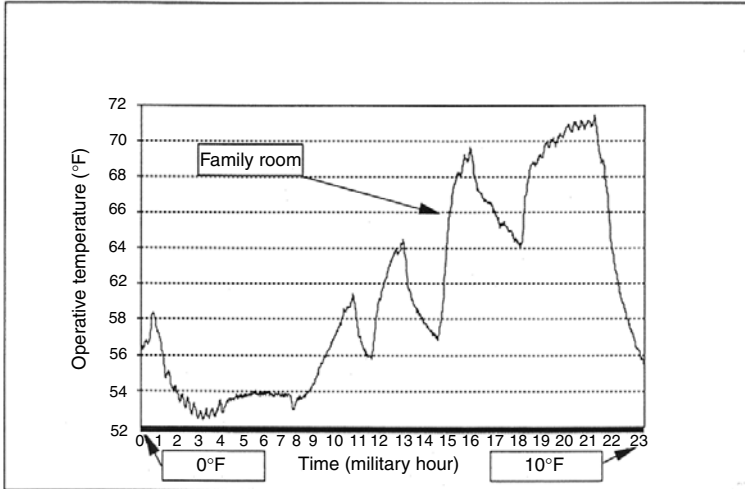


**FIGURE 5.54** Heat pump below design conditions. Average outdoor temperature, 7.6°F.

peaks and valleys from 9:00 A.M. to 5:00 P.M. suggests problems with maintenance of the 68°F set-forward temperature.

The cycling associated with the pattern may be more a problem of thermostatic control than sufficiency of installed capacity. On both floors, the forced-air thermostats were located approximately halfway down the hallways. Temperature feedback from a room isolated and distant from the thermostat can be a problem with floor-zoned heating systems.

Inspection of the other two monitored rooms for this 24-h period revealed better maintenance of setback and set point temperatures. The patterns of OT in the dining room and master bedroom suggest that the installed capacity of the forced-air system was sufficient.

Proving the sufficiency of the installed capacity for the forced-air system was not the point of this comparison—the sizing criteria for conventional heating systems are well established. Radiant panel sizing criteria are an issue because the undersizing of the radiant system is so dramatic compared with the sizing of conventional systems. The radiant system's performance down to and below design conditions supports the methodology for sizing that the manufacturer and university modeling employed for this installation, at least for steady-state conditions. The information available suggested that the installed capacity was adequate for recovery as well, but more specific investigation of this phenomenon may be required.

Calculating the heat loss of rooms and entire structures and subsequently establishing installed capacity is based on assumptions and often judgments by heating, ventilating, and air conditioning (HVAC) contractors. Sizing a heating system to meet the most severe possible weather for a location is clearly not economical (ASHRAE, 1993). The calculations and methodology of either the manufacturer or the university are certainly within the proper range. The significantly reduced installed capacity of the radiant system by either method of calculation appears appropriate to meet assumed design conditions given the evidence from this field study. The manufacturer's significant reduction in installed capacity with

nonmechanical radiant panels operating at lower average indoor air temperatures is credible.

### 5.3.9 Summary of Findings

**Air Infiltration.** The literature review provided consistent evidence of the reduced air infiltration rates with nonducted heating systems in comparison with forced-air ducted systems. The results of the two blower door tests performed on the AFSD house were in accordance with this evidence. The AFSD house demonstrated a 12.5 percent reduction in the natural air infiltration rate when in the radiant mode as compared with the forced-air mode. Previous research has shown that air infiltration during blower operation of a ducted system can double the air infiltration rate. The blower door tests performed at the AFSD house emphasized the validity and importance of effectively eliminating the duct system during operation of the radiant system. The sealing of all ducts and returns during operation of the radiant system served to increase the validity of the two-system comparison.

**Energy Consumption.** The radiant heating system demonstrated significantly better energy performance than either the heat pump or baseboard system. Translation of the three energy consumption–outdoor temperature relationships into expected energy savings for a given locale was accomplished with TRY data from Andrews Air Force Base. In the AFSD house, 33 percent savings could be expected by operating the radiant system instead of the heat pump, and 52 percent savings could be expected by radiant system operation in place of the electric baseboard system.

It is important to note that the comparative energy performance of the three systems is specific to the AFSD house and its occupancy by a working couple. Savings in other homes with varying numbers of occupants and their daily routines could have a significant impact on the comparative energy performance of the three heating systems.

**Installed Capacity.** The installed capacities of the radiant, heat pump, and electric baseboard systems support the radiant panel manufacturer's claim of significantly reduced installed capacity for the radiant system. The actual installed capacity of the radiant system was 40 percent less than recommendations for steady-state system operation, 50 percent less than the installed capacity of the heat pump system, and 60 percent less than the electric baseboard installation. (The installed capacities of both the heat pump and the electric baseboard were designed for day and night setback.) Review of data for outdoor conditions to and below design conditions (13°F) revealed that the installed capacity of the radiant system was adequate to maintain set indoor temperatures. There was insufficient information to determine definitively if the installed capacity of the radiant system was sufficient in the family room. Accurate information on the specific heat loss characteristics of a structure at the room-by-room level may be required to reduce the installed capacity of the radiant system to the extent presented in the AFSD house.

**Thermal Comfort.** Review of the thermal comfort surveys completed by the two AFSD house occupants suggested that comparable levels of thermal comfort were provided by the radiant and heat pump systems. Occupants found that their location in relation to the panels influenced thermal comfort. During recovery from setback, location for thermal comfort may be required. During steady-state conditions, the effect that viewing angle had on thermal comfort permitted individuals with varying

thermal requirements to locate in relation to the panel for comfort. Localized thermal comfort was found to be provided by the radiant system within 10 to 15 min during recovery, and roomwide comfort was provided in approximately 45 min. Both occupants found these delivery times acceptable, although the roomwide provision of comfort during recovery required anticipation of this room's use. The occupants, prior to any knowledge of the two systems' energy performance, indicated their preference for the radiant system because of greater flexibility and control on a room-to-room basis, silent operation, and fewer problems with sinus discomfort. Their preferences were based less on thermal comfort criteria than on features associated with system operation.

Lower air temperatures as the OT rises rapidly is central to energy savings claims with radiant heat. The rate of increase in the ambient air temperature in the monitored rooms of the AFSD house suggested reduced ambient air temperatures for 2 to 4 h, with prevailing outdoor conditions having a significant impact on the duration of reduced air temperatures. The specific geometry and heat loss characteristics of the room also had a significant impact on duration.

During some periods of extended panel operation, individuals located directly beneath a radiant panel registered thermal discomfort when a panel cycled off. Although the individual found the environmental conditions acceptable while the panel was energized, the rapid and sharp drop in OT associated with the panel cycling off caused thermal discomfort. Thermal discomfort due to panel cycling was only registered by individuals located beneath a radiant panel. (See Sec. 6 of this Handbook for information on proportional thermostats.)

The comfort analysis in this report is limited to the evaluation of subjective input from two occupants of the AFSD house. Although the evaluation of completed thermal comfort surveys provided valuable information on thermal comfort, their specific thermal requirements, standards of dress, and backgrounds cannot be ignored as limiting factors in the thermal comfort analysis.

Quantitative analysis, such as predicted mean vote (PMV) analysis or comparison with computer modeling results, would provide an additional basis for thermal comfort evaluation. Quantitative analysis would be complicated by the lagged response time of currently available operative or mean radiant sensors and the present inability of computer models to analyze thermal comfort delivery with radiant heating systems under transient conditions.

The complete report appendix included an illustration of the test house. See Figs. 5.55 through 5.59.

## **5.4 RESEARCH FOUNDATION IS FIRM**

---

Radiant panel research provides information removing mystery and uncertainty from radiant panel heating and cooling system design. In fact, the advantages of radiant panel systems becomes very clear when systems are designed to operative instead of dry-bulb air temperature. The range of radiant panel selection facilitates the provision of thermal comfort through radiant specification under almost any architectural scenario.

Before the National Association of Home Builders Research Center (NAHBRC) radiant heating study we just reviewed, there were few performance data available and little distinction between ceiling radiant systems. The NAHBRC case study monitored thermal comfort and energy performance in an occupied home during the 1993–1994 heating season. The project was conducted to expand the base of information on which heating systems are based.



FIGURE 5.55 Fire-safe adaptable demonstration house.

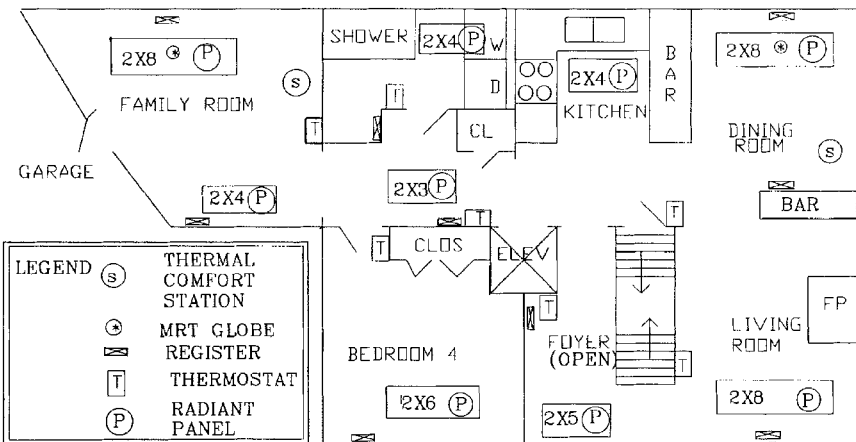


FIGURE 5.56 First floor of modular house.

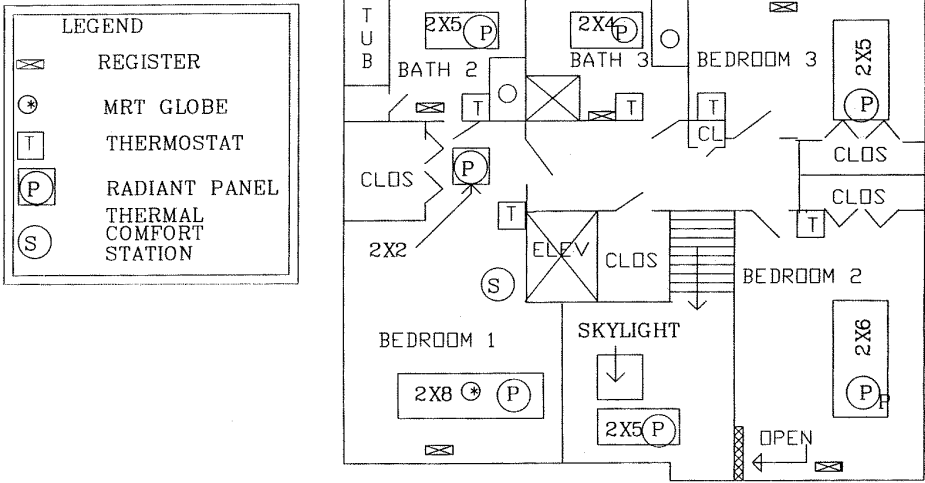


FIGURE 5.57 Second floor of modular house.

The case study found:

The magnitude of savings obtained for the working couple occupying the research home suggests that energy saving would be obtainable in a great portion of U.S. households. It is important to note that the comparative energy performance of the three systems is specific to the Adaptable Fire Safe Demonstration (AFSD) house and its occupancy by a working couple. Savings in other homes with varying numbers of occupants and their daily routines could have a significant impact on the comparative energy performance of the three heating systems.

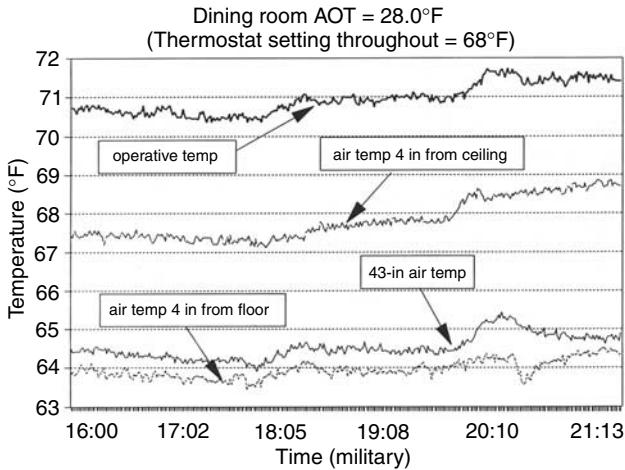
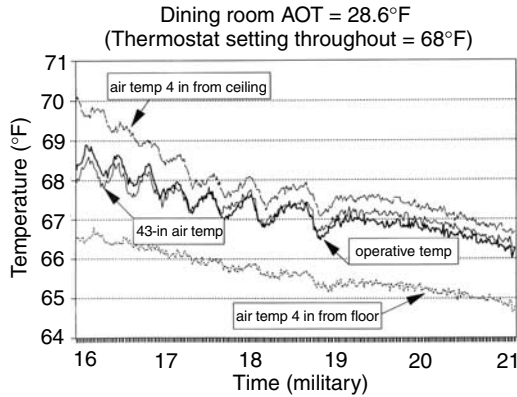


FIGURE 5.58 Temperature characterization: panels.



**FIGURE 5.59** Temperature characterization: heat pump.

Interest in the results of the NAHB Research Center study led to the development of the following case study, which was inclusive of both original and retrofit heating system comparison. The study extends the base of knowledge about the complex process of heating system performance evaluation and comparison. The next case study, which is benchmarked with the NAHBRC study, provides comparative information through retrofit installation, resulting in comparative information on seven different heating systems, ASHRAE, Transactions, SF-98-9-4, and is provided with the permission of ASHRAE.

### **5.5 CASE STUDY: SEVEN-SYSTEM ANALYSIS OF THERMAL COMFORT AND ENERGY USE FOR A FAST-ACTING RADIANT HEATING SYSTEM**

Falling real estate prices and rising maintenance and repair costs prompted the condominium association to develop a program to enhance its competitive attractiveness as a retirement community. Therefore, the case study focused on the relative performance of various heating technologies in relation to the needs of the retirement community. The information developed in the Radiant Demonstration Program (RDP) may be used with the NAHB case study to compare the comfort and energy performance of various heating systems in new and retrofit applications.

#### **5.5.1 Background**

The rural northeastern retirement community was built in the late 1960s and early 1970s for persons 55 years old, or older “empty nesters.” Members of the active retirement community now average 77 years of age. The bucolic 2700-unit complex includes single- and two-story duplex and quadplex cedar-sided buildings clustered in 24 condominium groupings. The buildings are slab construction with open-air-vented attics, outside-wall brick fireplaces, metal-framed sliding doors and windows with thermopane glass, noninsulation certified overhead recessed lighting, and bath-

room ceiling heat-fan units. Duplex units have 9-ft living and dining room ceilings; other ceilings are 8 ft. Some duplex units have garages underneath and/or crawl spaces. Four hundred units heat with electric furnaces. The rest are heated by concealed resistance heat wire preembedded in sheetrock serving as the ceiling. Six-inch fiberglass batts insulate the vented open-air attics. Standard correction of heating system failure involved removing the “ceiling” and reinstalling new sheetrock heater panels, which required taping, sealing, and texturing the entire contiguous ceiling area. Floor heaters, 750 or 1500 W, connected to the radiant system thermostat supplemented entry and sliding glass door areas. Installed watt capacity was 11 kW for the quadplex units, 17 kW for the duplex, and 20 kW for the electric furnaces.

The pocketbook issues were basically broken down into three categories: real estate value, energy cost, and condo fees. Although the market value drop is partly explained by area economic indexes, the “electric heat” image and high maintenance fees were also blamed. Rising electric rates spawned increased high-bill complaints, whereas the age-related repairs were escalating condo fees. Replacement of failing and drooping ceiling heat panels created a major and increasing expense. The condominium association was concerned that repairs were not taking advantage of new technologies that would improve comfort and lower costs while eliminating the problems that necessitated replacement or repair. The RDP followed a high-bill heat pump utility initiative that had unattractive capital costs. The condominium association was searching for programs to increase the economic attractiveness of the retirement community.

The comfort deficit inherent to the original buildings was also of major concern to the aging occupants. Owners reported discomfort sitting on window seats or near living room or bedroom sliding glass doors, unused living room fireplaces, kitchen dining table windows, and in the bathrooms and dressing areas. Temperature setback is impractical due to the lengthy recovery period inherent with high-mass, concealed radiant systems. Moreover, the association prohibited setback because frozen pipes were a recurring problem. Some residents didn't feel comfortable regardless of how much money they spent on heating.

### 5.5.2 Methodology

A lottery drawing was used to select one condominium to represent each of 18 building designs. A surface-mounted, modular, fast-acting ceiling radiant heating system was installed in each unit. Pre- and postenergy consumption was monitored during several heating seasons. Occupants compared the new fast-acting radiant system with concealed radiant heating and electric forced-air central furnaces. In addition, 12 high-bill complaints represented four designs that were previously retrofitted with standard air-to-air, high-efficiency air-to-air, and groundwater heat pumps (four of each), with monitored pre- and postenergy consumption over the same 3- or 4-year period. Four units were retrofit with compact, modern gas forced-air furnaces, which also provided hot water.

Separate metering was employed for the heat pumps for a period of time. The weather data normalization appeared to have very close correlation with the base bill average method during the mild 1994–1995 winter. The apparent impact of the resistance backup resulted in significantly higher kilowatt-hour per degree-day figures for the normal 1993–1994 and 1995–1996 winters, invalidating normalization as a tool for analysis of energy use. Next, a popular weatherization model, Princeton Score Keeping Method (PRISM) was employed to evaluate the 1995–1996 energy use in the radiant panel installations. The intent was to determine the impact of a limited weath-

erization program that involved caulking and sealing and the addition of attic fiberglass batt insulation to a total of  $R$ -38, which were not already in place. PRISM utilizes whole-house meter readings and average outdoor temperatures to develop normalized annual (energy) consumption (NAC) for pre- and postweatherization periods. According to the PRISM manual, "A static mode, PRISM is not appropriate, as some dynamic models are, for the management of a building to schedule thermostat setbacks." A feature of fast-acting radiant panels is dynamic occupancy oriented setup and setback, making use of PRISM inappropriate due to the "interventions" characteristic of the retrofit radiant equipment.

In the absence of instrumentation and/or appropriate dynamic modeling, the method of choice for analysis is the base bill method. A large sample population monitored over a period of several years provides an opportunity to detect distortions and benefits from time period averaging. The results of this approach tracked the experience documented in the DOE AHTP Project 4183 Case Study. The information developed in the RDP shows the range of energy use that might be anticipated in an elderly population with various residential retrofit heating system alternatives. The resident energy use range relates to the comfort of the original system, savings motivation, lifestyle, and the performance features of the retrofit system.

***Original Concealed Ceiling Radiant and Electric Furnace.*** The installing contractor appears to have followed general sizing and equipment practices in use before the 1973 energy crunch led to more demanding building codes. The concealed radiant sheetrock panels (14 wsf) were sized at 10 watts per square foot ( $W\ ft^2$ ) of floor space. Additional in-floor convection heaters (750 to 1500 W) were installed in front of sliding glass doors. It is normal practice to employ practicable, usually space-limited, oversizing to reduce the multiple-hour system recovery from vacation temperature setback. Individual room thermostats were designed for zone control.

The electric furnaces were 20-kW units, which reflected 30 percent or more oversizing, again to improve setback recovery. Metal ducting was incorporated with the slab to provide heat delivery at floor level. As with most central systems, control was by a single low-voltage thermostat.

***Heat Pump and Gas Furnace.*** Standard and high-efficiency air-to-air heat pumps, as well as geothermal heat pumps, were sized according to *Manual J* and ASHRAE methodology by the electric utility and the installing contractor. All heat pumps were installed with emergency resistance backup of 15 kW, according to standard practice in the harsh northeastern winter climate. Both equipment failure and the needs of the elderly population validated the necessity of installing emergency backup heat for all heat pumps. Due to the prohibitive cost of running new ducting, the existing air-conditioning ducts were used with appropriate modification (additional outlets, etc.). Control was by a single programmable heat pump thermostat.

The installing contractor sized the high-efficiency gas forced-air furnaces. Installation was in the former electric water heater "closet," requiring continuous mechanical ventilation. Again, due to cost, existing air-conditioning ducts were used with minor modification. Sizing reflects current multiple-equipment capacity options and setback recovery oversizing of 30 percent. Control is by a single low-voltage thermostat.

***Fast-Acting Surface Radiant System.*** The manufacturer, based upon extensive field experience in relation to established ASHRAE heat loss calculations, sized the fast-acting surface radiant system. Sizing was consistent with the methodology used for the NAHBRC case study, which incorporated thermal comfort monitoring based upon ASHRAE Standard 55 (ASHRAE, 1992). The Building Comfort Analysis Program (BCAP) was employed to fine-tune installations. The unique characteris-

tics inherent in the retirement complex construction and the occupant requirements necessitated sizing review. Yet installed capacity was 40 to 60 percent less than the comparative system. The multisized, higher-watt density (50 W/ft<sup>2</sup>), surface radiant panels are sized to the nearest 100 W of heated area and located in relation to heat loss requirements. Ceiling coverage is approximately 15 percent, compared with 80 percent for the concealed radiant. Control is by replacement, radiant sensing line-voltage controls.

***Thermal Comfort and Mean Radiant and Operative Temperatures.*** ASHRAE design philosophies continue to be focused upon obtaining a specific indoor air temperature for a given *design* outdoor air temperature. Referred to as the *envelope* calculation, the designer requires information on the number and type of walls, windows, and doors, the ceiling, and floors—but does not need information detailing the relative locations of these building components. An *energy balance* is then performed using regional weather data to determine the design outdoor temperature.

The thermal comfort approach incorporates the philosophy of providing occupant thermal comfort in the built environment rather than simply establishing a design air temperature. This procedure is not new. In fact, ASHRAE Standard 55 has stood the test of updating every 5 years for more than 25 years. The complexity of radiant heat transfer calculations was an obstacle to implementation of the standard until ASHRAE Research Project 657, *Simplified Method to Factor Mean Radiant Temperature (MRT) into Building and HVAC System Design* (Jones and Chapman, 1994), produced the Building Comfort Analysis Program (BCAP), covered in detail in Sec. 8. The *MRT* is defined as “the uniform temperature of an imaginary enclosure in which the radiation from the occupant equals the radiant heat transfer in the actual nonuniform enclosure” (Fanger, 1967).

*Thermal comfort* is defined in the standard as “the state of mind that expresses satisfaction with the thermal environment.” The standard defines thermal comfort as a function of air temperature, MRT, air velocity, relative humidity, clothing, and activity level. Activity level and clothing requirements are normally consistent with the building environment, air velocity is maintained low enough to prevent drafts, and the effect of humidity on thermal comfort is usually a function of the overall HVAC system. Therefore, the air temperature and MRT are the parameters controlled by the design engineer in a specific built environment. Nonuniformity in the radiation field, which leads to occupant discomfort, is expressed in terms of the difference between the mean radiant and mass-averaged air temperatures. Though MRT provides an indication of the radiation field in the room, Fanger (1967) found that the ambient air temperature cannot be ignored. Operative temperature, which combines the relative effects of the air temperature and the MRT by weighting convective and radiative heat transfer coefficients, is the best parameter to judge local thermal comfort.

The BCAP model incorporates radiation, conduction, convection, and air infiltration. This preciseness leads to enhanced, reliable MRT calculations coupled with calculated dry-bulb temperatures that provide an excellent indication of thermal comfort. The methodology provides a myriad of results in addition to the MRT and OT, including radiant asymmetry and dry-bulb air and surface temperatures. This methodology was useful in selecting heater output and design location for the fast-acting radiant panels to optimize room thermal comfort signature (TCS).

### 5.5.3 Field Test Results

A substantial quantity of electrical meter data were collected over several years to assess the results of the modified heating system. Table 5.64 presents the difference

**TABLE 5.64** Comparison Between the Various Units Before and After the Heating System Upgrades

Unit	Concealed 1993–1994	Surface radiant 1994–1995	Surface radiant 1995–1996	Surface radiant 1996–1997
Berkshire	2.52	2.46	2.43	2.00
Carriage H	1.89	1.92	1.72	N/A
Country H	1.87	1.80	1.80	1.66
Country H	2.59	2.11	1.76	1.70
Ethan Allen	0.90	0.69	1.00	.8
Franklin	1.62	1.69	1.75	1.61
Heritage	1.23	1.04	0.89	N/A
Kent	1.68	1.64	1.84	1.65
Hawthorne	1.72	1.76	1.51	1.72
Twain L	0.85	0.71	0.59	.73
Twain U	1.06	0.86	1.02	.9
New England	1.64	1.49	1.53	1.51
Roxbury II	3.23	1.90	2.29	1.96
Sherman	2.92	2.64	2.39	2.06
Sherman	1.93	1.84	1.81	1.82
Winthrop	1.94	2.03	2.02	N/A

in unit electrical consumption in 1993–1994 (before the modification) and in 1994–1997 (after the modification). The electrical consumption records are for the November-through-April billing periods. The first column in the table lists the housing unit style, and the second column lists the actual kilowatt-hour difference between the two billing periods (before and after). The last two columns express this difference in a percentage of the before-modification electrical consumption. The last column bases this percentage on the heating-only electrical consumption, which was calculated to be 64 percent of the total winter electrical consumption.

From the first column in Table 5.65, the difference in electrical consumption between the “before” and “after” heating systems ranges from a seasonal high of 5956 kWh to a low of 286 kWh. The average savings were 1736.75 kWh per unit, which is indicative of several of the units. The highest percentage of savings was 29.8 percent, with an average percent savings of 10.3 percent (14.6 percent over the heating-only electrical consumption). The extreme range of savings indicates the difficulty in designing heating systems. The distribution of the savings is also illustrated graphically in Fig. 5.60. This figure shows a histogram of the number of units that fall into each range. As shown, three samples fall into the negative category (i.e., required additional energy for operation). However, the majority of the 16 samples fell into the 500- to 2500-kWh savings categories.

This broad range is due mainly to the operational choices of the occupants, which can be explored more by referring to Table 5.64. This table shows a wide range of information based on the kWh consumption per heating degree-day (HDD). As this index increases, so does the electrical consumption. Again, the first column shows the housing unit style, followed by the electrical consumption before modification (concealed radiant). The second and third columns list the kWh/HDD for each unit during the 1994–1995 and 1995–1996 heating seasons. In some cases, the electrical consumption is greater for the modified system than for the original concealed system. For example, the occupants of the Ethan Allen style unit showed substantial

**TABLE 5.65** Radiant Demonstration Program Comparison of 16-Unit Composite Sample Size Data for November-Through-April Billing Periods (October Through March Degree-Days Equal Approximately 5500)

	Actual kWh difference	Difference compared with gross kWh	Difference applied to heating kWh only*
Country House	5606	29.8%	36.3%
Roxbury II	5956	29.2%	31.9%
Heritage	2274	22.6%	31.2%
Mark Twain L	1875	18.5%	35.9%
Sherman	3973	16.0%	26.2%
Carriage House	1698	12.0%	15.0%
Hawthorne	1658	11.5%	16.4%
Sherman (cir)	1665	8.5%	14.3%
New Englander	1291	8.4%	10.9%
Country House (cir)	1136	6.4%	10.3%
Mark Twain U	527	4.4%	8.2%
Berkshire	719	3.6%	5.0%
Winthrop	85	-0.1%	0.8%
Franklin	-217	-1.8%	-2.3%
Kent (crest)	-286	-1.9%	-2.8%
Ethan Allen	-172	-2.0%	-3.1%
Average	1736.75	10.3%	14.6%
Total gross savings	27788		

\* Base bill estimate method used to determine heating kWh. Total heating kWh averaged 64 percent of 6-month winter gross kWh used.

savings from 1993–1994 to 1994–1995. The kWh/HDD decreased from 0.9 to 0.69, a change of 23.3 percent. However, the next heating period, shown in the table as 1995–1996, resulted in an increase to 1.0, a change of 11.1 percent. The differences in the second and third columns are suspected to be due to the operational differences of the occupants. The occupants of the Kent, Twain U, New England, and Roxbury II units experienced this same trend.

In general, the Ethan Allen occupants knew that the original concealed system was extremely expensive to operate. Consequently, they chose to remain thermally uncomfortable when facing the prospect of receiving large electrical bills. As stated earlier, the original concealed radiant system, relying primarily on high thermal mass, exhibited poor thermal response. This characteristic was due to the combination of high thermal mass and a low power level of 14 W/ft<sup>2</sup>. Because of this long thermal response, thermostat setback was rarely used. Instead, the occupants kept the thermostat at a constant cool setting. The radiant surface panel system, however, responds quickly to thermostat adjustments, allowing the residents to use thermostat setback features at night and during unoccupied periods. Following the setback period, the occupants experienced comfortable conditions in minutes instead of hours. By operating the system in this manner, the occupants found they could stay thermally comfortable for the same, or often lower, cost as with the concealed radiant system. During this reeducation process, the residents learned to use the radiant system to attain thermal comfort in a cost-effective manner.

The heat pump, baseboard, and gas installations replaced concealed radiant units. As shown in Table 5.66, the heat pumps averaged 2.07 kWh/DD in the mild 1994–1995 winter compared with the concealed radiant of 2.25. In the harsh 1995–1996 winter, the

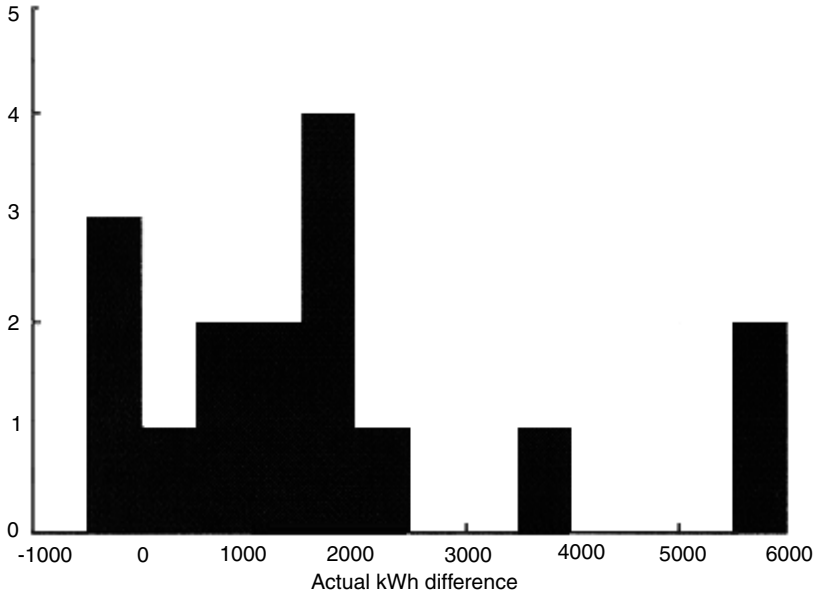


**FIGURE 5.60** Histogram showing the distribution of actual kilowatt-hour differences between the examined units.

relationship was still favorable at 2.48 to 2.66, although the resistance backup significantly reduced the overall efficiency. Both systems were higher than the fast-acting radiant, which averaged, respectively, 2.04 and 1.96 kWh/DD. Four heat pump owners have since converted to fast-acting radiant units and one to a baseboard unit.

The four gas conversions averaged the same actual annual dollar expenditure, adjusted to include the summer minimum charge necessitated by the hot-water conversion to gas. The actual Btu consumption averaged almost 50 percent higher than the concealed radiant, presumably due to the required furnace ventilation and increased building forced-air infiltration and exfiltration.

Baseboard electric averaged 2.36 kWh/DD compared with 2.00 kWh/DD for fast-acting radiant. The controls and setback for the baseboard units were not known. Baseboard heating was seldom used due to safety concerns, building design, and the reluctance to sacrifice wall space—characteristic of occupants with a lifetime of possessions.

**TABLE 5.66** Radiant Demonstration Program Comparison of 50-Unit Composite Sampling (kWh/DD) for the Entire Heating System

Equipment	92/93	93/94	94/95	95/96	96/97	Average	NAHB
Heat pump	n/a	2.78	2.07	2.48	1.96	2.32	2.29
Electric furnace	n/a	2.59	n/a	n/a	n/a	2.59	n/a
Concealed radiant	2.34	2.23	2.25	2.66	n	2.37	n/a
Surface radiant	n/a	n/a	2.04	1.96	1.49	1.83	1.54
Baseboard	n/a	n/a	2.14	2.33	n/a	2.33	3.21
Gas	n/a	n/a	n/a	3.66	n/a	3.66	n/a

## 5.6 RESEARCH OUTLOOK

---

ASHRAE and organizations operating under work statements funded by ASHRAE have conducted basic research for decades. Solid information and design methodology are largely proven through research already conducted. However, there has been little application of this information in the development of computer design and simulation programs. RP-657 and subsequent related research has demonstrated that this can be done. The applications research projects have validated the results. It is clear that there are substantial benefits that are in the national interest, both in terms of energy conservation and occupant health.

There is need for more comparative information. The Radiant Panel Association (RPA), electric and gas utilities, and government agencies are organizations that may have access to data on large numbers of installations that could be aggregated into a database or comparative study. Research organizations allied with particular interests or that might favor a particular product or company are not good candidates for comparative studies. In addition, large studies are costly and usually practical only when utility consumption figures are readily available for other reasons. In any event, large-scale studies are relatively uncommon, and those that do exist were for convection systems that are now outdated by code and technological building and equipment change.

Yet, the body of research and case study that does exist for radiant heating confirms that radiant heating systems do provide occupant thermal comfort with equipment sizing that is below that which is indicated by ASHRAE design guidelines for convection systems.

## CASE STUDIES\*

S · E · C · T · I · O · N · 6

**CONTROL OPTIONS  
FOR RADIANT  
HEATING AND  
COOLING PANELS**



---

# CHAPTER 1

---

## INTRODUCTION

---

This section focuses primarily on the governing control that provides the initial signal to the component(s) that are appropriate to operate each type of radiant heating panel, equipment, and system. The initial control is normally either a low- or line-voltage thermostat.

Thermostats usually operate in relation to the air temperature that is sensed or measured in the occupied space. For nonconcealed or visible electric systems, such as wall or ceiling radiant panels, a room or area thermostat may be the only control required. A single low-voltage control is also often used for gas-fired radiant heaters.

For concealed or hydronic systems, more complex control design may be required. Embedded electric or hydronic floor heating may also have an over-temperature-limit sensor or temperature control located in the radiant floor panel to prevent the panel from exceeding a maximum temperature or to control surface temperature to a specific maximum comfort temperature. For floor warming, the only control parameter may be the actual floor surface temperatures, not in-space air temperature.

The hydronic system's master thermostat may have an array of supportive flow and temperature control sensors and valves that interact in response to the master control. Slave or independent area controls may be employed to implement zone control. The entire system may also be further governed by an outdoor reset control that communicates changing outdoor temperatures so that the interior controls can control the system in anticipation of the heat loss conditions that the insulated interior space will ultimately experience (Fig. 1.1). Variable-temperature radiant hydronic systems utilize motorized mixing valves to adjust water temperature in relation to the change in outdoor temperatures.

An energy management system may further manage all system components in harmony with a centrally managed control protocol primarily designed to optimize mechanical system operating efficiency. Finally, safety controls can override other controls to prevent malfunction, protect the equipment, and reduce risk of damage.

Downstream flow, control, and temperature valves and related mechanical and electronic equipment controls are complex, varied, and installation specific. Furthermore, a number of issues such as "control valve differential pressure selection is considered by many to be part art, part experience" (Hegberg, 2000). This chapter focuses on the issues involved in selection of governing controls related to in-space occupant thermal comfort. The reader is advised to consult the ASHRAE handbooks, application-specific resources, and equipment manufacturers for information on how best to design the interactive hydronic support system to ensure optimal radiant system control set point response (Fig. 1.2)

The primary objective of in-space thermostatic controls of any type is to operate a given device or system in relation to the control set point, based on whatever mea-

6.4 CONTROL OPTIONS FOR RADIANT HEATING AND COOLING PANELS

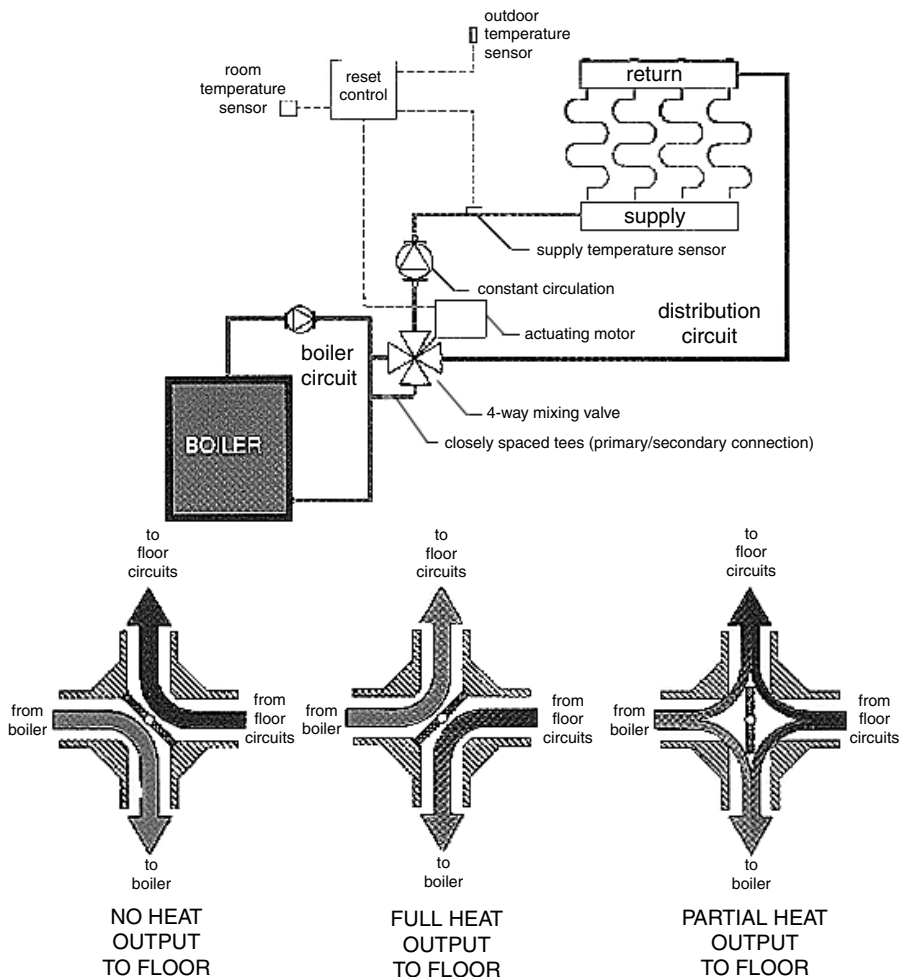
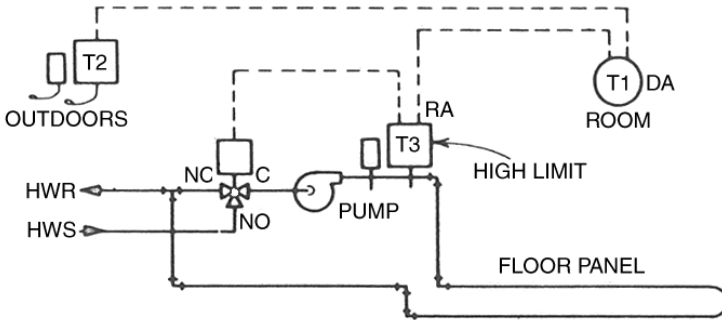


FIGURE 1.1 Four-way motorized mixing valve. (Source: Siegenthaler, Plumbing & Mechanical, 1996.)

surement protocol is used to define the set point. For heating and cooling systems in the built environment, the set point has historically been defined in degrees Fahrenheit or Centigrade based on capability to measure dry-bulb air temperature. Measurements of air temperature normally occurred at the thermostat that contains the sensor. Central to the assumption that occupant comfort is provided at a dry-bulb air temperature set point is the assumption that average unheated surface temperatures are equal to the dry-bulb air temperature, and that dry-bulb air temperature is uniform throughout the space that the thermostat controls.

People have grown accustomed to setting thermostats at 72°F, assuming that this number is the key to comfort. President Jimmy Carter actually used national television and donned a red sweater during the “energy crunch” in the 1970s to show peo-

ple how to be comfortable and save energy. He explained that lowering thermostats from 72°F to 68°F, a 4° temperature setback, would result in approximately 12 percent energy savings. With radiant heating, occupants are comfortable at dry-bulb air temperatures that are often below 68°F.



**FIGURE 1.2** Floor panel heating: hot water. (Source: Haines, Hittle, Chapman & Hall, 1983.)

Radiant designers sought to capture the energy savings that radiant heating can achieve through providing in-space occupant comfort at lower dry-bulb air temperatures. They replaced temperature markings on some controls with such words as *comfort zone*, *warm*, *cool*, *low*, *medium*, and *high* rather than dry-bulb air number settings (Fig. 1.3). The idea was that the occupant would select a comfort setting, without prejudice to air temperature. It was expected that the comfort setting would reflect energy savings due to the lower dry-bulb air temperatures at which in-space occupant comfort may be achieved in a radiantly heated environment. Although the concept may be sound, many people are uneasy with a control without numbers for selection, a thermometer or temperature display for performance comparison, and a “click,” indicator light, or other sign that the system is off or on.

The commonly chosen dry-bulb air set point temperature numbers relate to controls used for convection heating systems that are in the great majority of U.S. buildings. The common set point temperatures are not based on actual in-space occupant thermal comfort analysis, or operative temperature. In fact, many built environment heating and cooling control books do not even define comfort or relate to the extensive research conducted to define the parameters of human thermal comfort.

Control capabilities have improved markedly with the introduction of electronic sensors, improved switches, digital display, and multiple programming and communication features. Accurate air sensing is inexpensive using a thermistor that communicates dry-bulb air temperature changes through the resulting change in thermistor resistance that temperature change causes. However, actual set point control continues to be based solely on dry-bulb air temperature because few controls sense, measure, or respond to mean radiant temperature. Thermostat sensing is generally of the dry-bulb air temperature encountered in, on, or around the thermostat housing, and the system heating or cooling the space monitored by the thermostat is designed to respond accordingly.

The local air temperature sensed will not be indicative of the actual in-space conditions unless they are representative of (1) dry-bulb air temperatures prevailing

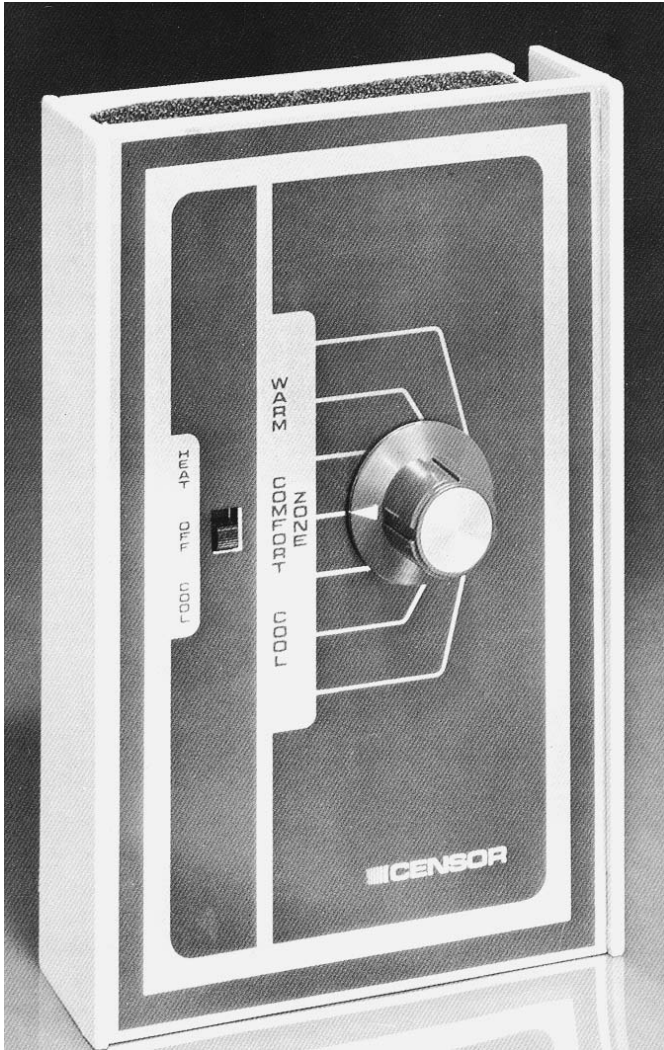


**FIGURE 1.3** Example of comfort zone electronic thermostat.

throughout the heated space and (2) average unheated surface temperature (AUST) also matches sensed dry-bulb air temperature. Such conditions are more likely to occur in new Model Energy Code (MEC), superinsulated residential buildings, and in buildings conforming to ASHRAE Standard 90.1-1999 for commercial buildings. However, occupant thermal comfort is not ensured by the application of these guides or codes. Such buildings, by specification or definition, embody specific design and insulation features to improve building energy performance by minimizing building heat loss, such as exposure-defined glass percentages and infiltration

limits under various conditions. However, these codes and standards do not incorporate ASHRAE Standard 55 as either an objective for, or prescriptive measure of, building performance.

However buildings are constructed, air-sensing thermostats are only reactive to heating and cooling system load changes resulting from human occupancy, solar or night radiation, and other temperature, wind, heat transfer, and use influences after the change in dry-bulb air temperature has occurred. Radiant thermostats embody sensors that quickly recognize changes in mean radiant temperature (MRT), whether structural or occupancy based. The heating or cooling system is operated to reflect the change in MRT so that the system does not overshoot or undershoot the dry-bulb air temperature. Over- and undershoot are common complaints with conventional convection heating and air-conditioning control systems that only respond to influence of MRT after it is reflected in dry-bulb air temperature. This means the responding HVAC system is always playing catch-up to the changing room conditions.

The improvement in comfort control achieved through the load anticipation that sensing of MRT provides is not to be confused with the heat anticipation feature built into many heating controls. The heat anticipator is designed to anticipate the flywheel effect of the heating system so that temperature overshoot does not occur. This is accomplished by use of a resistor that provides localized heat to cause the thermostat to shut off heat just prior to reaching set point.

Control to operative temperature (OT) optimizes building thermal control in relation to occupant thermal comfort because the impact of surface temperatures is taken into account. However, control selection, whether based on dry-bulb air temperature or operative temperature, impacts system performance and should be integrated into design analysis. We explore the range of control options and their significance in terms of equipment sizing, energy use, and occupant thermal comfort. We relate the impact of control operation to the building architectural features and building materials  $R$  values.

Finally, we review operating characteristics of various thermostat options. Thermostat operational basics include cycle frequency, set point accuracy, droop, power requirements, unit power consumption, setback-setup functionality, off-on and proportional operation, and system design and performance factors impacted by central system management.

## INTRODUCTION

---

# CHAPTER 2

---

## ROLE OF THE HEAT OUTPUT

---

### 2.1 INTERFACE WITH THE SPACE BEING CONDITIONED

---

#### 2.1.1 CONVECTION SYSTEMS

Traditional design procedure has been focused on locating convection heat output where it will address heat loss and provide relatively uniform space conditions in terms of dry-bulb air temperature. Convector design and location are designed to provide unobtrusive heat delivery. However, convection air temperature depends on the heat generation system and varies with the length of run from the source among other lesser factors. Regardless of the factors impacting the temperature of warm air flowing from the diffuser or convector, the design protocol is developed with the objective of heating or cooling space in the built environment to a given temperature set point, usually 72°F for heating.

For convection furnace and heat pump, the registers were usually placed in the floor facing up to “wash” the window with warm air. Sometimes, the diffusers open directly over the window, and the floor returns are located to pull the warm air down and across the floor. This approach has become more common because ducting is commonly shared for both heating and cooling. With dual use, there is also a need to set system pressurization controls for each mode, adjust for the seasonal change-over, and recognize that alterations that affect airflow will require a complete system pressure rebalance. In hydronic convection systems, the radiators and baseboards were generally placed under windows and along outside building walls of the rooms being heated.

The air temperature that is measured for many central systems is at the single thermostat that is located in an interior hallway on only the first, or perhaps in an interior hallway on each, floor. Variances in area heat loss or related heat Btu supply result in a temperature imbalance that a central control is unable to detect. Examples are the “cold blow” associated with the heat pump and the “scorched air” associated with gas furnaces. Perhaps this is why it is reported that “50–60 percent of all homes have serious comfort, and by default, energy-related problems” (Guarino, Contracting Business, 1998).

There are many factors that can lead to multiroom central system-conditioned space temperature inequality. Among them are heat gain from appliances, lights, and occupancy. The “cold back or feet syndrome” occurs when the occupant’s body heat radiates to a cold wall or window, or conducts to the floor. Conversely, excessive radiant gain may occur when the occupant is standing next to a radiator, stove, fireplace, or other heat-generating object.

**6.10 CONTROL OPTIONS FOR RADIANT HEATING AND COOLING PANELS**

Aside from the normal heat loss variation caused by use, wind, solar, day, and night impacts, the simple act of closing a door, activating an exhaust fan, or closing the drapes, blinds, or window shades may unbalance an otherwise well-designed convection system. Zoning, remote sensing, and interactive heat delivery are a few control options that are designed to cope with the dynamics of space conditioning. But they are usually reactive systems, because they are responding to changes in dry-bulb air temperature readings as the thermostat is impacted by change in the heat loss variables and mean radiant temperature (MRT).

Convection registers, grills, diffusers, and baseboards each contribute a small radiant component to heat delivery as they are warmed by the heated outcoming or convecting air. However, the dominant MRT input, in terms of human thermal comfort in the conditioned space, is the temperature of the surrounding surfaces, especially those that occupants are likely to be near, such as a slab-on-grade floor or a large window. A radiant system may be required to ensure that MRT design requirements are met when average unheated surface temperature (AUST) deviates very much from desired room dry-bulb air temperature set point.

**2.1.2 RADIANT SYSTEMS**

Radiant central systems may be controlled from a single thermostat with a similar hallway location, which also measures dry-bulb air temperature. However, because the building is not pressurized by the design of the heating system, performance of a well-designed radiant system is less impacted by draft, convection, and other thermal comfort factors, except solar, that are characteristic of convection systems.

Transmission losses are significantly lower for radiant systems. ASHRAE Standard 152, *Residential Thermal Energy Distribution Efficiency*, provides methodology for determining thermal energy loss for single-family residences with independent air, hydronic, or electric distribution systems. Energy transmission losses for either cooling or heating are much less significant factors for equipment sizing, control, and energy use performance analysis for radiant electric or hydronic systems than they are for convection systems, where losses range from 15 to 40 percent.

On the other hand, each high-mass floor panel has unique design and control requirements. The possibility that performance-affecting changes (e.g., room use, lifestyle, furnishings, or alterations) can be made during the long panel life requires that appropriate flexibility is built into system control. The documentation should record what was done and note limitations. Factors, such as panel location within the building and distance from heat source, impact heat loss to be met by the system. Flooring *R*-value differences and the possibility of alteration, as well as room use, occupancy, and heat loss dynamics, are reasons that room-by-room zoning is essential to optimizing system occupant thermal comfort performance and operating efficiency.

Almost all electric and most hydronic radiant heating systems are easily zoned. Closing a door usually will impact convective system balance but will not impact the performance of a radiant zone, except to reduce natural infiltration or exfiltration through the door opening. However, the impact of solar gain added to a radiant floor that is already operating at peak heat delivery could result in significant in-space temperature overshoot. Factors such as these are only manageable if the control design is comprehensive and flexibility to respond by zone is both timely and effective.

High-mass radiant systems, which to a greater or lesser comparative degree include all concealed radiant systems, have a response time related to the heat transfer characteristics of the panel mass. Outdoor reset controls are used to com-

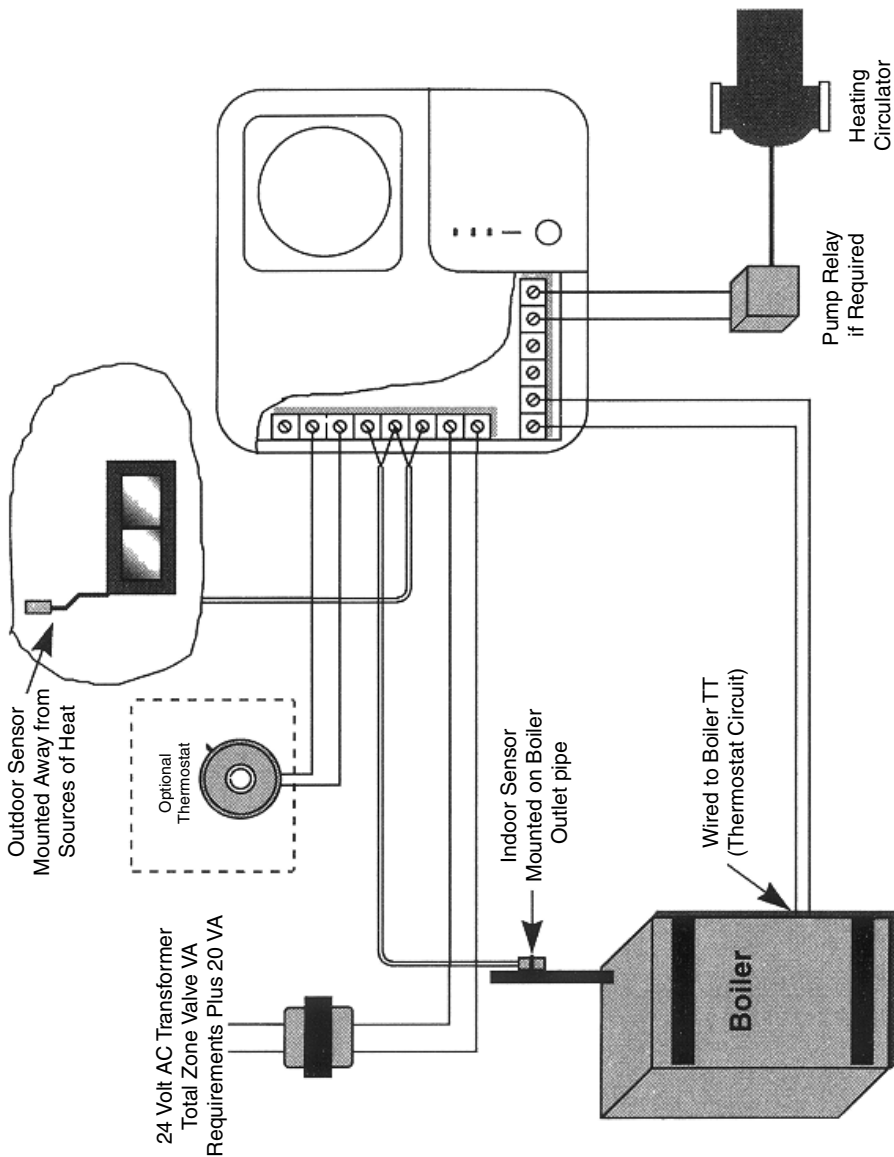
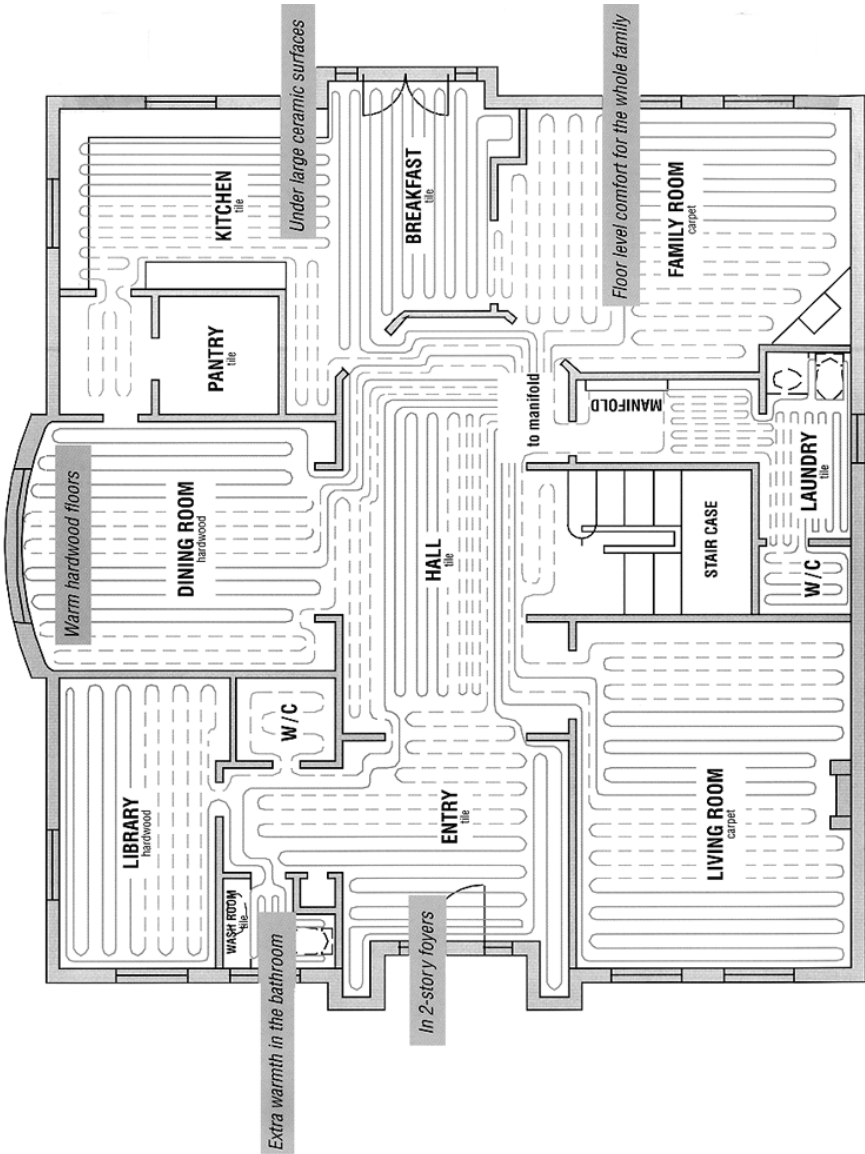


FIGURE 2.1 Basic wiring schematic for a hydronic system.



**FIGURE 2.2** Schematic shows differences that make room control important for radiant floor heating.

municate exterior temperature changes to the control system. The control uses the information to effect mass charge and discharge to maintain thermostat dry-bulb air temperature set point. If outdoor reset was not used, the system could only respond very slowly to the change, resulting in temperature deviation from set point (Fig. 2.1).

Unlike convection systems, radiant systems deliver more than half of panel heat output radiantly. Whether the heat is delivered from the floor, wall, or ceiling, the panel surface temperature during the “on” cycle is elevated from the dry-bulb, set point air temperature in an amount related to a variety of factors. The MRT is higher than with convection systems. Controlling the radiant system to the same dry-bulb air temperature as convection systems results in a warmer in-space thermal environment that would be apparent in the operative temperature.

Radiant panel heat delivery surface temperatures are sometimes panel-specific, sometimes a system variable, and sometimes a matter of panel selection. Radiant panel heat output and placement dictate the range of surface temperature constraints, as well as the split of radiant and convection heat delivery. Control selection and system management capability must be matched with these radiant panel performance parameters (Fig. 2.2).

## **2.2 INTERFACE WITH THE SPACE BEING HEATED**

---

Because all radiant heating systems heat occupants and objects, which then reradiate heat, thereby warming the space, it makes sense to measure MRT as well as dry-bulb air temperature to determine occupant thermal comfort. Controls that incorporate MRT are on the horizon, but for now dry-bulb air temperature control is the standard means that operates heating and air-conditioning systems.

The result is that systems are designed to heat space, not people, and therefore, buildings, not occupants. Convection system capacity, although often made up of separate heat generation modules, is generally much less efficient and requires oversizing when operated by zone and using temperature setback-setup, although the modules can ramp up or down with building-wide heat loss demands. Convection heat losses are generally increased by the process of zoning and attendant pressure balance changes. The impact of such changes must be factored into the economics of convection system operating analysis.

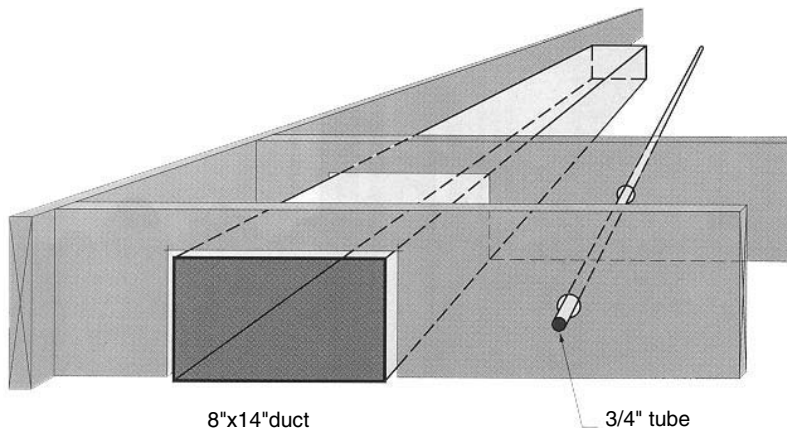
Radiant systems have small transit heat loss compared with convection systems (Fig. 2.3). Zones can be controlled to dry-bulb air temperature. Radiant systems develop natural convection but experience less heated air migration and maintain a higher MRT than convection systems. Radiant heat interacts directly with occupants. Human skin is an excellent radiant receptor. The radiant field, or MRT, is an important determinant of the dry-bulb air temperature at which occupant thermal comfort may be achieved in a radiant heat environment.

Fast-acting radiant systems restore comfort quickly and do not require capacity up-sizing for moderate setup or setback recovery. The sizing of radiant and convective systems for setback-setup based on occupant thermal comfort using operative temperature (OT) is being addressed in ASHRAE Research Project 1114, *Develop Simplified Methodology to Incorporate Thermal Comfort Factors for Temperature Setback/Setup into In-Space Heating and Cooling Design Calculations*.

Common practice is to oversize the convection heating system by 20 percent if day setback-setup is to be practiced and 40 percent if both day and night setback-

6.14 CONTROL OPTIONS FOR RADIANT HEATING AND COOLING PANELS

setup are used. The reason for significant oversizing is to reduce the recovery period for comfort restoration. In practice, oversizing is often even greater as furnace or boiler size is dictated by the available equipment match for both convective and hydronic radiant systems. This is further complicated for heat pumps where the dominant load—cooling or heating—determines equipment sizing. Electric radiant and baseboard heating designs may be more precise because equipment gradations are much smaller. Oversizing or capacity beyond what is required to satisfy the heat loss of concealed radiant systems has traditionally been dictated by impact of surface coverings, the need for uniform heat across the surface, and the level of tolerance for the duration of setback or vacancy recovery.



The 3/4" tube can carry as much heat as the 8"x14" duct when both are operated under typical conditions.

**FIGURE 2.3** Hydronic conduit compared with forced air duct.

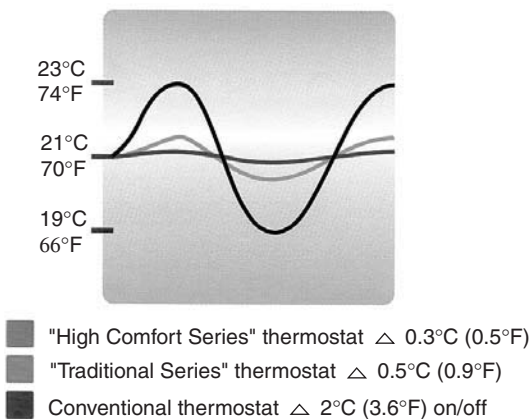


**FIGURE 2.4** Graph of range of thermostat comfort performance.

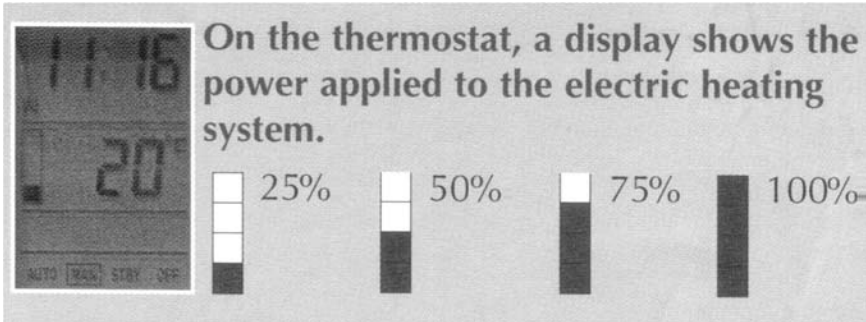


**FIGURE 2.5** Range of power supplied.

Surface-mounted radiant panels generally respond very quickly compared with concealed radiant systems and most convection systems. Minimal oversizing is required for normal occupancy setback of 5°F. Oversizing for recovery from long-term vacancy setback of 20°F or more is determined by the recovery tolerance.

There are restraints and consequences to oversizing. For any system, there could be short cycling during moderate periods that would impact occupant thermal comfort and operating efficiency. For radiant panels, the constraints of surface temperature and radiant asymmetry limit the acceptable level of panel heat output under the entire range of operating conditions.

The use of proportional or modulating controls can address panel heat output variation concerns in relation to occupant thermal comfort (Fig. 2.4). The use of remote access or programmable controls may eliminate concerns about the duration of recovery ramps. In all cases, the system design must be comprehensive to be certain that the solution to one problem does not create another (Fig. 2.5).

Management of heat output, whether by convection, radiation, or the combination of each, is the objective of the control protocol for occupant comfort and energy efficiency.

## ROLE OF THE HEAT OUTPUT

---

# CHAPTER 3

---

## CONTROLS IN COMMON USE

---

Many different types of controls are in common use. Most operate with low-voltage or line-voltage electric current. Some commercial systems operate with pneumatic pressure or wireless communication. For residential and light commercial centrally convection-heated buildings, use of a single low-voltage interconnected thermostat is common for each unit or dwelling area. Line-voltage thermostats are generally used in conjunction with electric resistance heating systems that are installed and operated on an independent room-by-room or area-by-area basis utilizing separate controls for each room or area. Low-voltage thermostats are used for central heating systems, large electric heater loads, and for interconnected zoned electric room systems.

Traditional thermostats are reactive to changes in dry-bulb air temperature and were designed primarily for convection heating systems. Thermostats measure the temperature of air that circulates past the sensor that is shielded by, enclosed inside, or exposed on the thermostat cover. Thermostats are normally installed on an inside wall, away from extraneous heat sources. The thermostat has traditionally been positioned 5 ft above the floor in a convenient location where the air being sensed is representative of the air temperature in the space being controlled.

The built environment into which a control is to be installed must be fully defined in terms of thermal conditions as well as range of performance requirements. The demands placed on a control are impacted by a variety of factors, including new or existing building construction materials, nature of construction, as well as configuration and use: an atrium, factory, meeting room, office, rest room, basement, and so forth. The control design must also be carefully analyzed and defined by the objectives of building operation, space conditioning, and occupant thermal comfort.

Factors for consideration include cost, control specification conformance, installation location, electrical service options, resistive and/or inductive load, control energy use, control performance efficiency, setback-setup, and communication and program capability, set point accuracy, “droop” or operational temperature set-point deviation, cycle frequency, accuracy, and so forth. In hydronic systems there are the additional factors of multiple downstream mechanical functions that must be safely and harmonically synchronized to achieve the response required to satisfy the control command.

### **3.1 BIMETAL AND ELECTRONIC LOW-VOLTAGE THERMOSTATS**

---

Perhaps the most familiar low-voltage thermostat is the familiar round thermostat often located in a first-floor residential or light commercial hallway to control a cen-

**6.18 CONTROL OPTIONS FOR RADIANT HEATING AND COOLING PANELS**

tral heating system. Low-voltage controls are used for electric, oil, or gas hydronic and forced-air heating system. Low-voltage thermostats operate on 24-V current. UL listing is not required for low voltage. However, to use a low-voltage thermostat, a transformer usually must be installed to convert line-voltage to low-voltage power supply to the thermostat. Low-voltage bimetallic thermostats do not generate heat or experience line droop. They are generally accurate, yet inexpensive, basic thermostats.

However, in zoned electric baseboard or radiant heat, the cost of the thermostat, plus the relay transformer, and attendant wiring and installation usually exceed the cost of using one or even two electronic line-voltage thermostats. However, for larger loads or where multiple zones are involved, low-voltage thermostats remain a viable electric baseboard or radiant heat option. The design feature in comparison with line-voltage thermostats is that a larger electrical load can be designed by using low-voltage thermostats to control a series of circuits through the use of transformers and relays.

The contacts are very responsive to the current settings, usually measured in milliamps, and result in comparatively better control than bimetal snap-action line-voltage controls. Bimetal low-voltage thermostats provide consistent performance over the full range of loads for which they may be used. Line control performance is impacted by amperage draw resistance heat. Mercury-activated contacts have been replaced for environmental reasons by sensitive bimetal air temperature-sensing coils that are usually dust shielded and positioned for optimum sensing within the low-voltage thermostat housing.



**FIGURE 3.1** Electronic “round.”  
(Photo courtesy of Honeywell International.)

Low-voltage thermostats are commonly used for in-space control of radiant hydronic central and zoned systems, with remote controls for each zone. Low-voltage controls are also used to control larger, multicircuit electric panel system loads, in combination with the required transformer(s) and relay(s).

Low-voltage thermostats include basic off-on models, as well as programmable models, and models that can also control blowers, fans, and air conditioning. The controls are generally low in cost and high in traditional air-sensing temperature control performance. The programmable models are electronic, with accurate dry-bulb air temperature electronic sensing and, in some cases, battery-free memory storage capability in the event of a short-

term power failure. A good example of the electronic evolution of low-voltage thermostats is found in the common trademarked round thermostat (Fig. 3.1).

### **3.2 SNAP-ACTION BIMETAL AND ELECTRONIC LINE-VOLTAGE THERMOSTATS**

Snap-action thermostats are named for the familiar click that is made by the opening and closing of their electrical contacts due to a permanent magnet that accelerates final circuit closure and ensures chatter-free electrical contact closure. Snap-action thermostats were used for almost all electric resistance heat installations, which were dominant before the advent of the heat pump. A bimetal temper-

ature-sensing plate is adjusted, or calibrated, by means of a setscrew, which is adjusted so that the contacts are open at the thermostat set point temperature that matches the actual air temperature reflected by the position of the bimetal plate (Fig. 3.2). Bimetal thermostats have a long life, although their accuracy usually declines over time as the bimetal sensor oxidizes, corrodes, gets dusty, and the springs and contacts become corroded, pitted, and otherwise worn.

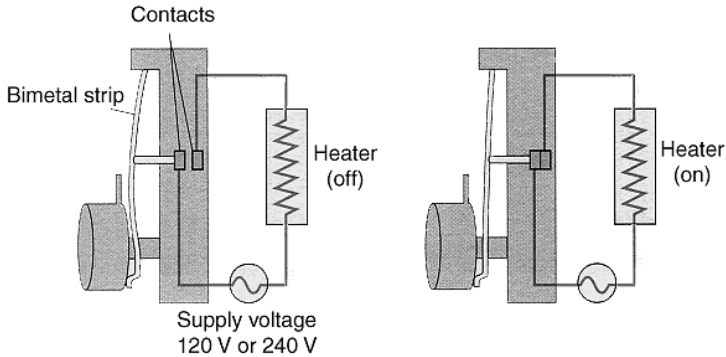


**FIGURE 3.2** Operation of bimetallic thermostat.

The heating system operates in response to current flow through contacts, which either close (make contact) to enable the flow of current when heat is needed, or break (open) to stop current flow when the load is satisfied. The sensitivity of the bimetal sensor to the surrounding air determines how often the contacts open and close to maintain thermostat set point. It is important to know the contacts' capability in relation to current flow so that the correct thermostat is installed. Some thermostats require a minimum load, or amperage draw, to activate. Others are damaged by the current surge from a fan, motor, or any inductive load and may only be used for control of electric resistive loads. Manufacturers' instructions will detail the ability of the control to handle resistive and/or inductive loads, and the minimum and maximum amperage draws for each.

A bimetal line-voltage thermostat is usually designed for use on all common line voltages. Electronic thermostats are usually voltage specific and will only operate on the specified voltage. However, some electronic models are designed to operate on either 120 or 240 V or 208 and 240 V. Bimetal thermostat design includes two-circuit models that can handle 5000 W in total. Some electronic thermostats can handle as much as 4800 W on a single circuit. Manufacturers' specifications will detail the control voltage, amperage, and wattage capability. As technology advances are extended to all types of controls, the features and capabilities will continue to broaden.

Line-voltage controls that are double-pole four-wire controls have the capability to break both electrical lines, thus providing a "positive" off. Some building codes require double-pole thermostats. The use of double-pole thermostats is advised for safety and equipment protection during periods of system shutdown (Fig. 3.3).

Single-pole thermostats are two-wire controls that only break one line. They may be used on 240-V systems but are most commonly used for 120-V systems to reduce wiring or deal with an existing single electrical feed. Many electronic line-voltage controls are only available as single-pole models.

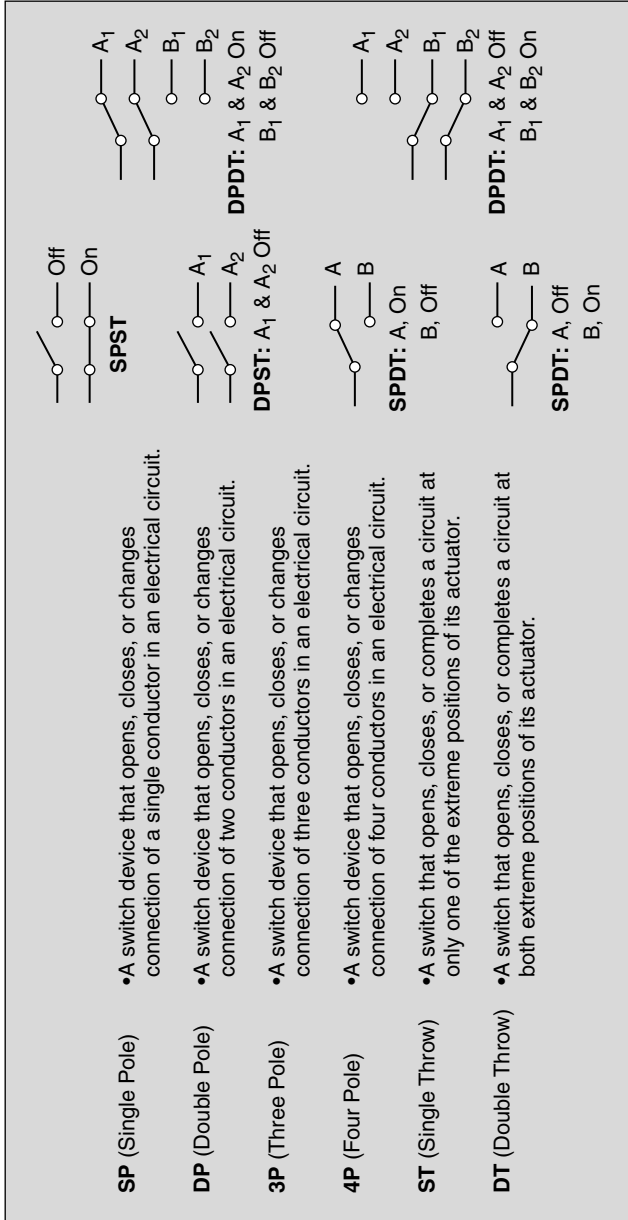


**FIGURE 3.3** Switch terms.

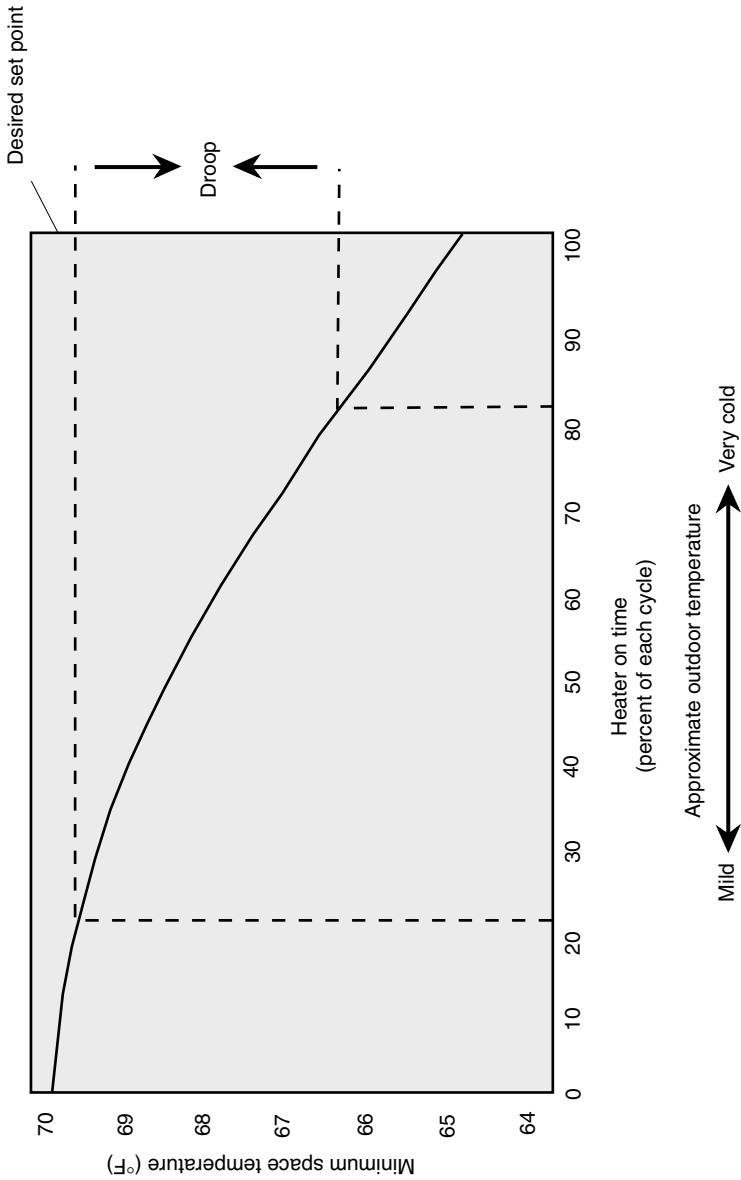


**FIGURE 3.4** Profile of 3°F thermostat droop.

**6.22 CONTROL OPTIONS FOR RADIANT HEATING AND COOLING PANELS**

Line-voltage controls have historically depended on temperature-sensing accuracy in relation to actual room dry-bulb air temperature. In fact, the term *droop* was introduced to characterize the deviation from set point experienced by line-voltage thermostats whose construction and electrical load created heat that impacted temperature-sensing and operational accuracy (Fig. 3.4). Bimetal line-voltage thermostats were normally calibrated for droop that occurred between the 20 and 80 percent duty cycle band, to improve performance at maximum load—normally 16 A. The resulting line resistance heat at maximum load would increase the temperature of the bimetal sensor by 3 to 7°F or more. As a result, the contact would open when the actual-space dry-bulb air temperature was correspondingly below set point. Occupants would be uncomfortable. They would raise the set point to compensate.

In an effort to prevent premature heat shutoff from occurring, the calibration was offset by the same amount. The opposite problem would occur if the installed heater load fell below the maximum load by 50 percent to 8 A, because the thermostat would overshoot the set point due to the maximum load calibration offset. Inaccuracy would also occur during periods when heat cycles were very short, such as those that commonly occur during the spring and fall “shoulder” season. Technology and thermostat redesign has produced models with significantly reduced droop as the line heat influence has been all but eliminated on newer bimetallic control designs.

A similar problem existed in electronic thermostats due to internal triac or triac-relay component heat generation. This was often compounded by circuit design location without regard to sensor impact. Some components in early models also generated heat due to constant 3- to 5-W current draw that not only generated temperature-distorting heat but also consumed considerable annual energy, which was frequently unaccounted for in the energy-saving justification for installation conversion. As these problems were detected, solutions were developed to make heat generation and standby current consumption nonissues. However, each electronic thermostat and control scheme should be evaluated to be sure that temperature-sensing accuracy and control current consumption are in line with design parameters.

---

**3.3 ENERGY IMPACTS OF CONTROL CHOICE**

---

Much has been written about the energy impacts of control selection and operation. A survey in *Contracting Business* found that more than 50 percent of homeowners were only “somewhat” or “not at all” satisfied with their present comfort systems. They listed energy savings and comfort as the two most important factors in purchasing a new home comfort system (Fig. 3.5).

Energy savings potential ranges to 25 percent, but the bulk of the savings are more related to energy management than to actual control operation (Fig. 3.6). In fact, the magnitude of savings depends more on how the control is used, the nature of the heating system design and management, and control features than the actual operation of the control itself. And, of course, the chart does not reflect the savings potential of control to operative temperature (OT). However, there are certain basic thermostat operational characteristics that do impact how closely the thermostat maintains the temperature set point.

For the sake of this discussion, we are talking about the use of the control in a convection heating environment where dry-bulb air temperature and mean radiant temperature (MRT) are equal. The only factor being discussed is thermostat performance. Earlier discussions defined droop and its effect on set point accuracy.

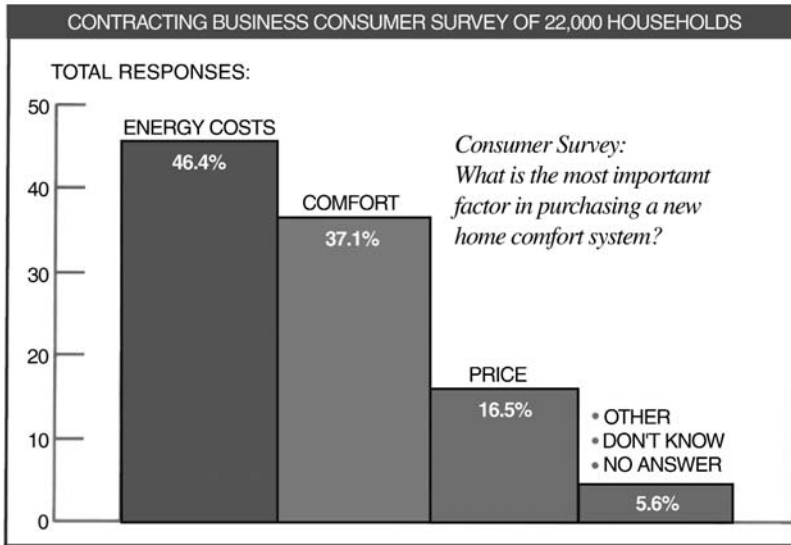


FIGURE 3.5 Rank of comfort system purchase factors.

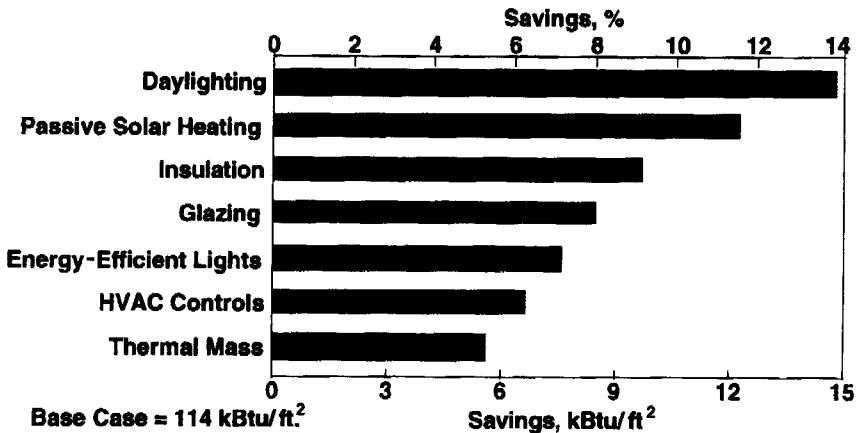
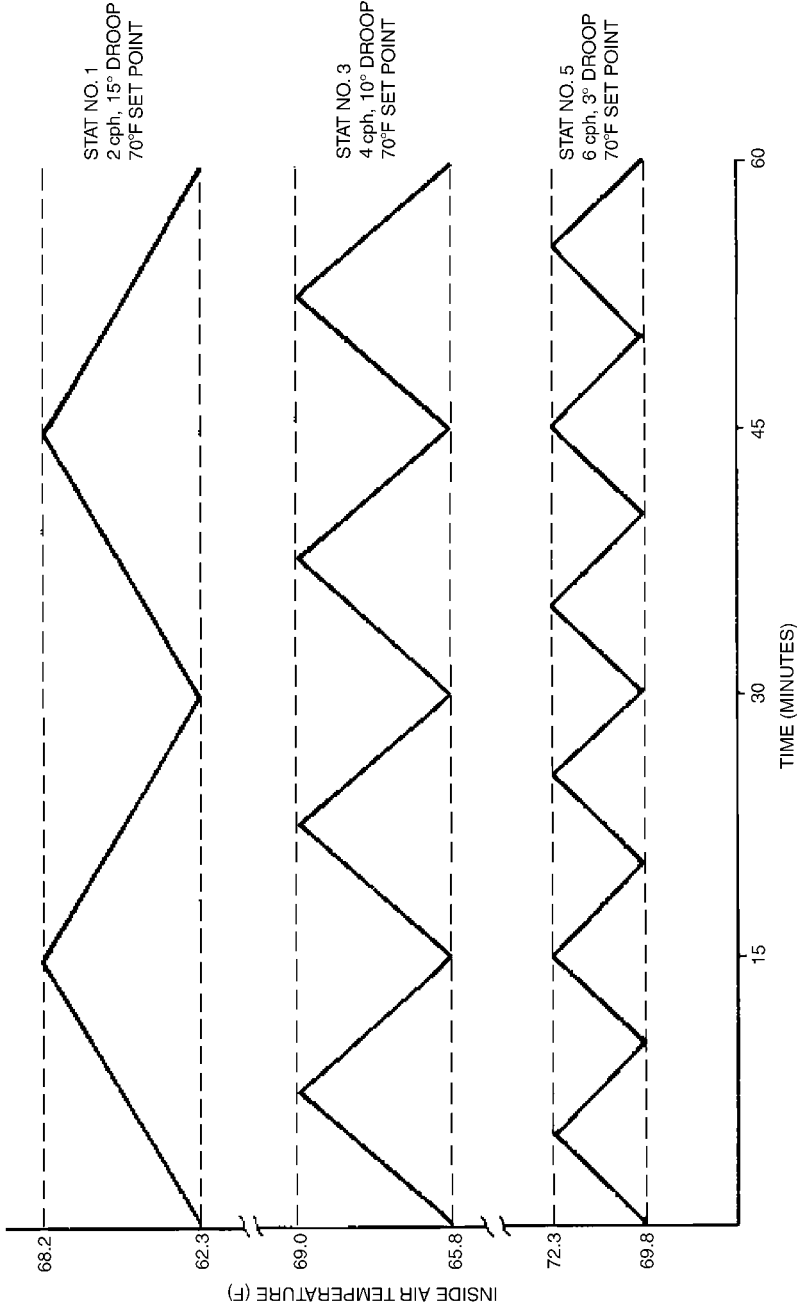


FIGURE 3.6 Ranking of energy-efficient strategies.

Although this is very important in heating climates, this may be a relatively insignificant factor in mild climates, where light loads are being controlled. Where the “on” cycle is brief, the time period does not result in an internal thermostat heat buildup. For most electronic thermostats, droop is likely to be between 1 and 2°F at maximum load if the control is properly designed.

Thermostat cycles occur when the control turns heat “on” or “off.” Bimetallic thermostat cycle frequency is usually between two and five cycles per hour in the most common operating range for the heating season (Fig. 3.7). By comparison, electronic thermostat cycles are frequent and are measured in minutes or even fractions



**FIGURE 3.7** Effect of thermostat cycle rate on room swings.

of a second. Some electronic thermostats have almost instant temperature sampling that is averaged over the time period selected for cycle frequency. Frequent cycling is an obvious advantage to maintaining set point (Fig. 3.8).

Differential, normally measured at 50 percent duty cycle, is the difference that a control tolerates between cycles. Differential is inversely proportional to the cycle rate. The more frequent the cycle, the closer to set point the dry-bulb air tempera-

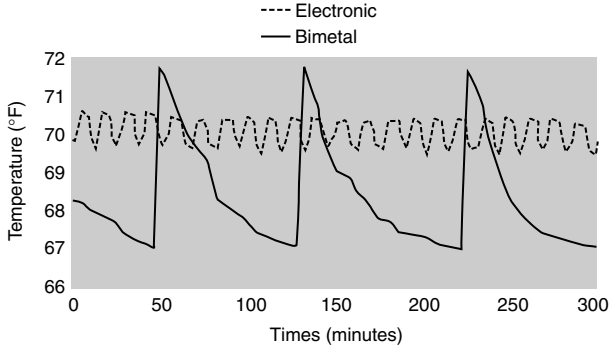


**FIGURE 3.8** Differential and cycle frequency of electronic versus bimetal thermostats. (Source: EPRT.)

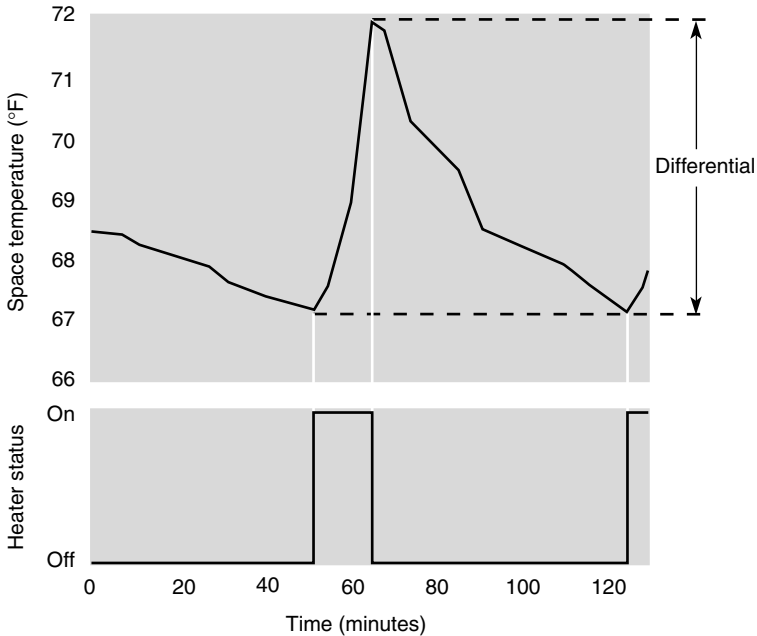


**FIGURE 3.9** Representation of 5°F temperature differential.

**6.26** CONTROL OPTIONS FOR RADIANT HEATING AND COOLING PANELS

ture is maintained. This temperature swing, deadband, or hysteresis is the Achilles' heel of the bimetal thermostat, because bimetal by its nature is a relatively slow sensing instrument compared with electronic thermistors controlled by logic and switching component (Fig. 3.9). One way to measure the deadband on a bimetal thermostat is to listen for the "on" and "off" click and note the number of degrees difference or dial space between clicks. Although the best bimetal thermostats have a 1 to 2°F differential, most old, and some new, units have differentials as large as from 5 to 7°F, and even larger. Although calibration could reduce the differential in some units, not all units have this feature.

It should also be noted that the term *deadband* is also used to define the temperature band within which a thermostat used for heating and cooling is designed to call for neither heating nor cooling. The premise is based on the assumption that occupants will be comfortable within the temperature band applied to the particular circumstances of the design involved without the use of either the heating or cooling system. Such a designed energy conservation deadband is not to be confused with a

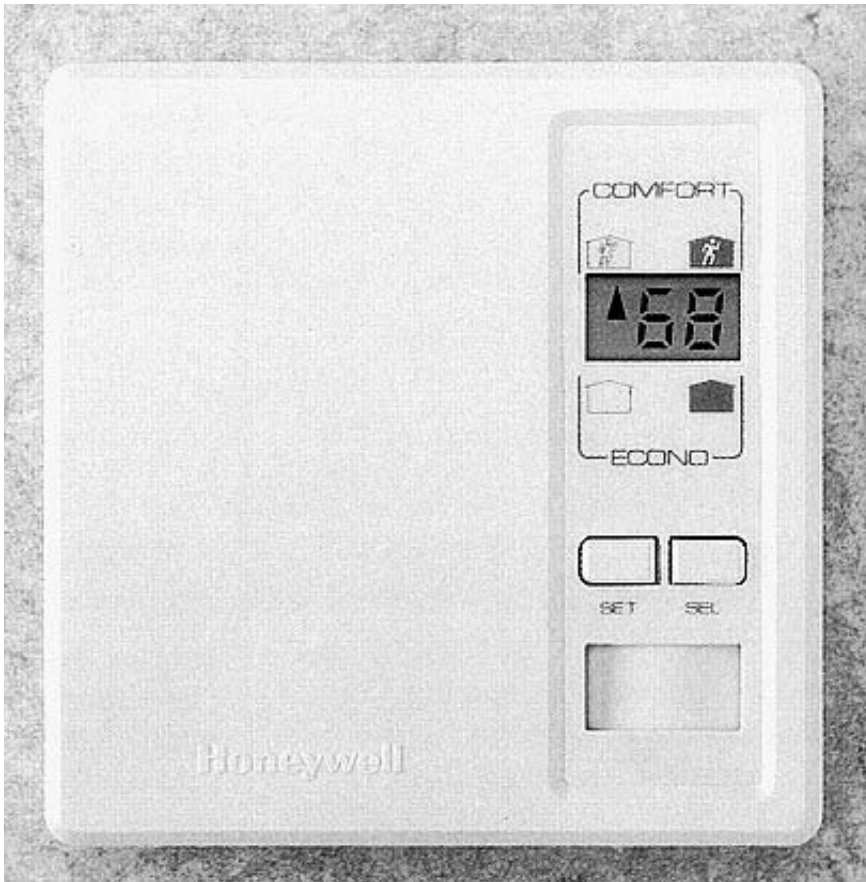


**FIGURE 3.10** Programmable motion- and light-sensing thermostat.

nonperforming temperature band that results in temperature set point differential referred to in the preceding paragraph.

Perhaps the most widely perceived test of a thermostat is its accuracy or ability to maintain average room temperature in relation to set point. It is when you try to discuss this point that you see how closely intertwined droop, cycling, differential, accuracy, and yes, MRT are in determining just what the cause of temperature deviation from set point actually is in real-world applications. And to further complicate matters, the role of the individual is just that, individual action, which impacts the use and operation of the thermostat.

A thorough report on performance comparison of thermostat replacement programs concluded, “. . . energy savings achieved . . . depend greatly on how the occupants use the products, as well as the performance of the products themselves . . . and potentially reduce heating energy consumption by about 7 to 10 percent” (“Advanced Line-Voltage Thermostats for Electric Resistance Heating,” by J. Gregerson, *E-Source*, January 1997).

### 3.3.1 ELECTRONIC AND PROGRAMMABLE THERMOSTATS

Dynamic, programmable thermostats are able to capture savings in addition to those related to set point accuracy. Programmable and remote access thermostats relate temperature set point to occupancy based on a programmed schedule. Light- and motion-sensing thermostats respond to changes in occupancy (Fig. 3.10). The performance of either control must be matched with the capability of the heating or cooling system to achieve set point. The controls may anticipate set point change, proportionally control heat or cool input in relation to set point, or communicate with other “smart” devices.

Occupants have deep-seated feelings about how to operate a thermostat. Such feelings surface when they are uncomfortable. Experience has taught the authors that most people are reluctant to yield control of their comfort to the discipline of programmable thermostats, except where a system in which setback set-up is imperceptible to the occupant. Just as with lighting, significant energy savings are achievable when unoccupied space is heated or cooled minimally without impacting or involving the occupants.



---

# CHAPTER 4

---

# THERMOSTATS AND THERMAL COMFORT

---

*Comfort* is one of the most casually used words in the English language. It is almost impossible to find a piece of heating or air-conditioning equipment or systems, thermostats, or energy management systems that do not claim to provide comfort. Yet, the leading building and HVAC publications routinely publish the results of surveys showing more comfortable or energy-efficient heating in the top five reasons for moving to a new house, or reports of some dissatisfaction with the heating system by almost 50 percent of respondents. Building occupants apparently are not enjoying the comfort being so widely promised.

Section 3, “Thermal Comfort,” details the history, background, and basis for ASHRAE Standard 55-92, *Thermal Environmental Conditions for Human Occupancy*. This section will be brief because the focus is only on the potential for implementation of the standard as it relates to application of operative temperature (OT) in thermostats and controls for the built environment. The impact of OT-sensing thermostats on occupant thermostat interaction and energy consumption has not been studied.

However, the computer simulation, “Operating a Space Under Comfort Conditions, Not Temperatures,” clearly shows that the energy necessary to maintain the required conditions is less than with conventional systems (Simmonds, 1993). Studies that are discussed in other sections of this Handbook indicate that substantial energy savings and productivity gains due to the elimination of occupant thermal discomfort could result if OT, rather than dry-bulb air temperature, was the input factor operating heating and cooling systems.

## 4.1 MEAN RADIANT TEMPERATURE

---

Mean radiant temperature (MRT) is the uniform surface temperature of a radiantly black enclosure in which an occupant would exchange the same amount of radiant heat as in the actual nonuniform space. Along with air speed, humidity, and the more common dry-bulb temperature, thermal radiation control is essential to human thermal comfort. That condition of mind that expresses satisfaction with the thermal environment is defined as *thermal comfort*.

Because air speed and relative humidity in an occupied space are normally within recommended limits, the main comfort variables are air and MRT. Yet, because dry-bulb air temperature is the only input factor to the thermostat, the impact of MRT is unrecognized.

**6.30** CONTROL OPTIONS FOR RADIANT HEATING AND COOLING PANELS

Everyone has experienced some MRT impacts. Perhaps the number one MRT impact is that caused from ever-changing solar radiation that is impacted by clouds, the rotations of the earth, and building design. A change in the presence of solar radiation can easily produce a double-digit in-space MRT swing. A totally different MRT influence comes from floors that are more than a few degrees above or below room dry-bulb air temperature. This may be due to factors such as the impact of location above an unheated garage, a hot boiler room, or a vacated space. Mean radiant temperature swings occur in low-thermal mass materials such as windows, corrugated steel, and uninsulated partition walls. Mean radiant temperature influences occupant thermal comfort throughout the year in the built environment.

Another significant, though generally overlooked, MRT impact appears when space occupancy is materially changed. An auditorium fills or empties. The traditional thermostat is reactionary—it will not recognize the MRT occupancy change but will only respond when the dry-bulb air temperature in the vicinity of the control rises or falls in response to the impact of the occupancy change on air temperature. In the case in which the heating system is on when the space fills, the system continues to heat to the thermostat set point. This could result in significant temperature overshoot, because each occupant contributes approximately 100 W of heat to a space being heated. Alternatively, the additional 100-W occupancy load will not be seen by the cooling system until the air temperature reaches the set point. In either case, if MRT were sensed, the control would respond immediately to the increased or decreased load requirements, avoiding the conditions caused by the inability of a conventional thermostat to maintain the dry-bulb set point.

Morris L. Markel, a man with a lifetime of experience designing electric heating equipment, developed a device, the Comfort-Check Meter (Fig. 4.1), which analyzes in-space occupant thermal comfort. The device is quick, handheld, and can be set up to record 24 h of readings for subsequent download through the RS-232 port directly into a computer spreadsheet for analysis. The Comfort-Check Meter is discussed in more detail in Sec. 4.2 of this chapter.

The building and design community has recognized the MRT impact on occupant thermal comfort. They have sought to reduce or manage MRT impacts by building tighter buildings; requiring higher building material  $R$  values; installing thermally broken doors and windows to reduce thermal bridging; and using spectrally selective glazing, favorable building orientation design, and other factors. The objective is to reduce MRT swings so that radiant asymmetry is reduced to acceptable occupant thermal comfort levels.

These changes, as positive as they are, do not eliminate the impact of MRT on daily occupant thermal comfort because systems are controlled solely by dry-bulb air temperature. For example, along with the improvement in building construction and materials, the practice of temperature setback is becoming a building code standard. But the MRT impact of internal building surface temperatures is not taken into account in the economic analysis, productivity, or equipment sizing. People are cold (and possibly less productive) on Monday morning, as the warm-up recovery is in progress.

ASHRAE Research Project 1114, *Develop Simplified Methodology to Incorporate Thermal Comfort Factors for Temperature Setback/Setup into In-Space Heating and Cooling Design Calculations*, should provide important information that will include MRT and define temperature setback-setup in terms of occupant thermal comfort. It will do this with a mathematical model that will predict the time-dependent thermal comfort characteristics of vacant or occupied space.

In addition to those MRT influences that occur naturally or in the course of building use, there are situations in which hybrid systems, a subject covered in Sec. 7,

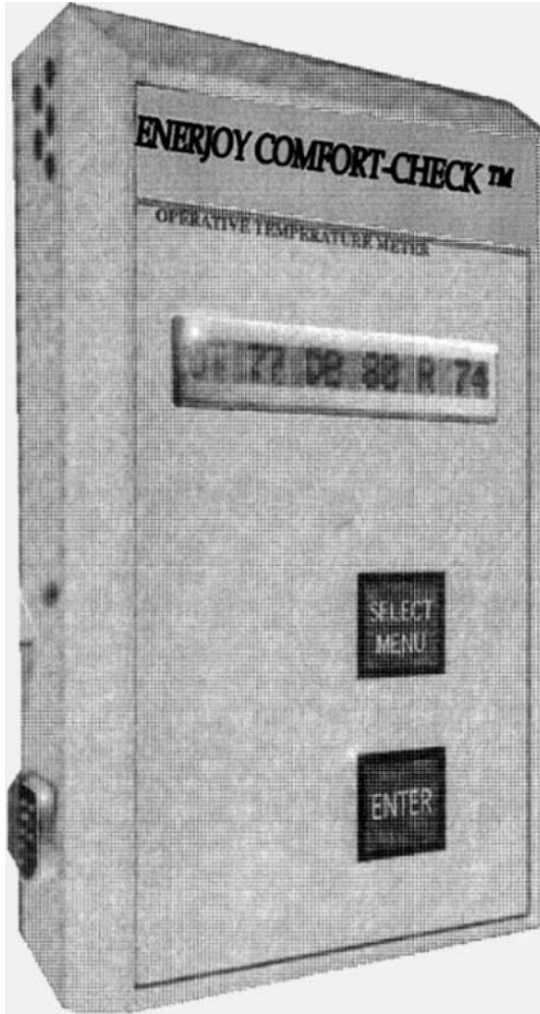


**FIGURE 4.1** Operative temperature (OT) meter averages air (DB) and radiant (MRT) temperatures.

involve using both radiant and convective systems. ASHRAE Research Project 907, *Design Factor Development to Obtain Thermal Comfort with Combined Radiant and Convective In-Space Heating and Cooling Systems*, developed information that is covered in detail in Sec. 7. Although the focus is on system analysis, this information assists in understanding the in-space thermal comfort impacts of common-spot comfort influences, such as wall cooling units, fireplaces, hot-air registers, radiators, baseboards, space heaters, and radiant ceiling, wall, or portable heaters.

Mean radiant temperature is an obvious and important determinant of thermal comfort and energy efficiency. It must be incorporated into design and engineering programs to demonstrate the benefit. Obvious comparative benefit will drive build-

ing, system, control, and energy management system MRT implementation. When that occurs, the building and HVAC industry use of the word *comfort* will accurately project occupant experience in the built environment.

## 4.2 OPERATIVE TEMPERATURE

Operative temperature is the uniform temperature of a radiantly black enclosure in which the occupant would exchange the same amount of heat by radiation plus convection as in the actual nonuniform environment, thereby experiencing thermal comfort, or thermal neutrality. This condition is represented by the term *operative temperature* (OT). Within the temperature range common to the built environment, OT is the simple average of dry-bulb air temperature and MRT. It is that simple.

The trailblazing work of P. O. Fanger resulted in the development of a methodology called *predicted mean vote* (PMV), which provided for the evaluation of thermal comfort based on clothing and activity levels under a given set of thermal conditions (Fig. 4.2). The entire subject of thermal comfort is covered in detail in Sec. 3 of this Handbook.

The attractive feature of the Comfort-Check Meter described earlier in this chapter is that all three figures are shown digitally almost instantly. The MRT represents 120° solid-angle view, and the air temperature is sensed in the housing. A micropro-

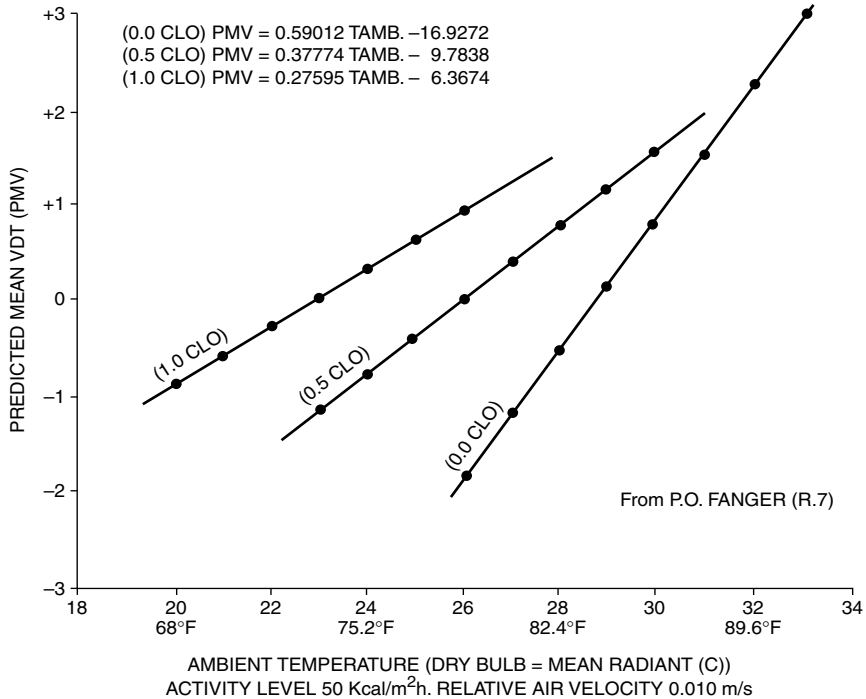


**FIGURE 4.2** Predicted mean vote (PMV) versus average temperature.

cessor calculates the OT every 6 s. The MRT impact may be quickly demonstrated by using a glass of ice water or a hot coffee cup. The tool demonstrates the ease with which the concept may be implemented, as well as the significance of its impact. It also demonstrates the downside of blindly controlling to OT.

Consider, for example, a second home that is kept operating, but used occasionally. There is poor insulation and a lot of glass. If a thermostat, which is sensitive to MRT, replaces a convection bimetal thermostat, you will naturally find that a higher air temperature is called for as defined by OT. Yet, if this is a vacant vacation house, where setback is designed to lower energy costs, the exact opposite will occur—bills will go up! Under such conditions, the OT set point can be lowered to reflect the MRT that is considered acceptable. This was the net effect of the bimetal thermostat that only sensed air temperature and was kept at 50°F, which was the minimum setting considered to keep pipes from freezing.

The use of OT may also open up the field of task heating. Many believe task heating holds as much promise for energy savings as task lighting, which swept the country with support from the EPA, DOE, and the nation's electric utilities. A recent study by the authors and ASHRAE Student Member Jamie Howell, entitled *Radiant Panel Surface Temperature over a Range of Ambient Temperature*, develops guidelines for placing and sizing radiant heaters in large occupied spaces where the indoor temperature is below occupant thermal comfort levels to provide localized thermal comfort. The project was performed by using the methodology described in detail in Sec. 8 of this Handbook.

There are many obvious benefits to using OT. The purpose of a heating or cooling system, aside from shielding the building and its contents from damaging temperatures, is to make people comfortable. The shift in focus from heating space to heating people demands recognition of MRT. The recognition of MRT makes it possible to harness the benefits of radiant, as opposed to or in combination with convective, heat transfer. One of the key benefits is energy conservation resulting from heating people before or instead of space.



---

# CHAPTER 5

---

# ENERGY MANAGEMENT SYSTEMS

---

Energy management systems (EMS) may be used for the control of radiant heating panels for in-space occupant thermal comfort or space conditioning in the same way they are used to control the conditioning of space with convection heating systems. Such systems are normally designed to optimize the performance of the central heat delivery system. In the process, heat delivery to each space or area to be conditioned is designed to satisfy the local sensing device signal.

In the case of radiant panels that are centrally supplied with a heated or cooled fluid, the focus of the EMS is efficient operation of the central system in response to in-space or area dry-bulb air temperature-sensing signals. Such control is part of a complex electrical, and usually electronic, control design that includes area and boiler thermostats, transformer, outdoor reset, valve prioritization, and control for temperature, flow, and zoning, plus whatever related systems are integrated into the EMS (Fig. 5.1).

Whatever the energy source, the radiant panel control may be entirely local or by an EMS. In the case of local control, line-voltage thermostats are often used. Either programmable or nonprogrammable proportional controls ensure radiant output in direct relation to heat loss for electric radiant ceiling and floor systems and include remote floor sensing where floor temperature control, such as floor warming, is required (Figs. 5.2 and 5.3). For EMS participation, a low-voltage thermostat designed to operate within an EMS protocol is usually required. However, an EMS may operate all radiant systems.

Energy management systems operate under proprietary and universal protocols. ASHRAE *Building Automation and Control Networking Protocol* (BACnet) is detailed in ASHRAE Standard 135. BACnet is based on a four-layer collapsed architecture that corresponds to the physical, data link, network, and application layers of the International Standards Organization/Open Systems Interconnection (ISO/OSI) model. The application layer and a simple network layer are defined in the BACnet Standard (Fig. 5.4).

Other protocols use local area network (LAN) and specific integrated circuit chips that communicate with all of the devices in which they are implanted. Ethernet has become one of the most widely used LANs. Proprietary architectures are used by numerous EMSs developed by building management contractors, consultants, and other related organizations. The technology is moving so rapidly that detailed discussion would likely be outdated by publication. The bottom line is that whatever control one might envision is probably technically, though not

6.36 CONTROL OPTIONS FOR RADIANT HEATING AND COOLING PANELS

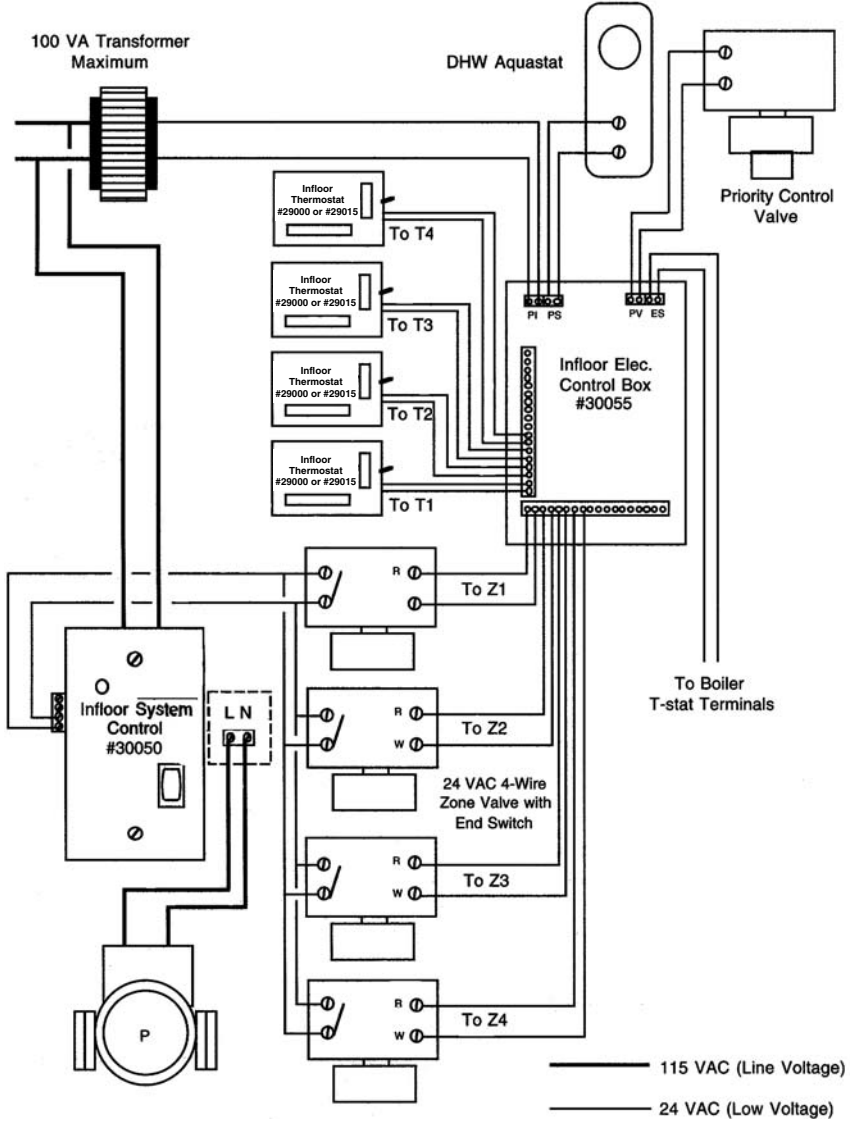


**FIGURE 5.1** Schematic showing electric control box, system control, and multiple zone valves for floor hydronic radiant heating system.

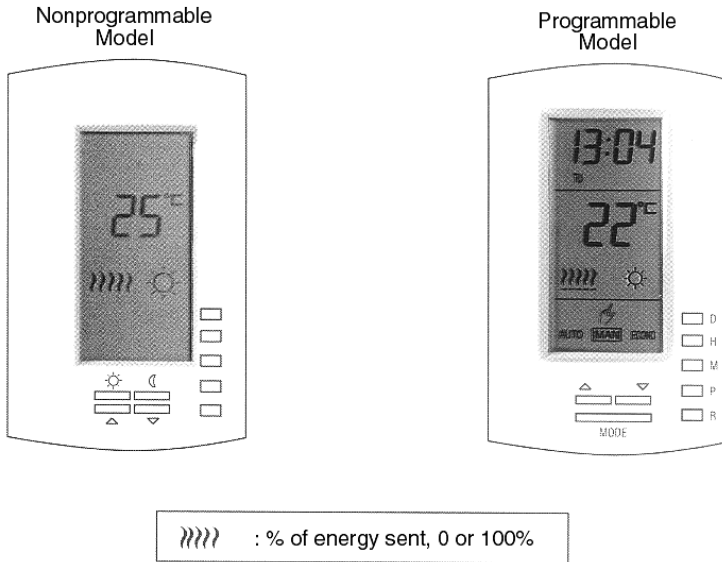
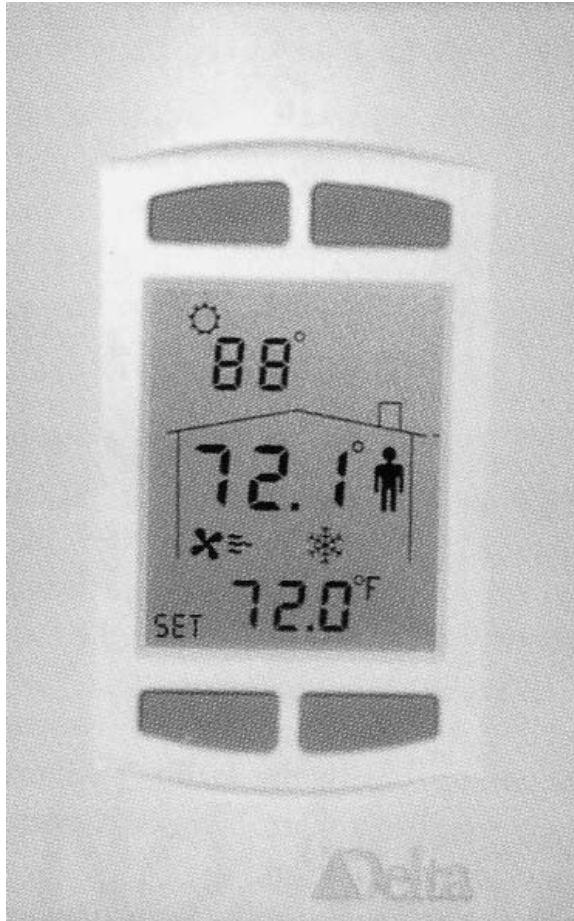


FIGURE 5.2 Programmable and nonprogrammable proportional thermostats.



FIGURE 5.3 Floor sensing programmable thermostat.

## 6.38 CONTROL OPTIONS FOR RADIANT HEATING AND COOLING PANELS



**FIGURE 5.4** BACnet thermostat.

necessarily economically, feasible. Yet component prices continue to decline steadily, making more options affordable daily, including remote telephone control (Fig. 5.5).

From the point of discussion in this section, the main point to be made is that radiant systems can participate in any of the network systems as long as the communicating thermostats used are appropriate for the particular radiant panel system components being centrally managed. However, until operative sensing thermostats are developed and adopted by EMS programs, the radiant system in-space performance will be based on dry-bulb air temperature-sensing signals. Other important control components, such as those required with hydronic sys-

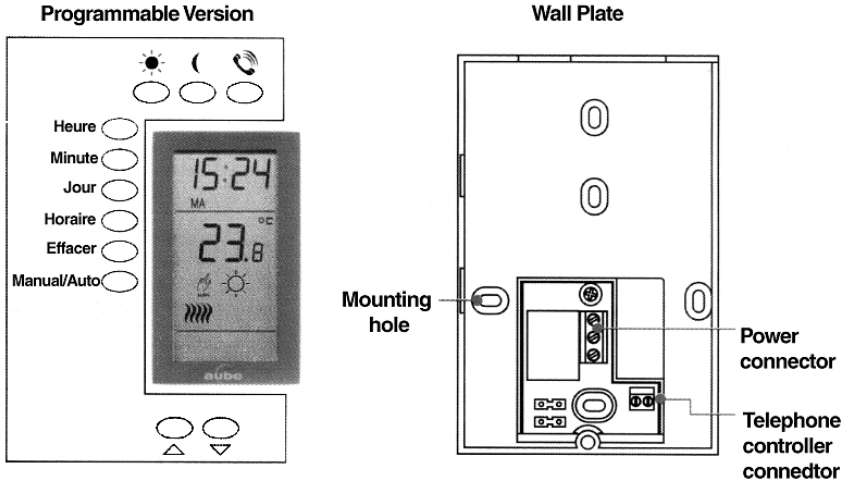


**FIGURE 5.5** Remote telephone control thermostat.

tems to control fluid temperature, flow rate, and so forth, can be managed in the same way as traditional hydronic convection systems, but care must be taken to ensure both comfort and equipment operation are uncompromised or endangered, respectively.

When OT-sensing controls are incorporated into an EMS, the full benefits of radiant heating will be optimized.



S · E · C · T · I · O · N · 7

**RADIANT HEATING  
AND COOLING  
HYBRID SYSTEMS**



---

# CHAPTER 1

---

## WHEN TO USE HYBRID SYSTEMS

---

### 1.1 HEATING SYSTEM DEFINITIONS

---

Heating systems are used to condition and protect buildings and their contents. However, the second and most commonly identified threshold for heating system use is to provide occupant thermal comfort. Gan and Croome (1994) reported that almost 40 percent of the world's nonrenewable energy is used to achieve thermal comfort in buildings. Thermal distribution systems can use one or both of two different modes of heat transfer, convection and radiation, to deliver thermal comfort to an occupant.

Figure 1.1 illustrates the difference in heating modes. The forced-air system [Fig. 1.1(b)] uses primarily convection to deliver the heat energy to the occupant. The system heats the air first. Then the air heats the occupant. With a radiant system [Fig. 1.1(c)], the occupant is first heated. Then the occupant and the other room surfaces heat the surrounding air. To accurately mathematically model a heating system and predict the thermal comfort of an occupant, it is necessary to know the relative amounts of energy transferred by each mode, called the radiative-convective split.

Section 7 briefly describes three major types of heating systems: in-space convective heating systems, radiant heating systems, and combination or hybrid systems. In addition, the search to find documentation on the radiative-convective split for specific heaters and the results of the search are described.

#### 1.1.1 In-Space Convective Heating Systems

In-space heaters convert fuel to heat in the space to be heated (ASHRAE, 1996). Examples of in-space heaters are wall and floor furnaces, baseboard heaters, cord-connected portable heaters, stoves, and fireplaces. The fuel may be gas, oil, electricity, or solid fuel. In-space heaters provide thermal comfort to a room by a combination of forced and natural convection and radiation. Chapter 29 in the 1996 ASHRAE *Systems and Equipment Handbook* provides detailed information about in-space heaters including descriptions, minimum annual fuel utilization efficiencies, and control information.

#### 1.1.2 Radiant Heating Systems

As described previously in this text, radiant heating systems transmit energy to the occupant and objects in a space by electromagnetic waves. It is important to note that

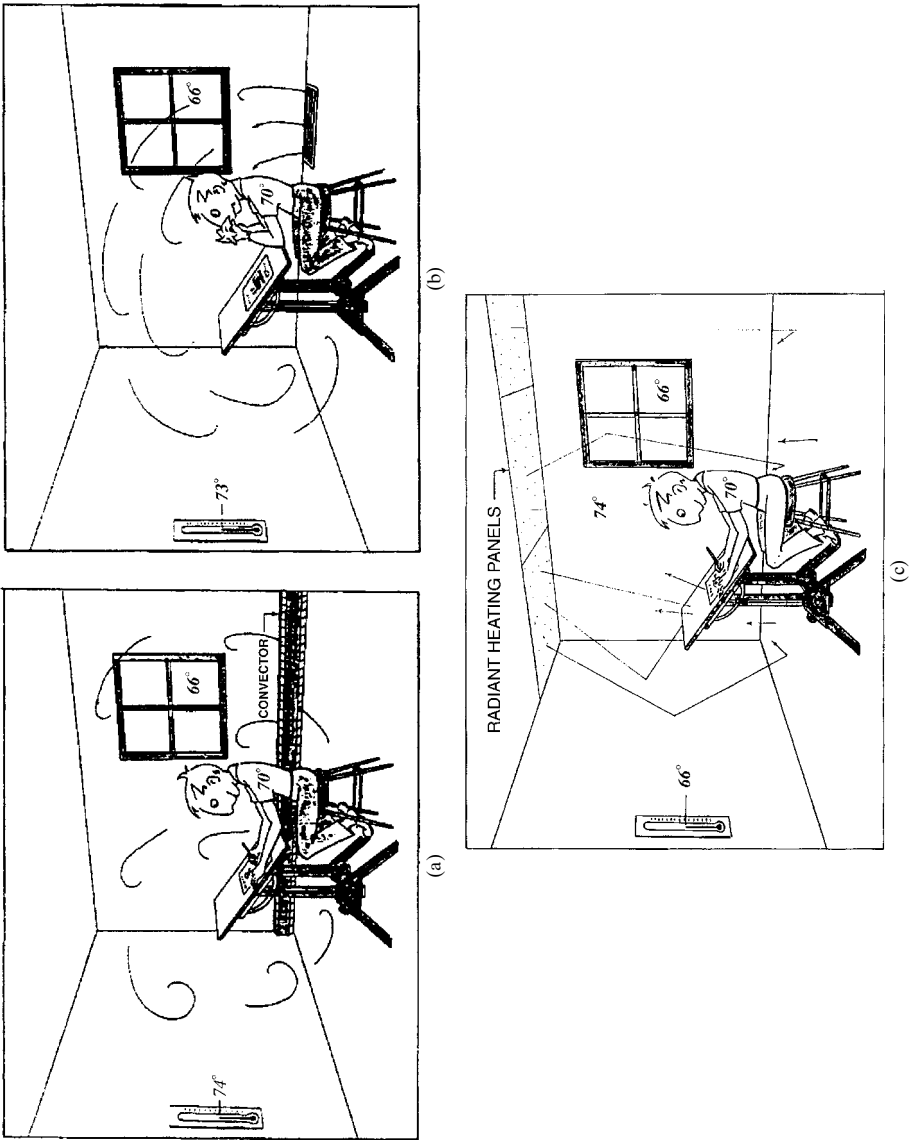


**FIGURE 1.1** Radiant-convective heaters. (a) Natural convection. (b) Forced-air convection. (c) Radiant heating panels. (Courtesy of Morris L. Markel.)

radiation travels through the air at the speed of light and does not directly heat the air except under conditions where the air is laden with moisture. Examples of radiant heaters are embedded hydronic conduit in ceilings, walls, or floors, electric ceiling, or wall panels, and embedded electric heating conduit in ceilings and floors (ASHRAE, 1995). Chapter 49 in the 1995 ASHRAE *HVAC Applications Handbook* and Chapter 15 of the 1996 *HVAC Systems and Equipment Handbook* provide more information on radiant heating including types of radiant heaters and design considerations.

### 1.1.3 Hybrid Systems

Hybrid systems combine convective and radiant heaters. The goal is to leverage the heat transfer advantages of each system to minimize fuel consumption and increase occupant thermal comfort. The convective system is normally used to maintain a baseline dry-bulb air temperature. The radiant system is used to achieve the desired mean radiant temperature (MRT). In a combination system, the convective system is undersized—either by design or default—and the sizing deficit is addressed by the radiant heating system.

The combination system is designed to the occupant thermal comfort specifications. The specification may call for provision of uniform, varied, or localized occupant thermal comfort. The radiant system ensures that the thermal comfort specification is met. The goal of a hybrid system is to eliminate unacceptable operative temperature gradients in a room while at the same time creating a thermally comfortable environment using the least fuel.

The definition of a *hybrid system* is an optimal integration of different distribution and delivery systems with specific functions, served from the same or different plant or energy sources.

ASHRAE-funded research provides examples of energy use reduction under specified occupant thermal comfort conditions, using hybrid heating systems. Currently, the ASHRAE handbook series does not contain a specific chapter on this type of heating system.

### 1.1.4 Heater Output Characteristics

To accurately predict the thermal comfort distribution in a room, the relative portions of heat contributed by convective and radiant heat transfer must be known. Although some manufacturers provide these data, a comprehensive, documented equipment-specific radiative-convective split reference source is not available.

The radiative-convective split for fireplaces, stoves, wall and floor furnaces, baseboard heaters, portable cord-connected heaters, and radiant panels is essential to optimal hybrid system design. Without accurate heat transfer information, designers are ill equipped to determine mean radiant temperature and ensure provision of occupant thermal comfort. ASHRAE research has established the radiant-convective split for flat wall, floor, and ceiling radiant heating panels.

ASHRAE Research Project 876 confirmed the influence of location on radiant-convective split for an insulated, fast-acting electric radiant panel when moved from the ceiling to the wall, and the corresponding Btu increase required to maintain equality of radiant output. Table 1.1 shows radiant panel convective split factors developed by the University of Illinois research. The results are consistent with research conducted at Kansas State University, and much earlier at the former ASHRAE Laboratories.

**TABLE 1.1** Percentage of Panel Output Due to Radiation for Various Tests

Test and surface	Location		
	Ceiling (% output radiant)	Side wall (% output radiant)	Floor (% output radiant)
plastic 35	91.5	75.3	78.7
plastic 45	92.5	72.5	72.3
plastic 55	91.1	71.3	70.5
vinyl 35	93.0	75.5	74.6
vinyl 45	91.7	72.3	66.1
vinyl 55	89.7	70.3	67.4
textured 35	93.1	72.2	72.5
textured 45	89.4	72.1	68.1
textured 55	89.3	70.9	68.5
carpet 35	93.9	71.1	67.3
carpet 45	87.0	71.7	69.9
carpet 55	89.4	—	—
white 35	—	74.1	73.9
white 45	—	71.9	70.4
white 55	—	71.2	68.4
mid texture 35	—	75.6	—
mid texture 45	—	72.0	—
mid texture 55	—	71.2	—
Average	91.0	72.4	70.6

*Source:* ASHRAE RP-876.

Recently, an ASHRAE project was completed to identify the radiative-convective split of common office equipment such as printers, computers, monitors, and copiers. This information provides useful input for optimizing thermal comfort in an office environment. Comprehensive information on system components and options regarding the radiant-convective split is essential for sizing and designing combination systems.

## 1.2 EXAMPLES OF COMMON HYBRID SYSTEMS

A good example of a combination system is the room that is heated by an in-space gas-fired wall heater. The wall heater is undersized so as to provide a moderate but cool indoors dry-bulb air temperature. A radiant panel has been installed in the ceiling to raise the operative temperature field in the room. The temperature relationship is shown in Fig. 1.2.

In this example, the in-space heater maintains the room at a dry-bulb air temperature of 60°F. Without the radiant heater, the operative temperature field hovers around 55°F, obviously cooler than an occupant pursuing normal low metabolic rate indoor activities would prefer. The radiant ceiling panel increases the operative temperature to 70°F; this increase comes from the increased radiant intensity field generated by the radiant panel surface temperature.

The benefits of this system are as follows: (1) the capital outlay could be lower due to the sizing of smaller equipment; (2) the radiant heater does not have to be sized for “freeze” protection; (3) the in-space heater needs to be sized only to main-

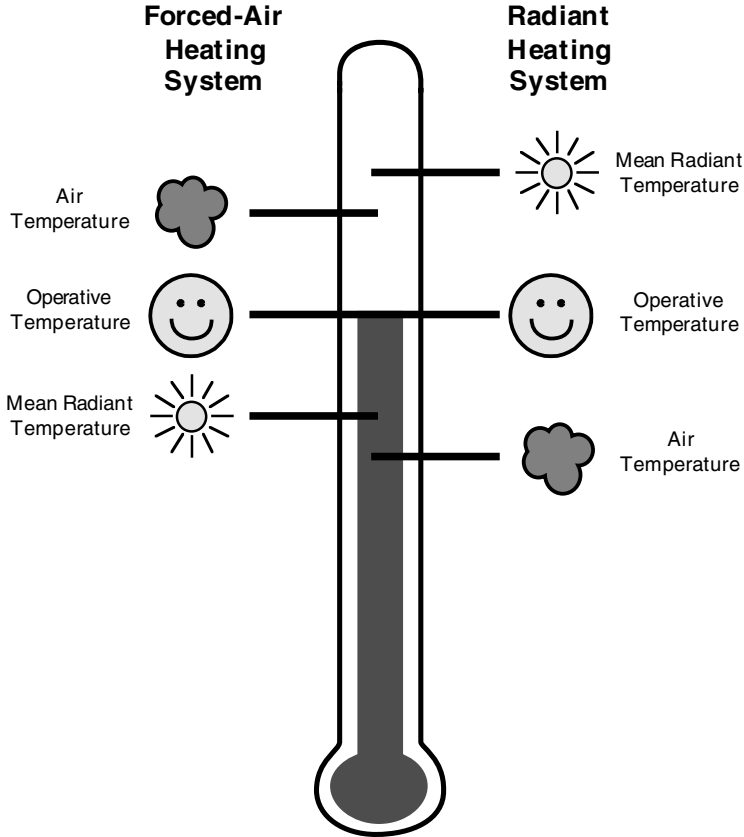


**FIGURE 1.2** Combination system.

tain an indoor dry-bulb air temperature that is several degrees cooler than a “thermally comfortable” environment; (4) the area of unacceptable radiant asymmetry in front of the wall heater is minimized; and (5) the radiant heater needs to be powered only when occupants are in the room. The last benefit could result in large energy savings. In the case of a room heated by an in-space heater alone, the thermostat would be set to provide a thermally comfortable environment only when the room is occupied. In the case of the combination system, the thermostat needs to be set only to the baseline temperature until the area is occupied. With fast-acting radiant systems, an occupant entering the room would feel thermally comfortable almost immediately following system activation.

### 1.3 RETROFIT HYBRID SYSTEM OPTIONS

Any radiant system can be retrofit to create a hybrid system. The first task is to identify radiant panel systems that optimize the performance of the combination system in meeting the thermal specification. The second task is to determine site-specific

installed system feasibility, cost, and acceptance criteria. On the basis of answers to these questions, the appropriate equipment category is identified to select the equipment that best meets specification requirements.

In general, concealed electric and hydronic systems are more costly to install than visible hydronic or electric systems. Expense and complexity are reduced for radiant conversions or additions where hydronic input or electric wiring that could support the equipment required is already in place. The cost and complexity increase significantly when the retrofit option involves installation of new electrical service, new hydronic heat generation equipment, or ceiling, wall, or floor replacement or enhancement.

The increasing demand for radiant comfort is spawning design innovation and equipment development that continues to simplify installation and reduce cost. Radiant retrofit product evolution, including electric and hydronic mats, panels, conduit, and combination electric hot water and hydronic heaters, all challenge the validity of cost generalizations. It is very important that product information is up to date. Factors in addition to cost include the availability of fuel, installation trades, and site accessibility.

Warm floors are no longer considered a luxury, but a standard comfort feature much like air conditioning. One of the most common circumstances in which hybrid system installation is considered occurs when installation of so-called “cold surface” flooring, such as wood, tile, stone, slate, marble, ornate or plain concrete, or terrazzo, is specified. Occupant barefoot heat conduction to these surfaces makes them feel colder than carpet surfaces. Radiant ceiling, wall, or floor systems are used to warm any surfaces that feel or are cold.

Hybrid systems should be considered in the process of initial building design. The driving force for employment of hybrid systems is operating cost reduction and provision of occupant thermal comfort. However, hybrid systems often develop out of necessity by default to correct mean radiant temperature deficiency. Hybrid systems are designed to ensure occupant thermal comfort, to lower energy costs by reducing dry-bulb air temperatures, or to reduce central system operating costs by task heating. Radiant retrofit is sometimes the solution of last resort. In fact, if mean radiant analysis is part of the initial design methodology, hybrid systems will become an integral part of many building specifications to meet comfort and operating cost objectives.

Common architectural feature and area usage candidates for hybrid systems include atriums, entry buffers, lobbies, split level designs, areas of sparse, localized, or transient occupancy, unbalanced system performance, undersized or aging systems, cathedral ceilings, large bathroom or patient areas, large window expanse, skylights, special needs areas, and surgical, nursery, and areas where system zoning is ineffective, impractical, or inefficient. In essence, a hybrid system should be employed to avoid the problems inherent in “one-size-fits-all” heating and cooling system design.

The most active emerging hybrid HVAC application is in sustainable building design. Natural environmental conditions are harvested to enhance building performance, provide occupant thermal comfort, and minimize energy consumption. Solar gain and nocturnal radiation heat loss present energy design opportunity for heating and cooling. Examples of sustainable building design are described in Chapter 4, “Hybrid Heating and Cooling Demonstration Projects.”

## **1.4 SYSTEMS WITH RADIANT COOLING**

---

Radiant cooling is not new in commercial applications. One of the earliest approaches involved the use of torchiere fixtures to remove excessive incandescent light heat in offices and hotels in the summer. The system was hydronic and normally

involved a continuous circulation of water in circular fixtures that surrounded the light fixture and only operated when the lighting was operating. The advent of cooler fluorescent lighting and central air conditioning eliminated the need for this novel approach to reduce interior heat increase from lighting.

Current applications include both ceiling and floor panels. Museums, office buildings, airports, retail stores, and homes are a few of the building types that are fully or partially radiantly cooled (Fig. 1.3). One of the large-scale buildings most readers are familiar with in the United States is the original section of Chicago's O'Hare Airport.

#### 1.4.1 Hydronic Radiant Cooling

Combination systems that provide cooling as well as heating require special attention. The big issue is relative humidity. In almost all buildings, there are times when air needs to be recycled through a dehumidifier to continuously remove moisture from the air. The radiant panel surface temperature determines the percentage of heat that can be removed from the space through radiant cooling. The capacity constraint is the least likely dew point temperature that may be encountered in the space served by the radiant panel. In other words, radiant panel temperature cannot be lower than the temperature at which there is any reasonable probability that condensation could occur.

Floor cooling is practical for almost all buildings, but the indoor and outdoor climate limitations must be recognized. Even dry climates have times when dehumidification is necessary and condensation is a factor. The most common floor applications are slab on grade or suspended slabs (Fig. 1.4). Slabs in contact with wood are not a good application, and floor coverings, such as carpet, vinyl, or wood, must be avoided.

Radiant cooling floor surface temperature limitations are commonly about 65°F (20°C) (Fig. 1.5). Depending on tube spacing, encapsulation heat transfer factors, and room air temperature, actual water temperature is in the range of 40° to 50°F (12° to 16°C), with a usual design for a maximum of 5°F (2°C) supply-return tem-



**FIGURE 1.3** Berne office building with cold façade, alternative energy generation, and chilled ceilings.



**FIGURE 1.4** Floor cooling.

## Floor Cooling Capacity

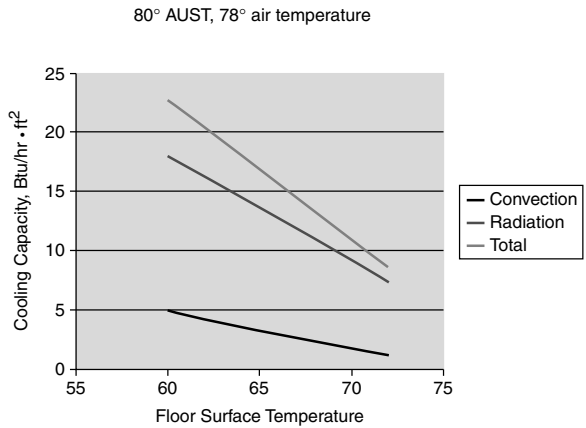


**FIGURE 1.5** Floor cooling capacity.

## Water Temperature - Floors

For 79° room air temperature, 12" tube spacing

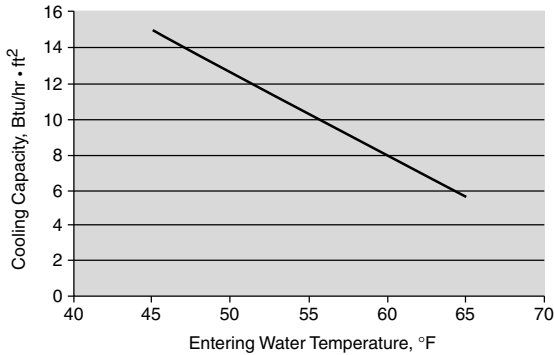


**FIGURE 1.6** Floor temperature of floors.

perature difference (Springer, 2000) (Fig. 1.6). Although the primary floor temperature comfort limitation is 65°F (20°C), condensation must not occur under any circumstances. Finally, the chilled water source may limit the water temperature, particularly in natural, nonmechanical applications. Common chilled water sources include water chillers, air or ground heat pumps, condensing units with heat exchangers, cool ground or surface water, and cooling tower or other evaporative source, including “night sky” cooling.

Hydronic radiant ceiling panels (Fig. 1.7) are used for both radiant heating and cooling. Ceiling location offers the usual advantage of preserving floor treatment flexibility. The entering water temperature is typically 1°F above the dew point

## Ceiling Panels

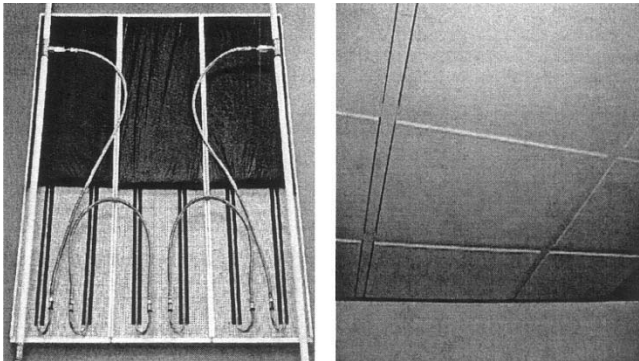


**FIGURE 1.7** Ceiling panels.

(Fig. 1.8). Under normal room and panel operating temperatures, radiant ceiling cooling panels can remove  $30 \text{ Btu/h} \cdot \text{ft}^2$  ( $95 \text{ W/m}^2$ ) by radiation and about  $15 \text{ Btu/h} \cdot \text{ft}^2$  ( $47 \text{ W/m}^2$ ) by convection. A typical VAV system supplying  $1 \text{ cfm/ft}^2$  of  $55^\circ\text{F}$  ( $13^\circ\text{C}$ ) air has the capability of removing  $21.6 \text{ Btu/h} \cdot \text{ft}^2$  ( $68 \text{ W/m}^2$ ) of sensible heat. Continuing the example with ventilation air supply of  $0.2 \text{ cfm/ft}^2$  at the same temperature, the remaining sensible load is 80 percent of  $21.6 \text{ Btu/h} \cdot \text{ft}^2$  ( $68 \text{ W/m}^2$ ), or slightly more than  $17 \text{ Btu/h} \cdot \text{ft}^2$  ( $54 \text{ W/m}^2$ ). In this example, the ratio panel to ceiling area is  $17/30$  or less than 60 percent. If it were practical to drop ventilation air to  $45^\circ\text{F}$  ( $7^\circ\text{C}$ ), the radiant cooling panel area would drop to 50 percent (Mumma, 2001).

Advantages cited (Mumma, 2001) for radiant ceiling panels are as follows:

- First cost (with experienced contractors) is about 15 percent less than installing a conventional air system.
- Long-term savings are dramatic (i.e., approximately 20 to 30 percent, as a result of reduced fan power).
- Panels provide reduced operation and maintenance costs (minimal moving parts and no filters).
- Testing and balancing during commissioning before occupancy is simpler and less expensive to perform.
- Comfort levels can be better than those of other conditioning systems because radiant loads are treated directly, and air motion in the space is at normal ventilation levels.
- Supply air quantities usually do not exceed those required for ventilation and dehumidification.
- A 100 percent outdoor air system may be installed with smaller penalties, in terms of refrigeration load, because of reduced outdoor air quantities [multiple spaces (Eq. 6.1) of Standard 62-1999 does not apply to this situation].
- Wet surface cooling coils are eliminated from the occupied space.

Depending on the climate and application, it is important to provide for dual protection against freezing, condensation, and equipment damage. Suggested check

## Water Temperature - Ceilings

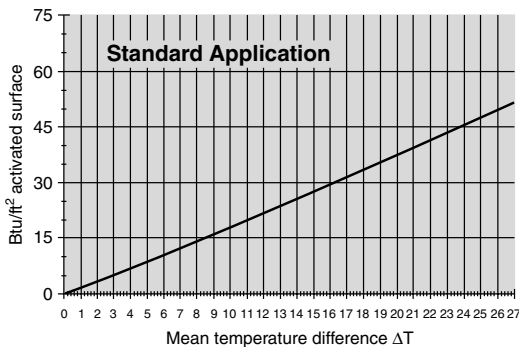


**FIGURE 1.8** Water temperature of ceilings.

devices include freeze thermostat, flow switches, floor temperature sensors, dew point controls, and humidistat, and buffer tanks, respectively (Springer, 2000).

Clearly, radiant hydronic cooling is an option to be studied whenever radiant hydronic heating is specified. Radiant floor heating capacity makes hydronic floor heating a viable option in almost any application (Fig. 1.9). Although radiant cooling is normally used to satisfy part of the load, it may well be the only cooling required during the shoulder seasons and may serve capacity constrained electric utilities by facilitating load shift or peak shaving.

#### 1.4.2 Radiant Cooling Has Wide Application

David Schaetzle, Arizona State University, is currently developing a comprehensive radiant cooling database under ASHRAE Research Project RP 981. The project is noteworthy in the detail of data collection. In addition to developing data that will be important to the evaluation of the potential for performance enhancement through hybrid system design, the project is expected to demonstrate the practicality for cool thermal storage during periods of off-peak, lowest-price electric rates.

The residence involved in the study is of Adobe construction (Fig. 1.10). The high-mass concrete walls provide the mass required for cool thermal storage. Hydronic, narrow capillary mats embedded in the ceiling structure facilitate heat removal from the building mass during periods of low, off-peak nighttime electric rates. One of the objectives of the research is to determine what portion of heat removal can be handled by the high-mass radiant cooling design. Another objective is to develop performance data based on operative temperature as the measure of occupant thermal comfort.

A different set of conditions were addressed in a Museum Project in Ankara, Turkey, conducted by Birol Kilkis et al. (Fig. 1.11). The project is unusual in its analysis of the preservation of antiquities while at the same time addressing the thermal comfort requirements of visitors interested in viewing the antiquities under conditions of occupant thermal comfort. The issues of humidity, thermal comfort, and

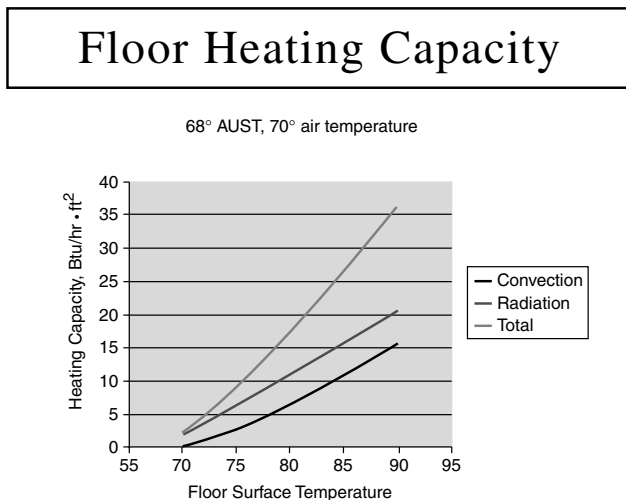


**FIGURE 1.9** Floor heating capacity.



**FIGURE 1.10** Adobe construction study.

operating cost are addressed from the perspective of a hybrid system designed to optimize the requirements of exhibit preservation and viewer comfort.

A radiant cooling project conducted by Davis Energy Associates, Richard Bourne and David Springer, demonstrated the practicality under certain conditions of nocturnal roof misting for the purpose of facilitating radiant cooling in buildings.



**FIGURE 1.11** Ankara Museum in Turkey.

The project involved detailed documentation of performance of a proprietary roofing system that enables the downsizing of conventional cooling equipment by taking advantage of nocturnal radiation and dry climate evaporation to cool water at night for the purpose of facilitating daytime cooling.

Hybrid systems are an integral part of the “whole-building approach” being advanced under the U.S. Department of Energy’s High-Performance Commercial Building Program. The program was initiated by pioneering solar advocate, Douglas Balcomb, who developed the comprehensive energy evaluation design program Energy 10. Paul Torcellini and Sheila Hayter et al. at the National Renewable Energy Laboratory have developed a broad array of sustainable building demonstration projects. Of particular interest to the authors is the fact that the very design of these buildings and their energy systems starts with an analysis to harness radiant impacts and requirements to optimize building energy consumption in relation to occupant thermal comfort.

One project of particular interest is the demonstration of low-energy design and renewable energy at the BigHorn Home Improvement Retail Center (Fig. 1.12). The state-of-the-art building incorporates radiant hydronic floor heating in the retail space, gas-fired radiant heaters in the warehouse, and careful building design to facilitate the entrance of cool air, the exit of hot air, and the prevention of high summer sun entry through window overhangs and shading. Sky lights, clerestory windows, compact fluorescent lighting, and optimum building orientation help to minimize lighting and heating loads.

Another NREL project incorporated novel, locally formed, insulated concrete structural forms for a modular residential one-story building to demonstrate the potential for natural heating and cooling in Pueblo, Colorado. Cooling was entirely through nocturnal radiation and the appropriate window operation routine. Electric radiant panels in bathrooms and bedrooms provided heat supplement to provide for heat control under special needs conditions. One fireplace gas log insert was provided to satisfy the hearth customs characteristic of the area and to ensure resale financing for reluctant passive solar lenders. The demonstration confirmed the potential for energy conservation by taking advantage of natural local climatic patterns.

Yet another building for the twenty-first century project demonstrated a sustainable building for the future, Zion National Park Visitor Center (Fig. 1.13). The focus of this remote structure was demonstration of natural cooling and ventilation for

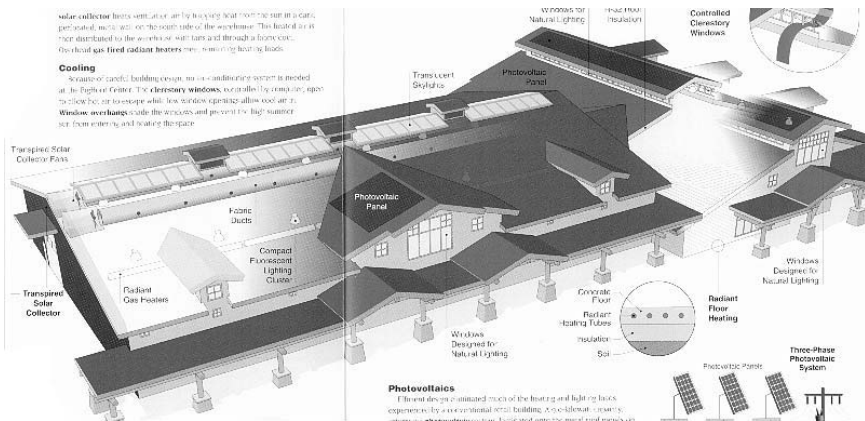


FIGURE 1.12 BigHorn Home Improvement Retail Center.

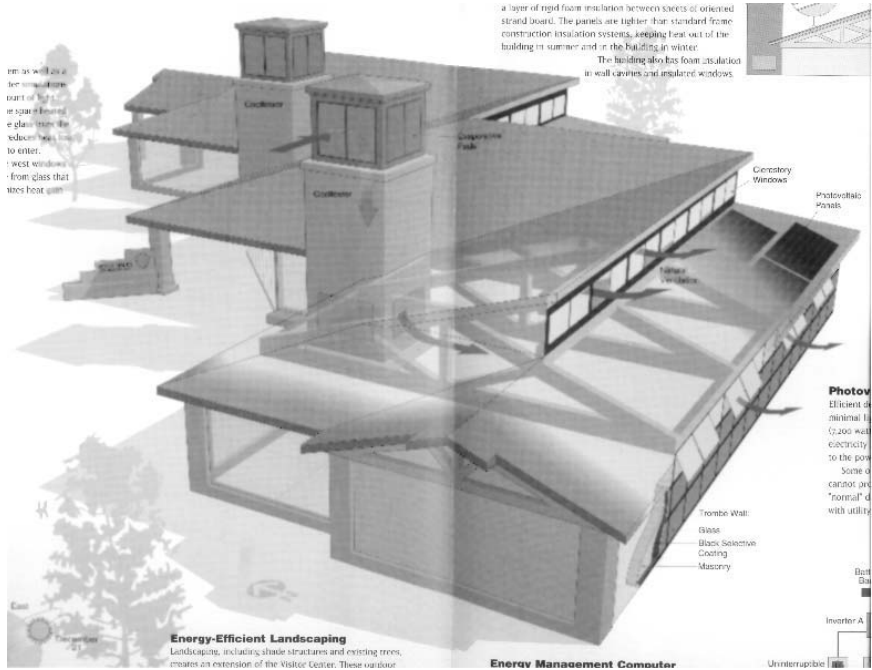


FIGURE 1.13 Zion National Park Visitor's Center.

interior climate control based on occupant thermal comfort. NREL performed computerized analysis for building design and orientation, as well as the application of trombe wall, building and glass materials coatings, clerestory windows, evaporative cooling tower pads, photovoltaic panels, and energy management. Electric radiant ceiling and personal space panels were used to ensure that the optimum mass natural heat charge was maintained during deficit charging, as well as occupant thermal comfort during all occupancy periods.

Under *CANMET's C2000* program for commercial buildings, sustainable buildings such as Green on the Grand are being constructed. These buildings incorporate a goal of 50 percent energy reduction from ASHRAE 90.1 1989 and additional environmental criteria beyond the scope of the ASHRAE Standard. Green on the Grand includes hydronic heating and cooling among the features specified to meet the objectives.

Green on the Grand also sought to use the most benign fuel and equipment, which in Ontario at the time implied DFC/HFC—free equipment and natural gas as fuel. Space heating and cooling was provided through the use of water-based radiators. Also, because water is a more efficient heat transfer medium than air, the motor energy required to move heat through water-based radiators is less than the electricity required to move heat through air-based ducts.

To accomplish cooling, 30 percent of the ceiling area was dedicated to hydronic radiant ceiling panels. Some of the panels were mounted in frames directly on the ceiling surface and others were placed in a T-bar grid ceiling. In the case of Green on the Grand, a natural gas-fired boiler-absorption chiller handled both heating and cooling. The unit was installed outdoors to maximize usable interior space, required less space than typical heating and cooling equipment, and was rated to operate at 85 percent efficiency. (See Figs. 1.14 and 1.15.)

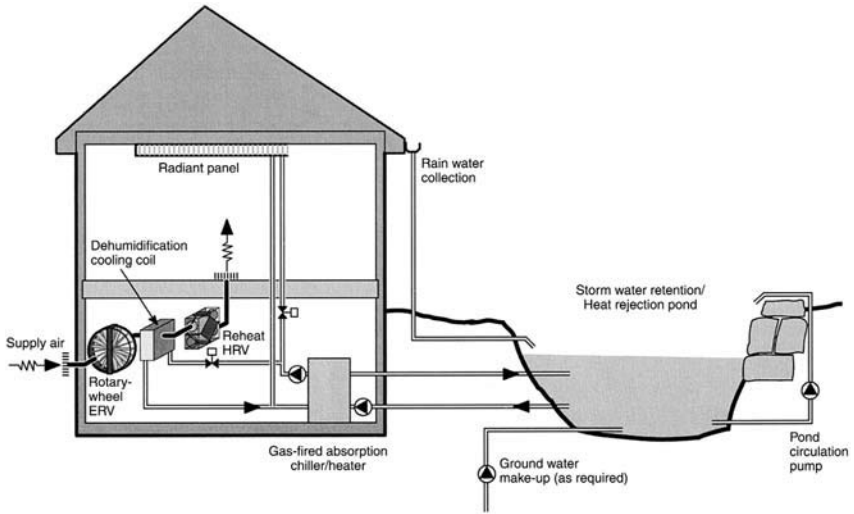


**FIGURE 1.14** Complete cooling system.



**FIGURE 1.15** Radiator panels, shown mounted on the cathedral ceiling, provide both heating and cooling.

Although the designers of the system recognized that the chiller was not as efficient as an electrical air conditioner (COP of 0.95 versus a COP of 2.5), they felt that the lower fuel cost and environmental considerations were overriding at the time. The designers also incorporated a manmade pond to serve in place of a cooling tower to facilitate rejecting heat to the outside through scenic evaporation-enhancing flow over decorative rocks during the distribution cycle.

Because cooling has become an accepted standard or necessity in more and more buildings worldwide, the magnitude of the electric air-conditioning load has resulted in a summer load peak for most electric utilities. Natural and radiant cooling provide an opportunity to significantly contribute to cooling load reduction, and energy use optimization in relation to occupant thermal comfort. The reader is referred to the Annotated Bibliography for more sources of information on radiant cooling, design, control, and installations. There is also more detailed information in Chapter 4 on the Museum, Adobe, and Night Cooling, and sustainable building projects.

---

## CHAPTER 2

---

# CONVECTIVE SYSTEMS WITH RADIANT PANELS

---

### 2.1 AIR AND GEOTHERMAL HEAT PUMPS

---

Both air-to-air and geothermal heat pumps are broadly promoted by electric utilities for residential and commercial heating and cooling. Each system boasts a coefficient of performance ratio above 1 to 1 due to extraction or exchange of energy from or to the air, earth, or fluid. Air-to-air heat pumps accomplish heating through convection, whereas geothermal heat pumps can accomplish heat delivery by using either air or water for convection or radiation, respectively.

Radiant hydronic ceiling and floor heating use lower water supply temperature than conventional hydronic convective systems (Fig. 2.1). Heat pumps can usually meet the demand at lower outside air temperatures, perhaps eliminating supplementary boiler or chiller (Kilkis, 1993). The combination of radiant heating or cooling improves the performance (COP) of heat pumps (Fig. 2.2).

The attainment of significant geothermal market share has proven to be a challenging task despite joint multimillion dollar government, manufacturer, and electric utility programs. Perhaps the appeal of radiant comfort that is reflected in the rapid growth of hydronic floor heating would bring both radiant floor heating and geothermal heat pumps into the mainstream if the synergies of their combination were fully appreciated.

The incorporation of radiant hydronic into a geothermal system may be at least twice the challenge of selling each alone. The frustration is obvious in the Oak Ridge National Laboratory report *Geothermal Heat Pumps in K-12 Schools*, that could just as well be written about radiant heating, in the following explanation of designers' reluctance to specify geothermal systems:

... some barriers remain to the increased use of GHPs in institutional and commercial applications. First, because GHPs are perceived as having higher installation costs than other space conditioning technologies, they are sometimes not considered as an option in feasibility studies. When they are considered, it can be difficult to complete the information required to compare them with other technologies. For example, a life cycle cost analysis requires estimates of installation costs and annually recurring energy and maintenance costs. But most cost estimators are unfamiliar with GHP technology, and installed costs tend to be very conservative, furthering the perception that GHPs are more costly than other technologies. Because GHP systems are not widely represented in the software used by engineers to predict building energy use, it is also difficult to



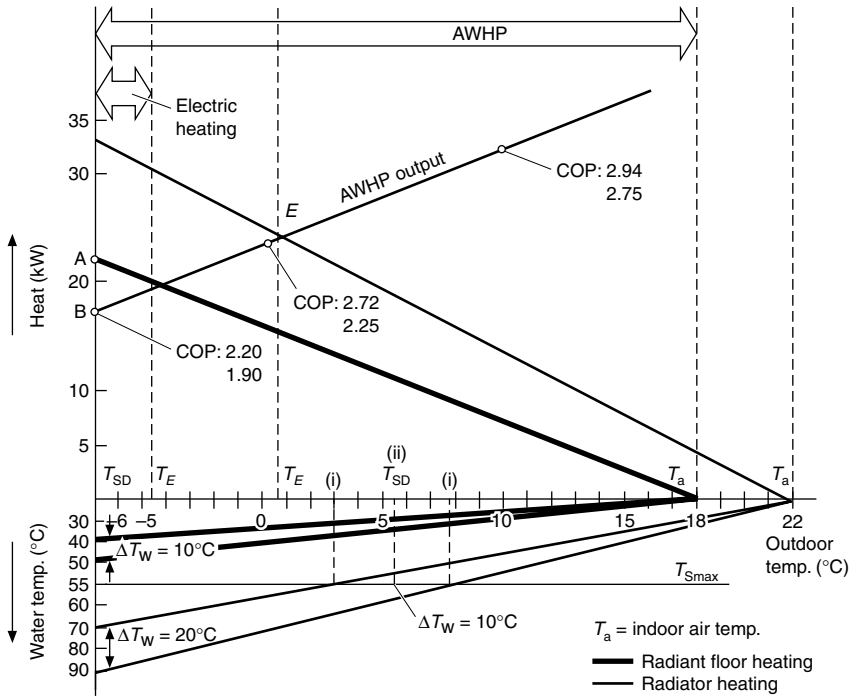


FIGURE 2.2 Radiant panels enable improved performance of an air-to-water heat pump.

wherever building design merits. And radiant panels in many forms are an excellent complement to the convective geothermal and air-to-air heat pumps.

**2.2 WARM-AIR FURNACES**

Central forced-air heating gas, oil, and electric furnaces generally distribute hot air through a ducted distribution and cold air return system designed to provide uniform temperatures throughout the space controlled by a single thermostat. Warm air systems are normally designed to create slightly positive internal air pressure under operating conditions to minimize cold exterior air infiltration. Ducting design and interior damper adjustment is set up so that airflow, and therefore heat transfer, match each space's heat loss so that uniform conditions result from the setting of a single central system thermostat.

The basic laws of physics and the increasingly diverse architectural features becoming common to all types of buildings place very difficult design challenges in the quest for achievement of uniform in-space comfort under both occupied and unoccupied conditions. For example, consider the pressure changes that occur when heat delivery ducts or room doors are closed for whatever reason, and the normal duct and stairway stack effect that is present in multifloor structures. The increased use of windows, open spaces, and cathedral ceilings presents comfort challenges.

Structural design and occupancy demands provide opportunities for successful conflict resolution through radiant hybrid design.

### **2.3 RADIANT HEATING AND COOLING**

---

Radiant heating and cooling in combination with convection systems are used to make up the deficit load by design or default. In the case of radiant cooling, the objective is normally defined and driven by the economics of the part load contribution that the site-specific conditions and use will permit. As seen in the Arizona project described in detail in Chapter 4, the incentive for investigating the potential for radiant cooling is usually framed by the costs of peak load electricity in relation to the use requirements of the facility.

The thermal sailing that the hydronically cooled mass affords is an important factor for designers to investigate in relation to anticipated power interruption periods, or brownouts. In addition, it is important to compare pump versus fan cost as it relates to the delivery of cooled air. Make up air for ventilation purposes must conform to the requirements of ASHRAE Standard 62-1989, *Ventilation for Acceptable Indoor Air Quality*, regardless of whether the system incorporates radiant cooling.

In cases in which radiant heating is combined with convection heating, the main determinant is usually the desired level of occupant thermal comfort. For example, warm floors are often specified. Yet, whether electric or hydronic is considered usually depends on the size of the application. Electric is almost always more economically installed in small places, whereas hydronic systems may be justified when the applications are extensive, and in fact, encompass enough floor space to permit the radiant system to be the primary system. However, when floor warming is the sole objective, the normal practice is to maintain the floor at a set temperature all year long, usually about 70°F.

In the case of large window expanse and localized need for supplemental heat, electric radiant wall or ceiling panels or floor mats are usually the most economic and satisfactory solution. Where hydronic supply is available, hydronic wall panels may also be an economic option.

The reader is referred to the chapters in Sec. 5 that describe the various radiant heating and cooling products to determine which option is the most practical for new or retrofit design.

---

# CHAPTER 3

---

## VENTILATION WITH RADIANT HEATING AND COOLING

---

### 3.1 INDOOR AIR QUALITY

---

The requirements for indoor air quality are detailed in ASHRAE Standard 62-1989, *Ventilation for Acceptable Indoor Air Quality*. There are also requirements defined in local building codes. The reader is referred to these sources for specific information regarding indoor ventilation requirements for buildings.

Building construction and use are major determinants of ventilation requirements. In other words, the number of building occupants, the activities being performed, and inherent building structure air changes per hour provide the input to determine whether mechanical ventilation is required. Public buildings have ventilation requirements that are very different from residences.

Radiant heating is appropriate for all types of buildings; residential buildings seem to be the most common application. The popularity of radiant heat in homes is probably explained by the fact that heat type is owner specified, and homes are usually owner occupied. In any event, except in cases in which building construction reduces air change below 1/3 air change per hour, it is common to provide mechanical ventilation in bathrooms and the kitchen. For homes in which inherent structural air change is considered inadequate or for cases in which additional ventilation is desired, heat recovery ventilators or air-to-air heat exchangers may be installed.

Exhaust-only ventilation for small areas is another approach to providing additional ventilation as desired. The advent of low Sone [one (1) Sone being the sound a refrigerator makes], low-energy exhaust fans designed for continuous running has made exhaust-only ventilation a practical, low-cost ventilation option. However, it is important to analyze the requirements and entry points for supply air to avoid potential mold, mildew, and comfort problems from random supply. Control may be set up so that the volume of air in cubic feet per minute (cfm) may be adjusted as well as the frequency and duration of fan operation.

An example of a radiant hybrid system is the combination of a radiant electric ceiling panel with a centered exhaust fan that may also incorporate a light and night-light, for use in bathrooms. The use of this single product combination, the Bathroom Comfort Center<sup>®</sup>, provides for all bathroom comfort needs. The radiant ceiling panel warms the floor, walls, windows, and mirrors, reducing or eliminating condensation and mirror fog. The exhaust fan evacuates moisture and odors and draws in air conditioning if required in the summer (Fig. 3.1).



**FIGURE 3.1** ENERJOY Bathroom Comfort Center heat panel, with a centered exhaust fan, light, and night-light. (Photo courtesy of SSHC, Inc.)

The use of the combination product, or a mix of electric radiant heating products and exhaust, provides the opportunity to separate the bathroom from a central heating system. The elimination of ducting for central heat pumps or forced-air systems reduces installation cost, eliminates potential for odor and moisture backdrafting, and separates control of the heating function for an area where heat requirements are seldom in sync with the rest of the building. The use of radiant heat in bathrooms may well become a building standard, much like air conditioning, and perhaps, floor warming.

Radiantly heated homes do not normally require additional ventilation. However, whole-house ventilation is also becoming more popular as growing awareness of chemical sensitivities and allergies make air purification a priority. One of the characteristics of radiant heating is the absence of fans and ducting to facilitate heat distribution. The only mechanical air movement that is required is that which is prescribed by codes and standards or occupant preference. The result is elimination of heat distribution-related airborne pollens, dust particles, and chemicals, as well as related fan energy and system-induced air infiltration.

### **3.2 CONTROLLING INFILTRATION**

---

A characteristic of radiantly heated homes is reduced air infiltration and exfiltration. There are several reasons for reduced air transport. Depending on building design and construction, the largest factor influencing air infiltration and exfiltration may be the presence and operation of the forced-air mechanical distribution system. Although great care may be exercised in balancing the system during installation, there are many factors that make pressure balance a fleeting occurrence.

In a November 2000 ASHRAE Journal article, “Improving Humidity Control for Commercial Buildings,” Joseph Lstiburek et al. said, “In theory, the designer can bal-

ance the airflows entering and leaving the building so that, apart from wind gusts, no pressure difference exists across the exterior wall. However, wall systems and HVAC systems are complex assemblies of small, connected chambers. Contrary to intuition, a building is not a simple large vessel in which interior pressure can be equal at all points. Just because most of the building has an average neutral air pressure with respect to the outdoors does not prevent some parts of the interior from being positive with respect to the building cavities. Humid air can be forced to leak outwards in some places while at same time, cold air is leaking *inwards*.”

Contributing determinants are the high air temperature of gas forced-air systems, which increases the relative indoor-outdoor temperature differential and related air pressure, and the high air volume required due to the lower air temperature characteristic of heat pumps. Occupancy patterns of use are ever-changing as doors are opened and closed, space use is altered, and occupant preference changes. In addition, ducting often serves two masters, both heating and cooling. Each requires different adjustments for proper balance and seasonal changeover, either of which is unlikely to be done in practice. Meanwhile, the stack effects that result from forced hot and baseboard air temperature gradients are also largely absent with radiant systems.

Building materials selection, quality of construction, and simple caulking and sealing are all determinants of building air infiltration. In addition, building site selection and orientation is also an important factor as wind speed is a factor impacting infiltration regardless of heating system selection. However, the selection of a heating system and how it is installed is one of the largest infiltration determinants. Yet the influence of the heating system on air infiltration is often overlooked in energy, comfort, and building performance analysis.

Radiant systems minimize the indoor-outdoor temperature differential because the warmed objects and surfaces warm the air indirectly. Therefore, the air is only as warm as the temperature setting for the heating requirement, resulting in a smaller indoor-outdoor temperature and related pressure differential. This characteristic of radiant systems is an especially important feature in many applications, such as clean rooms, laboratories, and hospitals. The utilization of radiant systems for heating and cooling is an option to be explored wherever indoor-outdoor air exchange needs to be minimized.

### **3.3 HUMIDITY CONTROL**

---

Radiant heating does not directly impact humidity. The reduced infiltration of cold, dense, dry outside winter air enables the normal occupant aspiration, bathing, cooking, and other occupancy functions to be the primary influence of interior residential building humidity. The reduced infiltration characteristic of a radiant system is a factor to consider in analyzing the factors involved in humidity control. In general, radiantly heated buildings have higher relative humidity than forced warm air convection heated buildings.

For radiant cooling, humidity control is the major determinant of the radiant percentage contribution to required cooling capacity. The mechanical cooling system design must account for the potential extreme or boundary temperature and humidity conditions that might occur in the space employing the hybrid radiant cooling system. Radiant cooling may be synchronized with mechanical cooling, desiccant dehumidification, and dedicated outdoor air systems (DOAS).

Desiccant systems are used for dehumidification and sensible cooling as part of a total air-conditioning package. The basic desiccant dehumidification and cooling process is referred to as the Pennington cycle (Fig. 3.2). The cycle takes air through a dehumidification and regeneration process. The rotary wheel is the desiccant technology generally used in HVAC applications (CLER, 1998) (Fig. 3.3). The processed air may be from the inside or the outside exclusively, respectively, or in combination, depending on conditions and whether the dehumidification or ventilation mode is in operation (Fig. 3.4).

Engineers are seriously considering dedicated outdoor air systems (DOAS) (Mumma, 2001) (Fig. 3.5). DOAS decouple the building latent and sensible load, supplying approximately 20 percent of the normal VAV design flow, which requires that the dew point must be suppressed more than is typical with an all-air VAV system. Parallel building sensible cooling choices includes radiant panels as well as tra-

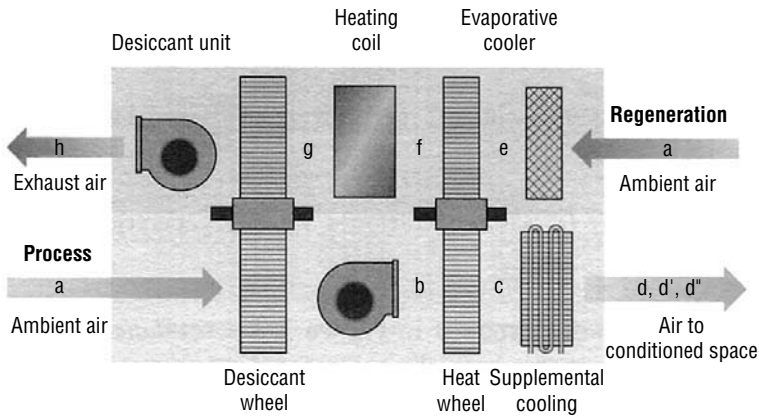


FIGURE 3.2 The Pennington cycle.

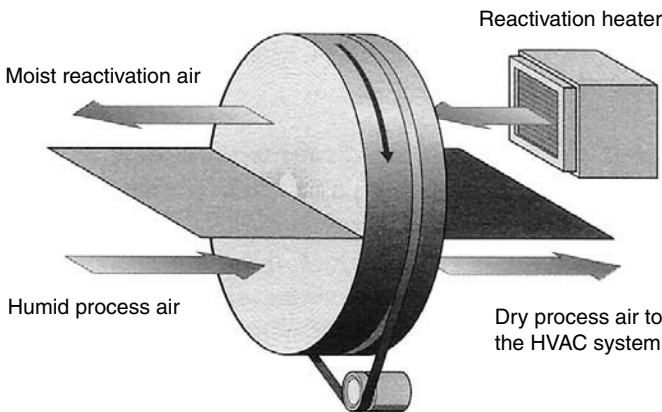


FIGURE 3.3 The rotary wheel desiccant dehumidifier.

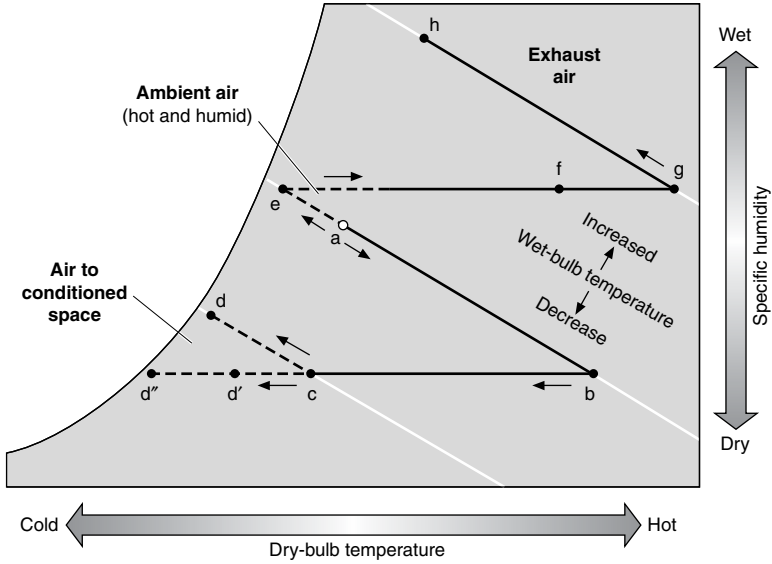


FIGURE 3.4 Humidity temperature graph.

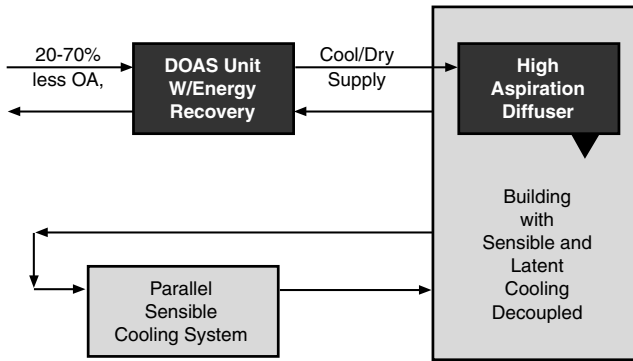


FIGURE 3.5 Dedicated outdoor air and parallel sensible cooling system.

ditional fan coil units, packaged unitary equipment or water-source heat pumps, and parallel all-air VAV systems.

Detailed analysis of companion mechanical air conditioning systems is beyond the scope of this book. The caveat is that boundary conditions for the hybrid system space to be conditioned be determined without error so that the radiant panel operation specification is flawless.



---

# CHAPTER 4

---

## HYBRID HEATING AND COOLING DEMONSTRATION PROJECTS

---

Following is a selection of hybrid HVAC system projects that are noteworthy in their creativity and contribution to documentation on the characteristics and performance of hybrid systems. Most of these projects continue to be monitored, and complete information is available for the reader to analyze in even greater detail. In fact, the quest for information continues as the early information confirms the economic and comfort advantages inherent in hybrid systems despite the additional investment in time resources that may initially be required for innovative design.

The detailed examples provide a real-world excursion through multiple design paths developed in pursuit of trend setting, comfort, and contents-based interior HVAC conditioning.

The exciting aspect of these hybrid projects is their comprehensiveness. And, indeed, the very introduction of radiant analysis enables much more comprehensive engineering than convection-focused output characteristics of common HVAC design methodology. In a world with changing energy cost, availability, and suitability parameters, the focus must shift to a better building HVAC engineering harvest of comfort and conservation potential. It is a challenge almost like the hog butcher finds a use for everything but the oink! So, read with interest about the robust options available through application of the hybrid system approach to HVAC system design.

---

### 4.1 ANKARA MUSEUM RETROFIT

---

ASHRAE member Ibrahim Birol Kilis has pursued the optimization of HVAC functions through the use of hybrid systems. His strong interest in furthering the quality of HVAC system performance led to his interest in providing the opportunity to edit for inclusion in the Handbook his comprehensive *ASHRAE Journal* article, “Hybrid HVAC Systems—When Should the Sensible, Latent, and Other Functions of an HVAC System be Decoupled?”

#### 4.1.1 To Couple or Decouple HVAC Functions

During the technological quest for human comfort, improved indoor heating was the first priority. An important late-nineteenth-century development was the

widespread use of central heating systems. These systems had only one function, namely, to transfer sensible heat to indoor spaces. Industrial necessity, rather than a desire to improve human comfort, prompted the early recognition of other indoor requirements.

Willis Carrier developed a humidity control device in 1902 for a lithographing and publishing plant to preserve paper from the effects of excess humidity. Later, indoor humidity control and comfort cooling were determined to improve the productivity by about 51 percent in a factory. Soon after, new HVAC components like cooling, ventilation, humidity control and indoor air quality assurance were defined. In the meantime, buildings became function specific, and the special indoor requirements were also identified.

Radiant temperature asymmetry, vertical air temperature profile, operative temperature (OT), mean radiant temperature (MRT), effective radiant flux (ERF), air velocity, and turbulence intensity ( $Tu$ ) are especially important for spaces with special functions like offices, schools, hospitals, museums, and libraries, as well as various industrial spaces.

As a consequence of new comfort vectors and indoor air quality requirements, new functions were superimposed on the sensible heat transfer function. In other words, although diverse functions were identified and assigned, the central forced-air system eventually became, by default, a multifunction system. This concept of coupling the HVAC functions at the plant, distribution, and delivery levels dominated the industry until recently.

The diversity of HVAC functions and precise control requirements overloaded the central system and created conflicts by performing too many tasks simultaneously. When the sensible, latent, and other functions are decoupled, it becomes possible to employ more function-specialized, dedicated, and alternative distribution and delivery systems. Increases in efficiency, system agility, and response flexibility are benefits that are indicated by the following factors.

1. Human thermal comfort. Recent studies have indicated a stronger relationship between thermal comfort and mean radiant temperature, operative temperature, and radiant asymmetry. An air system cannot directly control the mean radiant temperature. It is difficult to sustain the operative temperature by manipulating the indoor air temperature.

2. Control precision for humidity and air temperature. In libraries and museums two simultaneous HVAC functions are required. The first function is precise and object-specialized climate control to enhance preservative conservation of the collections. Relative humidity should stay within  $\pm 2$  percent, and the air temperature must be kept within  $\pm 0.5^\circ\text{C}$  ( $1^\circ\text{F}$ ). Most of the organic artifacts require a year-round relative humidity of 50 percent which also corresponds to the condition for lowest survival rate of airborne bacteria affecting humans.

In many cases, however, lower indoor air temperatures than are normally comfortable for humans are desirable. If the temperature is decreased from  $20^\circ\text{C}$  ( $68^\circ\text{F}$ ) to  $17.5^\circ\text{C}$  ( $63.5^\circ\text{F}$ ), the folding endurance half-life of paper will increase from 490 years to 750 years. This temperature requirement conflicts with the second function, which is the provision of human thermal comfort. The question then becomes, how can we avoid the compromise of artifact preservation for human comfort, or vice versa? If the functions can be properly decoupled and coordinated, both objectives can be met.

Another controversy arises from the assumption that energy conservation and the environmental requirements shown in Table 4.1 are in strong conflict. Actually, the relationship between energy consumption and climate control is not robust. The

effects on operating cost of different relative humidity and air temperature levels at different control limits were examined at various climatic locations.

The major conclusions were that it would be cheaper to keep relative humidity at 50 percent year-round than to maintain either 40 or 60 percent relative humidity year-round. The difference in operating cost between maintaining  $\pm 2$  percent RH and  $\pm 7$  percent RH is slight. Manipulating space temperature on a yearly basis from 18°C (64.4°F) in winter to 24°C (75.2°F) in summer has little effect on operating costs. These findings do not contradict the requirements where the stability of relative humidity is more important. Referring to part II in Table 4.1, if the humidity level is compromised, air temperature may be manipulated to offset the side effects, and there is no need to compromise other factors.

**3. Stability.** Using decoupled systems, energy demand profiles may be suitably modified, reduced, and stabilized. Although some functions are interrelated, it may be necessary to ensure the stability of each function through use of separate systems. For instance, with fluctuating outdoor conditions, precise control of indoor relative humidity will be easier if the air temperature is partly stabilized by a system that does not control indoor relative humidity.

**4. Efficiency and performance enhancement.** From the perspective of energy efficiency, air is not normally an efficient medium to deliver or extract heat. An air distribution system is more suitable for sustaining indoor air quality, which is vital.

**TABLE 4.1** Indoor Conditions in Museums and Libraries

Part I. Winter and summer design conditions				
Material	Winter		Summer	
	Air temperature	Relative humidity	Air temperature	Relative humidity
Paper <sup>a</sup>	18 ± 0.5°C	50 ± 2% RH	24 ± 0.5°C	50 ± 2% RH
Scrapbook, albums	18 ± 0.5°C	45 ± 3% RH	22 ± 0.5°C	45 ± 3% RH
Leather, wood	18 ± 1°C	50 ± 3% RH <sup>b</sup>	24 ± 1°C	50 ± 3% RH
Parchment, vellum	18 ± 1°C	50 ± 2% RH	24 ± 1°C	50 ± 2% RH
Microfilm	18 ± 1°C	35 ± 3% RH	18 ± 1°C	35 ± 3% RH
Inorganic materials (including metals)	18 ± 1°C	35 ± 5% RH <sup>c</sup>	24 ± 1°C	35 ± 5% RH

<sup>a</sup> Lower temperature and humidity levels are desirable, see Part II.  
<sup>b</sup> 55%RH is the upper safe limit for macro-environmental control against mold growth.  
<sup>c</sup> 30%RH is the absolute lowest limit in museums and libraries.

Part II. Degradation of paper				
Indoor air temperature	Degradation rate relative to 21°C and 50%RH			
	30	40	50	75
25°C	0.90	1.30	1.60	2.40
21°C	0.60	0.80	1.00	1.50
20°C	0.53	0.71	0.89	1.30
18°C	0.44	0.58	0.73	1.10
15°C	0.29	0.39	0.49	0.74

5. Zoning. Precise and flexible zoning is becoming a common requirement for many spaces. Hydronic or electrical systems can best accomplish definite zoning. A challenging problem in museums is how to adjust conditions to the requirements of radically changed display areas. Variability of space conditioning requirements is common not only to museums but also to laboratories, hospitals, and a host of other spaces for whatever reason.

Each may require a separate and definite variable zone protocol. When displays or conditions are changed frequently, zone conditioning must respond accordingly.

6. Precise and diverse control and management. Sophisticated control strategies and electronic equipment now available for total building management far exceeded the accuracy and response capabilities of conventional, multifunctional central HVAC systems. Direct digital control (DDC), building automation systems (BAS), and computer-aided facility management (CAFM) all made multifunction a requirement rather than an option. The control strategies seek to allocate dedicated, function-specific, and diverse distribution and delivery systems each with compatible accuracy and response.

#### 4.1.2 Hybrid Systems

The basic idea in a hybrid system is to decouple certain HVAC functions at the central plant and distribution level and to orchestrate them at the zone (delivery) level. For example, a conventional air-conditioning system serving primarily latent loads, and other functions related to air quality, may be complemented by a hydronic, electric (if heating is the only mode), or separate air system. Decoupling takes place primarily between the latent and sensible functions. A large portion of the sensible load is assigned to a hydronic system. Sensible load split may be dynamically controlled. Figure 4.1 shows the hybrid system for a museum. It consists of an all-air system and an all-water (panel) system that is integrated with the sprinkler system. When a single type of HVAC system is diversified, this may also be regarded as a hybrid system. Therefore, the term “hybrid” applies to the functions rather than the type of systems. With this in mind, a proper definition of a *hybrid HVAC system* is an optimal integration of different distribution and delivery systems with specific functions, served from the same or different plant or energy sources.

This definition emphasizes that a decoupling process consists of diversifying and complementing the HVAC functions of an air-conditioning system, rather than eliminating them. Decoupling requires a careful optimization and rationing of diverse functions for several design objectives including, but not limited to, space conditioning objectives, minimization of installation and operation costs, and maximization of energy efficiency.

#### 4.1.3 Panel Heating and Cooling in Hybrid Systems

Each building and its HVAC solution are unique, and a complete evaluation of the pros and cons of a hybrid system must be made. A hybrid system designed for a specific application that includes panel heating (hydronic or electric) and cooling (hydronic) systems used in combination with conventional HVAC systems offers unique advantages. Attributes of panel systems when combined with hybrid systems are summarized as follows:

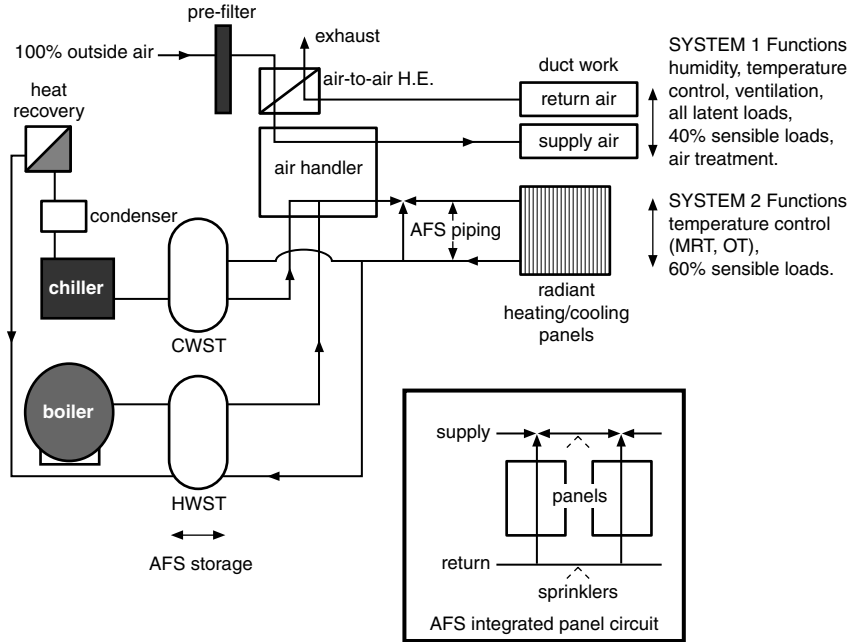


**FIGURE 4.1** Schematic diagram for the hybrid system.

**1. Human thermal comfort.** Radiant panels directly control the mean radiant temperature, which is an essential factor for human thermal comfort that is not controlled directly by conventional, convective HVAC systems. Management of MRT is important because the human body exchanges sensible heat by radiation and convection at approximately a 60 to 40 percent ratio, respectively.

Radiant floor and wall panels further enhance comfort because they normally operate at a similar split, 50 to 50 percent and 60 to 40 percent respectively. Radiant ceiling panel location can result in a higher radiant convection split approaching virtually 100 percent radiant heat output, depending on panel design, ceiling location proximity, and local casual or mechanical air movement. Objects heated radiantly reradiate heat thereby warming the air. The fact that radiant panels transfer heat by radiation and convection makes a radiant panel system a hybrid system in and of itself. Through the convective component, a radiant panel influences air temperature.

**2. Precise humidity and temperature control.** In a hybrid radiant panel system, although the convective heat transfer component of panels may influence air temperature, the forced-air system may be used for the stabilization and control of other functions, including the precise control of air temperature.

In museums and libraries, panel systems can substantially increase the half-life of artifacts by permitting lower air temperatures without compromising human comfort in winter, through an increase in MRT. This hybrid design strategy will also decrease energy consumption. (See ASHRAE RP-907.)

A central air system cannot differentiate humidity among zones. However, Table 4.1 indicates that paper and similar artifacts can be satisfactorily preserved at more than one combination of humidity and temperature. However, a hybrid radiant panel system may improve the preservation quality in each individual zone by manipulating MRT, which therefore requires less air temperature manipulation to control the humidity in each zone.

**3. Stability.** Radiant panel systems exhibit greater in-space thermal stability in comparison with convection systems due to the thermal mass of some panel designs and radiant heat transfer to furnishings and building mass. In these ways, radiant panels are coupled with thermal mass. Depending on the capability of the control, panels respond to changes in surface and/or air temperatures by controlling the surface heat transfer flux. Precise control of surface heat flux enables maintenance of thermal stability of an in-space environment.

**4. Efficiency and performance enhancement.** In a panel-heated or -cooled room, air temperature and air velocity distribution are generally more uniform than for a convection system. For example, air temperature stratification is minimal with floor heating, and the absence of mechanical ventilation means that system-related indoor air velocity are those of natural convection, which are comparatively very low.

Coupled with the influence of thermal mass introduced by the radiant panel system, sensible loads are reduced and their peaks are leveled. Significant reduction in energy occurs when air distribution fan electricity requirements are replaced by pumping energy for hydronic water distribution, or eliminated completely with electric panel systems.

Panel system design generally requires moderate supply water temperatures of 16°C (61°F) in cooling and 32°C (90°F) in heating (see Table 4.2). This enables the tie-in of panels in tandem to the return end of other HVAC elements in the system. Although panels satisfy large portions of the sensible loads, the latent loads govern the supply-water temperature for air handlers. This cascaded temperature moderation may increase the performance of the central equipment and allow the use of alternative energy sources.

**5. Definite and flexible zoning.** Radiant panels provide definite thermal zoning. The modular ceiling or vertical (partition) panel provides flexibility in partitioning and zoning. A recent application in a Dutch museum demonstrated that a dual floor heating and cooling system could compensate for substantially all base loads, enabling design of ventilation air volumes around minimal requirements.

**6. Other attributes and potential limitations.** Interconnection of hydronic HVAC systems with automatic fire sprinkler systems could provide sizable savings. According to NFPA-13 standard, water temperatures cannot exceed 49°C (120°F) or drop below 4.4°C (40°F). Hydronic radiant panel systems can easily comply with these limits.

In panel-hybrid systems, a common central air system can serve both the interior and perimeter zones. Smaller air handling units and ductwork reduce the ceiling and utility space requirements. This may be important in museums, libraries, and any building in which the value of space is appreciated.

Risk from inhalation of infectious droplet nuclei may be decreased by an increase of ventilation air up to a certain point where benefit of further ventilation diminishes. A hybrid radiant panel system enables maintenance of optimal ventilation, which is at rates below what is characteristic of mechanical HVAC systems.

Concerns expressed about potential limitations of hydronic panel systems must be addressed in design and construction. These concerns are that panels may leak

**TABLE 4.2** Sample Design for Ankara Museum of Ethnography

Location and climate												
Location: Ankara, Turkey, 39°57'N-32°55'E. Altitude: 861 m.												
Annual heating degree-days (based on 18°C): 2700.												
Outdoor design temperatures: -12°C, in winter; 34°C dry bulb, 20°C wet bulb, in summer.												
Outdoor relative humidity %RH	Months											
	1	2	3	4	5	6	7	8	9	10	11	12
45-year averages												
at 7 A.M.	85	83	80	73	71	64	57	57	63	73	84	86
at 2 P.M.	69	64	50	41	40	34	28	26	30	39	51	68
at 9 P.M.	79	78	67	58	60	52	43	40	46	58	73	82
Building function	Museum, floor area 500 m <sup>2</sup> , ceiling height: 6 m.											
Artifacts	Historical books and writings.											
Panel area	350 m <sup>2</sup> at the ceiling, 233 m <sup>2</sup> at partitions.											
Ceiling panels	3 mm aluminum with 13 mm ID attached tubing, back and sides are insulated with 2-cm-thick spray insulation.											
Partition panels	13-mm rubber tubing, sandwiched in 6-cm-thick plywood-drywall partitions. All tubing are spaced 20 cm on centers.											
Ventilation	100% fresh air with air-to-air heat recovery; air filtration: better than 95%.											
Min. air change	3 air changes per hour (10,000 m <sup>3</sup> /h).											
Air handling	Humidity control method, draw through, fan and motor in air stream.											
Indoor conditions	18 ± 1°C, 50 ± 2% RH in winter, 24 ± 1°C, 50 ± 2% RH in summer.											
Design parameters and results		Sensible load split PR										
		0.0	0.20	0.40	0.60	0.80	1.00					
Winter 60% RH	Sensible heating load W	100.000	96.000	90.000	85.000	80.000	70.000					
	Panel flux W/m <sup>2</sup>	N/A	33	62	87	110	120					
	Panel mean water temp. °C	N/A	30	30	32	33	35					
	Relative humidity %RH	50 ± 4	50 ± 3	50 ± 2	50 ± 2	50 ± 2	50 ± 2					
	Indoor air temp. °C	18.0	17.6	17.2	16.8	16.4	16.0					
	Mean radiant temp. °C	16.5	17.5	18.5	19.2	20.0	20.7					
	Operative temp. °C	17.2	17.5	17.8	18.0	18.2	18.3					
	Reheater capacity kW	170	128	86	62	40	12.5					
Summer 28% RH	Sensible cooling load W	70.000	69.000	68.000	67.000	67.500	68.000					
	Latent cooling load W	21.000	21.000	21.000	21.000	21.000	21.000					
	Panel flux W/m <sup>2</sup>	N/A	23	45	65	84	99					
	Panel mean water temp. °C	N/A	18	17	16	14	12					
	Relative humidity %RH	50 ± 4	50 ± 3	50 ± 2	50 ± 2	50 ± 2	50 ± 2					
	Indoor air temp. °C	24.0	24.0	23.7	23.5	23.3	23.1					
	Mean radiant temp. °C	24.6	24.2	23.7	23.3	23.0	22.8					
	Operative temp. °C	24.3	24.1	23.7	23.4	23.1	23.0					
Delivery	Cooling coil capacity kW	291	221	155	129	111	121					
	Reheat coil capacity kW	—	—	—	—	9.4	22.5					
	Indoor air velocity m/s	0.23	0.19	0.14	0.12	0.13	0.13					
	Supply air volume m <sup>3</sup> /h	41150	29786	18855	11580	14260	16205					
	Fan motor capacity kW	62	45	28	24	22	24					
	Hydronic pump capacity kW	N/A	0.3	0.5	1.0	1.5	2.0					
	Zone water flow rate m <sup>3</sup> /h	N/A	4.0	8.0	12.0	16.0	20.0					

fluid and condensation may occur on panels used for cooling. Buildings using air water systems are without incident of either leakage or condensation, including those with the addition to automatic fire sprinklers. Condensation on cooling panels is virtually eliminated by proper design, control, and split of the loads the panels are to address.

The heat flux from a ceiling panel directly above a display area may be limited if artifacts are sensitive to thermal radiation. Electric panel output is easily modulated within the range of panel capability. In a four-pipe hydronic system without a central zoning, heating and cooling may be simultaneous among different panels. However, the response may be slow. The relative importance of all factors may influence the equipment choice. The essence of hybrid system design is choosing the components providing exactly the set of localized space conditions required.

#### 4.1.4 Split of Sensible Loads

Although it is reasonable that sensible loads should be satisfied by sensible systems (panels), there are many factors that require an optimum split, defined by the term  $PR$ .

$$PR = \frac{\text{sensible load assigned to panel system}}{\text{total sensible load}} \quad (1)$$

$PR$  is a number ranging between 0 and 1. In a hybrid system,  $PR$  is greater than 0 and less than 1. An important factor influencing the selection of a suitable  $PR$  is the cost of the hybrid system. Installation cost, energy consumption of the plant, and operating cost of the distribution and delivery systems have to be compared and analyzed. Energy consumption of the plant will be relatively low in a panel hybrid system, and the installation cost is comparable with an all-air system. In addition, the operating cost of the distribution and delivery systems may be substantially lower. Because performance is site-specific, the optimal split ( $PR$ ) rendering the minimum operating cost should be carefully investigated.

To facilitate analysis, the merit of hybrid systems diagram (MOH) was developed, which is shown in Figure 4.2 for the following example. The specific power consumption ratio (SPC) is related to the total power required to run auxiliaries, such as fan motors and pumps to satisfy a specified sensible load.

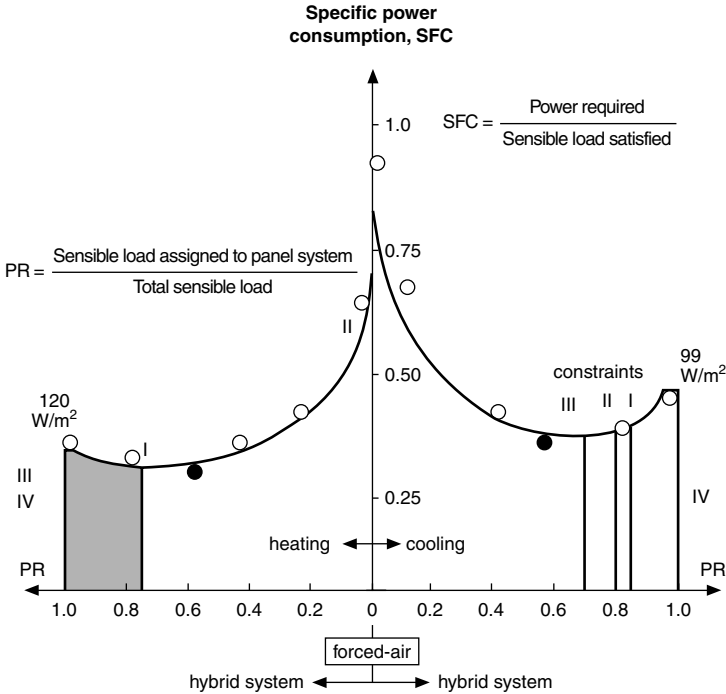
$$SPC = \frac{\text{power required by the system}}{\text{sensible load satisfied by the system}} \quad (2)$$

Figure 4.2 reveals the optimal  $PR$  for minimum operating cost, which is at the same time a good indicator for the overall cost. Optimal conditions may be preserved at part loads by adjusting  $PR$  at the zone level. There are four upper bound constraints for  $PR$ .

Constraint I: A portion of the sensible load is assigned to another convection system (e.g., forced air) to quickly and precisely control the indoor air temperature.

Constraint II: The reheat process is costly. Options that would replace it should be investigated. Energy code requirements, where they apply, must be met in the analysis.

Constraint III: Cooling panel loads should not exceed the predetermined safety level at which condensation would occur on panel surfaces under anticipated indoor conditions. Heating panel surface temperature design and/or control



**FIGURE 4.2** Merit of hybrid systems (MOH) diagram for the sample design.

should not exceed ASHRAE limits for relevant design factors including radiant asymmetry, 29°C (84°F) for heated floors, and other limits that may be appropriate for the application.

Constraint IV: Ideally, the amount of sensible loads that can be handled at minimum ventilation conditions should be assigned to a forced-air ventilation system.

The upper bound for *PR* is determined by whichever of the above constraints comes first.

Available duct space, cost, or permissible air velocity (constraint V) generally determines the lower bound.

**EXAMPLE 4.1** *The Ankara Museum of Ethnography has a display section for historical manuscripts and calligraphies. In accordance with the concept outlined in Figure 4.1, the hybrid system couples a forced-air system with fast response, low-mass hydronic metal ceiling panels, covering 70 percent of the total ceiling area. This ratio provides sufficient uncontrolled ceiling surface to enhance thermal convection in the heating mode. In addition to ceiling panels, removable partitioning panels with embedded tubing provide subzoning flexibility for frequently changing display arrangements. Each side of these panels may be individually served and controlled by drop-down tubing from the ceiling. When all partitioning panels are used, they make up 40 percent of the total panel area in the zone.*

The fundamental equations used for panel design are detailed in Chapter 5, *ASHRAE Handbook*. Two computer programs, *HEATP* and *COOLP*, were employed for the design and analysis of the panel system for heating and cooling, respectively. Calculating the plane radiant temperature in six directions can approximate MRT by using an area weighted mean value. At given indoor conditions, heat flux on the panel surface depends on the effective panel surface temperature. Due to the presence of artifacts that are sensitive to thermal radiation, the maximum designed heat output is  $120 \text{ W/m}^2$  ( $38 \text{ Btu/h} \cdot \text{ft}^2$ ). This corresponds to surface temperatures of  $31^\circ\text{C}$  ( $88^\circ\text{F}$ ) and  $29^\circ\text{C}$  ( $84^\circ\text{F}$ ) for ceiling and partitioning panels, respectively.

Panels are served by the automatic fire sprinkler piping (see the inset in Fig. 4.1). Two parallel tanks, namely, hot water storage and chilled water storage tanks, satisfy storage tank requirements for the automatic fire sprinkler system. These tanks serve for heat and cold storage, and at the same time minimize the short cycling of the chiller in mild weather. The chiller condenser has a heat recovery system.

Table 4.2 gives the design conditions for the  $500 \text{ m}^2$  ( $5382 \text{ ft}^2$ ) zone. Outdoor supply air passes through a prefilter and an air-to-air heat exchanger. At winter and summer design conditions, the program *PSYCNRO17* was used to analyze the psychrometrics, to size the air-handling system, and to optimize the air temperature difference ( $DT$ ) and the coil bypass factor for different  $PR$  values.

At summer outdoor design conditions, namely  $34^\circ\text{C}$  ( $93^\circ\text{F}$ ) dry-bulb and  $20^\circ\text{C}$  ( $68^\circ\text{F}$ ) wet-bulb temperatures, outdoor relative humidity is 28.6 percent at an elevation 861 m above sea level. The 45-y averages are shown in Table 4.2. The summer outdoor design conditions correspond to the monthly average readings for July, taken at 2 P.M.

In winter, 60 percent outdoor relative humidity approximates the monthly average conditions at 2 P.M. in February. At 50 percent indoor relative humidity and 100 percent outdoor supply air conditions, Table 4.2 reveals that both humidification and dehumidification are necessary in every season.

#### 4.1.5 Results

The hybrid system was designed for different  $PR$  values, ranging from 0 to 1, with increments of 0.2. Accounting for the attributes of panel systems 10 and 11, sensible heating and cooling loads were adjusted for  $PR$  values greater than 0. Latent loads were assumed to be independent of  $PR$ . From Eq. (1), a given  $PR$  value determines the split of the sensible load between the panel system and the forced-air system.

For example, when  $PR$  equals 0.6, 60 percent of the design sensible load is assigned to the panel system. The forced-air system is coupled according to the remaining 40 percent of the design sensible load and the latent load of the zone. Results for winter and summer design conditions are given in Table 4.2. The MOH diagram shown in Figure 4.2 was drawn using these results.

**4.1.4.1 Winter Operation** Sensible heating load decreases when  $PR$  is increased above 0 (all-air system) partly because increasing the mean radiant temperature for human comfort can decrease the air temperature. When  $PR$  is increased to 0.6, and the indoor design air temperature is decreased from  $18.0^\circ\text{C}$  ( $64.4^\circ\text{F}$ ) to  $16.8^\circ\text{C}$  ( $62.2^\circ\text{F}$ ), the operative temperature increases from  $17.2^\circ\text{C}$  ( $62.9^\circ\text{F}$ ) to  $18.0^\circ\text{C}$  ( $64.4^\circ\text{F}$ ). Operative temperature increases because MRT increases from  $16.5^\circ\text{C}$  ( $61.7^\circ\text{F}$ ) to  $19.2^\circ\text{C}$  ( $66.5^\circ\text{F}$ ). Consequently, the sensible heating load decreases by 15 percent.

A threefold advantage is achieved: (1) human comfort is improved, (2) the indoor air temperature is decreased, which reduces the sensible load, and (3) the

half-life of paper is increased. At PR-0.6, heating panels can be operated at a mean water temperature of 32°C (89.6°F). In humidifying mode, reheat is not totally eliminated, but its required capacity is substantially reduced. Only constraint II is active. According to Figure 4.2, PR-0.6 is shown to be an optimum split.

**4.1.4.2 Summer Operation** Sensible cooling load slightly decreases with *PR* up to 0.6, although the indoor air temperature and MRT both keep decreasing, yielding better artifact preservation and human comfort. This is primarily due to the decrease in the exfiltration losses.

Because of the reheat process required after PR-0.6, the supply air volume, indoor air velocity, and fan capacity required increase slightly. At PR-0.6, indoor air velocity is less than 0.13 m/s (0.43 ft/s), which is the limit indicated in the ASHRAE Handbook. Surface condensation starts at PR-0.70 at a maximum permitted indoor relative humidity of 55 percent. To ensure a proper indoor air temperature control, the upper limit for *PR* is around 0.85. Figure 4.2 reveals that the optimum *PR* is 0.6.

At PR-0.6, cooling panels deliver 65 W/m<sup>2</sup> (20.6 Btu/h · ft<sup>2</sup>) at a mean water temperature of 16°C (60.8°F) at 3°C (5.4°F) DT. The last section in Table 4.2 shows that required fan capacity decreases from 62 to 24 kW, where the required circulation pump capacity remains in the range of 1 kW. The required cooling coil capacity is 129 kW, compared to 291 kW for an all-air system (PR-0).

#### 4.1.6 Conclusions

Hybrid system design decouples the functions normally handled in their entirety by a single centralized HVAC forced-air system. Hybrid systems utilize the components that best resolve the conflicts that are unresolved by using a single system to address all HVAC needs. The merit of hybrid systems (MOH) diagram shows how hybrid system design optimizes each important HVAC function.

The design of a panel hybrid system for a museum indicates that power consumption of distribution and delivery systems may be reduced by 50 percent. The HVAC functions are improved, despite the presence of conflicting indoors space heating and/or cooling requirements. Cited articles indicate that the decoupling of HVAC functions is emerging as a viable option. The museum design example quantifies hybrid concepts through a successful demonstration project.

## 4.2 NIGHT SKY COOLING SYSTEM SAVES ENERGY IN A COMMERCIAL BUILDING

---

### 4.2.1 Project Description

The night sky cooling system enables downsizing of conventional cooling equipment and reduces annual energy costs by cooling water in a radiative and evaporative fashion. Water is sprayed over a flat or low-slope roof surface at night, filtered and stored, and delivered the following day for cooling. The system is comprised of a roof spray assembly, a thermal storage component, and a microprocessor control unit.

The process is most applicable to arid climates where hot days are followed by cool nights with minimum temperatures below 18°C. The product was tested in a Los Angeles state government office building.

Operationally, system storage water is sprayed over the low-slope, single-ply membrane roof that is divided by a north-south ridge. The spray water, typically chilled to 5° to 10°C below the minimum night air temperature, from the east and west roof sections is collected at roof drains, filtered, and stored in an underground tank north of the building.

This tank water is delivered on a thermostat demand to custom cooling coils added at rooftop HVAC units, serving a large open plan section of the building. The water chilled on the west roof slope is also filtered and then circulated through underfloor plastic tubing to store cooling in the concrete slab floors of rooms located along the west and south walls. This passive radiant cooling from the floors provides first-stage cooling for these areas, with second-stage cooling provided by 12 small rooftop HVAC units. Annual cooling energy consumption was reduced by more than 50 percent.

#### **4.2.2 Technical Data**

The system installed includes a copper and brass roof spray assembly composed of piping, pumps, sand filters, and spray heads, an underground Fiberglas storage tank (56.9 m<sup>3</sup>), plastic underfloor tubing (approximately 2700 m), and four chilled water coils. Typical capacities are 3.4 MJ/m<sup>2</sup> of roof surface in peak conditions. For buildings with peak loads exceeding this amount, the WhiteCap system allows for significant downsizing of conventional cooling equipment.

#### **4.2.3 Energy and Economic Data**

Conventional cooling energy consumption was over 70 percent lower with system operation in September than without the system in July. Adjusting for system pump energy uses and climate changes, net annual cooling energy savings are over 50 percent (over 74.4 GJ saved annually). Simple payback period is less than 2.5 y. The cost of the system totaled \$10,100, with annual savings of \$4,400.

### ***4.3 LOW-ENERGY DESIGN AND RENEWABLE ENERGY AT THE BIGHORN RETAIL CENTER***

---

#### **4.3.1 Building Envelope**

By using whole-building design, an energy-efficient building is created with many interrelated features to improve the quality and efficiency of lighting, heating, and cooling. The envelope or the structure of the building is itself part of the building's lighting, heating, and cooling system. The building has a translucent skylight along the length of the warehouse roof and north- and south-facing clerestory windows along the length of the retail space to provide lighting. The clerestory windows also provide some passive solar heating in the winter and natural ventilation for cooling in the summer.

Insulation is an integral part of the building envelope. Because the building is heated by using radiant heating in the concrete slab floors, completely insulating the bottom of the floor and foundation walls was important to minimize heat loss to the

ground. The roof and walls are also more insulated than conventional commercial buildings.

#### 4.3.2 Lighting

Natural light from the translucent skylight and clerestory, dormers, and other windows, called *daylighting* meets most of the building's lighting needs.

Additional lighting needs in both the retail store and the warehouse are met with compact fluorescent lamp fixtures. The fixtures are made of eight 26-W lamps grouped within a domed glass shade. Motion sensors turn on the lights in the interior offices, employees' break room, and restrooms. In the rest of the building, an energy management computer automatically balances the electric lighting with the daylighting for maximum savings.

Using daylighting and the compact fluorescent fixtures to light the building is expected to reduce energy use for lights by 79 percent compared to conventional retail buildings.

#### 4.3.3 Heating

In the retail space, radiant floor heating provides comfort without heating the air in the space. Tubes in the concrete floor circulate hot water that has been heated by natural gas. In addition, south-facing clerestory windows allow some solar heat into the space in the winter when the sun is low in the sky (passive solar heating). Computer simulations helped design the windows and overhangs to collect the right amount of light and heat. Special glass reduces heat loss from the building while allowing light and heat to enter.

In the open warehouse, two separate systems provide heating. A transpired solar collector heats ventilation air by trapping heat from the sun in a dark perforated metal wall on the south side of the warehouse. This heated air is then distributed to the warehouse with fans and through a fabric duct. Overhead gas-fired radiant heaters meet remaining heating loads.

#### 4.3.4 Cooling

Because of careful building design, no air-conditioning system is needed at the BigHorn Center. The clerestory windows are controlled by computer and open to allow hot air to escape while low window openings allow cool air in. Window overhangs shade the windows and prevent the high summer sun from entering and heating the space.

#### 4.3.5 Photovoltaics

Efficient design eliminated much of the heating and lighting loads experienced by a conventional retail building. A 9.0-kW capacity, integrated photovoltaic system laminated onto the metal roof panels on south-facing roofs of the building is expected to provide an average of 25 percent of the electricity needed to run the building. The photovoltaic system is tied directly to the building's three-phase electrical system. The BigHorn Center is the first retail center in Colorado to have a net metering agreement in which electricity produced over the amount used is sold back to the utility at the same rate that the utility sells electricity for the building.

#### 4.4 AN ALTERNATIVE APPROACH—THE NEXT GENERATION OF COMFORT CONTROL

##### 4.4.1 High-Mass Construction

Insulation outside the thermal mass has the greatest benefit in decreasing operational costs and increasing comfort. Although the times of peak heat gain and loss remain the same as those of the same weight of uninsulated mass, the insulation can greatly reduce the amount of the peak. In addition, the mass on the inside of the insulation maintains a more stable temperature and can be charged and discharged of energy as desired for the season; these conditions can be held without rapid transfer to the exterior. With low-energy methods, the mass can be discharged of heat in the cooling season or charged in the heating season. A minimum of 2-in-thick mass with a maximum of surface area can stabilize the interior environment, whether mechanically or passively conditioned (Fig. 4.3). The heavy mass also has sound

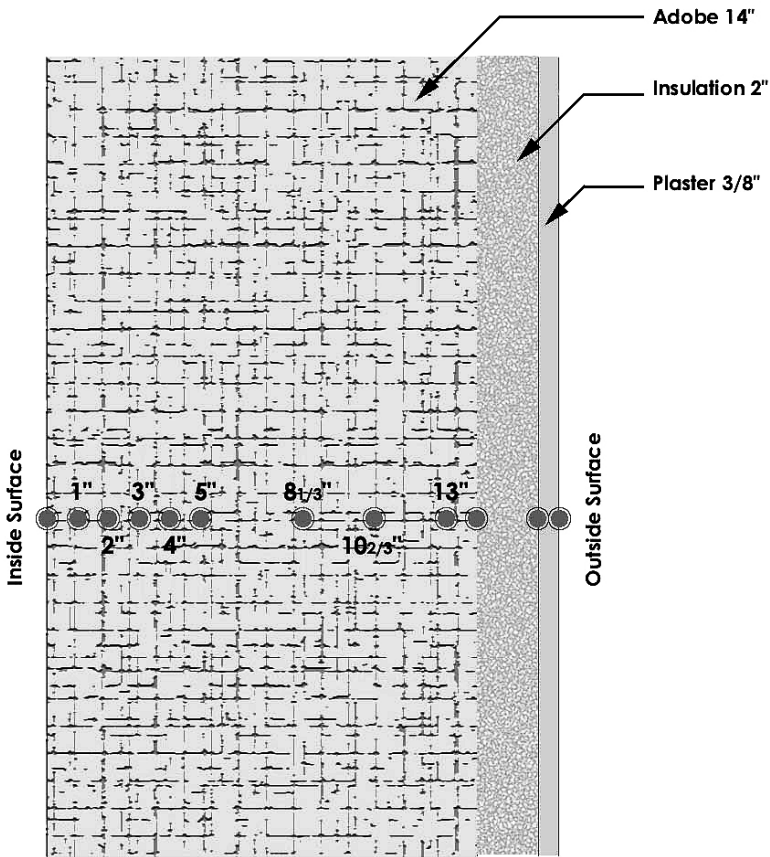


FIGURE 4.3 Typical wall section.

transmission and fire safety advantages. Combined with a hydronic radiant system and proper controls, the heavy thermal mass should provide superior interior comfort conditions.

#### **4.5 HYBRID RADIANT-CONVECTIVE SYSTEMS**

---

The system combines the heat transport mechanism benefits of both the radiant and convective systems. The following benefits (Feustel and Stetiu, 1993) would be brought about by the addition of a radiant cooling and heating system.

1. The system will significantly reduce the amount of air transported through the home. For thermal comfort reasons, low-turbulence air supplies are assuming increased importance. Using the convection system only for air renewal and humidity control reduces fan transportation energy. The cooling is provided mainly by radiation using water as the transport medium. Hydronic cooling systems can remove a given amount of thermal energy using less than 5 percent of the otherwise necessary fan energy.
2. Due to the large surfaces available for the heat exchange in hydronic radiant cooling systems (usually almost the whole ceiling), the coolant temperature is marginally lower than the room air temperature. The small temperature difference allows the use of either heat pumps with high coefficient of performance (COP) values or indirect evaporative cooling to further reduce the electrical power requirements.
3. Because of the hydronic energy transport, the hydronic system has the potential to interact with thermal energy storage devices—both thermal energy storage (TES) equipment and/or the thermal mass in the building's construction. A hydronic system can charge and discharge thermal storage with lower energy means, such as with indirect evaporative cooling equipment in the summer or hot water generated by solar panels in the winter. By providing thermal mass that can be charged and discharged hydronically, the size of the thermal storage equipment, if used, can be reduced.
4. Daytime energy distribution by a fractional horsepower pump can be operated by photovoltaic cells. Fan coil units, if needed for humidity control, could also be operated by photovoltaic cells during the day.
5. Indirect evaporative cooling using a cooling tower can be used longer into the extreme season than can the standard direct evaporative cooler.
6. Since no refrigerant would be brought into the occupied space, ammonia would be a possible refrigerant for the chiller.
7. It can provide higher levels of year-round comfort, more uniform air temperatures, cleaner surfaces, and a more healthful environment.
8. The radiant heating and cooling system has indoor air quality (IAQ) advantages. Many people in the Phoenix area suffer from allergies caused by pollens, mold, fungi, and dust. During the pollinating season, allergy sufferers must stay indoors and keep the windows and doors closed as much as possible. The evaporative cooler is an ideal growth medium for many types of molds and fungi. So, the indirect evaporative cooler has benefits from this perspective. Recirculated (well-filtered) air from an air conditioner is preferred to outdoor air brought in

through ventilation or an evaporative cooling system. But a radiant method of heating and cooling can offer relief to the allergy sufferer. Only a minimum amount of air (makeup required by ASHRAE Standard 62) must be provided (ASHRAE, 1989). Most of the load is satisfied by radiant means.

#### 4.5.1 System Controls

Technological developments in sensors and microprocessors make a higher standard of comfort control possible. Sensors have recently become much more reliable as well as relatively inexpensive. Microprocessors, which also have become inexpensive, allow sophisticated decision making and can use expert system methods for selecting and operating the most appropriate system at its optimum performance.

There are two options for a new generation of control using the combination radiant-convective system. One is using the “comfortstat,” patterned after the work of P. O. Fanger, which takes into account six variables of human comfort. A second method would be to use the operative sensor, which accounts for two comfort variables—ambient temperature and mean radiant temperature.

**4.5.1.1 PMV Control** The most innovative recent work related to the prediction of comfort was done by Fanger (1982). He merged physiological theory and statistical evidence of human response and developed a predictive mathematical model of thermal sensation. The benefit of the mathematical model developed by Fanger is that it includes all six comfort variables (activity level, clo value, ambient air temperature, mean radiant temperature, air velocity, and relative humidity) and produces a single index that can be used to produce comfort conditions. The mathematical model’s dependent variable is a thermal sensation index known as the predicted mean vote (PMV). It predicts how the “average” person would vote using the ASHRAE thermal sensation scale.

Fanger suggested that his mathematical model could be the basis for a device for controlling comfort called a comfortstat. Like a thermostat, the comfort index would maintain conditions within a range of acceptable values. The comfort index used in the comfortstat is the calculated predicted mean vote (PMV). In a regular thermostat, the comfort index used is dry-bulb air temperature. As mentioned previously, it accounts for only one of the six comfort parameters, whereas the PMV accounts for all six comfort parameters.

The thermostat can only effectively control devices that affect the ambient air temperature, whereas the comfortstat can also control additional devices that affect radiant temperature, air motion, and humidity (MacArthur, 1986; Int-Hout, 1986).

**4.5.1.2 Operative Sensor Control** The two primary variables in most sedentary comfort situations are ambient air temperature and the mean radiant temperature. This second variable is absolutely necessary in evaluating comfort when radiant systems are used. The two variables are combined in what is known as operative temperature (ASHRAE, 1992). Achieving a reliable and economical sensor to measure the operative temperature has been elusive. This project plans to field-test an operative sensor. This sensor was recently tested for the New York State Energy Research and Development Authority (Berglund, 1994). Initially, the operative sensor will be the primary sensor and basis of control for the Arizona Residence. Later, the use of PMV control will be explored by using input from the operative sensor.

## 4.5.2 Design of a Radiant-Convective Hybrid Demonstration House

The carefree Arizona house is designed as an appropriate style and construction technology for a desert home that can incorporate environmental radiant control systems.

**4.5.2.1 The Envelope** The single-story slab-on-grade house is approximately 250 m<sup>2</sup>, constructed of 36-cm (14-in) adobe exterior walls. The sloping roofs have no attic space but are insulated between wood joists with R-40 batts. The exterior adobe walls, enclosed in insulation, represent considerable thermal storage.

The exterior wall length is approximately 300 ft, the height averages 8 ft, and the thickness is 1.16 ft. The volume of adobe is 2772 ft<sup>3</sup> and has a mass (at 120 lb/ft<sup>2</sup>) of 285,000 lb. The ceiling (1-in cement plaster) represents another 25,000 lb and the floor (considering an effective 4-in thickness) is another 87,000 lb, thus with a mass totaling 397,000 lb. Each pound of these materials can store approximately 0.20 Btu/lb · °F. Therefore, the thermal capacitance of the exterior adobe walls is (397,000 × 0.20 Btu/lb · °F) = 79,500 Btu/°F. By lowering the mass temperature 1°F, almost 6.5 ton-hours of cooling can be stored. According to the load calculation, during the peak electrical rate period (9 A.M. to 9 P.M.), there is a requirement for 28.6 ton-hours. If, at the start of the peak demand period, the mass temperature were lowered 4.4°F below maximum 78°F, the compressor could be inactive during the peak demand period.

## 4.5.3 Types of Systems Used

For research purposes, the house has both a radiant floor and a radiant ceiling.

- *System sizing:* The peak equipment load for the house is considerably reduced because of the thermal storage capabilities of the adobe. The radiant cooling panels have been sized for climate loads, including outside air load. In addition, the air handler is sized for 50 percent of the climate loads. It is responsible for covering peaks and humidifying. Air distribution is sized for full load in case a future homeowner desires a standard convection system. Inside design temperature is 24°C (75°F). The peak chiller load is 3.8 tons, and the total number of ton-hours for the design day is 52. Because of the thermal storage, a three-ton reciprocating chiller was selected. If the unit is shut down for a length of time, the homeowner will be aware that the pull-down time of the massive home will be considerable.
- *The radiant floor:* The slab-on-grade floor contains tubing with a 10-mm ( $\frac{3}{8}$ -in) diameter at a spacing of 23 cm (9 in). This is a decrease in spacing of the 12 in (31 cm) required for winter heating design. As one aspect, the project will investigate whether floor cooling alone can provide satisfactory comfort.
- *The radiant ceiling:* For a predominantly cooling climate, theory predicts that a cool ceiling would provide better room convection patterns in the summer season, whereas radiant floors would be best for the heating season. Most of the ceiling area of the home is radiant panel, sized for the cooling load of approximately 60 W/m<sup>2</sup>.

To prevent condensation problems, a continuous vapor barrier is installed below the wood roof joists to prevent moisture from reaching a surface below the dew point, then 1 in of Styrofoam insulation board, a galvanized metal lathe fastened to the joist with cadmium screws, and 1 in of sand plaster. At a depth of 6 mm in from the surface of the plaster is a capillary tube mat. The tubes are plastic with a 2-mm

diameter spaced at 12 mm. A 16-mm supply header and another 16-mm return header connect them (Fig. 4.4).

- *Hydronic plants:* Chiller options include electrically driven or gas-driven compressor, or a gas absorption unit. The load calculation indicates a peak chiller load of 3.8 tons at 9 P.M., but, because of the thermal storage capacity of the envelope, the capacity of the chiller is reduced to a little more than 3 tons. The 52 ton-hours required during a design day can be generated during off-peak hours. The 3-ton chiller would not be sufficient for peak requirements if only a convective system were used. With an electric chiller, either air or water cooling is an option.
- *Ventilation-heat exchanger:* An energy recovery ventilator will provide replacement ventilation to/through the fan-coil unit. Sizing is for 0.35 air changes per hour (ACH) ( $0.06 \text{ cfm/ft}^2$ ). Because of the heat recovery capabilities, the outdoor air load on the system was assumed at 0.175 ACH ( $0.03 \text{ cfm/ft}^2$ ). Exhaust air is taken from the two bathrooms, the laundry room, and the kitchen. The unit will normally be operated when the house is occupied. The humidity sensor can also activate it
- *Convection system dehumidification:* One fan coil unit supplies air to the entire house. It is sized for 50 percent of the climate load and operated in peak conditions and when dew-point control is needed. Supply ducts are sized for an air supply that could provide the entire cooling requirement by convection with velocities around 500 fpm. Ducts will be inside the insulated building envelope. Humidity control is an essential requirement of the control system. Condensation on radiant panels or on supply piping is unacceptable. A high-quality dew point sensor will activate dehumidification achieved by means of a fan coil using chilled water.
- *Ceiling fans:* Multiple-speed ceiling fans over seating beds will add to comfort choices and extend the capacities of conditioning equipment by providing comfort at higher air and radiant panel temperatures.

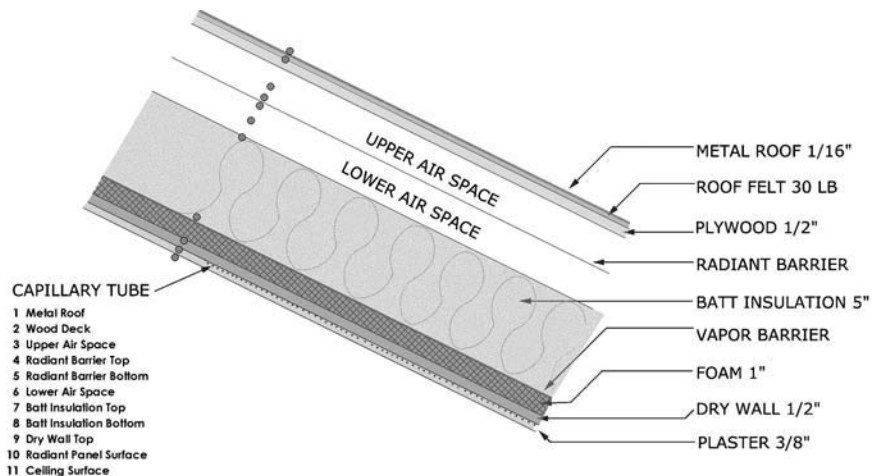


**FIGURE 4.4** Typical roof section.

- *Zoning:* Zoning is arranged to reduce energy consumption in unoccupied areas. There are three for the radiant floor system and the radiant ceiling system. Only one convective system is provided for the entire house. Its primary function is to provide humidity control. It is supplied by a separately piped and pumped hydronic circuit (Fig. 4.5).
- *Operative sensors:* Newly developed operative sensors will be field-tested. One to two sensors will be used in each zone.
- *Control program:* A programmable controller will allow the incorporation of the operative sensors and control of the out-of-the-ordinary plant equipment, including the chiller, a cooling tower, a plate-and-frame heat exchanger, and a ventilator-heat exchanger. The underlying strategy in the development of the control program is to provide comfort conditions in the occupied space within a range that is acceptable to the occupants at the lowest energy cost. If operative temperature is not within the comfort envelope, the logic program determines which sub-system can most efficiently restore comfort.
- *Zone master controllers:* Zone controllers provide information to the master controller, which maintains historic information and operates the various appliances, such as the chiller, the indirect evaporative cooler (cooling tower/plate heat exchanger), the ventilator, and the boiler. A zone controller would operate devices specific to the zone (e.g., ventilator, a ceiling fan, or hydronic valves). The zone controller also incorporates an occupancy sensor so that conditioning will only be provided to the zone when needed. The zone controller will also require the capability to receive input manually from the occupant (Fig. 4.6).

#### 4.5.4 Design Calculations

- *Load calculations:* The heating and cooling loads were simulated on a commercial load program with the results shown in Table 4.1.
- *Radiant ceiling:* The analysis and calculation of the thermal capacity of the radiant ceiling cooling for the master bedroom area was developed from the manufacturer's literature and originated from a test conducted at a German university in 1988 to 1989.
- *Radiant floor:* In floor cooling, the thermal comfort of a human foot with a shoe requires that the minimum floor surface temperature should not be below 18°C (ASHRAE, 1992). Following the design nomograph (Kilkis, ASHRAE, 1997) for panel heating and cooling, the maximum sensible cooling effect that can be obtained at an 18°C floor temperature and a 25°C indoor air temperature and  $AUST - t_a = +1^\circ\text{C}$  is around 65 W/m<sup>2</sup>. The concrete floor panel with the absence of any cover has about 0.11 m<sup>2</sup> · K/W characteristic panel thermal resistance ( $r$ ). Corresponding to this thermal resistance, the required mean water temperature is  $(t_a - 14^\circ\text{C}) = 12^\circ\text{C}$ . In floor heating, the maximum heat flux required also is around 60 W/m<sup>2</sup>. The den has the highest heat loss. In this case, the mean water temperature required in winter will be  $AUST = 13^\circ\text{C}$ .  $AUST$  is assumed to be 18°C in winter. Thus, the mean water temperature is about 31°C. At design conditions, the floor surface temperature will be about 24°C (assuming  $t_a = 20^\circ\text{C}$ ). When both the floor and the ceiling panels are used for cooling, the ceiling panel temperature will be the lead system. At full load, the ceiling requires an entering water temperature of 18°C. If this same entering water temperature is used for the floor, the

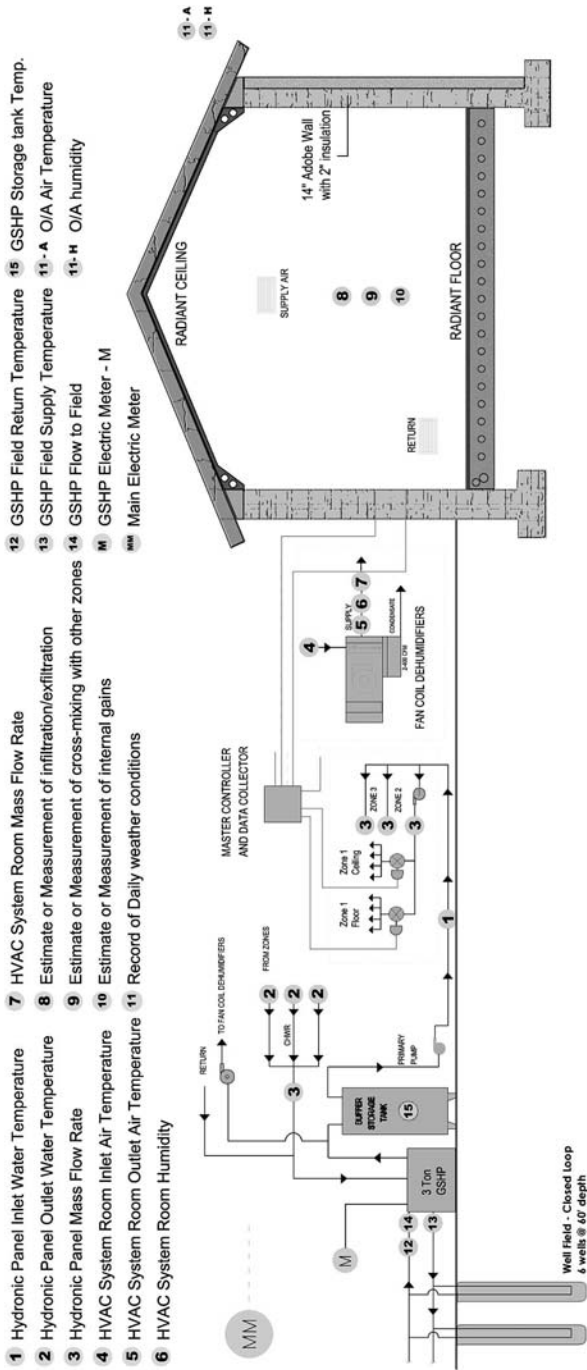


FIGURE 4.5 Radiant diagram.

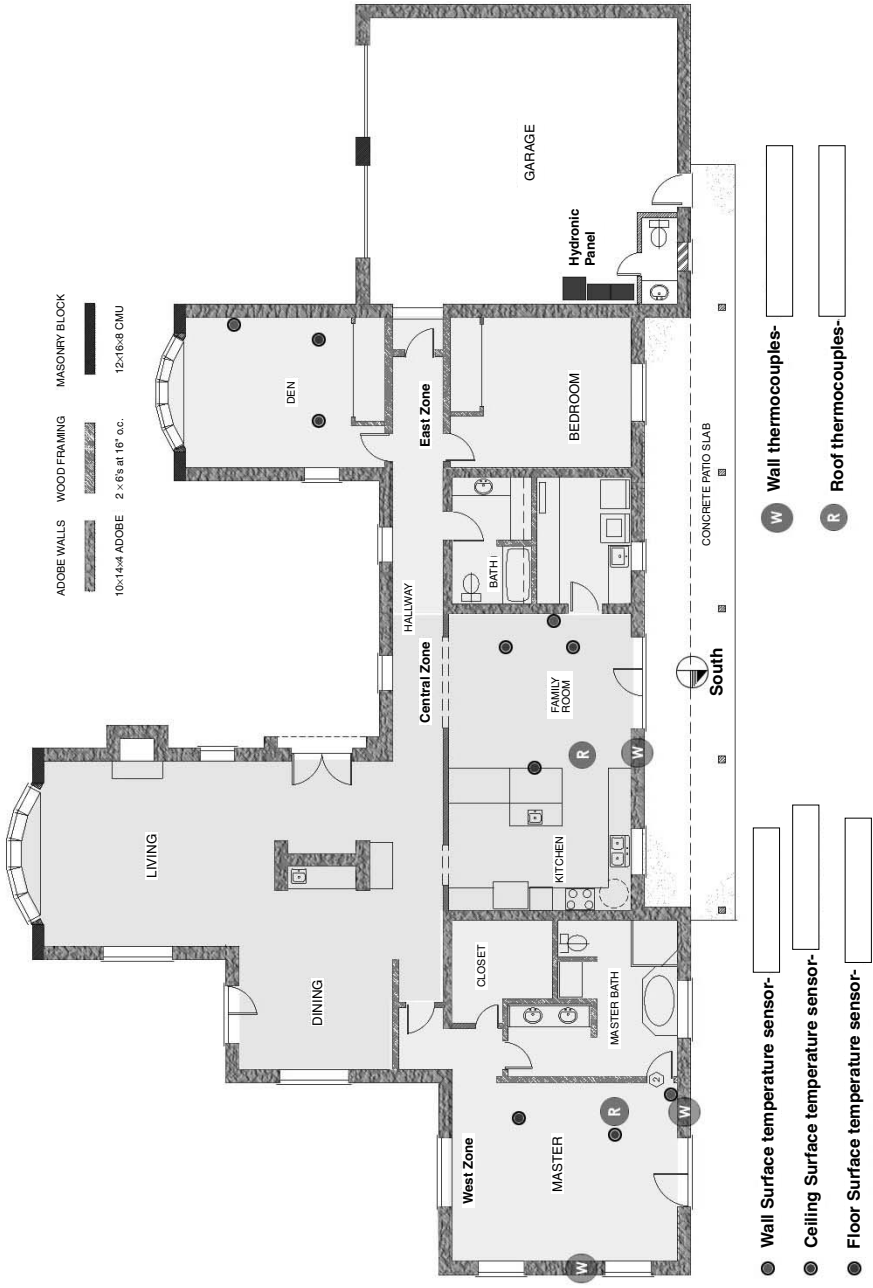


FIGURE 4.6 Building diagram.

cooling capacity of the floor panel will be  $27 \text{ W/m}^2$ . When the floor panel is operated at an entering water temperature of  $18^\circ\text{C}$ , the nomograph shows that the floor surface will be  $23^\circ\text{C}$ .

#### 4.5.5 Knowledge to Be Gained Through the Data Set Collection

1. Can a hybrid radiant-convective system provide superior comfort and at a lower cost than a conventional convective system?
2. Can a hybrid radiant-convective cooling system be operated in the extremes of the Arizona climate without moisture condensation problems?
3. Can operative sensors be used with a programmable control system to provide superior comfort?
4. For what percentage of the cooling season can noncompressive (indirect evaporative) cooling be used to achieve acceptable comfort?
5. What thickness of thermal mass is optimum for storing energy in the hot, arid region?
6. What percentage of the cooling load can be shifted to off-peak hours?

#### 4.5.6 Hybrid Heating Project Conclusions

The projects included in detail in Chapter 4 are indicative of the breadth of hybrid HVAC knowledge and interest manifest in engineering design in significant building projects. Interestingly, the projects also represent diverse sponsorship: university, engineering firm, federal government agency, and radiant manufacturer. The authors believe that broad interest is evolving because the hybrid concept is so compelling—buildings must serve their intended purpose.

The reader has no doubt observed that the analytical demands are really only unique in their breadth from standard heat loss only approaches to HVAC system design. The fundamentals are universal and will be further tied together in the next and final handbook section on radiant heater and cooler sizing.

S · E · C · T · I · O · N · 8

**ENGINEERING DESIGN  
TOOLS TO ASSIST IN  
HEATER-COOLER  
SIZING**



---

# CHAPTER 1

---

## INTRODUCTION TO COMPUTER-AIDED THERMAL COMFORT DESIGN TOOLS

---

Almost since the advent of computerized applications, researchers have worked to computerize the methodologies that are necessary to do the following:

- Calculate the heating-cooling load for a building
- Calculate thermal comfort parameters for a given heating, ventilating, and air-conditioning (HVAC) installation
- Optimize thermal comfort relative to energy consumption

These programs have progressed to the point where they are classified as one of the following:

- Whole-building simulations
- Localized thermal comfort simulations
- Auxiliary applications

Whole-building simulations help the user to select the equipment needed and to necessarily incorporate the efficiencies of the heat generation equipment and heating or cooling distribution design. Localized thermal comfort simulations determine the amount and design of heating or cooling required to meet the specification for the room or area, but they do not incorporate energy conversion or transmission factors. Auxiliary applications are specialized programs that enhance the capability of the master program for particular building components or performance features.

### 1.1 WHOLE-BUILDING SIMULATIONS

---

The most comprehensive and well-known whole-building applications are the BLAST™ and DOE/DOE-2™ building models. These complex programs reportedly have had fewer than 500 users in the United States, mainly government laboratories and departments, corporations, and large engineering design firms. These computer simulations treat each room in a building as a cell that is at a uniform temperature. Energy transfer is calculated throughout the building in response to weather conditions, heating and cooling system activation, and other triggers. The most recent version is the merged simulation—EnergyPlus™—which includes the best features of BLAST and DOE-2. At the time of this writing, EnergyPlus is in the beta stage, so the complete features of EnergyPlus are not well known or fully developed, but the program remains complex and is a whole-building simulation program that requires a considerable time investment to learn.

## 1.2 LOCALIZED THERMAL COMFORT SIMULATIONS

At the other end of the spectrum, localized thermal comfort simulations determine the conditions in one or more rooms and sometimes provide a variety of what-if comparisons from a range of preprogrammed energy efficiency options. The most recent example of localized thermal comfort analysis is the Building Comfort Analysis Program (BCAP), which was developed through ASHRAE Research Projects 657 and 907. Figure 1.1 illustrates the procedure as a flow diagram (Jones and Chapman, 1994). Rather than a particular program, BCAP is a methodology that incorporates localized radiation heat transfer, convection heat transfer, and other room conditions to determine localized thermal comfort throughout the occupied space. The first task shown in Fig. 1.1 is to describe the input parameters that ultimately prescribe the environmental conditions that surround the room. These include the following: the room geometry, heater size and location, heater characteristics, and room thermal properties like wall  $R$  values. The next step is to calculate the radiation intensity field within the occupied space. In the BCAP methodology, the radiant intensity field is determined with the discrete-ordinates model, which directly solves the most fundamental radiant transfer equation (RTE). Once the radiant intensity field is calculated, surface radiative heat fluxes are determined from the radiant intensity field. These radiant fluxes, coupled with heat conduction through the walls and convection heat transfer to the surfaces, fully prescribe the surface temperatures and the air temperature within the occupied space. Because the radiation calculations depend on the surface temperatures, the next task is to recalculate the radiation field as illustrated by the converged diamond-shaped box in Fig. 1.1. This iterative process continues until the energy entering and leaving the room comes

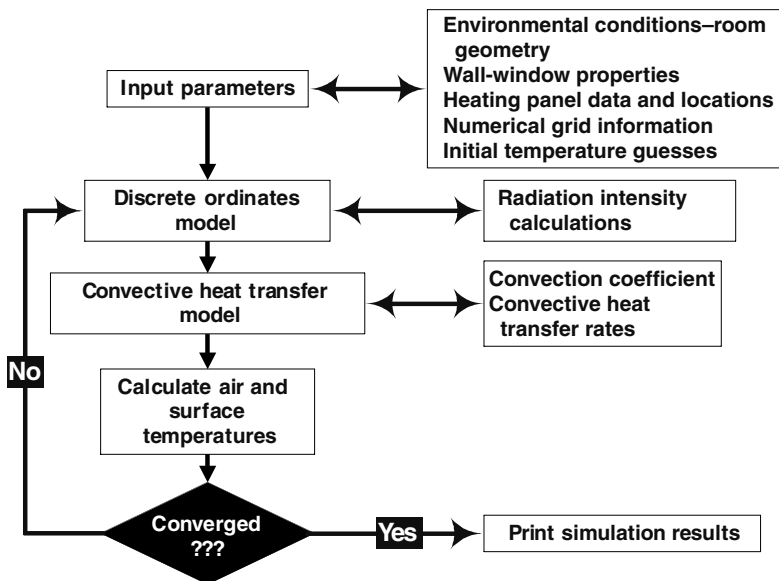
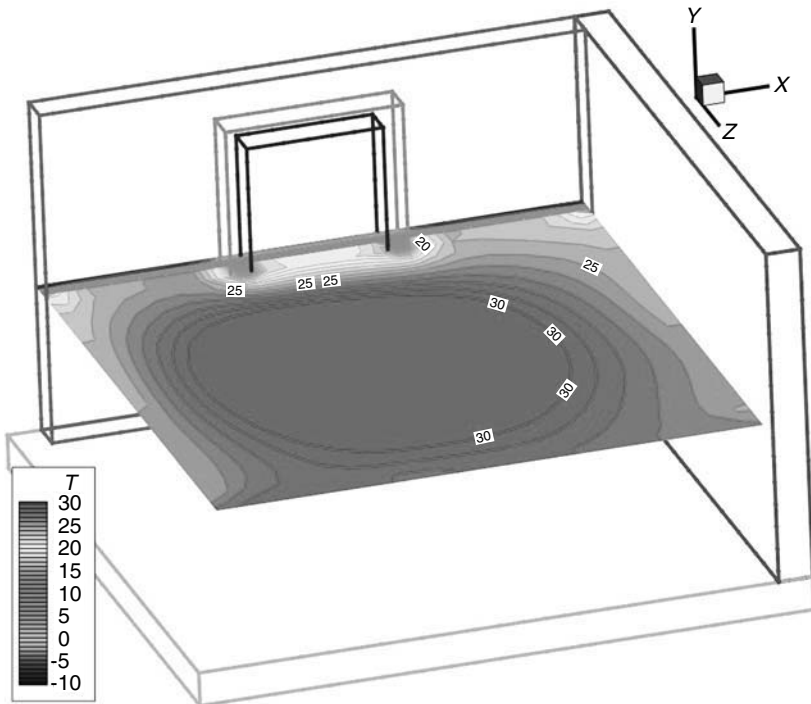


FIGURE 1.1 The BCAP flow chart.

into balance. At this point, the localized  $T_{mrt}$  and  $T_{op}$  are calculated. This procedure is described in detail in Chap. 3 of this section.

Using this procedure provides substantial information that is not available in whole-building simulations. For example, the whole-building simulations assume the dry-bulb air temperature and the wall surface temperatures within a room are uniform, which is not likely to be the real-world condition. An objective of a localized thermal comfort program using the BCAP methodology is to deal with the heat transfer conditions of the room through comprehensive design analysis. The analysis requires that we incorporate the details of the room, such as dimensions, insulation, orientation, glazings, air changes, and so forth, to provide additional information such as the  $T_{mrt}$  and  $T_{op}$  localized conditions throughout the room. Figure 1.2 shows an example of these localized conditions within the room. These results were produced using a computerized adaptation of the BCAP methodology. The particular output in Fig. 1.2 illustrates the thermal comfort signature (TCS™) that is created from the combination of the room structure and the radiant panel heater. In this figure, the room is characterized by cold outside conditions and a window system on the back wall of the room. The window frame chosen was aluminum to show the impact of the window and the frame on the  $T_{mrt}$ . The impact of the frame is seen by moving from the left to right across the room near the back wall. On the far left, the  $T_{mrt}$  is relatively high. As an occupant moves to the right along the back wall, the  $T_{mrt}$  becomes substantially lower in areas adjacent to the frame. Moving further to the right, the  $T_{mrt}$  increases slightly in front of the window, and then again decreases near the right side



**FIGURE 1.2** Example of the localized thermal comfort as determined by the TCS.

## 8.6 ENGINEERING DESIGN TOOLS TO ASSIST IN HEATER-COOLER SIZING

of the frame. A similar relationship occurs when there is not a thermal break to the exterior surrounding the perimeter of a radiant panel, such as a slab-on-grade.

This example clearly shows the importance of assessing the impact of room characteristics (e.g., dimensions, insulation, orientation, glazing, air change, etc.) on thermal comfort parameters. The BCAP methodology allows for details to be evaluated to determine optimal placement and sizing of all radiant heat panels, regardless of energy source. Other localized thermal comfort simulations do not offer this flexibility.

Programs that design in-space occupant thermal comfort systems also generate equipment sizing information based on the energy requirements for that space. In the case of electric in-space heating products (e.g., baseboard, portable, ceiling and wall panels, and concealed floor or ceiling cable or mats), the recommended equipment size may only meet the thermal comfort specification for that space. If a system, however, must also heat or cool outside of the space being designed, then further provisions must be made to account for heating and cooling generation and distribution efficiencies. The reader is referred to ASHRAE Standard 152, *Method of Test for Determining the Design and Seasonal Efficiencies of Residential Thermal Distribution Systems*.

In Chap. 3 of this section, several examples illustrate the importance of positioning and sizing radiant panel heating and cooling systems to achieve the lowest energy consumption and the highest level of thermal comfort. In these simulations, it is important to think of thermal comfort as a field property. A field property is one that varies with position in the room. Referring again to Fig. 1.2, the horizontal plane illustrates the characteristic of field with the localized mean radiant temperature (MRT) at a distance of 3 ft from the floor. The heater in this figure is positioned at the ceiling in the center of the room. As one can see, the  $T_{mrt}$  varies from a high under the heater to a low at some position from the walls. Also of interest from this field visualization is that  $T_{mrt}$  decreases near the window, especially in the vicinity of the window frame. The other interesting fact from this figure is that the  $T_{mrt}$  varies substantially with position in the room, just as it does in rooms with convection heating. A person standing directly under the heater would feel warmer than a person standing near a wall. Consequently, it is not appropriate to say that the level of thermal comfort in a room is a certain value, but, rather, that the thermal comfort in a room varies between the range of high and low  $T_{mrt}$  readings. The objective of using the BCAP methodology for design is to develop a solution that meets the occupant thermal comfort specification for the room being designed. One last observation from this example is that in-space heating and cooling systems can be used to impact thermal comfort in critical areas of the room. For example, if the design requirement is that the  $T_{mrt}$  reach a certain point in one portion of the room, but is not important in other parts of the room, then the designer can use a localized program based on the BCAP methodology to design for precisely those conditions. Without the use of a localized design tool, one would have to resort to a building envelope program and, by doing so, would lose the ability to design for localized thermal comfort conditions.

A second method that can be used to determine local thermal comfort is *computational fluid dynamics* (CFD). Although CFD provides extreme localized details, these simulations fall outside the realm of engineering tools. To be classified as an engineering tool, a simulation must be able to complete the calculations in a reasonably short time period. The question now is, What is a reasonably short period of time? Our opinion is that a reasonably short period of time is defined as starting a program on a modern desktop computer and then having that simulation complete within the time it takes to get a cup of coffee. Though this definition is not directly

quantifiable with a stopwatch, it is a definition to which most people can relate, and it is one that has not become dated as computational power increases.

By their very nature, CFD programs strive to identify detail at a very microscale level. In this sense, a CFD program is actually an experimental procedure to investigate features (e.g., turbulence, extremely localized temperature, etc.). To accomplish this level of detail requires at least one high-powered computer. Preferably, a CFD researcher will enlist the power of several high-powered workstations that work in parallel to solve a problem. Even with these high-powered computer systems, a solution will not be obtained for several days or weeks. Consequently, CFD simulations are not typically used as engineering design tools. Instead, CFD programs provide an excellent resource that can be used to develop or enhance engineering programs. Because of the substantial resources necessary to use a CFD program, this classification of programs is not discussed in this section.

### 1.3 AUXILIARY DATABASE PROGRAMS

---

Another category of computer programs is the auxiliary database programs that provide access to extensive databases. These databases have been developed over several years and represent a development cost of several hundred thousand, if not millions, of dollars. The most comprehensive and well-known auxiliary database program is Window 4.1™ from Lawrence-Berkeley Laboratories. This program contains an extensive database of almost every kind of window glass used in the built environment and was developed over a period of many years with ongoing government funding. The utility of the program is that it can generate inputs for use in the simulation programs. Essentially, a user enters a window description and then runs Window 4.1. The program then writes the output to a data file. Table 1.1 shows an example output for a window that has two glazings separated by an air gap. This example output illustrates the wealth of information that has been developed over the past several years such as the thermal conductivity and radiation properties of window systems. This information can be incorporated into other programs that use the BCAP methodology. The impact of up-to-date features of common window treatments on thermal comfort can be determined. Additional thermal comfort-based auxiliary programs for other building categories, such as floor, wall, and ceiling constructions, would offer similar benefits.

The other important category of databases is that of weather data, which can then be used to provide the information required for design temperature, as well as solar, wind, and other climate impact. The information developed by the U.S. Weather Service and other organizations, such as the National Renewable Energy Laboratory, are available in several formats. The *ASHRAE Handbook of Fundamentals* also contains weather data for HVAC calculations, and is being prepared in an interactive electronic format.

The vast majority of buildings that have contractor-designed HVAC systems rely upon rules of thumb, experience, the Associated Conditioning Contractors of America manuals, including *J* and upgrades, and manufacturer manuals or computer programs. Even though the word *comfort* guides system design and explains system performance, in practice design continues to be defined in terms of dry-bulb temperature performance, frequently from a central control thermostat. ASHRAE Standard 55 is seldom referenced. Manufacturer computer programs normally are used to size and design the particular equipment and materials involved for an entire building. These programs are based upon ASHRAE methodologies, product perfor-

8.8 ENGINEERING DESIGN TOOLS TO ASSIST IN HEATER-COOLER SIZING

TABLE 1.1 Example Output from Window 4.1™

WINDOW 4.1 DOE-2 Data File: Multiband Calculation													
Unit system	: SI												
Name	: DOE-2 WINDOW LIB												
Desc	: Sample												
Window ID	: 1												
Tilt	: 90.0												
Glazings	: 2												
Frame	: 0 None 0.000												
Spacer	: 0 0.000 0.000 0.000												
Total height	: 1219.2 mm												
Total width	: 914.4 mm												
Glass height	: 1219.2 mm												
Glass width	: 914.4 mm												
Mullion	: None												
Gap	Thick	Cond	dCond	Vis	dVis	Dens	dDens	Pr	dPr				
1 Air	12.7	0.02410	7.600	1.730	10.000	1.290	-0.0044	0.720	0.00180				
2	0	0	0	0	0	0	0	0	0				
3	0	0	0	0	0	0	0	0	0				
4	0	0	0	0	0	0	0	0	0				
5	0	0	0	0	0	0	0	0	0				
Angle	0	10	20	30	40	50	60	70	80	90	Hemis		
Tsol	0.703	0.702	0.700	0.693	0.679	0.647	0.579	0.441	0.211	0.000	0.603		
Abs1	0.101	0.102	0.103	0.106	0.110	0.115	0.122	0.130	0.133	0.012	0.113		
Abs2	0.067	0.067	0.068	0.070	0.072	0.073	0.072	0.065	0.047	0.000	0.068		
Abs3	0	0	0	0	0	0	0	0	0	0	0		
Abs4	0	0	0	0	0	0	0	0	0	0	0		
Abs5	0	0	0	0	0	0	0	0	0	0	0		
Abs6	0	0	0	0	0	0	0	0	0	0	0		
Rfsol	0.129	0.129	0.129	0.131	0.140	0.165	0.227	0.365	0.610	0.987	0.206		
Rbsol	0.129	0.129	0.129	0.131	0.140	0.165	0.227	0.365	0.610	0.987	0.206		
Tvis	0.814	0.814	0.812	0.808	0.796	0.765	0.692	0.536	0.272	0.000	0.711		
Rfvis	0.150	0.150	0.150	0.153	0.164	0.192	0.264	0.418	0.682	1.000	0.238		
Rbvis	0.150	0.150	0.150	0.153	0.164	0.192	0.264	0.418	0.682	1.000	0.238		
SHGC	0.757	0.757	0.755	0.750	0.737	0.707	0.639	0.498	0.257	0.002	0.659		
SC: 0.88													
Layer ID#	102		102	0	0	0	0						
Tir	0.000		0.000	0	0	0	0						
Emis F	0.840		0.840	0	0	0	0						
Emis B	0.840		0.840	0	0	0	0						
Thickness (mm)	3.0		3.0	0	0	0	0						
Cond [W/(m <sup>2</sup> · °C)]	295.3		295.3	0	0	0	0						
Spectral File	CLEAR_3.DAT					CLEAR_3.DAT	None	None	None	None			
Overall and center of glass I <sub>g</sub> U values [W/(m <sup>2</sup> · °C)]													
Outdoor temperature				-17.8°C				15.6°C		26.7°C		37.8°C	
Solar (W/m <sup>2</sup> )	Wd <sub>spd</sub> (m/s)	hc <sub>out</sub>	hr <sub>out</sub>	h <sub>in</sub>									
		[W/(m <sup>2</sup> · °C)]											
0	0.00	12.25	3.30	7.89	2.58	2.58	2.66	2.66	2.73	2.73	2.96	2.96	
0	6.71	25.47	3.24	7.93	2.79	2.79	2.86	2.86	2.94	2.94	3.20	3.20	
783	0.00	12.25	3.40	7.57	2.61	2.61	2.80	2.80	2.96	2.96	3.10	3.10	
783	6.71	25.47	3.30	7.70	2.82	2.82	2.96	2.96	3.17	3.17	3.33	3.33	

mance ratings, field experience, and equipment availability in terms of watts or Btu output. As of this printing, the authors are unaware that any of these programs provide  $T_{op}$  information or output.

#### **1.4 THE REST OF SECTION 8**

---

The remainder of this section, which is separated into three more chapters, demonstrates the variety of calculations that can be completed with the BCAP methodology, based upon steady-state and transient conditions. Because the BCAP methodology describes very complex calculations that were previously unavailable to the design community, users can, for the first time, obtain thermal comfort details within a room.

Chapter 2 in this section provides a design methodology that has been developed over the last 10 years. This design process leads the designer through the selection, placement, and analysis of in-space heating and cooling systems. Chapter 3 then applies this process to several cases. The cases, selected to cover a wide range of situations, lead the user through the setup, calculations, and analysis process. Some of the examples compare the design factor differences between various types of radiant heating and cooling panels. Chapter 4 ties all of the information together in this section to provide a comprehensive understanding of designing for thermal comfort. The reader will gain a thorough understanding of the value of developing in-space occupant thermal comfort design information before drawing conclusions about HVAC system energy and comfort performance.



---

## CHAPTER 2

---

# THE DESIGN PROCESS FOR LOCALIZED THERMAL COMFORT

---

This chapter presents a design process for a design engineer to choose, position, and analyze a room's heating or cooling system. This process illustrates the importance of thermal comfort analysis in a room through a careful consideration of all of the design factors for the specific situation. First, it is instructive to work through the basis of how to design an in-space heating or cooling system for occupant thermal comfort.

### 2.1 HOW IS THERMAL COMFORT CONNECTED TO THE ROOM STRUCTURE?

---

This portion of the chapter conceptually explains how the room structure connects to the localized mean radiant temperature ( $T_{\text{mrt}}$ ) and to the localized operative temperature ( $T_{\text{op}}$ ). For the purpose of this section, room structure is defined to include any component that affects occupant thermal comfort. For example, windows and walls are included in the room structure, as are the heating and cooling systems.

The localized  $T_{\text{mrt}}$  and  $T_{\text{op}}$  are functions of the localized room air temperature and the localized radiant intensity field. The radiant intensity field is, in turn, a function of the surface temperatures within the room and the geometry of the room. Consequently, components of the room structure that need to be included are those that affect the surface temperatures within the room.

To gain a complete understanding of the necessary components that determine the impact of room structure on occupant thermal comfort, the following three topics are discussed:

1. Calculation of  $T_{\text{mrt}}$  and  $T_{\text{op}}$
2. Calculation of the localized intensity field,  $I_{\lambda}(\mathbf{r})$
3. Development of the window structure that is necessary to accurately determine the localized intensity field,  $I_{\lambda}(\mathbf{r})$ .

#### 2.1.1 What Is Ultimately Desired—Thermal Comfort Parameters As Impacted by Room Structure

ASHRAE Standard 55 defines thermal comfort as “the condition of mind that expresses satisfaction with the thermal environment.” This definition loosely translates to the question, Does the occupant feel too hot, too cold, or just right? The simplest way is to ask all of the occupants if they are satisfied with their thermal environment. This method, however, may result in numerous thermostat adjustments or, as a worst case, reinstallation of the entire heating or cooling system.

Rather than responding to occupants' perceptions of their thermal comfort, the ultimate goal is to *predict* the thermal comfort in a room without resorting to a polling system.

The six primary variables that determine thermal comfort are: (1) activity level, (2) clothing insulation value, (3) air velocity, (4) humidity, (5) air temperature, and (6) mean radiant temperature ( $T_{mrt}$ ) (Fanger, 1967). For most design situations, the room usage dictates the activity level and clothing insulation value. For example, an office situation implies sedentary activity with business attire. In contrast, an exercise room implies a high activity level with shorts and a T-shirt. The humidity depends on the heating or cooling system for the entire building and may not be controlled at the room level. Usually, the air velocity is maintained at a level that avoids a draft yet provides the necessary fresh air for the occupants.

In an individual room, the dry-bulb air temperature and  $T_{mrt}$  are two variables that the design engineer may control on an individual room level. The dry-bulb air temperature measures the temperature of the air in the room, and the  $T_{mrt}$  measures the radiant energy exchange between the room surfaces and the occupant. In most design situations, only the air temperature is used, whereas the  $T_{mrt}$  is ignored. Consequently, the primary goal of the design process is to incorporate the effect of room structure on the localized  $T_{mrt}$  in the enclosed space.

Of the several ways to calculate  $T_{mrt}$ , only two are discussed. The first method is presented in the *ASHRAE Fundamentals Handbook* (1997) and uses wall temperatures and view factors to calculate  $T_{mrt}$ . The second method, developed during ASHRAE Research Project RP-907 (Chapman and DeGreef, 1997), directly employs the local radiant intensity field.

**ASHRAE Standard Method to Calculate  $T_{mrt}$ .** The classical method to calculate  $T_{mrt}$  uses the values of the surrounding surface (i.e., wall, window, sofa) temperatures (ASHRAE, 1997). Each temperature is weighted according to its position relative to the person. The equation assumes the surface materials have a high-enough emittance,  $\epsilon$ , to be considered radiatively black or ideal. This assumption is reasonably valid for most rooms, but its effect should be considered when analyzing the results. If the surfaces of the analyzed enclosure do not have a high emittance, then the results are not reliable. This assumption imposes a critical limitation on this method of calculating the  $T_{mrt}$ .

In addition, this method does not take into account low-E glass or other types of advanced glazing systems. The published emissivity of low-E glass is less than 0.1 in the infrared wavelength range (Carmody et al., 1996). Because the glass is opaque in that range, the rest of the radiant energy is reflected back into the room. The classical  $T_{mrt}$  method does not have the capability to handle this situation. The ASHRAE method also fails to consider short-wavelength solar radiation shining through a window, fails to consider any window transmission, and only considers the wall surface temperatures as boundary conditions.

Each of the surfaces is considered to be isothermal or has a uniform temperature,  $T_N$ . If this assumption is not valid for a single large surface, then the surface is subdivided until the assumption is valid. The view factors,  $F_{P \rightarrow N}$ , between the point  $P$  to be analyzed and all the surfaces  $N$  are calculated by some method. The  $T_{mrt}$  is then calculated as (ASHRAE, 1997)

$$\bar{T}_{mrt}^4 = T_1^4 F_{P \rightarrow 1} + T_2^4 F_{P \rightarrow 2} + \dots + T_N^4 F_{P \rightarrow N} \quad (2.1)$$

The temperatures for the calculation are in Kelvins, and the view factors are dimensionless. For rectangular surfaces, ASHRAE (1997) and Fanger (1967) provide view factor charts for the human body. View factors for standard geometric shapes can be

found in a standard heat transfer text, such as Incropera and DeWitt (1990) or Siegel and Howell (1981).

**Radiant Intensity Method.** The second method, and the one used in this text, takes advantage of the fundamental  $T_{\text{mrt}}$  definition to calculate  $T_{\text{mrt}}$  in terms of the radiant intensity balance at a particular point in the room. This fundamental definition states that the  $T_{\text{mrt}}$  is “the uniform surface temperature of an imaginary black enclosure in which the radiation from the occupant equals the radiant heat transfer in the actual non-uniform enclosure” (Fanger, 1967). In a room where all of the surfaces and the air are at the same temperature, the  $T_{\text{mrt}}$  and the air temperature are equal. As the difference between the surface temperatures and the air temperature increases, the difference between the  $T_{\text{mrt}}$  and the air temperature increases.

The radiant intensity approach determines the radiant intensity field within a room and then uses that intensity field to calculate the actual radiant heat transfer from the occupant. The two primary advantages of this method are that: (1) determination of the view factors is unnecessary; and (2) the intensity field includes the effect of wall surface properties and any other intensity boundary condition, such as solar insolation.

The basic formulation begins with writing the definition of the  $T_{\text{mrt}}$  in terms of mathematical quantities instead of words. Doing so results in

$$\dot{Q}_{p,b}(T_{\text{mrt}}) = \dot{Q}_{p,\text{act}} \quad (2.2)$$

In this equation, the term  $\dot{Q}_{p,b}$  represents the radiant heat transfer from the occupant in a room with radiatively black walls and a uniform surface temperature. According to this definition, this term is determined by

$$\dot{Q}_{p,b} = A_{\text{eff}} \sigma T_{\text{mrt}}^4 \quad (2.3)$$

The effective area is determined by (ASHRAE, 1996)

$$A_{\text{eff}} = f_{\text{eff}} A_D \quad (2.4)$$

The effective radiation area of a person,  $f_{\text{eff}}$ , equals 0.73 for a standing person (ASHRAE, 1996) and the DuBois area,  $A_D$ , is estimated from a person’s height and mass. For an average person,  $A_D$  equals  $1.821 \text{ m}^2$  (ASHRAE, 1996).

The term on the right side of the equation represents the actual radiation heat transfer experienced by an occupant. This term is directly related to the intensity field by Siegel and Howell, 1981

$$\dot{Q}_{p,\text{act}} = \int I_\lambda(\Omega) A_p(\Omega) d\Omega \quad (2.5)$$

This equation is a continuous summation (i.e., an integral) over all the directions represented by the solid angle  $\Omega$  (Siegel and Howell, 1981; Modest, 1993). The intensity and projected area in the direction  $\Omega$  are represented by  $I_\lambda(\Omega)$  and  $A_p(\Omega)$ , respectively.

Figure 2.1 shows a sample two-dimensional intensity distribution for a

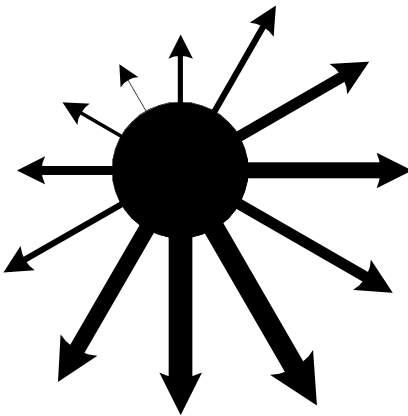


**FIGURE 2.1** Sample two-dimensional intensity distribution at a point in the enclosed space.

point. At this point in the development, some method must be employed to determine the intensity field. The development is discussed in the next subsection.

The net radiation at a particular point in the room as represented by the intensity around in Fig. 2.1 is calculated using an approximation of the continuous form around the point. [See Eq. (2.5).] This approximation was first employed in the early 1960s as a technique to determine neutron transport. Since then, the approximation has been validated extensively and used in radiation heat transfer studies. The approximation is given by

$$\dot{Q}_p \cong I^j A_p^j w^j \quad (2.6)$$

where the variable  $I^j$  is the intensity coming from a given discrete direction  $j$ ,  $w^j$  is the quadrature weighting function for that direction, and  $A_p^j$  is the projected area in the given direction. The projected area from direction  $j$  is provided in the *HVAC Systems and Equipment Handbook* (ASHRAE, 1996). The general equation for the projected area is

$$A_p^j = f_p^j f_{\text{eff}} A_D \quad (2.7)$$

where  $f_p^j$  is the projected area factor in direction  $j$ . Factor charts for sitting and standing people are given by Fanger (1967) and ASHRAE (1996).

Combining Eqs. (2.2) through (2.7) results in the final form of a very generalized method for determining the  $T_{\text{mrt}}$

$$T_{\text{mrt}} = \left[ \frac{\sum_j I^j A_p^j w^j}{f_{\text{eff}} A_D \sigma} \right]^{1/4} \quad (2.8)$$

This equation provides a more generalized approach to calculating the  $T_{\text{mrt}}$  than using the surrounding surface temperatures given in the classical method. This approach, using the localized radiant intensity field, was extensively validated in the paper by DeGreef and Chapman (2000) and has been used to accurately incorporate the various emissivities and nonuniform surface temperatures of room structures.

### 2.1.2 Calculating the Radiant Intensity Field

Equation (2.8) provides a robust and general method to calculate the  $T_{\text{mrt}}$  at any point in an enclosed space. The radiant intensity field, however, must be highly accurate in order to calculate occupant thermal comfort reliably in the form of  $T_{\text{mrt}}$ . The following paragraphs describe the very fundamental radiative transfer equation (RTE) and the preferred method employed to solve this equation. Once the solution method is developed, then the key components and information of the room structure that are necessary to incorporate the impact of the room structure into the thermal comfort analysis are determined.

**The Radiative Transfer Equation.** The RTE represents the most fundamental engineering equation that describes radiation transfer within an enclosure. Of note is that the RTE simplifies to the more familiar RTEs that include view factors and the temperature to the fourth power. These simplifications, however, introduce inaccuracies into the calculations and eliminate the generality of the RTE.

The radiative intensity  $I(\Omega)$  is determined from the RTE by (Viskanta and Mengüç, 1987; Siegel and Howell, 1981; Özisik, 1977):

$$\begin{aligned}
 (\nabla \cdot \Omega)I_\lambda(\mathbf{r},\Omega) &= \mu \frac{\partial I_\lambda}{\partial x} + \xi \frac{\partial I_\lambda}{\partial y} + \eta \frac{\partial I_\lambda}{\partial z} \\
 &= -(\kappa_\lambda + \sigma_{s,\lambda})I_\lambda + \kappa_\lambda I_{b,\lambda} + \frac{\sigma_{s,\lambda}}{4\pi} \int_{\Omega'} \Phi(\Omega' \rightarrow \Omega)I_\lambda(\Omega')d\Omega'
 \end{aligned}
 \tag{2.9}$$

For the special case of a typical occupied room, the equation reduces to the form:

$$\mu \frac{\partial I_\lambda}{\partial x} + \xi \frac{\partial I_\lambda}{\partial y} + \eta \frac{\partial I_\lambda}{\partial z} = \kappa_\lambda(I_{b,\lambda} - I_\lambda)
 \tag{2.10}$$

The associated boundary conditions depend on the emitted radiation from the boundary, the radiation reflected from the boundary, and the radiation transmitted through the boundary via a window. In equation form, the boundary condition in the  $x$ -direction is:

$$I_{\text{bnd},\lambda} = I_{b,\lambda} + (1 - \varepsilon_\lambda - \tau_\lambda) \int I_\lambda \mu d\lambda + \tau_\lambda I_{t,\lambda}
 \tag{2.11}$$

Equations (2.10) and (2.11) are solved in all directions and at all wavelengths to determine the spectral intensity field within the enclosure. Direct solution of this equation is only possible with numerical methods.

**The Discrete-Ordinates Method.** The discrete-ordinates method was first applied to neutron transport theory and is described by Carlson and Lathrop (1963). Today, the discrete-ordinates method is used by the Building Comfort Analysis Program (BCAP) methodology (Jones and Chapman, 1994; Chapman and Zhang, 1995, 1996; Chapman et al., 1997) to consider discrete directions and nodes, and calculates the radiant intensity at each point and direction within the enclosure. The enclosure space is divided into finite control volumes as illustrated in Fig. 2.2, and Eq. (2.10) is

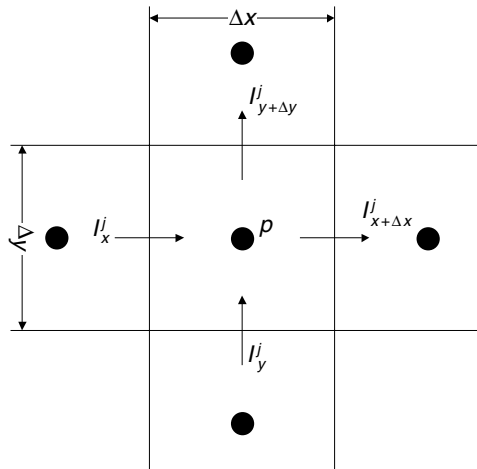


**FIGURE 2.2** Control volume for the discrete-ordinates method.

8.16 ENGINEERING DESIGN TOOLS TO ASSIST IN HEATER-COOLER SIZING

integrated over each three-dimensional control volume. The resulting equation in a discrete direction,  $j$ , is:

$$\int_z^{z+\Delta z} \int_y^{y+\Delta y} \int_x^{x+\Delta x} \left[ \mu \frac{\partial I^j}{\partial x} + \xi \frac{\partial I^j}{\partial y} + \eta \frac{\partial I^j}{\partial z} \right] dx dy dz = S \Delta V \tag{2.12}$$

The discrete-ordinates method designates the directions for  $j$ .

The control volume intensity along one side is assumed to be independent of the other two directions. For example, the intensity along the  $x$  interface is not affected by the  $y$  and  $z$  directions (Patankar, 1980). The equation then becomes:

$$\mu^j \Delta z \Delta y (I_{x+\Delta x}^j - I_x^j) + \xi^j \Delta z \Delta x (I_{y+\Delta y}^j - I_y^j) + \eta^j \Delta x \Delta y (I_{z+\Delta z}^j - I_z^j) = S_j \Delta V \tag{2.13}$$

This equation contains six interface intensities. Assuming the intensity profile across the control volume is linear, the intensity at the center of the control volume, point  $p$ , is (Truelove, 1988; Fiveland, 1988):

$$I_p^j = \alpha I_{x+\Delta x}^j + (1 - \alpha) I_x^j = \alpha I_{y+\Delta y}^j + (1 - \alpha) I_y^j = \alpha I_{z+\Delta z}^j + (1 - \alpha) I_z^j \tag{2.14}$$

The interpolations factor,  $\alpha$ , is set equal to one to avoid negative intensities, which are physically impossible and will yield unstable solutions. Fiveland (1987, 1988) reports that when  $\alpha$  equals one, the intensities will be positive. Substituting Eq. (2.14) into Eq. (2.13) yields:

$$I_p^j = \frac{\mu^j \Delta z \Delta y I_x^j + \xi^j \Delta z \Delta x I_y^j + \eta^j \Delta x \Delta y I_z^j + S \Delta V}{\mu^j \Delta z \Delta y + \xi^j \Delta z \Delta x + \eta^j \Delta x \Delta y} \tag{2.15}$$

Equation (2.15) is written for all the discrete directions for each control volume. For the  $S_4$  approximation, each control volume has 24 discrete directions. The values for  $\mu^j$ ,  $\xi^j$ , and  $\eta^j$  must satisfy the integral of the solid angle over all the directions, the half-range flux, and the diffusion theory (Truelove, 1987, 1988). Table 2.1 provides the values for  $\mu^j$ ,  $\xi^j$ , and  $\eta^j$  for the first quadrant. A complete table of values satisfying these conditions is tabulated and available from Fiveland (1988) and Chapman et al. (1992). The solution for Eq. (2.15) is an iterative solution that necessarily includes the boundary condition. Once solved, Eq. (2.15) provides the sought-after radiant intensity field within the enclosure.

The accuracy of the discrete-ordinates method has been validated by Fiveland (1987, 1988), Fiveland and Jamaluddin (1989), Truelove (1987, 1988), Jamaluddin and Smith (1988), Sanchez and Smith (1992), Yücel (1989), and Chapman (1992). The  $S_4$  approximation has been found to be a reasonable compromise between accurate results and low computational resources (Fiveland, 1988; Jamaluddin and Smith, 1988).

**TABLE 2.1** First-Octant Values for Directional Cosines and Weighting Factor

Ordnate direction	$\mu^j$	$\xi^j$	$\eta^j$	$w^j$
1	-0.2959	-0.9082	0.2959	0.5236
2	-0.9082	-0.9082	0.2959	0.5236
3	-0.2959	-0.2959	0.9082	0.5236

### 2.1.3 Determine the Necessary Room Structure Components

The necessary components of the room structure can be identified from the requirements of the RTE. The most critical information comes from the boundary conditions [Eq. (2.11)] since this is where the room conditions are incorporated into the RTE and then, in turn, into the  $T_{\text{mrt}}$  calculations. This section describes the necessary properties. For convenience, Eq. (2.11) is repeated:

$$I_{\text{bnd},\lambda} = \varepsilon_{\lambda} I_{b,\lambda} + (1 - \varepsilon_{\lambda} - \tau_{\lambda}) \int I_{\lambda} \mu d\lambda + \tau_{\lambda} I_{t,\lambda} \quad (2.11)$$

The first term on the right side of Eq. (2.11) represents the intensity that is emitted from a room surface. This quantity depends exclusively on the surface emissivity  $\varepsilon$  and on the surface temperature. The middle term represents the intensity that is reflected from the surface back into the enclosed space. The parenthetic term represents the surface reflectivity, and the term inside the integral represents the radiant intensity that is coming into the surface. The last term represents the intensity that is transmitted through a window into the enclosed space.

To capture the impact of the room structure, the foregoing discussion illustrates the necessity of accurately defined boundary conditions. In addition, the following three parameters must be known to define the boundary conditions:

1. The surface temperature
2. The surface properties (emissivity, reflectivity, and transmissivity)
3. The intensity coming into the surface [Eq. (2.9) calculations]

**Surface Temperature.** The surface temperatures of the room structure are calculated using the BCAP methodology. This methodology employs an energy balance at the surface:

$$\frac{(T_o - T_i)}{R_{\text{th}}} + h_i(T_{\text{air}} - T_i) + \left[ \alpha_i \int_{n \cdot \Omega < 0} |\mathbf{n} \cdot \Omega| I(\Omega) d\Omega' - \varepsilon_i \sigma T_i^4 \right] = \frac{\partial E_i}{\partial t} \quad (2.16)$$

Equation (2.16) describes the energy balance for a surface at  $T_i$ . The first term is the conduction through the surface, where  $T_o$  is the outside air temperature and  $R_{\text{th}}$  represents the thermal resistance of the surface-wall system. The second term is the convective flux between the room air and the wall surface. The third term is the net radiant heat flux from incident energy and emissive energy. The term on the right side of the equation represents the change in energy of the surface with time. At steady-state conditions, this term is zero. Equation (2.16) is rearranged to solve for the surface temperature once the air temperature and intensity field are known.

**Surface Properties: Emissivity, Reflectivity, and Transmissivity.** Many surface properties are tabulated in the *ASHRAE Handbook*. Unfortunately, surface properties for window systems represent a unique difference between a window system and a conventional surface. Window surface properties generally are strong functions of wavelength and therefore spectrally filter thermal radiation. Conversely, regular walls are opaque and thus are impervious to thermal radiation. Because of the strong wavelength dependence of certain window glazings, the surface properties and the RTE solution method must retain this dependency. Not doing so would eliminate the effect of solar heat gain on thermal comfort, as well as other inaccuracies.

## 8.18 ENGINEERING DESIGN TOOLS TO ASSIST IN HEATER-COOLER SIZING

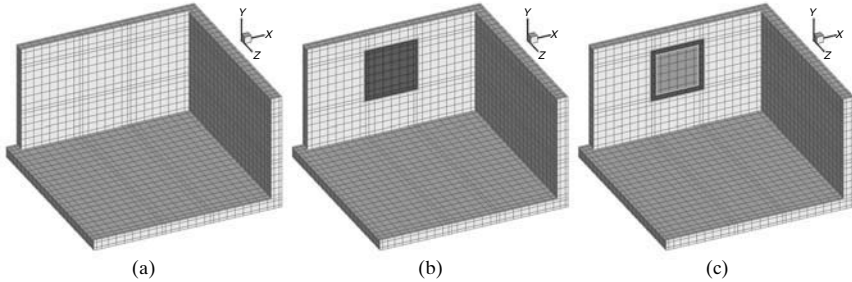


**FIGURE 2.3** Example of frame and window placement on a wall in the room. (a) Room, (b) frame added to back wall, (c) window added to frame.

The surface properties, along with the window system thermal conductivity, can be obtained from an auxiliary program, such as Window 4.1™. The DOE-2 output from Window 4.1 lists the dimensions of the window and, more important, provides the name of the file that lists the radiative properties for the glazing as a function of wavelength. By integrating the spectral data over four or five wavelength bands, a wavelength band-averaged radiative property can be obtained. The thermal conductivity is used in Eq. (2.16) to calculate the surface temperature of the window.

Figure 2.3 demonstrates the five steps that are necessary to incorporate a window system into the BCAP methodology.

1. Create one or more window systems using Window 4.1.
2. Describe the dimensions and thermal properties of the room.
3. Create an opening in a wall to position a window and a frame.
4. Select one of the window systems created in step 1 and position it in the frame created in step 3. This links the properties from the Window 4.1 DOE-2 file and from the spectral database used to create the window system to the BCAP methodology.
5. Repeat steps 3 and 4 as necessary.

Figure 2.3 demonstrates the sequence of events. Note that the software is able to draw upon the extensive window databases of Window 4.1.

## 2.2 SYSTEM EVALUATION CRITERIA

It is clear that specific details of the room structure are necessary to accurately evaluate the impact of the room structure and the heating and cooling system on occupant thermal comfort. This entire process is illustrated in Fig. 2.4. The box in the center represents a localized  $T_{op}$  and  $T_{mrt}$  simulation program that is based on the BCAP methodology. The arrows into the left and the top side of the box represent the design criteria for the enclosed space. The arrows out of the right side of the box represent information that is used to evaluate occupant thermal comfort within the room. The arrows on the right, the  $T_{mrt}$  gradient and power consumption, are performance variables that result from the analysis. These are used to assess the adequacy of the particular design.

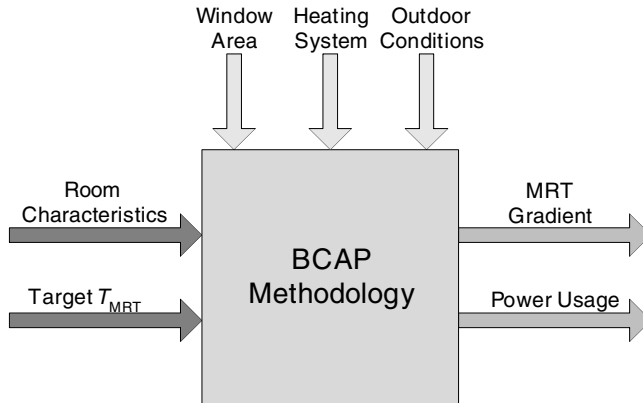


**FIGURE 2.4** The BCAP methodology by Jones and Chapman (1994) and Chapman and DeGreef (1997).

### 2.2.1 Performance Variables

The two variables used to evaluate heating and cooling systems are the operative temperature  $T_{op}$  gradients across the room and the power consumption. The severity of the  $T_{op}$  gradient across the room measures the variation of thermal comfort. The energy fuel consumption can vary as well and depends on the installed heating system. The balance between  $T_{op}$ ,  $T_{op}$  uniformity, and fuel consumption must be considered for each individual design situation.

### 2.2.2 The Difference Between Room Energy and Centralized Energy

Note that when comparing energy consumption in this section, the heating and cooling systems are in-space systems. That is, these systems are physically located somewhere within the enclosed space and are not centralized systems that convert fuel to heat energy at a centralized location that is then transported to individual rooms within the building.

In-space systems do not suffer from “transmission” losses, whereas the centralized systems experience some transmission losses. Transmission losses, as defined by ASHRAE Standard 152, are losses that occur between the point where the heat energy is created from the fuel (a central furnace, for example) and the point where the heat energy is applied to the room. According to Standard 152, the primary transmission losses for centralized warm-air systems are duct and stack losses. Transmission losses for hydronic systems typically are less, and range between 5 and 10 percent, whereas duct losses may range between 20 and 40 percent and higher with poor design or installation.

Because in-space systems convert fuel (e.g., natural gas, electricity, fuel oil, etc.) directly to heat within the enclosed space, these systems do not suffer from transmission losses. Similarly, in-space electric systems do not lose energy during conversion, either. These observations are important factors when comparing the energy requirements of in-space systems with centralized furnace or boiler systems. If only the energy required in the room is considered, then the centralized system will

## 8.20 ENGINEERING DESIGN TOOLS TO ASSIST IN HEATER-COOLER SIZING

- |   |
|---|
| <ul style="list-style-type: none"> <li>• Equipment sizing factors</li> <li>• Room power requirements</li> <li>• Product energy conversion loss</li> <li>• Transmission loss</li> <li>• Setup-setback sizing factor</li> <li>• Contingency factor</li> </ul> |
|---|

**FIGURE 2.5** Equipment-sizing factors.

appear to perform at a level greater than it will when installed. The difference is due to transmission and generation losses.

To fully appreciate how in-space thermal comfort analysis fits into the total system energy and performance specification, consider the equipment-sizing chart in Fig. 2.5 that provides the power requirements. To this factor, add the product energy conversion loss and energy transmission loss. Additionally, if temperature setup and setback are practiced, ASHRAE recommends oversizing of 20 to 40 percent for convection systems. ASHRAE Research Project 1114, *Develop Simplified Methodology to Incorporate Thermal Comfort Factors for Temperature Setback/Setup into In-Space Heating and Cooling Design Calculations*, will provide specific design information for both radiant and convective systems. Finally, standard practice often adds a safety or contingency factor of 10 percent, to accommodate as-built design changes, changes in area usage and temperature requirements, or other factors that impact energy supply requirements.

### 2.2.3 System Performance Index

An energy index is defined so that various heating and cooling systems can be compared. While this index does not include thermal comfort directly, it does provide an initial step in determining the best heating or cooling system for a specific design case. This index is defined as

$$PI = \frac{\text{system power, } \dot{P}_a}{\text{windowless room 100\% central forced air, } \dot{P}_B} \times 100 \quad (2.17)$$

The system power is the actual power needed inside the room to create a design average  $T_{op}$ . For consistency, the average  $T_{op}$  is specified as the weighted average of the localized  $T_{op}$  at a height 3 ft above the floor. The denominator in Eq. (2.17) is the same except that windows are removed from the design, and average  $T_{op}$  is obtained entirely by a centralized forced-air heating or cooling system.

As mentioned previously, this performance index does not consider transmission losses between the point where fuel is converted to heat and the room. Hence, the designer is responsible for taking these losses into consideration for a central heating and cooling system.

## 2.3 THE DESIGN PROCESS

Figure 2.6 illustrates the design process that is used in the remainder of Sec. 8. The first step is to specify the design conditions. For example, the designer specifies the

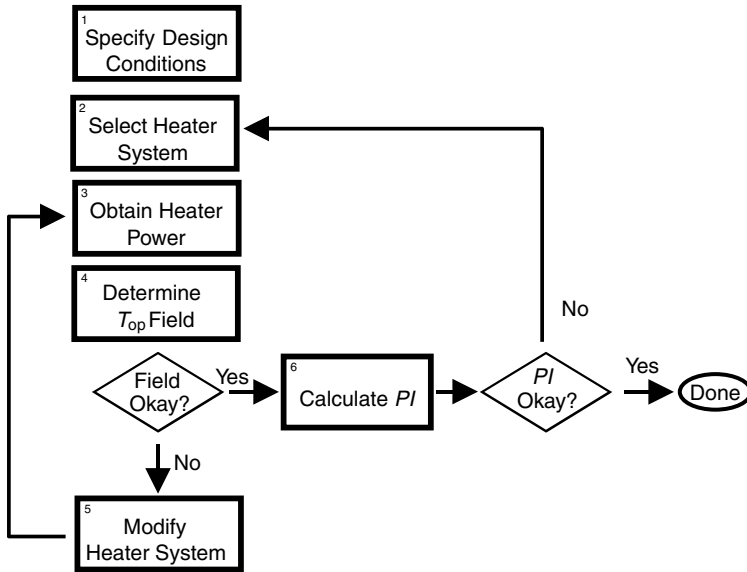


**FIGURE 2.6** Complete design process for sizing and placing in-space radiant heating and cooling panels.

targeted design operative temperature  $T_{op,d}$  for the occupied space along with the outdoor design temperature. The room structure is specified in this step as well. The next step is to choose a heating or cooling system. The designer may select a hydronic floor heating system, a modular radiant panel heating system, or for that matter a convective system. Discrete heat delivery equipment, such as a diffuser or a wall or ceiling heat panel, requires specification of the position of the panel or heat delivery source within the enclosed space.

Third, determine the power required by the heating or cooling system to achieve the design level of thermal comfort. The boundaries to be respected include safety, equipment output, and thermal comfort limits. The process used to determine this power level is shown in Fig. 2.7. The first step illustrated in the figure is the design process. This is the same block that is shown in Fig. 2.6 and is shown here only to reinforce the importance of this step. The second step in Fig. 2.7 is to estimate the heater power. This step is not that critical because the process itself will determine the appropriate power level of the heater that is necessary to deliver the design thermal comfort. We shall designate this power level as  $\dot{P}_1$ . With the heater specified, determine the average  $T_{op}$  that is developed by the heater specification and the design conditions. The design  $T_{op}$  is calculated at 1 ft above the floor. We shall designate this  $T_{op}$  as  $T_{op,1}$ . Next is the fourth step, which is to select a second heater power level and again calculate an average  $T_{op}$  at this second power level. We shall call these  $\dot{P}_2$  and  $T_{op,2}$ . Armed with two power levels and two associated  $T_{op}$ 's, the next step is to refine the actual heater power level by calculating a new estimate of the exact power level

$$\dot{P}_a = \left[ \frac{T_{op,d} - T_{op,1}}{T_{op,2} - T_{op,1}} \right] (\dot{P}_2 - \dot{P}_1) + \dot{P}_1 \quad (2.18)$$

8.22 ENGINEERING DESIGN TOOLS TO ASSIST IN HEATER-COOLER SIZING

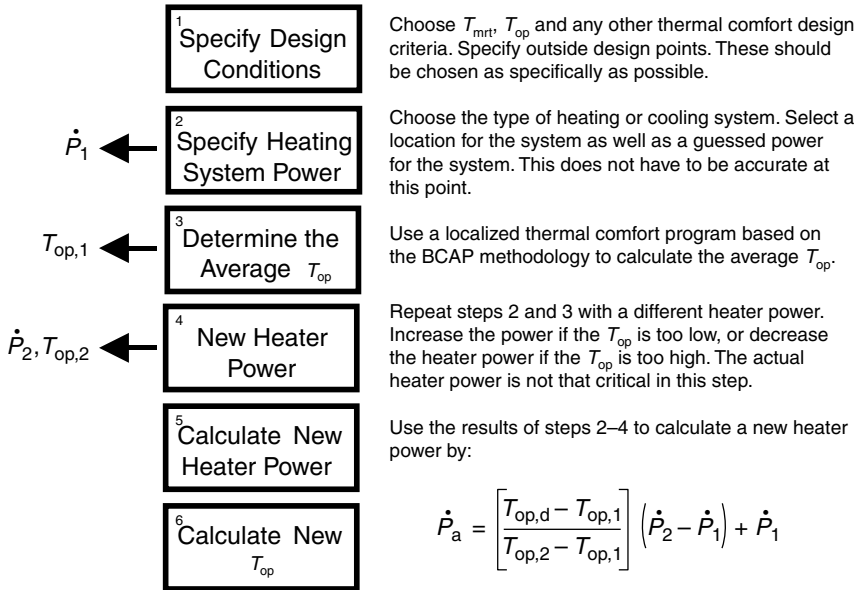


FIGURE 2.7 Determination of the heater power that is required to achieve a design level of thermal comfort.

Finally, recalculate the  $T_{\text{op}}$  at the power level calculated from Eq. (2.18) and then fine-tune the power level as necessary. The process described in Fig. 2.7 is fairly forgiving in that the guesses for  $\dot{P}_1$  and  $\dot{P}_2$  are not critical to achieve the final design power level and, hence, the size of the in-space heating system. As some guidance, though, use 15 Btu/(h · ft<sup>2</sup>) for  $\dot{P}_1$  and 25 Btu/(h · ft<sup>2</sup>) for  $\dot{P}_2$ . In fact, the most critical step in the process is to specify the thermal comfort design conditions and the environmental design point for the enclosed space. We hope that, at this point in the Handbook, you are thinking in terms of creating a specific  $T_{\text{op}}$  as opposed to setting a thermostat at 72°F (22.2°C)!

Once the heater power  $\dot{P}_a$  is determined from Fig. 2.7, the fourth step in Fig. 2.6 is to determine the  $T_{\text{op}}$  field throughout the occupied space. Of importance is to determine if the  $T_{\text{op}}$  gradients and radiant asymmetry are acceptable, and if the portions of the room that need to be thermally comfortable are thermally comfortable. If the  $T_{\text{op}}$  field is unacceptable, then the designer must reassess the heating system. This can include selection of a different heating system, or, in the case of panel, baseboard, or wall heaters, or convection diffusers, adjustment of the heaters' position within the occupied space. The idea is to repeat steps 3 through 5 until the  $T_{\text{op}}$  field is acceptable.

Once the  $T_{\text{op}}$  field meets the design conditions, the next step is to calculate the performance index PI using Eq. (2.18). If the PI is acceptable, then the design process is complete. If the PI is not acceptable, then the designer must revisit the heating system and possibly even the room structure.

Chapter 3 demonstrates each of the steps shown in Figs. 2.6 and 2.7 that are used to design a radiant heating or cooling installation. By the end of Chap. 3 in this section, the reader will have a thorough understanding of the design process as well as the impact that in-space heating and cooling systems have on thermal comfort.

---

# CHAPTER 3

---

## EXAMPLE

# DESIGN CALCULATIONS

## USING ABOVE<sup>®</sup>

---

This chapter illustrates how to use a localized thermal comfort design program to optimize the built environment for occupant thermal comfort. Essentially, this chapter pulls together all of the tools and methods discussed in this Handbook and shows how they can be put to use by the heating, ventilating, and air-conditioning (HVAC) designer. As one can surmise, the methods and calculations begin to become quite complex, even when the built environment is simple. Hence, it becomes logical to computerize the calculations to lift the tedium and complexity from the designer. Computerizing the calculations permits the designer to focus on the environment (e.g., building construction, orientation, use, and thermal comfort specifications) rather than the particular calculations.

Two important concepts are critical for the reader to remember. First, the fundamental radiation parameter is the intensity at various wavelengths in all directions. Many people reduce the complexity by using view factors. Although view factor analysis is acceptable for some cases, it is not acceptable for cases in which window glass is involved due to the wavelength dependency of the window glass. As daylighting and passive solar design become more important determinants of building design, the glass percentage of the building envelope increases dramatically.

Second, use proper design methodology to effectively harvest the benefits that daylighting and passive solar produce. Our choice is to calculate the directional, wavelength-dependent intensity using a sophisticated radiation solver, and then calculate heat fluxes, mean radiant temperatures (MRTs), and other parameters from the fundamental radiation field. This has been done in the following demonstration cases.

The demonstration cases presented in this chapter are described in Table 3.1. Table 3.2 provides properties of common insulating materials that are used in the examples. These cases represent a wide variety of radiant panels and demonstrate how design decisions impact localized thermal comfort. The first two demonstrations provide very specific details on how to implement a design methodology, while the remaining cases show how heating and cooling panels affect thermal comfort. Each case is fully explored to determine the benefits of designing for local thermal comfort.

The calculations are completed with a program called ABOVE<sup>®</sup>. ABOVE is a localized thermal comfort simulation that is based on the BCAP methodology described in the Handbook. At the time of this writing, ABOVE is in a prebeta release state. However, the output has been thoroughly compared with outputs presented in ASHRAE Research Projects 657 and 907, which developed the BCAP methodology.

In the demonstration cases, the following conditions are used unless specifically stated otherwise within the demonstration:

1. Ground temperature is 50°F (10°C).
2. Radiant panel heaters are positioned in the center of the ceiling.
3. A window is positioned in the center of the back wall and occupies 40 percent of the back wall.
4. The simulation output is represented by a figure that shows the back wall, the floor, and the right wall. A contour slice showing the operative temperature (OT)

**TABLE 3.1** Description of Each Case Included in Sec. 8, Chap. 3

Case	Description	$W \times D \times H$ (ft)	R value, W/F/C	Vent/ infil	$T_{amb}$ (°C)	Surface $\epsilon$	Target $T_{op}$ (°C)	Exceptions
1	Living area	15 × 12 × 9	11/30/30	0.7/0.4	-10	0.9	22	Back wall only is exposed to outside. Remaining walls are exposed to indoor temperature of 20°C. Window on back wall with $\epsilon$ of 0.6 and R-2. Window area is 40% of the back wall.
2	Heater position	15 × 12 × 9	11/30/30	0.7/0.4	-20	0.9	22	Back wall, ceiling, and two side walls are exposed to outside. Remaining surfaces are exposed to indoor temperatures of 20°C. Window area is 70% of the back wall. Heater is 3 × 3 ft that is moved along a center line from the back of the room to the front of the room.
3	Cooling	12 × 12 × 9	9/11/22	0/0.5	30	0.9	22	The ceiling panel cooling system is a 2 × 2 ft panel grid. Each is powered at the same level. Insulation backing is R-9.
4	Power density	30 × 30 × 12	4/4/4	0.5/0.5	0	0.9	20	First case is an imbedded ceiling heating system that is powered at 14 W/ft <sup>2</sup> . There is no backing insulation for this system other than the ceiling itself. The heater can only come to within 1 ft of the perimeter.
5	Surface emissivity	9.8 × 9.8 × 8.2	9/11/22	0.5/0.5	-10	Various	22	Compare power necessary for each surface emissivity.
6	Hydronic floor	20 × 15 × 9	9/11/22	0.5/0.5	-10	0.9	22	Assess the impact of a heated floor.
7	Heater power	12 × 12 × 9	2.5/2.5/2.5	0/0.4	-5	0.9	22	Show that radiant calculations are important even when the heating system is not an in-space radiant heater.

**TABLE 3.2** Thermal Properties of Common Building Materials

Material description	Specific heat [J/(kg · °C)]	Mass density (k/m <sup>3</sup> )	Thermal conductivity [W/(m · °C)]	Emissivity	
				Ratio	Surface condition
Aluminum (alloy 1100)	896	2,740	221	0.09 0.20	Commercial sheet Heavily oxidized
Aluminum bronze (76% Cu, 22% Zn, 2% Al)	400	8,280	100		
Alundum (aluminum oxide)	779				
Asbestos fiber	1,050	2,400	0.170		
insulation	800	580	0.16	0.93	“Paper”
Ashes, wood	800	640	0.071 (323)		
Asphalt	920	2,110	0.74		
Bakelite	1,500	1,300	17		
Bell metal	360 (323)				
Bismuth tin	170		65.0*		
Brick, building	800	1,970	0.7	0.93*	
Brass					
Red (85% Cu, 15% Zn)	400	8,780	150	0.030	Highly polished
Yellow (65% Cu, 35% Zn)	400	8,310	120	0.033	Highly polished
Bronze	435	8,490	29 (273)		
Cadmium	230	8,650	92.9	0.02	
Carbon (gas retort)	710		0.35 (256)	0.81	
Cardboard			0.07		
Cellulose	1,300	54	0.057		
Cement (Portland clinker)	670	1,920	0.029		
Chalk	900	2,290	0.83*	0.34*	About 394 K
Charcoal (wood)	840	240	0.05 (473)		
Chrome brick	710	3,200	1.2		
Clay	920	1,000			
Coal	1,000	1,400	0.17 (273)		
Coal tars	1,500 (313)	1,200	0.1		
Coke (petroleum, powdered)	1,500 (673)	990	0.95 (673)		
Concrete (stone)	653 (473)	2,300	0.93		
Copper (electrolytic)	390	8,910	393	0.072	Commercial, shiny
Cork (granulated)	2,030	86	0.048 (268)		
Cotton (fiber)	1,340	1,500	0.042		
Cryolite (AlF <sub>3</sub> · 3NaF)	1,060	2,900			
Diamond	616	2,420	47		
Earth (dry and packed)		1,500	0.064*	0.41*	
Felt		330	0.05		
Fireclay brick	829 (373)	1,790	1 (473)	0.75	At 1,273 K
Fluorspar (CaF <sub>2</sub> )	880	3,190	1.1		
German silver (nickel silver)	400	8,730	33	0.135	Polished
Glass					
Brown (soda-lime)	750	2,470	1.0 (366)	0.94	Smooth
Flint (lead)	490	4,280	1.4		
Pyrex	840	2,230	1.0 (366)		
“Wool”	657	52.0	0.038		
Gold	131	19,350	297	0.02	Highly polished
Graphite					
Powder	691*		0.183*		
“Karbate” (impervious)	670	1,870	130	0.75	

8.26 ENGINEERING DESIGN TOOLS TO ASSIST IN HEATER-COOLER SIZING

TABLE 3.2 Thermal Properties of Common Building Materials (Continued)

Material description	Specific heat [J/(kg · °C)]	Mass density (k/m <sup>3</sup> )	Thermal conductivity [W/(m · °C)]	Emissivity	
				Ratio	Surface condition
Gypsum	1,080	1,200	0.43	0.903	On a smooth plate
Hemp (fiber)	1,352.3	1,500			
Ice (0°C)	2,040	921	2.24	0.95*	
(-20°C)	1,950		2.44*		
Iron					
Cast	500 (373)	7,210	47.7 (327)	0.435	Freshly turned
Wrought		7,770	60.4	0.94	Dull, oxidized
Lead	129	11,300	34.8	0.28	Gray, oxidized
Leather (sole)		1,000	0.16		
Limestone	909	1,650	0.93	0.36*	At 336 to 467 K
				to 0.90	
Linen			0.09		
Litharge (lead monoxide)	230	7,850			
Magnesia					
Powdered	980 (373)	796	0.61 (320)		
Light carbonate		210	0.059		
Magnesite brick	930 (373)	2,530	3.8 (478)		
Magnesium	1,000	1,730	160	0.55	Oxidized
Marble	880	2,600	2.6	0.931	Light gray, polished
Nickel	440	8,890	59.5	0.045	Electroplated, polished
Paints					
White lacquer				0.80	
White enamel				0.91	On rough plate
Black lacquer				0.80	
Black shellac		1,000	0.26	0.91	“Matte” finish
Flat black lacquer				0.96	
Aluminum lacquer				0.39	On rough plate
Paper	1,300*	930	0.13	0.92	Pasted on tinned Plate
Paraffin	2,900	900	0.24 (273)		
Plaster		2,110	0.74 (348)	0.91	Rough
Platinum	130	21,470	69.0	0.054	Polished
Porcelain	750	260	2.2	0.92	Glazed
Pyrites (copper)	549	4,200			
Pyrites (iron)	569 (342)	4,970			
Rock salt	917	2,180			
Rubber					
Vulcanized (soft)	2,000*	1,100	0.1	0.86	Rough
Vulcanized (hard)		1,190	0.16	0.95	Glossy
Sand	800	1,520	0.33		
Sawdust		190	0.05		
Silica	1,320	2,240	1.4 (366)		
Silver	235	10,500	424	0.02	Polished and at 500 K
Snow (freshly fallen)		100	0.598		
(At 32°F)		500	2.2		
Steel (mild)	500	7,830	45.3	0.12	Cleaned
Stone (quarried)	800	1,500			

**TABLE 3.2** Thermal Properties of Common Building Materials (*Continued*)

Material description	Specific heat [J/(kg · °C)]	Mass density (k/m <sup>3</sup> )	Thermal conductivity [W/(m · °C)]	Emissivity	
				Ratio	Surface condition
Tar					
Pitch	2,500	1,100	0.88		
Bituminous		1,200	0.71		
Tin	233	7,290	64.9	0.06	Bright and at 323 K
Tungsten	130	19,400	201	0.032	Filament at 300 K
Wood					
Hardwoods	1,900/2,700	370/1,100	0.11/0.255		
Ash, white		690	0.172		
Elm, American		580	0.153		
Hickory		800			
Mahogany		550	0.13		
Maple, sugar		720	0.187		
Oak, white	2,390	750	0.176	0.90	Planed
Walnut, black		630			
Softwoods	See Table 3A,	350/740	0.11/0.16		
Fir, white	Chap. 24,	430	0.12		
Pine, white	ASHRAE	430	0.11		
Spruce	Handbook	420	0.11		
Wool					
Fiber	1,360	1,300			
Fabric		110/330	0.036/0.063		
Zinc					
Cast	390	7,130	110	0.05	Polished
Hot-rolled	390	7,130	110		
Galvanizing				0.23	Fairly bright

\* Data source not determined.

distribution across the room is also shown. The slice is 3 ft above the floor to approximate the midlocation of an occupant. This particular contour slice is called the *Thermal Comfort Signature*<sup>™</sup> (TCS<sup>™</sup>) because it represents the localized thermal comfort that is produced by the combination of the room structure and the radiant heating and/or cooling panels. In this regard, the TCS is, in all practicality, a signature of the particular combination. Changing one or more parameters will change the TCS.

5. Window radiative properties are an emissivity of 0.6, a transmissivity of 0.2, and an  $R$  value of 2.

### 3.1 HEATER POSITIONED ABOVE A WINDOW IN A LIVING AREA

The first demonstration case is a  $15 \times 12 \times 9$  ft living area with a large window located on the back wall. The outdoor temperature is  $14^\circ\text{F}$  ( $-10^\circ\text{C}$ ). The only wall exposed to the outdoor conditions is the back wall. The  $R$  values and other room structure properties are provided in Table 3.1. The goal is to design and position a radiant panel heater that will provide a TCS with an average  $T_{\text{op}}$  of  $70^\circ\text{F}$  ( $21.1^\circ\text{C}$ ).

## 8.28 ENGINEERING DESIGN TOOLS TO ASSIST IN HEATER-COOLER SIZING

## 3.1.1 Design Step 1: Specify Design Conditions

The design conditions for this room are predominantly listed in Table 3.1. The target average  $T_{op}$  with an outdoor temperature of 14°F (−10°C) is 70°F (21.1°C). For the purposes of the design procedure, the  $T_{op}$  is averaged over an area that is 3 ft above the floor of the room.

## 3.1.2 Design Step 2: Select the Heater for This Application

The heater selected for this application is a radiant panel heater positioned in the middle of the ceiling. The radiant panel heater exhibits a power density of up to 50 W/ft<sup>2</sup>. The first heater chosen for this example is a 4 × 4 ft heater panel. The completed room design is illustrated in Figure 3.1. The window is located on the back wall and the radiant panel heater is positioned in the center of the ceiling.

3.1.3 Design Step 3: Determine the Heater Power Necessary to Meet the Design  $T_{op}$ 

Determining the appropriate heater power is itself an iterative process. Referring to Fig. 2.7 in this section, the second and third step of determining the heater power requirements require the designer to estimate a heater power and then calculate the average  $T_{op}$  that results from that heater power. As a first guess, the heater power is estimated at 800 W. Using ABOVE to calculate the average  $T_{op}$  in the room produces the following results:

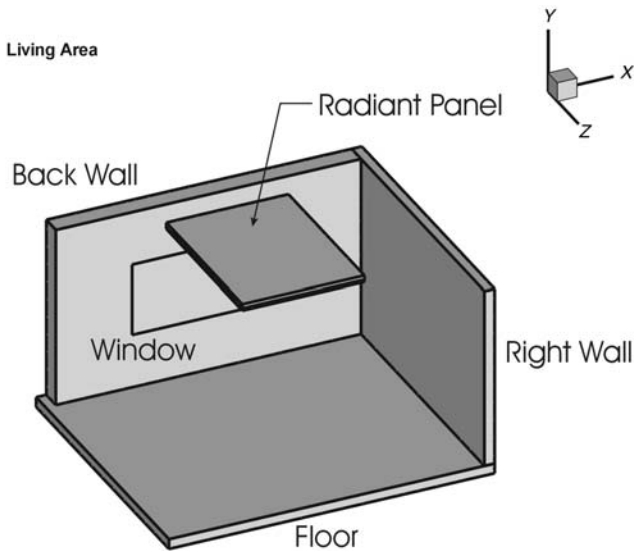


**FIGURE 3.1** Drawing of heater and window placement, and the orientation of the coordinate axes.

$$\dot{P}_1 = \left( \frac{50 \text{ W}}{\text{ft}^2} \right) \times (16 \text{ ft}^2) = 800 \text{ W}$$

$$T_{\text{op},1} = 73.5^\circ\text{F}$$

The next step in the power calculation is to estimate a second heater power and then recalculate the resulting average operative temperature. Again, the reader should keep in mind that the actual values for the heater power are not that important. The result is:

$$\dot{P}_2 = 600 \text{ W}$$

$$T_{\text{op},2} = 65.7^\circ\text{F}$$

Next, calculate a new estimate of the heater power based on the first two estimates. This is accomplished using linear interpolation [refer to Eq. (3.18)]:

$$\begin{aligned} \dot{P}_a &= \left[ \frac{T_{\text{op,d}} - T_{\text{op},1}}{T_{\text{op},2} - T_{\text{op},1}} \right] (\dot{P}_2 - \dot{P}_1) + \dot{P}_1 \\ &= \left[ \frac{70.0^\circ\text{F} - 73.5^\circ\text{F}}{65.7^\circ\text{F} - 73.5^\circ\text{F}} \right] (600 \text{ W} - 800 \text{ W}) + 800 \text{ W} \\ &= 710.3 \text{ W} \end{aligned}$$

The final step in determining the power is to recalculate the average OT with the 710.3 W. The result is precisely 70°F (21.1°C).

*Note.* The panel heater chosen for this application is a 4 × 4 ft panel heater with a watt density of 50 W/ft<sup>2</sup>, or a total available power input to the room of 800 W. Because the design calculation shows that only 710.3 W is required to maintain an acceptable level of comfort in the room, the chosen heater will do the job by only operating 88.8 percent of the time (710.3/800). Of note is that this particular heater leaves a heating margin of 11.2 percent relative to the design condition. The designer may choose to add a second heater to the room to add capacity if the outdoor conditions could become more severe.

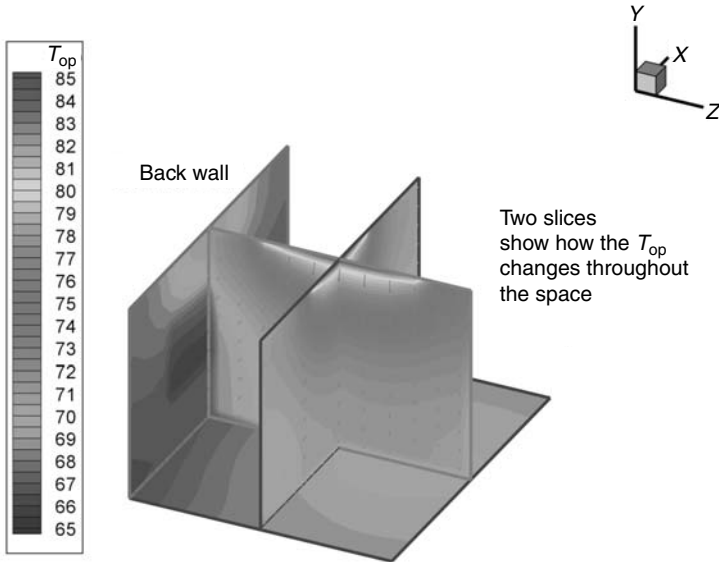
Some designers feel that a minimal heating margin is acceptable with the understanding that the radiant panel itself will store a certain amount of energy within the structure. For example, in the case of a heated concrete floor, the floor itself will store a substantial amount of energy that will overcome transients outside the design conditions. Similarly, radiant ceiling panel heaters tend to store energy in the furnishings and other components near the panel. As with the hydronic system, the energy from these furnishings and other interior components will help overcome transients outside the design conditions.

In contrast, a floor covering such as carpeting increases the insulating value of the floor and, therefore, increases the heat transfer resistance of a heated floor. This additional insulation limits the amount of heat that can be transferred from the panel surface to the occupied space. Consequently, in some cases, it may be beneficial to slightly oversize the heating system to provide for a potential change in room use or floor coverings by present or prospective owners or tenants.

### 3.1.4 Design Step 4: Evaluate the OT Distribution Within the Room

Figures 3.2 and 3.3 illustrate the OT distribution throughout the room in several different planes. Each slice within the room represents measurements of the OT at a particular point in the room. For example, Fig. 3.3 shows a slice that is 3 ft above the

8.30 ENGINEERING DESIGN TOOLS TO ASSIST IN HEATER-COOLER SIZING



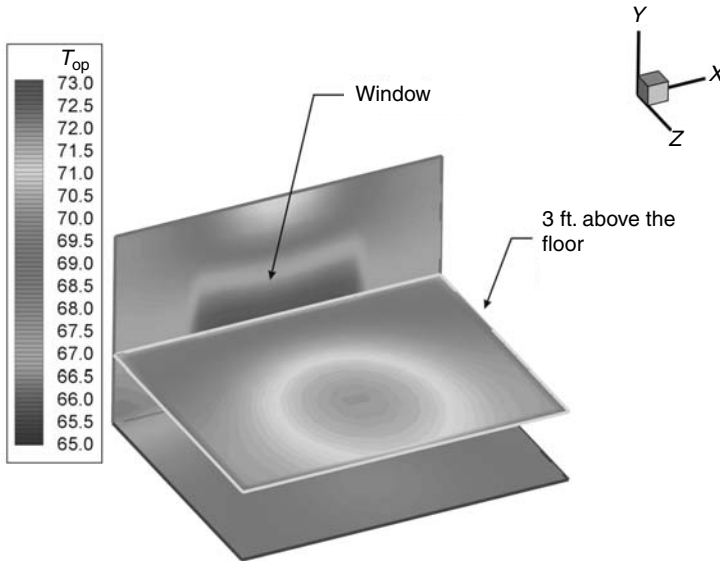
Avg. MRT = 71.5°F  
 Avg  $T_{op}$  = 71.5°F  
 Convection = 0.0 W  
 Radiation = 710.3 W  
 Ventilation = 0.71 ACH  
 Vent temp = 32°F  
 Infiltration = 0.4 ACH  
 Infil. temp = 32°F

**FIGURE 3.2** Operative temperature distribution throughout the occupied space.

floor of the room. The way to interpret this slice is to imagine a person measuring the  $T_{op}$  across the surface of the room, always 3 ft above the floor. These measurements are then plotted, as shown in Fig. 3.3. As shown in the figure, the  $T_{op}$  is highest directly under the heater and decreases near the window on the back wall of the room.

There are several interesting observations from these two figures.

1. Referring to Fig. 3.3, the surface temperatures on the back wall clearly show the location of the window. As expected, the surface temperature of the window is lower than the surface temperature of the rest of the back wall.
2. The location of the window has a direct impact on the local thermal comfort near the window. Again referring to Fig. 3.3, it is clear that the window lowers the  $T_{op}$  in the vicinity of the window. The window impacts the  $T_{op}$  as much as one-third of the way toward the back of the room.
3. The heater in the center of the ceiling mitigates the impact of the window to a large extent. The radiant panel heater creates a  $T_{mrt}$  that is higher than the room air temperature. Coupling the  $T_{mrt}$  with the room air temperature produces the  $T_{op}$  that is in a relatively comfortable region of 70°F (21.1°C).
4. The wall area above the window is warmed by the heater. This surface is warmed by absorbing radiant thermal energy from the heater, and then it reemits radiant



Avg. MRT = 71.5°F  
 Avg  $T_{op}$  = 70.0°F  
 Convection = 0.0 W  
 Radiation = 710.3 W  
 Ventilation = 0.70 ACH  
 Vent temp = 32°F  
 Infiltration = 0.4 ACH  
 Infil. temp = 32°F

**FIGURE 3.3** Illustration of the OT at an elevation of 3 ft above the floor.

energy into the room. This emission partially mitigates the impact of the window by increasing the  $T_{mrt}$  in the vicinity of the window.

5. It may be possible to make the  $T_{op}$  field more uniform by repositioning the heater. The  $T_{op}$  distribution is relatively uniform, however, because it varies by at most 3°F (1.7°C) from the area directly underneath the heater to a position near the back wall and is, therefore, not of great concern in this demonstration.

This demonstration case shows the methodology that is used to design for acceptable occupant thermal comfort. The next example expands on this concept by repositioning the radiant panel heater and evaluating the impact on occupant thermal comfort.

### 3.2 HEATER POSITIONED ABOVE A WINDOW

This demonstration is similar to the previous case in that it illustrates a room with a large window on one wall. The outdoor temperature is -4°F (-20°C). In this case, the back and side walls, as well as the ceiling, are exposed to the outdoor temperature. The front wall and the floor are exposed to interior temperatures of 68°F (20°C).

## 8.32 ENGINEERING DESIGN TOOLS TO ASSIST IN HEATER-COOLER SIZING

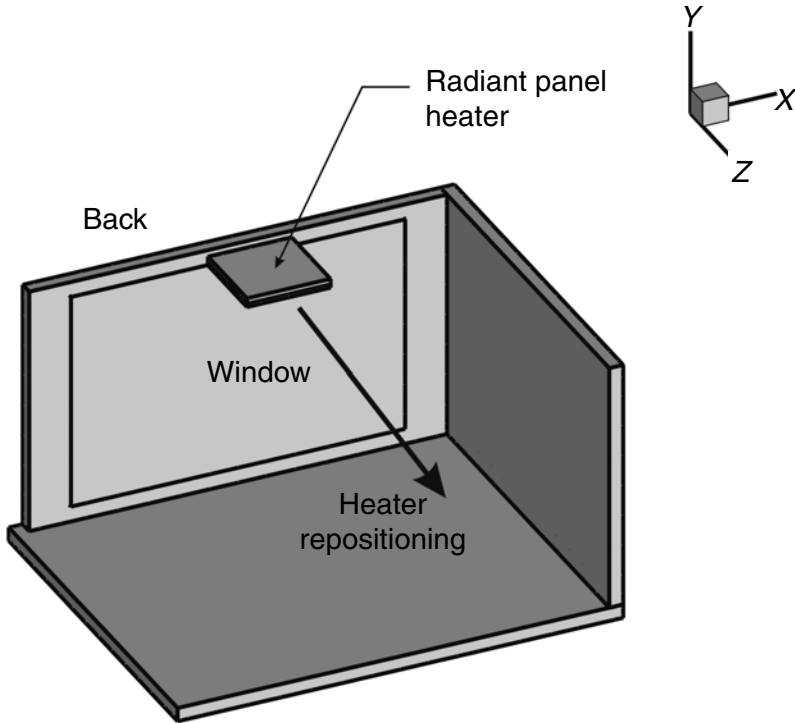


**FIGURE 3.4** Heater position impact on thermal comfort.

Figure 3.4 illustrates the room configuration and shows the position of the heater for the base case. The goal is to develop an appreciation of the importance of the radiant panel heater position. The heater is positioned along a center line extending from the back of the room to the front of the room. For the purposes of comparison, the position where the heater center is 20 percent of the distance from the back wall is considered the base case. The heater is sized to provide the design average  $T_{op}$  of 72°F (22°C). Once the heater power is established, it remains constant for each position of the heater.

### 3.2.1 Design Step 1: Specify Design Conditions

The design conditions for this room are predominately listed in Table 3.1. The target average  $T_{op}$  with an outdoor temperature of -4°F (-20°C) is 72°F (22°C). For the purposes of the design procedure, the  $T_{op}$  is averaged over an area that is 3 ft above the floor of the room.

### 3.2.2 Design Step 2: Select the Heater for This Application

The heater for this application is a radiant panel heater centrally positioned from left to right, but only 20 percent of the distance from the front to the back (refer to Fig. 3.4). The heater chosen for this example is a 3 × 3 ft heater panel.

### 3.2.3 Design Step 3: Determine the Heater Power Necessary to Meet the Design $T_{op}$

The heater power is determined in exactly the same manner as with the previous demonstration case. First, two heater power levels are chosen, and then the average  $T_{op}$  over an area that is 3 ft above the floor is calculated. Using ABOVE, the results from these steps are:

$$\begin{aligned}\dot{P}_1 &= 1350 \text{ W} & T_{op,1} &= 61.5^\circ\text{F} \\ \dot{P}_2 &= 1900 \text{ W} & T_{op,2} &= 82.7^\circ\text{F}\end{aligned}$$

The actual heater power needed to satisfy the design conditions is, then, calculated by:

$$\begin{aligned}\dot{P}_a &= \left[ \frac{T_{op,d} - T_{op,1}}{T_{op,2} - T_{op,1}} \right] (\dot{P}_2 - \dot{P}_1) + \dot{P}_1 \\ &= \left[ \frac{72.0^\circ\text{F} - 61.5^\circ\text{F}}{82.7^\circ\text{F} - 61.5^\circ\text{F}} \right] (1900 \text{ W} - 1350 \text{ W}) + 1350 \text{ W} \\ &= 1622 \text{ W}\end{aligned}$$

The final step in determining the power is to recalculate the average OT with the 1622 W. The result is, as expected, precisely 72°F (22.2°C).

*Note.* A 3 × 3 ft heater designed for 8-ft ceiling applications will generally have a power density of no more than 50 to 60 W/ft<sup>2</sup>. Consequently, the heater for this application will have to be much larger. However, it is instructive to observe the impact of a ceiling radiant panel heater that is 180 W/ft<sup>2</sup>.

### 3.2.4 Design Step 4, Attempt 1: Evaluate the OT Distribution Within the Room

At this point, it is important to evaluate the OT distribution within the room. Even though the *average* OT across the room is at the design guideline, the OT gradients may be too severe to provide an acceptable level of thermal comfort.

Figure 3.5 shows the Thermal Comfort Signature that represents this particular radiant panel heater in this particular room. The TCS shows the OT distribution at the 3-ft elevation above the floor. Although the radiant panel heater maintains an acceptable level of comfort in certain areas around the heater, some designers may decide that the  $T_{op}$  gradients are too steep as one moves away from the heater. The  $T_{op}$  gradients are shown in Fig. 3.5 by how close the contour temperature lines are to each other. The closer the lines, the steeper the temperature gradients. Referring to Fig. 3.5, the temperature of the back wall changes rapidly as one moves from the top center of the wall toward the floor. This rapid change represents a steep temperature gradient. In contrast, the surface temperature of the right wall changes very little from back to front. Hence, the temperature gradient of the right wall is relatively small. In this case, the difference between the high and low  $T_{op}$  within the TCS is 12°F (6.7°C).

There are several alternative configurations that can be employed to reduce the severity of the  $T_{op}$  gradients. The first that is investigated is repositioning the heater along a line from the back to the front of the room. Figure 3.6 illustrates the impact of heater position on the average  $T_{op}$  and on the  $T_{op}$  gradient. The heater is first placed on the ceiling very close to the outside wall. The heater is then moved progressively farther from the wall. Figure 3.6 shows the OT field that is created with

## 8.34 ENGINEERING DESIGN TOOLS TO ASSIST IN HEATER-COOLER SIZING

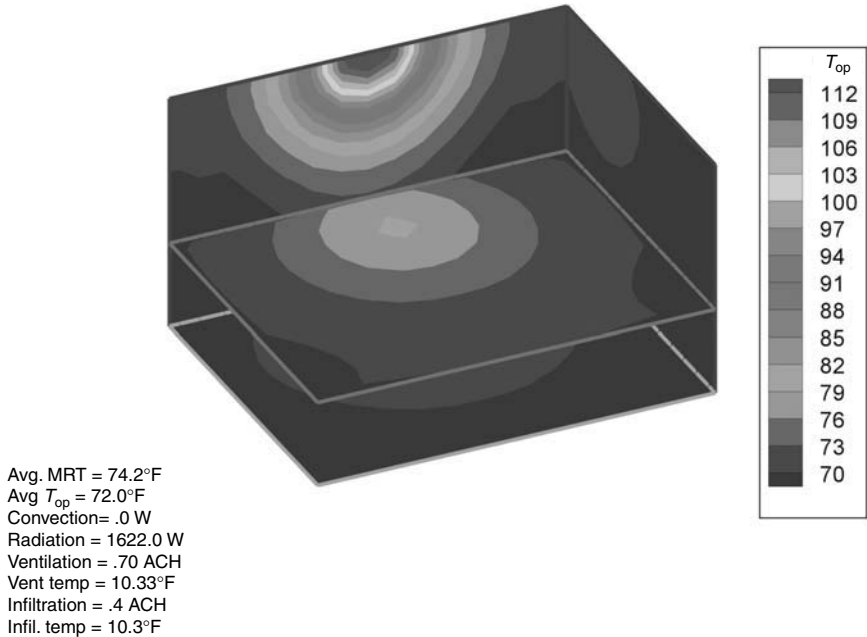


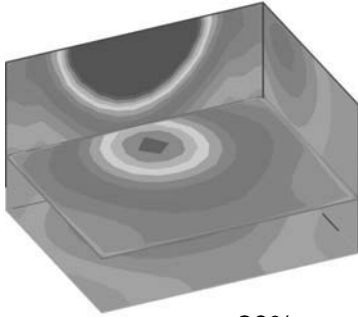
**FIGURE 3.5** Results from the base case where the center of the heater is positioned 20 percent of the distance from the back wall.

each of the four cases. The first case, where the heater is closest to the window, shows that the effect is to warm the area just in front of the window. As the heater is moved farther from the window, the illustration shows how the OT field changes. Of note is that the area just in front of the wall becomes somewhat less comfortable, whereas the impact or potentially adverse impact under design conditions of the window becomes less pronounced deeper into the room. Also noticeable is that the  $\Delta T_{op}$  at the 3-ft elevation becomes slightly larger as the heater is moved from the window toward the front of the room. The conclusion is that the heater is best placed in the vicinity of the relatively cold area to reduce the  $T_{op}$  gradients and, therefore, enhance occupant thermal comfort.

### 3.2.5 Design Step 4, Attempt 2: Evaluate the OT Distribution Within the Room

A second alternative is to select an entirely different heater system, namely, one that comprises two heaters with a total power output equal to the single heater and, therefore, with a proportional lowering of the heater power density. The positioning and subsequent results are illustrated in Fig. 3.7. One heater is positioned near the window, and a second heater is positioned toward the middle of the room.

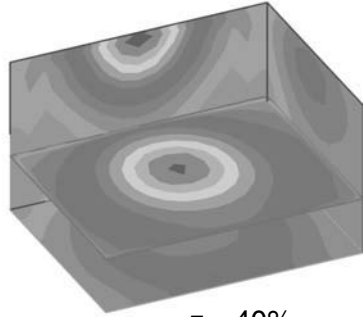
From Fig. 3.7, it is apparent from the TCS that this configuration provides more uniform  $T_{op}$  and, therefore, a more uniform distribution of occupant thermal than those in Fig. 3.6. Using two radiant panel heaters as opposed to one radiant panel



$$z = 20\%$$

$$T_{op} = 72^\circ \text{ F}$$

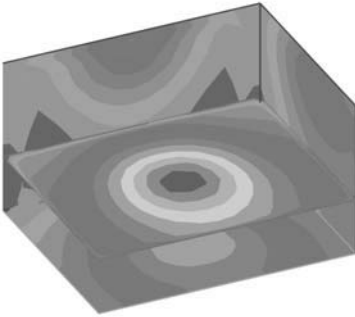
$$\Delta T_{op} = 12^\circ \text{ F}$$



$$z = 40\%$$

$$T_{op} = 73.2^\circ \text{ F}$$

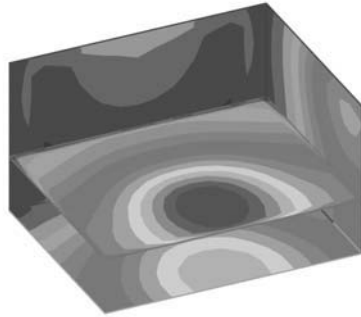
$$\Delta T_{op} = 12.7^\circ \text{ F}$$



$$z = 50\%$$

$$T_{op} = 73.5^\circ \text{ F}$$

$$\Delta T_{op} = 13^\circ \text{ F}$$



$$z = 70\%$$

$$T_{op} = 73.5^\circ \text{ F}$$

$$\Delta T_{op} = 17^\circ \text{ F}$$

**FIGURE 3.6** Impact of heater location on OT field.

heater creates a difference between the high and low  $T_{op}$ , which along the TCS is  $6^\circ\text{F}$  ( $3.3^\circ\text{C}$ ), while maintaining an average OT of  $72^\circ\text{F}$  ( $22.2^\circ\text{C}$ ). In contrast, the difference between the high and low  $T_{op}$  in Fig. 3.6 is between  $12^\circ\text{F}$  ( $6.7^\circ\text{C}$ ) and  $17^\circ\text{F}$  ( $9.4^\circ\text{C}$ ), depending on the location of the radiant panel.

One final comment on this analysis is directed toward the utility of a direct radiation solver. Looking at the bottom panel in Fig. 3.7, one sees how the heaters create a thermal comfort profile that is directional in nature. Additionally, this figure shows the actual flow of radiant energy from the heater to other parts of the room. The flow of radiant energy is represented by the arrows that leave the heater surfaces and disperse throughout the room. Longer arrows represent regions of more intense radiant energy. A goal is to design the heating system so that the arrows are relatively short in occupancy regions.

Again, because this analysis program solves the fundamental form of the radiant transfer equation, the user does not have to input things such as view factors and profiles that represent the assumed shape of how radiant energy leaves the surface

## 8.36 ENGINEERING DESIGN TOOLS TO ASSIST IN HEATER-COOLER SIZING

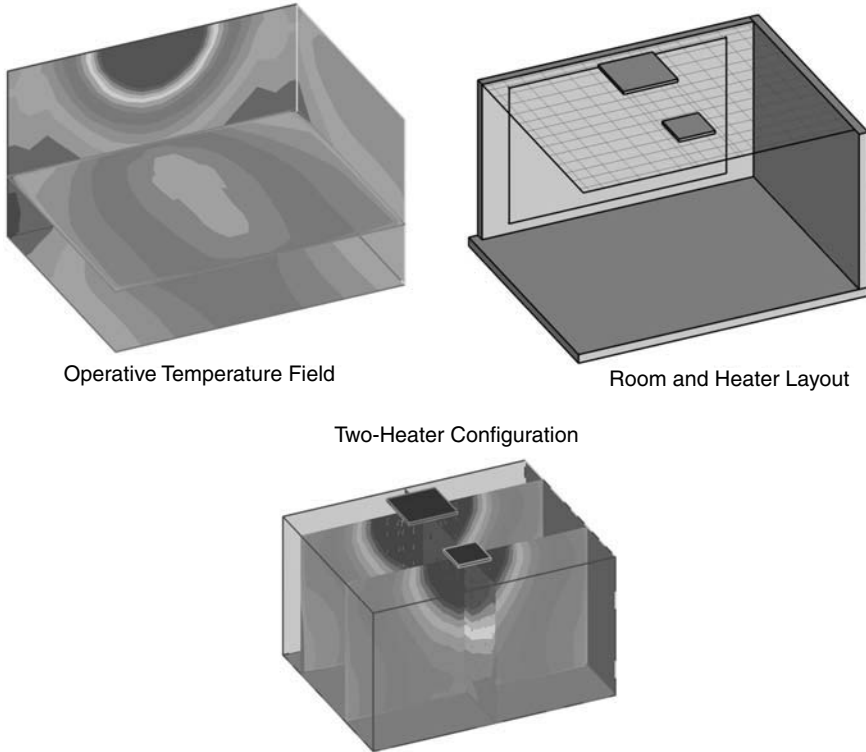


**FIGURE 3.7** Layout and results from the two-heater configuration.

of a heater. Instead, the direct radiation solver determines the radiant flow path as a direct consequence of solving the most fundamental equations. This leaves the designer free to focus on which radiant panel design and panel power density provides the specified occupant thermal comfort profile under the conditions defined.

### 3.3 HEATER POWER AND INDOOR TEMPERATURE

This demonstration considers a simple room with three walls exposed to the outside. The remaining wall and the ceiling and floor are interior walls. The surrounding temperatures above the ceiling, below the floor, and outside of the back wall are 69.8°F (21°C). The remaining walls experience the outside temperature. All walls exhibit an  $R$  value of 2.5. Two-heater configurations are used in this example, one that will accommodate an outdoor temperature of 41°F (5°C) and a second configuration that will accommodate an outdoor temperature of 14°F (-10°C). The goal is to see how the heater power changes to maintain an MRT of 71.6°F (22°C). The heater, in this case, is a simple convective heater. The point is to demonstrate that radiation heat transfer plays a significant role even for conventional heating systems.

The first case utilizes the outdoor temperature of 41°F (5°C). The heater is sized at 245.60 W to achieve an average MRT of 71.6°F (22°C). The second case, which uses an outdoor temperature of -10°C, requires a heater of 669.6 W to maintain the average MRT at 71.6°F (22°C). For the first case, the average room dry-bulb air temperature is 72.57°F (22.54°C), and for the second colder case, the room air temperature is actually 1°C higher at 74.37°F (23.54°C). At first, one may think that the indoor dry-bulb air temperature should be lower when the outdoor temperature is lower. The following analysis explains why the air temperature is higher for the colder case.

The resulting MRT distribution at a height of 0.9 m from the floor is illustrated in Fig. 3.8. The top panel shows the first case [41°F (5°C)], and the bottom panel shows the second case [14°F (-10°C)]. In each case, the MRT is higher toward the back of

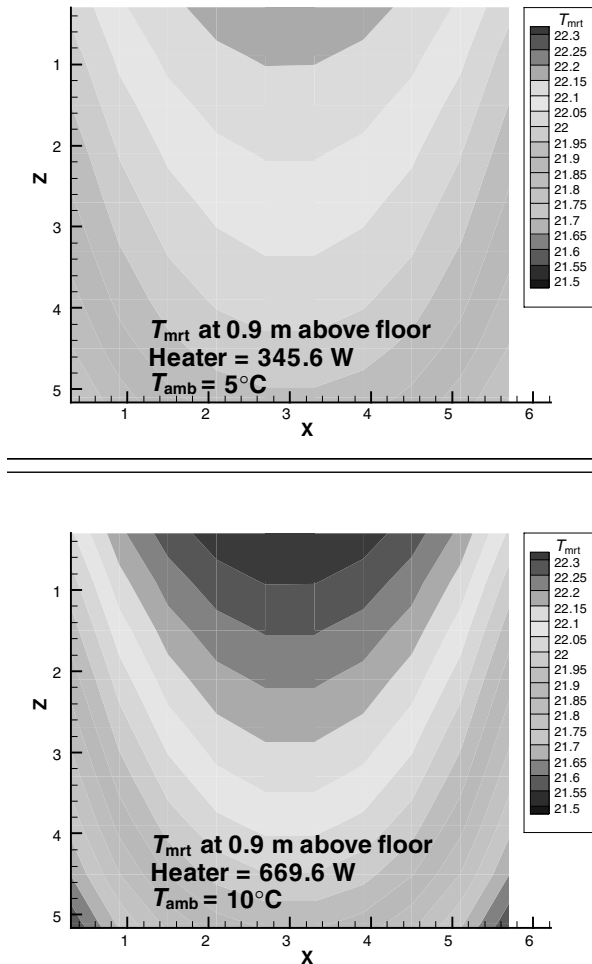


**FIGURE 3.8** Mean radiant temperature distribution as a function of heater power and outdoor temperature.

8.38 ENGINEERING DESIGN TOOLS TO ASSIST IN HEATER-COOLER SIZING

the room and decreases as one moves away from the center of the back wall toward the front of the room. This is expected as the front and side walls are exposed to the outdoor temperature, and the back wall is exposed to an adjacent temperature of 69.8°F (21°C).

Comparing the two cases shows that even though the average MRT is the same, the first case exhibits a more uniform MRT distribution. To find the reason for this, the wall surface temperatures are shown in Fig. 3.9. Again, the top panel shows the first (warmer) case, and the lower panel shows the second (colder) case. As illustrated, the warmer case exhibits warmer walls, and the cooler case exhibits cooler walls. The net effect should be to lower the room air temperature for the cooler case below that of the warmer case. This result is contradictory, however, to the stated increase in air temperature for the colder case.

Investigating further, Fig. 3.10 shows the surface temperature distribution of the ceiling (which should be the same as that of the floor because the room is symmetrical). In this case, the ceiling exhibits a higher surface temperature for the colder case than for the warmer case. Because the surfaces of the ceiling and floor areas are larger than the surface areas of the side walls, the net effect of heat exchange between the ceiling, floor, and two walls and the air will be higher for the colder case than for the warmer case.

A second way to look at this problem is to consider how the surface temperatures of the three exterior walls and the three nonexterior surfaces (floor, ceiling, and back wall) will change for each case. The exterior walls will be cooler for the colder

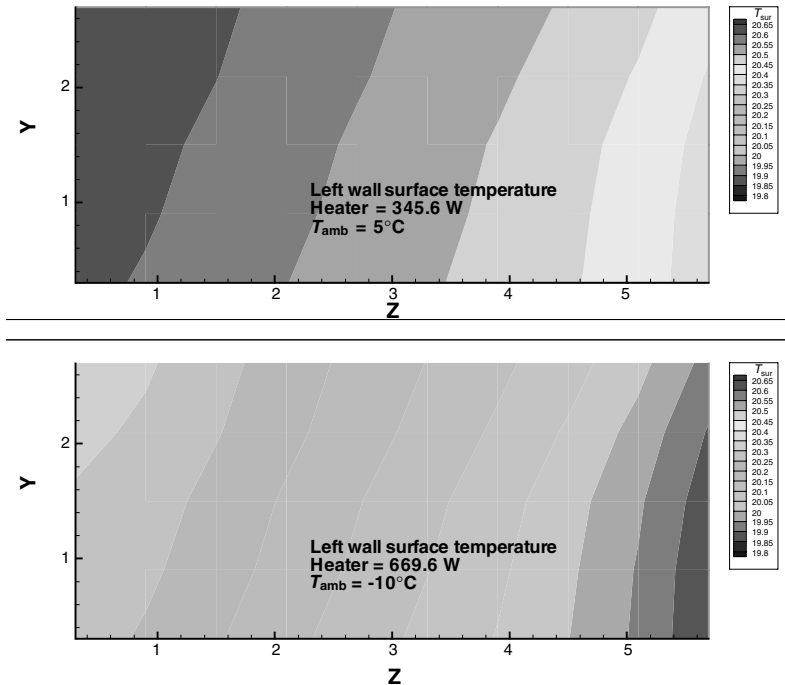
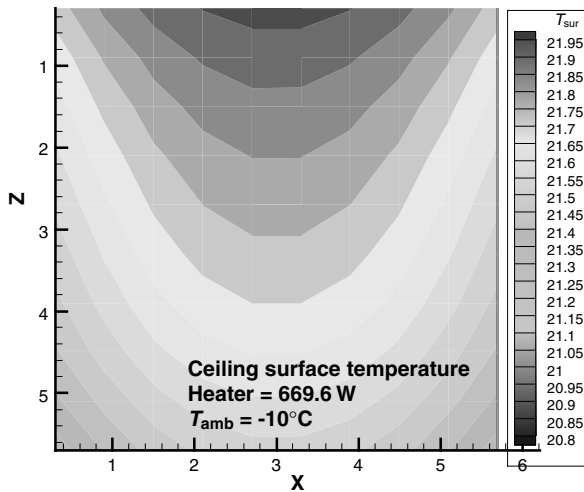
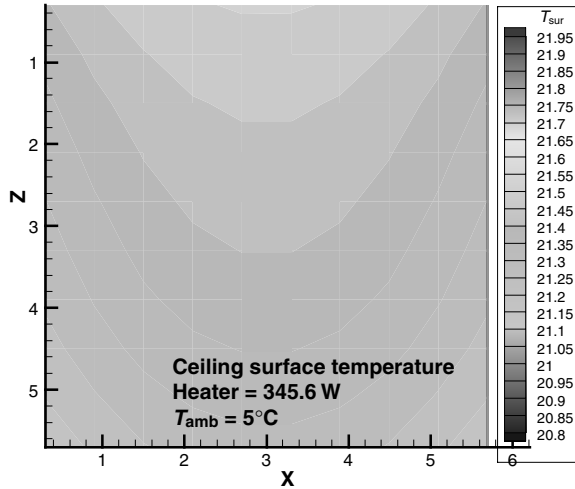


FIGURE 3.9 Wall surface temperatures as a function of heater power and outdoor temperature.



**FIGURE 3.10** Ceiling surface temperatures as a function of heater power and outdoor temperature.

(second) case than for the first case because of the colder outside temperature. Because these temperatures contribute directly to the MRT distribution in the room, the net effect from the cooler exterior walls is to lower the average MRT. Consequently, for the average MRT to stay the same between the two cases, something must happen to increase the temperatures of the nonexterior walls to offset this decreasing effect of the exterior walls. The only way to increase the temperature of the nonexterior walls is to increase the heat transfer through these walls.

**8.40** ENGINEERING DESIGN TOOLS TO ASSIST IN HEATER-COOLER SIZING

The two modes of heat transfer to the nonexterior walls are radiation from the surrounding walls and convection from the room air. The radiation heat transfer rate should be lower because the exterior wall temperatures are lower. Again, this is an effect that will tend to lower the temperature of the nonexterior walls, which, in turn, will lower the average MRT. Because of all these offsetting effects, the convection heat transfer rate to the nonexterior walls for the colder case must be significantly higher than for the warmer case. We know that this must be true because:

1. These walls are the only possible way to offset the decrease in MRT from the exterior walls.
2. The radiation heat transfer rate to the nonexterior walls is lower for the cold case because the surrounding walls are colder.

Finally, there are only two ways to increase convection heat transfer to the nonexterior walls:

1. Increase the room air temperature
2. Decrease the temperature on the other side of the walls

Because the adjacent temperature stays the same, the air temperature in the room must increase in order for the average MRT to remain the same between the two cases. Figures 3.9 and 3.10 verify this explanation.

### **3.4 POWER DENSITY VERSUS HEATER AREA**

---

This example demonstrates the differences in spreading the heater power over a small or large area. A radiant panel heater can be specified such that the power output is 1000 W spread over several hundred square feet or an area that is half that size, or other combination and power density based upon the particular radiant panel design and power density options. The designer is encouraged to refer to Sec. 5 of this Handbook to review the many radiant panel design options that encompass the full variety of available energy sources and panel locations.

This case compares the efficiency of a concealed electric radiant panel with smaller, higher-power density radiant panel heaters positioned on the ceiling throughout the room. The target  $T_{op}$  for this example is 61°F (16.1°C) and represents a large enclosure that is 30 × 30 ft with a 12-ft ceiling. The outside temperature is 14°F (−10°C). Figure 3.11 illustrates the room structure of the concealed electric radiant panel in the ceiling. To closely simulate real life, the concealed panel heater comes within 1 ft of each wall and is not insulated on the back side of the ceiling with the exception of the ceiling itself. The dimensions and other pertinent room structure are provided in Table 3.1. The layout of the other four heater cases are illustrated in Fig. 3.12. The difference between these cases and the concealed radiant panel heater is that the power input from the cases illustrated in Fig. 3.12 comes from four radiant panel heaters positioned in each quadrant of the room. The only difference between each four-heater case is that the heater size is reduced and, therefore, the heater power density increases proportionally. Each heater power density and size is provided in Fig. 3.12.

Concealed ceiling electric radiant heater panels are usually limited to 14 W/ft<sup>2</sup>. The calculations from ABOVE show that a power density of 11.33 W/ft<sup>2</sup> is needed to achieve an average  $T_{op}$  over the TCS of 61°F (16.1°C). Multiplying the power density

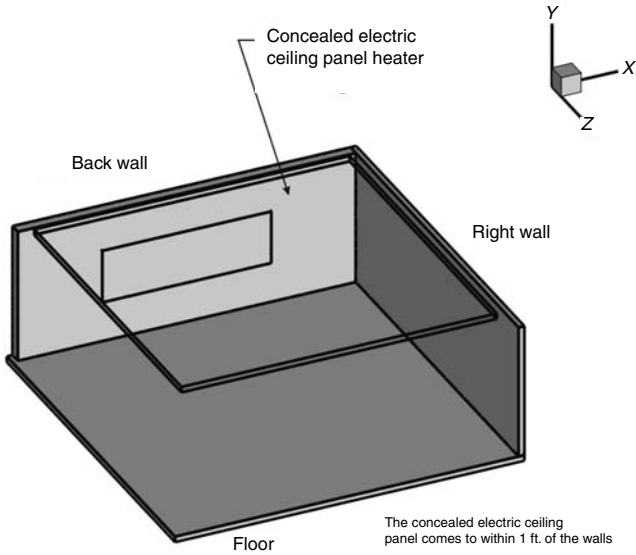


**FIGURE 3.11** Schematic showing the room structure for a concealed electric radiant heater.

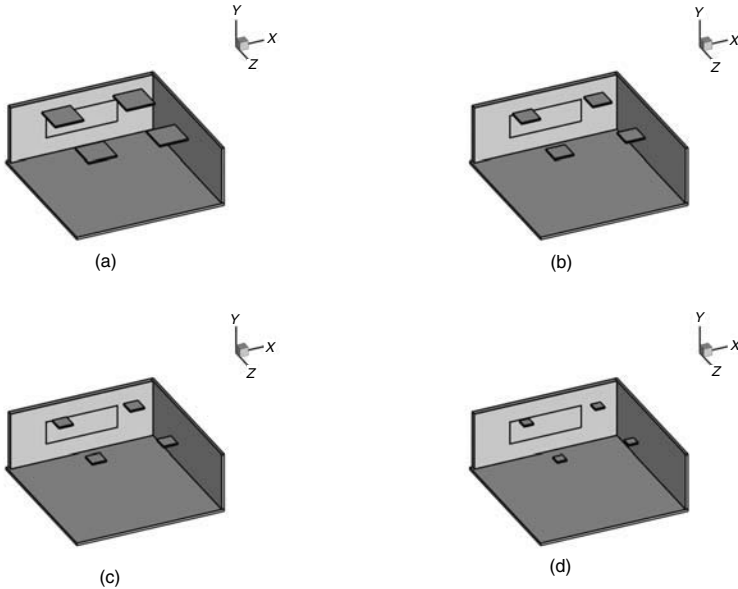


**FIGURE 3.12** Room structure showing the four-heater configuration and heater power density. (a)  $6 \times 6$  ft,  $26.5 \text{ W/ft}^2$ ; (b)  $4 \times 4$  ft,  $60 \text{ W/ft}^2$ ; (c)  $3 \times 3$  ft,  $106 \text{ W/ft}^2$ ; (d)  $2 \times 2$  ft,  $239 \text{ W/ft}^2$ .

8.42 ENGINEERING DESIGN TOOLS TO ASSIST IN HEATER-COOLER SIZING

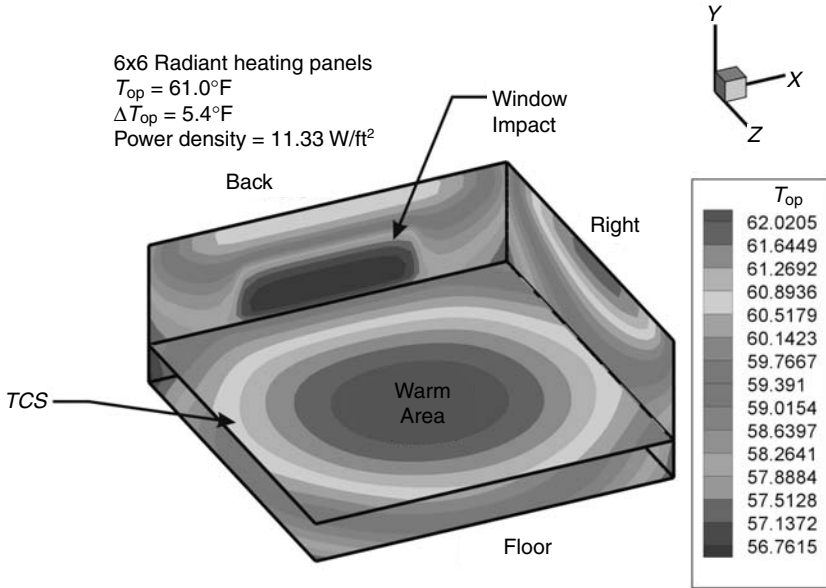


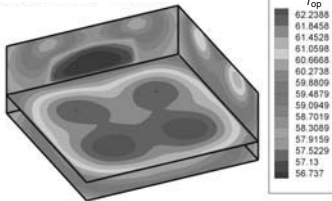
**FIGURE 3.13** Operative temperature field for the imbedded ceiling electric heaters powered at  $11.3 \text{ W/ft}^2$ .

of  $11.33 \text{ W/ft}^2$  by the heated surface area ( $28 \times 28 \text{ ft}$ ) provides a total power input of  $8883 \text{ W}$ . The results from ABOVE are shown in Fig. 3.13. There is nothing spectacularly surprising about the TCS for the concealed radiant panel. As expected, the center of the room is the thermally warmest portion, and the  $T_{op}$  along the TCS decreases near the walls. The impact of the cooler window is seen by the depressed  $T_{op}$  near the back of the room. As a measure of the OT gradient across the TCS, the difference between the maximum and minimum  $T_{op}$  at the 3-ft elevation is  $5.4^{\circ}\text{F}$  ( $3.0^{\circ}\text{C}$ ).

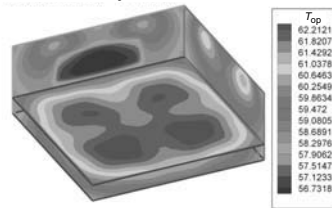
Figure 3.14 illustrates the TCS for the each of the four cases where four radiant panel heaters were used to achieve the design OT conditions. In each of the four cases, the total power added to the room was  $3816 \text{ W}$ , which is in stark contrast to the  $8883 \text{ W}$  necessary for the concealed panel heater in Fig. 3.13. This power input of watts is only 43.0 percent of the power that is necessary for the concealed panel heater. As mentioned previously, the entire ceiling acts as one large heat panel. These were oversized in the example because they experience edge- and backloss, but in practice they would also be oversized to compensate for the start-up thermal lag. The radiant panels used to produce the results in Fig. 3.14, on the other hand, are insulated on the back to prevent substantial backlosses through the ceiling.

There is at least one interesting observation by comparing the four cases in Fig. 3.14. Starting with the TCS in the top left panel that is produced by  $6 \times 6 \text{ ft}$  heaters with a power density of  $26.5 \text{ W/ft}^2$ , there is a distinct area under each heater that is thermally warmer than the areas in the rest of the room. The window along the back wall of the room cools the area near the back of the room. Also apparent from Fig. 3.14 is that the radiant panel heaters create areas of higher temperature on the walls

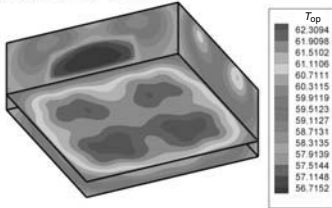
6 x 6 Radiant heating panels  
 $T_{op} = 61.3^{\circ}\text{F}$   
 $\Delta T_{op} = 5.0^{\circ}\text{F}$   
 Power density = 26.5 W/ft<sup>2</sup>



4 x 4 Radiant heating panels  
 $T_{op} = 61.4^{\circ}\text{F}$   
 $\Delta T_{op} = 4.8^{\circ}\text{F}$   
 Power density = 60.0 W/ft<sup>2</sup>



3 x 3 Radiant heating panels  
 $T_{op} = 61.4^{\circ}\text{F}$   
 $\Delta T_{op} = 5.2^{\circ}\text{F}$   
 Power density = 106.0 W/ft<sup>2</sup>



2 x 2 Radiant heating panels  
 $T_{op} = 61.4^{\circ}\text{F}$   
 $\Delta T_{op} = 5.3^{\circ}\text{F}$   
 Power density = 239.0 W/ft<sup>2</sup>

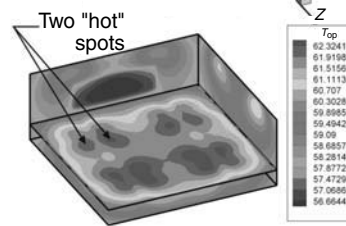


**FIGURE 3.14** TCS created by replacing the concealed radiant panel with four 6 x 6 ft radiant panels of various sizes and power densities.

near the ceiling. These warmer areas will then reemit radiant energy into the room to augment the  $T_{op}$  in areas near these surfaces. The difference between the maximum and minimum  $T_{op}$  is 5.0°F (2.8°C), which is, surprisingly, 0.4°F (0.22°C) less than for the concealed radiant panel. The reason for this is that the concealed radiant panel focuses most of its radiant energy into the symmetrical region in the center of the room. Because this region does not see the walls as easily as the regions toward the exterior portions of the room, the MRT is less affected by the wall surface temperatures. Similarly, the concealed radiant panel is at a lower temperature near the exterior walls of the room and, therefore, does not have as large of an impact on the occupied areas near the exterior walls. The highest  $T_{op}$  in the concealed case is 62°F (16.7°C), and the lowest  $T_{op}$  is 57.0°F (13.9°C).

The distributed system, on the other hand, actually focuses the bulk of its radiant energy in areas that are near the exterior walls. Because of this placement, the exterior portions of the room that exhibited a cooler  $T_{op}$  in the concealed case now exhibit a slightly higher  $T_{op}$  for the distributed case. The high and low  $T_{op}$  for the distributed case are 62.6°F (17.0°C) and 57.6°F (14.2°C), respectively. Of note is that the highest  $T_{op}$  from the distributed case is 0.2°F (0.11°C) greater than the high  $T_{op}$  for the concealed case, but the lowest  $T_{op}$  for the distributed case is 0.6°F (0.33°C) greater than the low  $T_{op}$  for the concealed case.

**8.44** ENGINEERING DESIGN TOOLS TO ASSIST IN HEATER-COOLER SIZING

Comparing the four TCSs in Fig. 3.14 shows an interesting trend in the difference between the high and low  $T_{op}$  and in the shape of the TCS. First, it is interesting to note that the lowest difference between the high and low  $T_{op}$  is for the case of the  $4 \times 4$  ft heaters with a power density of  $60.0 \text{ W/ft}^2$ . This trend suggests that there is an optimum power density and/or heater size that provides the design level of  $T_{op}$  that also minimizes the  $T_{op}$  gradient within the TCS. The second observation is that as the power density increases, the thermally warm spot under the heater begins to separate into two hot spots. The reason for this is that the smaller, higher-power density heaters focus an increased amount of energy on a smaller area within the room and within TCS. At the same time, the wall surface near the heater also increases. This increased wall temperature then reemits radiant energy into the occupied space. The combination of the radiant energy from the heater and from the wall creates a second warm spot where one might normally expect only one. A similar observation can be seen if a portion of the wall surface is reflective, such as with a large mirror.

### 3.5 RADIANT COOLING PANEL

---

Radiant cooling panels may be located on the floor, wall, or ceiling. The risks of condensation and the limits of occupant thermal comfort bound them. The examples demonstrate the percentage of cooling that can be handled radiantly under several different conditions. The balance of cooling may be addressed in whatever way is most appropriate for the geographic area and building usage design. In some areas, the primary role of radiant floor cooling is the removal of solar gain from the building mass. The balance of space conditioning may be accomplished through the normal ventilation required for maintaining indoor air quality if the outside temperature is moderate. Wherever hydronic radiant heating panels are employed, radiant cooling is an option to be explored.

In stark contrast to the examples of radiant heating, this demonstration considers the capabilities of providing radiant cooling. At first, it may seem unnatural to provide radiant cooling. After all, radiant panels appear to be panels that deliver radiant heat to the occupied space. Radiant cooling panels do just the opposite in that they lower the MRT and, therefore, make the occupant feel thermally comfortable by radiantly removing energy from the occupied space. To accomplish this task, the radiant cooling panel must be at a lower surface temperature than the surrounding spaces so as to create an environment that has a net absorption rate rather than a net emission rate of radiant energy.

Figure 3.15 illustrates a room with eight  $2 \times 2$  ft radiant cooling panels mounted on the ceiling. These panels are cooled by relatively cold water to radiatively cool the occupied space. The potential problem with a radiant cooling panel is that the panel surface temperature may become lower than the dew point temperature of the air in the room.

The dew point temperature is a function of the relative humidity and the pressure within the room. In most cases, the ambient pressure will be 29.92 inHg. The dew point temperature is seen in practical situations when pipes carrying cold water sweat in the summer. The concept is that the air contains sufficient moisture such that it condenses when the air comes into contact with a cold surface. In humid climates, condensation can occur on the outside of window panes. Again, as with the water pipes, the outside of the window is sufficiently cooled such that the moisture in the outside air condenses on the outside of the window pane.

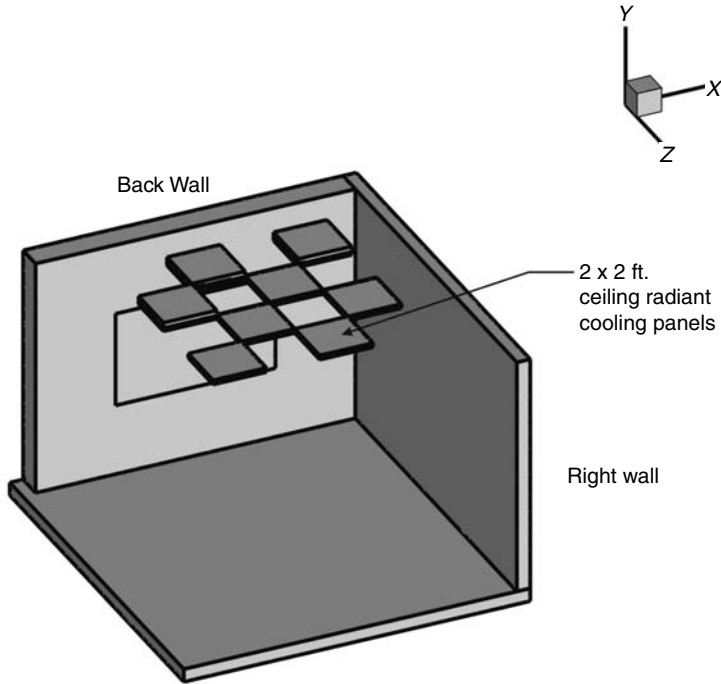


**FIGURE 3.15** Layout of radiant cooling panels.

So, just how cold can surfaces become before condensation becomes a problem? Fortunately, there are straightforward equations that can be used to answer this question.

This first step is to gain a clear understanding of the problem. To do this, consider the afternoon conditions in, for example, Manhattan, Kansas, during August. The dry-bulb temperature is 100°F (37.8°C), and the relative humidity is 40 percent at 100°F (37.8°C). For this particular scenario, the amount of moisture in the air is approximately 0.017 lbm water/lbm air. This term is called the *humidity ratio* and is designated by the Greek symbol  $\omega$ . The only way to change the humidity ratio is to add or subtract water from the air. Conversely, the relative humidity changes with air temperature, hence, the word *relative*. To grasp the fact that the relative humidity changes with temperature, let us cool the afternoon air to 90°F (32.2°C). We have done nothing to change the humidity ratio of the air, so it is still 0.017 lbm water/lbm air. The relative humidity, however, increases to about 56 percent. This leads one to believe that as the air is cooled with a constant humidity ratio, there is some temperature at which the relative humidity reaches 100 percent. In our example, the temperature at which the relative humidity is 100 percent is 72°F (22.2°C).

The question now is, What happens if the air is cooled to a temperature below 72°F (22.2°C)? Because we cannot have a relative humidity above 100 percent, the only possible solution is that some of the moisture must condense from the air. This is precisely what happens when moisture condenses on the outside of a cool window pane or water condenses on the cold-water pipes in a house. The surface tempera-

**8.46** ENGINEERING DESIGN TOOLS TO ASSIST IN HEATER-COOLER SIZING

ture is lower than the condensation temperature and, therefore, the moist air in the vicinity of the cold surface loses liquid water to the cold surface.

To put some numbers to these calculations, we must first define some parameters. The first two parameters are the relative humidity and the humidity ratio. In equation form, these parameters are defined as:

$$\omega = \frac{0.622p_v}{p - p_v} \quad \text{Humidity ratio} \quad (3.1)$$

$$\phi = \frac{p_v}{p_{\text{sat}}(T)} \quad \text{Relative humidity} \quad (3.2)$$

The term  $p$  is the barometric pressure, the term  $p_v$  is the vapor pressure, and the term  $p_{\text{sat}}$  is the saturation pressure at the dry-bulb temperature. The barometric pressure and the dry-bulb temperature generally are known. The saturation pressure is strictly a function of temperature and is approximated by the following curve fit to experimental data:

$$p_{\text{sat}}(T) = 0.8159 - 2.6243 \times 10^{-2}T + 2.78113 \times 10^{-4}T^2$$

$$T \rightarrow \text{°F} \quad (3.3)$$

$$p_{\text{sat}} \rightarrow \text{psia}$$

The only remaining unknown is the vapor pressure,  $p_v$ , which is a function of how much moisture is contained in the air. Assuming that one can measure either relative humidity or the humidity ratio, the vapor pressure can be used to calculate the dew point temperature of the air. This is accomplished with either Eq. (3.1) or Eq. (3.2):

$$p_v = \frac{p\omega}{0.622 + \omega} \quad (3.4)$$

$$p_v = \phi p_{\text{sat}}(T) \quad (3.5)$$

Once  $p_v$  is calculated, the dew point temperature is determined by:

$$T_{\text{dp}} = 37.908 + 91.4305p_v + -25.8623p_v^2$$

$$p_v \rightarrow \text{psia} \quad (3.6)$$

$$T_{\text{dp}} \rightarrow \text{°F}$$

The significance of Eq. (3.6) is that if any surface in the room is lower than the dew point temperature, then one should expect condensation on that surface. In our particular example, if the air temperature is 100°F (37.8°C) at a relative humidity of 40 percent, then any surface that is lower than 72°F (22.2°C) will produce condensation.

In humid climates, condensation presents a major obstacle for radiant cooling applications. If one desires to produce an  $T_{\text{op}}$  of 72°F (22.2°C), then it is mandatory that the panel surface temperature be lower than 72°F (22.2°C). As demonstrated by our simple example, panel temperatures lower than 72°F (22.2°C) will produce copious quantities of condensation that can severely damage interior furnishings.

The moral of the story is that when designing a radiant cooling panel installation, one must consider the possibility of condensation. Fortunately, the methodologies developed in this Handbook apply equally to cooling scenarios as they do to heating scenarios. Referring again to Fig. 3.15, the power applied to the cooling panels is necessarily negative so that heat is removed from, rather than supplied to, the room. Figure 3.16 illustrates the TCS that is developed if each radiant cooling panel illustrated

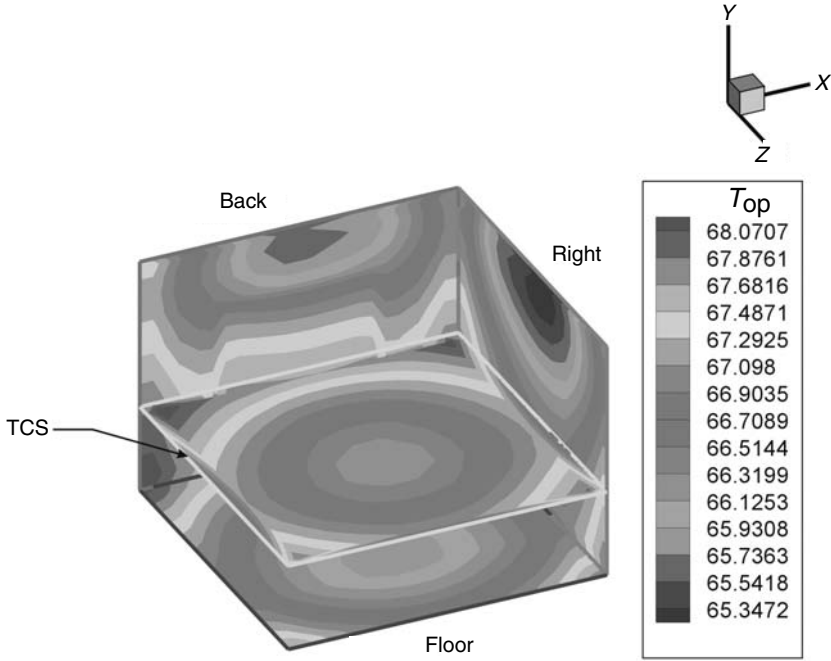


FIGURE 3.16 Operative temperature distribution created by the radiant cooling panels.

in Fig. 3.15 removes 56 W of heat from the room. The radiant cooling panels are cooled to provide an average TCS of 70°F (21.1°C). Although the TCS looks to be very uniform [the difference between the high and low  $T_{op}$  is less than 2°F (1.11°C)], the next step is to determine if any of the panel surface temperatures are below the dew point temperature. For this particular example, we will assume that the dew point temperature is 66°F (18.9°C). Figure 3.17 illustrates the temperature of the

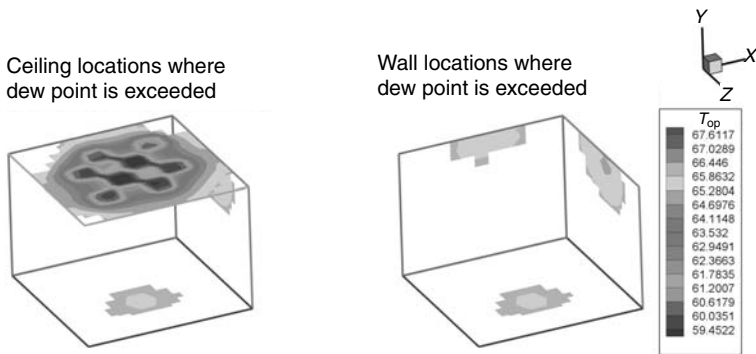


FIGURE 3.17 Portrayal of the ceiling and wall surface temperatures showing potential problem areas for condensation.

## 8.48 ENGINEERING DESIGN TOOLS TO ASSIST IN HEATER-COOLER SIZING

ceiling, walls, and floors, including the radiant cooling panels. The shaded areas are those where the surface temperature is lower than the dew point temperature. Of interest is that room surfaces other than the radiant cooling panels are cooled below the dew point temperature. Because of this, this particular radiant panel installation will not be acceptable unless the dew point temperature can be lowered through a dehumidification system.

The conclusion is that radiant cooling panels contain an additional level of design complexity. It is important for the designer to consider the dew point of the occupied space and the surface temperature of the radiant cooling panels, as well as the surface temperature of other surfaces in the room.

### 3.6 WALL SURFACE COATINGS

---

One concept that often puzzles the designer and the consumer alike is how the surface emissivity in the enclosed space impacts thermal comfort and energy consumption. The standard ASHRAE tables present the radiation emissivity of common building materials. Well-developed information is also available on a variety of building envelope constructions. In the process of refining an understanding of the building as a system, considerable research has been conducted on the role of radiant heat transfer and rejection through the use of radiant barriers. It is now common building practice to evaluate the role of reflectivity, transmissivity, and emissivity in optimizing building heating and cooling loads.

Within the built environment, Brookhaven Laboratory's John W. Andrews and J. H. Saunders conducted a project, "The Effect of Wall Reflectivity on the Thermal Performance of Radiant Heating Panels." The research developed several charts that show potential energy savings with various room surfaces, various infiltration rates, and relevant temperature readings. The results shown in these charts coincide with output from ABOVE, which uses the BCAP methodology.

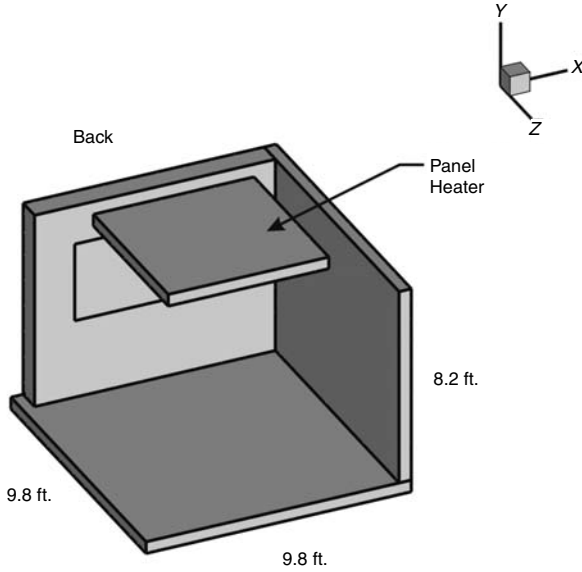
To shed some light on the concept of surface emissivity, this demonstration examines the energy consumption and the TCS for the room and heater shown in Fig. 3.18. The heater is positioned in the center of the ceiling, and a window is centered on the back wall of the room. The emissivity and  $R$  value of the window remain constant throughout this demonstration at  $\epsilon = 0.6$  and an  $R$  value of 2.

The first calculation was completed with all surfaces exhibiting an emissivity equal to 1.0. Note that this is not too far removed from the real case where the surface emissivity ranges from 0.85 to 0.90. From the base case, a heater power of 1000 W was necessary to achieve an average  $T_{op}$  of 61.3°F (16.3°C).

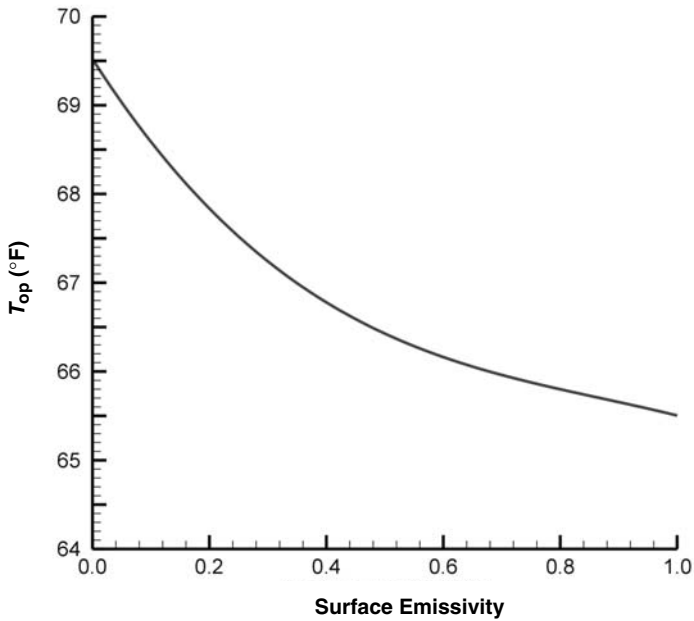
Using an emissivity of 1.0 as the benchmark, the case was repeated with surface emissivities of 0.8, 0.6, 0.4, 0.2, 0.1, and 0.005. All surfaces except the ceiling, the heater surface, and the window were changed to these values. This series of calculations was completed twice, first holding the heater power constant at 1000 W and then holding the OT constant at 61.3°F (16.3°C).

Figure 3.19 shows the results of the first set of calculations. The figure illustrates the variation of  $T_{op}$  with surface emissivity. As the surface emissivity decreases, the OT increases, but at the same rate that the emissivity decreases. Of interest is that the OT changes very little between an emissivity of 1.0 and about 0.50. Any true gain in OT is seen only for very small emissivities.

Figure 3.20 shows the results of the second set of calculations. This figure illustrates the savings in power that could be achieved if the surface emissivities were reduced with a constant  $T_{op}$  of 61.3°F (16.3°C). The key observation from this figure



**FIGURE 3.18** The room structure and heater position used to investigate the impact of surface emissivity on thermal comfort and energy consumption.



**FIGURE 3.19** Impact of surface emissivity on OT with constant power input.

## 8.50 ENGINEERING DESIGN TOOLS TO ASSIST IN HEATER-COOLER SIZING

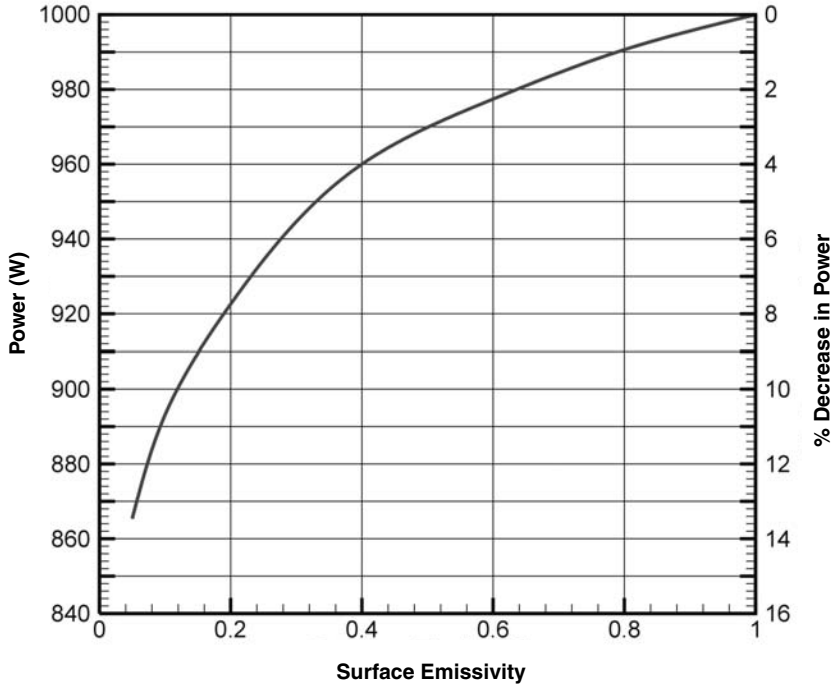


**FIGURE 3.20** Impact of surface emissivity on power input to maintain a constant  $T_{op}$  of 61.3°F (16.3°C).

is that reducing the surface emissivity from 1.0 to 0.6 would produce a power savings of about 2.2 percent. Reducing the surface emissivity from 1.0 to 0.4 would produce a power savings of 4.0 percent.

Figure 3.21 compares several parameters from each of the cases. The visualizations in Fig. 3.21 result from the first set of calculations where the heater power output was held constant at 1000 W. Each graph shows the following: (1) wall surface temperatures, (2) a vertical slice through the room that shows how the OT varies with height and depth, and (3) vectors illustrating the flow of radiant energy. From a casual observation, the top row of graphs, representing surface emissivities of 1.0, 0.8, and 0.6, look very similar. The bottom row of visualizations, representing from left to right emissivities of 0.4, 0.2, and 0.05, begins to show some difference in the wall surface temperatures, and in the OT near the ceiling.

Of primary interest are the vectors that represent the flow of radiant energy. Heat transfer of any kind is defined as a *vector*. This means that at any point in the enclosed space, radiant heat transfer has a magnitude and a direction. The direction shows where the radiant energy is going. Another way to think about this is to consider a packet of radiant energy that is just leaving the surface of the radiant panel heater. By knowing the direction of this packet, one could trace the path that the packet will take until it finally impacts a surface and is absorbed by that surface. Note that the concept of vectors inherently incorporates the effect of surface reflection. This is explained in the following discussion.

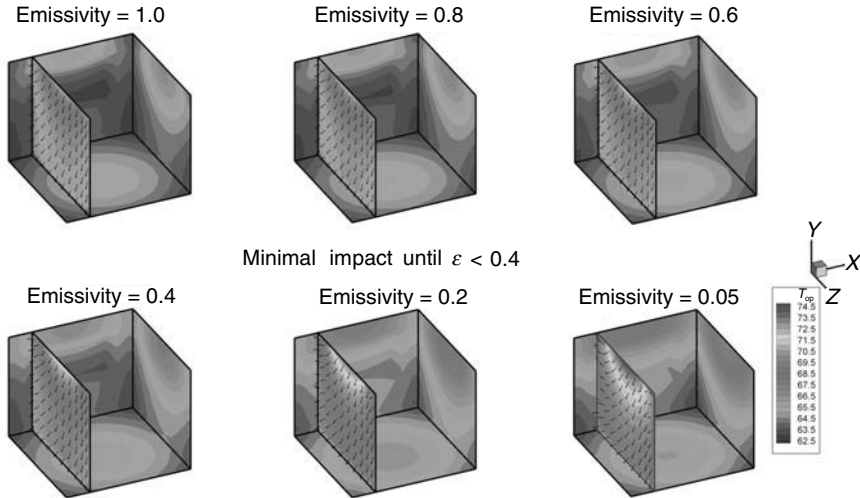


**FIGURE 3.21** Variation in radiation flow, surface temperature, and OT with surface emissivity.

The vectors in Fig. 3.21 show that, for an emissivity greater than or equal to 0.6, the radiant energy predominately leaves the heater surface and impacts on the other room surfaces. Jumping to the other end of Fig. 3.21 where the surface emissivity is 0.05, one first notices that the vector directions are substantially different. In fact, the vectors appear to turn toward the back of the room a short distance above the floor. This happens because the floor is highly reflective. Hence, the packets of radiant energy are forced to flow toward the back of the room where the window surface still exhibits a surface emissivity of 0.6. Looking at the other visualizations in the bottom row of the figure shows that the vectors begin turning toward the back of the room, but not at the extreme that is shown for the 0.05 emissivity case.

The conclusion from this calculation is that the surface emissivity must be very low to meaningfully impact the energy consumption and thermal comfort within a room. Also, keep in mind that in this demonstration, we set the floor to the same emissivity as the walls. This would most certainly not be true because floor coverings exhibit an emissivity of 0.9 or higher. Using a realistic floor material will further minimize the impact of surface emissivity on thermal comfort and energy consumption.

The results from Figs. 3.19 and 3.20 beg the question of how low of an emissivity is practical. To answer this question, consider the surface emissivity of a white sheet of paper. Some might consider this to at least be in the midrange of emissivity. In fact, the emissivity of a white sheet of paper is 0.86! The emissivity of granite is 0.44 and that of smooth (extensively polished) marble is 0.56. The point here is that it is difficult to achieve a surface emissivity that is much lower than 0.80. If one is successful at achieving a low emissivity, the benefit is lost as soon as the surface becomes dusty. Additional information on impact of surface emissivity on energy consumption is contained in the thorough report from Brookhaven Laboratories.

**3.7 HYDRONIC RADIANT HEATING SYSTEM**

This final demonstration explores a floor heating system. This particular system could be powered hydronically or via electric cable. The system considered is installed in a slab-on-grade in a relatively large building, 20 ft wide  $\times$  15 ft deep. The ceiling is 9 ft high. The  $R$  values of the walls and ceiling are 11, and the  $R$  value of the concrete slab is 1. The outside temperature is 14°F (-10°C), and the ground temperature is 50°F (10°C). In each demonstration case, the power density of the hydronically heated slab is 10 W/ft<sup>2</sup>. The goal is to achieve an average OT somewhere in the range between 60°F (15.6°C) and 75°F (23.9°C). The thermal conductivity for the soil was approximated as 1 W/(m · K).

The purpose of this demonstration is to explore thermal charging of the ground underneath the slab, and how the hydronically or electrically heated slab delivers thermal comfort to the enclosed space. Two separate calculations are completed: The first considers the case where the concrete slab is not insulated, and the second set of calculations uses a layer of  $R$ -10 insulation underneath the slab. The average OT is determined for each case.

Several interesting observations come from Figs. 3.22 and 3.23. Figure 3.22 shows two visualizations that represent the results from the uninsulated calculations. The graphic on the left side of the figure illustrates the wall and floor surface temperatures, along with a slice through the center of the room showing the OT. The lower right panel in Fig. 3.22 shows the same case, except that the room is

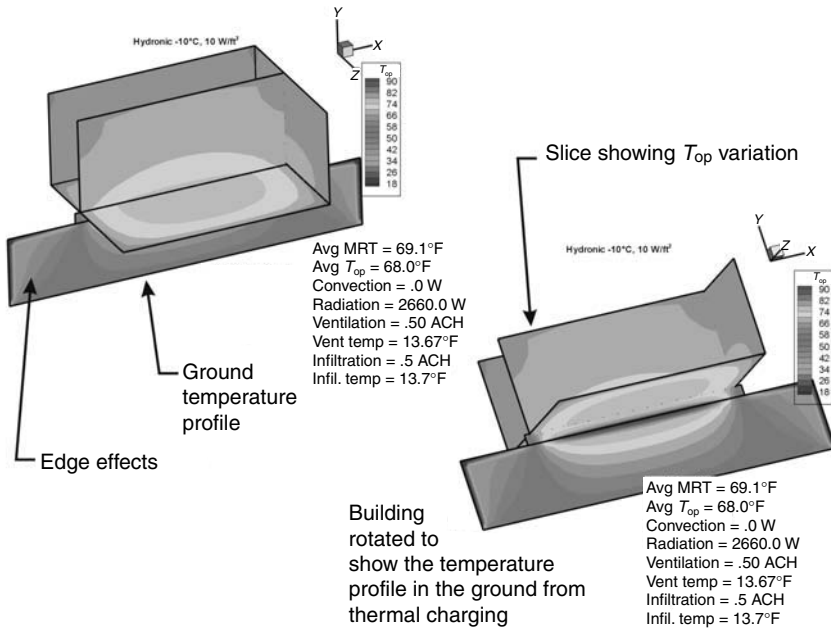


**FIGURE 3.22** Temperature distribution of the slab that is not insulated showing thermal charging of the soil underneath the slab.

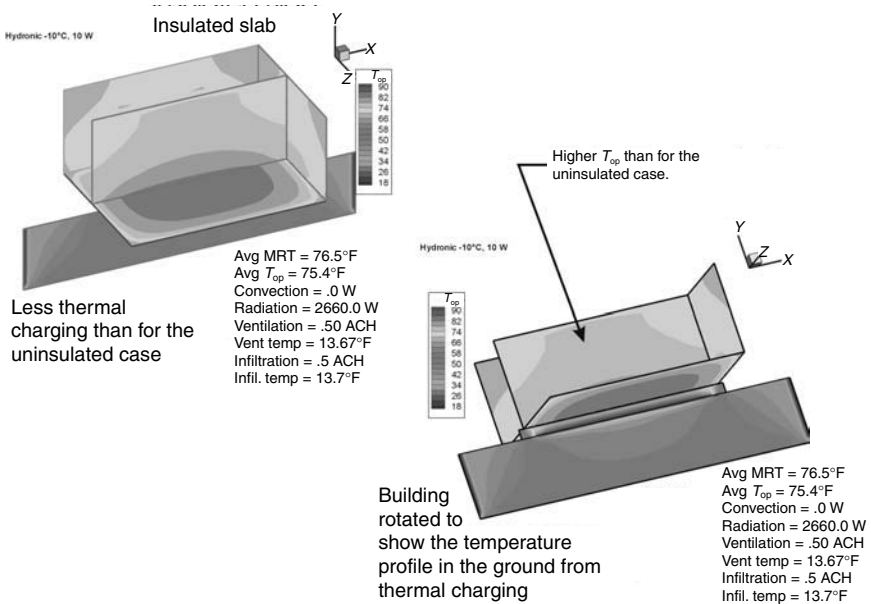


**FIGURE 3.23** Temperature distribution of the wall and floor of the insulated slab.

slightly rotated to show the temperature distribution in the ground underneath the slab. Looking first at the ground temperature distribution, it is apparent that the slab contributes significantly to increasing the soil temperature. The effect, however, does not extend too far down or to the side of the slab. Remembering that heat transfer is driven by temperature difference, and referring to Sec. 2 of this Handbook, once the ground is fully charged, heat transfer losses to the ground are minimized. This occurs because the soil temperature just beneath the slab is heated to a temperature that is very close to the temperature of the slab. The temperature difference between the bottom of the slab and the soil is very small so that the amount of heat that is transferred from the slab to the soil also is very small. Keep in mind, though, that this only occurs when the soil is thermally charged. Otherwise, the soil acts more like a heat sink, absorbing every Btu that it can from the slab. One point that needs to be made is that the soil conditions control, in a very large way, the amount of energy that is absorbed from the slab. The type of soil and the moisture content play a huge role in determining the soil thermal conductivity and specific heat. As shown in Sec. 2 of this Handbook, these two parameters control how far thermal energy is transferred through the soil, and how much energy the soil can store.

Figure 3.24 illustrates additional detail of the right wall and the floor. In general, the wall surface temperatures are approximately 67°F (19.4°C) in the vicinity of the floor, and they reduce to as low as 60°F (15.°C) near the corners of the wall. The floor temperature is highest in the center and decreases toward the edge of the slab. The high point is 74°F (23.3°C), and the lowest temperatures are about 65°F (18.3°C) at the slab corners. These temperatures are relatively cool because the slab edges are not insulated, and the corners are exposed to two sides.

## 8.54 ENGINEERING DESIGN TOOLS TO ASSIST IN HEATER-COOLER SIZING

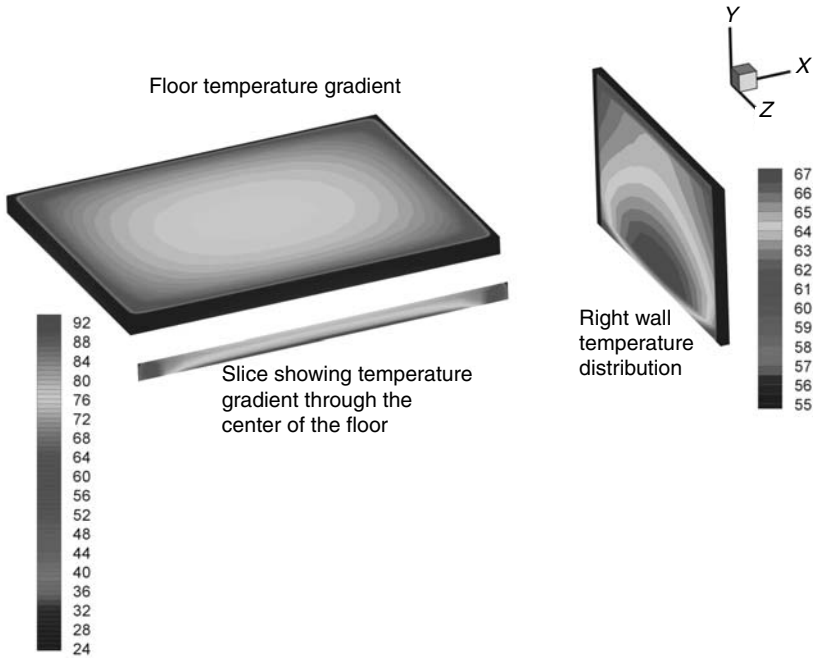


**FIGURE 3.24** Temperature distribution of the wall and floor of the slab that is not insulated.

Figure 3.22 shows the same configuration as the insulated slab but with the  $R$ -10 insulation between the slab and the soil. Because the  $R$ -10 insulation provides a thermal barrier between the slab and the soil, a larger temperature difference is necessary to drive heat transfer from the slab into the soil. Consequently, the soil is not charged to as high a level, and the slab operates at a higher temperature than for the uninsulated case. Because the temperature scales are the same in Figs. 3.22 and 3.23, it is easy to see the difference in thermal charging and the temperatures in the enclosed space. Very little thermal charging occurs in the insulated case as demonstrated by the lack of elevated temperatures underneath the slab. Also of note is that the average OT is about  $6^{\circ}\text{F}$  ( $3.33^{\circ}\text{C}$ ) higher for the insulated case. This higher OT field is created by the elevated floor temperatures that range from a low of  $70^{\circ}\text{F}$  ( $21.1^{\circ}\text{C}$ ) to a high in the center of the floor of about  $80^{\circ}\text{F}$  ( $26.7^{\circ}\text{C}$ ). This impact on surface temperature makes it very important to define the heat transfer variability and characteristics of the soil and insulation surrounding the slab.

### 3.8 SUMMARY OF CASES

The cases in this chapter show the flexibility of creating thermally comfortable and energy-efficient environments with in-space radiant panel heating and cooling systems. Our hope is that you now have an understanding of the design features of radiant systems, and that the mystery has been removed. The final objective of this

chapter is to demonstrate the utility and the importance of a localized thermal comfort program based on the BCAP methodology. As mentioned previously, ABOVE, which uses the BCAP methodology, was used to complete the thermal comfort and heat transfer calculations. We consider a working program that utilizes the BCAP methodology a large step forward in the goal of designing HVAC systems for thermal comfort, and we hope that you will likewise use such a program for your needs.



---

# CHAPTER 4

---

## SIZING, DESIGN, AND METHODOLOGY CONCLUSIONS

---

We have reviewed a broad array of formulas, calculations, design programs, and methodologies that can be employed to design a radiant heating or cooling system. The focus of this Handbook has been on the design of the radiant panel based upon occupant thermal comfort. We have been concerned not only with the power requirement, but also with the design of the radiant panel required to meet the thermal comfort specification. There are many ways to achieve the objectives and multiple building design options that impact energy consumption and system power capacity requirements.

The case studies in Sec. 5 of this Handbook provide a variety of system comparisons, radiant panel construction analyses, and a review of ASHRAE comparative sizing analyses. Although it is clear that refinements are going to be made as computer programs, such as EnergyPlus™ and ABOVE©, are fully developed, the major design differences between the methodologies stand out when the design parameter becomes the operative temperature (OT). Another significant influence that is covered in detail in this Handbook is the wavelength dependency of window glass and the thermal performance of window glasses in the built environment. It is important to understand that the room structure can create a fairly substantial radiant environment, even when radiant panel heaters are not used.

The primary message of this Handbook is that the inclusion of mean radiant temperature (MRT) in heating, ventilating, and air-conditioning (HVAC) design analysis is essential in order to provide in-space occupant thermal comfort as defined by ASHRAE Standard 55, as well as to properly address window heat loss and influence on thermal comfort. There are many methods, however, that a careful designer can employ to achieve radiant system design objectives. The ASHRAE Handbooks provide a wealth of information as do manufacturers, industry trade groups, and a multitude of national, state, and local governmental organizations that facilitate the design of more comfortable and energy-efficient buildings. Having the proper design tools is important, but proper design perspective and product knowledge is essential to harvesting the tools' full potential for increasing building comfort and economy.

### **4.1 RADIANT PANEL EFFICIENCY AS A DESIGN FACTOR**

---

It is also very important to carefully define the radiant panel heat transfer design and insulation characteristics to ensure that the panel configuration will meet the performance specification for the space being designed. The radiant panel heat transfer surface provides in-space heat delivery. Each type of radiant panel as well as its location will impact the in-space sizing requirement. Good design starts with definition of the panel performance boundaries based upon safety, thermal comfort,

codes, and product ratings. It is essential to define the limitations or boundaries under which the design must be developed.

In fact, the determination of the heat transfer efficiency of a radiant panel involves defining the back and edge losses, the radiant-convective split relative to panel location, and the heat transfer efficiency to the panel from the energy-bearing fluid in the case of hydronic panels. The calculation of these deductions from input energy follows normal ASHRAE methodology and is essential to determine radiant panel sizing. This information is covered in detail in the case studies in Sec. 5.

Once the panel heat efficiency has been determined, the relationship between area and power requirements determines actual panel design. Or, if other boundary conditions prevail, the designer may alter the design where possible to increase panel heat transfer efficiency, or select a more efficient panel configuration. In any event, panel heat delivery efficiency is the remaining variable that will determine panel capacities that need to be added to fuel conversion and energy transmission loss to determine minimum power requirements. Depending upon the type and application of radiant panel, power capacity may be added to address the potential for panel coverings (increasing  $R$  values) in the case of floors or to shorten the setup recovery from periods of extended vacancy.

Whether the radiant panel selected is a preinsulated ceiling panel or a concealed floor panel, there is likely to be a significant reduction in equipment sizing from convection systems. In the case of central systems, the reductions in transmission losses will be a major influence. For in-space insulated ceiling panels with very high efficiencies, the building heat delivery system capacity difference compared with central systems of all types will be dramatically lower, as shown in the ENERJOY case study in Sec. 5 of this Handbook.

Whether a designer uses old-fashioned room-by-room hand calculations or a sophisticated program like ABOVE<sup>®</sup>, careful attention to design seasoned with experience should produce an excellent radiant installation. By now, the reader should be as comfortable with designing the radiant panel heating and cooling system as a diffuser or baseboard convection system. Both systems require attention to how heat is delivered to the occupied areas. The difference is that convection system thermal comfort design is dominated by the influence of air buoyancy, whereas the radiant system design is governed by radiant intensity. In the absence of sophisticated computer programs that calculate these factors, the design engineer draws upon knowledge and experience to produce a design that provides occupant comfort, in spite of the limitations of dry-bulb air temperature as the control parameter.

Radiant heating and cooling are becoming more popular as a primary HVAC approach, so it is clear that the design methodologies in common use, although not optimal, are working quite well. In fact, the emergence of hybrid HVAC systems attests to the growing recognition of the role of radiant heating and cooling in managing building surface temperatures. The reader is encouraged to work with the tools that are readily available to design and specify radiant heating and cooling in concert with the building as a system. The opportunities for reducing energy consumption by linking power application directly to the provision of occupant thermal comfort during in-space occupancy are enormous. Radiant heating panels are uniquely equipped to capture occupancy-based comfort savings due solely to the nature of radiant heat transfer and the related control options.

One of the more interesting conclusions drawn from the cases is that the power density and the location of the heater play an important role in determining the thermal comfort signature (TCS<sup>™</sup>). Referring to Figs. 3.13 and 3.14 of this section, it

is apparent that the TCS varies with the power density and the location of the heaters. This is in contrast to the belief that a room needs a certain amount of power to provide a certain level of thermal comfort. These studies show that this statement needs to be refined to include not only the heater power, but also the position of the heater and the power density of the heater. Figure 4.1 shows the variation in the maximum  $T_{op}$  difference within the TCS as a function of power density. The figure shows that power densities that are too low can increase the  $\Delta T_{op}$  and power densities that are too high can likewise increase the  $\Delta T_{op}$ . Finding the most favorable power density requires a careful study of how the  $\Delta T_{op}$  varies with the particular heater, especially because the results shown in Fig. 4.1 most undoubtedly will vary with the room structure.

The bottom line is that the HVAC designer must continue to use the most technologically advanced tools that are available. Prior to this Handbook, these tools were manufacturer and other computer programs buttressed by the ASHRAE Handbooks. The designer now has the information contained in this Handbook, as well as a computerized version of the Building Comfort Analysis Program (BCAP) methodology that gives the capability to design for localized thermal comfort. Once one knows how the TCS varies with the room structure and with the radiant panel position and type, the opportunities are endless to reduce power consumption and to bring thermal comfort parameters to the forefront of building design.

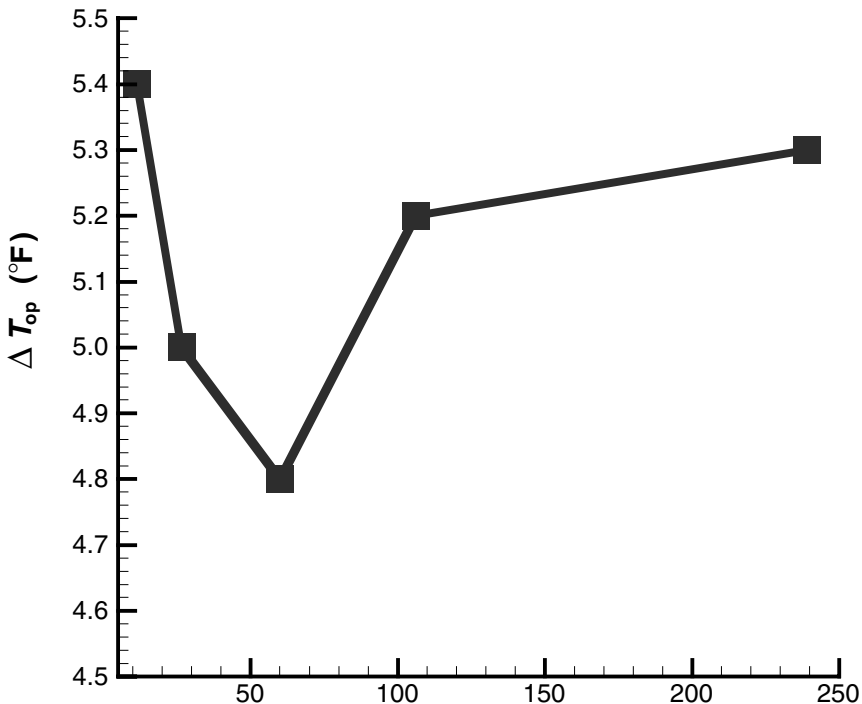


FIGURE 4.1 Variation in OT with radiant panel heater power density.

## 4.2 PARTING COMMENTS

---

Several important key points to remember are the following:

- The built environment should be designed as a trade-off between achieving an acceptable level of thermal comfort and energy consumption.
- The focus of HVAC design is to create a thermally comfortable environment over a wide range of conditions. Having said that, the dry-bulb temperature is not necessarily a good measure of thermal comfort. Instead, one should use the  $T_{op}$  as a metric for thermal comfort.
- In-space heating and cooling systems operate differently than centralized systems. The primary difference is that the conversion from fuel to either heat removal (in the case of a cooling system) or heat addition (in the case of a heating system) takes place in the occupied space for the in-space system and in a centralized location for the centralized system. Consequently, losses occur through fuel conversion in the centralized system or in moving the heat to or from the occupied space. Transmission losses do not occur for the in-space systems and, therefore, in-space systems reduce the overall building capacity requirement and increase heat delivery efficiency compared with centralized systems.
- Designing for thermal comfort entails substantially more than just adding energy to the occupied space. With radiant panels, the power density, how the energy is added, and the location where the energy is added are of critical importance. The power density demonstration in Chap. 3 of this section shows how the designer would choose to minimize the  $T_{op}$  gradient across the room if he or she were working with a sophisticated design methodology such as BCAP.
- Hydronic or electric systems function to warm the floor of the occupied space, such as in slab-on-grade systems; the energy consumption rate during the early part of the heating season will be high because the system thermally charges the ground under the slab. As the season progresses, the energy consumption will decrease as energy is no longer required to charge the ground mass. Losses (as in the case of climates where the system does not short-cycle) due to thermal charging can be minimized by insulating the slab from the ground, especially at the edges of the slab and extending under the ground away from the building in a manner prescribed by the climate and soil conditions. For electric systems, the thermally charged mass can be designed so that it will have the capacity to warm the space during periods of peak power usage when the system is turned off.
- Radiant cooling presents the unique design problem of how to cool the occupied space without creating a rainstorm within the space. The calculations in Chap. 3 of this section show that the surfaces within the space must be maintained above the dew point temperature. In climates that are not continuously arid, precautions must be taken to lower the dew point temperature within the space. This can be accomplished with dehumidifiers or desiccants. As a further precaution, an interactive control system should be installed to deactivate the radiant cooling system should the dehumidification system fail to work properly.
- Windows create a unique design opportunity for the management of radiant energy because of the wavelength dependency of the window glass properties. There is a wealth of window data compiled by the window glass manufacturers and by the federal government that are easily obtained with the Window 4.1™ program referenced in Chap. 1 of this section. Of particular importance is that window glass is opaque to the long-wave radiant energy produced by low-

temperature, in-space radiant heating panels. In contrast, window glass is normally transparent to the short-wavelength radiant energy produced by high-temperature radiant heating systems.

- Radiant systems have better in-space thermal stability than do forced-air convection systems. However, the thermal response of radiant panels is a function of panel mass, power density, and location. Setback recovery design based upon usage requirements is essential to satisfactory system performance.
- Radiant panel covering or obstruction impacts heat delivery or removal, which will impact radiant output and the TCS. Radiant design must consider these impacts in order for the design to serve the needs of future owners or tenants.

The final parting thought to remember is that radiant panel heating and cooling empowers the designer with the opportunity to approach occupant thermal comfort in the full range of architectural designs for the built environment with the precision that a skilled surgeon brings to cosmetic surgery.

